

## Session C11: Unified Theories Including Strong Interactions

*Chairman :* E. C. G. SUDARSHAN

*Organizer:* H. TERAZAWA

*Scientific Secretaries:* K. AKAMA  
A. SUGAMOTO

1. Unification of the Basic Particles and Their Forces at Low and High Energies  
J. C. PATI
2. Unifying All Elementary Particle Forces Including Gravity  
H. TERAZAWA
3. Grand Unified Schemes and Spontaneous Compactification  
L. PALLA
4. New Gravitational Instantons and Universal Spin Structure  
P. G. O. FREUND

## C 11 Unifying AH Elementary-Particle Forces Including Gravity

H. TERAZAWA

*Institute for Nuclear Study, University of Tokyo, Tanashi, Tokyo 188*

It is a final goal in physics to unify all the four basic forces, strong, weak, electromagnetic, and gravitational. I have found it hard to make one story out of many different models and diverse interests existing at this stage of the game in this field. The following is the best I can do.

In this talk, I would like to review some of the contributed papers allocated to this Session other than what Pati,<sup>1</sup> Palla,<sup>2</sup> and Freund<sup>3</sup> will give us talks on. Let me first discuss unified gauge theories of strong, weak, and electromagnetic interactions. There are two standard models: the model of Pati and Salam<sup>4</sup> in which leptons have the fourth color and the model of Georgi and Glashow<sup>5</sup> in which a simple group SU(5) is assumed for grand unification. Since Fritzsche<sup>6</sup> has given in Session CIO and Pati will give us here some features of these "orthodoxies," I shall pick up only new ideas contributed to this Session.

In the original Georgi-Glashow model,<sup>5</sup> leptons and quarks are assigned to a fundamental quintet and an antisymmetric decuplet of SU(5):

$$\frac{1}{\sqrt{2}} \begin{pmatrix} 0 & \bar{t}_3 & -\bar{t}_2 & -u_1 & -d_1 & -b_1 \\ -\bar{t}_3 & 0 & \bar{t}_1 & -u_2 & -d_2 & -b_2 \\ \bar{t}_2 & -\bar{t}_1 & 0 & -u_3 & -d_3 & -b_3 \\ u_1 & u_2 & u_3 & 0 & e^+ & -E^+ \\ d_1 & d_2 & d_3 & -e^+ & 0 & \bar{E}^0 \\ b_1 & b_2 & b_3 & E^+ & -\bar{E}^0 & 0 \end{pmatrix}_L, \quad \frac{1}{\sqrt{2}} \begin{pmatrix} 0 & \bar{g}_3 & -\bar{g}_2 & -c_1 & -s_1 & -h_1 \\ -\bar{g}_3 & 0 & \bar{g}_1 & -c_2 & -s_2 & -h_2 \\ \bar{g}_2 & -\bar{g}_1 & 0 & -c_3 & -s_3 & -h_3 \\ c_1 & c_2 & c_3 & 0 & \mu^+ & -M^+ \\ s_1 & s_2 & s_3 & -\mu^+ & 0 & \bar{M}^0 \\ h_1 & h_2 & h_3 & M^+ & -M^0 & 0 \end{pmatrix}_L,$$

( $\bar{\nu}_e$ )<sub>L</sub>, and ( $\bar{\nu}_\mu$ )<sub>L</sub>.

They also form two right-handed 15-plets and two right-handed singlets with suitable combinations of leptons and quarks. Assuming two 35-plet Higgs scalars, the one breaking SU(6) down to SU(3)<sub>c</sub> x SU(3)<sub>V</sub> x U(1) and the other breaking 811(3)<sup>^</sup>, as well as a 15-plet Higgs scalar and also a singlet one, he has derived two mass relations for leptons and quarks:

$$\begin{pmatrix} d_1 \\ d_2 \\ d_3 \\ l^+ \\ \bar{\nu} \end{pmatrix}_R \quad \text{and} \quad \frac{1}{\sqrt{2}} \begin{pmatrix} 0 & \bar{u}_3 & -\bar{u}_2 & -u'_1 & -d_1 \\ -\bar{u}_3 & 0 & \bar{u}_1 & -u'_2 & -d_2 \\ \bar{u}_2 & -\bar{u}_1 & 0 & -u'_3 & -d_3 \\ u'_1 & u'_2 & u'_3 & 0 & -l^+ \\ d_1 & d_2 & d_3 & l^+ & 0 \end{pmatrix}_L.$$

It is then very tempting to enlarge the gauge group so that these fifteen leptons and quarks may be put in a same multiplet. Such an extension of the Georgi-Glashow model to a grand unified model of SU(6) gauge group has been made by Inoue, Kakuto, Nakano, Abud, Buccella, Ruegg, Savoy, Lee, Weinberg, and Yoshimura.<sup>7</sup> In the contributed paper, "Unified SU(6) Gauge Theory of the Strong, Weak, and Electromagnetic Interactions" by S. K. Yun,<sup>8</sup> the eight leptons, ( $e^-, E^-, \nu; E^0$ ) and ( $\bar{\nu}_L, M^-, \nu^+; M^0$ ), and the eight quarks, ( $t, U, g, C$ ) with charge 2/3 and ( $d, b, s, h$ ) with charge -1/3, form two left-handed 15-plets and two left-handed singlets:

$$\frac{m_d}{m_b} = \frac{m_s}{m_h} \quad \text{and} \quad m_d + m_s + m_b + m_h = m_e + m_\mu + m_{E^-} + m_{M^-},$$

the latter of which is weaker than the original one of Georgi and Glashow,  $m_d = m_s, m_{\bar{\nu}} = m^{\wedge}$  etc., in a model with a single quintet Higgs scalar. From these relations, he has predicted

$$m_b = 3.5^{+1.3}_{-0.4} \text{ GeV} \quad \text{and} \quad m_h = 4.6^{+1.7}_{-0.5} \text{ GeV}.$$

The quantization of electric charge of elementary particles is one of the most satisfactory features in grand unified gauge theories. In order for electric charge to be quantized, it is not, however, necessary that the strong gauge group  $G_c = SU(3)_c$  and the weak and electromagnetic gauge group  $G_w \times G_A$  (where  $G_A$  is an Abelian factor) be unified into a simple or semisimple group. What is necessary is either that the group  $G_w \times G_A$  is unified by a semisimple flavor gauge group  $G_f$  or that the group  $G_w \times G_c$  is unified by a semisimple strong gauge group  $G_s$ . In the contributed paper, "Embedding Weak-hypercharge in Strong Gauge Group" by Inoue, Kakuto, Komatsu, and Nakano,<sup>9</sup> the latter possibility has been investigated in great detail. The first example of their models is the case where  $G_s = SU(4)$ .<sup>4</sup> Since  $SU(3)_c$  should be electrically neutral, the charge operator  $Q$  is written as

$$Q = Q_w + Q_s \quad \text{with} \quad Q_s = 2\sqrt{6} x F_{15},$$

where  $F_{15}$  is a generator of  $SU(4)$  and  $x$  is a parameter to be determined. Due to the color constraint that fermion representations should contain only  $\mathbf{1}$ ,  $\mathbf{3}$ , and  $\mathbf{3}^*$  of color  $SU(3)_c$ , allowed candidates are  $\mathbf{1}$ ,  $\mathbf{4}$ ,  $\mathbf{6}$ , and  $\mathbf{4}^*$  of  $SU(4)$ . They are decomposed into representations of subgroup  $SU(3)_c \times U(1)$  in the notation  $(d_c, Q)$  as

$$\begin{aligned} \mathbf{1} &= (\mathbf{1}, 0), \quad \mathbf{4} = (\mathbf{3}, x) + (\mathbf{1}, -3x), \\ &\text{and } \mathbf{6} = (\mathbf{3}, -2x) + (\mathbf{3}^*, 2x). \end{aligned}$$

The relation between the gauge coupling constants of  $SU(3)_c \times U(1)$  is given by

$$g_c = 2\sqrt{6} x g'.$$

They take two choices:  $G_V = SU(2)$  or  $SU(2)_L \times SU(2)_R$ . In the case of  $G^A = SU(2)$ ,

$$Q_w = h$$

where  $h$  is a  $SU(2)$  generator. They have found that one of the most interesting models is given by

$$x = \frac{1}{6}, \quad I(f_1) = 0, \quad I(f_4) = \frac{1}{2}, \quad \text{and} \quad I(f_6) = 0.$$

The leptons and quarks are assigned as

$$\begin{aligned} (f_4^{I=1/2})_L &= \begin{pmatrix} u \\ d \end{pmatrix}_L + \begin{pmatrix} \nu_e \\ e \end{pmatrix}_L, \\ (f_4^{I=1/2})_R &= \begin{pmatrix} u \\ b \end{pmatrix}_R + \begin{pmatrix} N \\ e \end{pmatrix}_R, \end{aligned}$$

$$(f_6^{I=0})_R = d_R + b_R^*, \quad \text{and} \quad (f_6^{I=0})_L = N_L.$$

Following the renormalization group analysis of Georgi, Quinn, and Weinberg,<sup>5</sup> they obtain

$$\ln\left(\frac{m_Y}{\mu}\right) = \frac{2\pi}{11} \left[ \frac{3}{2} \alpha^{-1} (1 - \sin^2 \theta_w) - \alpha_G^{-1} \right].$$

This indicates that  $m_Y$ , the mass of superheavy gauge bosons, must be of order  $10^{33} \sim 10^{40}$  GeV, far above the Planck mass. In this way, they have studied every combination of  $SU(4)$ ,  $Sp(3)$ ,  $Sp(4)$ ,  $SO(7)$ , and  $SO(8)$  for the strong gauge group, and  $SU(2)$  and  $SU(2)_L \times SU(2)_R$  for the weak gauge group. One of their conclusions is that, in this approach, the constraint relations between the gauge couplings, the weak mixing angle and the mass scale of symmetry breaking owing to the renormalization effect are not so severe compared with those in the grand unified models. The mass scale, however, becomes far above the Planck mass in some cases, or becomes too small to ensure the proton stability in some other cases.

In grand unified gauge theories, there is only one gauge coupling constant. The Higgs potential and the Yukawa coupling between fermions and Higgs scalars are, however, arbitrary so that one can choose whatever hierarchy of spontaneous symmetry breakdown one wants by adjusting Higgs representations and their parameters. In the contributed paper, "Eigenvalue Conditions and Asymptotic Freedom of  $SO(7V)$  Gauge Theories" by Chang and Perez-Mercader,<sup>10</sup> it is demonstrated that this is not true if the theory is required to be asymptotically free.<sup>11</sup> In order to make the theory asymptotically free, they have imposed "eigenvalue conditions"<sup>12</sup> on all the coupling constants other than the gauge coupling. The new features of their grand unified scheme are 1) The number of "carbon copies" of the basic fermion family ( $w, d, \nu, e, \dots$ ) is limited. 2) Each fermion multiplet of  $SO(N)$  unifies the light fermions ( $w, d, \nu, e, \dots$ ) with superheavy fermions ( $I, D, \dots$ ). The superheavy fermions have masses which are of the order of the superheavy gauge boson masses. 3) Even though  $SO(12)$ <sup>13</sup> contains  $SU(4) \times SU(2) \times SU(2)$ ,<sup>13</sup> the structure of the vacuum indicates a breakdown of manifest left-right invariance, already at super-high energies. For  $SO(7V)$  gauge theories, the renormalization group equations<sup>14</sup> for the

gauge coupling  $g$ , the Yukawa coupling  $h$ , and the quartic Higgs couplings  $X$  and  $A$  are given by

$$16\pi^2 \frac{dg}{dt} = -g^3 \left[ \frac{22}{3}(N-2) - \frac{2n_F n_D}{3} - \frac{n_B}{3}(N-2) \right],$$

$$16\pi^2 \frac{dh}{dt} = h^3 \left[ 2n_F n_D + \frac{N(N-1)}{2} + (N-4)^2 - N \right] - 6g^3 h(N-2) - \frac{3}{4}g^2 h[(N-4)^2 - N],$$

$$16\pi^2 \frac{d\lambda}{dt} = \lambda^2 [4N(N-1) + 64] + \lambda A(16N-8) + 12A^2 - 24(N-2)g^2\lambda + 18g^4 - 6n_F n_D h^4 + 8n_F n_D \lambda h^2,$$

and

$$16\pi^2 \frac{dA}{dt} = A^2(8N-4) + 96\lambda A - 24(N-2)g^2 A + 6(N-8)g^4 - 24n_F n_D h^4 + 8n_F n_D \lambda h^2,$$

where  $n_f$  and  $n_d$  are the number of identical fermion and the dimension of spinor representation, respectively.

They assume a special solution of the type  $h(t) = \bar{h}g(t)$ ,  $\lambda(t) = \bar{\lambda}g^2(t)$ , and  $A(t) = \bar{A}g^2(t)$ .

Then, the coupled set of differential equations is reduced to a coupled set of algebraic equations for the constants  $A$ ,  $X$ , and  $\lambda$ , which can be solved. For example, in the SO(12) model with  $n_f=7$ , the solutions are

$$A^2 = 0.1171 g^4 \quad X = -0.012 g^4$$

and  $1 - 0.6166 g^4$

Since the parameters of Higgs potential are fixed, the structure of the vacuum after spontaneous symmetry breakdown is also fixed. It is  $U(2) \times SO(10)$  in this case. They emphasize that, in this kind of asymptotically free grand unified theory, the hierarchy of symmetry breaking is dictated by the theory. There is no longer room to declare a range of quartic self-couplings so as to choose one vacuum vs another.

The baryon number non-conservation is one of the most intriguing features common to grand unified gauge theories. In the contributed paper, "Unified Gauge Theories and the Baryon Number of the Universe," Yoshimura<sup>15</sup> has made a very interesting suggestion that the dominance of matter over antimatter

in the present universe is a consequence of baryon number non-conserving reactions in the very early fireball. Grand unified gauge theories provide a basis for such a conjecture. He has made a computation in a specific SU(5) model of the Georgi-Glashow type<sup>5</sup> and within the standard big-bang cosmology,<sup>16</sup> and found a small ratio of baryon to photon number density in rough agreement with observation. Let me quickly sketch his idea in the following. The time development of the baryon number density  $N_b(t)$  in a hot universe is given by

$$\frac{dN_b(t)}{dt} = -3 \frac{\dot{R}}{R} N_b + \sum_{a,b} (\Delta n_B) \langle \sigma v \rangle N_a N_b$$

where  $R$  is the cosmic scale factor,  $\langle \sigma v \rangle$  is the thermal average of the cross-section for  $a+b \rightarrow *$  anything times the relative velocity of  $a$  and  $b$ ,  $\Delta n_B$  is the change of baryon number in this process, and  $N_a$  is the number density of  $a$ . In the universe (the temperature  $T$ ) dominated by highly relativistic particles, the following relation holds:<sup>16</sup>

$$R/\dot{R} = -T/\dot{T} = (\frac{8}{3}) \frac{cpG}{13y} e$$

where  $p$  is the energy density

$$\rho = d_f \pi^2 T^4 / 15.$$

The effective number of degrees of freedom  $d_f$  is 1/2 or 7/16 for each boson or fermion species, respectively. From these relations, he obtains the rate equation

$$\frac{dF_b}{df} = -v \left( \frac{WG_b d_b}{45} - v^* (3 \dots) \right)$$

where  $\delta = X(J_n Xov)$ ,  $F_b = N_b/T$  and  $F_f = N_f/T$  with the photon number density  $N$ . Next, he claims that to obtain a nonvanishing baryon number one must break the microscopic detailed balance because otherwise the inverse reaction would cancel the baryon number gained. This necessity of simultaneous violation of the baryon number and the CP- or T-invariance is one of the points in his suggestion. To illustrate the idea, he adopts a grand unified SU(5) gauge model of the Georgi-Glashow type with six or more flavors of quarks and leptons. The baryon number non-conservation is caused by exchange of the superheavy lepto-quark gauge bosons  $W$  and also by exchange of colored Higgs scalars  $H_1$  and  $H_2$  (the Yukawa coupling constants  $f$  and  $h$ ). For CP-violation, he adopts the

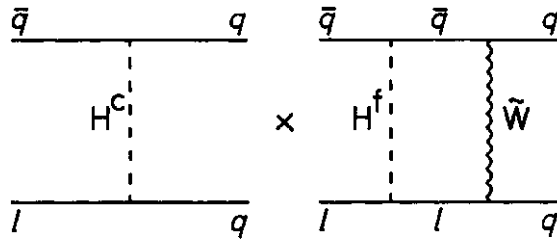


Fig. 1.

Weinberg model<sup>17</sup> in which complex dimensionless parameters,  $a$  and  $1/3$ , are introduced in the Higgs propagators by

$$i\langle T(H_1^{\dagger a} H_2^a) \rangle_{q=0} = \alpha/m_W^2 \text{ for } a=4, 5 \\ = \beta/m_W^2 \text{ for } a=1-3.$$

He has found that the dominant contribution to  $\delta$  comes from interference of the diagrams in Fig. 1 and that

$$\frac{\delta}{T^2} \simeq \frac{3g^2}{8\pi^2 m_W^4} \text{Im} \beta \alpha^* (\text{tr } hh^\dagger \text{tr } f^2 - \text{tr } hh^\dagger f^2).$$

Under the reasonable assumption  $N_b \ll N_s$ , the rate equation is integrated to

$$\frac{N_B(T)}{N_\gamma(T)} \simeq - \left( \frac{8\pi^3 G_N d_F}{5} \right)^{-1/2} \left( \frac{3}{8} \right)^2 \frac{\delta}{T^2} \\ \times N_\gamma(T_{\text{initial}}).$$

To obtain a rough quantitative idea of this ratio, he has made a drastic extrapolation of this formula up to  $T_{\text{min}} = m^{\wedge}$  to get the numerical result

$$\frac{N_B}{N_\gamma} \simeq 2 \times 10^{-9} \left( \frac{m_t}{10 \text{ GeV}} \right)^2 \left( \frac{m_b}{5 \text{ GeV}} \right)^2 A \\ \text{with } A \simeq 0(1).$$

An estimate of this ratio<sup>16</sup> from experimental data ranges from  $10^{-8}$  to  $10^{-10}$ , which agrees with this result. Although the numerical result should not be taken too seriously because of crudest approximations involved, I have found that his suggestion is extremely interesting and really working.

Next, I would like to discuss unified models of all elementary-particle forces including gravity. Recently, possible unification with supergravity has been extensively investigated and it has been discussed by Freedman<sup>18</sup> in Session C6. There have been proposed some other ideas on this super-grand unification. The strong gravity proposed by Isham, Salam, and Strathdee and by Zumino<sup>19</sup> is one of them. In the contributed paper, "Emergence of a (possibly) Strong Component in a Poincaré-

Quadratic Gauge Theory of Gravity" by Hehl, Ne'eman, Nitsch, and von der Heyde,<sup>20</sup> a related but quite distinct picture has been proposed for unifying gravity and the confining strong force. It is also a completely new description of gravity which is quite different from Einstein's general relativity. In their gauge approach to the Poincaré group the vierbein  $e^{\mu}$  represents the translational potential and the vierbein connection  $r_{\mu}^{\nu} = -\text{Tipa}$  the rotational potential. The corresponding field strengths are torsion and curvature,

$$F_{ij}^{\alpha} \equiv 2(\partial_{[i} e_{j]}^{\alpha} + \Gamma_{[i\beta}^{\alpha} e_{j]}^{\beta})$$

$$\text{and } F_{ij\alpha}^{\beta} \equiv 2(\partial_{[i} \Gamma_{j]\alpha}^{\beta} + \Gamma_{[i\gamma}^{\beta} \Gamma_{j]\alpha}^{\gamma}),$$

respectively. Let  $\langle f \rangle$  and  $S_f$  be a matter field and a matter Lagrangian. The total Lagrangian is then given by

$$\mathcal{L}_{\text{tot}} = \mathcal{L}(\psi, \nabla^{\Gamma} \psi, e) + \mathcal{V}(e, \partial e, \Gamma, \partial \Gamma)$$

it one supposes minimal coupling in accordance with the equivalence principle. In analogy with electrodynamics, they assume the quadratic Lagrangian for  $\wedge$

$$\mathcal{V} = (\det e) \left[ \frac{1}{4l^2} (-F^{ij}_{\alpha} F_{ij}^{\alpha} + 2F^{i\gamma}_{\gamma} F_{i\delta}^{\delta}) \right. \\ \left. + \frac{1}{4\kappa} (-F_{ij\alpha}^{\beta} F^{ij\alpha}_{\beta}) \right],$$

where  $l$  is the Planck length and  $\kappa$  is a dimensionless coupling constant. In assuming this Lagrangian, they suppose that the coupled equations derived from it result in a restructuring of the two initial gauge potentials into one long-range Einstein-Newton-like potential with  $l^2$  dimensional coupling, and a second, Yang-Mills-like, short-range one with dimensionless (strong) coupling. The latter would be asymptotically-free and confining, and would thereby produce a natural "strong gravity" component. They have proved that such a confining contribution does indeed arise in the linearized approximation.

Assume

$$e_i^{\alpha} = \delta_i^{\alpha} + \frac{1}{2} h_i^{\alpha} \text{ with } |h_i^{\alpha}| \ll 1 \text{ and } |I'_{i\alpha}{}^{\beta}| \ll 1,$$

and define

$$\gamma \equiv \gamma_k^k \text{ with } \gamma_{ij} \equiv h_{(ij)} - \frac{1}{2} \eta_{ij} h_k^k \text{ and } \Gamma'_i = \Gamma_{ki}^k.$$

Then, the linearized field equations for  $y$  and  $Fi$  turn out to be

$$\square\square\gamma = -2\kappa(\Sigma - 2\partial_k\tau^k) - 2I^2\square\Sigma$$

and

$$\square\partial_k\Gamma^k = (\kappa/2)(\Sigma - 2\partial_k\tau^k)$$

where  $S$  and  $v_i$  are the trace of momentum and spin current, respectively. For a spinning point particle of mass  $m$  located at the origin,  $r^i=0$  and  $Z=-md(r)$ . Then the first equation yields the solution

$$\gamma(r) = -\frac{I^2}{2\pi}\left(\frac{m}{r}\right) + c_1 - \frac{\kappa}{4\pi}(mr) + c_2 r^2$$

for some  $r_{min} < r < r_{max}$ . The constant multiplying the Newton potential and the one in front of the confinement potential are both fixed. They have further demonstrated that their Lagrangian reproduces the Schwarzschild solution, and therefore proves to be a viable one. There is only one problem: how do leptons avoid strong gravity? They suggest that even leptons might yet display the same features at shorter ranges and larger energies, or alternatively that the color degree of freedom is involved.

In the rest of my talk, I would like to review the recent work by Akama, Chikashige,

Matsuki, and myself<sup>21,22</sup> on the unified model of the Nambu-Jona-Lasinio type for all elementary-particle forces including gravity. We start with a nonlinear fermion Lagrangian of the Heisenberg type for a Weinberg-Salam multiplet of massless leptons and quarks:

$$\begin{aligned} \mathcal{L} = & \bar{l}_L i \not{\partial} l_L + \bar{l}_R i \not{\partial} l_R + \bar{q}_L i \not{\partial} q_L + \bar{u}_R i \not{\partial} u_R \\ & + \bar{d}_R i \not{\partial} d_R + f_1 (Y_{l_L} \bar{l}_L \gamma_\mu l_L + Y_{l_R} \bar{l}_R \gamma_\mu l_R \\ & + Y_{q_L} \bar{q}_L \gamma_\mu q_L + Y_{u_R} \bar{u}_R \gamma_\mu u_R + Y_{d_R} \bar{d}_R \gamma_\mu d_R)^2 \\ & + f_2 (\bar{l}_L \gamma_\mu \boldsymbol{\tau} l_L + \bar{q}_L \gamma_\mu \boldsymbol{\tau} q_L)^2 \\ & + f_3 (\bar{q}_L \gamma_\mu \lambda^a q_L + \bar{u}_R \gamma_\mu \lambda^a u_R + \bar{d}_R \gamma_\mu \lambda^a d_R)^2 \\ & + f_4 (b_l \bar{l}_L l_R - b_u \bar{q}_R^c u_L^c + b_d \bar{q}_L d_R) \\ & \times (b_l \bar{l}_R l_L - b_u \bar{u}_L^c q_R^c + b_d \bar{d}_R q_L). \end{aligned}$$

By using the Kikkawa's algorithm<sup>23</sup> to analyze this nonlinear Lagrangian and by imposing the massless conditions of Bjorken<sup>24</sup> on vector fields, we construct an effective Lagrangian which combines the unified SU(2) X U(1) gauge theory of Weinberg and Salam for the weak and electromagnetic interactions of leptons and quarks, and the Yang-Mills gauge theory of color SU(3) for the strong interaction of quarks:

$$\begin{aligned} \mathcal{L}' = & \bar{l}_L i \gamma^\mu \left( \partial_\mu + ig' \frac{1}{2} Y_{l_L} B_\mu - ig \frac{1}{2} \boldsymbol{\tau} \cdot \mathbf{A} \right) l_L + \bar{l}_R i \gamma^\mu \left( \partial_\mu + ig' \frac{1}{2} Y_{l_R} B_\mu \right) l_R \\ & + \bar{q}_L i \gamma^\mu \left( \partial_\mu + ig' \frac{1}{2} Y_{q_L} B_\mu - ig \frac{1}{2} \boldsymbol{\tau} \cdot \mathbf{A}_\mu - if \frac{1}{2} \lambda^a G_\mu^a \right) q_L \\ & + \bar{u}_R i \gamma^\mu \left( \partial_\mu + ig' \frac{1}{2} Y_{u_R} B_\mu - if \frac{1}{2} \lambda^a G_\mu^a \right) u_R + \bar{d}_R i \gamma^\mu \left( \partial_\mu + ig' \frac{1}{2} Y_{d_R} B_\mu - if \frac{1}{2} \lambda^a G_\mu^a \right) d_R \\ & - G_l (\bar{l}_L \phi l_R + \bar{l}_R \phi^\dagger l_L) - G_u (\bar{q}_L \phi^a u_R + \bar{u}_R \phi^{a\dagger} q_L) - G_d (\bar{q}_L \phi d_R + \bar{d}_R \phi^\dagger q_L) \\ & - \frac{1}{4} (B_{\mu\nu})^2 - \frac{1}{4} (A_{\mu\nu})^2 - \frac{1}{4} (G_{\mu\nu}^a)^2 + |D_\mu \phi|^2 - \mu^2 |\phi|^2 - \lambda (|\phi|^2)^2. \end{aligned}$$

Let me emphasize the difference between our model and the ordinary gauge models. In our picture of unification, the photon the weak vector bosons  $W^\pm$  and  $Z$ , and the physical Higgs scalar  $\phi$  appear as collective excitations of lepton-antilepton or quark-antiquark pairs while the color-octet gluons  $G^a$  appear as those of quark-antiquark pairs. Also, in the ordinary gauge models, the coupling constants  $f, g, g', K, G_u, G_v,$  and  $G_d$  and the mass parameter  $\mu^2$  are arbitrary, whereas in our model they are completely fixed by the quantum numbers of leptons and quarks, the cutoff momentum, and the coupling constants in the original Lagrangian. The most important

results of our unified model of the Nambu-Jona-Lasinio type for strong, weak, and electromagnetic interactions are the following: the Weinberg angle  $\theta_w$  is determined to be  $\sin^2 \theta_w = (2/3^2) / (S_0^2) = 3/8$  where  $I$  and  $Q$  are the weak isospin and charge of leptons and quarks. The gluon coupling constant is also determined to be  $8/3$  times the fine-structure constant  $\alpha$ . These results coincide with those of Georgi and Glashow<sup>5</sup> in their unified SU(5) gauge model. However, our results are due not to such an assumed higher symmetry as SU(5) but to the Nambu-Jona-Lasinio dynamics in our model with only SU(3)<sub>color</sub> x [SU(2) x U(1)]<sub>weib.e.r.g.</sub>.

The masses of the weak vector bosons are predicted to be

$$m_w = (7ia/V \ 2 \ G_f \ \sin^2 \ d_{y^*} = 60.9 \ \text{GeV}$$

$$\text{and } m_z = m_w / \cos \theta_w = 77.0 \ \text{GeV}.$$

Entirely new and proper to our model are the following relations between the masses of the physical Higgs scalar and weak vector boson and those of leptons and quarks:

$$m_\eta = 2[(\sum m^4)/(\sum m^2)]^{1/2}$$

$$\text{and } m_W = \sqrt{3}[\langle m^2 \rangle]^{1/2}$$

where  $\sum$  and  $\langle \rangle$  denote the summation and arithmetic average over all leptons and quarks. These relations together with the previous results predict the arithmetic-like-average mass of leptons and quarks to be

$$[\langle m^2 \rangle]^{1/2} = 35.2 \ \text{GeV}$$

and the mass of the physical Higgs scalar to be bounded by

$$m_\eta \leq (2/V \sim 3) m_w = 703 \ \text{GeV}.$$

Another important result is the relation between the fine-structure constant and the sum of the charge squared of leptons and quarks:

$$\alpha = 3\pi/(\sum Q^2) \ln (A^2/m^2),$$

where  $A$  is the universal cutoff momentum and  $m$  is the geometric-like-average mass of charged leptons and quarks defined by

$$m = \prod m^{Q^2/(\sum Q^2)}.$$

This relation is essentially the old result of Gell-Mann and Low<sup>25</sup> in their renormalization group approach.

In our model of the Nambu-Jona-Lasinio type for gravity, the graviton is also a collective excitation of a fermion-antifermion pair.<sup>26</sup> We start again with a very simple nonlinear fermion Lagrangian

$$\mathcal{L}_0 = \bar{\psi} i \frac{1}{2} \vec{\partial} \psi + f_0 (T_{\mu\nu})^2$$

$$\text{with } T_{\mu\nu} = \bar{\psi} i \frac{1}{4} (\gamma_\mu \vec{\partial}_\nu + \gamma_\nu \vec{\partial}_\mu) \psi$$

and impose the massless condition on a tensor field, the gravitational field. Then, we derive the effective Lagrangian

$$\mathcal{L}'_0 = \bar{\psi} i \frac{1}{2} \vec{\partial} \psi + \frac{1}{4} (\partial_\lambda h_{\mu\nu})^2 - g_0 T_{\mu\nu} h^{\mu\nu}$$

$$\text{with } g_0 = 4\pi/(\kappa_0 N_0 A^2)^{1/2},$$

where  $\kappa_0 = 2/3$  or  $1/3$  depending on the invariant

or Pauli-Villars cutoff procedure. This Lagrangian reproduces the familiar Newtonian gravitational potential if the gravitational constant  $G$  is related with the total number  $N_0$  of leptons and quarks:

$$G = g_0^2/4\pi = 4\pi/\kappa_0 N_0 A^2.$$

It is also shown that a more sophisticated model of this type defined on the curved space effectively reproduces the Einstein-Weyl's theory of general relativity.

We further unify the unified model of strong, weak, and electromagnetic interactions and the model of gravity into a unified model of the Nambu-Jona-Lasinio type for all elementary-particle forces including gravity. The most exciting result of this grand unification is a simple relation (the  $G \sim a$  relation) between the fine-structure constant and the Newtonian gravitational constant:

$$\alpha = 3\pi/(\sum Q^2) \ln (4\pi/\kappa_0 N_0 G m^2).$$

This relation can be easily derived from combining the above two relations for  $a$  and  $G$ . Historically, a relation of this type was conjectured by Landau<sup>27</sup> in 1955. Since this  $G \sim a$  relation is very sensitive to the total number of leptons and quarks, we can predict<sup>28</sup> based on it that there exist a dozen leptons (six neutrinos and six charged leptons) and a dozen flavors and three colors of quarks (6x3 up quarks and 6x3 down quarks). The geometric-like-average mass of the charged leptons and quarks is also predicted to be

$$m = (4\pi/\kappa_0 N_0 G)^{1/2} \exp [-3\pi/2\alpha (\sum Q^2)]$$

$$= 23.7 \ \text{GeV}.$$

It is now natural to ask why so many leptons and quarks. In concluding this talk, I shall present an answer to this question. It is a "spinor-subquark" model of leptons and quarks in which leptons and quarks are made of three subquarks of spin 1/2,

$$w_i \ (i=1, 2), \ h_i \ (i=1, 2, \dots, N),$$

$$\text{and } C_i \ (i=0, 1, 2, 3).$$

The left-handed  $w_L$  and the right-handed  $w_R$  and  $w_{2B}$  are a doublet and singlets of the Weinberg-Salam SU(2), respectively. The  $l/z/s$  form an Applet of the unknown H symmetry. Also, the  $C_0$  and  $C/s$  ( $z=1, 2, 3$ ) are singlet and triplet under the color SU(3) symmetry. Leptons and quarks are expressed in

terms of these subquarks as

$$\nu_j = (w_1 h_j C_0), l_j = (w_2 h_j C_0), u_{ji} = (w_1 h_j C_i),$$

$$\text{and } d_{ji} = (w_2 h_j C_i)$$

for  $j=1, 2, \dots, N$  and  $i=1, 2, 3$ .

In the unified subquark model of all elementary-particle forces, which is an alternative to the unified lepton-quark model, the gauge bosons  $W^\pm$  and  $Z$ , and the physical Higgs scalar  $t_j$  appear as collective excitations of a  $w$ - $w$  pair while the color octet gluons  $G^a$  appear as those of a  $C$ - $C$  pair. As a result, we derive the following relations between the masses of  $r_j$ ,  $W^\pm$ , and  $Z$ , and those of  $w$ 's:

$$m_\eta \cong 2m_w, m_W \cong \sqrt{3} m_w,$$

$$\text{and } m_Z \cong (\sqrt{3} / \cos \theta_w) m_w.$$

These relations predict the masses of the physical Higgs scalar and the  $w$  subquark to be

$$m_\eta \sim 70.3 \text{ GeV} \quad \text{and} \quad m_w \sim 35.2 \text{ GeV}.$$

This result strongly suggests that the masses of the physical Higgs scalar and weak vector bosons may be very close to the threshold of  $w$ -subquark pair production, if any (see Fig. 2).

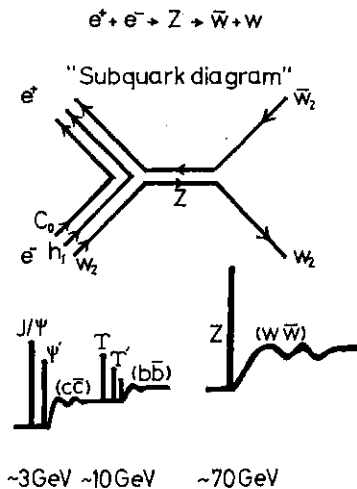


Fig. 2.

I, therefore, strongly urge experimentalists to be still alert for producing possible subquark pairs even after the anticipated exciting discovery of the weak vector bosons in 80's.

I wish to thank Drs. K. Akama and A. Sugamoto for their help in preparing for this review.

References

1. J. C. Pati: "Unification: Its Implications for Present and Future High Energy-Experimentation," in this Proceedings, C11.
2. L. Palla: "Spontaneous Compactification," in this Proceedings, C11.
3. P. O. G. Freund: "World Topology and Gauged Internal Symmetries," in this Proceedings, C11.
4. J. C. Pati and A. Salam: Phys. Rev. **D10** (1974) 275.
5. H. Georgi and S. L. Glashow: Phys. Rev. Letters **32** (1974) 438; see also H. Georgi, H. R. Quinn and S. Weinberg: *ibid.*, **33** (1974) 451.
6. H. Fritzsch: "Gauge Models of Weak Interactions," in this Proceedings, C10.
7. K. Inoue, A. Kakuto and Y. Nakano: Progr. theor. Phys. **58** (1977) 630; M. Abud, F. Buccella, H. Ruegg and C. A. Savoy: Phys. Letters **67B** (1977) 313; B. W. Lee and S. Weinberg: Phys. Rev. Letters **38** (1977) 1237; M. Yoshimura: Progr. theor. Phys. **58** (1977) 972.
8. S. K. Yun: contributed paper No. 28, COO-3533-99/SU-4210-99. (Syracuse Univ., Sept., 1977).
9. K. Inoue, A. Kakuto, H. Komatsu and Y. Nakano: contributed paper No. 534, KYUSHU-78-HE-8 (Kyushu Univ. and Kinki Univ., June, 1977).
10. N.-P. Chang and J. Perez-Mercader: contributed paper No. 937, CCNY-HEP-78-15 (City Coll. of the City Univ. of N.Y.); see also M. Chaichian: in this Proceedings, C 5.
11. D. Gross and F. Wilczek: Phys. Rev. Letters **26** (1973) 1343; H. Politzer: *ibid.*, **26** (1973) 1346.
12. N. P. Chang: Phys. Rev. **D10** (1974) 2706; M. Suzuki: Nucl. Phys. **B83** (1974) 269; E. Ma: Phys. Rev. **D11** (1975) 322; Phys. Letters **62B** (1976) 347; Nucl. Phys. **B116** (1976) 195; E. S. Fradkin and O. K. Kalashnikov: J. Phys. **A8** (1975) 1814; Phys. Letters **59B** (1975) 159; *ibid.*, **64B** (1976) 177.
13. H. Fritzsch and P. Minkowski: Ann. Phys. **93** (1974) 193.
14. D. Gross and F. Wilczek: Phys. Rev. **D8** (1973) 3633; T. P. Cheng, E. Eichten and L. F. Li: Phys. Rev. **D9** (1974) 2259.
15. M. Yoshimura: contributed paper No. 911 (Tohoku Univ.).
16. For a review, see S. Weinberg: *Gravitation and Cosmology*, (Wiley, New York, 1972) Chapter 15.
17. S. Weinberg: Phys. Rev. Letters **37** (1976) 657. For a review, see R. Mohapatra: "Theory of CP Violation," in this Proceedings, C 10.
18. D. Z. Freedman: "Supersymmetry and Supergravity," in this Proceedings, C6.
19. C.J. Isham, A. Salam and J. Strathdee: Phys. Rev. **D3** (1971) 867; *ibid.*, **D9** (1974) 1702; A. Salam: *Ann. N. Y. Acad. Sci.* **294** (1977) 12; see also B. Zumino: in *Lectures on Elementary Particles and Quantum Field Theory*, by S. Deser *et al.* (MIT Press, Cambridge, Mass., 1970) Vol. 2, p. 437.
20. F. W. Hehl, Y. Ne'eman, J. Nitsch and P. Van



- der Heyde: contributed paper No. 236 (Univ. of Colonge and Tel-Aviv Univ.).
21. H. Terazawa, K. Akama and Y. Chikashige: *Progr. theor. Phys.* **56** (1976) 1935; *Phys. Rev.* **D15** (1977) 480; see also T. Saito and K. Shigemoto: *Progr. theor. Phys.* **57** (1977) 242; **57** (1977) 643.
  22. H. Terazawa, Y. Chikashige, K. Akama and T. Matsuki: *Phys. Rev.* **D15** (1977) 1118; *Progr. theor. Phys.* **60** (1978) 868; contributed paper No. 103, KEK-78-11 (National Lab. for High Energy Phys., July, 1978).
  23. K. Kikkawa: *Progr. theor. Phys.* **56** (1976) 947; T. Kugo: *ibid.*, **55** (1976) 2032; see also T. Eguchi and H. Sugawara: *Phys. Rev.* **D10** (1974) 4257; H. Sugawara: "Gauge Invariant Spinor Theory," in this Proceedings, C9.
  24. J. D. Bjorken: *Ann. Phys.* **24** (1963) 174.
  25. M. Gell-Mann and F. E. Low: *Phys. Rev.* **95** (1954) 1300.
  26. P. R. Phillips: *Phys. Rev.* **146** (1966) 966; see also A. D. Sakharov: *Dokl. Acad. Nauk SSSR* **177** (1967) 70.
  27. L. Landau: in *Niels Bohr and the Development of Physics*, edited by W. Pauli (McGraw-Hill, New York, 1955) p. 52.
  28. H. Terazawa: *Phys. Rev.* **D16** (1977) 2373.
- Note added in proof: Recently, J. Arafune has pointed out that the baryon-number non conservation claimed by Yoshimura violates CPT invariance and unitarity.

PROC. 19th INT. CONF. HIGH ENERGY PHYSICS  
TOKYO, 1978

## C11                      **Unification: Its Implications for Present and Future High Energy-Experimentation**

J. C. PATI

*Department of Physics and Astronomy, University of Maryland,  
College Park, Maryland 20742*

### §1, Introduction

Since the last International Conference held in Hamburg a year ago, there is one marked difference in the experimental situation regarding the status of the structure of neutral current interactions. At present all experiments, which include neutrino-nucleon-scattering, neutrino-charged lepton scattering as well as parity violation in electron-deuteron-scattering, agree remarkably well with the predictions of the simple gauge-unification based on the symmetry-structure<sup>1</sup>  $SU(2)_L \times U(1)$ .

This raises two important questions:

(1) Do the set of data noted above single out  $SU(2)_L \times U(1)$  as the only allowed symmetry relevant for low energy electro-weak force, or do they allow for possible alternative symmetries, which would differ from the predictions of  $SU(2)_L \times U(1)$  even in the low energy regime in areas yet to be explored experimentally?

(2) Given that a gauge unification of the weak and electromagnetic forces is already

manifest at present energies through the discovery of neutral current interactions, what new phenomena and correspondingly fundamentally *new physics* may one look forward to discover next at higher energies through high energy accelerators to be completed in the near future and within the decade? Specifically, assuming that the three basic forces—weak, electromagnetic as well as strong—have a common origin, and so also do quarks and leptons,<sup>2,3</sup> one might look forward to discover next *tangible evidence* of such a "grand" unification. This evidence would arise if one could see traces of the new class of interactions (analogous to neutral current interactions) that are needed for putting quarks and leptons into one multiplet. The pertinent question is: can these new interactions and correspondingly "grand" unification manifest at an energy or mass-scale, within experimental reach in the near or conceivable future?

The purpose of my talk is two fold:

(i) First, to note that the present set of

data, which test only (a) left handed neutrino- or right handed antineutrino-scattering, and (b) the *parity violating part* of the electron-quark neutral current (nc) interaction do not single out  $SU(2)_L \times U(1)$  as the only allowed low energy electro-weak-symmetry, since they have not yet probed sensitively into the parity conserving part of the nc interaction.

The present set of data permit two alternative low energy forms for the electro-weak symmetry: (i) The left handed  $G_L = SU(2)_L \times U(1)$ , as well as<sup>4</sup> (ii) the left-right symmetric  $G_{LR} = SU(2)_L \times SU(2)_R \times U(1) \times U(1)$ . Both of these arise as alternative low energy forms relevant for electro-weak interactions within unifying symmetries<sup>3</sup> such as  $[SU(4)]^4$ . The two sub-symmetries  $G_L$  and  $G_{LR}$  coincide in their predictions as regards low energy neutrino-scattering as well as parity violating part of the nc interaction. But they can differ in general substantially from each other in their predictions as regards the parity conserving part of the nc interaction, and simultaneously as regards the masses and the number of the relatively light weak neutral gauge bosons. The symmetry  $G_{LR}$  permits in general a weak gauge boson  $Z_A$  substantially lighter than the  $Z^0$  ( $m_{Z_A} \lesssim 85 \text{ GeV}$ ) of  $SU(2)_L \times U(1)$  consistent with *all* available data. Such differences, in case they exist, can be probed sensitively through a measurement of the parity conserving forward-backward asymmetry-parameters for  $e^- e^+ \rightarrow u \bar{u}$  scattering at PETRA and PEP energies and also for high energy pp and pp scattering.

In other words, discovery of new physics, which could signal a structure beyond  $SU(2)_L \times U(1)$ , may still be awaiting PETRA and PEP experiments as well as high energy pp and pp experiments under planning. Any indication for the presence of the extra  $U(1) \times U(1)$  factor in the low energy electro-weak symmetry would be important in that it would greatly narrow down the choice of the superstructure  $G$  unifying weak, electromagnetic as well as strong forces.

(ii) The second and main point of my talk would be to emphasize that a manifestation of the postulated strong-electro-weak-unification need not necessarily await realization of ultrahigh centre of mass energies exceeding  $10^{15} \text{ GeV}$ , as traditionally claimed.<sup>5</sup> Within

unifying symmetries such as  $[SU(4)]^4$ , which gauge chiral color, such a unification can manifest at an energy scale as low as about  $10 M_0^6 \text{ GeV}$ , provided *chiral color*  $SU(3) \times SU(3)$  rather than vector color emerges as a good low energy symmetry.<sup>6</sup> This raises the possibility that "grand" unification may in fact be testable within the present generation. I shall remark that chiral color brings with it intriguing signatures without disturbing the familiar successes of the standard vector QCD; It supplements the familiar octet of vector color gluons with an octet of relatively light *axial color gluons* ( $m_{A_8} \lesssim (1/2 - 2) \text{ GeV}$ ), which generate spin-spin force in the leading term. This may help resolve some of the lingering discrepancies as regards level-splitting and transitions in charmonium physics.

In the course of my talk I shall briefly allude to a) left-right symmetry and CP violation, b) spontaneous breakdown of symmetry structures of the form  $[SU(4)]^4$ , in particular some new results<sup>7</sup> exhibiting that there is an intimate link between the emergence of the GIM-mechanism and the degree of nc parity violation within such a symmetry-structure, and c) the question of liberation versus confinement of quarks and gluons, especially the possible links between liberated color and the excess prompt neutrinos observed in beam dump experiments on the one hand and the indicated rise in  $\nu W_2$  at high  $W^2 > 100 \text{ GeV}^2$  for  $\nu p$ -scattering reported at this conference on the other.

The topics appear in the following sequence:

II. Grand Unification: Comparative Summary of Alternative Approaches

III. Salient Features of  $[SU(4)]^4$ : Left-Right-Symmetry CP Violation: Link Between GIM-Mechanism and Neutral Current Parity Violation: Integer Versus Fractional Quark-Charges: Liberated Versus Confined Quarks and Gluons

IV. Role of Chiral Color in Low Mass Unification: Possible Signatures of Chiral Color in Quarkonium-Physics and Deep Inelastic scattering

V. Summary: Important Questions: New Discoveries Within the Decade

Due to lack of space, I include only the second and last chapters in this Proceeding, which provide motivations, a comparative

summary and experimental consequences of grand unification. A complete outline may be found in the Proceedings of the Seoul Symposium on Elementary Particle Physics held September, 1978.

### §11. Grand Unification

The motivations for going beyond electro-weak unification (exemplified by the symmetry-structure  $SU(2)_c \times U(1)$ ) are that within the premises of electroweak unification: (a) there are more than one gauge coupling constants, which are unrelated; thus the weak angle  $\tan^2 \theta_w \sim (g'/g)^2$  is an arbitrary parameter; (b) there is no rationale for the existence of quarks and leptons; (c) there is no rationale for the existence of weak, electromagnetic and strong interactions; (d) there is no prediction for the charges of leptons vis-a-vis those of quarks; electric charge is not quantized; (e) there is no compelling reason why  $(V-A)$ -chiral weak interactions should work for  $(e^-$  and  $p^+)$  rather than for  $(e^+$  and  $p^+)$ .

These shortcomings are eliminated within the so-called "grand" unification-hypothesis, which is this:<sup>2,3,8</sup> quarks as well as leptons are members of one multiplet; weak, electromagnetic as well as strong interactions derive their origin from a single set of interactions characterized by a single basic gauge coupling constant. The observed distinctions between quarks and leptons as well as between weak, electromagnetic and strong interactions are not intrinsic to the basic equations of motion. The distinctions arise at low energies as a consequence of spontaneously induced asym-

metry in the ground state; these distinctions should disappear at appropriately high energies.

Such a broad view calls for the existence of a *new class of interactions* mediated by gauge particles ( $X$ ) coupled for example to quark-lepton-currents. These exotic gauge particles need in general to be much heavier than weak  $W^\pm$  and  $Z^0$  bosons both on grounds of absence of exotic interactions (such as  $K_L \rightarrow \pi l e$  and for some cases decay of the proton) as well as the observed low energy disparity between effective strong and electromagnetic coupling constants.

It is these exotic gauge particles (generically referred to as  $X$ ) and the interactions generated by them, which are the *hall marks* of grand unification. One thus needs to achieve centre of mass energies of order  $M_X$  to feel the effects of the new class of interactions and therefore of grand unification. At momenta exceeding  $M_X$ , one would expect to see the merging of the effective coupling constants of the three basic interactions characterizing strong, electromagnetic and weak forces; at such momenta (or energies) one may even produce the  $X$ -particles unless their production is forbidden by confinement. Thus the mass of the  $X$ -particles is an important property of grand unified theories. What is  $M_X$ ? Alternative models differ drastically from each other in their predictions on  $M_X$ .

There are two classes of unifying symmetries: *i.e.*, those based on *semi-simple groups*\* (*e.g.*,  $[SU(4)]^4$  or more generally  $[SU(rc)]^4$ ) with discrete symmetries linking the various  $SU(n)$  factors, and those based on *simple groups*<sup>8</sup>

Table I.

Unifying symmetries	Unif. mass scale* $M \sim M_X$	$\sin^2 \theta_w^{**}$	Quark charge***	Baryon No. violation	$\tau_{\text{proton}}$
$[SU(4)]^4$	Chiral color $10^4 - 10^6$ GeV	.28 - .30	Either ICQ or FCQ	Spontaneous for ICQ	$10^{26} - 10^{32}$ yrs for ICQ
	Vector color $10^{16}$ GeV	.20			
SU(5)	$10^{16}$ GeV	.20	FCQ	Intrinsic	$10^{34}$ yrs
SO(10)	$10^{16}$ GeV	.20	FCQ	Intrinsic	$10^{34}$ yrs
$E_7$	$> 10^{16}$ GeV	.67	FCQ	Intrinsic	$> 10^{34}$ yrs
$E_8$	$> 10^{16}$ GeV		FCQ	Intrinsic	$> 10^{34}$ yrs

\* The unifying mass-scale  $M$ , at which the effective coupling constants merge is typically few times  $M_X$  ( $M \sim 3$  to  $5 M_X$ ).

\*\* The values quoted correspond to the low energy electro-weak symmetry  $G_e$  being  $SU(2)_c \times U(1)$ . (See, *e.g.*, ref. 6 for consequences of other choice for  $G_e$ .)

\*\*\* See ref. 9 for a restriction on quark-charges within unifying symmetries.

(such as SU(5), SO(10),  $E_7$  and  $E_6$ ). A comparative summary of some of the salient features (including  $M_i$ ) of these symmetries is given in Table I.

From a glance at the table, we see that the semisimple unifying symmetries, e.g.,  $[SU(4)]^4$ , are singled out on the ground: they permit unification at a relatively low mass-scale  $M \sim 10^4$ - $10^6$  GeV, the others require a mass-scale ten orders of magnitude higher. It is thus clear that tangible evidence for grand unification could conceivably arise in the foreseeable future only within symmetry-structures such as  $[SU(4)]^4$  or extensions thereof. Even proton-decay should be testable for  $[SU(4)]^4$  in the near future assuming that quarks acquire integer charges. For the other cases, requiring lifetimes  $> 10^{34}$  years, the corresponding test would be harder. The predictions on  $\sin^2 \theta_w$  would thus appear to be essentially the only testable prediction of grand unified theories such as SU(5), SO(10) and  $E_7$ . Such a prediction can be used to eliminate certain unifying symmetries (e.g.,  $E_7$  with a prediction for  $\sin^2 \theta_w \sim 0.67$  is eliminated on this ground), but it can hardly be used to provide tangible evidence for grand unification. As noted earlier, one needs to see effects of exotic Z-interactions to realize evidence for grand unification. Only symmetry-structures of the form  $[SU(4)]^4$  or extensions thereof can provide such a scope through high energy accelerators under planning and cosmic ray experiments.

**§III Summary: Important Questions: New Discoveries**

To summarize,

(1) Grand unification mass-scale need not be ultraheavy ( $> 10^{16}$  GeV). It can be as low as about  $10^4$ - $10^6$  GeV. Low-mass unification hypothesis suggests that chiral color  $SU(3)_c \times SU(3)_f$  may underlie observed phenomena as a good low energy symmetry. The QCD-octet of vector color gluons must then be accompanied by an octet of relatively light axial color gluons. These axial gluons would be confined or liberated depending upon whether color in general is confined or liberated. Even for the confined case, the axial color gluons can exhibit characteristic signatures for example in charmonium physics and in deep inelastic

scatterings through inherent spin-spin force and small mass-dependent scaling violations respectively.

(2) The basic hypothesis of left-right symmetry, which turns out to be an essential ingredient of unifying symmetries such as  $[SU(4)]^4$ , suggest

(a) isoconjugate milliweak CP violation<sup>10</sup>; this predicts e.d.m. of neutron  $\sim 10^{-24}$ - $10^{-27}$  ecm and milliweak CP violation in  $1/\tau_{\beta}$ -decay.

(b) An era for the appearance<sup>11</sup> of (V+A)-interaction "on par" with V-A at centre of mass energies  $\sim m_{W_{\pm}} \pm (1/2) m_{W_{\pm}} \sim 1000$  GeV.

(c) Signatures at PETRA-PEP and LEP through possible departures from the  $SU(2)_L \times U(1)$  in the *parity conserving sector via* enhanced  $e^+e^- \rightarrow \nu\bar{\nu}$ -forward backward asymmetry parameter; which, if seen would call for a  $Z_{\nu}$  lighter than the  $Z^0$  of  $SU(2)_L \times U(1)$  and in turn for a symmetry-structure of the form  $SU(2)_L \times SU(2)_R \times U(1)_X \times U(1)_Y$ . Such departures will not reflect themselves either in neutrino-scatterings or in parity violating nc interactions, nor will they show themselves sensitively in  $e^+e^- \rightarrow u\bar{u}$  scatterings at the low SLAC energies.

(3) Unification-hypothesis implemented through semisimple groups of the form  $G_{flavor} \times G_{color}$  permit quark-charges to be either fractional or integral; correspondingly the octet of vector color gluons either remain massless or acquire light mass spontaneously. For the case of the former (i.e., fcq), confinement at least to a pretty good extent is obligatory on experimental grounds, since no stable fractionally charged quarks or massless gluons are seen; while for the latter integer charge quarks and gluons become unstable against decay into leptons; once liberated they become an abundant source of prompt neutrinos. For this case, confinement is not absolute but only partial in the sense that the effective Archimedes masses of the quarks and gluons are very light ( $\sim 10$  to few hundred MeV) inside the hadronic environment, while outside their liberated *physical* masses are heavier  $\sim$  few to 15 GeV, but not infinite.

Liberated integer charge quarks and gluons and in general liberated color will reflect themselves (a) through excess prompt neutrinos

in beam dump type experiments, (b) through rise  $\sim(15 \text{ to } 20)\%$  in deep inelastic structure functions, above color threshold, (c) through dilepton production by high energy pp and pp-experiments (*i.e.*,  $pp \rightarrow \text{virtual } \gamma \rightarrow e^+e^-$ ), (d) through production at PETRA or PEP and also at the Cornell Machine of the narrow ( $\Gamma \sim \text{few MeV}$ ) vector neutral gluon  $U$  decaying into (hadrons+T\*), hadrons,  $e^+e^-$  and  $fT/u$ , as well as production of the axial vector gluon  $U_A$  (if the axials exist) decaying into vector  $U+\gamma$ ,  $U+(c \text{ or } f)$  etc., and (e) finally directly through a search for quarks and gluons in emulsion bubble chamber experiments sensitive to detection of short-lifetimes  $\sim 10^{-12} - 10^{-15}$  sec. For purposes of such a search it should be noted that quark and gluon hadronic pair-production cross-sections are expected to be in the range of  $100 \mu\text{b}$  for quark and gluon-masses in the range of 2 to few GeV; on the other hand such cross sections may be several (4-6) orders of magnitudes lower if their masses are in the range of 10 GeV.

A further promising probe into the integer nature of quark-charges would also arise from a study of two-photon processes as well as the nature of the jet structures in  $e^+e^-$ -annihilation at high energies. The two-photon processes (*e.g.*,  $e^+e^- \rightarrow e^+e^- + \text{Hadrons}$ ) have the virtue that they can be sensitive to the integer-character of quark-charges even below threshold for color-production. These processes are at present under study.

The need for a massive experimental search for liberated quarks and gluons with a view to provide a definitive answer on the fundamental question of confinement versus liberation cannot be overemphasized.

I end this talk by listing a few questions, which I regard are important together with new discoveries, which could possibly be anticipated on the basis of such questions. The questions as well as the possible discoveries are motivated solely through unification ideas alluded to in the introduction. They are headed by the centre of mass energy-scales relevant for the purpose.

$E_{cm} < 100 \text{ GeV}$

(1) Is  $Z_A$  lighter than  $Z^0$ ? Is low energy electro-weak symmetry  $SU(2)_c \times U(1)$  or

$SU(2)_L \times SU(2)_R \times U(1)_L \times U(1)_R$ ?

Expt: Forward and backward asymmetry in  $e^+e^- \rightarrow \gamma^* \rightarrow \mu^+\mu^-$  at PETRA and PEP and in pp or  $pp \rightarrow \gamma^* \rightarrow \mu^+\mu^-$ . Will discover  $Z_A$  or  $Z^0$  at LEP and in high energy pp and pp-machines.

(2) *edm of neutron* = ?

$10^{-24} - 10^{-27}$  ecm \* CP violation isoconjugate milliweak

$< 10^{-29}$  ecm  $\rightarrow$  CP violation superweak

(3) *Quarks and gluons—liberated or confined?* Search for

a)  $e^+e^- \rightarrow C/\text{vector} \rightarrow (\text{hadrons}+; -)$ , hadrons,  $e^+e^-$ ,  $J/\psi$

b) Beam dump experiments: Excess prompt neutrinos

c) Rise in *jup*, vN-structure functions above color-threshold.

d) Signals in  $pp \rightarrow \text{ufts}$ , in jets and in 2-photon processes

e) Decaying quarks and gluons in emulsion-bubble chamber experiments.

(4) *Proton: Stable to what extent?*

Need search for many particle decay of protons (*e.g.*,  $p \rightarrow 3\pi + \gamma$ ) with sensitivity sufficient for lifetime in the range of  $10^{29} - 10^{32}$  years. A lifetime  $\tau_{\text{proton}} > 10^{32}$  years would be incompatible with relatively light liberated integer charge quarks. Proton is expected to be unstable on the basis of unification-ideas regardless of whether quarks are integer or fractionally charged, *i.e.*, irrespective of whether they are liberated or confined.

(5) *New flavors, heavy leptons*

PETRA, PEP and LEP

$e^+e^- \rightarrow$  successor of  $J/\psi, T, \dots$

$pp \rightarrow j/\psi, r, \dots$

$e^+e^- \rightarrow \tau^+\tau^-$  etc.

The decay modes and mixing angles of heavy quarks and leptons are of fundamental value.

$100 \text{ GeV} < E_{cm} < 1000 \text{ GeV}$

(1) *Signals of V+A-inter actions?*

Search for heavier neutral " $Z^0$ " bosons in the mass range 150-500 GeV through successors of LEP and pp and pp-machines in planning, which could indicate an intrinsic left-right symmetric nature of the basic lagrangian.

(2) *Production of  $W^{\pm}(jui) + \nu_e l$*

$10 \text{ TeV} < E_{cm} < 100 \text{ TeV}$  (Laboratory machines and cosmic rays)

(1) *Traces of exotic X-inter actions, signals for grand unification:*

- a) Anomalous lepton production:  $pp \rightarrow \mu^+ \nu_\mu$  at ISABELLE
- b) Anomalous lepton-lepton scattering etc.

To conclude, unification ideas provide scopes for a host of new fundamental discoveries. Such scopes call for construction of high energy  $e^-e^+$ , ep, pp and pp machines with centre of mass energies ranging from a few hundred GeV to about 10 TeV.

I thank Drs. Victor Elias, Subhas Rajpoot, Professor Rabindra N. Mohapatra, and especially Professor Abdus Salam for several collaborative discussions. I have benefitted from much helpful conversations with Prof. J. K. Kim, Mr. I. G. Koh and Mr. H. K. Lee. Research is supported in part by the National Science Foundation and in part by the General Research Board of the University of Maryland.

#### References and Footnotes

1. S. Weinberg: Phys. Rev. Letters **13** (1967) 168; Abdus Salam: in *Elementary Particle Theory, Nobel Symposium*, ed. by N. Svartholm (Almqvist, Stockholm, 1968) p. 367; S. L. Glashow, J. Iliopoulos and L. Maiani: Phys. Rev. **D2** (1970) 1285.
2. J. C. Pati and Abdus Salam: Phys. Rev. **D8** (1973) 1240; Phys. Rev. Letters **31** (1973) 661; Phys. Rev. **D10** (1974) 275.
3. J. C. Pati: *Proc. Second Orbis Scientiae (Coral Gables, Florida, January 1975)* p. 253-256; J. C. Pati and Abdus Salam: Phys. Letters **58B** (1975) 333.
4. J. C. Pati and S. Rajpoot: ICTP Trieste Preprint IC/78/1 and references therein, to be published in Phys. Letters; and Q. Shafi and Chr. Wetterich: Univ. of Freiburg preprint (1978).
5. H. Georgi, H. R. Quinn and S. Weinberg: Phys. Rev. Letters **33** (1974) 451.
6. V. Elias, J. C. Pati and Abdus Salam: Phys. Rev. Letters, **40** (1978) 920.
7. A. Davidson and J. C. Pati: preprint (in preparation).
8. H. Georgi and S. L. Glashow: Phys. Rev. Letters **32** (1974) 438; H. Fritzsch and P. Minkowski: Ann. Phys. (NY) **93** (1975) 193; F. Gursey and P. Sikivie: Phys. Rev. Letters **36** (1976) 775; P. Ramond: Nucl. Phys. **B110** (1976) 214.
9. R. N. Mohapatra, J. C. Pati and Abdus Salam: Phys. Rev. **D13** (1976) 1733.
10. R.N. Mohapatra and J. C. Pati: Phys. Rev. **D11** (1975) 566.
11. A comment is in order regarding the recently advanced astrophysical limit on the number of neutrinos (see S. Weinberg, this Proceeding). It ought to be stressed that this limit applies only to those neutrinos, which are light and which couple with order  $G^2$ -strength to the weak neutral  $Z^0$ . Thus the limit does not apply to right-handed neutrinos within  $L \leftrightarrow R$ -symmetric theories, in which SSB leads to  $SU(2)_L \times U(1)$ -like parity violating nc interaction as proposed in the last paper of ref. 2 and in ref. 10.
12. See J. C. Pati and Abdus Salam: Trieste Preprints IC/77/65 and IC/78/54 (to be published in Nucl. Phys.) for a review of some of these points.

PROC. 19th INT. CONF. HIGH ENERGY PHYSICS  
TOKYO, 1978

## C11

## Spontaneous Compactification

Presented by L. PALLA

*Institute for Theoretical Physics, Roland Eötvös University, Budapest*

It has been an ever alluring idea, after discovering the geometrical foundations of gravity, to give a similar description of the matter, too. The attempts unifying geometrically the Einstein theory with arbitrary gauge field theories led to the inclusion of extra dimensions.<sup>1</sup> In these constructions a specific structure was introduced for the extended space-

time, namely a fibre bundle with the Minkowski space as base space. Thus the extra dimensions have lost their physical sense as real space-time dimensions.

However, the example of dual models<sup>2</sup> suggests that it can happen that physically interesting models prefer dimensions greater than four. In the low energy region they lead to

Einstein theory of gravitation in interaction with gauge fields. As the extra dimensions in this case have a dynamical role, the only way to evade them is to show that in these directions the space is so curved that it closes upon itself, *i.e.*, gets compactified.

Spontaneous compactification is said to occur when we have a solution of the classical Einstein-Yang-Mills system in 4+D space time dimensions with a space-time being the direct product of the Minkowskian space by a compact space of constant curvature in the extra D dimensions. So far this phenomenon has been shown for a number of cases,<sup>3145</sup> and it also has been demonstrated that it generates masses of the order of Planck's mass.

On the other hand it has been indicated<sup>6</sup> that in grand unification (GU) models<sup>7</sup>—aiming to unify most of the known interactions using only one coupling constant—the first step (superstrong) symmetry breaking may not proceed *via* the Higgs mechanism but has a different origin. Our idea is therefore the following: we try to replace the usual first step of symmetry breaking in GU models by the mass generation *via* the spontaneous compactification. The fields surviving this with zero mass constitute an effective field theory at ordinary energies, where the second symmetry breaking may occur.

To exhibit the spontaneous compactification we start with a 4+D dimensional space time and an action—which is the sum of the Einstein action and the matter action with a cosmological term—containing as dynamical variables a set of gauge fields belonging to a local Lie group *G* and the gravitational field *g*<sup>^</sup> (indices with *û* refer to the 4+D dimensional space-time):

$$S = S_E + S_M = -\frac{1}{16\pi G} \int d_{4+D} \hat{x} \sqrt{-g} R - \int d_{4+D} \hat{x} \sqrt{-g} \left[ \frac{1}{2} \text{Tr} (G_{\hat{\mu}\hat{\nu}} G^{\hat{\mu}\hat{\nu}}) + \frac{1}{2} V_0 \right]$$

Here, as usual, *R* is the curvature scalar of the 4+D dimensional space-time, and

$$G_{\hat{\mu}\hat{\nu}} = G^i_{\hat{\mu}\hat{\nu}} \frac{\lambda_i}{2} = \partial_{\hat{\mu}} W_{\hat{\nu}} - \partial_{\hat{\nu}} W_{\hat{\mu}} - ie[W_{\hat{\mu}}, W_{\hat{\nu}}];$$

$$W_{\hat{\mu}} = W_{\hat{\mu}^i} \frac{\lambda_i}{2}$$

is the gauge field tensor, *V*<sub>0</sub> is the cosmological

term to be determined. *G* and *e* are the 4+D dimensional gravitational and gauge coupling constants, respectively; they can be related to their 4-dimensional counterparts.

The equations of motion can be derived from the variation of this action and they are the 4+D dimensional Einstein equ. plus the curved space gauge field equations. Both the action and the eqs. of motion are symmetric between all space-time variables, but we look for a solution which breaks this symmetry and gives the compactification of D dimensions. Therefore we split the *x*<sup>^</sup> into two sets, the first set, containing D coordinates (*0%* belonging to an internal space /, the other set containing four coordinates *x*<sup>^</sup>, belonging to a space which we identify with the ordinary space-time, *i.e.*, we assume for the metric:

$$ds^2 = g_{\mu\nu}(x) dx^\mu dx^\nu + g_{ij}(\theta) d\theta^i d\theta^j$$

and that *g*<sup>^</sup>=*V*<sup>^</sup> (*A*<sup>^</sup>)> while the / space is a D dimensional hypersphere of radius *i*?<sub>0</sub> (to be determined).

For the gauge fields we assume that they are independent of *x*<sup>\*</sup> and *W*<sup>^</sup>*O*.

All these assumptions together reduce the eqs. of motion to the gauge field equations on the / hypersphere and two sets of constraints originating from the Einstein-eqs. :

$$\frac{1}{2} \frac{D(D-1)}{R_0^2} = 8\pi G \left( \frac{1}{4} G^a_{ij} G^{ija} + \frac{1}{2} V_0 \right)$$

$$\frac{1}{2} \frac{(D-1)(D-2)}{R_0^2} g_{ij} = -8\pi G \left( G^a_{ik} G^a_{j} \right. \\ \left. - g_{ij} \left( \frac{1}{4} G^a_{lm} G^{lma} + \frac{1}{2} V_0 \right) \right)$$

Solutions to these equations were found for general D with *G*=*SO*(*D*+1),<sup>3</sup> for *D*=2 with any compact Lie group *G*<sup>\*</sup> and even in the case when the / space is a space of constant curvature and the *G* group acts transitively on / (*i.e.*, *I* is a coset space *G*/*H*).<sup>5</sup> We take these solutions as the ground state of our theory.

To use the spontaneous compactification for symmetry breaking purposes first we embed the compactifying gauge group *G* into a larger group *K* and couple in an invariant way 4+D dimensional matter fields (scalars, fermions) to *g*<sub>μ</sub> and assuming that these matter fields vanish in the ground state. Then the particle spectrum is obtained by studying

the fluctuations around this ground state. (i.e., keeping the compactifying and fixed.) In fact after the spontaneous compactification all fields can be expanded in series of hyperspherical functions defined on the space / with coefficients depending only on  $x^{**}$ . For these coefficients we get an effective action in the Minkowski space by integrating over the compactified coordinates in the  $4+D$  dimensional action.

The fields obtained this way from the fluctuations of  $g^\wedge$  and  $g_{ij}$  reproduce the local fields of the fibre bundle approach.<sup>1</sup> In particular they contain 0 mass gravitation and 0 mass vectors which are Yang-Mills bosons associated with the symmetry of the internal space.

However, more interestingly, we obtain 0 mass gauge vectors associated with  $G'$ —the maximal subgroup of  $K$  commuting with  $G$ —from fluctuations in  $Wp$  outside  $G$ .

To see it in some detail let us consider the  $D=2$  case with an arbitrary compact Lie group<sup>4</sup>: here to achieve compactification we put for the gauge fields a "magnetic monopole" ansatz described in the Wu-Yang formalism<sup>8</sup> ( $d^i=d$ ,  $\delta^i=ip$  are the usual polar and azimuthal angles on  $S^2$ ):

$$W_\theta=0, \quad W_\varphi=\frac{H}{e} \begin{cases} \cos\theta-1 \\ \cos\theta+1 \end{cases} \begin{matrix} \text{N.P.} \\ \text{S.P.} \end{matrix}$$

$$H=\frac{1}{2} n_i \lambda_i$$

(N.P. and S.P. stand for two overlapping regions, jointly covering the entire sphere and containing the north pole ( $\theta=0$ ) and south pole ( $\theta=\pi$ ) respectively).  $H$  is a linear combination of the generators of  $G$  and in the overlapping region  $W^{N.P.}$  and  $W^{S.P.}$  are connected by the gauge transformation  $\exp(i\lambda(pH))$ . This transformation must be single valued, this fixes the normalization of  $H$ :  $\exp(4\pi H)=1$ . This ansatz is a solution provided

$$V_0=\frac{e^2}{k(8\pi G)^2} \quad R_0^2=\frac{8\pi G}{e^2} k$$

$$k=2 \text{Tr} H^2=\sum n_i^2$$

Now if around this solution we make a perturbation of the following type:

$$ds^2=g_{\mu\nu}(x)dx^\mu dx^\nu + R_0^2 (\sin^2\theta d\varphi^2 + d\theta^2)$$

$$W_\mu(x)=A_\mu(x) \quad [A_\mu(x), H]=0$$

then after integrating out the  $0, <p$  coordinates we obtain 0 mass gauge fields  $\hat{A}_\mu(x)=(AnRl)^{-1/2}$  associated with the little group of the constant  $H$  matrix, ( $=(?)$ ) interacting with ordinary gravity. The 4-dimensional gauge and gravitational coupling constants turn out to be  $e_m=(4nRD)^{-1/2}e$  and  $G_m=G/4nRl$  respectively, therefore  $R_0^2=G_m e^2 l^2$  (i.e.,  $RQ'$  is of the order of the Planck mass.)

Expanding the fluctuations of  $Wp$  outside  $G'$  in terms of generalized Wu-Yang monopole harmonics we proved that they obtain super-heavy masses of the order of  $RQ'$ . Therefore the symmetry group of the 0 mass gauge vectors is  $SO(3)\times G'$  (the  $SO(3)$  comes from the symmetry of the internal space now being

For scalar fields in any representation of  $K$  we found<sup>4</sup> that the masses of the fluctuations are given by  $M^2=[J(J+1)-q_i^2]/R_0^2$  (here  $q_m$  is the diagonal element of the matrix representing  $H$  and  $J$  is the  $SO(3)$  quantum number of the representation;  $J>q_m$  therefore those scalar components which belong to  $q_m=0$  in the  $J=0$  ( $SO(3)$  singlet) case acquire no mass, while all the others obtain huge masses ( $OQR\delta'$ )).

As all of the non-zero masses are of  $O(i\sigma^\wedge)$ , at ordinary energies only the zero mass components have physical relevance in the sense that either they remain exactly massless or they obtain their non-zero, "physical" masses by some other mechanism. Therefore to build a sensible GU model we must have zero mass fermions too. We shall have them after integrating out on the internal space, if the Dirac equ.—written on  $S^2$  and containing as external fields the compactifying gauge fields—has zero eigenvalues. We found that for each  $q^\wedge O$  there are  $2|q^\wedge|$  elements of zero mass fermions in the  $J=|q^\wedge|-1/2$  representation of  $SO(3)$ . As in the Dirac equ. the compactifying gauge fields appear as a magnetic monopole potential (=field of non-trivial global topology) this result can be understood as a manifestation of the Atiyah-Singer index theorem.

If for example we take  $AT=SU(4)$  and place fermions in the  $\wedge$  representation and we choose an  $H$  matrix of the form:  $H=n \text{diag} (1/2 \ 1/2 \ 1/2-3/2)$  ( $n$  integer) breaking  $SU(4)$  down to  $SU(3)\times U(1)$ , then for  $n=l$  we have an  $SU(3)$



triplet SU(2) singlet of 0 mass fermions (quarks?) as well as 3 SU(3) singlets, SU(2) triplets (leptons?).

The neglected higher mass excitations may play an important role if we assume that strong interactions couple in a way gravitation does,<sup>9</sup> as in this case the Planck length becomes of the order of the size of elementary particles and these geometrical constructions may give a description of the hadronic world. However in this case we must face the problems arising from the relatively simple spectrum as well as from the complexity of the resulting infinite component field theory.

It is obvious that in the  $D=2$  case essentially we used only a topologically non-trivial U(1) gauge field to compactify the extra two dimensions on  $S^2$ . Based on this observation we determined the minimal gauge groups which allow topologically non-trivial compactifying gauge fields on even  $D$  dimensional spheres with  $SO(Z>+1)$  invariance.<sup>10</sup> Just like in the  $D=2$  case the "monopole" these gauge fields also guarantee the existence of 0 mass fermions, but they are now *singlets* under the  $SO(D+1)$  internal-space-symmetry group.

If, however, we compactify the extra even  $D$  dimensions on  $CP^{D/2}$ , then using recent results from the theory of generalized monopoles<sup>11</sup> it is possible to show that the minimal compactifying gauge group is U(1). Embedding this U(1) into  $K$  raises an interesting possibility as  $CP^{D/2} = SU(i)/2+1 / SU(i)/2 \times U(1)$

and therefore the symmetry group of the gauge fields is  $SU(Z)/2+1 \times G$  and in the physically most interesting case ( $D=6$ ) we can again have 0 mass fermions because  $CP^3$  allows a spin structure.

#### References

1. Th. Kaluza: Sitzungberichte der Preuss. Akad. Wiss. (1921) 966; O. Klein: Nature **118** (1926) 516; Y. M. Cho and P. G. O. Freund: Phys. Rev. **D12** (1975) 1711; Y. M. Cho and Pong Soo Jang: Phys. Rev. **D12** (1975) 3789; J. Rayski: Acta Phys. Pol. **XXVII** (1965) 89.
2. *Dual Theory*, ed. M. Jacob (North Holland, Amsterdam, 1974); J. Scherk: Rev. Mod. Phys. **47** (1975) 123.
3. E. Cremmer and J. Scherk: Nucl. Phys. **B103** (1976) 399; **B108** (1976) 409; **B118** (1977) 61.
4. Z. Horváth, L. Palla, E. Cremmer and J. Scherk: Nucl. Phys. **B127** (1977) 57.
5. J. F. Luciani: Nucl. Phys. **B135** (1978) 111.
6. E. Gildener: Phys. Rev. **D14** (1976) 1667.
7. J. C. Pati and A. Salam: Phys. Rev. **D8** (1973) 1240; H. Georgi and L. Giashow: Phys. Rev. Letters **32** (1974) 433; H. Georgi, H. Quinn and S. Weinberg: *ibid.*, **33** (1974) 451; M. Fritzsche, M. Gell-Mann and P. Minkowski: Phys. Letters **59B** (1976) 156.
8. T. T. Wu and C.N. Yang: Phys. Rev. **D12** (1975) 3845; Nucl. Phys. **B107** (1976) 365.
9. C.J. Isham, A. Salam and J. Strathdee: Phys. Rev. **D3** (1971) 867; **D8** (1973) 2600; A. Salam and J. Strathdee: Phys. Letters **B67** (1977) 429; Trieste preprint IC/77/153.
10. Z. Horváth and L. Palla: Trieste preprint IC/78/37, to be published in Nucl. Phys. **B**.
11. A. Trautman: Int. J. Theor. Phys. **16** (1977) 561.

PROC. 19th INT. CONF. HIGH ENERGY PHYSICS  
TOKYO, 1978

## C 11 World Topology and Gauged Internal Symmetries

P. G. O. FREUND

*Enrico Fermi Institute and Department of Physics, University of Chicago,  
Chicago 60637*

In the theory of gravitation there are two topological invariants that are the counterparts of the instanton number of Yang-Mills theory.<sup>1</sup> Of these I will concentrate on the index  $r$  of the space-time manifold defined by

the gravitational metric:

$$\tau = \int R R^* d^4x$$

with

$$RR^* = -\frac{1}{96\pi^2} \epsilon^{\mu\nu\rho\sigma} R_{\beta\mu\nu}^\alpha R_{\alpha\rho\sigma}^\beta$$

It is related to the first Pontryagin number  $P_1$  by  $P_1 = 2\pi^2 \int RR^*$ . It contributes to the Adler-Bell-Jackiw axial anomaly

$$\partial^\mu j_\mu^{(5)} = -\frac{N_D}{4} RR^*$$

+ usual Yang-Mills FF\* terms

as noted by Delbourgo and Salam,<sup>2</sup> and by Eguchi and myself.<sup>3</sup> Here, and below,  $N_D$  stands for the number of complex Dirac fields and  $N_M = 2N_D$  is the number of corresponding real Majorana fields. Thus the integral version of the axial anomaly gives the helicity change  $\Delta Q^5$  in terms of the index

$$\Delta Q^5 = -\frac{N_M}{8} \tau$$

We proposed<sup>3</sup> the complex projective plane  $P_2(C)$  as a gravitational instanton for this anomaly (in terms of three complex homogeneous coordinates  $z_0, z_1, z_2, z_3$ ,  $P_2(C)$  is defined by  $|z_0|^2 + |z_1|^2 + |z_2|^2 + |z_3|^2 = a^2$  and by identifying points that differ by an overall phase:  $(z_0, z_1, z_2, z_3) = (e^{i\theta} z_0, e^{i\theta} z_1, e^{i\theta} z_2, e^{i\theta} z_3)$ ). Fubini found a Kähler metric for  $P_2(C)$ . The corresponding 4-dimensional real (+ + + +) metric is a solution of Einstein's equations with cosmological term ( $A = 3/2a^2$ ). The index of  $P_2(C)$  is  $\tau(P_2(C)) = 1$ . This leads to the paradoxical value  $\Delta Q^5 = -N_M/8$ . The reason for this is that while fermion triangle (and loop) diagrams are responsible for the anomaly, fermions are Lorentz spinors (because of the spin-statistics connection) and spinors cannot "live" on  $P_2(C)$ .

It may be worthwhile to recall how spinors can be denied accomodation on some Riemann manifold  $M$ . Consider the bundle of oriented orthonormal frames of  $M$  and a closed curve situated completely in one of its fibres, say, over the point  $P \in M$ . Moreover, let this curve correspond to a vierbein rotation by  $2K$  SO that spinors at  $P$  change sign. Then it cannot be contracted to a point while staying within the fiber. But, for a sufficiently non-trivial topology of the manifold  $M$ , this curve when deformed through the whole bundle may be shrunk to a point leading to no spinor sign change. Thus, two curves obtainable from each other by continuous deformation give conflicting instructions as to spinor signs. Spinors cannot sort their signs out and find the manifold "deadly". Fortunately, what I called

"sufficiently nontrivial topology" above can be made precise: the second Stiefel-Whitney characteristic class  $w_2$  should not vanish.

Hawking<sup>5</sup> has proposed the Taub-NUT solution as a replacement for  $P_2(C)$ . Unfortunately,  $\tau(\text{Taub-NUT}) = 0$ , so that this does not work.<sup>6</sup>

At this point a more general aspect of this whole problem surfaces. In the transition from classical to quantum gravity a functional integration over gravitation fields, *i.e.*, over world manifolds is involved. The world contains Fermi-matter fields: quarks and leptons. Yet, not every manifold can support spinors (*Le.*, Fermi fields). To obtain a consistent quantum theory two alternatives can be contemplated:•

(A) restrict the functional integral to manifolds that have a spin structure: spin manifolds,

or;

(B) require all matter fields to appear in suitable multiplets of a gauged symmetry that permits the definition of a generalized spin structure on *all* 4-dimensional Riemann-manifolds.

Next, I shall explore these two alternatives, closely following recent work<sup>7</sup> of Back, Forger and myself.

First, let me consider alternative (A). It is automatically realized in all forms of supergravity theory, since the  $OSp(A, 4)$  and  $SU(N/2, 2)$  supergroups contain not the Lorentz group but its covering spin group which thus acts in the fibres of the supergravity bundle. In such theories a gravitational instanton is to be a 4-dimensional compact spin-manifold with positive metric forms and first Pontryagin number  $p \neq 0$ . To be of special physical interest it should also be an Einstein manifold (*i.e.*,  $R_{\mu\nu} = \Lambda g_{\mu\nu}$  for some  $\Lambda$ ).  $P_2(C)$ , not being a spin-manifold, will not do. It is incumbent on us to find new instantons. The trick is to look for algebraic submanifolds of  $P_3(C)$  other than  $P_2(C)$ . Let  $z_0, z_1, z_2, z_3$  be the homogeneous complex coordinates of  $P_3(C)$  and  $F_m(z_i)$  a homogeneous polynomial in  $z_i$  of degree  $m$ . If  $\text{grad } F_m \neq 0$  for  $z = 0$  then  $F_m(z) = 0$  defines a Kähler submanifold of  $P_3(C)$ . For even  $m = 2n$  the second Stiefel-Whitney class of  $V_{2n}$  vanishes so that it is a spin manifold. Standard topological methods then yield:

$$\tau(V_{2n}) = -16 \frac{(n+1)n(n-1)}{6}$$

Thus,  $r(V_2)=0$  while  $r(F_4) = -16$ . Notice that now  $JQ_6$  is an even integer and the  $P_2(C)$  "paradox" disappears. According to Yau,<sup>8</sup>  $V_4$  admits a metric that is a solution of Einstein's equations without cosmological term, and it is possible that the  $V_{2n}$  manifolds are Einstein for all  $n$ . Moreover, if  $M$  is any 4-dimensional spin manifold without boundary, then there exists a 5-dimensional spin manifold whose boundary is the union of  $M$  and of  $r = -r(M)/6$  copies of  $F_4$ :  $M$  is spin-cobordant to  $rV_{\pm}$ .<sup>9</sup> In this sense  $F_4$ 's are the fundamental gravitational instantons.

Supergravity, which implements alternative (A) is certainly not experimentally established. Therefore, it is in order to look for alternative resolutions of the " $P_2(C)$ -paradox".  $P_2(C)$  itself while not a spin-manifold, still is a complex manifold and as such can be given a generalized Spin<sup>0</sup> structure.<sup>10</sup> This is done<sup>11</sup> by having the matter fields carry a conserved charge, the corresponding current serving as the source of an abelian gauge field. The extra gauge phase freedom then allows the consistent definition of spinors on  $P_2(C)$  provided one has a "charge-statistics" connection: fermions (*i.e.*, spinors) carry odd (integer) values while bosons (*i.e.*, tensors) carry even values of the charge. The gauge field then also contributes to the anomaly and together with the gravitational contribution gives  $Jg^{\pm} = \text{integer}$ . There may exist a larger (non-abelian) gauge group  $G$  such that coupling all matter fields to gauge fields of  $G$ , all 4-dimensional Riemann manifolds (not only those that are also complex manifolds) can be given a generalized spin structure, again provided a certain "internal spin"-statistics connection is enforced. In 4-dimensions such a group  $G$  exists and must be at least  $SU(2)$  or more realistically  $SU(2) \times SU(2)$  or  $SU(2) \times SU(2) \times U(1)$ .

To see this, note that  $Spin(4) = SU(2) \times SU(2)$  can be homomorphically mapped onto  $Spin(4) \times SU(2)$  by the identity map to  $Spin(4)$  and projection onto one of the two  $SU(2)$  factors as the map to  $SU(2)$ . Define  $Spin(4) \rightarrow Spin(4) \times SU(2)/Z_2$  by identifying  $(g, h) \sim (-g, -h)$  for  $g \in Spin(4)$ ,  $h \in SU(2)$ . Now,  $SO(4)$  and  $Spin(4)$  differ from  $Spin(4)$  and  $Spin(4) \times SU(2)$

each by a  $Z_2$  factor. Either  $Spin(4) \rightarrow Spin(4) \times SU(2)$  homomorphism induces an  $SO(4) \rightarrow Spin(4)$  homomorphism that can be used to upgrade the  $SO(4)$  bundle into a  $Spin(4)$ -bundle. With a gauged internal  $SU(2)$ -symmetry one can thus define spinors on any 4-dimensional Riemann manifold. Physically one may attempt to identify this with the "weak isospin" factor of the unified weak-electromagnetic gauge group. But, there is one more consistency requirement. Any representation  $A$  of  $Spin(4)$  on a vector space  $V$  can be pulled back to a representation of  $Spin(4) \times SU(2) = SU(2) \times SU(2) \times SU(2)$ . But, we must require the element  $(-1 -1 -1)$  of  $SU(2) \times SU(2) \times SU(2)$  to map to the identity within  $A$ . Label  $A$  by three spins  $(j_1, j_2, j_3)$ . This requirement then means  $e^{i\pi(2j_1+2j_2+2j_3)} = 1$  so that  $j_1 + j_2 + j_3 = \text{integer}$ . Thus, the fermions, for which  $2j = \text{half odd integer}$  because of the spin-statistics connection, must have a half odd integer weak isospin. Similarly, bosons must have integer weak isospin. This is a weak isospin-statistics connection. Unfortunately, as it stands it would rule out both the right-handed leptons and Higgs fields of the Weinberg-Salam model. But, instead of the minimal  $SU(2)$  we can choose an internal symmetry like  $SU(2) \times SU(2) \times U(1)$  and reasonable "internal-spin"-statistics connections can be produced.

Notice a remarkable feature of all this. The natural realization for alternative (A) is in the framework of supergravity theories. These theories determine both the gauged internal symmetry ( $O(N)$  or  $U(N)$ ,  $N < 8$ ) and the multiplet spectrum. The seemingly unrelated alternative (B) again provides information on the gauged internal symmetry and on the multiplet spectrum this time in the form of an "internal spin"-statistics connection.

Before concluding I wish to briefly mention that one way to experimentally test supergravity—and the corresponding solution (A) of the spinor puzzle—is to test its prediction of  $SU(3)_{\text{color}}$  sextet quarks.<sup>12</sup> In this vein, it has been remarked recently,<sup>13</sup> that the  $Y \rightarrow Y$  mass splitting and the  $Y$  leptonic decay rate could be much more readily accounted for if the  $Y$ 's constituent  $\bar{c}$ -quark were a color sextet.<sup>14</sup> Admittedly, the absence of stable or very long-lived hadrons in the 5-6 GeV/c<sup>2</sup>

mass range<sup>15</sup> makes this interpretation less probable, although a final verdict should come from the measurement of the hadronic decay rate of the  $\rho$ -meson. Of course there could exist color sextet quarks of higher mass. If very long-lived, these would allow<sup>16</sup> for most exciting practical applications.

To conclude, let me venture a speculation. The new gravitational instantons we found are algebraic manifolds. Remarkably also the instantons of the SU(2) Yang-Mills theory are algebraic as noted by Atiyah and Ward.<sup>17</sup> Maybe in the "euclidean" sector all (finite action) solutions of a gauge theory—whether Yang-Mills or gravity—are algebraic just like the self-dual or anti-self-dual instantons. What would this mean? Think of a point particle in a central potential. There exist potentials for which all classical trajectories are algebraic curves: the Newton-Coulomb and the harmonic oscillator potentials. But, for these potentials both the classical and the quantum-mechanical problems are exactly analytically soluble. Maybe "euclidean" Yang-Mills and gravity (and supergravity?) are *exactly soluble* both classically and at the quantum level. Exactly soluble 2-dimensional field theories have been known for a long time. But, here I am suggesting the prospect of exactly soluble 4-dimensional gauge theories. The crucial ingredient, the algebraic nature of the classical solutions, would provide a peculiar vindication of Kepler's approach, that emphasized precisely the algebraic aspect for planetary motion. For gauge theories a global Keplerian approach may yet be as profitable as the prevalent local dynamical Newtonian approach.

## References

1. For a general discussion of anomalies and instantons in Yang-Mills theories see the beautiful review paper by S. Coleman, Harvard preprint HUTP/A004.
2. R. Delbourgo and A. Salam: Phys. Letters **40B** (1972) 381.
3. T. Eguchi and P. G. O. Freund: Phys. Rev. Letters **37** (1976) 1251.
4. R. Geroch: J. Math. Phys. **9** (1968) 1739.
5. S. Hawking: Phys. Letters **60A** (1977) 84.
6. T. Eguchi, P. B. Gilkey and A. J. Hanson: Phys. Rev. **D17** (1978) 423; H. Romer and B. Schroer: Phys. Letters **71B** (1977) 182; see also, M.J. Duff: Queen Mary College preprints (1976), (1977).
7. A. Back, P. G. O. Freund and M. Forger: Phys. Letters **77B** (1978) 181.
8. S. T. Yau: U.C.L.A. preprint.
9. J. Milnor: L'Enseignement Math. 2-Sér. **9** (1963) 198.
10. M. Atiyah, R. Bott and A. Shapiro: Topology **3** (Suppl. 1) (1964) 3.
11. S. Hawking and C. N. Pope: Phys. Letters **73B** (1978) 42; G. W. Gibbons and C.N. Pope: D.A.M.T.P. preprint, to be published.
12. A. Salam and J. Strathdee: Phys. Rev. **D11** (1975) 1521; M. Gell-Mann and Y. Ne'eman: unpublished.
13. Y. J. Ng and S.-H. H. Tye: Phys. Rev. Letters **41** (1978) 6; P. G. O. Freund and C. T. Hill: Chicago preprint EFI 78/21; H. Fritzsche: Wuppertal preprint WU-B78-19.
14. Color sextet quarks have also been considered from different points of view by G. Karl: Phys. Rev. **D14** (1976) 2374; by F. Wilczek and A. Zee: *ibid.*, **D16** (1977) 860.
15. D. Cutts *et al.* Phys. Rev. Letters **41** (1978) 363; L. Lederman: report at this Conference.
16. P. G. O. Freund and C. T. Hill: Chicago preprint EFI 78/23; R. Cahn: Phys. Rev. Letters **40** (1978) 80.
17. M. Atiyah and R. S. Ward: Comm. Math. Phys. **55** (1977) 117.
18. In a different context A. M. Polyakov has also speculated on the solubility of gauge theories.

## PI a: Hadron-Hadron Reactions, Low Multiplicity

*Chairman :* E. L. GOLDWASSER

*Speaker :* V. A. TSAREV

*Scientific Secretaries:* F. TAKASAKI  
K. OGAWA

## PIb: Hadron-Hadron Reactions, High Multiplicity

*Chairman:* L. VAN HOVE

*Speaker:* R. E. DIEBOLD

*Scientific Secretaries:* T. HIROSE  
H. KICHIMI

# Pl1a Hadron-Hadron Reactions, Low Multiplicity

V. A. TSAREV

*P.N. Lebedev Physical Institute, Moscow*

## Introduction

This report is a review of the recent results on two-body and quasi-two-body exclusive processes, submitted to the sessions A1 and A2 of this Conference. It includes four parts devoted to the elastic scattering, spin effects, diffractive dissociation and nondiffractive processes.

At the present level of understanding of hadron dynamics it is very difficult to present this varied material coherently from a unified point of view. The Regge model traditionally used for unifying the experimental data has lost some of its popularity in recent years. Although it is still often used for phenomenological discussions, the main interest shifted to those approaches which aim to reveal the underlying mechanisms and establish the connection with hadron structure. The quark model strengthened substantially its position. Besides many successful predictions, based on combinatorics, it in some cases also gives a dynamical description. Unfortunately this last possibility is still dubious for low- $\sqrt{s}$  processes constituting the main subject of this talk. In this situation the presentation of material inevitably gains the features of a gaily-coloured mosaic with experimental facts mixed with inserts of phenomenological comments.

A large amount of data is submitted to Sessions A1 and A2 and due to limited size of the talk, I can present only some of them. The summaries due to Kycia<sup>1</sup> and Yokosawa<sup>2</sup> will help to cover the rest results. I wish to apologize to all those authors whose results are out of the scope of this report. Earlier summaries on the subject can be found in papers.<sup>3-6</sup>

## I. Elastic Scattering

### *L* Scattering near forward direction

I begin with the most inclusive value, the

total cross section, which is connected via optical theorem with the imaginary part of the elastic scattering amplitude at  $t=0$ . Brookhaven-FNAL-Rockefeller group extended recently their earlier measurements of hadron total cross sections up to 370 GeV/c.<sup>7</sup> The results are shown in Figs. 1-3 and are seen to continuing the trend observed below 200 GeV/c. The pp accelerator data together with that obtained recently from the cosmic ray measurements<sup>8</sup> indicate that the  $\sigma_{tot}(s)$  rise is close to  $\log^2 s$  up to at least 40 TeV.

Measurements of the Coulomb-nuclear interference at small  $|t|$  yields the real part of the elastic scattering amplitude  $\text{Re } T_{el}$ . This information is important for checking theoretical models and fundamental dispersion relations together with some extra assumptions about the unmeasured values of  $a_{el}$  at high energies and the unmeasurable contribution of the

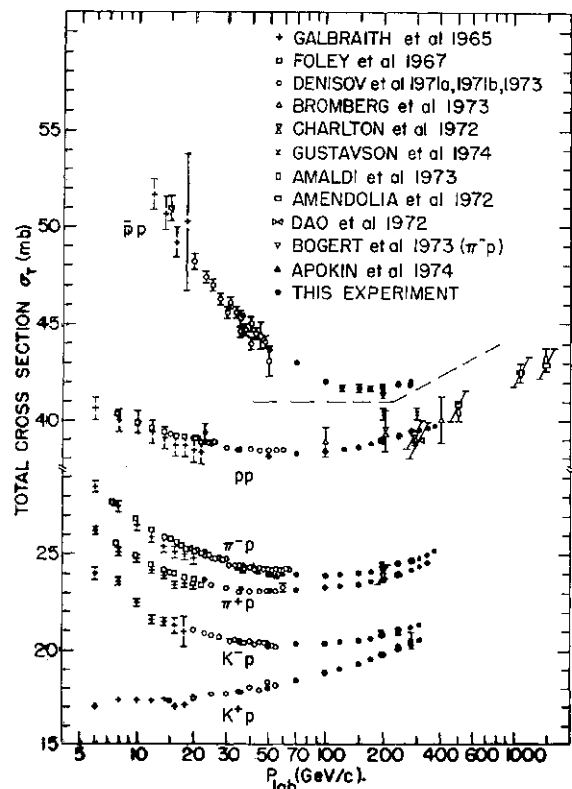


Fig. 1.

unphysical region.

New precise data on the  $\text{Re } T_{el}$  become available recently from measurements at

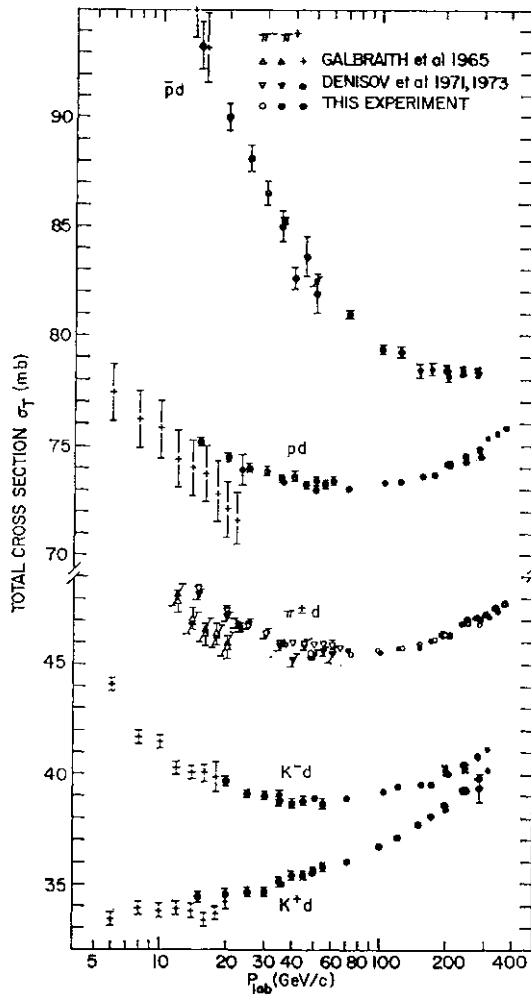


Fig. 2.

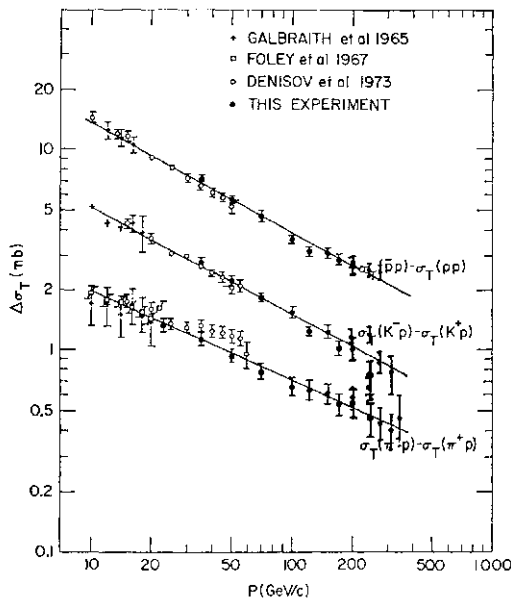


Fig. 3.

IHEP and CERN SPS on  $rc/p$  scattering<sup>9,10</sup> and at FNAL on  $pp$ ,  $pd$ <sup>11</sup> and  $p^4\text{He}$ <sup>12</sup> scattering.

7 T " p elastic scattering in the Coulomb region has been studied by the Dubna-Gatchina-IHEP collaboration at 40 GeV/c<sup>9</sup> and CCFL collaboration from 30 to 140 GeV/c.<sup>10</sup> These groups measured both the proton recoil and the forward scattered particles thus getting good resolution and background rejection. The results are shown in Fig. 4 together with

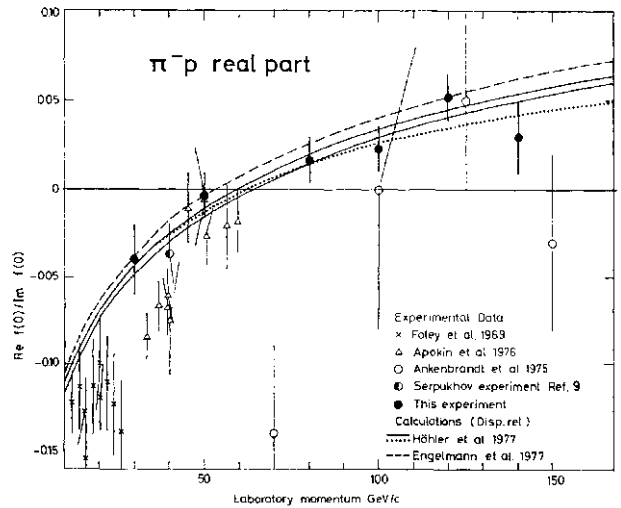


Fig. 4.

data from other experiments. The  $p_{-}(s)$  is seen to cross zero already below 80 GeV/c. The dispersion relations predictions are also shown and are in good agreement with the data, in particular near 30 GeV/c in contrast to results from some earlier experiments. The dispersion analysis indicates the rise of  $\text{Re } f_{el}(7\pi)$  up to at least 1000 GeV/c. The differential cross section slope in the low  $|t|$  region (typically  $11.2 \pm 0.3 (\text{GeV}/c)^{-2.8}$ ) is found significantly bigger than the slope at  $-f=0.2 (\text{GeV}/c)^2$ ;  $\delta(-0.2) \sim 8.2-8.3 (\text{GeV}/c)^{1.2}$ , the effect already known from  $pp$  scattering. The data show no significant  $s$  dependence of the slope.

Results of the Arizona-Dubna-Fermilab-Rockefeller collaboration on the ratio of the real to imaginary parts of the forward scattering amplitude  $p$  for  $pp$  scattering in the region: 50-400 GeV/c are depicted in Fig. 5a. An empirical expression:  $\rho_{pp}(5) = (-0.490 \pm 0.034) + (0.076 \pm 0.006) \ln s$  describes all existing points in the region 50-400 GeV/c and shows that  $p_{p}(s)$  crosses zero at about 335 GeV/c. The solid curve in Fig. 5a derived from dis-

person relations is seen to be in good agreement with data.

New data on  $\text{Re } \Gamma_{pd}^n$  are compared in Fig. 5b with pp data, shown by the solid curve. The small difference in slopes for  $p_n(s)$  and  $p_p(s)$  is well reproduced by the Glauber model with assumption of proton-neutron identity. Values of  $p_m$  extracted from pd and pp data are shown in Fig. 5c together with total error corridor for  $\wedge p p$ . No significant difference between  $p_{vp}$  and  $p_m$

is found.

Interesting results were obtained by Arizona-Dubna-Fermilab group with helium target.<sup>12</sup> The elastic proton-helium differential cross section have been determined from 40 to 400 GeV/c in the range  $0.003 < |*| < 0.52$  (GeV/c)<sup>2</sup> and is seen in Fig. 6 to display a beautiful diffractive minimum at  $-0.22$  (GeV/c)<sup>2</sup>. This dip is expected to be filled in partially by the real part of the nucleon-nucleon scattering amplitude thus allowing its deter-

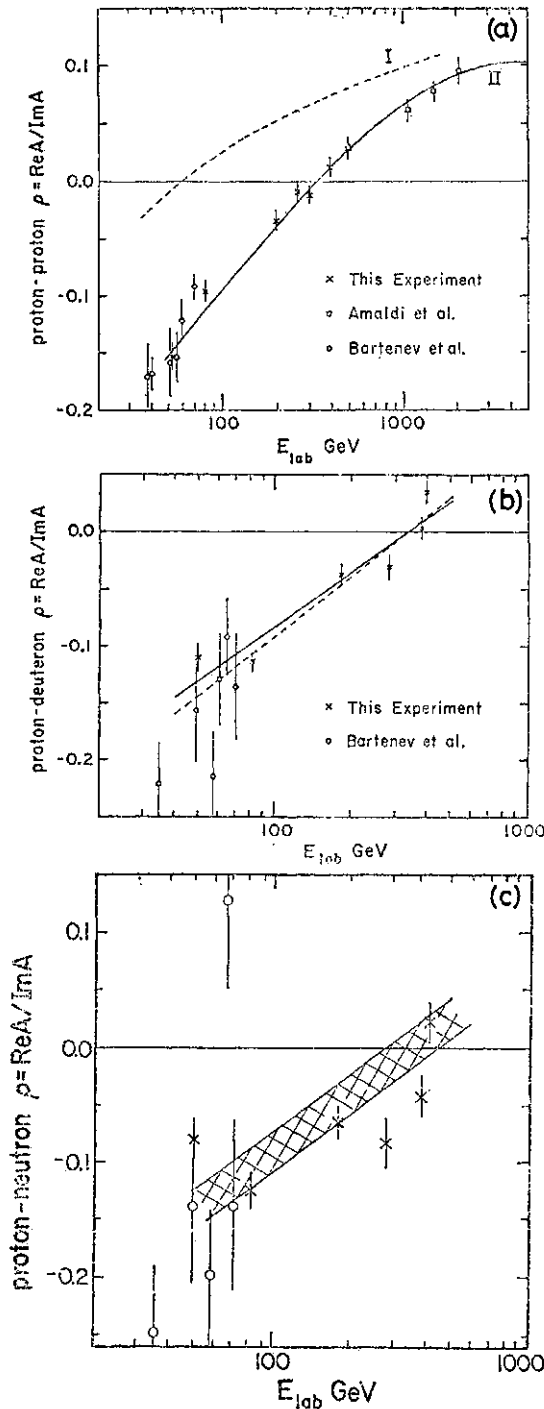


Fig. 5.

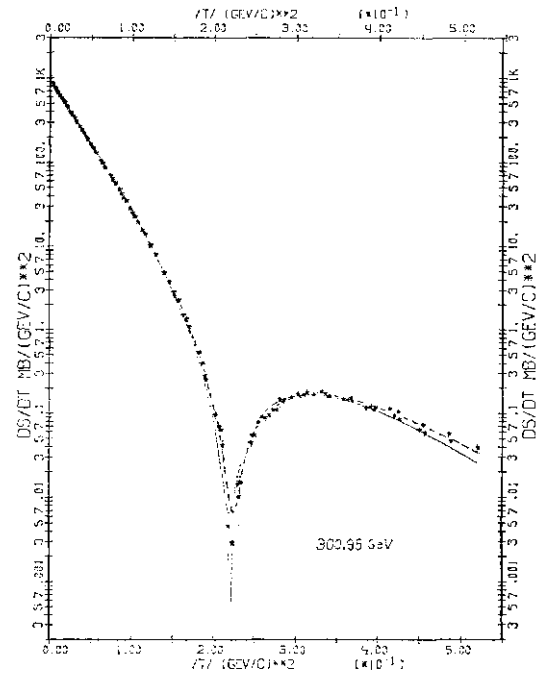


Fig. 6.

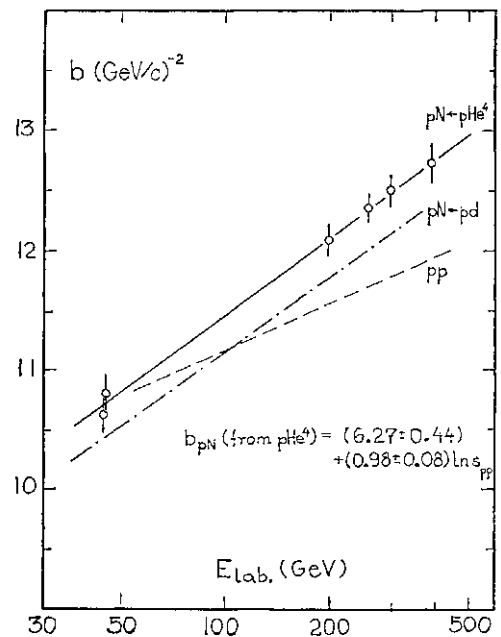


Fig. 7.



mination at  $t^{\wedge}0$ . This possibility is especially important in view of the fact that despite numerous data on the  $\text{Re } T_{el}$  at  $t=0$ , an information of its  $t$  dependence is still not available. A very preliminary Glauber analysis of the data has shown a  $\sqrt{|p_i|}$  term, the linear dependent term in  $p(t)=p_0+p_i|t|$ , of  $\sim -0.2$ .

I would say, however, that before discussing these  $p(t)$  values the data need more careful theoretical study, especially of inelastic screening, spin effects and possible non 2-body correlations.

The effective nucléon nucléon slope parameter  $b$  obtained from helium experimental values are significantly different from those known for proton-proton elastic scattering. This effect is also observed in pd elastic scattering.<sup>13</sup> These slopes are shown in Fig. 7 and may be parametrized as  $b(s)=b_0+b_1 \ln s$ , where for  $p^4\text{He}$   $Z_{>0}=6.27\pm 0.44$ ,  $b_0=0.90\pm 0.08$ ; for pd  $\bar{e}_0=6.3\pm 0.5$ ,  $b_1=0.92\pm 0.09$ ; for pp  $\bar{e}_0=8.27\pm 0.32$ ,  $\wedge=0.556\wedge: 0.028$ . The energy dependence of the  $p^4\text{He}$  and pd slopes is some 2 times greater than for pp. This difference could be attributed to the  $\mathcal{E}$  dependence of inelastic shadowing,<sup>5,12</sup> although there are some puzzling features, which indicate that something important is missed in our understanding of the inelastic screening: a) The rate of shrinkage  $b_1$  for pd turns out to be much faster than is expected from the simple triple Regge phenomenology;<sup>5</sup> b)  $b_1$  for  $p^4\text{He}$  is expected to be much larger than for pd in disagreement with data; c) The data also do not confirm prediction<sup>14</sup> of  $b_1$  rising when  $t$  approaches the dip. In particular the values  $6,0=-0.03)=1.35 (\text{GeV}/c)^{-2}$  and  $b_1 < 7 \sim 0.07)=2.85 (\text{GeV}/c)^{-2}$  are predicted<sup>14</sup> for  $p^4\text{He}$ , but within experimental errors the data give the same  $b_1$  values for different  $t$ .

Further evidence of the inelastic shadowing came from recent studies of the pd and dd elastic scattering at the CERN ISR<sup>15</sup> and FNAL.<sup>16</sup> The CERN data at 53 and 63 GeV/c extend from about  $-t=0.07 (\text{GeV}/c)^2$  to about  $-t=2 (\text{GeV}/c)^2$ , covering extensively the single and multiple scattering regions. The differential cross sections at 53 GeV are shown in Figs. 8 and 9. Contrary to the pd case, a narrow interference minimum is clearly present in dd case. Comparison with calculations shows that around the interference region the

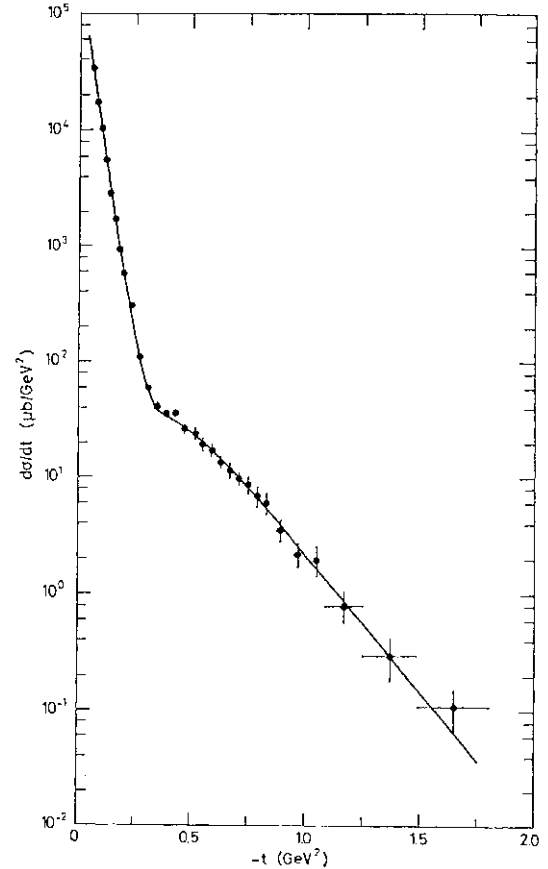


Fig. 8.

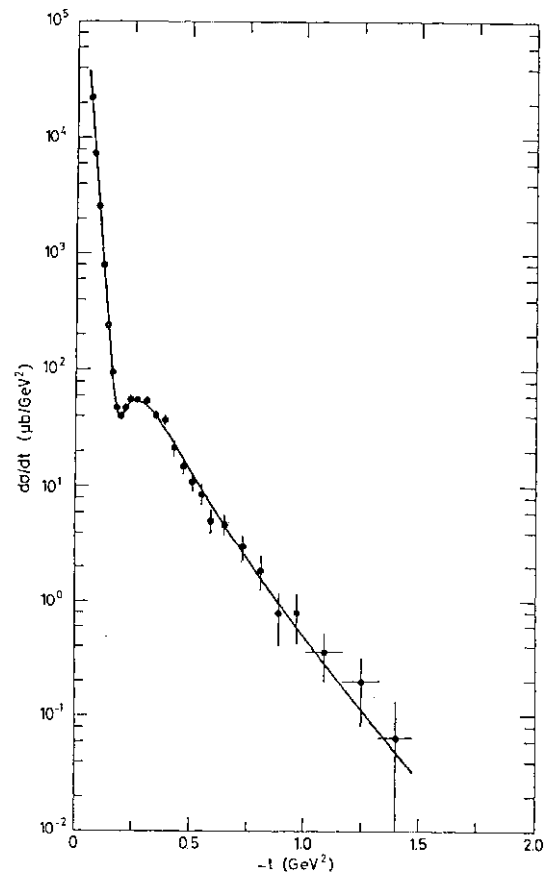


Fig. 9.

pure Glauber theory is inadequate to describe the detailed properties of the differential cross sections by factor as big as 30% in particular regions of  $t$  as illustrated in Fig. 10. These deviations are found to be adequately described by inclusion of inelastic screening as

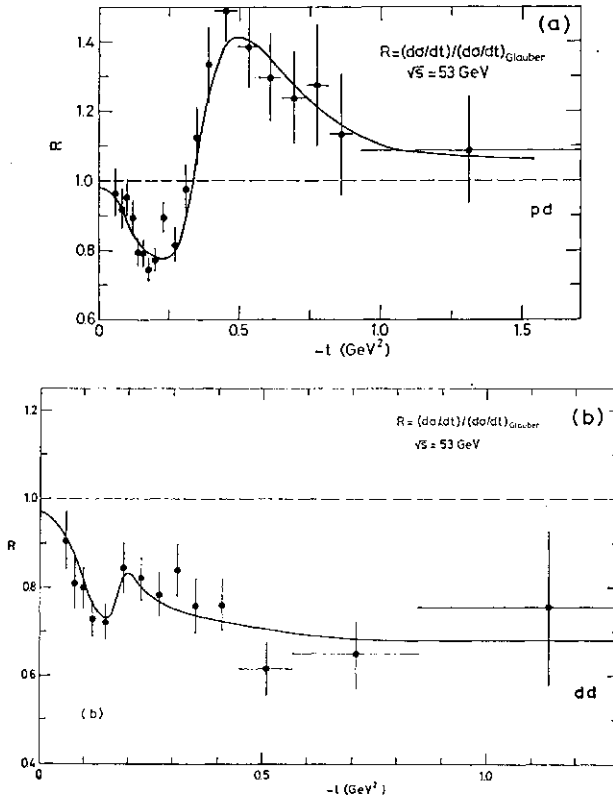


Fig. 10.

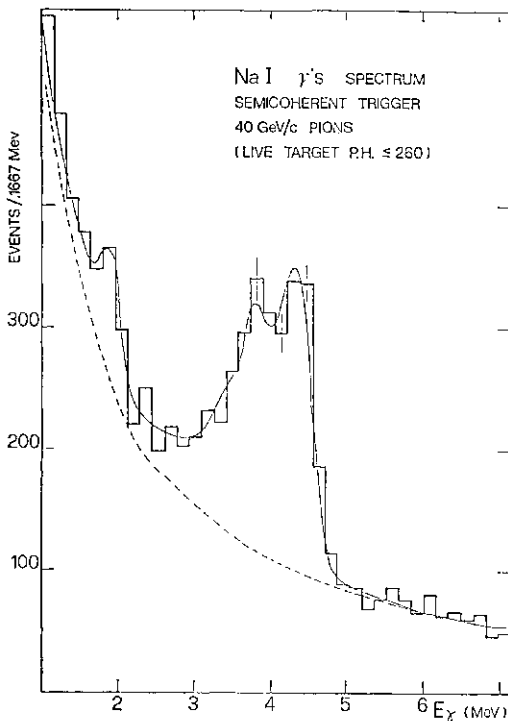
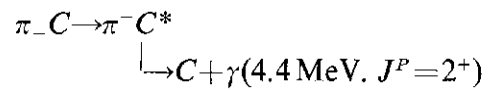


Fig. 11.

shown by solid curves in these figures. I would remind that such effect, which resembles the "small scale oscillations" in pp scatterings has been earlier predicted<sup>17</sup> and experimentally observed at Dubna in a-nuclei collisions.<sup>1\*</sup> The analysis of inelastic corrections of paper<sup>1\*</sup> demonstrates that hadron-nucleus collisions provide a sensitive test of different parametrizations of inclusive production in pp collisions.

One more result from studies with nuclei is submitted by Dubna-Milan Collaboration<sup>19</sup>. This group studied elastic semicoherent scattering (Fig. 11):



and demonstrated that at high energies semicoherent processes are evident, measurable and may be used for hadronic studies.

2. Medium-1 region

The differential cross section for TT-P elastic scattering has been recently measured between 2.1 and 3.5 GeV/c at all angles in a cm. angular range of  $-0.85 < \cos \theta^* < 0.95$ .<sup>20</sup> The results of this first experiment at the KEK synchrotron are shown in Fig. 12 and I am glad to congratulate Japanese physicists with this success.

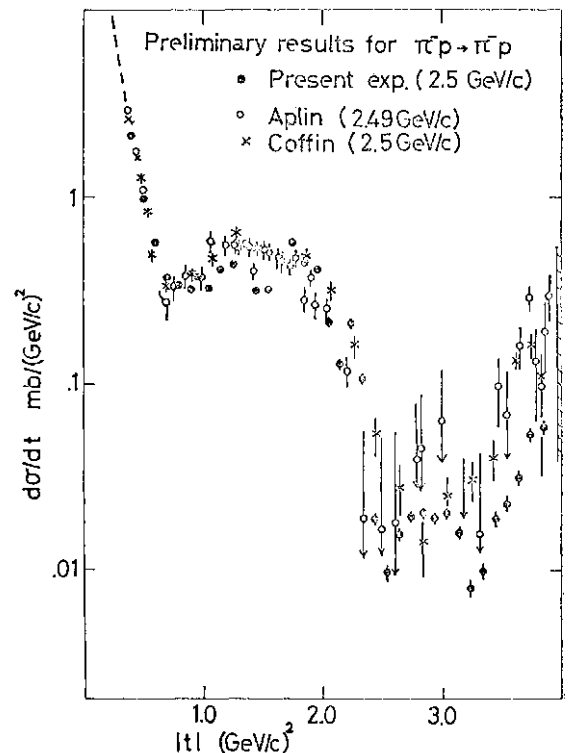


Fig. 12.

At higher energies different versions of the eikonal and Regge models, successfully describing the forward peak, predict a succession of diffraction minima and maxima and decreasing the slopes for higher order peaks:  $6_1-2Z>_2^{\wedge}36$ \_\_\_\_\_The Chou-Yang model<sup>21</sup> with an electromagnetic form factor and  $a_{em}$  as an input, gives especially strict predictions: the first minimum is predicted at  $-1.4$   $(\text{GeV}/c)^2$ , the second maximum at  $t \sim -1.8$   $(\text{GeV}/c)^2$ , and also the shift at higher  $s$  of the  $h(s)$  to lower  $|t|$  and rise of the height of the second peak as a result of the rise of  $a_{em}$ . It is well known that these predictions of the model have been beautifully confirmed at ISR and FNAL.

Recently the dip region has been studied at FNAL in  $pp$ <sup>22</sup> and  $pn$ <sup>23</sup> scattering and in  $pp$  at CERN<sup>24</sup>. Both the  $pp$  and  $pn$  data in Figs. 13, 14 and 15 show the gradual evolution of the dip near  $t \sim -|A|$   $(\text{GeV}/c)^2$  as the energy increases. While the dip is similar to that observed in  $pp$  data, the  $np$  cross sections are generally higher in this region. The comparison is shown in Fig. 16. At lower  $|t|$  the cross sections are compatible out to  $-s \sim 0.8-0.9$   $(\text{GeV}/c)^2$ . At larger  $|t|$ , they begin to diverge with  $np$  cross section approximately 3 times the  $pp$  cross section

near  $-t \sim 1.25$ . This difference extends to  $-t \sim 1.4$   $(\text{GeV}/c)^2$ . At the same time the 280  $\text{GeV}/c$  data are found to agree with 282 equivalent lab. energy ISR data. This comparison shows that near the dip and at lower energies the non-pomeron  $p$  and  $A_2$  contributions are compatible with that of pomeron, whereas at higher energies the  $p$ ,  $A_2$  contributions become significantly smaller.

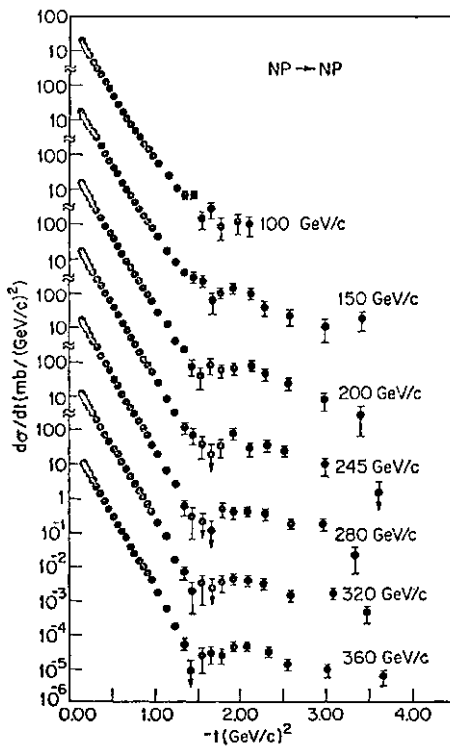


Fig. 13.

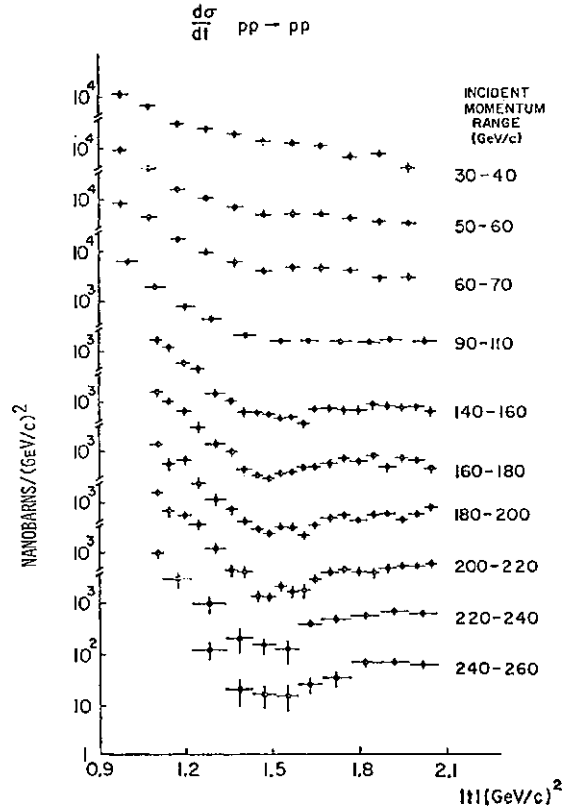


Fig. 14.

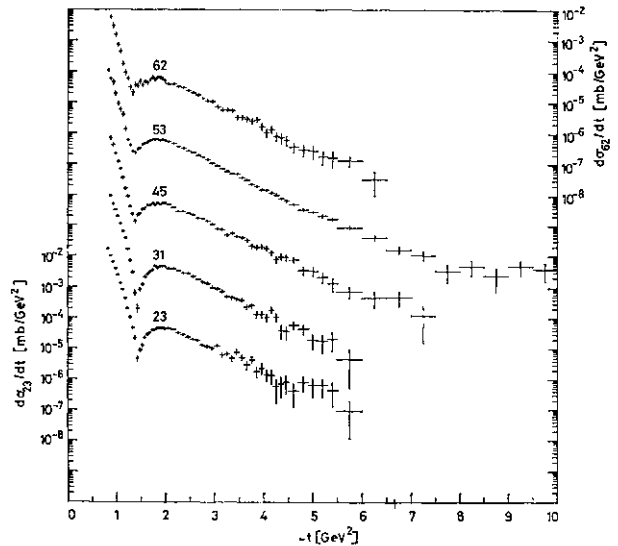


Fig. 15.

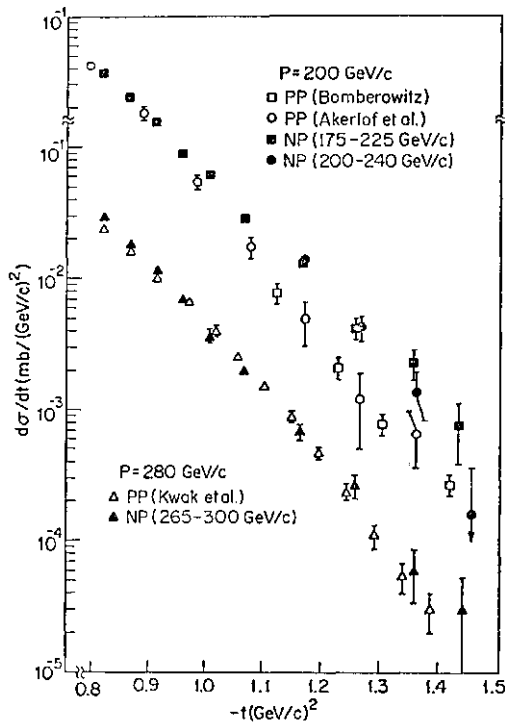


Fig. 16.

The position of the minimum and 2nd maximum in pp scattering is shown in Fig. 17 together with the geometrical scaling prediction. The cross section values at the second maximum and in the dip are shown in Fig. 18. At lower energies they drop and then start to rise in the ISR regions. Behind the 2nd maximum the cross section shows a remarkable simple exponential character. The slope values is constant up to  $-t=5$  (GeV/c)<sup>2</sup> where it starts to change for smaller values. The energy dependence at high  $s$  is very weak in contrast with trend of the data at lower energies. The CHHAV derived the phase of the amplitude from the energy dependence at fixed  $t$  neglecting spin and using derivative analyticity relations. The result is shown in Fig. 19. At high  $t$  (behind the 2nd maximum) the amplitude is predominantly imaginary whereas  $\text{Re } T_{jlm} T$  changes sign in the minimum region.

Concerning the energy dependence the CHHAV reaches the conclusion that  $GS^{25}$  is a valuable approximation which may be perfect for the full ISR range from  $\sqrt{s}=0.8$  up to the dip or for the full  $0.8 < \sqrt{s} < 5$  GeV/c from energies  $\sqrt{s} > 45$  GeV. This is illustrated in Fig. 20. On the other hand the other parametrization:

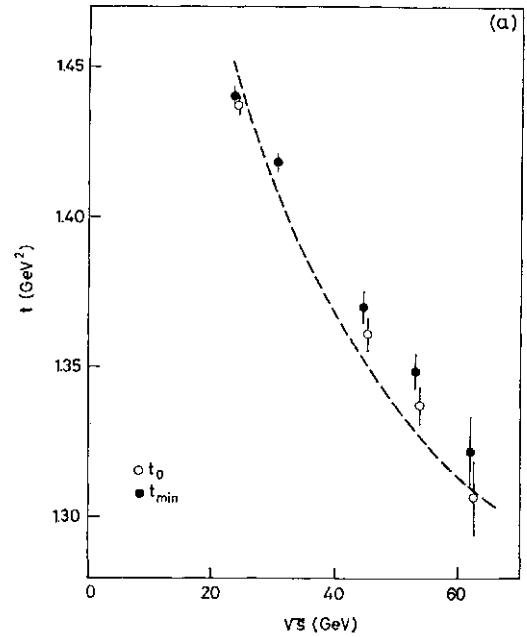


Fig. 17. (a)

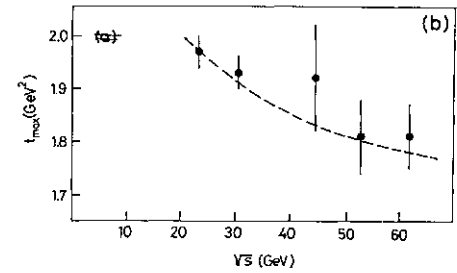


Fig. 17. (b)

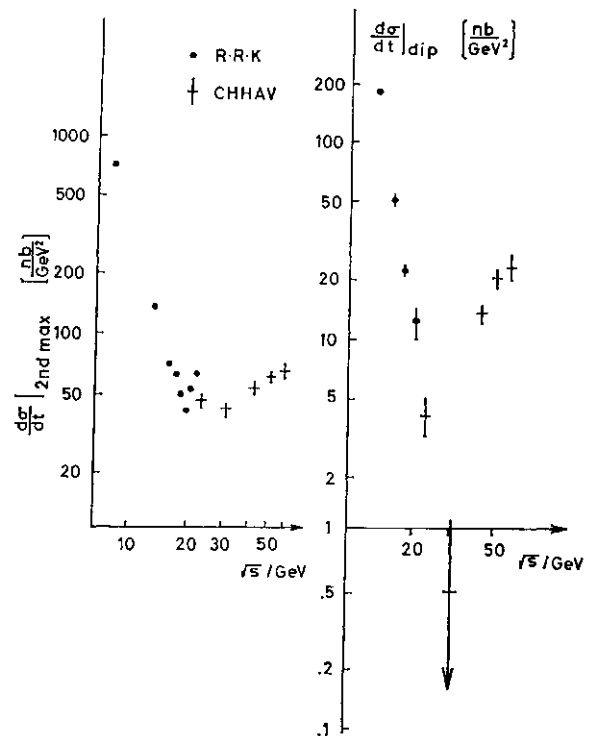


Fig. 18.

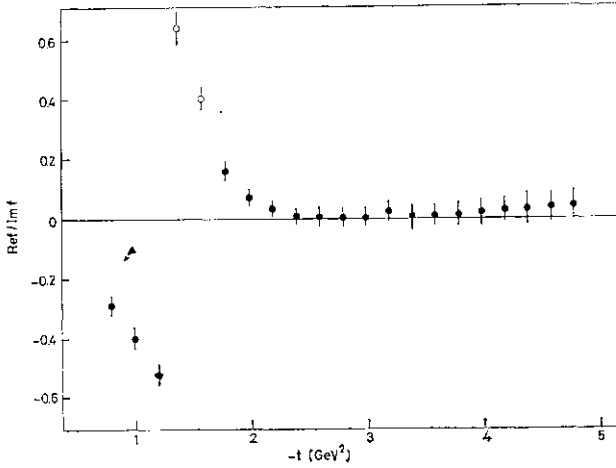


Fig. 19.

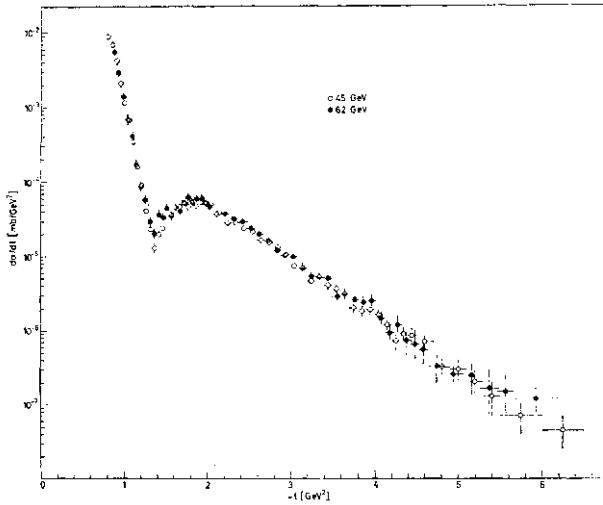


Fig. 20.

$$\frac{d\sigma}{dt} = |\sqrt{A} \sigma_{tot}(i+\rho) e^{B\sigma_{tot}(1-i\rho)/2} - \sqrt{c} e^{Dt/2} e^{-i\pi\alpha(t)/2} s^{\alpha(t)-1}|^2$$

was found describing these data excellently in the full  $s$  and  $t$  region investigated.

The main conclusions from these results can be summarized as follows. The scattering is very much diffractive with weak energy dependence and predominantly imaginary amplitude, except in the dip region, where  $\text{Im } r_{e1} \sim 0$ .

### 3. Large- $t$ scattering

Experimental discovery of the diffraction dip and second maximum in nucleon-nucleon scattering, predicted by theoretical models, gave rise to confidence in these models and optimism about their further verification at higher  $|t|$ . However experiments, performed in the last few years, yielded completely unexpected results. Recent measurements of the

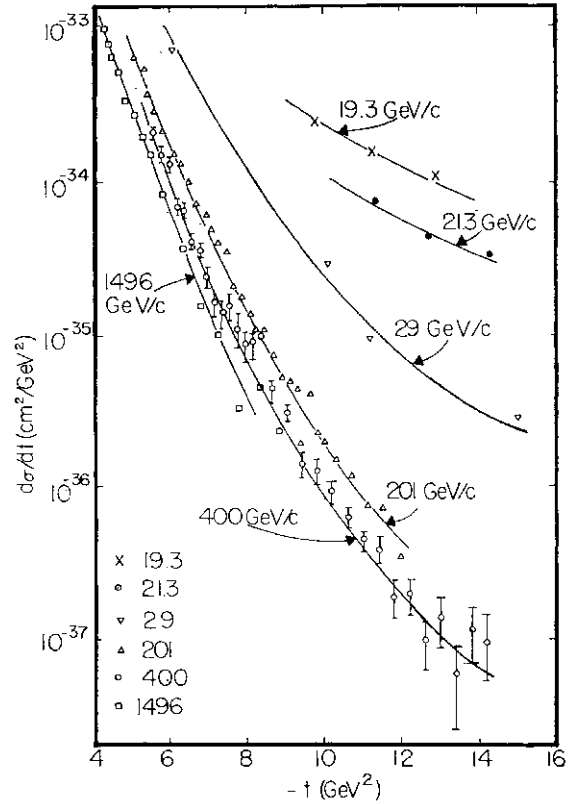


Fig. 21.

high- $|t|$  pp-scattering have been done at ISR by the CHHAV collaboration<sup>24</sup> at  $\sqrt{s}=53$  GeV up to  $|t|=10$  (GeV/c)<sup>2</sup> (the results were already shown in Fig. 15), and at FNAL by the CMNL collaboration at 200 GeV/c up to  $t=12$  (GeV/c)<sup>2</sup> and at 400 GeV/c up to  $t=14$  (GeV/c).<sup>26</sup> Results are shown in Figs. 21 and 22 and have the following important features: a) There is no second diffraction minimum expected by theoretical models at  $t \sim -4.5$  (GeV/c)<sup>2</sup>; b) The slope in the region  $2 < |t| < 6$  (GeV/c)<sup>2</sup> is  $f_{t_1} \sim 1.5$  (GeV/c)<sup>-2</sup> for FNAL and  $-1.8$  (GeV/c)<sup>-2</sup> for ISR. At larger  $|t|$  it smoothly changes to  $f_{t_2} = 0.9-0.7$  (GeV/c)<sup>-2</sup>. (Notice that the shape of  $da/dt$  becomes especially simple when it is plotted against  $p_s$ —Fig. 23. Such dependence has been discussed in on the base of unitarity relation.<sup>27</sup>

These features which are in sharp disagreement<sup>28</sup> with predictions of popular models impose a question on the validity of these models. Conjecture that beyond the second peak we are breaking into territory controlled by "hard" interaction of the constituents with the mainly real amplitude can probably be rejected. The arguments include relatively low angles  $< 15^\circ$ , small real part, estimated<sup>24</sup> from derivative analyticity relations,

and comparison with direct calculations in the framework of various versions of "hard" models.<sup>28</sup> However, this point needs further investigations in view of the fact that the FNAL data<sup>26</sup> show  $da/dt \sim S^{-n}$  dependence with

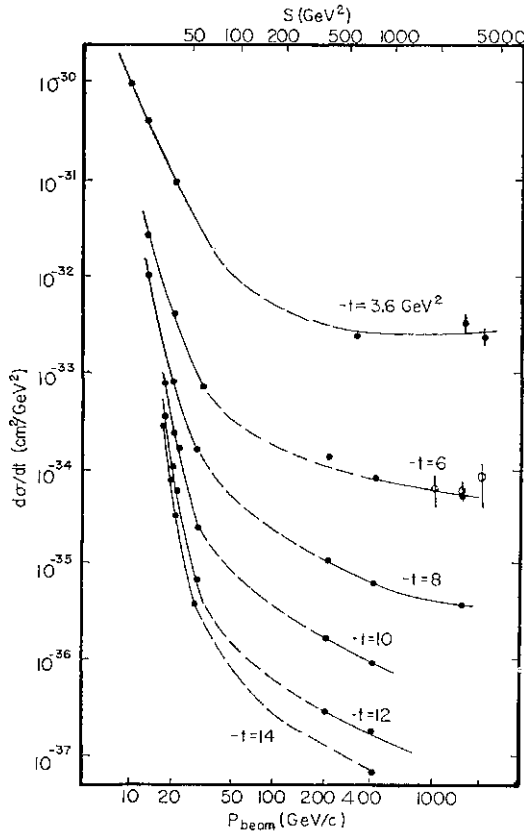


Fig. 22.

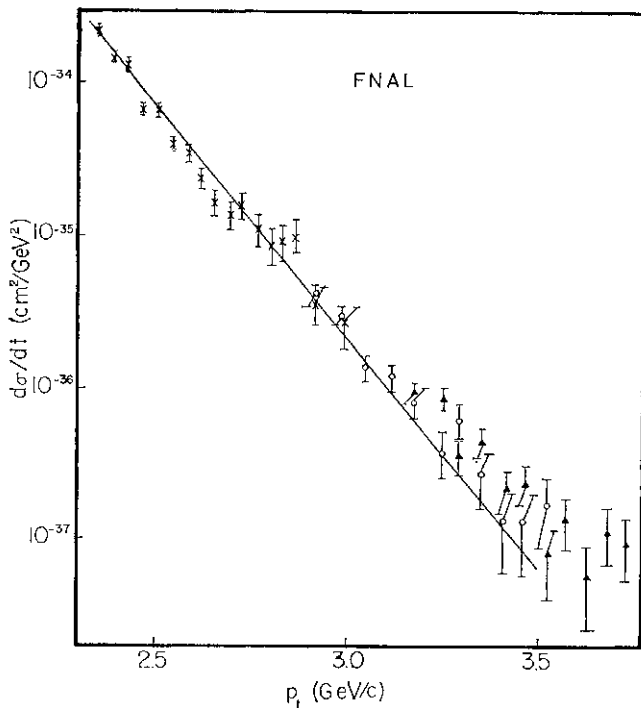


Fig. 23.

$rc=9.7 \pm 0.3$  at the largest fixed angle  $\theta=15^\circ$  which is in agreement with the value  $h=10$ , predicted by the constituent counting rules.<sup>29</sup>

One can think that the reason for the failure of the popular models is connected with their oversimplification. In particular, the failure can be caused by non-adequate treatment of inelastic diffraction. Its contribution importantly influences the shape of  $da/dt$ <sup>17,30</sup> and works in the proper direction.<sup>31</sup> Some other suggestions have been also used to improve traditional models.<sup>32-35</sup>

A very attractive suggestion is that the discovered features of  $da/dt$  are related to some peculiarities of the proton internal structure. The quark-gluon picture of hadrons, in the form of "dressed" quark model,<sup>36,37</sup> may be one of the possibilities. (This picture, resembling the light nuclei, has in fact been implied already in the early discussion of the additive quark model.<sup>38</sup> Calculations based on this "granular" model can explain observed slopes but have some problems with the value of  $da/d$ <sup>39,40,41</sup>

Another possibility to introduce "substructure" is related to the idea of "core," which can be traced back to nuclear physics and NN force theory. A specific realization may be different<sup>42-46</sup> and the slope in  $t$  of  $0.9$   $(\text{GeV}/c)^{-2}$  corresponds in different models to a size of the core of  $0.2-0.4$  fermi.

In concluding the discussion of the high  $t$  behaviour and the intriguing absence of the second dip, it's worth to note that the difference in the slopes  $Z_s, b_s$  at FNAL and ISR energies may indicate the tendency for the second dip to develop itself at  $-t \sim 4-5$   $(\text{GeV}/c)^2$  at very high energies.<sup>47</sup>

#### 4. Large angle scattering

"Hard" interaction of constituents is expected to control large angle hadron-hadron scattering revealing itself in the form of automodelity and dimensional counting rules for differential cross sections<sup>29</sup>  $d\sigma/dt$  ( $0, m, n = \text{fixed}$ )  $\propto y^{-n}$ ,<sup>(11)(12)</sup> where  $n$  is the sum of the number of quarks in the initial and final states of the interaction. The **existing** data **seem** to confirm these predictions but more full information is needed. A new high statistics experiment has recently been performed at ANL<sup>48</sup> to test the counting rule. The results

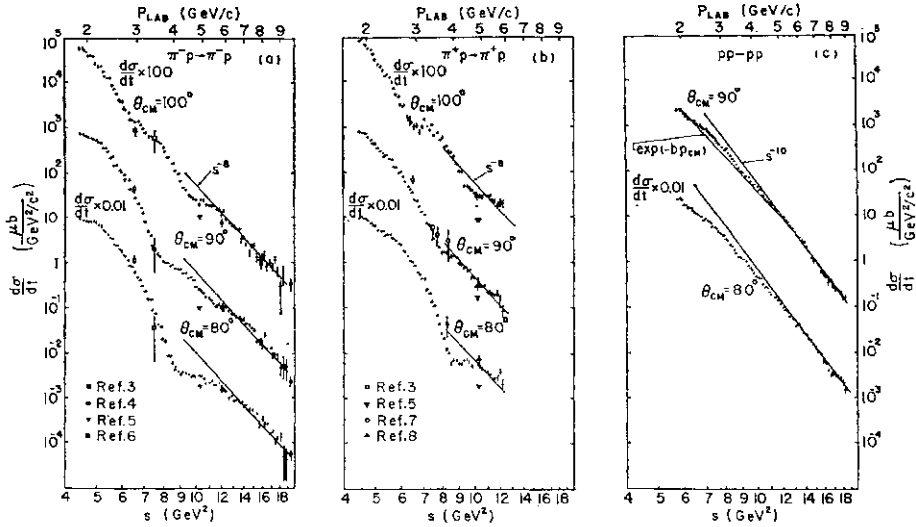


Fig. 24.

are shown in Fig. 24 together with earlier data. The  $pp$  data are inconsistent with one value of  $n$  over the entire energy range, but at  $s > 2 \text{ GeV}^2$  give  $n = -2 = 10.07 \pm 0.11$ . The  $\pi^+p$  data are more complicated but for  $s > 6 \text{ GeV}^2$  they are consistent with  $s^{-8}$  at all angles, suggesting an "asymptotic" agreement with the theory.

At smaller energies the same group<sup>49</sup> observed  $rep$  scattering cross section narrow structures with  $r = 100\text{--}200 \text{ MeV}$  which may be signal of Ericson's fluctuations, which are expected to feed into nonexotic channels as a result of resonance overlapping.

## II. Spin Effects in Elastic Scattering

In our previous discussion of elastic scattering we followed the old good tradition and completely neglected any spin effects. "Shadow" nature of high  $s$  small  $|t|$  elastic scattering related to the averaged effect of many inelastic channels may serve as justification. However at large angles the situation could be quite different. The progress in experimental technics crowned with development of the Argonne facility allowed last years precise measurements of the spin-orbit and spin-spin interactions. The very interesting and unexpected results were obtained, demonstrating structures in the cross sections and the importance of the spin effects especially at large  $p$ . Most of these data have been widely discussed at the special conferences very recently and here I limit myself to only brief discussion.

### 1. $Aa^\wedge$ , $C_{LL}$ and diproton resonance

A striking energy dependence has been observed<sup>50,51</sup> in the difference  $Jt_L = \langle 7_{tot}(\hat{\mathbf{i}}^\wedge) - a_{tot}(\hat{\mathbf{i}}^\wedge) \rangle$  of the total cross sections for longitudinally polarized initial protons with a maximum difference of  $-17 \text{ mb}$  at  $1.47 \text{ GeV}/c$  as shown in Fig. 25a. Simultaneous measurements<sup>51</sup> of  $C_{LL}$  covering around  $\theta_{cm} = 90^\circ$  from  $1.0$  to  $3.0 \text{ GeV}/c$  also shows a large variation—Fig. 25b. At the same energy range the  $pp$  polarization at fixed  $t$  also shows a remarkable energy dependence.<sup>52</sup> These features have been interpreted as evidence for the formation of diproton resonance.<sup>50,53</sup> Using dispersion relations for a forward  $pp$  scattering amplitude and the data on  $J < t$ , it was shown<sup>54</sup> that the Argand plot of the scattering amplitude has a clear resonance-like behaviour around  $1.5 \text{ GeV}/c$ . An analysis<sup>53,55,56</sup> of data indicates that  ${}^3F_3$  and possibly  ${}^1D_2$  and  ${}^3G_4$  states seem to resonate. The  ${}^*F_8$  exotic resonance would have  $J = 3^-$ ,  $M = 2260 \text{ MeV}$ ,  $r \sim 200 \text{ MeV}$  and elasticity  $20\text{--}30\%$ . It is interesting to see that this resonance, if exists, can be described together with previously indicated at Dubna  $AA$ ,  $Ap$  and  $AAP$  resonances (see ref. 57) by the quark bag model.<sup>58</sup> To clarify the resonance-like structure, measurements of  $C_{NN}$ ,  $C_{ss}$  and  $C_{LL}$  for angles from  $0^\circ$  to  $90^\circ$  will be made at Argonne ZGS.

The other issue of the  $Ja_n$  data emerging from its phenomenological analysis<sup>59,60</sup> is the revival of interest in low-lying Regge trajectories. It was shown in the Conference paper<sup>59</sup> that  $\hat{a}a^\wedge$  data seems to be consistent

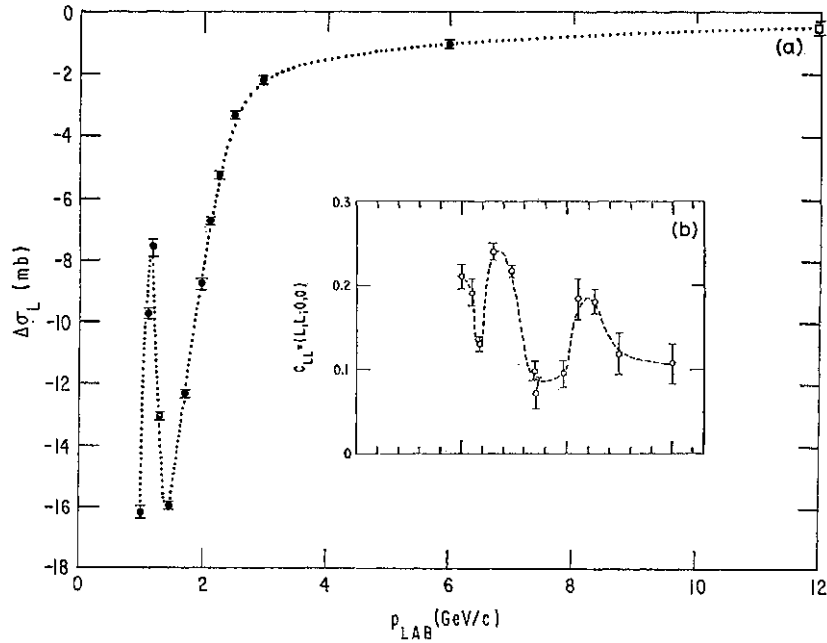


Fig. 25.

with the expected energy dependence from  $^4\text{He}$ -like exchange at  $j\pi_i, b > 3 \text{ GeV}/c$ . The low-lying isoscalar exchange was found to be consistent with estimations based on  $e(0^{++})$  exchange which is expected also from npolarization<sup>61</sup> and  $7\pi\text{N}$ -scattering.<sup>62</sup>

2. *pp Amplitudes at 6 GeV/c*

At least nine measurements are needed to determine five  $pp$  scattering amplitudes. Various  $pp$  scattering parameters have been measured at  $6 \text{ GeV}/c$ ,<sup>63,64</sup> including 3-spin parameters, which are sufficient to determine  $pp$  elastic scattering amplitudes in a model independent way at  $0.2 < |t| < 0.8 \text{ (GeV}/c)^2$ .<sup>51</sup>

I'll show only the results for  $C_{LL}$  which is negative at higher  $|t|$  and large in magnitude (Fig. 26). (This fact may shed some light on the nature of the constituents and their interactions.<sup>65</sup>) These data were used<sup>51</sup> to construct  $pp$  scattering amplitudes at  $6 \text{ GeV}/c$  and the result is shown in Fig. 27 at small  $tcz = 0.3 \text{ (GeV}/c)^2$ . The overall phase was adjusted assuming  $\text{Re } N_0 / \text{Im } N_0 = -0.35$ , the measured value at very small  $|t|$ .

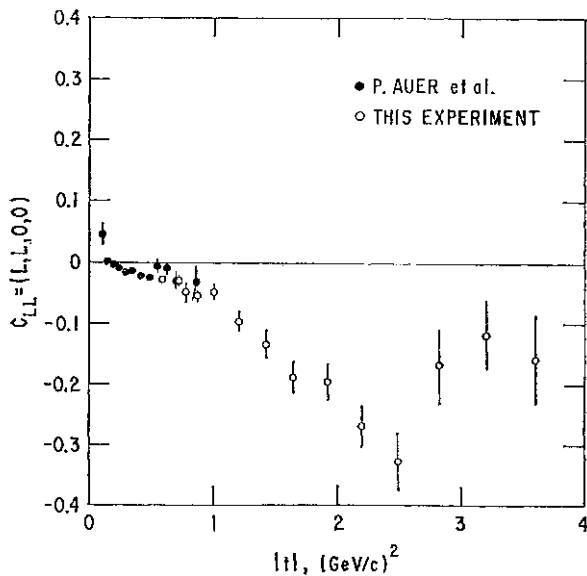


Fig. 26.

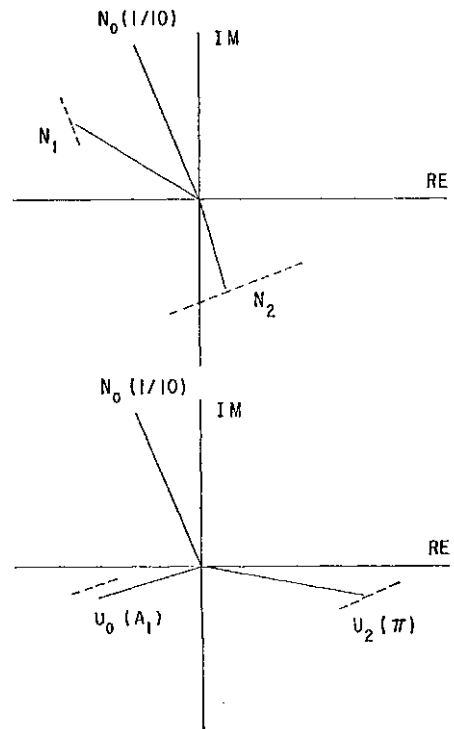


Fig. 27.



3. Measurements with spins normal to the scattering plane

The systematic study of the pp elastic scattering in pure transverse initial spin states at 6 GeV/c is presented by the Krisch group.<sup>66-69</sup> The measurements include eight pure three-spin cross sections  $da/dt$  ( $ij \rightarrow ol$ ), three two-spin cross sections  $da/dt$  ( $ij$ ), ( $da/d?$ ),  $A$ ,  $C_{NN}$ ,  $D_{NN}$  and  $AT_{NN}$ . These data allowed to determine the magnitudes of five independent transversity amplitudes and to test P- and P-invariance, showing that any P- and P-violating cross sections are consistent with being less than about 6% of  $\{da/dt\}$ . The most dramatic results of these studies are presented in Fig. 28 and show that the ratio  $da/dt$  ( $\uparrow\uparrow$ ):  $da/dt$  ( $\parallel$ ) has the sharp zero at  $P_i = 0.9$  (GeV/c)<sup>2</sup>, broad maximum at about  $P_i = 1.7$  (GeV/c)<sup>2</sup> and then rises rapidly at  $P_i = 3.6$  (GeV/c)<sup>2</sup> reaching a value of 4 at the maximum  $P_i$  presently available at the Argonne.

The energy dependence of the  $C_{NN}$  at  $\theta_{c.m.} = 90^\circ$ <sup>69</sup> displays dramatic decrease near 3.5 GeV/c followed by flat behaviour and then suddenly increases near 12 GeV/c.

Figure 29 shows a plot of the pure four-spin cross sections  $da/dt$  ( $\uparrow\uparrow \rightarrow \uparrow\uparrow$ ) obtained at 6 GeV/c<sup>66</sup>. The spin dependence is large, and becomes larger at high  $P_i$  beyond  $P_i \sim 0.8$  (GeV/c) where all cross sections have break. The double-flip cross sections  $da/dt$  ( $\hat{\uparrow}\hat{\uparrow} \rightarrow \hat{\uparrow}\hat{\uparrow}$ ) and  $da/dt$  ( $\hat{\uparrow}\hat{\uparrow} \rightarrow \hat{\downarrow}\hat{\downarrow}$ ) are typically 10 times smaller than the nonflip.

All considered data display importance of the spin-effects in the high  $P_i$  scattering. Since this region is expected to be controlled by the hard scattering of the constituents, the study of spin dependence becomes a powerful way to reveal the peculiarities of an interaction and the nature of the constituents involved in the hard scattering.<sup>65,70</sup>

4. Elastic scattering polarization

New data on polarization for pp, pn, Trp, Kp elastic scattering are submitted to the Conference.

At low energies backward polarization of  $n-p$  scattering has been measured from 2.25 to 3.50 GeV/c.<sup>71</sup> This experiment is another one of the first series of experiments of KEK proton synchrotron. In Fig. 30 preliminary

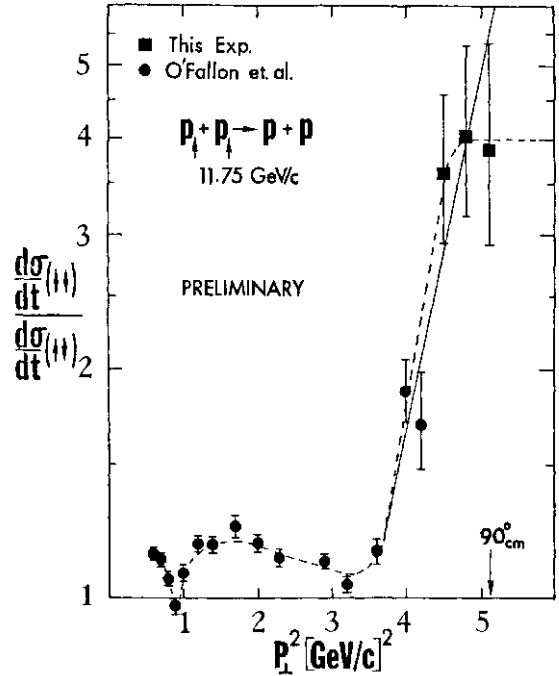


Fig. 28.

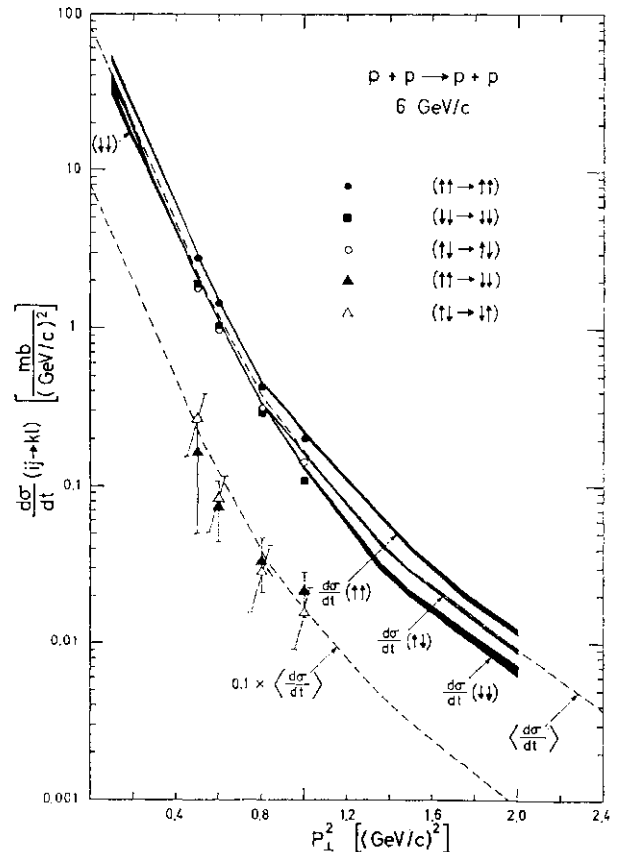


Fig. 29.

results are shown together with other data. Now with the new KEK data we have the landscape for the  $n-p$  polarization in the whole angle region and can admire the very interesting systematic patterns in  $t$  and their energy dependences. The data in Fig. 30

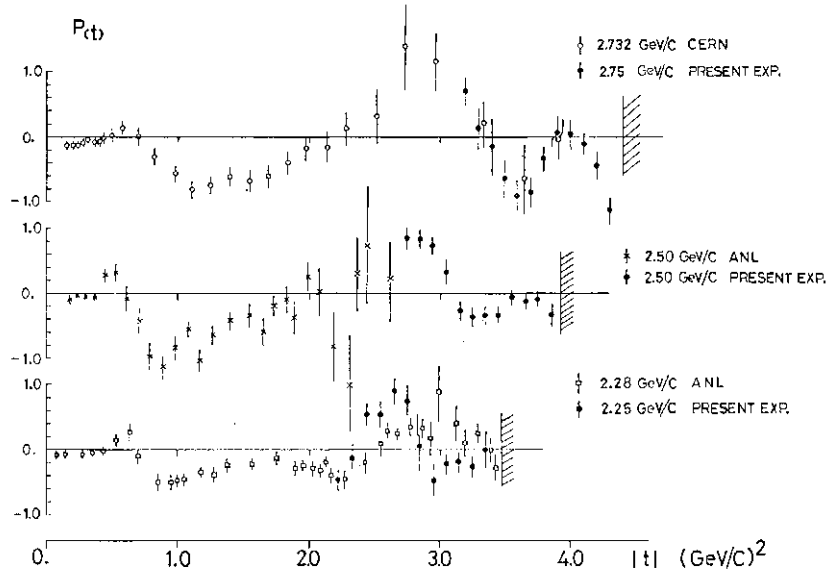


Fig. 30.

exhibit remarkable polarization thus giving an important information for understanding the interplay of different mechanisms governing

this intermediate energy region. The other KEK data on polarization in pp-pp and pp-pn at 0.7 GeV/c and results for inclusive polarization can be found in the Yokosawa's talk.<sup>2</sup>

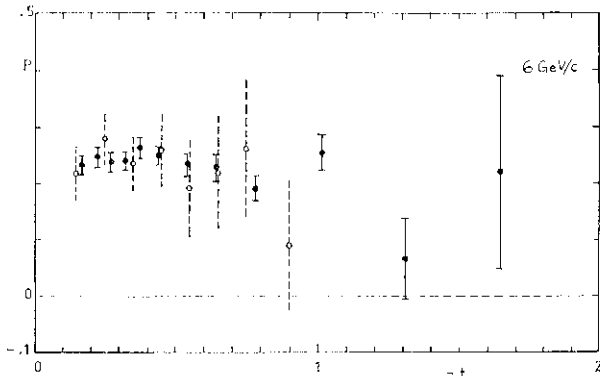


Fig. 31 a.

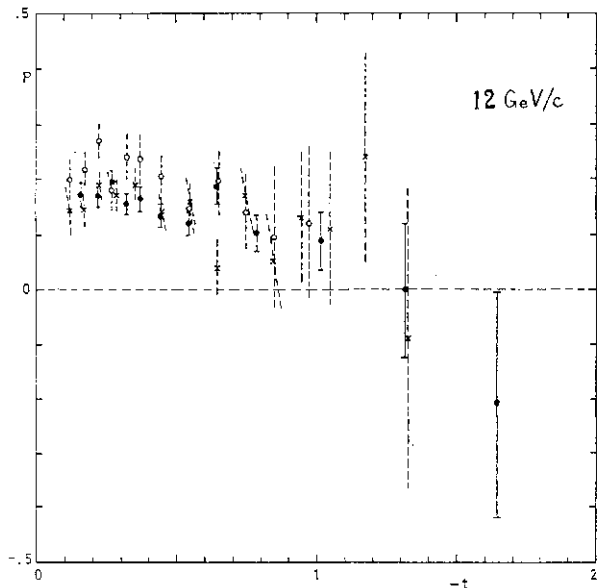


Fig. 31 b.

New results for the  $K^+p$  elastic scattering polarization at 6 and 12 GeV/c<sup>72</sup> are given in Fig. 31 and have statistics which is appreciably higher than in the previous experiments. There is evidence in Fig. 31 for the changing of the sign of polarization at 12 GeV/c and  $-t \sim 1.0$  (GeV/c)<sup>2</sup> which is expected from the strong absorption Regge model calculations.<sup>73</sup>

The preliminary results on pp and np polarization at 24 GeV/c<sup>74</sup> shows a mirror-symmetry indicating an importance of  $I=1$  exchange at this incident momentum. The pp polarization at 24 GeV/c in Fig. 32 shows a pronounced

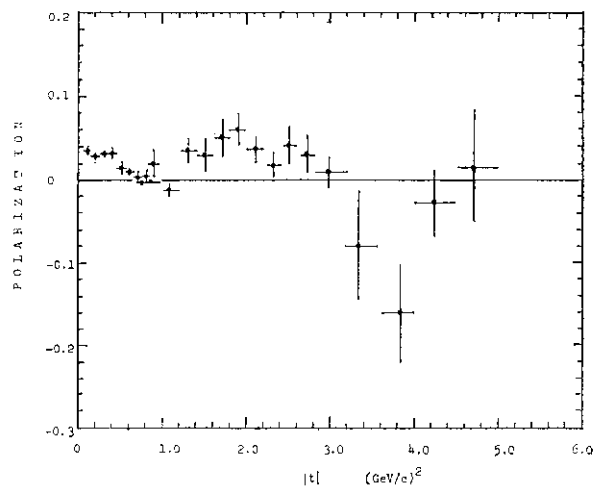


Fig. 32.

structure at large  $|t|$  region. In comparison with similar results obtained at 12 GeV/c at Argonne new data display rather a double-bump structure in a region  $1.0 < |t| < 3.0$  (GeV/c)<sup>2</sup> followed by a negative dip at  $\sim 4$  (GeV/c)<sup>2</sup>.

Figures 33, 34 show recent results for pp elastic polarization from CERN at 150 GeV/c<sup>75</sup> and FNAL at 100 and 300 GeV/c.<sup>76</sup> The 150 GeV/c data display rather clear shape of

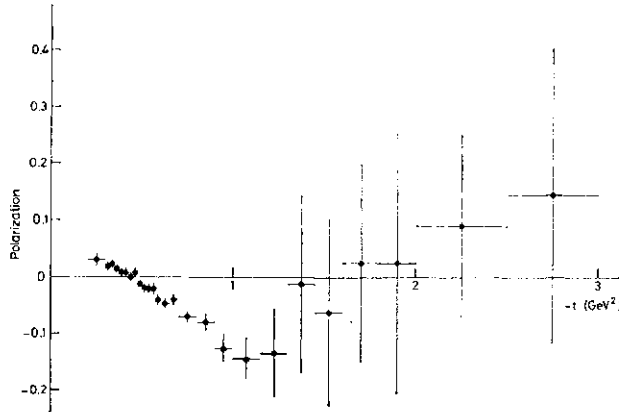


Fig. 33.

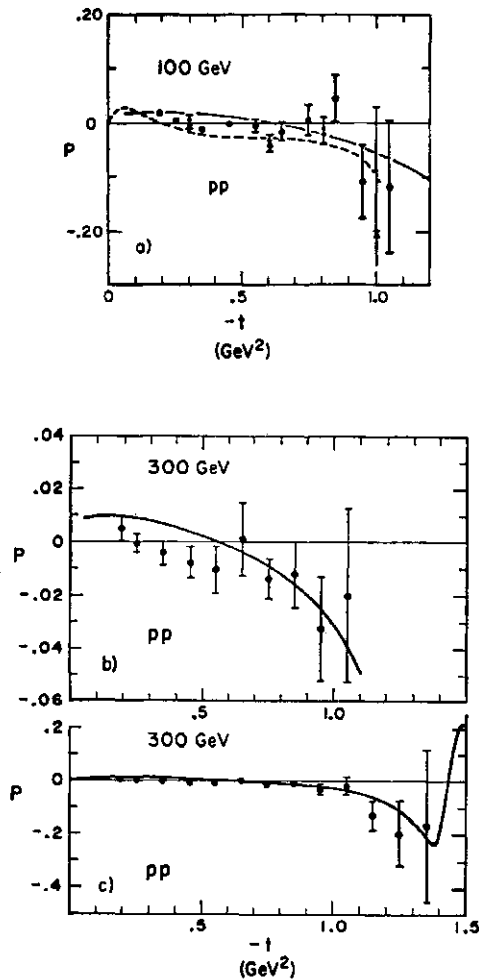


Fig. 34.

$t$  dependence, which is similar to the one indicated of the 45 GeV/c Serpukhov data.<sup>77</sup> At small  $|t|$  the polarization is small positive, and then at about  $t = -0.4$  (GeV/c)<sup>2</sup> it changes sign. The most remarkable feature of the data is a sizable negative polarization around  $t = -1$  (GeV/c)<sup>2</sup>. The FNAL results are somewhat different from CERN data and show smaller polarization at low  $|t|$ , although they are consistent with  $P \sim 15\%$  at  $-t \sim 1-14$  (GeV/c)<sup>2</sup>.

The  $7\pi^+p$  elastic scattering polarization at 100 GeV/c as measured at FNAL<sup>76</sup> is shown in Fig. 35 and displays expected mirror symmetry.

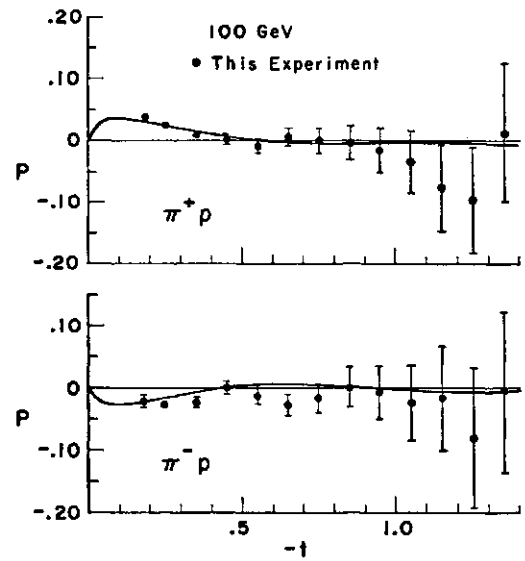


Fig. 35.

There are many theoretical models which could be compared with these new polarization data (see, for example refs. 73, 78-81), but I do not have possibility to discuss all of them. The only general remark is that the observation of negative pp polarization at high energies may be directly related to the rising pp total cross sections.<sup>78</sup>

### III. Inelastic Diffractive Scattering

Submitted to this Conference are results on different low multiplicity channels of diffractive dissociation (DD) in beams of  $\pi$ -mesons, K-mesons and nucleons and we will discuss some of them.

#### 1. $n \rightarrow 3n$ and the Ax-problem

The Ax resonance and its partners in the  $JPC = 0^{++}$  SU(3) nonet remain mysterious

objects, whose existence just as for flying saucers is debated for many years.<sup>82</sup> Both the quark model and chiral symmetry provide compelling reasons why an  $A_x$  meson should exist. Traditionally the  $A_x$  is associated with the broad enhancement observed around 1.1 GeV in the invariant mass of the diffractively produced  $3\pi$  system. However, phase analysis showed<sup>83</sup> that the  $1^+$  partial wave phase did not have resonance variation. Since that this peak is presented in different papers sometimes as a resonance, sometimes as a threshold kinematical bump. The new round of debates includes evidence both "for" and "against" the resonance. We begin with "for", a) Through analysis of  $DD \pi z \pi z$  has been carried out in paper<sup>84</sup> submitted to this Conference and also in recent papers.<sup>85,86</sup> The analysis includes as ingredients the Drell-Hiida-Deck model, direct production of the  $A_i$  resonance and resonance rescattering. The interference of the DHD mechanism with rescattering can reduce the variation of the phase<sup>85</sup> and its further suppression arises as a result of inelasticity due to  $K^*K$  channel.<sup>84,86</sup> As a result a modest phase variation found in experiment does not contradict the existence of the  $A_x$  resonance—see Fig. 36. The contribution of direct resonance production turns out to be very small—Fig. 37, and the interference results in a shift of the peak to smaller  $M$ . b) The new analytic of the IHEP-CERN data on  $DD \pi p \rightarrow (3\pi) p$  based on fully analysis, unitary functions<sup>88</sup> concludes that the data do not completely rule out the resonant nature of the  $A_x$ . The lesson which we learn from these studies is that the problem

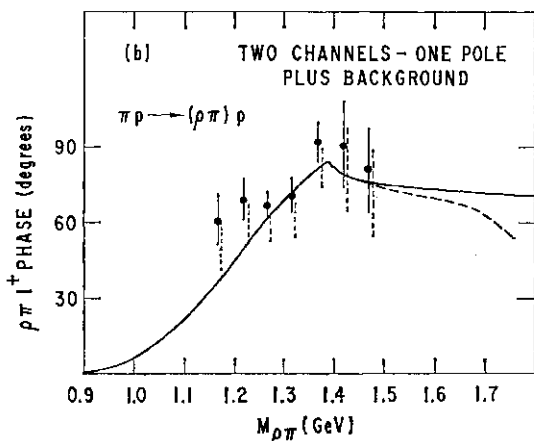


Fig. 36.

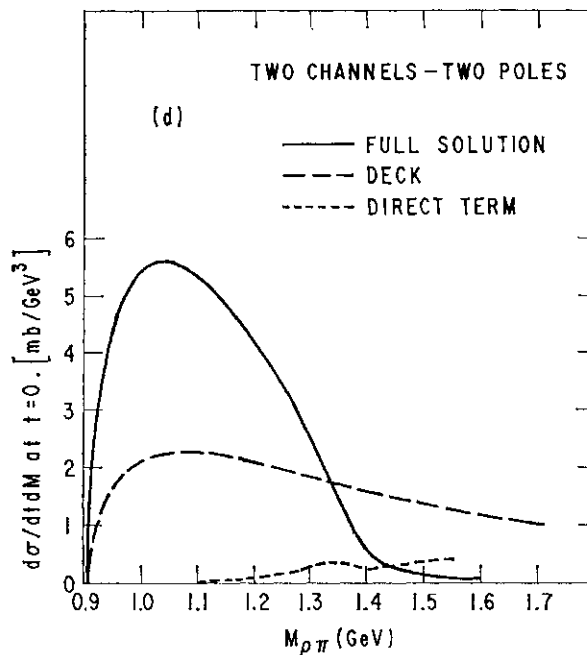


Fig. 37.

of extracting information about possible resonance like  $A_x$  which could be excited diffractively in the presence of strong resonance-like background, is nontrivial and demands not only excellent data but also rather sophisticated theory for the analysis and thus is strongly model dependent, c) One more piece of evidence in favour of diffractive  $A_x$  production was found<sup>89</sup> in coherent ( $3\pi$ ) production on nuclei, d) Evidence for  $A_x$  production was also found in nondiffractive reactions which do not contain large non-resonant background and so are more convenient for searching for the  $\Lambda_i$ . The peak at  $M = 1041 \pm 13$  MeV was observed in backward production in  $K^- p \rightarrow 2^-(\pi^+ \pi^- \pi^0) p$  at 4.15 GeV/c<sup>90</sup> and at  $M = 1050 \pm 10$  MeV in backward production in reaction  $\pi^- p \rightarrow \pi^0 (\pi^+ \pi^- \pi^0) p$  at 9 and 12 GeV/c<sup>91</sup> e) Some indirect evidence for  $A_x$  resonance exchange is given by study of the spin effects in reactions  $pp \rightarrow pp$ <sup>92</sup> and  $\Lambda^0 p \rightarrow \Lambda^0 n$ .<sup>92</sup> However none of these evidences is conclusive.

Among recent measurements a negative result on the  $A_x$  was obtained at SLAC,<sup>93</sup> where diffractive and charge-exchange reactions  $\pi^+ p \rightarrow (\pi^+ \pi^0 \pi^+) p$  (1) and  $\pi^+ p \rightarrow (\pi^+ \pi^0 \pi^+) p$  (2) were studied. In the diffractive channel (1) the  $A_1, A_2, A_3, A^+$  enhancements were observed but with only the  $A_1$  having a resonance phase variation. A partial-wave analysis of reaction

(2) shows clear evidence for resonant behaviour of the  $2^-(px)d$  and  $3^-(\rho\pi)f$  amplitudes, associated with  $A_1$  and  $\omega'$  (1975) production; however no evidence for  $A_1$  or  $A_2$  production in the  $1^+(px)S$  and  $2^-(\rho\pi)S$  waves is found. The upper limit for  $A_1$  production with  $M \sim 1.1$  GeV from these data is about ten times smaller than is expected from theoretical estimations.<sup>82</sup> Notice that the cross sections found for backward production<sup>90,91</sup> on the contrary are very close to theoretical estimates<sup>82</sup>: in  $K \sim p$   $a_{A_1} \sim 3.6 \pm 0.5$   $\mu\text{b}$ ,  $a_{\text{theor}} = 2J$   $\mu\text{b}$  and in  $\pi^- \sim p$   $a_{A_1} \sim 3.5 \pm 0.2$   $\mu\text{b}$ ,  $a_{\text{theor}} = 3.9$   $\mu\text{b}$ .

So the  $A_2$  problem is still lacking perfect clearness. Although the majority votes "for,"

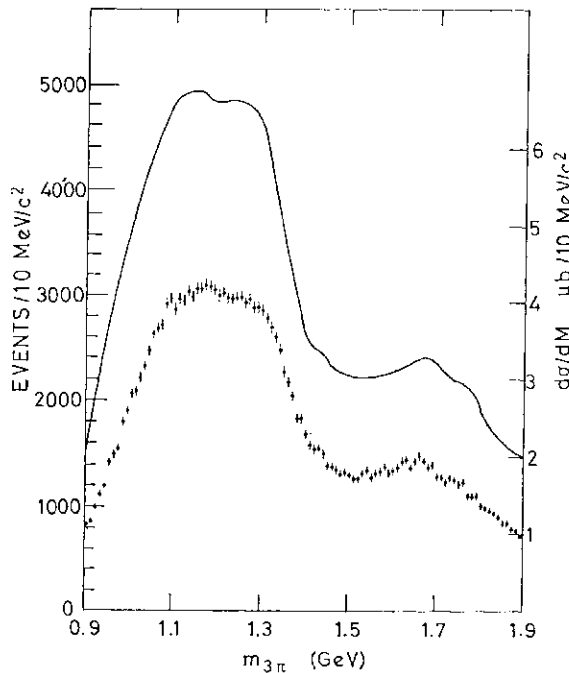


Fig. 38.

there is no still proof of the existence of the  $A_2$  resonance.

New data on  $DD \pi^+ \rightarrow (3\pi)^+ p$  are presented to this Conference from a measurement at 93 GeV/c.<sup>94</sup> The experiment was performed at the CERN SPS by Amsterdam-CERN-Cracow-Munich-Oxford-Rutherford collaboration and yielded almost one quarter of a million events.

The  $(3\pi)$  mass spectrum is shown in Fig. 38 together with the data corrected for acceptance and is similar to that obtained by experiments of lower energies and smaller statistics though there is now the possibility of structure in the flat top of the 1.1 to 1.3 GeV "A" region. The  $d\sigma/dt'$  in the region  $M_{3\pi} < 2$  GeV (Fig. 39) is, however, considerably different from previous observations. The usual slope-mass correlation is observed at low  $t' = t - t_{\text{min}}$ , but there is a clear break in slope in the region of  $0.4$   $(\text{GeV}/c)^2$ , this second component having a smaller and non-massdependent slope of about  $5$   $(\text{GeV}/c)^{-2}$ . The fit to a form  $pAe^{at'} + (l-p)Be^{bt'}$  leads to  $A(M)$ ,  $B(M)$  shown in Fig. 40. The  $A_2$  does have a perturbing effect, but the phenomenon is present throughout the entire  $(3\pi)$  mass spectrum. The intensity of the dominant  $1^+ S(\rho\pi)$  wave of the low mass region may be seen in Fig. 41 changing from low to high  $t'$  region.

The discovered two-component  $t'$ -dependence resembles that observed in the nucleon DD and may teach us an important lesson of significance of the absorptive effects in pion DD (see refs. 5 and 95). In particular the account of absorption may change some of the conclusions of the analyses of the  $A_2$ -problem.

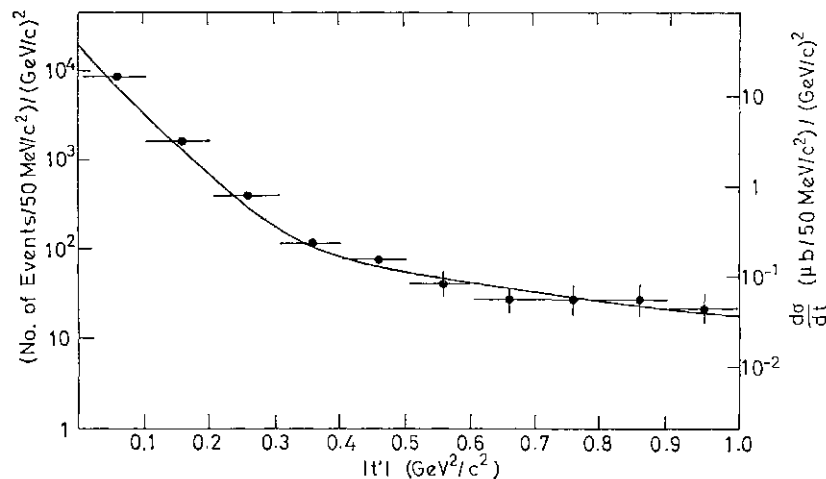


Fig. 39.

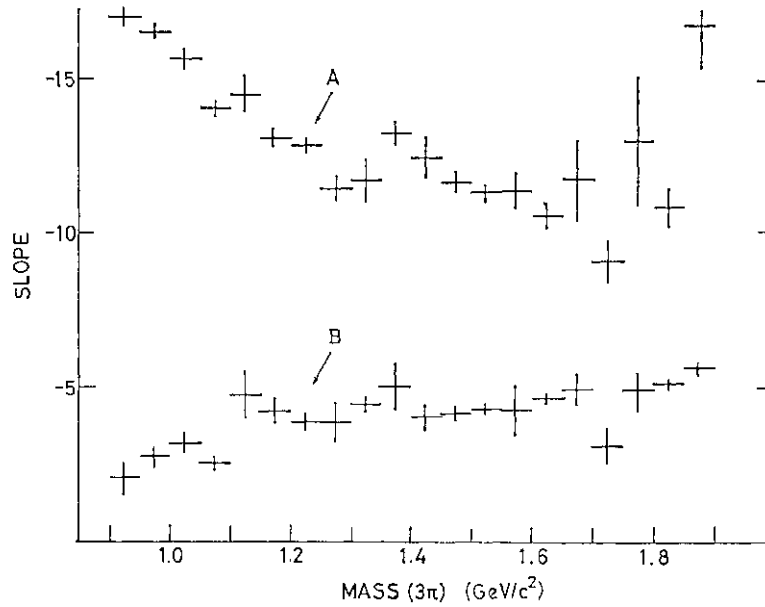


Fig. 40.

2. Coherent nucléon DD

Nucléon DD has been studied carefully in the last few years, especially in nucleon-nucleon collisions at Serpukhov, FNAL and CERN and these data significantly influenced the theoretical view of the DD mechanism.<sup>6,95</sup>

Recently these studies have been supplemented with new data from coherent DD on nuclear targets. The Arizona-Dubna-Fermilab group studied nucléon DD on helium target  $p^4\text{He} \rightarrow X^4\text{He}$ <sup>6</sup> and the most interesting preliminary results are the following: a) The  $t$  dependence in Fig. 42 shows a pronounced kink in the region of  $-t$  from 0.15 to 0.25  $(\text{GeV}/c)^2$  for all accessible masses and energies. In fact, there are two reasons for the structure in this  $t$  region. First, the low mass NN  $\rightarrow$  TTNN DD is known to exhibit the dip or break

around  $t = -0.2 (\text{GeV}/c)^2$ <sup>95</sup>. Second, the Glauber rescattering which gives rise the dip seen in  $p^4\text{He} \rightarrow p^4\text{He}$  at  $0.22 (\text{GeV}/c)^2$  are also expected to lead to a dip in low mass  $p^4\text{He} \rightarrow X^4\text{He}$  at somewhat smaller  $|t|$ . The reason why one sees only the kink remains to be analysed, b) New feature of the slope-mass dependence not seen in  $pp \rightarrow Xp$  data is an indication of a structure near the threshold and may be at  $M_x = 4 \text{ GeV}^2$ . If it is a true

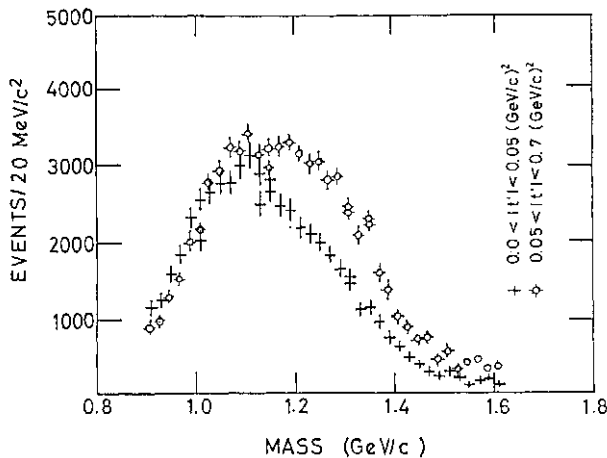


Fig. 41.

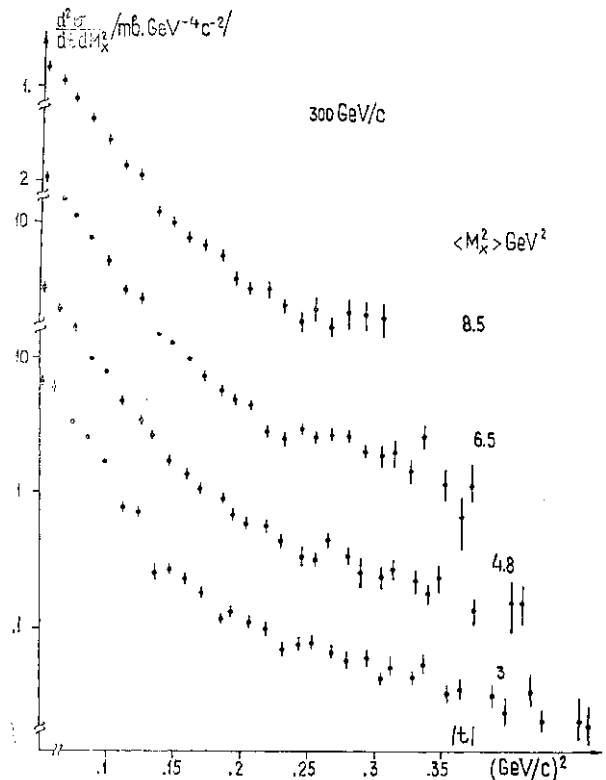


Fig. 42.

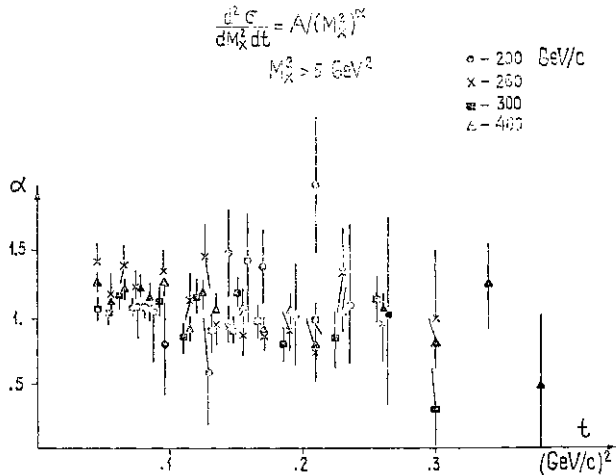


Fig. 43.

effect, it may indicate that the nucleus acts as a filter differently absorbing various components of the excited system, c) The cross section at fixed  $t$  and  $M_X > 5 \text{ GeV}^2$  has been fitted by the form  $d\sigma/dt dM_X = A(M_X)^{-\alpha}$  and yields the values of  $\alpha$  consistent with 1—Fig. 43. Such a behaviour has been found previously in the pd gas-jet experiments<sup>7</sup> and suggests the importance of the triple-pomeron interaction.

5. Double DD and double pomeron exchange

CERN-Pavia group,<sup>8</sup> extended their previous study of double DD  $pp \rightarrow (p7r7r\sim)(p7r7r\sim)$  to the reactions, involving neutron DD:  $nn \rightarrow (p;r'')(p7r\sim)$  and  $pn \rightarrow (p7r7r\sim)(p7r\sim)$  at  $\sqrt{s} = 26.4$  and  $37.2 \text{ GeV}$  using new data taken at the CERN ISR with dd and pd colliding beams. These results, supplemented by data on single DD  $pp \rightarrow p(p7r\sim)$  and  $pn \rightarrow p(p7r\sim)$  measured at some experiment allow to test in detail the pomeron factorization at different  $t$  and  $M$  values without use of elastic scattering data. The latter may be important in view of the apparent difference in absorption in elastic and inelastic

diffractive scattering. Invariance of the mass distribution at one vertex from the other vertex is demonstrated in Fig. 44 where the ratios of normalized cross sections are plotted as a function of mass, showing that the excitation properties of (Ntt) and (Nnn) systems are identical in different reactions. Figure 45 shows that the relation

$$d\sigma \sim [pn \rightarrow (p;r'7r\sim)(p7r\sim)] = \{ \wedge [PP \wedge (P \wedge \sim)(P \wedge \sim)] \} X \wedge [nn \rightarrow (,7r Xp^* )]$$

is nicely satisfied implying factorization in a wide  $t$  region up to  $-t=2 \text{ (GeV/c)}^2$ . However, despite of these impressive manifestations of the factorization, I believe, we need still more detailed investigation (say in  $d^2\sigma/dt dM$ ) to clarify the role of absorptive effects.

A search for double pomeron exchange contributions is of fundamental interest for hadron diffraction theory. A number of experiments have been performed in last few years to search for this mechanism, however, only recently clear enough signal of this contribution was detected. In the paper<sup>9</sup> submitted to this Conference the thorough study of the DPE in reaction  $pp \rightarrow pp \pi\pi$  has been carried out for the first time over the full energy range available at the ISR with complete kinematical reconstruction. The high available statistics allowed to use rather restrictive cuts to solve the main problem of suppression of the background due to single DD. The properly selected events with leading protons and centrally produced pions (say  $|x_p| < 0.9$ ,  $|y_\pi| < 1$ , "sample B") display features compatible with theoretical expectations for DPE.

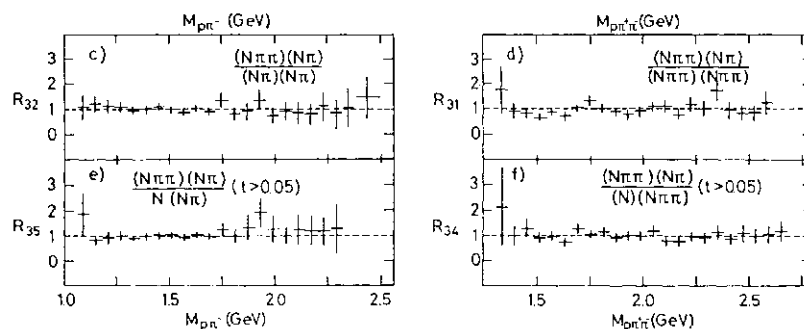


Fig. 44.

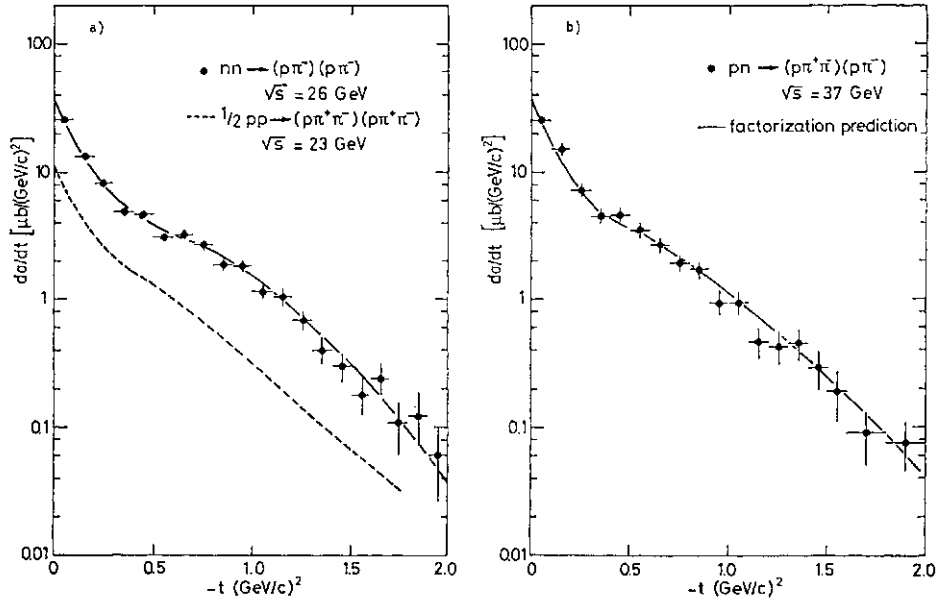


Fig. 45.

a) No correlation was found between protons. The distribution in the difference  $A < p$  of the proton angles  $\langle \hat{t}_{12} \rangle$  in Fig. 46 is uniform for sample B (shaded area) in contrast to more liberal "sample A" with  $|*|_p < 0.8$ . Furthermore, there is no correlation between the

momentum transfers  $t_{1,2}$  at the two proton vertices.

b) The observed slope  $b$  of the  $t$ -distribution — Fig. 47 is close to the expected value  $6 \sim (1/2) 6_{e1}^6 (\text{GeV}/c)^{-2}$  and in accord with factorization it also describes the two-dimensional distribution in  $(* + \epsilon, \dots)$ .

c) The allowed  $(KTL-)$  quantum numbers for the DPE are  $7=0, J^P=0^+, 2^+, 4^+$ . The  $(TT+TT')$  mass spectrum is dominated by an enhancement near threshold with no indication for  $\Lambda(765)$  meson and with signal of the  $f(1270)$  at high energy. The decay angular distribution of the  $K^+ K^-$  system is compatible with what one expects from a spin 0 state.

d) The energy dependence for different

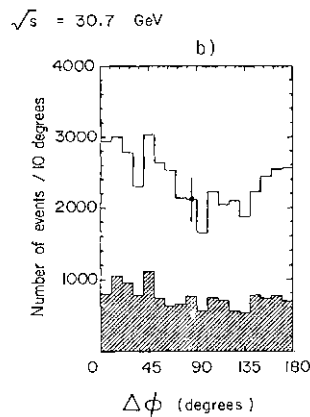


Fig. 46.

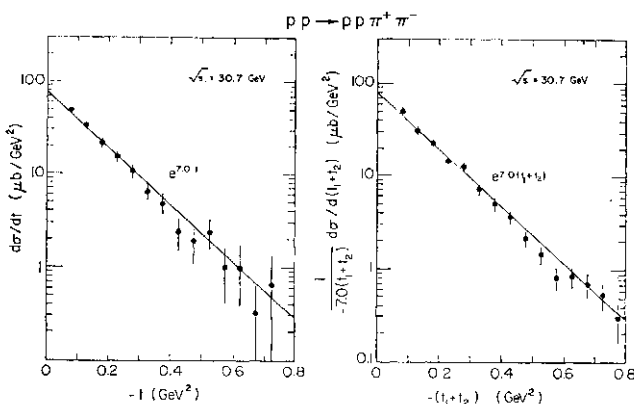


Fig. 47.

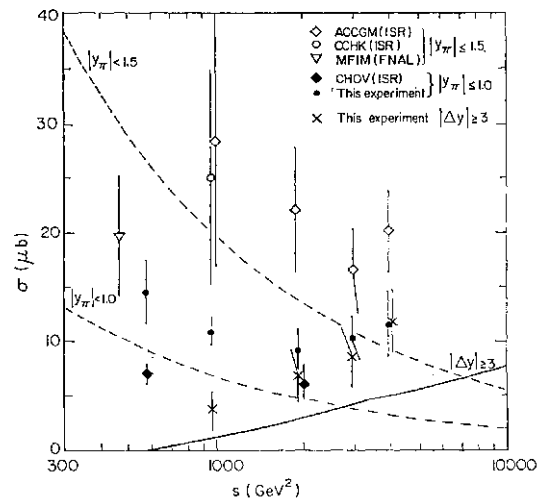


Fig. 48.



samples is shown in Fig. 48 also in reasonable agreement with theoretical predictions and allows to estimate the DPE contribution as  $\sigma = 9.5 / ah$  for the sample B.

4. Theoretical models for DD

Production of inelastic states in diffractive scattering is related to the composite nature of hadrons and different absorption of constituents in "shadow" scattering. So diffraction can provide valuable information on coherent interactions between hadronic constituents. This aspect has recently been emphasized in papers<sup>100,101</sup> and we touched on it already in connection with our discussion of elastic scattering. In the model<sup>102</sup> which stressing the role of gluons, hadron diffraction arises as a result of elastic diffractive scattering of "glueballs" belonging to the colliding hadrons. This point of view can motivate a revival of the old Morrison idea on a special nature of diffractive ("D"-) resonances<sup>103</sup>: They can be considered<sup>104</sup> as a bound system of quarks and excited glueballs. These models are certainly interesting from a heuristic point of view. However, in their current form they do not permit carrying out detailed calculations of exclusive channels and predict internal properties of produced states, mass spectra, correlations and so on. It makes their experimental verification difficult.

The quark model offers another possibility, however a priori it is not clear to what extent it can be applied to small- $t$  processes.<sup>101</sup> Here quarks are mainly at large distance and the confining interaction aims to hadronize them. In such situation the use of virtual hadrons as "constituents" may be more adequate. The well known example is given by various version of the Drell-Hiida-Deck model, widely used in practical calculations of DD. The model has been considerably developed recently to meet experimental and theoretical constraints (see refs. 5, 95 for review). Contrary to elastic scattering, where quark model gives reasonable description in a wide  $t$  region in DD the model is known to encounter some problems with  $t$  and M-distributions (see ref. 101). The quark model suggested in ref. 105 seems to avoid these difficulties and naturally unifies resonance and non-resonance contributions. The final state hadronizing interaction con-

trois the resonant or non-resonant character of diffractive excitation, as shown graphically in Fig. 49a, b. The model can be used also for inclusive excitation—Fig. 49c. Further development may include fluctuations of the active partons in the "dressed" quark.<sup>106</sup>

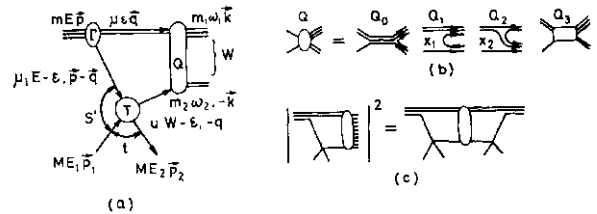


Fig. 49.

Until detailed calculations are absent, it is difficult to estimate how adequate to the experiment the quark-gluon models are. Nevertheless this approach seems to be very promising in relation information from lepton and hadron induced reactions.

IV. Nondiffractive Processes

7.

Considerable experimental activity remains in the study of quasi-two-body nondiffractive reactions while the bygone theoretical enthusiasm in this field diminished. Failures of the Regge cut calculations have led to a tendency of returning back to the pole phenomenology. Semiquantitative systematics reached on the base of Regge model and quark relations can be considered as satisfactory to a certain extent<sup>107,59</sup> and this is illustrated in many papers, submitted to this Conference. At the same time all attempts to obtain more detailed quantitative description and to get rid of arbitrary phenomenological elements are still unsatisfactory.

Since the substantial part of new data on non diffractive two-body processes has been covered by mini-rapporteurs, I'll confine myself here to only brief discussion of a few selected topics.

The charge exchange processes  $7r \sim p \rightarrow 7r \sim n$  and  $7r \sim p \rightarrow n$ , the simplest and classical from exchange model point of view, have been studied at low energies at KEK and Dubna. The KEK measurements<sup>108</sup> of  $n \sim p \rightarrow n \sim n$  differential cross section and polarization cover the region from 2 to 3 GeV/c,  $|\cos \theta| < 0.9$  and provide new important data to incorporate in

partial wave analysis. The Dubna group<sup>10\*</sup> studied  $\pi^-p \rightarrow \gamma^n$  at 3.3 and 4.75 GeV/c and a small  $|t|$ . The sizable minimum in the forward direction seen in Fig. 50 indicates a dominance of the helicity-flip amplitude and the data are in agreement with  $\Lambda$ -exchange.

Recently very interesting data on high energy single  $J^{++}$  production<sup>110</sup> and charge-exchange double dissociation of protons<sup>111</sup>

have been obtained at ISR, demonstrating the validity of Regge ideas at high energies. New information on the charge-exchange process  $pp \rightarrow (p7r^+)(p7r^-)$  at the ISR between  $\sqrt{s} = 23$  and 63 GeV/c is presented to this Conference.<sup>112</sup> Double resonance production is observed in both the  $\Delta^{++}$  and  $J^{++}N^0$  (1688) channels. The differential cross sections are seen in Fig. 51 having two separate components: a steep forward spike with a width about  $\text{ra}^{-2}$ , followed by a much shallower exponential tail. Both slopes show indication of shrinkage. A rather strong slope-mass correlation observ-

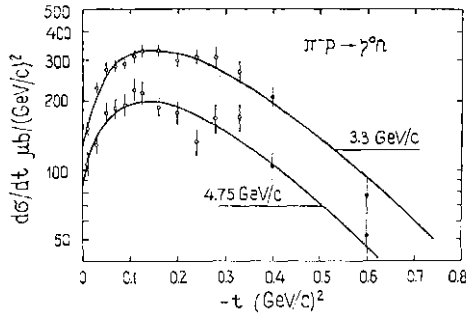


Fig. 50.

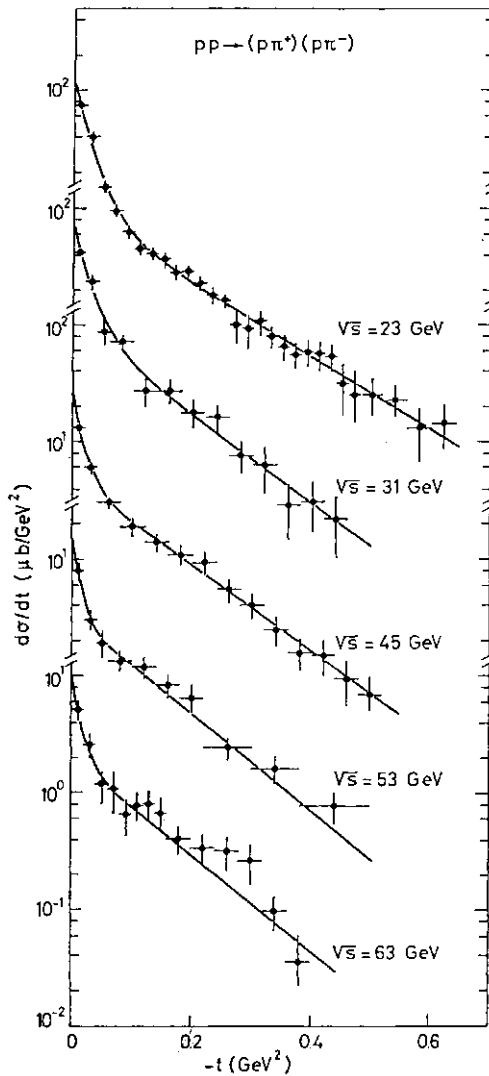


Fig. 51.

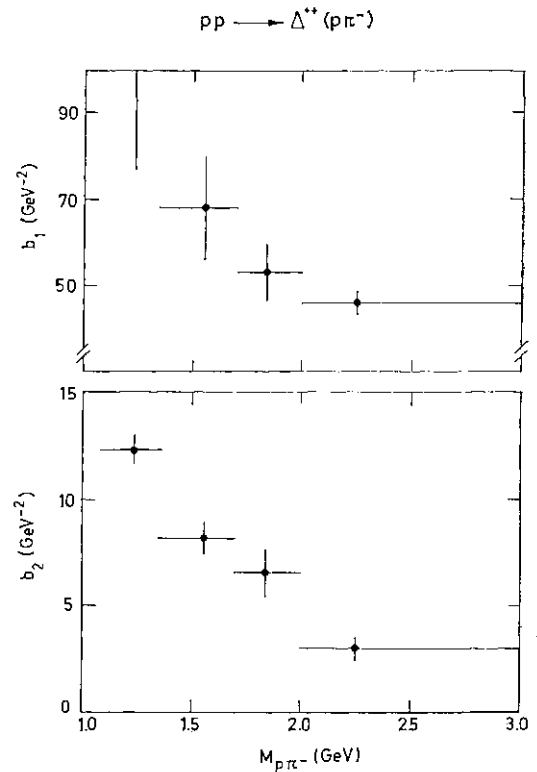


Fig. 52.

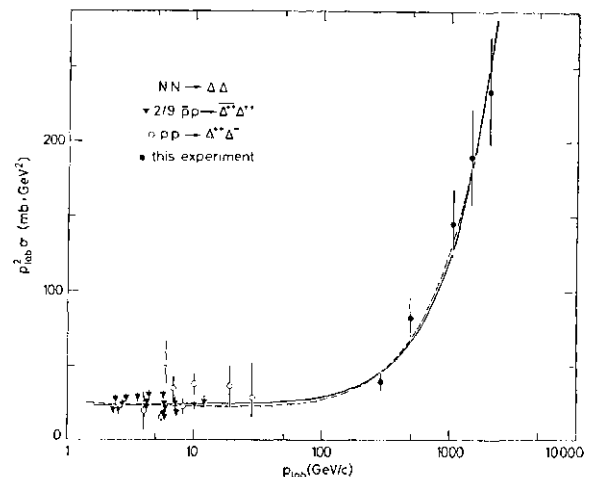


Fig. 53.

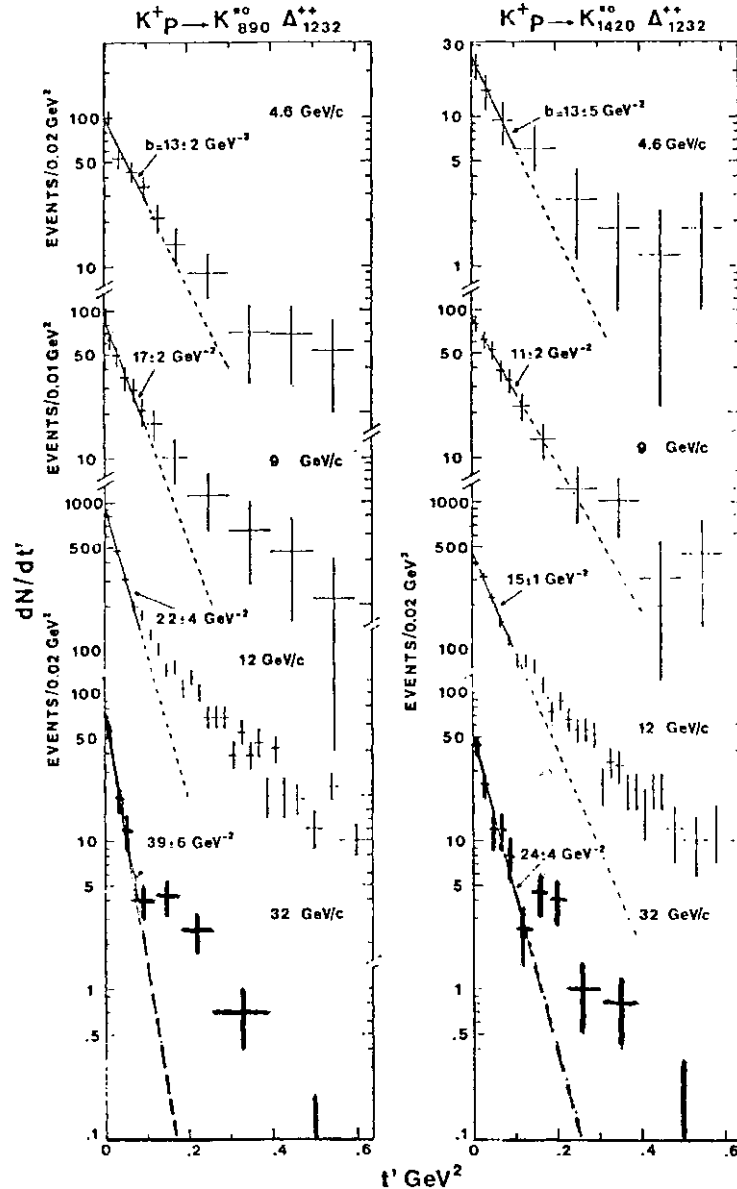


Fig. 54.

ed for  $J^{++}(p7r\sim)$  for both components (Fig. 52) resembles that of DD. The energy dependence displays also two regimes, seen in Fig. 53 for  $J^{++}J^0$  channel. All these pictures are in nice accord with expectation of the Reggeized absorbed pion- $H^0$ ,  $A_2$ ) picture, confirming previous observations.<sup>110111</sup>

The reaction  $7r\sim p\rightarrow 7r\sim 7r\sim n$  has been measured in a high statistics experiment on a transversely polarized proton target at 17.2 GeV/c by CERN-Munich collaboration<sup>92</sup> and unexpectedly large nucléon polarization effects have been observed. A model independent analysis of these data indicates a large lower limit ( $* > 30\%$ ) of the spin non-flip unnatural exchange amplitudes at low  $|t|$  apparently associated with the  $A_2$  meson. Partial wave

analysis performed by the same group<sup>113</sup> shows that the  $A_2$  contribution tends to decrease with the increasing  $ttz$  mass. These 17.2 GeV/c data have been successfully fitted<sup>114</sup> by the Regge model with  $A_2$ ,  $n$  and  $A_1$  meson exchanges plus  $n$ - and  $\Lambda$ -cuts and the predictions of this model turned out to be in excellent agreement with preliminary data on  $7r\sim p\rightarrow 7r\sim 7r\sim n$  at 63 GeV/c.<sup>114</sup>

A plenty of data on meson and baryon resonance production at 8 and 32 GeV/c in  $tt''p$  and  $K^+p$  collisions have been obtained in the bubble chambers studies at SLAC<sup>115</sup> and Serpukhov.<sup>116117</sup> The obtained results are also in agreement with Regge model. As an illustration Fig. 54 shows the shrinkage predictions of Regge of  $d\sigma/dt$  for two particular

channels.<sup>116</sup> The rate of fall at the total cross section of all reactions smoothly extrapolates the lower energy data. The values of exponent in the  $\langle J-PT \rangle$  dependence for  $K^+p$  reactions<sup>116</sup> with  $K^{*+}(890)P$ ,  $K^0J$ ,  $K^{*0}(1420)J^{++}$  final state is  $n \approx 1.65$ , for  $K^{*0}(890)i^{++}$  and for  $K^{*+}(1420)P \ll 1.45$ .

A very nice confirmation of the  $\alpha$ -exchange Regge picture has been also obtained in the K-regeneration experiment by Chicago-Wisconsin-UCSD collaboration<sup>118</sup> from 35 to 130 GeV/c. The results for the value and the phase of the amplitude are shown in Fig. 55. Taking the trajectory and the residue for  $p$  Regge pole from  $\pi^+p$  the authors obtained for  $a(JO)$  the value  $0.494 \pm 0.014$ .

Finally I want to present the results of a high statistics study of the charge exchange reaction  $\pi^-p \rightarrow M^0+n$  which has been carried

out in Sepukhov at 40 GeV/c.<sup>119</sup> Invariant mass distribution for  $\gamma$  pairs shown in Fig. 56 displays a distinct enhancement for  $M \approx 2.85$  GeV/c<sup>2</sup>. The position of the enhancement coincides with the mass value of the resonance  $\rho(2.82 \pm 0.02)$  GeV which has been observed at DESY via the  $J/\psi \rightarrow \rho^* X \gamma$ ,  $X \rightarrow 2\gamma$  decay,<sup>120</sup> and which is considered as the possible lowest pseudo scalar state  $r_{j_c}$  of the hidden charm family (c, c). The authors<sup>119</sup> interpreted the observed events in the X peak as  $\gamma_c$  production

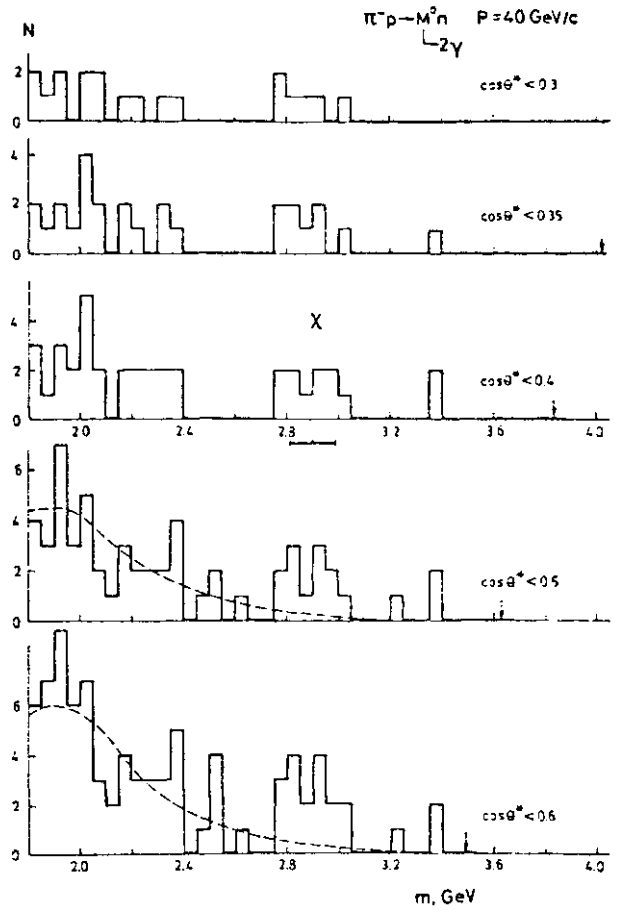


Fig. 56.

and estimated  $M_{\gamma_c} = 2.88 \pm 0.06$  GeV and  $\sigma(\pi^-p \rightarrow X(2.85)n) = 4.10 \cdot 10^{-32} \text{ cm}^2$ , assuming  $2\gamma$  branching ratio as  $5.10 \cdot 10^{-3}$ . This is two orders of magnitude lower than the  $\pi^-p \rightarrow \rho^0 n$  cross section at the same energy.

2. Exchange degeneracy

New data on the line-reversed charge-exchange<sup>121</sup> and hypercharge-exchange<sup>122,125</sup> processes, submitted to this Conference, allow to test the exchange degeneracy. In the simplest picture, the two line-reversed processes, say  $\pi^+p \rightarrow K^+2^+$  and  $K^+p \rightarrow \pi^+2^+$ , should be dominated at high energies and small  $|t|$  by a pair of exchange Reggeons (here  $K^*(890)$  and  $K^{*+}(1420)$ ). If these trajectories and residues are equal (strong exchange degeneracy), we would expect equal cross sections and zero polarization. If only trajectories are degenerate (weak exchange degeneracy), we expect equal cross sections and mirror symmetric polarizations.

A very thorough study of the reactions  $\pi^+p \rightarrow K^+2^+$ ,  $K^+p \rightarrow \pi^+2^+$  (1) has been done at 7 and 10.1 GeV/c in the paper.<sup>122</sup> Figures 57, 58 show the polarization and the value of

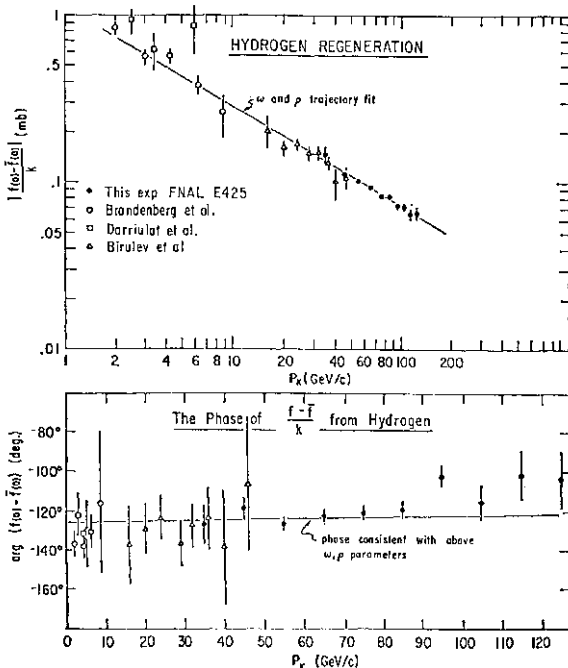


Fig. 55.

J, the ratio of the difference to the sum of  $da/dt$  for both reactions. It is seen that at  $|t| < 0.5$  (GeV/c)<sup>2</sup> and  $P_{L,a,b} = 10.1$  GeV/c the cross sections are near equal and  $P$  is small. In the region  $0.6 < |t| < 0.8$  (GeV/c)<sup>2</sup> the differential cross sections at both momenta show a cross-over. These results suggest that the non exchange-degenerate contribution may be vanishing in this  $t$  region. Beyond the cross-over point the cross sections seem diverging from one another when energy grows.

One can conclude that SED is violated for reactions (1) at all considered  $t$  and  $p$  while WED is well satisfied at the intermediate  $t$

values, but is violated at large  $|t|$ . As to small  $|t|$ , here EXD violating contribution seems to decrease at larger energies. The WED for reactions (1) is also confirmed at 11.6 GeV/c in paper<sup>24</sup> whereas SED is ruled out at 70 GeV/c by observation of nonzero  $2-p^0$  polarization.<sup>126</sup>

At the same time for the line-reversed pair  $TT^*P + K^*Y^{*+}$  (1385),  $K^-p \rightarrow \Lambda^+ \pi^- Y^{*+}$  (1385) (2) at 11.6 GeV/c nearly equal cross sections have been found together with  $P \sim 0$  indicating SED. The cross section measurements [123] at 10 and 16 GeV/c for (1), (2) and  $K^-n \rightarrow \Lambda^+ \pi^- A$ ,  $7\pi^+ p \rightarrow KM$  pair are also consistent with EXD. Whether it is weak or strong is unclear due to the lack of polarization measurements.

In contrast the comparison of the cross sections for the line reversed reactions  $K^-p \rightarrow \Lambda^+ \pi^- A$  (1520) and  $7\pi^+ p \rightarrow KM$  (1520) at 4.2 GeV/c<sup>123</sup> has shown strong violation of EXD.

For charge exchange reactions  $K^-n \rightarrow K^0 p$ ,  $K^-p \rightarrow K^0 n$ , controlled by  $p$  and  $\Lambda$ -exchanges, the nonzero polarization observed at 6 and 12 GeV/c confirms that predictions of SED are not satisfied<sup>121</sup>. The deviations from the mirror symmetry of  $P(K^-n \rightarrow K^0 p)$  and  $i^*(K^-p \rightarrow K^0 n)$  suggest WED violating contributions at these energies. The amplitude analysis of these reactions shows<sup>129a</sup> that the violation of WED corresponds to a lower  $A$ , trajectory by approximately  $Aa \sim 0A$ .

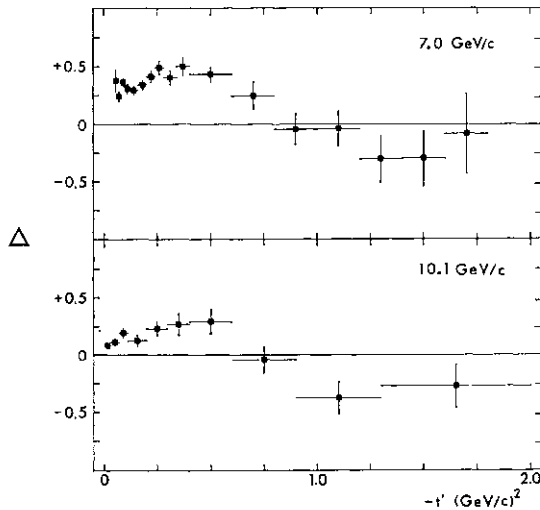


Fig. 57.

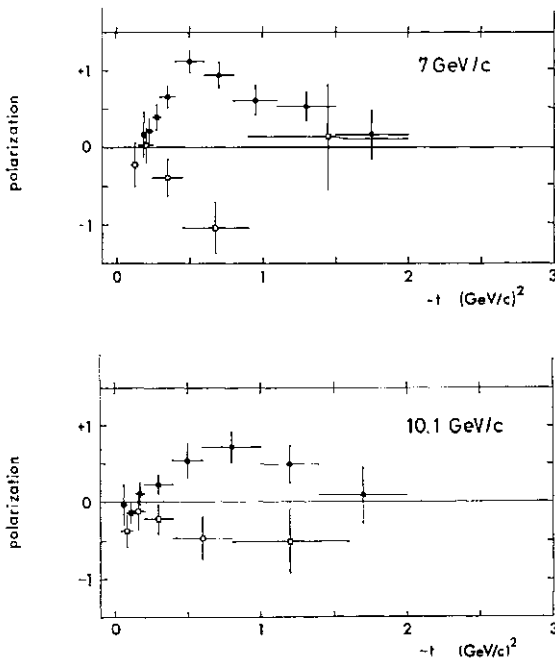


Fig. 58.

### 3. Test of the quark model relations

Hypercharge exchange reactions offer many opportunities to test quark model predictions. The quark model relations applied to the meson vertex in peripheral meson-baryon interactions are known to be well satisfied. New confirmation came from a studies of relations

$$\frac{d\sigma}{dt}(K^-p \rightarrow \omega A) = \frac{d\sigma}{dt}(K^-p \rightarrow \rho A),$$

$$\frac{d\sigma}{dt}(K^-p \rightarrow \phi A) = \frac{d\sigma}{dt}(\rho^- p \rightarrow K^* A) \quad (1)$$

at 4.2, 10 and 16 GeV/c, presented to this Conference.<sup>125,127</sup> On the other hand the  $\eta$ - $\eta'$  involving sum rules

$$\sigma(K^-p \rightarrow \eta Y) + \sigma(K^-p \rightarrow \eta' Y)$$

$$= \sigma(K^-p \rightarrow \pi^0 Y) + \sigma(\pi^- p \rightarrow K^0 Y)$$

are found to be in violent disagreement with data both for  $Y=A$  and  $A^*$  (1520).<sup>123,125</sup> The failure of this relation could be due to the

inadequacy of the standard  $rj-rj'$  mixing scheme assumed in the quark model.

The success of the meson-vertex relations (1) should be contrasted with the serious disagreement observed for quark baryon-vertex relation. The SU(6) sum rules

$$\frac{d\sigma}{dt} (K^-p \rightarrow MA^0) = 3 \left\{ \frac{d\sigma}{dt} (K^-p \rightarrow M^0 \Sigma^0) + \frac{d\sigma}{dt} (K^-p \rightarrow M^0 Y^{0*}(1385)) \right\}$$

has been found<sup>127, 128</sup> to be broken by a constant factor of roughly three for a large variety of reactions. At the same time the relations between polarizations are found to be in good agreement with predictions of the additive quark model. This fact may indicate that the symmetry requirements of SU(6) for baryons should be somehow relaxed. One particular model is discussed in refs. 127, 128. This model<sup>129</sup> assumes that the baryon is a bound state of a (more tightly bound) two-quark system (the diquark) and a third quark. Thus one avoids the necessity of complete three-quark symmetrization by treating the diquark as an "object" distinguishable from the remaining quark. It has been found<sup>128</sup> that the diquark hypothesis is capable of explaining a large number of discrepancies between the symmetric quark model predictions and the experimental data for strangeness- and charge-exchange two-body processes.

Concluding discussion of tests of the quark model, I want to mention also new results on the test of Okubo-Zweig-Iizuka rule in  $\psi$  production. The reaction  $\gamma r \sim p \rightarrow K^+ K^- K^+ K^- n$  has been measured at 22.6 GeV/c<sup>130</sup> and strong  $\psi$  signals in the  $K^+ K^-$  effective mass plots has been detected. The expected OZI rule suppression of the  $\langle f_{10n}$  final state did not observed and the conclusion is that the OZI rule is working poorly in the observed production processes. The same conclusion has been also reached<sup>131</sup> from the study of reaction  $pp \rightarrow \pi^+ \pi^+ \pi^-$  at 0.76 GeV/c.

### Summary and Conclusions

1) Dispersion relations are in good agreement with data.

2) Inelastic diffractive contributions in elastic scattering amplitude on nuclei and perhaps on hadrons are important.

3) GS works at FNAL-SPS and ISR energies.

4) The small and medium  $t$  scattering is very much diffractive.

5) Large  $t$  elastic scattering may probe the constituents.

6) There is a good evidence for dibaryon.

7) Spin effects are important at high  $P$ .

8) Large negative  $P$  in pp at high  $s$  may be connected with  $a_{\text{res}}$  rise.

9)  $A_i$  is still a problem.

10) Factorization works in DD but needs further study.

11) There is a good evidence for double pomeron contribution.

12) Regge+quarks give satisfactory semi-quantitative systematics.

13) EXD is satisfied at high  $s$  HE reactions but not so good in CE reactions.

14) Quark relations are in good agreement with data for meson vertex (except  $rj-rj'$ ) but in disagreement for baryon vertex.

### Acknowledgements

I am very indebted to E. Berger, A. Bujak, T. Kycia, E. Malamud, S. V. Mukhin, E. Nagy, J. Softer, D. L. Soloviev, F. Takasaki, A. Yokosawa, and N. P. Zotov, for useful discussion and help in preparation of this talk. I would like to thank also the Organizing Committee of the Tokyo Conference for hospitality during my stay at Tokyo.

### References

1. T. F. Kycia: Summary of A1, this Conference.
2. A. Yokosawa: Summary of A2, this Conference.
3. A. B. Kaidalov: *Proc. XVIII Int. Conf. High Energy Physics (Tbilisi, 1976)*.
4. K. Winter: *Proc. Eur. Conf. Particle Physics (Budapest, 1977)* vol. 1, p. 55.
5. V. A. Tsarev: *ibid.*, vol. 1, p. 83.
6. V. Simak: *ibid.*, vol. 1, p. 129.
7. A. S' Carroll *et al.*: paper K8, this Conference.
8. R. Nam *et al.*: *Yadernaya Fizika* 26 (1977) 1038.
9. V. D. Apokin *et al.*: paper 940, this Conference; IHEP preprint 78-80.
10. J. P. Burg *et al.*: paper 476, this Conference.
11. D. Gross *et al.*: paper 158, this Conference; *Phys. Rev. Letters* 41 (1978) 217.
12. E. Jenkins *et al.*: private communication from E. Jenkins.
13. Y. Akimov *et al.*: *Phys. Rev. D* 12 (1975) 3399.
14. E. M. Levin *et al.*: *JETP Letters* 23 (1976) 131.
15. G. Goggi *et al.*: paper 1070, this Conference.

16. D. Gross *et al*: paper 1074, this Conference.
17. V. A. Tsarev: *Proc. XVIII Int. Conf. High Energy Physics (Tbilisi, 1976)* p. A M.
18. V. G. Ableev *et al*: paper submitted to *XVIII Int. Conf. High Energy Physics (Tbilisi, 1976)*.
19. P. L. Frabetti *et al*: paper 631, this Conference.
20. M. Fukushima *et al*: paper 455, this Conference.
21. T. T. Chou and C. N. Yang: *Phys. Rev. Letters* 20 (1968) 1213.
22. D. Gross *et al*: paper 1074, this Conference.
23. C. E. De Haven, Jr. *et al*: paper 671, UMHE 78-2.
24. E. Nagy *et al*: paper 36, this Conference.
25. J. Dias de Deus: *Nucl. Phys. B* 59 (1973) 231.
26. J. L. Hartmann *et al*: *Phys. Rev. Letters* 39 (1977) 975; S. Conetti *et al*: *Phys. Rev. Letters* 41 (1978) 924.
27. I. V. Andreev *et al*: *Nucl. Phys. B* 10 (1969) 137.
28. V. P. Sukhatme: *Phys. Letters* 38 (1977) 124.
29. V. A. Matveev, R. M. Muradyan and A. N. Tavkhelidze: *Letters Nuovo Cimento* 7 (1973) 719; S. J. Brodsky, G. R. Farrar, *Phys. Rev. Letters* 31 (1973) 1153.
30. P. J. Crozier and B. R. Webber: *Nucl. Phys. B* 115 (1976) 509.
31. P. J. Crozier and B. R. Webber: Cambridge preprint HEP 77/4.
32. C. Bourrely, J. Soffer and T. T. Wu: preprint CNRS 77/p. 966 (1977).
33. H. Fujisaki and K. Tsukahara: paper 124, this Conference; preprint ROP-78-4 (1978).
34. L. L. Jenkovszky and B. Y. Struminsky: preprint ITP-77-112E (1978).
35. P. D. B. Collins and F. D. Gault: *Phys. Letters* 73 B (1978) 330.
36. G. Altarelli *et al*: *Nucl. Phys. B* 69 (1974) 531.
37. E. M. Levin, Y. N. Shehter: *Proc. IX Leningrad Winter School, 1974*, p. 28; Y. Y. Anixovitch: *ibid.*, p. 106.
38. A. M. Baldin: *Proc. Int. School Theor. Phys. Haukova Dumka, (Kiev, 1976)* p. 469; S. B. Gerasimov: JINR preprints p. 2439 (1965); p. 2619 (1966).
39. S. Wakaisumi: preprint HORD-7809 (1978).
40. S. Wakaisumi and M. Tanimoto: *Phys. Letters* 70 B (1977) 55.
41. A. Bialas *et al*: *Acta Pol.* B8 (1977) 855; A. Bialas *et al*: preprint TPJU-26/77 (1977).
42. A. D. Krisch: *Phys. Letters* 11 (1963) 217.
43. T. Gerrity and A. Pagnamenta: Univ. of Chicago Circle preprint 5/1/77.
44. M. M. Islam and G. W. Heines: Univ. of Connecticut preprint (1977).
45. J. Orear: Cornell preprint CLNS 384 (1978).
46. L. YanHove: *Nucl. Phys. B* 122 (1977) 525; T. Kuroda, T. Uchiyama: Preprint RIEP-326, 327 (1977).
47. T. T. Chou and C. N. Yang: Stony Brook preprint ITP (1977).
48. H. Courant *et al*: paper 464, this Conference.
49. H. Courant *et al*: paper 463, this Conference.
50. I. P. Auer *et al*: paper 447, this Conference.
51. L. P. Auer *et al*: paper 446, this Conference.
52. M. G. Albrow *et al*: *Nucl. Phys. B* 23 (1970) 445.
53. K. Hidaka *et al*: *Phys. Letters* 70 B (1977) 479.
54. W. Grein and P. Kroll: Wuppertal Report, WU B77-6 (1977).
55. N. Hoshisaki: *Progr. theor. Phys.*, 57 (1977) 1099.
56. N. Hoshisaki: paper 520, this Conference.
57. B. A. Shahbazian *et al*: paper 143, this Conference.
58. R. J. Jaffee: *Phys. Rev. Letters* 38 (1977) 195; J. J. De Swart *et al*: THEF-HMY-71.1 (1978); Y. Matveev: *Proc. V Int. Seminar Particle Physics, (Dubna, 1978)*.
59. E. L. Berger, C. Sorensen and A. C. Irving: paper 29, this Conference.
60. R. Stacey: Westfield College preprint (1978).
61. S. L. Kramer *et al*: Argonne Report ANL-HEP-77-74 (1977).
62. R. A. Morrow: *Nuovo Cimento* 43 A (1978) 212.
63. D. Miller *et al*: *Phys. Rev. Letters* 36 (1976) 763; *Phys. Rev. D* 16 (1977) 2016.
64. I. P. Auer *et al*: *Phys. Rev. Letters* 37 (1976) 1727.
65. C. K. Chen: Argonne Report ANL-HEP-77-71, ANL-HEP-77-64 (1977).
66. M. Borghini *et al*: paper 427, this Conference; *Phys. Rev. D* 17 (1978) 24.
67. J. R. O'Fallon *et al*: paper 425, this Conference; *Phys. Rev. Letters* 39 (1977) 733.
68. D. G. Crabb *et al*: paper 423, this Conference.
69. A. Liu *et al*: paper 424, this Conference; *Phys. Letters* 74 B (1978) 273.
70. J. Ranft and G. Ranft: paper 487, this Conference.
71. M. Fukushima *et al*: paper 456, this Conference.
72. M. Fujisaki *et al*: paper 233, this Conference.
73. G. L. Kane and A. Seidl: *Rev. mod. Phys.* 48, (1976) 309.
74. J. Antille *et al*: paper 663, this Conference.
75. G. Fidecaro *et al*: paper 715, this Conference.
76. M. E. Zeller *et al*: paper 683, this Conference.
77. A. Gaidot *et al*: *Phys. Letters* 61 B (1976) 103.
78. L. D. Soloviev and A. V. Shelkachev: paper 190, this Conference.
79. C. Bourrely, *et al*: CERN preprint TH-2471 (1978).
80. M. I. Dzhagarkava *et al*: preprint E2-10971, Dubna (1977).
81. H. R. Gerhold and W. Majerotto: paper 692, this Conference.
82. H. E. Haber and G. L. Kane: *Nucl. Phys. B* 129 (1977) 429.
83. Yu. M. Antipov *et al*: *Nucl. Phys. B* 63 (1973) 141, 153.
84. J. L. Basdevant and E. L. Berger: paper 209,

- this Conference.
85. M. G. Bowler *et al*: Nucl. Phys. B 97 (1975) 227.
  86. R. S. Longacre and R. Aaron: Phys. Rev. Letters 38 (1977) 1509.
  88. R. L. Schult and H. W. Wyld: Phys. Rev. D 16 (1977) 62.
  89. J. Perneger *et al*: Nucl. Phys. B 134 (1978) 436.
  90. Ph. Gavillet *et al*: Phys. Letters 69 B (1977) 119.
  91. A. Ferrar *et al*: Phys. Letters 74 B (1978) 287.
  92. H. Backer *et al*: paper 472, this Conference.
  93. C. Baltay *et al*: Phys. Rev. Letters 39 (1977) 591.
  94. B. Alper *et al*: paper 696, this Conference.
  95. V. A. Tsarev and N. P. Zotov: Fizika tchastits i atomnogo yadra v. 9 (1978) 651.
  96. E. Jenkins *et al*: private communication.
  97. Y. Akimov *et al*: Phys. Rev. Letters 35 (1975) 766.
  98. G. Goggi *et al*: paper 1071, this Conference.
  99. D. Drijard *et al*: paper 274, this Conference.
  100. A. Bialas: Proc. Eur. Conf. High Energy Physics {Budapest, 1977} p. 351.
  101. V. A. Tsarev: Proc. V Int. Seminar Particles Physics {Dubna, 1978}.
  102. L. Van Hove and K. Fialkowski: Nucl. Phys. B 107 (1976) 211; A. Murayama *et al*: paper 519, this Conference.
  103. D. R. O. Morrison: Proc. XV Int. Conf. High Energy Physics {Kiev, 1970}.
  104. A. Bialas and A. Czachov: preprint TP SU-25/77, TPJU-1/78.
  105. V. A. Tsarev: Lebedev Inst, preprint No. 59 (1978).
  106. H. I. Miettinen and J. Pumplin: Fermilab-Pub-78/21-THY (1978).
  107. A. C. Irving and R. T. Worden: Phys. Reports 34 C (1977) 117.
  108. K. Miyake *et al*: paper 544, this Conference.
  109. V. Y. Arkhipov *et al*: paper 140, this Conference.
  110. H. de Kerret *et al*: Phys. Letters 69 B (1977) 372.
  111. G. Goggi *et al*: Phys. Letters 72 B (1977) 265.
  112. G. Goggi *et al*: paper 1072, this Conference.
  113. H. Backer *et al*: paper 473, this Conference.
  114. B. Alper *et al*: paper 693, this Conference.
  115. T. Kitagaki *et al*: paper 548, this Conference.
  116. A. Givernaud *et al*: paper 222, this Conference.
  117. M. Yu. Bogoljubsky *et al*: paper 1054, this Conference.
  118. K. Freundenreich *et al*: paper 898, this Conference.
  119. W. D. Apel *et al*: paper 246, this Conference.
  120. W. Braunschweig *et al*: Phys. Letters 67 B (1977) 243.
  121. M. Fujisaki *et al*: paper 233, this Conference.
  122. A. Berglund *et al*: paper 9, this Conference.
  123. S. J. M. Barlag *et al*: paper 396, this Conference.
  124. J. Ballam *et al*: paper 957, this Conference.
  125. Aachen-Berlin-Bonn-CERN-Cracow- London-Vienna Collaboration: paper 276, this Conference.
  126. M. W. Arenton *et al*: paper 1023, this Conference.
  127. J. C. Kluyver *et al*: paper 397, this Conference.
  128. M. Zralek *et al*: paper 336, this Conference.
  129. D. B. Lihtenberg and L. J. Tassie, Phys. Rev. 155 (1967) 1601.
  - 129a. M. Fujisaki *et al*: paper 234, this Conference.
  130. A. Etkin *et al*: paper 649, this Conference.
  131. A.M. Cooper *et al*: paper 864, this Conference.



## P1b Hadron-Hadron Reactions, High Multiplicity

R. DLEBOLD

Argonne National Laboratory, Argonne, Illinois 60439

### §1. Introduction

This talk covers results presented in four parallel sessions:

	Contributed Papers
A3 —High Energy Hadron Reactions, High Multiplicity	75
B7—Charm Searches and Related Topics	29
BIO—Ultrahigh Energy Events and Exotic Phenomena (Cosmic Rays)	18
B11—Nuclear Effects in High Energy Collisions and Related Topics	58 180

It thus has a broader range of topics than the title would suggest. As can be seen by the number of contributed papers, these fields are quite active; in particular, many results were contributed on high multiplicity or inclusive type studies and on reactions taking place off nuclei.

Although these topics have generally been studied for several years now, many of the contributions add valuable data at new energies or for different beam particles, and are useful in making compilations and detailed fits to the data. Such a multitude of numerical results is, however, somewhat difficult to cover adequately in a rapporteur talk. Fortunately, many of these subjects were covered in detail by the mini-rapporteurs in the parallel sessions. In any case, with 180 papers, roughly 16% of the total contributed to the Conference, I cannot possibly cover all the results and I apologize to those whose hard work has not been adequately covered.

### §2. Two and Three Body Correlations

Kenney *et al* (paper 496) have looked at TT<sup>+</sup>P reactions at several energies in bubble chambers, including 30,000 events at 360 GeV/c. They have analyzed the dependence of the two-body correlation function

$$R = \frac{\rho_2(y_1, y_2)}{\rho_1(y_1)\rho_1(y_2)} - 1, \quad (1)$$

$$\rho_1(y) = \frac{1}{\sigma} \frac{d\sigma}{dy}, \quad (2)$$

$$\rho_2(y_1, y_2) = \frac{1}{\sigma} \frac{d^2\sigma}{dy_1 dy_2}, \quad (3)$$

on multiplicity and incident momentum.

The 360-GeV/c data are combined with results at 18.5, 100, and 200 GeV/c to evaluate cluster parameters. Some of the two-body correlations for unlike charged particles near  $71 = \Delta^2 = 0$  are shown in Fig. 1, both as a function of multiplicity and as a function of energy. Note that the authors use only  $>8$  prongs in order to avoid diffractive effects. In the Berger cluster model<sup>1</sup>

$$R_n^{+-}(0, 0) = \frac{\langle k \rangle^{+-}}{n} \left[ \frac{\ln s}{2\sqrt{\pi\delta}} - 1 \right] \quad (4)$$

where  $\langle k \rangle^{+-}$  is the numbers of charged particles per cluster and  $\delta$  is the correlation length,  $\langle j_i - j_i \rangle_{rms}$ . When plotted using the scales shown in Fig. 1, the model expects straight lines, as observed. Note that unlike most experiments, with results at only one energy, these authors can use the various energies to give a consistency check on the method. After checking the consistency, they simultaneously fit the dependence on multiplicity and energy and find that on average there are  $1.60 \pm 0.12$  charged particles per cluster and  $a = 0.99 \pm 0.03$ .

With the present high statistics available from bubble chamber experiments the same set of authors (paper 497) were able to observe three-body dynamical correlations. For this purpose they use the definition

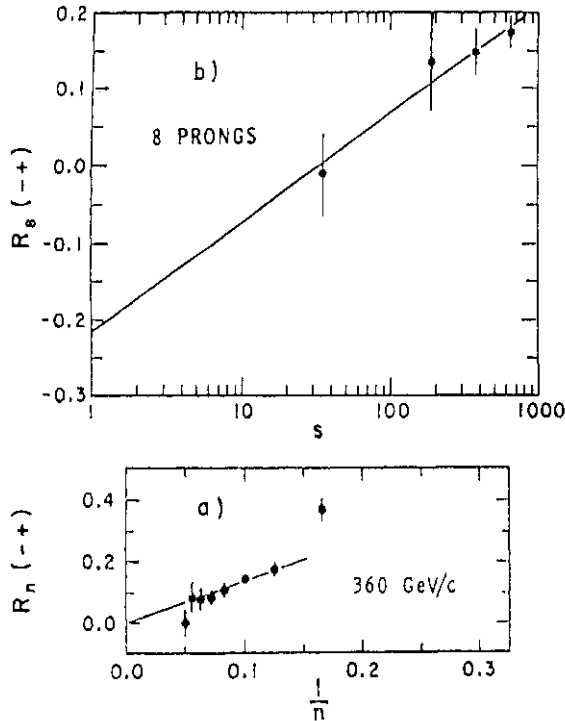


Fig. 1. Energy and multiplicity dependence of the two body correlation functions for unlike-charge pairs produced in TT-P reactions at  $y_1=y_2=0$  (Kenney *et al.* paper 496).

$$R_3 = \frac{(123)_{--} - (12)(3)_{--} - (23)(1)_{--} - (31)(2)_{--} + 2(1)(2)(3)_{--}}{(1)(2)(3)}, \quad (5)$$

where

$$(123)_{--} \equiv \rho_3(y_1, y_2, y_3) = \frac{1}{\sigma} \frac{d^3\sigma}{dy_1 dy_2 dy_3}, \text{ etc.} \quad (6)$$

Note that the effects coming from two-body correlations are explicitly removed. Figure 2 shows the results, both for all three particles having negative charge and for the  $-|-$  combination. As expected, they do not observe any correlation between three negatively charged particles. They do, however, see a significant effect near  $y_1 = y_2 = y_3 = 0$  for the  $-|+$  combination; this effect is apparently narrower than the two-body correlations, with a width of perhaps  $\pm 1/2$  unit of rapidity. The three-body correlation observed is considerably smaller than found for the two body case:

	$R_2(0, 0)$		$R_3(0, 0, 0)$
$+ -$	$0.69 \pm 0.05$	$- + -$	$0.26 \pm 0.07$
$--$	$0.23 \pm 0.07$	$---$	$0.01 \pm 0.06$

A smaller three-body correlation would, of course, be expected if the average cluster does

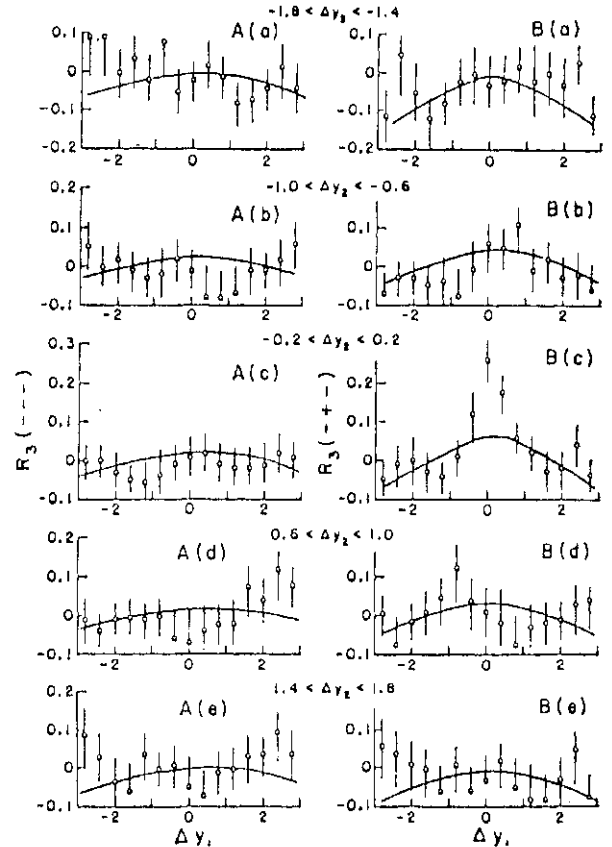


Fig. 2. Dynamical three-body correlation for  $7r-p$  reactions at 200 GeV/c as a function of  $Jy' = y_i = y_j$ , for various intervals of  $\Delta y_2 = y_2$ ,  $-J > 3$ . Values for the  $(---)$  charge combination are shown on the left, and for the  $(-+-)$  on the right. The smooth curves are from a Monte Carlo simulation which includes no explicit short-range correlations (Kenney *et al.* paper 497).

indeed have only 1.6 charged particles.

We next consider the results of a high statistics ISR experiment carried out in the split field magnet at  $\sqrt{s} = 52$  GeV by the CCHK collaboration (Drijard *et al.* paper 273). To avoid diffractive effects they cut on  $-7$  reconstructed tracks, leaving a sample of  $\sim 200,000$  events. Figure 3 shows the two-body correlation function, with positive correlations for  $y_2 = 0$  and 2, but a negative correlation out near the kinematic limit,  $y_2 = -4$ . Qualitatively this effect is well fit by various cluster models, the results of the independent emission of charged clusters being shown in the figure. They find a correlation length very similar to that of the **previous experiment**, an average of 1.8 charged particles per cluster, and one cluster per unit rapidity.

Figure 4 shows the change in charge density at  $y_i$  when the trigger particle at  $y_2$  of negative

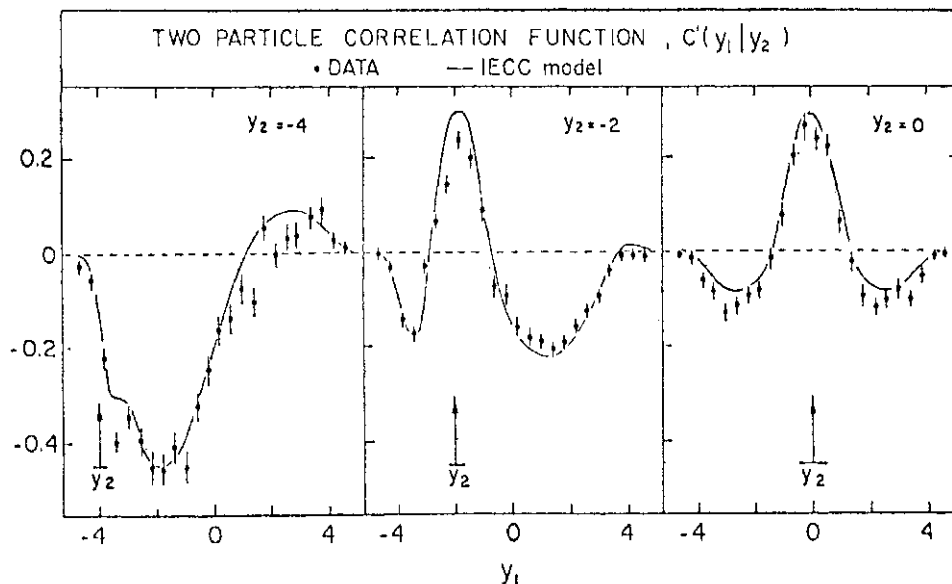


Fig. 3. Two body correlation function in non-diffractive ( $n_{ch} > 7$ ) pp collisions at  $\sqrt{s} = 52.5$  GeV for different values of  $y_2$ . The lines are the predictions of a cluster model with independent emission of charged clusters (Drijard *et al.* paper 273).

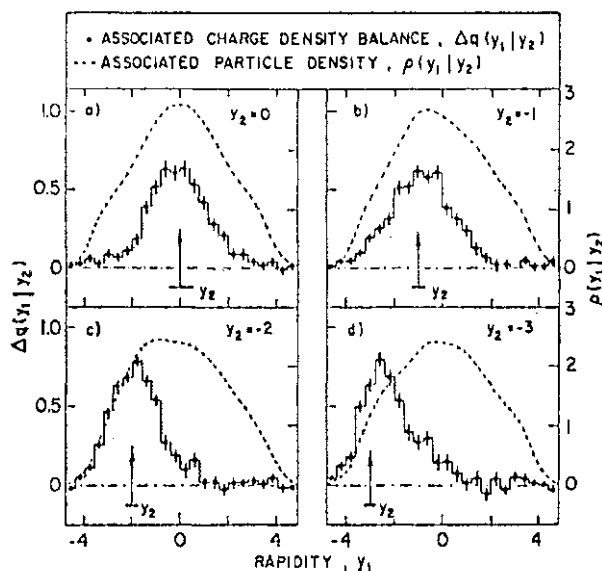


Fig. 4. Associated charge density balance (Drijard *et al.* paper 273).

charge is replaced by one of positive charge. The data show a local compensation of charge, much narrower than the associated particle density distribution; this allows a partial discrimination between the various models considered by these authors.

They have also looked at the distribution of transverse momentum compensation, and find that unlike charge compensation,  $p_T$  is compensated globally in agreement with both their uncorrelated jet model and correlated cluster link model. The authors tend to favor the latter model which can be used to obtain<sup>2</sup>

$$\alpha'_p(0) = 0.26/\text{GeV}^2 \quad (7)$$

for the slope of the Pomeron trajectory. They also obtain an average mass for the clusters of  $1.3$  GeV, with an average transverse momentum of  $(0.65 \pm 0.10)$  GeV/c, comparable to that observed for meson resonances in this mass region.<sup>3</sup>

Other methods have also been used to define clusters in attempts to understand multi-particle reactions. Pless *et al.* (paper 551) use charge distributions to define zones; they find that most of the multi-particle events can be described as having two leading particles or clusters, plus a central isotropically decaying fireball. An alternate method finds clusters of charged particles using a nearest neighbor technique.<sup>4</sup> This latter technique yields a  $p_T$  distribution for clusters of charged particles which matches on rather well to the jet cross sections found by Bromberg *et al.* at larger  $PT$ .

### §3. Second Order (Bose-Einstein) Interference

A few years ago Kopylov, Podgoretsky and Cocconi<sup>6</sup> suggested the use of like-particle (*e.g.*,  $\pi^+\pi^+$ ) correlations to estimate the dimensions and lifetime of emission (not interaction) regions. This is similar to a method used over the past 20 years by radioastronomers and has been used in other fields as well.

In principle, this technique is of particular interest because one can examine the emis-

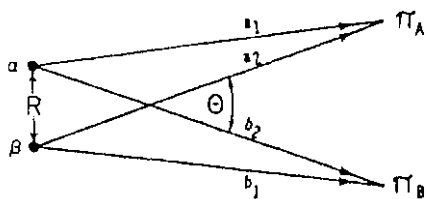


Fig. 5. Sketch showing two identical pions combing from two sources; used to derive eq. 8.

sion regions for the various classes of events such as high —  $p_T$  events, events having  $p'$ 's, or as a function of multiplicity.

For example, consider the two  $\pi$ 's ( $K_1$  and  $\pi_2$ ) coming from points  $a$  and  $b$  in Fig. 5. Since we can't tell which source gave which  $\pi$ , we must add the amplitudes:

$$|\text{Amp}|^2 = \left| e^{ika_1} e^{ikb_1} + e^{ika_2} e^{ikb_2} \right|^2 = 2(1 + \cos Rk\theta) \quad (8)$$

Integrating these points over a sphere yields the relation

$$\frac{N_{\pi^+\pi^+}}{N_{\pi^+\pi^-}} = C \left[ 1 + \lambda \frac{(2J_1(Rq_t)/(Rq_t)^2)}{1 + (q_0\tau)^2} \right] \quad (9)$$

where

$$q = \text{component of } \mathbf{P}_1 - \mathbf{p}_2 \text{ transverse to } \mathbf{P}_1 + \mathbf{P}_2$$

$$q_0 = E_1 - E_2 \quad (\text{in CM system}).$$

The coefficient  $\lambda$  allows for the fact that not all of the  $\pi$ 's may be able to interfere with one another, and the normalization on the left-hand side neglects possible resonant effects in the low-mass  $\pi^+\pi^-$  system.

Three sets of bubble chamber data are shown in Fig. 6 (Deutschmann *et al.*) together with fits to eq. 9. The data are well fit by this form, with the enhancement being largest near  $q_0 \approx 0$  as expected. These authors find that the radius of the emission region is independent of the reaction, and also, at least for the high-statistics  $\pi^+\pi^-$  data, independent of multiplicity,  $R = (1.85 \pm 0.15) f$ . They also find the lifetime parameter to be  $c\tau = (1.2 \pm 0.3) f$ . The interference is strongest for the  $pp$  case with  $X$  close to unity, while it is only half this value for the higher energy  $\pi^+$  and  $K^-$  beams.

These values are compared with results from other experiments in Fig. 7, which includes several new results presented to this Conference. While there is considerable spread in the results from the different experiments, the radii of Deutschmann *et al* appear larger than found in most of the previous experiments. They have reanalyzed some of the previous data, in particular allowing  $\lambda$  to vary

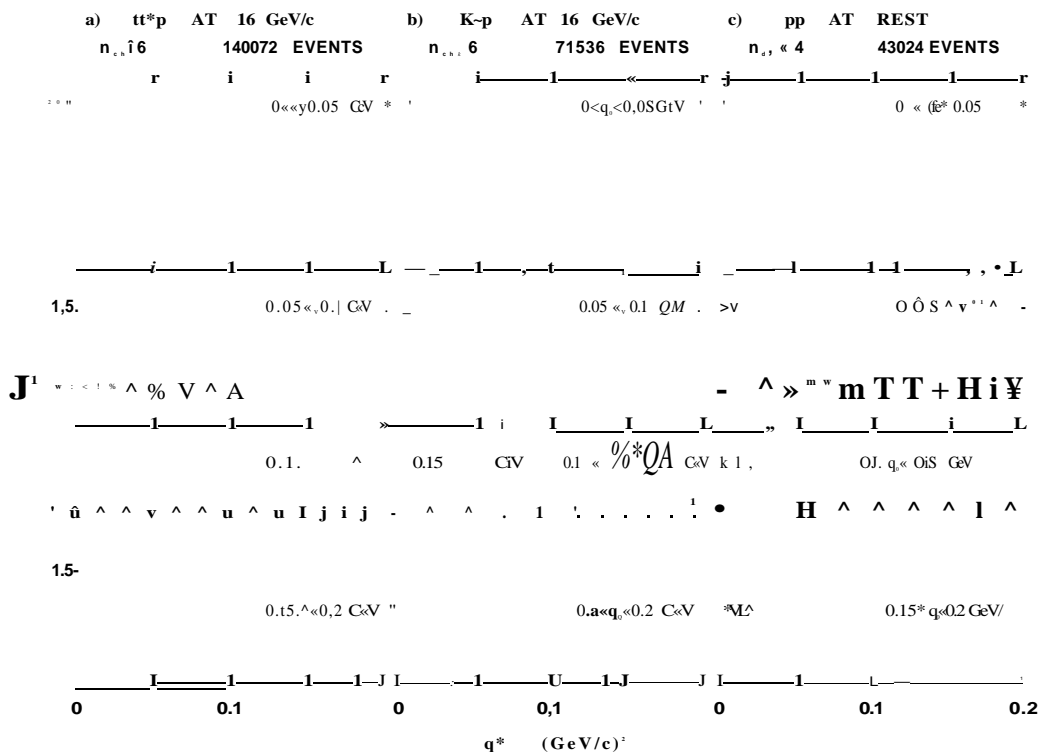


Fig. 6. Normalized ratio of the numbers of pion pairs of like and unlike charges, fit to eq. 9. From ref. 7.

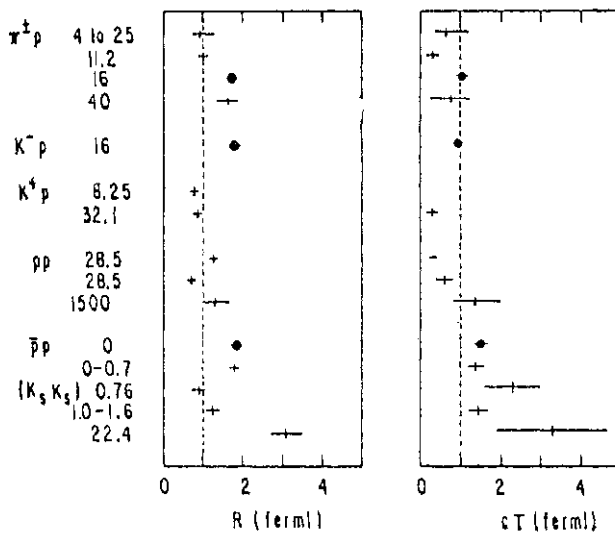


Fig. 7. Compilation of results on the source parameters obtained from Bose-Einstein interference fits. The circles are from Deutschmann *et al.* (réf. 7); see réf. 8 for the other points.

rather than fixing it to unity, and find results closer to their own than to the values given by the original authors. It thus appears that the variation from reaction to reaction, or energy to energy; shown in the figure more likely comes from systematic effects, rather than from a true variation of the emission region. As additional high statistics results become available, it will be of interest to analyze all experiments using the same method in order to search for true variations.

#### §4. Meson Resonance Production

This subject is closely related to that of clusters; indeed some of the clustering effects discussed previously must come from resonance production. There has been a controversy, however, as to whether resonances are a dominant or negligible effect in the cluster analyses.

The average number of  $p^\circ$ 's per produced charged pion pair is shown in Fig. 8, taken from a compilation by Kenney *et al.* (paper 500); they find that at high energy about 12% of the produced charged pions come from  $p^\circ$ - $\pi^+ \pi^-$ . It should be noted that the  $p^\circ$  signal is difficult to estimate due to the large combinatorial background. One might expect similar contributions from  $p^\pm$  and from  $\omega$  decays; further, the decays of  $\gamma$ ,  $K^*$ ,  $N^*$ , and so on, will also contribute and thus the fraction of charged pions coming from resonant production and decay is probably 3 to 6 times

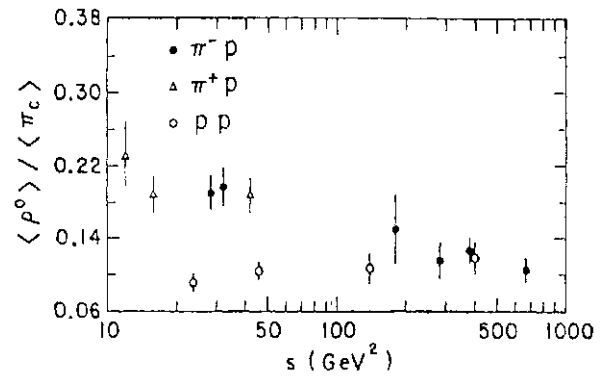


Fig. 8. Compilation of the average number of  $p^\circ$ 's per produced pion pair as a function of energy for  $7T^+ p$  and  $pp$  interactions (Kenney *et al.* paper 500).

larger than the 12% from  $p^\circ$ 's alone. In fact, Dao *et al.* (paper 495) estimate that resonances can account for 80% of all charged pions in their  $pp$  data at 300 GeV/c. This can be compared with a recent estimate<sup>9</sup> that (10 to 30)% of the pions produced in 16-GeV/c  $7T^+ p$  interactions are "direct" and do not come from resonance decay.

At Fermilab-SPS energies only a small percentage of the  $p^\circ$ 's come from diffraction dissociation (this process is only 10 or 20% of the total cross section and the multiplicity is low). Thus, the various estimates of 50 to 80% of the charged pions coming from resonance production must still be approximately valid for the high multiplicity events used to study clustering in the central region. This means that a majority of the so-called clusters are in fact old fashioned resonances, in which case "clusters" may not be the most appropriate language.

A compilation of the energy dependence for inclusive  $p^\circ$ ,  $K^*$ , and  $K_s$  production is shown in Fig. 9 (Kichimi *et al.*, paper 545); the figure shows that the inclusive production of  $p^\circ$ ,  $K_s$ , and  $K^*$  all scale together with energy, in approximately the ratio 1/0.6/0.3. The  $K^*$  rises somewhat faster at lower energy and eventually becomes equal to  $K_s$  above  $\sim 50$  GeV. These authors find that approximately two thirds of the  $K_s$  already come from  $K_s^*$  and  $K_{f_{420}}$ , similar to the  $TT^*$  case where a large fraction also appears to come resonant production and decay.

Analyses of inclusive pion or kaon data is thus not at all straightforward. The contributions from resonance production and decay distort both the  $x$  distributions<sup>9,10</sup> and  $p_T$

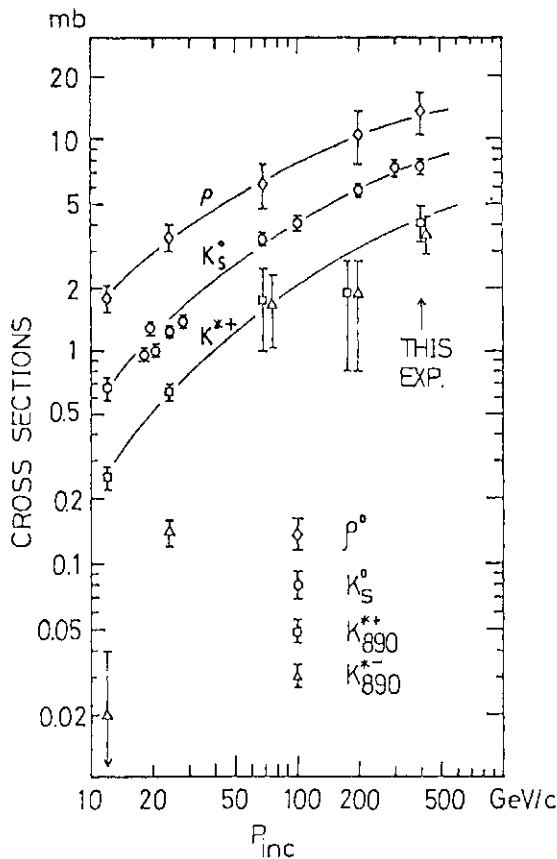


Fig. 9. Compilation of the inclusive cross sections for  $p^0$ ,  $K$ , and  $K^{*}(890)$  production in  $pp$  interactions (Kichimi *et al.* paper 545).

distributions,<sup>11</sup> and can give misleading results if not taken into account in analyses such as triple Regge or parton fits. The  $x$  distortion caused by this effect depends on the process; one of the largest effects is that coming from  $p^0$  decay contributing to  $7r^+ \rightarrow 7r^-$ .

We turn now briefly to the production of meson systems via diffractive dissociation. As is well known, this process gives a strong peak in the effective mass distribution near threshold. At larger masses the process becomes more difficult to identify, but Morrison *et al.* (paper 97) have developed a technique to identify the diffractive component using the energy dependence of the charge-exchange

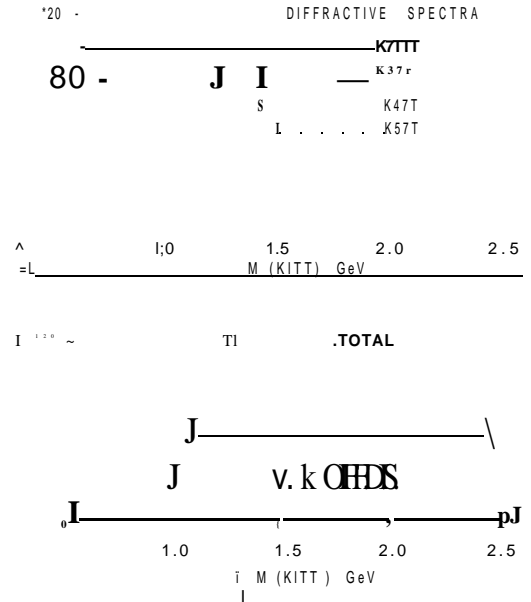


Fig. 10. The diffractive spectra for kaon diffractive dissociation: a) for different multiplicities; b) compared with the total spectrum (Morrison *et al.* paper 97).

states to subtract off the non-diffractive part of the  $\pi^+$  states. Using this method they obtain a substantial diffractive component, even at the higher masses as shown in Fig. 10. For example, from their  $K \sim p$  data at 10 and 16 GeV/c they find that at a  $K^*$  mass of 2.5 GeV  $\sim 1/2$  of the events come from diffractive dissociation. They obtain an integrated cross section  $\sim 1.2 \text{ mb}$  ( $\sim 5\%$  of  $a_{tot}$ ) each for diffractive  $K^*$  and diffractive  $N^*$  production.

### §5. Triple Regge Phenomenology

Although several papers contributed to the Conference included triple Regge fits, I will have to limit myself to the recent experiment of Barnes *et al.* (paper 1065 and ref. 12) on  $7T^0$  and  $-q$  production by 100-GeV/c  $TT^*$  beams. Not only do they have very high statistics, but they also have an interesting

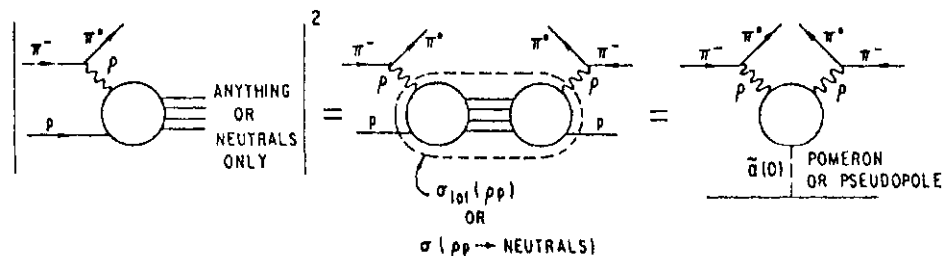


Fig. 11. Outline of triple Regge theory for  $7r^+p \rightarrow 7r^+X$  full inclusive and for neutrals only.

new twist to add to the game: using the same apparatus they did two experiments, first for the usual full-inclusive distribution and, secondly, for the zero-prong, neutrals-only final state. The theoretical models for these two cases are outlined in Fig. 11. For the full inclusive case one has the usual dominant

term, Pomeron exchange at  $l=0$  with  $a(0)=\lambda$ . For the neutral-only final state they introduce the concept of a pseudopole with trajectory at  $\lambda=0$  determined by the energy dependence of the zero-prong cross section (from which they estimate a value of  $d(0)=-0.08\pm 0.2$ ). For each case they can then obtain the  $t$  depen-

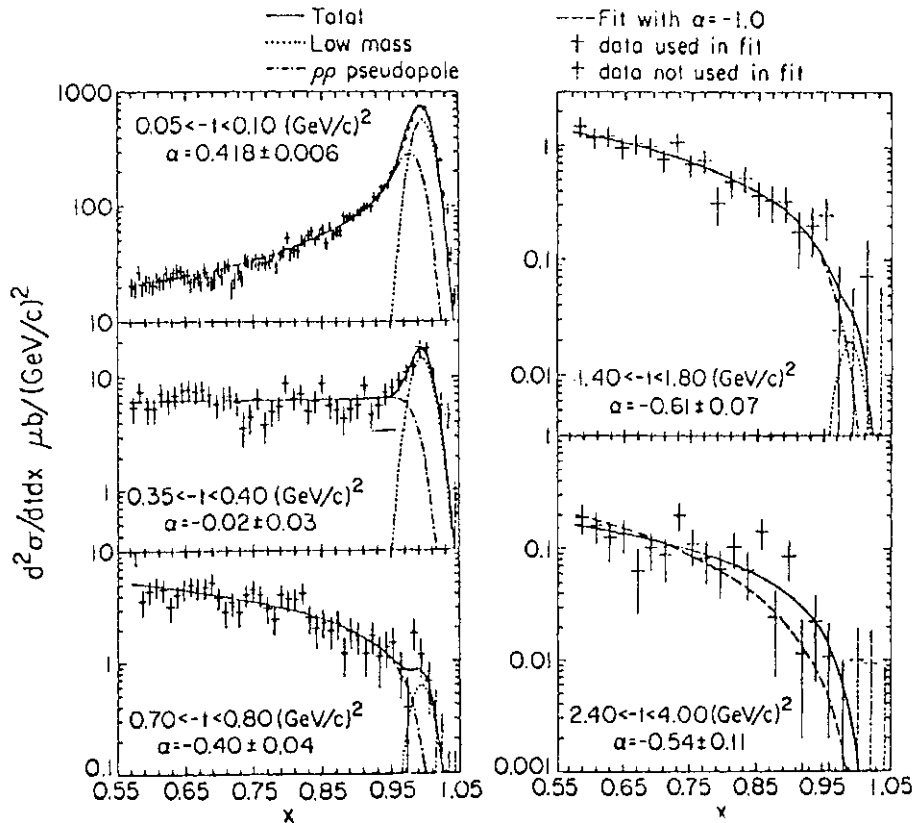


Fig. 12. The  $x$  dependence for  $n$   $p \rightarrow 7\pi^+$  plus neutrals only for different  $t$  bins, together with the triple Regge fits (ref. 12).

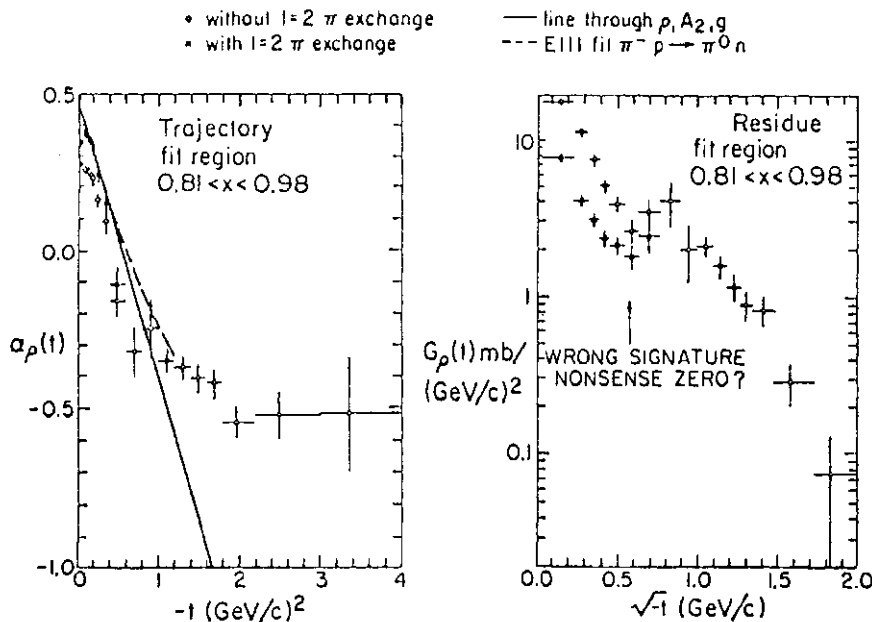


Fig. 13. The  $p$  trajectory and residue function found by fits to the full-inclusive  $n^+$  data (Barnes *et al.* paper 1065), compared with the  $p$  trajectory from the exclusive data (ref. 13).

dence of the exchanged trajectory,  $p(A_2)$  for  $n\backslash rj$  production, using the form

$$\frac{d^2\sigma}{dt dx} = f(t) \frac{(1-x)^{\tilde{\alpha}(0)-2\alpha} \rho^{(t)}}{s^{1-\tilde{\alpha}(0)}} + \text{low-mass contribution from exclusive states} \quad (10)$$

A sample of the neutral-only inclusive data is shown in Fig. 12 together with the fit. Note that the shape of the spectrum does in fact change with  $t$ , as expected in the triple Regge model from the variation in  $a(t)$  with momentum transfer. The results for the  $\text{TT}^{\text{full-inclusive}}$  case are shown in Fig. 13. The  $p$  trajectory is in qualitative agreement with that obtained<sup>13</sup> from the exclusive channel  $\pi^+p \rightarrow \pi^0 n$ , while the  $p$  residue shows some structure in the neighborhood of  $-t=0.5 \text{ GeV}^2$ , the exact nature of the structure depending somewhat on the details of the fit.

Trajectories from the fits to the neutrals-only data are shown in Fig. 14.

The results of this work can be summarized as follows:

1. There is good qualitative agreement for the  $p^*$  and  $A_2$  trajectories obtained from the three final states:
  - a) exclusive-neutron using energy dependence;
  - b) full-inclusive using spectrum shape;
  - c) neutrals-only using a different spectrum shape.
2. There are some systematic uncertainties from the value of  $a(0)$  used for the pseudopole and from the details of the fit (such as the  $x$  range used).
3. The trajectories appear to level off for momentum transfers  $> 1.5 \text{ GeV}^2$  at  $a \sim -0.6$ . This latter value can be compared with the constituent interchange model

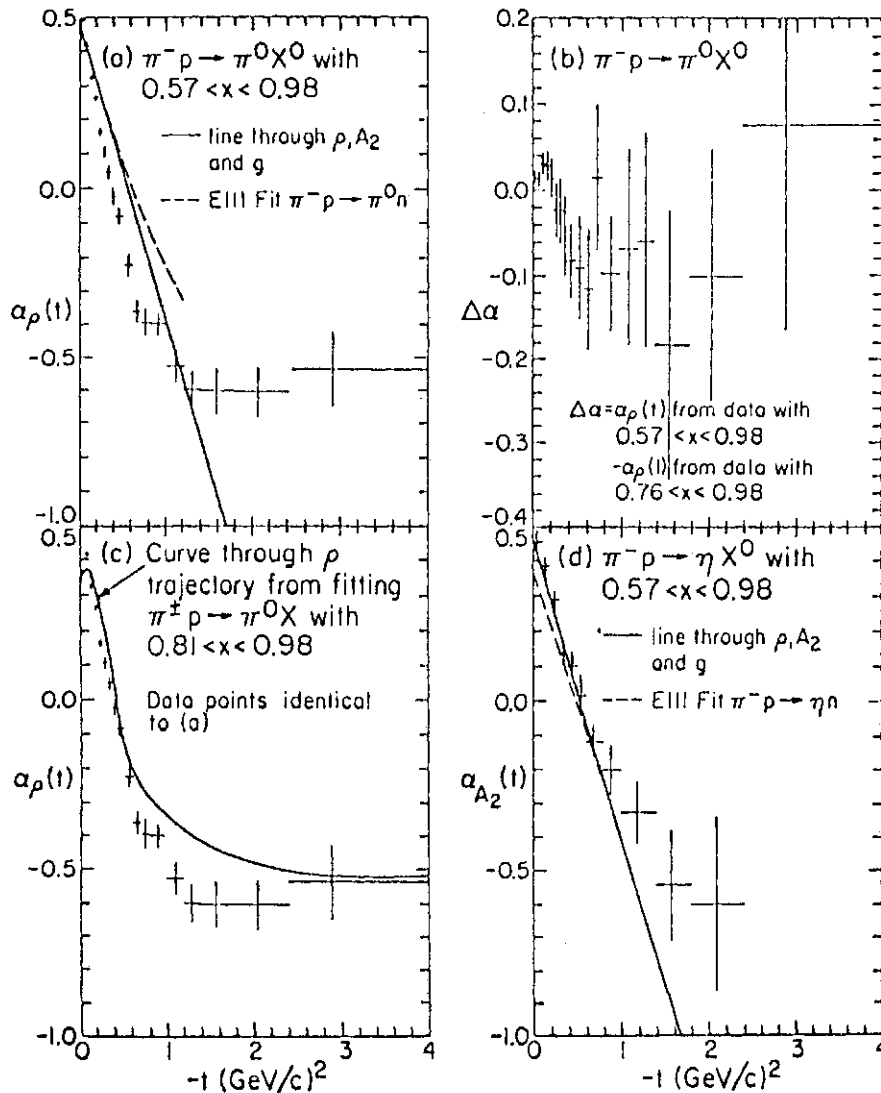


Fig. 14. The  $p$  and  $A_2$  trajectories determined by fits to the neutrals-only data (ref. 13).



- prediction of  $-1$ .
4. The  $\Lambda$ -exchange residues show structure (or a dip) near  $-t=0.5 \text{ GeV}^2$ , whereas the  $A_1$  residues are smooth in this region. The structure is presumably due to the wrong signature nonsense zero at  $a_p=0$ .
  5. From a detailed examination of their fits, the authors conclude that the simple Regge theory appears to work over a wider range of  $x$  for the neutrals-only final state as compared to the full-inclusive reactions. They suggest that this may be due to the weak coupling nature of the neutral final state and the corresponding pseudopole.

**§6. Parton Ideas for Leading Particles**

We turn now to a possible connection between low and high  $p_T$  phenomena. There has been a great deal of activity in this area during the last year or two, especially in explaining the momentum (or  $x$ ) distribution of fast particles at low  $p_T$  with parton structure functions. The simple idea of fragmentation, sketched in Fig. 15a, does not work well; it gives too rapid a decrease in cross-section as  $x$  increases. The trouble is that momentum is lost at each of two stages: first, the single quark carries off only part of the initial pion momentum; and, secondly, it then fragments into the leading particle plus other particles which compete for momentum.

There are several ways to fix this; Andersson *et al.*<sup>14c</sup> have suggested that the quark which

interacts with the target is a wee quark with little momentum, leaving nearly the full energy for the fragmenting quark. Data presented to this Conference by the Fermilab Single Arm Spectrometer Group (Cutts *et al.*, paper 413), however, show that while this prediction gives approximately the correct shape for the  $x$  distribution, it generally does not have the correct normalization.

A more popular scheme is the recombination model sketched in Fig. 15b; this model assumes that the leading quark somehow dresses itself, or recombines, with a soft ( $x_2 \sim 0$ ) quark from the sea. This idea goes back several years<sup>15</sup> but received renewed interest from the observation of Ochs<sup>16</sup> that the ratio of  $7r^+$  to  $7T \sim$  inclusive production by protons follows very closely the ratio  $u(x)/d(x)$ , where  $u$  and  $d$  are the quark structure functions found in deep inelastic lepton scattering. This idea has also been used successfully by Eisenberg *et al.* (paper 768) to fit the  $rc^+jn^-$  ratio from similar reactions.

While Ochs neglected the momentum  $x_2$  carried by the quark picked up from the sea, Das and Hwa<sup>17</sup> developed a model in which this  $x_2$  distribution is folded in using a somewhat arbitrary recipe. This model has been used to estimate the sea-quark distributions

$$f_{\text{sea quarks}} \propto (1-x)^{n_q} \tag{11}$$

Examples of such fits obtained by Duke and Taylor<sup>18</sup> are shown in Fig. 16. By fitting simultaneously to several particle ratios, they obtained both the shape and normalization of the sea-quark distributions. Similar fits have

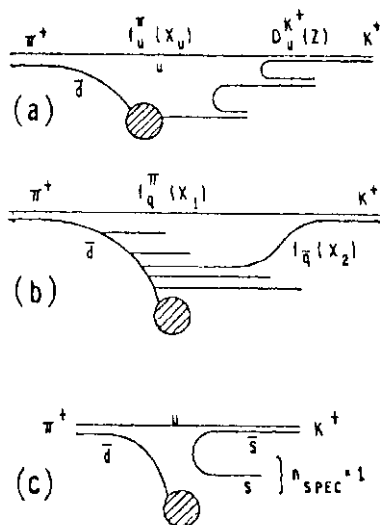


Fig. 15. Sketches of parton models used to describe low- $p_T$  leading particles: a) fragmentation; b) recombination; c) spectator.

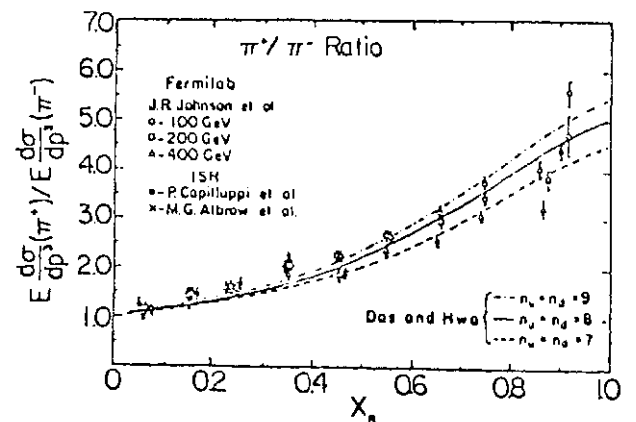


Fig. 16. Das-Hwa type fits to the  $(p \rightarrow 7r^+) / (p \rightarrow 7r^-)$  ratio using several choices for the exponent in eq. 11 (ref. 18).

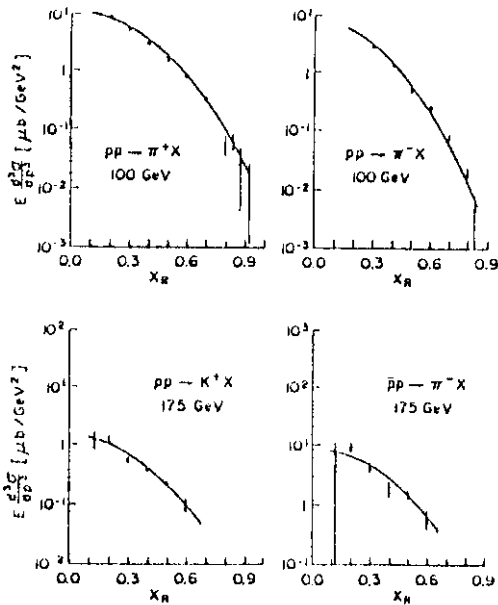


Fig. 17. Das-Hwa type fits to the invariant cross sections at  $p_T=0.3$  GeV/c (D. Cutts *et al*, paper 413).

also been obtained by the Fermilab Single Arm Spectrometer Group, Cutts *et al.* (paper 413), as shown in Fig. 17. Again, reasonable fits are obtained to the data by adjusting the parameters of the sea-quark distributions. The exponents in eq. 11 obtained for the sea-quark distributions from the two Fermilab experiments are as follows

	Cutts	Duke-Taylor
$\bar{u}$	$7.5 \pm 0.6$	} $8 \pm 1$
$\bar{d}$	$12.8 \pm 2.3$	
$\bar{s}$	$6.5 \pm 0.2$	$6 \pm 2$

There is good agreement between the two analyses, and the results are also in qualitative agreement with those obtained from dilepton production.<sup>19</sup>

Such fits have also been made<sup>20</sup> to the ISR data of the CHLM collaboration,<sup>21</sup> as shown

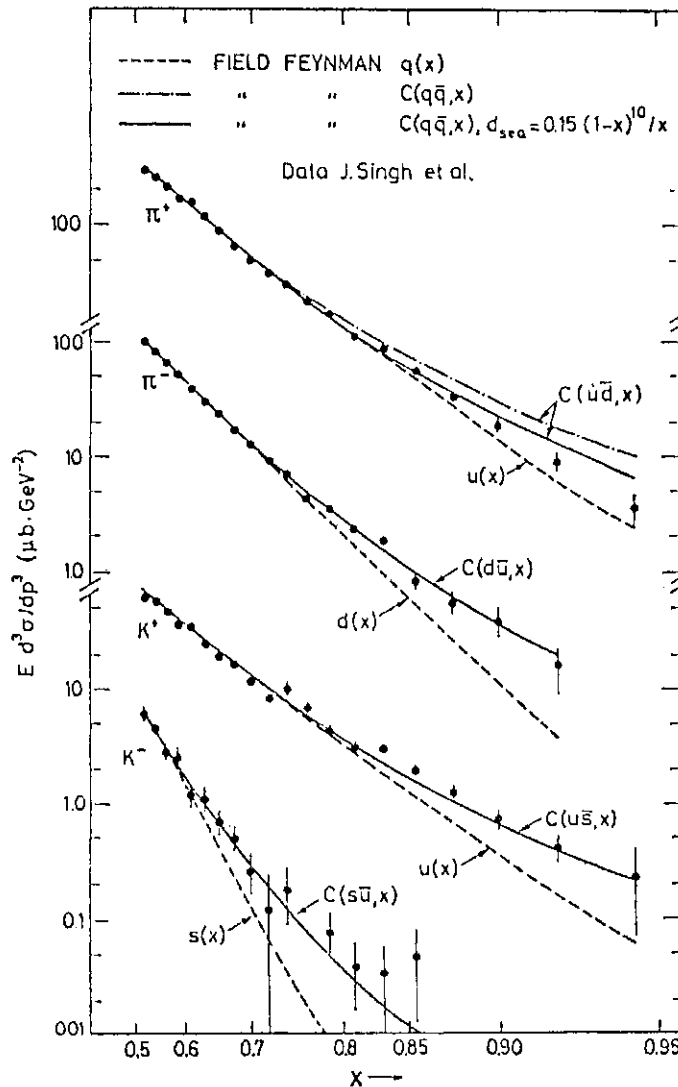


Fig. 18. Invariant cross sections for the production of particles in pp reactions at  $\sqrt{s} = 45$  GeV and  $p_T=0.75$  GeV, compared with the appropriate quark distributions (dashed lines) and with the convoluted distributions (Das-Hwa); from ref. 20. Data from ref. 21.

in Fig. 18 for  $\sqrt{s} = 0.75$  GeV/c. The dashed curves show the appropriate valence-quark distributions, and are the results one would obtain by neglecting the momentum contribution from the sea-quark. Better agreement with the data is obtained after convolution with the sea-quark distributions *à la* Das and Hwa.

In two papers presented to this Conference these ideas have been applied to data from incident pions and used to calculate the quark distributions within the pion:

Cutts <i>et al.</i> (paper 413)	Kenney <i>et al.</i> (paper 498)
valence $\propto (1-x)^{1.5 \pm 0.6}$	fix valence distribution to various models, <i>e.g.</i> , Field-Feynman, then get sea $-(1-x)^{-4}$
nonstrange sea $\propto (1-x)^{3.0 \pm 0.3}$	
strange sea $\propto (1-x)^{0.9 \pm 0.3}$	

The valence quark exponent of  $1.5 \pm 0.6$  is in qualitative agreement with that obtained from the lepton pair experiments.<sup>19</sup>

These results should be taken with a degree of skepticism, however; it's amazing that the analysis works so well considering that:

1. The model is not well-founded on basic theoretical principles and is somewhat arbitrary (for example, the choice of the recombination probability to be  $x^2/x^2$ ).
2. The fits end up with so much momentum in the sea that there is none left over for gluons (compared with lepton scattering, hadron interactions take place over a relatively long time scale, and it is suggested in ref. 18 that the gluons convert their momentum into quark pairs during the interaction).
3. For some of these reactions there are substantial contributions from resonance production and decay which is usually not taken into account.

4. For some reactions triple Regge contributions are important.
5. Scaling violations and other gluonic effects inherent in the parton-quark model may mask the true quark distributions.

The problem of resonant production and decay has been particularly stressed by Pokorski and Van Hove.<sup>15</sup> The effect of  $p$  contributions to the  $p - \Lambda^*$  inclusive spectra has been examined by Erne and Sens;<sup>20</sup> they find that while the effect is not dominant, it could well affect detailed quantitative fits such as those done to obtain the sea quark distributions.

The same data have been fit<sup>21</sup> for  $x > 0.7$  to the triple Regge model; the resulting Regge trajectories are shown in Fig. 19. The reactions  $p \rightarrow \pi^+ \pi^+, \pi^+ \pi^-, K^+$  all give similar values for  $a(t)$ , even though somewhat different values were expected for the different reactions. Perhaps one should simply be pleasantly surprised that the fits gave answers this close, since the inclusive production is a sum of not only triple Regge type terms, but also parton type processes, as well as resonance production and decay.

In spite of the complexity of low  $p_T$  physics the parton concepts do appear to be useful for an intuitive grasp of the data. For example, we can ask what happens to the  $n/\pi^+$  ratio, so beautifully explained by Ochs,<sup>16</sup> if we now require also an additional fast  $n^-$ . Naively, one might have thought the ratio would remain invariant under the requirement of the extra  $\pi^-$ ; however, the first  $\pi^-$  uses up the only d valence quark in the proton and for the second  $n^-$  both the quark and anti-quark must come from the sea. This requirement is similar to that for  $K^-$  production, and as shown<sup>22</sup> by Fig. 20 the  $\pi^+ x^- / n^- \pi^+$  ratio is

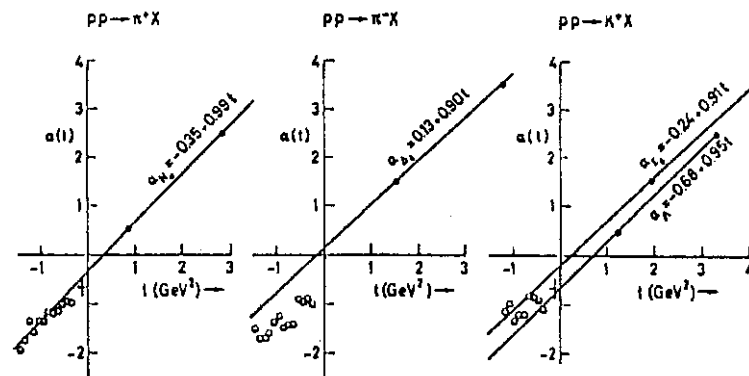


Fig. 19. Effective trajectories from one-term triple-Regge fits to the region  $x > 0.7$  (ref. 21).

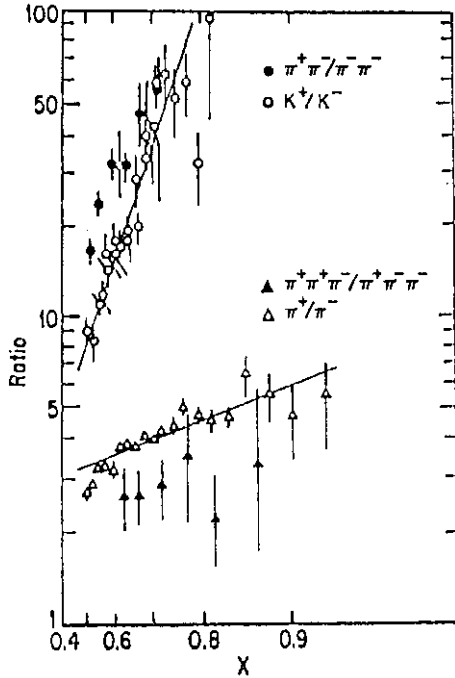


Fig. 20. Cross section ratios from pp interactions at  $\sqrt{s} = 53 \text{ GeV}$  (ref. 22).

indeed in qualitative agreement with the  $K^+ / K^-$  ratio. Other situations of this sort can also be studied; for example, the  $nJ/\psi$  ratio has been predicted<sup>23</sup> to change dramatically for events which contain lepton pairs of high effective mass. In the Drell-Yan model such pairs will be made preferentially by  $u\bar{u}$  annihilations which would then leave behind a different distribution of quarks available for hadron production.

An alternative, more superficial method for estimating the leading particle momentum distributions is given by the spectator counting rules of Brodsky and Gunion.<sup>24</sup> The best results are obtained if one assumes that one of the beam quarks is absorbed on the target, and the produced particle is accompanied by the minimum number of spectator quarks, as shown, for example, in Fig. 15c. Since the momentum must be shared with these spectators, one expects for the fast particles

$$x(d\sigma/dx) \propto (1-x)^{2n} \text{spec}^{-1}. \quad (12)$$

This is obviously a cruder model than those discussed previously. For example, both  $K^+$  and  $J/\psi$  produced from incident protons would then be expected to go as  $(1-x)^3$ , whereas it was the ratio of these two reactions which was fit so well by Ochs using the difference between the  $u$  and  $d$  quark valence distributions.

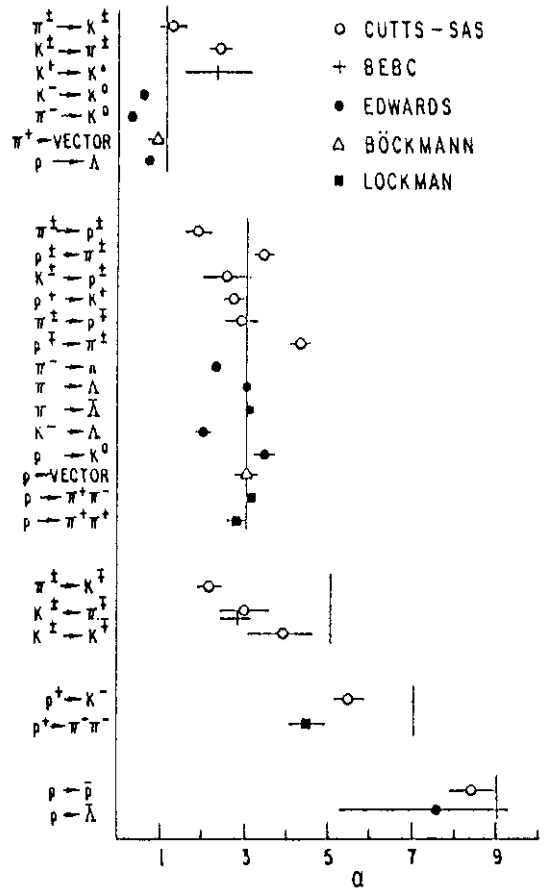


Fig. 21. Compilation of the exponent  $a$  used to characterize the dependence of inclusive processes at large  $x$ ;  $x da/dx = (1-x)^a$ . The data come from the sources listed in ref. 25 and are compared to that expected by spectator counting in the quark exchange model (ref. 24).

In Fig. 21 I have compiled some of the recent experimental results<sup>25</sup> and compared them with the predictions of the spectator counting model. At best, the model gives a rough measure of the difficulty in creating a fast particle of a given type. While some reactions are described well, others miss by one or sometimes two units in the exponent. Since the data are typically being fit over a range in  $1-x$  of a factor of five, this means that the model often gives a fall off which disagrees with the data by a factor of 5 to 25. The model is particularly unreliable for those processes with three or four spectator quarks. In some cases one can make excuses based on resonant contributions, triple Regge effects, helicity flip dominance, etc., but this means that the predictive power of the model is limited.

Some of the worst disagreements with the spectator quark counting rules are shown by the recent SPS hyperon beam results (Bourquin

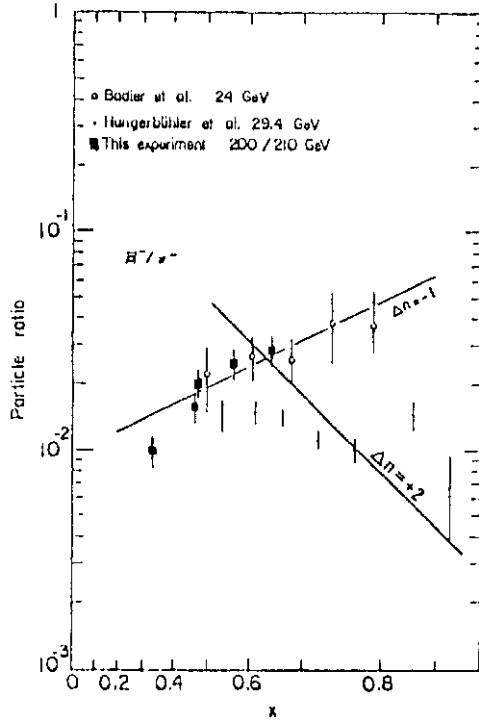


Fig. 22. Ratio for  $S^-$  produced in the forward direction by protons (M. Bourquin *et al.*, paper 777).

*et al.*, paper 777) such as the  $E^-/\pi^-$  ratio shown in Fig. 22. While the previous low-energy experiments disagree with one another, it is clear that this ratio is far from compatible with the prediction of the spectator model.

**§7. Heavy Stable Particle Surveys**

Here we will discuss the production of particles with lifetime sufficiently long to be observed in a secondary beam. We begin with three experiments which looked in vain for particles with mass in the region of 5 GeV. While it is always good to look for new effects on general principles, these experiments are of particular interest in view of the speculation

by Cahn<sup>26</sup> that the new quark in the  $Y$  might form stable or highly metastable compounds with the lightest of the old quarks, yielding a relatively stable meson with mass in the region 5 GeV. Two Fermilab experiments were performed recently with the parameters and results outlined in Table I. The Single Arm Spectrometer results of Cutts *et al.* are somewhat more sensitive, setting a 90% confidence upper limit roughly 20 times smaller than that for  $Y$  production. The results of Bourquin *et al.* (paper 777) using the SPS charged hyperon beam are also shown in Table I. While their cross section limit is several orders of magnitude less stringent than those of the Fermilab experiments, they are able to see down to lifetimes of order  $10^{10}$  seconds; again, no significant signal was observed.

The beam survey experiment of Bozzoli *et al.* (paper 915 and reported by Giacomelli in section A3) also searched for particles with lifetimes  $>10^{-8}$  seconds. They were able to set upper limits on the flux of such particles,  $<10^{-7}$  that of pions for new particles with  $M < 1$  GeV; at higher masses, 3-10 GeV, the limit is of order  $10^{10}$  of pion flux. This group also measured the flux of light nucleons and anti-nucleons. As one tries to make more and more nucleons (or antinucleons) stick together the cross section falls rapidly, the price being a factor of 2,000 per nucleon and 6,000 per anti-nucleon. These results can be compared with the sticking model which predicts

$$\frac{d^2N}{dx dx} \sim (\text{oplop})^2 \tag{13}$$

The observed  $d/d$  ratio is actually found to be three times this prediction.

The last experiment of this type which I

Table I. Searches for quasi-stable particles of  $M \approx 5$  GeV; upper limits are 90% confidence level.

	Cutts <i>et al.</i> , RPL 41, 363 (1978)	Vidal <i>et al.</i> , Fermilab-Pub 78-48	Bourquin <i>et al.</i> , Paper 777
Primary beam-target	pBe	p(BeO)	p(BeO)
Primary, secondary mom. (GeV/c)	400-70	400-70	200-95
Beam line	M6+SAS	NI	SPS Chgd. Hyp.
Length (m)	500	920	10-30
$\tau$ for $e^{-2.3} = 1/10$ (sec)			
at $M = 5$ GeV	$0.6 \times 10^{11}$	$1 \times 10^{11}$	$0.7 \times 10^{11}$
No. of Cerenkov counters	8	2	3
Mass range searched (GeV)	4 to 10	4.5 to 6	2 to 10
Number of light particles	$10^{11}$	$0.5 \times 10^{11}$	$X/\tau c < 10^{11}$
$E(d^* < j/dp^*) (cm^2/GeV^2)$	$< 1.1 \times 10^{11}$	$< 3 \times 10^{11}$	

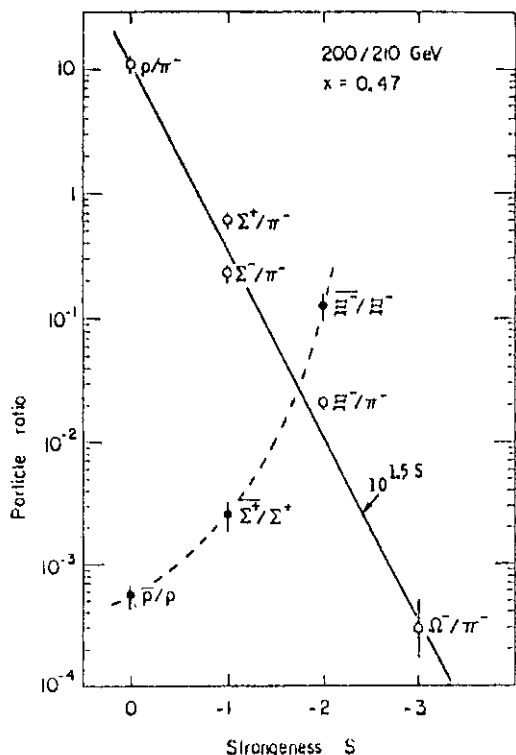


Fig. 23. Particle production by protons as a function of S (M. Bourquin *et al*, paper 777).

shall discuss is the survey of charged hyperons from 200 GeV interactions shown in Fig. 23. Here one pays a price of a factor of 30 in rate for each unit of strangeness. Note the rapid increase in the anti-baryon to baryon ratio as the strangeness increases; for  $S=2$  the ratio is already  $<10\%$ , leading one to speculate that

the ratio of anti  $Q\sim jQ\sim$  may be close to unity.

### §8. Non-Emulsion Searches for Charm

In a previous section we considered inclusive production of some of the old meson resonances; in a similar vein this section considers the inclusive production of charm resonances by hadron beams. This subject is obviously important since inclusive charm production gives another dimension to the study of dynamics, namely, the production of massive quarks or particles which can be compared with that of the lighter particles.

A list of some of the non-emulsion charm searches<sup>27</sup> is given in Table II; in general, I have limited myself to experiments well above threshold,  $\sqrt{s} > 10 \text{ GeV}$ . One must treat the cross sections listed in the table with caution. In general, the experiments are sensitive to only a small fraction of the  $4\pi$  solid angle, and a large extrapolation must be made using some theoretical model; different models have been used by the different groups. Further, the A dependence assumed for production off nuclei is often not mentioned and this can lead to an uncertainty of a factor of three in the cross section extrapolated to hydrogen. Also, it is sometimes not clear whether the cross section limit being quoted is for all D's, or only for a particular charge state, or whether the cross section is

Table II. Non-emulsion searches for inclusive charm production; limits are generally 95% confidence level on statistics, but do not include the systematic uncertainties of typically a factor of three.

First author	Decay modes	Reaction	$\sqrt{s}$ GeV	$\sigma(pp \rightarrow DD\bar{X})$ $\mu\text{b/nucleon}$
Antipov	$K\pi; K\pi$	$\pi^- \text{Be}$	10	$<(2-9)$
	$K\pi; \mu$			$<(10-20) (A^1)$
Albrecht	$K^0\pi^\pm$ (or $K\pi\pi$ )	nC	10	$<\sim 25$
Jonckheere	$\mu; \mu V^0$	$\pi^- \text{C}$	20	$<22 (A^1)$
Abolins	$K\pi$	nBe	22	$<15$
Spelbring	$K\pi; \mu$	nBe	24	$<100$
Lipton	$e^\pm; \mu^\mp$	nBe	24	$<30$
Lauterbach	$\mu$	pCu	27	$<\sim 1$ (using longit. pol.) $<\sim 10$ (without pol.)
Ditzler	$K\pi$	pBe	27	$<30$
Baum	$e^\pm; \mu^\mp$	pp	55	$<76$
Clark	$e^\pm; \mu^\mp$	pp	55	$\begin{cases} 76 \pm 36 \\ 25 \pm 10 \end{cases}$
Brown	single $\mu$	pFe	27	$30-80 (A^1)$
Soukas	beam dump $\rightarrow \nu$	pCu	7	1
Asratyan	beam dump $\rightarrow \nu$	pFe	12	$19 \pm 15$
Hansl	beam dump $\rightarrow \nu$	pCu	27	40
Alibrán	beam dump $\rightarrow \nu$	pCu	27	$100-200$
Bosetti	beam dump $\rightarrow \nu$	pCu	27	$100-200$

per D meson or per pair of D mesons. Thus the upper limits quoted generally have systematic uncertainties of a factor of three or more. In making the table, I have normalized the results to a set of standard branching ratios.<sup>28</sup>

The experiments range from those with a good direct signature, such as searches for bumps in the mass spectrum of  $\kappa^+ \pi^-$ , to those where the signature is rather indirect. Unfortunately, those experiments with potentially good signatures observe no conclusive evidence for charm production by hadron beams; in general, the upper limits are in the neighborhood of 10 to 20 *ub*. The upper limit of Lauterbach is only 1 *ub*, but this result is model dependent since it assumes that the muons from semi-leptonic D decay have a high longitudinal polarization; if this polarization information is ignored, the upper limit is of order <10 *ub*. Another of the more indirect experiments (Clark *et al.*, paper 115) looks at  $c/\bar{c}$  pairs at the ISR, and claims to see a two standard deviation effect after a large background has been subtracted.

Recently, two types of experiments have observed significant signals. Brown *et al.* (paper 1011) run a proton beam into a large hadron calorimeter and observe events with *single* muon production. After correcting for the decays in flight of pions and kaons they conclude that they are observing a cross-section in the region 30-80 *ub* (under the assumption of an  $i^+$  dependence). At the present time the most straightforward explanation of the single muon events would be the production and semileptonic decay of charmed particles. However, the cross-section quoted is larger than the upper limits set by many of the previous experiments.

The SPS neutrino beam dump experiments observed signals consistent with the production and fast decay of charmed particles in the beam dump, although the three experiments disagreed on the size of the effect, with cross sections for charm production now quoted from 40 to 200 *ub* (under the assumption of an  $A^0$  dependence). Again, these cross sections seem high when compared with the upper limits obtained by the other experiments listed in Table II; the disagreement can be reduced if an  $A^+$  dependence is assumed, in which case the

cross sections would fall in the range 10 to 50 *ub*. For comparison, the 28-GeV/c beam dump experiment at Brookhaven of Soukas *et al.* (paper 1156) set an upper limit of  $\sim 1$  *ub*.

A search for charm was carried out in BEBC by looking for prompt single electron (or positron) production by 22-GeV/c  $\pi^+$  in hydrogen (Calligarich *et al.*, paper 1150). Out of 25896 interactions they found one unambiguous event of this type:

$$\pi^+ p \rightarrow e^+ \Lambda^+ \pi^+ (K^0) \pi^+ X^0$$

where  $X^0$  is the unobserved system of neutral particles (missing mass  $\sim 1.4$  GeV). The presence of the  $K^0$  suggests that this could well be charm production. The one event corresponds to  $d \times B R \sim 1$  *ub* (10 *ub* for a 10% semileptonic branching ratio).

Albrecht *et al.* (paper 149) used a Serpukhov wire spark chamber spectrometer to look at 45 GeV nC interactions and have found the

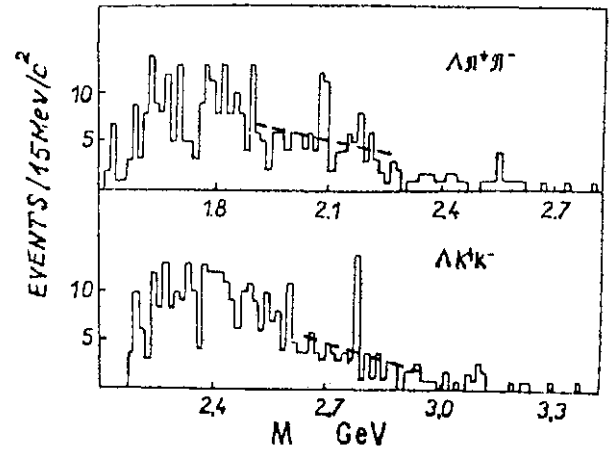


Fig. 24. Invariant mass distributions from 45-GeV nC interactions (Albrecht *et al.*, paper 149)

two narrow bumps in Fig. 24. The first bump is seen in the  $\Lambda \pi^+ \pi^-$  system at a mass of 2085 MeV, 23 events compared with  $\sim 10$  expected. The second bump is in the  $\Lambda K^+ K^-$  mass spectrum at 2790 MeV; 13 events compared to  $\sim 4$  expected. These bumps could be interpreted as decays of charmed baryons, but with  $\sim 4$  standard deviations per bump they clearly need confirmation; the authors quote a  $d \times B R \sim 1$  *ub*/nucleon each.

While bare charm is indeed proving difficult to observe in a reliable manner with hadron beams, hidden charm in the form of  $\langle p \rangle$  and  $\langle p' \rangle$  has been observed over the years and I have nothing qualitatively new to report here.

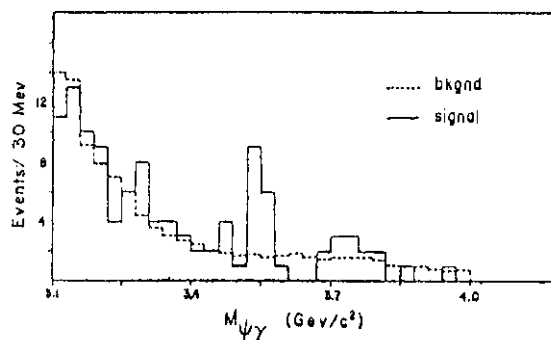


Fig. 25. The  $(pj)$  mass spectrum produced by a beam of 215 GeV/c  $\pi^-$ ; the background distribution was generated by taking uncorrelated  $\Lambda^+$ 's and  $f_0$ 's (Holloway *et al.*, paper 440).

Since the  $T$  is discussed in the talk of Lederman, I will not discuss it either. The one piece of hidden-charm physics that I do want to discuss is shown in Fig. 25. The Fermilab Chicago-Cyclotron-Magnet Spectrometer was used by Holloway *et al.* (paper 440) to observe the production of  $\psi$  states by a 215-GeV/c  $n^-$ -beam. They find events with  $(f_0 \rightarrow j\bar{j}) + u\bar{u}$  and then look for an additional  $j$  ray; the  $cpj$  mass distribution shows a bump of  $11 \pm 4$  events at 3550 MeV. This is just the mass of one of the  $\chi$  states and after correcting for their  $\gamma$ -ray acceptance they find that  $(38 \pm 13)\%$  of the  $\psi$ 's are produced *via*  $\psi(3555)$  production and decay. This number compares

well with the value  $(43 \pm 21)\%$  observed previously at the CERN ISR by Cobb *et al.*<sup>29</sup>

### §9. Short Lived Particles in Emulsions

The observation of production and decay of charm particles in emulsion should have the advantage of a clean signature and of relative independence of decay modes. Such experiments do depend, however, on possible biases and the lifetime; indeed, measurements of the lifetimes of charmed particles are also of great interest. In a simple, bare emulsion experiment one would actually observe the superposition of several different lifetimes from the different charm particles. In principle, this problem is avoided by some of the newer experiments which back up the emulsion stack with a large spectrometer or bubble chamber, both to locate interesting events in the emulsion and to separate the different charm particles through their decay products. Other uncertainties in the lifetime measurements come from possible scanning biases, both at very short and very long distances, as well as from the estimate of the Lorentz factor  $\gamma = E/M$ .

A list of emulsion experiments is shown in Table III. Several of these experiments have been presented to this Conference and claim

Table III. Some emulsion experiments on short-lived particles.

Paper	Beam	Comments	Events/Interaction	$\sigma$ ( $\mu\text{b/nucleon}$ )	$\tau$ ( $10^{-13}$ sec)
Bannik <i>et al.</i> (paper 154)	70 GeV p 60 GeV $\pi^-$	only search $l \leq 100 \mu$	4 events/ $\sim 20000$ ints. (each with an electron)	$5 \pm 3$	$\sim 0.6$
Coremans-Bertrand <i>et al.</i> PL 65B, 480 (1976)	300 GeV p	first decay $< 150 \mu$ , second $< 2$ mm	no pairs/60000	$< 1 1/2$ 90% conf. ( $A^{2/3}$ )	—
Bozzoli <i>et al.</i> L. N. Cim. 19, 32 (1977)	300, 400 GeV p	first decay 10 to 600 $\mu$ second $< 2$ mm	no pairs/16000	$< 7$	—
Ushida <i>et al.</i> (paper 492)	400 GeV p	first decay at 320 $\mu$ , second at 2930 $\mu$	one pair/312	$\sim 30$	$\sim 1$
Chernyavsky <i>et al.</i> (paper 308)	400 GeV p	search $\leq 1$ mm	9 singles/1120	$\sim 120$ ( $A^1$ )	$\sim 0.2$
Fuchi <i>et al.</i> (paper 491)	10–20 TeV	cosmic ray com- pilation of assoc. prod.	1 pair or cascade per 20–40 ints. (20 decays observed)	$\sim 500$	$X^0 \sim 4$ $X^\pm \sim 12$
Diambri-Palazzi	20–80 GeV $\gamma$	$< 3$ mm (along relativistic tracks)	2 possible singles (16, 30 $\mu$ ) per 482 ints.	$\sim 1/2$	0.02–0.05
Burhop <i>et al.</i> PL 65 B, 299 (1976)	$\nu$	broad-band beam from 400-GeV p	1 single/16 ints.		$\sim 6$
European $\nu$ Collab. (paper 798)	$\nu$	broad-band beam from 350-GeV p	0/31 charged current ints.		—



to have positive results. In general, these positive results are in contradiction to the upper limit  $\sim 1 / \mu b$  set by the two earlier experiments listed in the table, which were unable to find associated pairs in a search of the region down-stream of 76,000 primary interactions.

Two new experiments claim to have seen short-lived decays, based on the observation of single decays. In an experiment performed at Serpukhov Bannik *et al.* (paper 154) have observed four events having an electron associated with the secondary vertex. While Gaisser and Halzen<sup>30</sup> have estimated that backgrounds in single-decay samples (from interactions and decays of non-charm particles) are expected at the few to 50% level, Bannik *et al.* claim that the requirement of an electron should result in a very small background.

Chernyavsky *et al.* (paper 308) have found nine charm candidates out of 1120 primary stars produced by 400-GeV/c protons. Although they scan out to 1000  $ju$  these events show flight paths of only 12-90  $\mu$ . With such short flight paths there should be little probability of background from interactions. Their integral distribution of lifetimes is shown in Fig. 26. As indicated by the straight line, a lifetime in the neighborhood of  $2 \times 10^{-14}$  represents the data well; the systematics on such a lifetime may be large, however, due to possible scanning biases. These authors suggest a reason for the nonobservation of associated events: perhaps charm production proceeds mainly through associated production

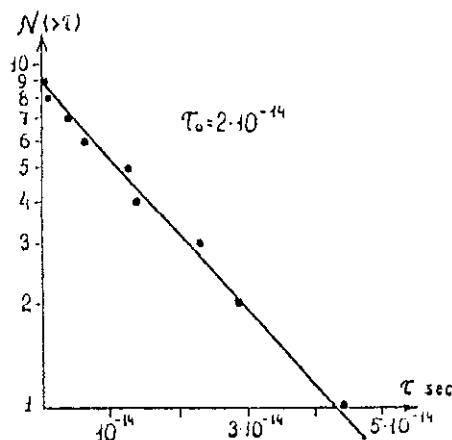


Fig. 26. Integral distribution of the lifetimes of the nine short-lived particles observed by Chernyavsky *et al.* (paper 308). The lifetime value shown should be considered preliminary due to possible scan biases.

of a charmed meson together with a charmed baryon, the meson having a lifetime too short to be observed reliably in the emulsion. Indeed, for most of these nine events one must assume that the observed decays are of baryons, rather than mesons, if the mass is to be in the neighborhood of 2 GeV.

Still, this does not explain why the two earlier experiments with much higher statistics did not observe such events. Although these earlier groups emphasized their nonobservation of associated pairs, in fact they also looked at single production and found only a few events, consistent with the flat lifetime distribution expected from interactions or hyperon decays. For example, Bozzoli *et al.* only observed 8 events with decay paths  $< 100 JU'S$  even though they looked at 15 times as many interactions as Chernyavsky *et al.*

Fuchi *et al.* (paper 491) have made a compilation of short-lived particles produced by cosmic rays in the energy region 10-20 TeV. To reduce backgrounds they accept only events having two or more short-lived particles. Out of six interactions, some of them from exposures 20 or 30 years ago, they find 20 candidates. The integral lifetime spectra for both charged and neutral candidates are shown in Fig. 27. The six neutral short-lived particles suggest a lifetime in the neighborhood of  $0.4 \times 10^{-12}$  seconds, while the 14 charged particles give a lifetime of roughly 3

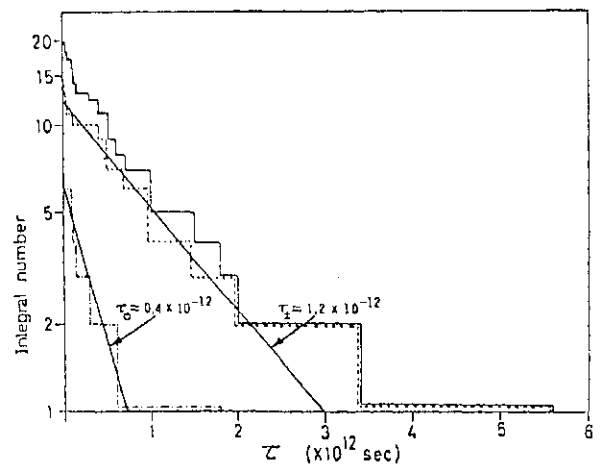


Fig. 27. Integral lifetime distributions for short-lived particles from associated production by cosmic rays of 10-20 TeV; solid line shows charged plus neutral particles, dashed line for charged, dash-dot for neutrals. No correction has been made for scan biases. Compilation by Fuchi *et al.* (paper 491).

times as long. It is interesting to note that Fig. 27 is consistent with the theoretical suggestion<sup>31</sup> that the lifetime of the charged D meson is longer than that of the neutral. The authors estimate that short-lived particles are produced every 20-40 events at these energies, *i.e.*, a cross section of  $\sim 500$  //b/nucleon.

For completeness, Table III also shows results obtained from  $\gamma$ -ray and neutrino interactions in emulsions. The results of the Omega Photon Emulsion Collaboration were presented in session B4 by Diambri-Palazzi. So far, they have found two possible candidates, both with rather short flight paths, suggesting a lifetime of  $< 10^{-14}$  seconds. While one event was found in a previous neutrino emulsion experiment, the most recent experiment (paper 798) has thus far been unable to find any candidates in a search of 31 charged-current interactions. As with the  $\gamma$ -ray experiment, this latter neutrino experiment has really only begun the long and tedious task of scanning, so additional results can be anticipated within the next year or two; other emulsion experiments are being set up at Fermilab as well.

I would now like to summarize the present inclusive charm situation. Can all of these experiments be consistent with one another? With enough *ad hoc* assumptions one could probably get consistency between the majority of the experiments; however, my guess is that at least some of them are wrong or have been given a wrong interpretation. One of the worst discrepancies is between the old high-statistics emulsion experiments and the more recent beam dump experiments. This has been investigated in some detail by Crennell *et al.*<sup>22</sup> who combine the  $DD$  production model of Halzen and Matsuda<sup>33</sup> with the scan criteria of the Coremans-Bertrand experiment. They conclude that the experiments could be consistent if the average lifetime of the charmed particles were either  $< 0.5 \times 10^{-31}$  or  $< 10^{-12}$  seconds. This can be compared with the theoretical expectations<sup>31</sup> of  $0.5 \times 10^{-12}$  seconds; the theorists claim they would be surprised if the lifetime lay outside the range  $10^{-14}$  to  $10^{-11}$  seconds and this would prejudice one against the very fast lifetime possibility. The lifetime cannot be much more than  $10^{-12}$  seconds, however, or various bubble chamber

experiments would have been able to detect the finite decay length. Since both the emulsion experiments and beam dump experiments assume the same  $A$  dependence, this possible systematic error cannot explain the discrepancy between the two experiments. If the charm particles were produced more diffractively, a smaller cross section could produce the observed number of neutrino interactions from the beam dump experiments. Much more than a factor of 2 or 3 is improbable, however, because the neutrino spectrum would then disagree with that observed.<sup>34</sup> Systematic errors of a more experimental nature are also possible, of course, and are even strongly suggested by the fact that neither the emulsion experiments nor the beam dump experiments agree well amongst themselves.

More exotic explanations are also possible, although these are perhaps premature. One possibility would be that the neutrinos in the beam dump experiments originate primarily from the decay of some other type of particle, such as mesons with one of the new  $T$  quarks. Another possibility suggested to this Conference (Banerjee and Subramanian, paper 437) involves new, relatively-light neutral bosons produced in pairs with a small cross section and long lifetime.

My own guess is that the charm cross section at Fermilab-SPS energies is of order  $10$  //b/nucleon with lifetimes hiding in the shadows near  $10^{-12}$  seconds. With all of the present experimental effort being brought to bear on this problem, it should be well understood by the time of the next Conference.

## §10. Centauro Events

The only way to study interactions above  $\sqrt{s} = 60$  GeV at present is to use cosmic rays. Although these experiments are very difficult, they have over the years indicated the trends to be expected at higher energies. Rising total cross sections, the increase in transverse momentum, and a rapid increase in average multiplicity have all been shown by these experiments. Rather than trying to cover all of the results from the cosmic ray experiments, I will concentrate instead on one topic, the so-called Centauro events.

While such events are not observed at present day accelerator energies they are

apparently produced relatively frequently, at least a few per cent of the total cross section, at lab energies of 1,000 TeV. They are characterized by a high multiplicity of strongly interacting particles, roughly 80, but are consistent with having no  $\gamma$  rays, and thus no  $7r^0$ 's, coming from the primary interaction. Five such events have been observed by a Brasil-Japan collaboration (paper 434) using emulsion chambers on Mount Chacaltaya in Bolivia, 5200 m above sea level.

These interactions take place in the atmosphere, typically a few hundred meters above the apparatus. Only the height of the first event could be measured directly; it was found to be 50 m above the apparatus and gave an average  $p_T$  of  $1.7 \pm 0.7$  GeV/c. The heights of the other events have been calculated assuming the same average transverse momentum. The characteristics of these events are outlined in Table IV.

**Table IV. Characteristics of the Centauro and Mini-Centauro events (Brasil-Japan Collaboration, paper 434).**

	Centauros	Mini-Centauros
No. events	4+1	13
Interaction height (m)	50, 80, 230, 500	300-1900
Hadronic mult.	70-90	$\sim 15$
Fireball mass (GeV)	$\sim 200$	$\sim 30$
Total energy (TeV)	1000-1400	250-2500

It was found that the energy and transverse momentum of the secondary particles are exponential and that the angular distributions are consistent with isotropy, making it natural to speak of the production of a fireball. They have calculated the mass of the fireball using two methods, each giving  $M \sim 200$  GeV. The first method uses the average transverse momentum to deduce the average energy in the center of mass to be 2.3 GeV per particle; the mass of the fireball is then just calculated as the number of particles times this average energy. The second method assumes a forward-backward symmetry in the center of mass system; the median angle,  $\theta_m$ , then corresponds to  $90^\circ$  in the center of mass and the mass can be simply calculated as

$$\tan \theta_m = \frac{p_T}{p_H} = \frac{p_T^*}{\gamma \beta E^*} \approx \frac{1}{\gamma} = \frac{M}{E}$$

$$M \approx E \theta_m$$

where  $E$  is the total laboratory energy of the fireball. This energy is measured in the emulsion chambers by allowing the particles from the Centauro events to interact in the apparatus, converting about one-fifth of their energy to  $7r^0$ 's, the  $\gamma$  rays of which can be measured in the emulsion chambers. They then observe a sum of  $\gamma$ -ray energies,  $E_{\gamma} \approx 200$  to 300 GeV, implying a total energy for these events in the neighborhood of 1,000 to 1,400 TeV, and this result gives a fireball mass quite consistent with that obtained by the average transverse momentum.

As shown in Table IV, these authors have now also observed 13 events which they call mini-Centauro. While these events only have  $\sim 15$  strongly interacting particles, a somewhat low multiplicity, they share with the Centauro events the characteristic of having little or no  $\gamma$  rays from  $7r^0$ 's.

While the Centauro events need confirmation from other experimental groups, their presence could help to explain some of the other effects such as high multiplicity and large average transverse momentum seen by the various cosmic ray experiments. The colliding beam projects being planned for the next few years at CERN, Fermilab, and Brookhaven will probably have sufficient energy to observe this new type of interaction; for example,  $\sqrt{s} = 800$  GeV corresponds to a laboratory energy of 340 TeV. With their large cross section such events should be relatively easy to see, even at the low luminosities which may be present during the initial operation of these colliding beam systems. Whether or not the Centauro events are eventually confirmed, they do hold a lesson for us as we seek to expand our energy horizons with accelerators: we should not simply imagine that nature continues on in a unimaginative and dull fashion; she may in fact have some real surprises up her sleeve, in this case a totally new type of strong interaction setting in above some high-energy threshold. Judging from the high multiplicities observed in extensive air showers at even higher cosmic ray energies, more than one surprise may be waiting for us.

## §11. Interactions Off Nuclei

There has been considerable work, both experimental and theoretical, in this field,

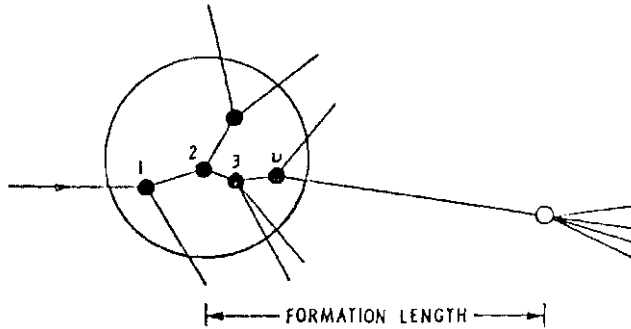


Fig. 28. Schematic view of interactions in nuclei.

particularly in the Soviet Union. Here I will mention just a few of the points to give a flavor of the physics and to remind those not working directly with nuclei of this very active sub-culture.

A simple, naive picture of an interaction in a nucleus is shown in Fig. 28. Experiment shows that the fast, high-energy stuff acts much like the incident beam particle while inside the nucleus. In particular, there is very little cascading of the sort observed in a hadron calorimeter, where the first interaction might produce 10 particles, each of which in turn interact to produce several more particles, and so on, leading to a rapid build up of the shower. This is not observed. If we define  $\nu_i$  to be the number of interactions of an incident proton in the nucleus, then the average number can be expressed as

$$\begin{aligned} \bar{\nu}_p &\approx A\sigma_{\text{inel}}(pp)/\sigma_{\text{inel}}(pA) \\ &\approx 0.7 A^{0.3} \end{aligned} \quad (14)$$

The number of fast charged secondaries coming from nuclear reactions normalized to those from hydrogen,

$$R_A = \langle n \rangle_A / \langle n \rangle_{\text{hydrogen}}, \quad (15)$$

is plotted in Fig. 29 (ref. 35) as a function of both  $A^{1/3}$  (proportional to the nuclear radius) and the variable  $\nu$ . As shown by the figure, the data lie on the straight line

$$\hat{A} = 0.47 + 0.61 \nu \quad (16)$$

when plotted as a function of  $\nu$ , but do not show a simple relationship when plotted as a function of the nuclear radius. This result shows a surprising simplicity of these high energy interactions: the high-energy stuff propagating through the nucleus acts much as the beam particle itself, even though it becomes an excited system which eventually decays out-

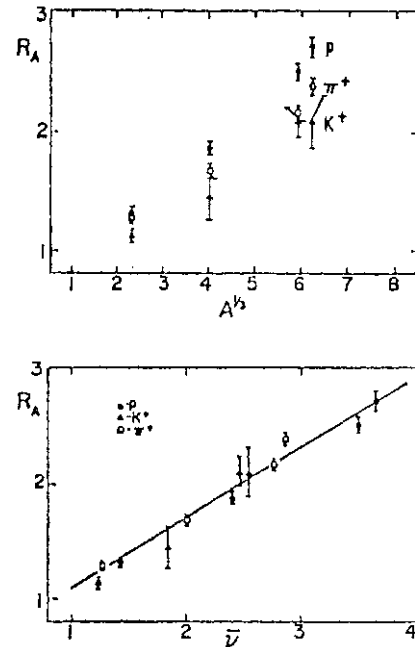


Fig. 29. Charged particle multiplicity ratio (eq. 15) at 100 GeV/c as a function of  $A^{1/3}$  (proportional to the nuclear radius) and  $\nu$  (eq. 14); from ref. 35.

side the nucleus. Dimensional arguments give for this decay or formation length

$$l \sim p / (M^2 + P_T^2), \quad (17)$$

in which case the forward going high-energy stuff tends on average to decay well outside the nucleus radius, and to first order these fast particles do not depend upon the thickness of the nucleus. For the slow particles one expects a multiplicity roughly proportional to  $\nu$ , the number of interactions in the nucleus. Equation 16 is not far from the simple mnemonic,  $1/2 + 1/2\nu$ , where the first term comes from that part of the multiplicity generated by the beam, while the second term would correspond to that coming from target fragmentation.

Actually the slow recoils from the target fragmentation region have a short enough formation length that some cascading in this region is possible. Such cascading can give particles in kinematic regions which would normally be forbidden in reactions off single nuclei. Numerous experiments have looked at slow backward protons, for example, and a whole class of theories has been developed to describe such interactions.<sup>36</sup> These theories go under various names such as coherent tube model, cumulative effect, and big hadron model. The physical picture in such models is different from that shown in Fig. 28; these

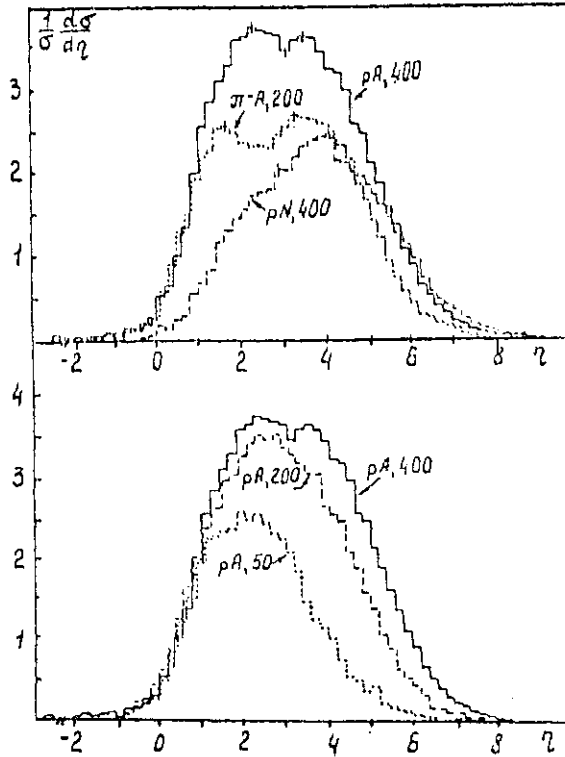


Fig. 30. Compilation of inclusive pseudorapidity distributions of fast ( $0.7 < \eta < 0.7$ ) particles in emulsions compared with that off single nucleons, and also at the different incident laboratory momenta indicated in GeV (Boos *et al.* paper 307).

models assume that the interaction takes place off  $\nu$  nucleons which act together as a single coherent target and thus give a higher  $s$  value (by a factor of  $\nu$ ) than one would normally achieve with a hydrogen target.

Pseudorapidity distributions observed in emulsions are shown in Fig. 30. This compilation was taken from the very nice review paper of the Alma-Ata *et al.* collaboration (paper 307). While the target fragmentation region ( $0 < \eta < 1$ ) depends strongly on  $A$ , it is independent of the beam identity and energy, as expected for limiting fragmentation. The dependence on  $A$  of the target extends well into the central region near  $\eta = 3$ , a relatively long-range correlation between the target and central regions which is not expected in many models. In the beam fragmentation region there is a slight loss of particles as  $A$  increases. The central region grows and the curves move out in the beam fragmentation region as more phase space becomes available at higher energies. There is an indication of these distributions developing a double peak, one from the multiplication of slowish particles in the target fragmentation region, and the second from

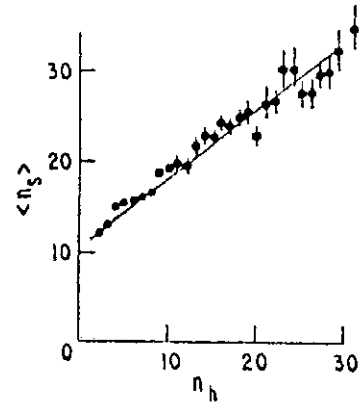


Fig. 31. Average multiplicity of fast particles from inelastic 400-GeV p-emulsion reactions as a function of the number of associated "heavy" tracks (Boos *et al.* paper 307).

the usual peak near  $x=0$ .

One advantage of emulsion experiments is that they can count the number of heavily ionizing tracks,  $n_h$ , mainly recoil protons with ( $3 < 0J$ ). As shown by Fig. 31, the average number of fast particles,  $\langle n_s \rangle$ , depends strongly on  $n_h$ , the data in the figure being well represented by the straight line

$$\langle n_s \rangle = 10.5 + 0.76/n_h^* \quad (18)$$

The intercept of 10.5 is roughly 15% higher than the average value ( $n_{ch,y=9}$  found for pp reactions. The dependence of  $\langle w \rangle$  on  $n_h$  can be compared with Eq. 16, suggesting that  $n_h$  is a measure of  $\nu$  for a given event.

A relatively clean testing ground for ideas about reactions off nuclei is afforded by the deuterium nucleus, and many bubble chamber experiments have looked at such interactions. For example, a recent experiment<sup>37</sup> using a 360-GeV/c  $n^-$  beam found the double scattering probability to be (15±2) % in deuterium. They further found the ratio of negatively charged particles produced in double scattering reactions to those from  $n-p$  collisions to be  $L36+.07$ , a value somewhat larger than, but consistent with, predictions based on AGK cutting rules or the coherent tube model.

A recent experiment on the  $A$  dependence of inclusive neutron production by 400-GeV protons has been carried out at Fermilab using a calorimeter to detect the forward-going neutrons. From their lead and beryllium data they obtain the values for  $a$  shown in Fig. 32, where  $a \propto A^{-1}$ . As the neutron momentum increases above  $x=0.15$ ,  $a$  falls

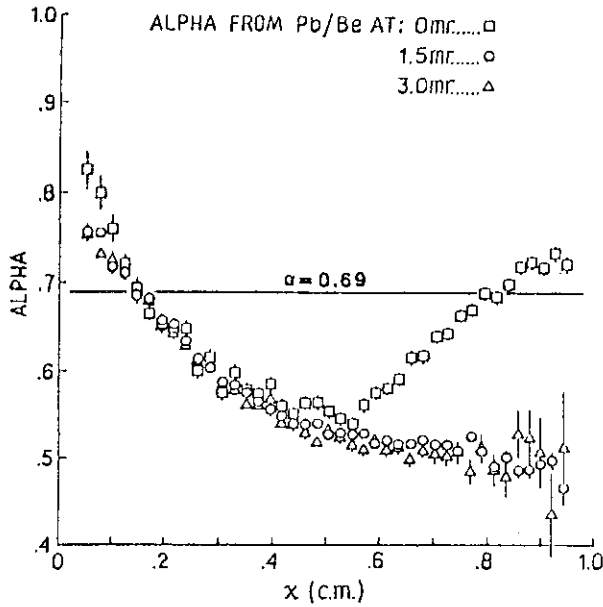


Fig. 32. Values of a calculated from lead/beryllium ratios of neutrons produced by 400-GeV protons (Whalley *et al* paper 673).

below the value of 0.69 for the overall inelastic cross section, and fewer high-momentum neutrons are produced per interaction from lead than from beryllium. A similar effect is shown in Fig. 30 for fast charged particles in emulsions and has been observed in other counter experiments<sup>38</sup> as well. An exception to this trend is the 0-mrad neutron production shown in Fig. 32 where  $\alpha$  increases again above  $x=0.6$ ; this effect is not observed in the corresponding copper data, suggesting that the increase of fast neutrons off lead comes from coherent electromagnetic production processes (one- $\pi$ - exchange) which would have a  $Z^2$  dependence.

Another nuclear effect has been studied with an experiment<sup>39</sup> using  $\text{Ti}^*$  beams on neon at 10 GeV; neglecting the production of  $K^+$ ,  $p$  and assuming charge symmetry, one can estimate the momentum distribution of protons including those normally too fast to be identified in the usual way with ionization measurements. The average longitudinal momentum carried off by protons is shown in Fig. 33 as a function of the number of fast particles,  $n_s$ ; for  $n_s > 8$ , the protons carry off on average  $\sim 2 \text{ GeV}/c$  per event. Assuming an equal amount for the neutrons, this becomes a total of  $4 \text{ GeV}/c$ , a surprisingly large number considering that the experiment was carried out at only  $10 \text{ GeV}/c$ .

3 r-

**r / r**

Z \_\_\_\_\_ | \_\_\_\_\_ | \_\_\_\_\_ |  
O            4            a            12

Fig. 33. Average laboratory longitudinal momentum per event carried off by protons produced in 10-GeV/c  $\wedge$  Neon collisions, as a function of the number of fast particles in the event (ref. 39).

A summary of some of the more important points concerning reactions off nuclei is as follows :

1. *Little cascading*—long time development.
2. Multiplicity *depends on  $\nu$*  rather than  $A^{1/2}$ ; the hadronic state blasting it's way through the nucleus remembers the nature of the incident beam.
3. *KNO scaling approximately valid*, although  $(n)/D$  changes by  $\sim 40\%$  depending on  $\nu$  as measured by slow protons ( $n_s$ ).
4. *Fast nucléons* often blasted out of nucleus;  $\langle j^+, | \rangle \sim 4 \text{ GeV}/c$  per event for  $7r^- \text{ Ne}$  at  $10 \text{ GeV}$  and  $n_s > 5$ .
5.  $\nu A$  induced events much like *TZA* : multiplicity distributions, fast protons, slow backward protons etc., are all very similar.<sup>40</sup>
6. *Many different models* can follow the data, but with little predictive power.

**§12. Conclusions**

1. The results of many experiments on multiplicities and correlations at different energies and with different beam particles have been presented to this Conference. With ever-increasing statistics, detailed effects such as three-body dynamic correlations can now be observed.
2. The compensation of charge and transverse momentum has been studied at the ISR with high statistics and has been used to discriminate between various cluster models.
3. Second order (Bose-Einstein) interference effects have been observed in several experiments and interpreted in terms of the

dimensions of the emission region. While this method holds promise for the study of the variation of these dimensions with different parameters, the variations thus far observed appear to come from differences in the treatment of the data.

4. Resonance production and decay appear to account for the majority of pions and kaons coming from high energy interactions, and analyses of inclusive distributions must take this into account if reliable results are to be obtained.

5. The  $p$  and  $A_z$  trajectories have been obtained from a triple Regge analysis of pion charge exchange and  $nj$  production, from both full-inclusive and neutrals-only final states; the results are in good qualitative agreement with those obtained from the energy dependence of the exclusive reactions.

6. Parton ideas, particularly as formulated by Das and Hwa, appear to be highly successful in describing the  $x$  distributions of leading nondiffractive particles at low  $p_T$ .

7. Charm production by hadron beams continues to be elusive; experiments with good signatures have thus far only been able to set upper limits, while more indirect experiments such as the SPS neutrino beam dump and the Fermilab single muon experiments observe signals which in some cases are larger than the previously quoted upper limits.

8. Emulsion experiments looking for short-lived charmed particles are also contradictory. Several experiments claim to have such events, but with different lifetimes and in violation of upper limits set by previous experiments.

9. My own guess is that inclusive charm production at Fermilab-SPS energies is of order  $10^{-6}$  b/nucleon with lifetimes of order  $10^{-12}$  sec, but this will be resolved in the next year or two as much experimental effort is being devoted to the question.

10. The cosmic ray experiments continue to tantalize the rest of us who are tied to accelerator energies; they promise new types of strong interactions, Centauro events with high multiplicity but no  $7r^0$ 's, at the next generation of colliding-beam machines.

11. Interactions off nuclei are being actively pursued as a laboratory in which to study the space-time development of hadronic matter. The strong suppression of cascading inside

nuclei is of fundamental importance and shows the relatively long evolution times involved.

### Acknowledgments

In developing this talk I have greatly benefited from innumerable discussions with many different people, both before and during this Conference, and I am grateful for their help. I would like also to thank my scientific secretary, Prof. T. Hirose, for his assistance in the preparation of the talk. The hospitality and efficient organization of our Japanese hosts have contributed greatly to the success of this Conference and is very much appreciated.

### References

1. E. L. Berger: Nucl. Phys. B 85 (1975) 61.
2. M. LeBellac: Rapp. talk, Budapest Conf. (1977).
3. H. Kirk *et al*: Nucl Phys. B 128 (1977) 397.
4. Irwin A. Pless: IX Int. Sym. High Energy Multiparticle Dynamics (Tabor, Czechoslovakia, July 1978).
5. C. Bromberg *et al*: Phys. Rev. Letters 38 (1977) 1447.
6. G. Kopylov and M. Podgoretsky: Sov. J. Nucl. Phys. 18 (1973) 656; 19 (1974) 434; G. Cocconi: Phys. Letters 49B (1974) 459.
7. M. Deutschmann *et al*: CERN/EP/PHYS 78-1 (Jan. 1978).
8. The K+p data at 32.1 GeV/c are from M. Goossens *et al*, paper 444; the pp data from the ISR are from D. Drijard *et al*, paper 273; and the pp->K,K,X data at 0.76 GeV/c are from A. M. Cooper *et al*, Nucl. Phys. B 139 (1978) 45. The other points are taken from the compilations presented in the above papers.
9. H. Grassier *et al*: Nucl. Phys. B 132 (1978) 1.
10. D. Cutts *et al*: Phys. Rev. Letters 40 (1978) 141.
11. H. Kirk *et al*: Nucl. Phys. B 128 (1977) 397.
12. A. V. Barnes *et al*: Caltech preprint CALT-68-667 (June 1978).
13. A. V. Barnes *et al*: Phys. Rev. Letters 37 (1976) 76; O.I. Dahl *et al*: Phys. Rev. Lett 37 (1976) 80.
14. B. Andersson: Phys. Letters 69B (1977) 221.
15. Hyman Goldberg: Nucl. Phys. B 44 (1972) 149; S. Pokorski and L. Van Hove: Acta Phys. Pol. B5 (1974) 229; Nucl. Phys. B 86 (1975) 243; and CERN preprint TH. 2427 (Nov. 1977).
16. Wolfgang Ochs: Nucl. Phys. B 118 (1977) 397.
17. K. P. Das and R. C. Hwa: Phys. Letters 68B (1977) 459.
18. D. W. Duke and F. E. Taylor: Phys. Rev. D 17 (1978) 1788.
19. L. Lederman: rapporteur talk at this Conference.
20. F. C. Erne and J. C. Sens: CERN preprint (Jan. 1978).
21. J. Singh *et al*: Nucl. Phys. B 140 (1978) 189.

22. W. Lockman *et al*: Phys. Rev. Letters 41 (1978) 680.
23. T. A. DeGrand and H. I. Miettinen: Phys. Rev. Letters 40 (1978) 612.
24. S. J. Brodsky and J. F. Gunion: Phys. Rev. D 17 (1978) 848.
25. Data used for Fig. 21 come from a) D. Cutts *et al*, paper 413 (100, 175 GeV/c); b) M. Barth *et al*, paper 338 (70 GeV/c); c) R. T. Edwards *et al*, Phys. Rev. D 18 (1978) 76 (200 GeV/c); d) K. Bôckmann, Talk at the Symposium on Hadron Structure and Multiparticle Production, Kazimierz (1977) (16 to 225 GeV/c); e) ref. 22 ( $\sqrt{s} = 53$  GeV).
26. R. N. Cahn: Phys. Rev. Letters 40 (1978) 80.
27. Yu. M. Antipov *et al*: papers 204 and 941; K.-F. Albrecht *et al*: paper 149; A. M. Jonckheere *et al*: Phys. Rev. D 16 (1977) 2073 and H. Lubatti: private communication; M. A. Abolins *et al*: Phys. Rev. Letters 37 (1976) 417; D. Spelbring: Phys. Rev. Letters 40 (1978) 605; R. Lipton *et al*: Phys. Rev. Letters 40 (1978) 608; M. J. Lauterbach: Phys. Rev. D 17 (1978) 2507; W. R. Ditzler: Phys. Letters 71 B (1977) 451; L. Baum: Phys. Letters 77 B (1978) 337; A. G. Clark: Phys. Letters 77 B (1978) 339; K. W. Brown: paper 1011; A. Soukas *et al*: paper 1156; A. E. Asratyan: paper 288; T. Hansl *et al*: Phys. Letters 74 B (1978) 139; P. Alibrant *et al*: Phys. Letters 74 B (1978) 134; P. C. Bosetti *et al*: Phys. Letters 74 B (1978) 143. For a review of the CERN beam dump experiments see also H. Wachsmuch, talk at the Oxford Neutrino Conf. (July 1978).
28. Particle Data Group: Phys. Letters 75 B, No. 1 (Apr. 1978).
29. J. H. Cobb *et al*: Phys. Letters 73 B (1978) 497.
30. T. K. Gaisser and F. Halzen: Phys. Rev. D 14 (1976) 3153.
31. C. Quigg: Fermilab preprint Conf.-78/37-THY (April: 1978) and minirapporteur talk in Session B8.
32. D. J. Crennell *et al*: Rutherford preprint RL-78-051 A (June, 1978).
33. F. Halzen and S. Matsuda: Phys. Rev. D 17 (1978) 1344.
34. Private communication from E. L. Berger and T. Kamae.
35. J. E. Elias *et al*: Phys. Rev. Letters 41 (1978) 285.
36. For a comparative review of various models describing high energy interactions in nuclei see B. Andersson: *Proc. Int. Colloq. on Multiparticle Reactions* (Tutzing, 1976 p. 109).
37. K. Moriyasu *et al*: Nucl. Phys. B 137 (1978) 377.
38. K. Heller *et al*: Phys. Rev. D 16 (1977) 2737; D. Chaney *et al*: Phys. Rev. Letters 40 (1978) 71; however, the neutron induced data of D. L. Burke *et al*: paper 676, show little change in the yield per inelastic collision of particles with pseudorapidity  $> 5.5$ .
39. W. M. Yeager *et al*: Phys. Rev. D 16 (1977) 1294.
40. T. H. Burnett *et al*: U. of Wash, preprint VTL-PUB-55 (1977) and H. Lubatti: private communication; J. P. Berge *et al*: Fermilab Pub.-78/55 (1978).



## P2a: Large $PT$ Phenomena, Jet Structure

*Chairman :* G. VON DARDEL

*Speaker:* R. SOSNOWSKI

*Scientific Secretaries:* K. NAKAMURA  
T. INAGAKI

## P2b: Prompt Dilepton Production by Hadron Reaction

*Chairman:* P. FALK-VAIRANT

*Speaker:* L. LEDERMAN

*Scientific Secretaries:* M. MISHINA  
A. MAKI

## P2a Large $p_T$ Phenomena and the Structure of Jets

R. SOSNOWSKI

*Institute of Nuclear Research, Warsaw*

The modern history of the high transverse momentum phenomena started in 1972 when it was found that the spectrum of the transverse momentum,  $p_T$ , of secondaries produced in hadronic collisions did not drop as fast as expected from its behaviour at low  $p_T$  values. Since this discovery the effort of many experimental teams supplied us with a global information concerning collisions of two hadrons with a large transverse momentum secondary produced. It is rather difficult to discuss in the present review the details of experiments the results of which have been submitted to this Conference. Nevertheless one has to stress that a big effort of experimentalists allows us to study the production of secondaries at transverse momenta as large as 16 GeV/c. It is also of great importance that new detectors cover a large fraction of the phase space recording other particles produced in the collision. This enables us to study globally the large transverse momentum phenomena. The aim of this review is to systematize the existing experimental knowledge in the field.

It is rather widely believed that the production of objects with a large transverse momentum in collisions of two hadrons is due to the hard scattering of their constituents. We will not discuss here any specific model of this type. We will use however the hard scattering picture as a guiding line in our survey of the experimental data. According to this picture a collision in which a hard scattering occurs should look like that in Fig. 1. Two

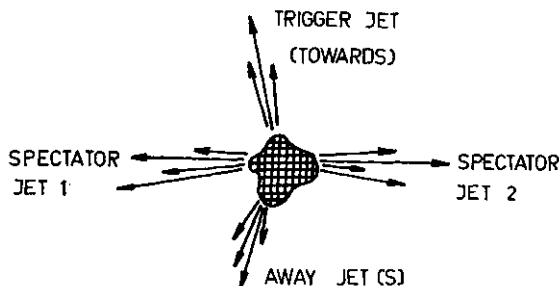


Fig. 1.

scattered constituents with large transverse momenta should show up as two jets of hadrons. One of them which is used to trigger the apparatus we call a *Trigger Jet* and the other one—an *Away Jet*. Two incoming hadrons, each with one constituent removed by the hard scattering are expected to create two *Spectator Jets*. *The present review will be then a guided tour through the four-jet world.* Figure 1 tells us how this world is expected to look like. Using other coordinates:—rapidity,  $y$ , and azimuthal angle,  $\langle p \rangle$ ,—the four jets should be seen as it is shown in Fig. 2. In this figure

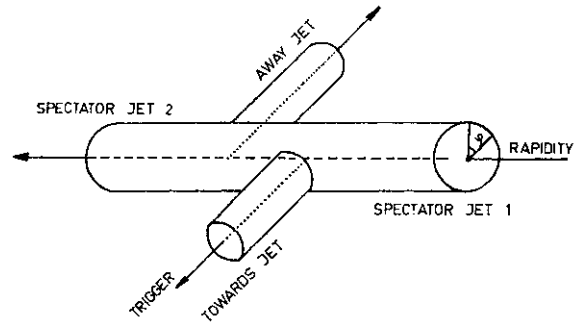


Fig. 2.

the number of charged particles per interval of  $y$  and  $\langle p \rangle$  is plotted. Of course this figure has been drawn by an optimist. The reality looks

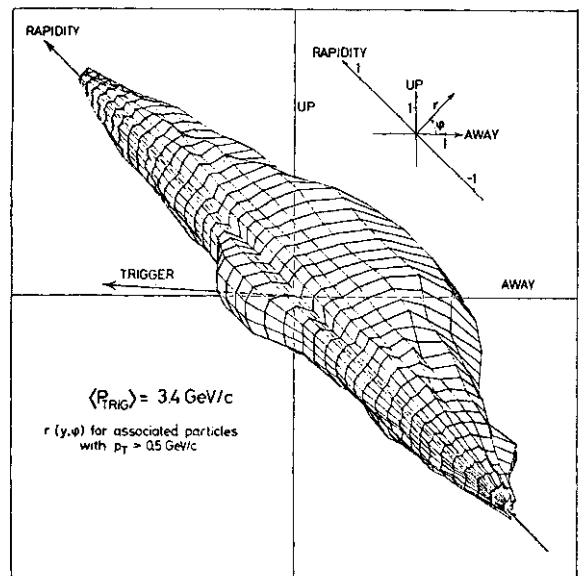


Fig. 3.

as shown in Fig. 3 obtained by the British-French-Scandinavian Collaboration (BFS)<sup>1</sup> who studied p-p collisions using the Split Field Magnet detector (SFM) at the CERN Intersecting Storage Rings (ISR). The large- $p_T$  charged particles were observed at  $90^\circ$ . In the same experiment a sample of average inelastic collisions called minimum bias events was recorded. To avoid the acceptance problem the data are presented in the form of the particle density ratio for large- $p_T$  events and minimum bias events.

The four regions where we expect to see four jets are not as distinct as it was shown in Fig. 2, nevertheless we can see a small hump towards the triggering high- $p_T$  particle, two spectator jets and a broad away bump which could be due to many superimposed "away" jets.

### §1. Trigger Jet

The simplest trigger used to study high transverse momentum phenomena is that indicating the presence of one secondary particle with a large  $p_T$ . The spectrum of transverse momentum has been recently measured up to 16 GeV/c. This has been performed for neutral pions produced in p-p collisions at the CERN Intersecting Storage Rings.<sup>2,3,4</sup> The inclusive spectrum has been measured for different collision energies and the data could be compared to the expression

$$E \frac{d^3\sigma}{dp^3} \sim p_T^{-n} f(x_T). \quad (1)$$

In the simplest version of the hard scattering model the first term describes the dynamics of the scattering whereas the second one reflects the momentum spectrum of constituents inside the hadrons. The quantity  $x_T$  denotes here the ratio of the transverse momentum to its kinematically allowed maximum value. At transverse momenta below 6-7 GeV/c inclusive distributions were well described by the formula (1) with  $w=8$ . All three experimental groups, who extended measurements to higher momenta, have shown that the exponent  $n$  decreases in the region of higher  $p_T$ . This is shown in Fig. 4. The exponent  $n$  is smaller than the value  $n=S$  obtained at lower  $p_T$  values. Nevertheless it is still larger than 4—the value expected for the

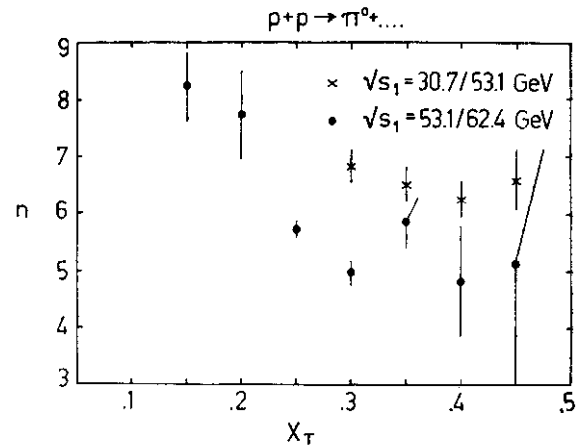


Fig. 4.

scattering of two spin 1/2 quarks interacting *via* a vector gluon exchange. However the mechanism of a vector gluon exchange is not ruled out because there exist many reasons why  $n$  is not equal 4. These are:

1. Scattered quarks have a substantial transverse motion.
2. Distribution of the normalized longitudinal momentum,  $x$  of quarks depends on the four-momentum transfer squared,  $-t$ .
3. The quark-gluon coupling constant depends on  $t$ .
4. At lower  $p_T$  other processes such as quark-gluon and gluon-gluon scattering are present.
5. Observed particles with a large  $p_T$  are the decay products of resonances produced with a relative rate which varies with  $p_T$ .
6. Single particle emission decreases with  $p_T$ .

Quantum chromodynamics justifies or predicts the first four effects. The fifth one—the production of resonances at large- $p_T$ —is based only on experimental observation. Two contributing papers by the CERN-College de France-Heidelberg-Karlsruhe (CCHK) Collaboration<sup>5</sup> and by the British-French-Scandinavian (BFS) collaboration<sup>1</sup> show that resonances give a rather important contribution to the production of charged particles with large  $p_T$  (Figs. 5 and 6). The analysis performed by the CCHK collaboration shows that in the region of  $p_T$  of 2-3 GeV/c there are as many  $\Lambda$ -mesons as pions coming from other sources than  $p^*$  decay. There is a slight evidence that the relative rate of  $p^0$  might increase with  $p_T$ .

The  $rf$  production was studied by the

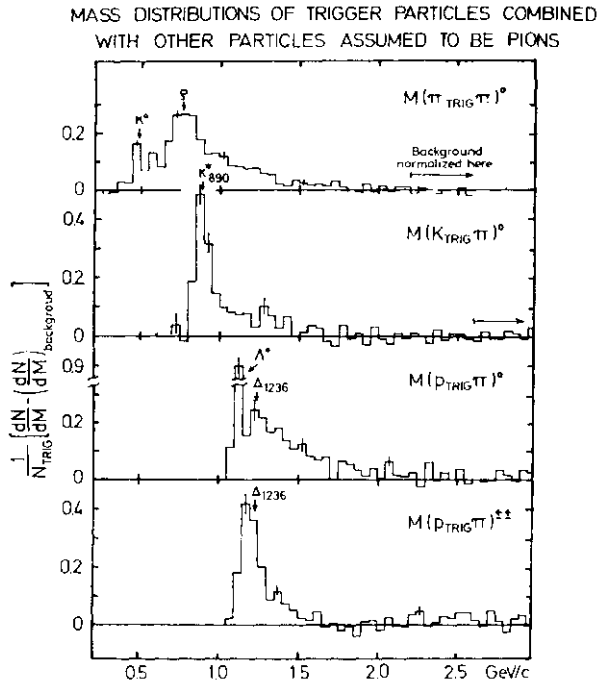


Fig. 5.

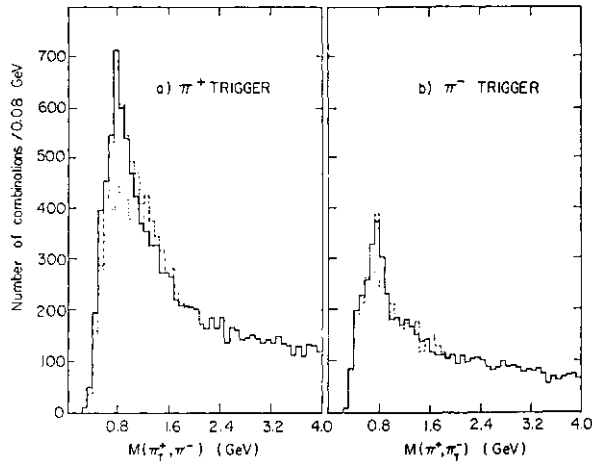


Fig. 6.

CERN-Saclay<sup>6</sup> and Brookhaven-CERN-Syracuse-Yale<sup>4</sup> Collaborations (Fig. 7). The latter showed that the rate of  $7r^0$ -mesons was  $0.56 \pm 0.02$  of the  $7r^+$  rate and depends neither on  $p_t$  nor on the energy of collisions.

The variation of the resonance contribution with  $p_t$  may affect the exponent  $n$  in formula (1). We should not worry too much that this means a non scaling  $z$  distribution where  $z$  stands for the fraction of the longitudinal momentum taken by a particle in a jet. The single particle trigger accepts only a small fraction of hard scattering collisions. Even if this fraction does not scale the overall effect of scaling violation will be weak.

The measurements of the Fermilab-Lehigh-

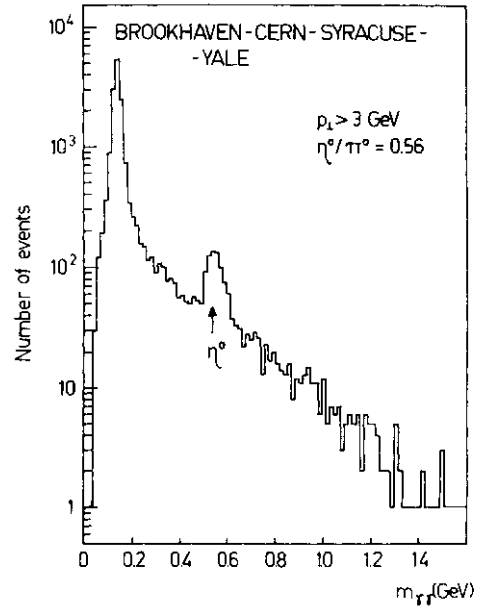


Fig. 7.

Pennsylvania-Wisconsin Collaboration<sup>7</sup> show that the inclusive cross section for the production of large- $p_t$  jets decreases with  $p_t$  less rapidly than does that for single particles (Fig. 8). We would rather believe that the  $p_t$  spectrum of scattered constituents is closer to the spectrum of jets than to that of single particle triggers. We should therefore analyze the validity of the formula (1) using the invariant inclusive cross section for large- $p_t$  jets.

A large transverse momentum particle is accompanied rather often by other secondaries emitted roughly in the same direction. This

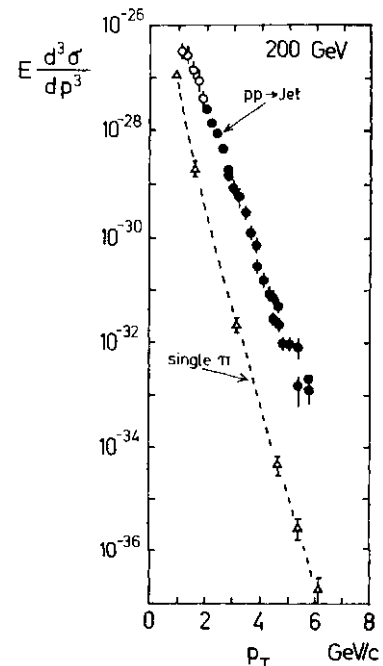


Fig. 8.

effect could be already seen in Fig. 3. The central slice of this figure cut perpendicularly to the rapidity axis is shown in Fig. 9. There is a clear excess of particles following the

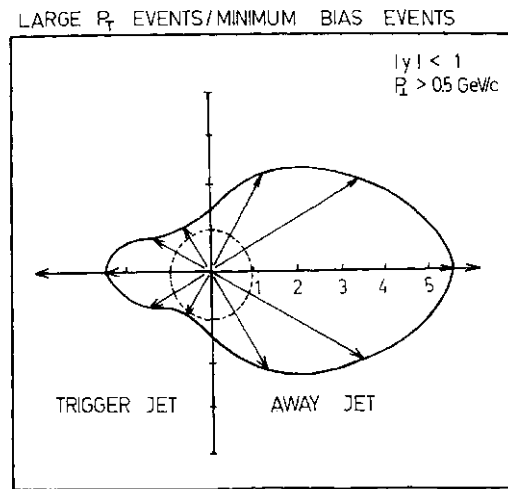


Fig. 9.

large- $p_T$  triggering particle and having therefore angles not very much different from that of the trigger. The collimation of particles in the direction of the large- $p_T$  trigger is also seen in the rapidity distributions.<sup>8</sup> In Fig. 10 se-

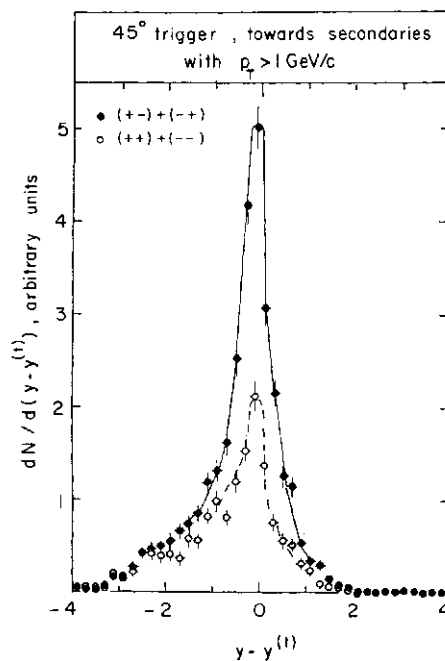


Fig. 10.

condaries with angles close to the trigger azimuthal angle are plotted versus the rapidity difference,  $y - y(\text{trigger})$ . Only secondaries with  $p_T > 1 \text{ GeV}/c$  are plotted. The sharp peak can not be explained by two-body resonances. It is seen in both charge combina-

tions and suggests the existence of the "trigger" jet.

The BFS Collaboration<sup>1</sup> has estimated the transverse momentum of jet fragments,  $q_T$ , measured with respect to the jet axis. Secondaries with  $p_T > 1 \text{ GeV}/c$  from the  $y$  and  $\langle p$  regions surrounding the trigger particles have been used. Results are shown in Fig. 11.

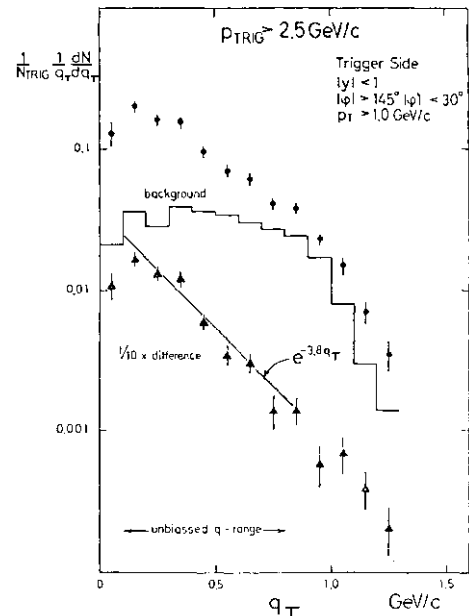


Fig. 11.

The background distribution was obtained by combining high- $p_T$  triggering particles with secondaries from minimum bias events. The authors conclude that

$$\langle \Lambda \rangle = (0.52 \pm 0.05) \text{ GeV}/c.$$

The CERN-Saclay Collaboration<sup>6</sup> has studied at ISR p-p collisions with a large transverse momentum seen as electromagnetic showers in the segmented lead-glass calorimeter. In addition charged tracks emitted in the same direction were also recorded. The direction of the trigger jet was approximated by a vector sum of the neutral particle momenta. The average transverse momentum with respect to this axis was found to be

$$\langle \#_i \rangle = 0.39 \pm 0.01 \text{ GeV}/c$$

for neutral particles and

$$\langle 0_i \rangle = 0.59 \pm 0.05 \text{ GeV}/c$$

for charged particles. The difference between two values is due to the definition of the jet axis. It has been found that the value of  $\langle q_T \rangle$  does not depend on the transverse momentum of the trigger (Fig. 12). The

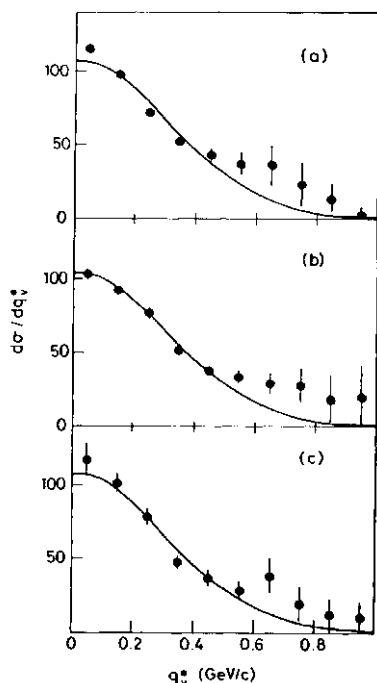


Fig. 12. Trigger transverse momentum: (a) 5~6 GeV/c; (b) 6-8 GeV/c; (c) >8 GeV/c.

trigger jet is therefore an object with fragments limited rather in  $q_t$  and not in their angular divergence.

Let us now summarize the experimental facts concerning the "trigger" jet.

- "Trigger" jet does exist. However, usually it is distorted by experimental conditions imposed by the trigger requirements.
- The invariant cross section for the large- $p_t$  particle production when fitted with formula (1) gives  $n > 4$ . However this does not rule out the quark-quark scattering via a vector gluon exchange.
- The ratio of the cross section to produce a large- $p_t$  jet to that for the single particle production is large and increases with  $p_t$ .
- A rather high rate of the resonance production is observed.
- The average transverse momentum of jet fragments with respect to the jet axis,  $\langle q_t \rangle$  is  $\sim 0.5$  GeV/c. This value does not depend on the momentum of jets.
- Little can be said about the distribution of jet fragments along the jet axis due to the trigger biases.

## §2. Away Jet

In Figs. 3 and 9 we can observe an excess of particles in the region where the away jet is expected to occur. It may be, however, only

the momentum conservation which sends particles to this region. To answer this question Cobb *et al.*<sup>9</sup> analyzed collisions with two neutral pions produced with large transverse momenta. It has been found that the two  $7c^0$ 's are usually emitted at azimuthal angles the difference of which is close to  $180^\circ$ . A possible reason for that is shown in Fig. 13.

AZIMUTHAL ANGLE BETWEEN TWO LARGE  $p_t$   $\pi^0$ 's

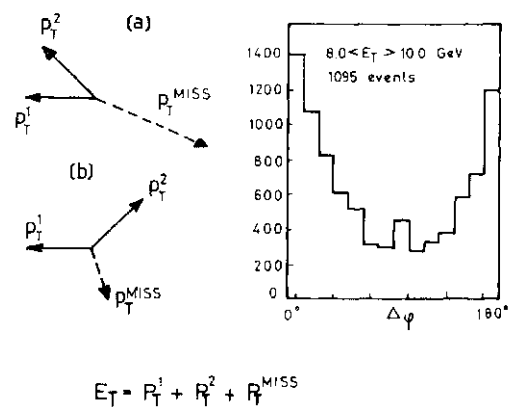


Fig. 13.

The configuration (a) is less frequent than (b) because in this case an extra object with a large- $p_t$  has to be produced to balance the momentum. In order to eliminate this effect the missing transverse momentum,  $p_T^{MISS}$  was determined for each event and the quantity  $E_T = p_T^1 + p_T^2 + p_T^{MISS}$  was calculated. If two  $7r^0$ 's and the object carrying missing transverse momentum are not correlated and are produced each with the probability  $\sim \exp(-Ap_t)$  the probability to observe a two  $7r^0$ 's event depends only on  $E_T$ . Selecting events with  $8 < E_T < 10$  GeV the authors obtained the distribution of the difference of azimuthal angles of two pions,  $\Delta\phi$ , as displayed in Fig. 13. We see that the particles show correlation at small  $\Delta\phi$  (trigger jet) as well as at large  $\Delta\phi$ . The latter correlation is of the dynamical nature and not the consequence of the momentum conservation.

It has been known from previous experiments<sup>8,10</sup> that the away particles show a strong positive correlation both in rapidity and azimuthal angle. Such a correlation is expected if away jets exist. Results submitted to the present conference support the previous observations. The British-French-Scandinavian Collaboration<sup>1</sup> presented in Fig. 14 the

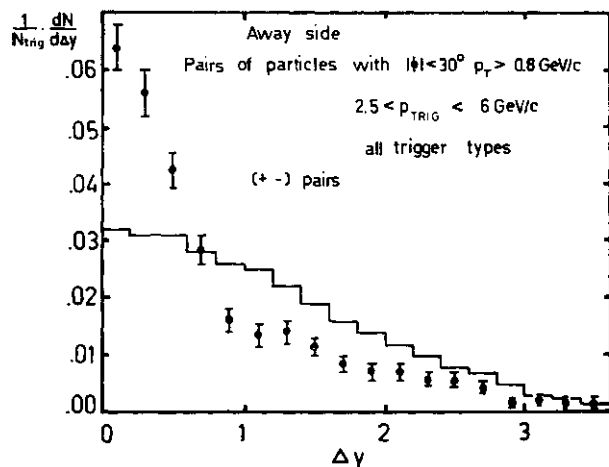


Fig. 14.

distribution of the rapidity difference of two away particles produced in the same collision. In this figure the distribution for uncorrelated pairs of particles coming from different events is also plotted. The comparison of two distributions shows that the emission of particles with similar rapidities is more frequent than expected for uncorrelated pairs. The CERN-Saclay Collaboration<sup>11</sup> displayed the same effect by plotting the correlation function

$$R = \frac{\text{observed distribution}}{\text{uncorrelated distribution}} - 1$$

versus the difference of pseudorapidities of two away particles (Fig. 15). The correlation is stronger for particles with larger transverse momenta.

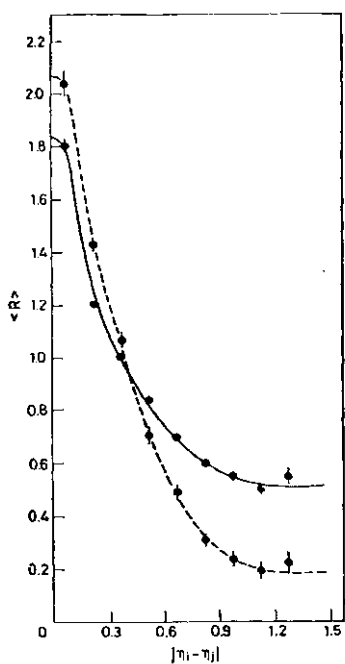


Fig. 15.

The collaboration estimated also the average value of the transverse momentum of jet fragments with respect to the jet axis. It was found to be identical for charged and neutral particles and equal to

$$\langle \#_j \rangle = 0.55 \pm 0.6 \text{ GeV}/c.$$

No dependence on the away jet momentum was observed. The average value of  $q_t$  was obtained assuming the gaussian distribution of each of two components of  $q_t$  and the cylindrical symmetry of the away jet.

Free from above assumptions is the result of the CERN - Columbia - Oxford - Rockefeller Collaboration.<sup>12</sup> Using the detector covering full azimuthal region for particles with pseudorapidities  $M < 0.7$  the collaboration measured independently the average values of two components of  $q_t$ . The component  $q_t$  was parallel to the plane given by momenta of incoming protons and the away jet axis whereas the component  $q_{\perp}$  was perpendicular to this plane.

The average values of two components versus the transverse momentum of away particle are plotted in Fig. 16. Both average

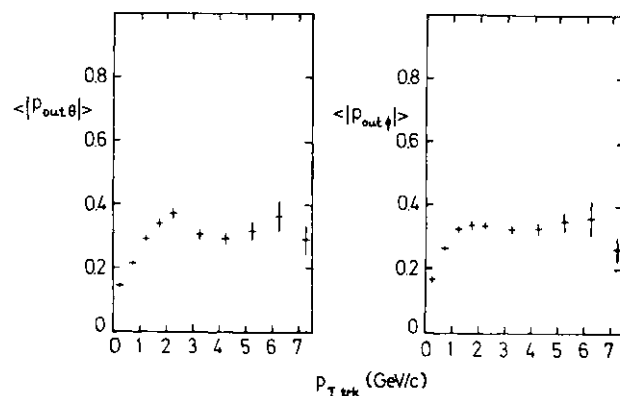


Fig. 16.

values are equal to 0.35 GeV/c and do not depend on the transverse momentum of particles.

The away jet fragments are often studied in terms of two quantities  $p_{out}$  and  $x_E$  defined in Fig. 17. We call "trigger plane" the plane containing the momenta of incoming hadrons and the momentum of a triggering particle. The momentum of an away particle is in general not parallel to this plane. Its component perpendicular to the plane we call  $p_{out\perp}$ . The transverse momentum component parallel to the trigger plane,  $p_{ft}$  and the trigger transverse momentum,  $p^{\wedge}$  define  $x_E$ .

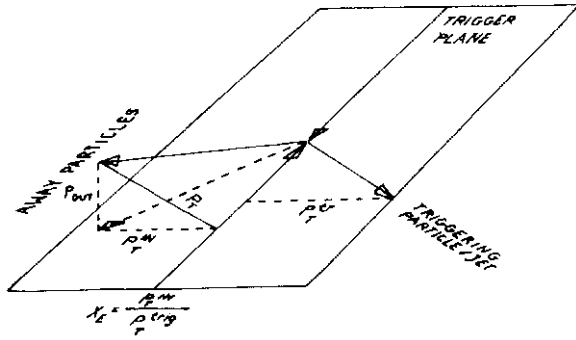


Fig. 17.

$$x_E = |p_T^{in}| / p_T^{trig}$$

It has been found previously that the  $p_{out}$  distribution is rather wide and that its average value increases with  $x_E$ .<sup>8</sup> This can be due to any of the following effects :

- the away jet is a diverging bunch of particles,
- there are more than one away jets,
- the away jet and the trigger jet are not coplanar, e.g., because interacting constituents have a transverse motion.

We have seen already that the average value of  $q_T$  for away jet fragments does not depend either on the jet momentum or on the momentum of the fragments. This observation rules out two first possibilities. We have to accept therefore that interacting hadronic constituents have a substantial transverse motion.

The Fermilab - Lehigh - Pennsylvania - Wisconsin Collaboration<sup>7</sup> has determined the transverse momentum of constituents,  $k_T$  using the double arm calorimeter detector. They triggered for events whenever the sum of the transverse momenta deposited in both calorimeters exceeded the threshold value. Two large- $p_T$  jets have been observed. It has been found, however, that their transverse momenta do not balance each other as it can be seen in Fig. 18. The distribution of the unbalanced transverse momentum was used to estimate the average  $k_T$  of constituents before collision. The value of  $k_T$  as high as 1 GeV/c was obtained. This value is consistent with that required in order to explain the wide spectrum of  $p_{out}$ . The experimental results presented at this conference have shown that for trigger momenta larger than 5 GeV/c and  $x_E$  close to one the average value of  $p_{out}$  reaches 1.2 GeV/c.

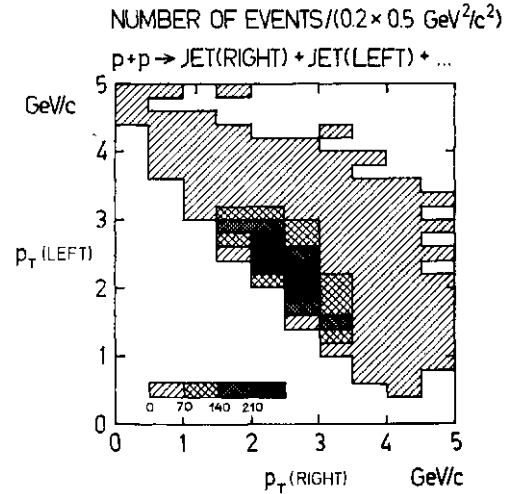


Fig. 18.

More details on the average value of  $p_{out}$  was presented by the CERN-Columbia-Oxford-Rockefeller Collaboration<sup>12</sup> as is shown in Fig. 19. According to this figure  $\langle p_{out} \rangle$  depends not only on  $x_E$  but also on the trigger transverse momentum. The authors warn a reader that the presented results are not corrected for the momentum resolution. There are however two other measurements which support the observation shown in Fig. 19. The

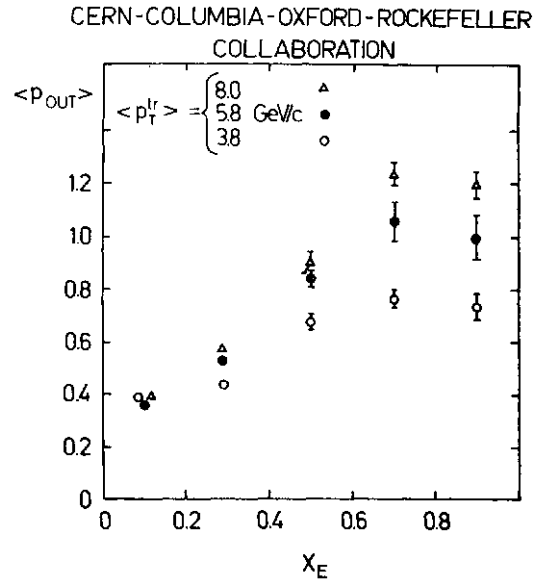


Fig. 19.

CERN-College de France-Heidelberg-Karlsruhe Collaboration<sup>8</sup> measured  $\langle p_{out} \rangle$  vs  $x_E$  for trigger transverse momenta in the region 2-3 GeV/c and the value  $\langle p_{out} \rangle = 0.7$  GeV/c was obtained. On the other hand the Brookhaven - CERN - Syracuse - Yale Collaboration obtained  $\langle p_{out} \rangle = 1.2$  GeV/c for very large



trigger transverse momenta. We can conclude therefore that the transverse momentum of constituents inside a hadron increases with the trigger transverse momentum. The harder is the collision the larger is transverse motion of colliding constituents.

From experiments on jets in  $e^+e^-$  and lepton-nucleon collisions it follows that fragments of jet scale in the normalized longitudinal momentum,  $z = p_{\text{out}}/p_{\text{in}}$ . For hadronic largely collisions the variable  $x_E$  is a good approximation of  $z$  for the away jet and therefore should exhibit a scaling behaviour. It has been shown however by the CCHK Collaboration<sup>8</sup> that the distribution  $dN/dx_E$  does not scale and depends on the transverse momentum of the trigger. This effect was interpreted as the consequence of the transverse motion of constituents inside incoming hadrons. Due to this motion  $x_E$  differs significantly from  $z$ . The difference between  $x_E$  and  $z$  should be, however, less important for collisions with a very largely values of a trigger. The results of the BFS Collaboration<sup>1</sup> show in fact that the  $dN/dx_E$  distribution of charged particles scales for transverse momenta of a trigger larger than 3 GeV/c (Fig. 20). Similar results were obtained by

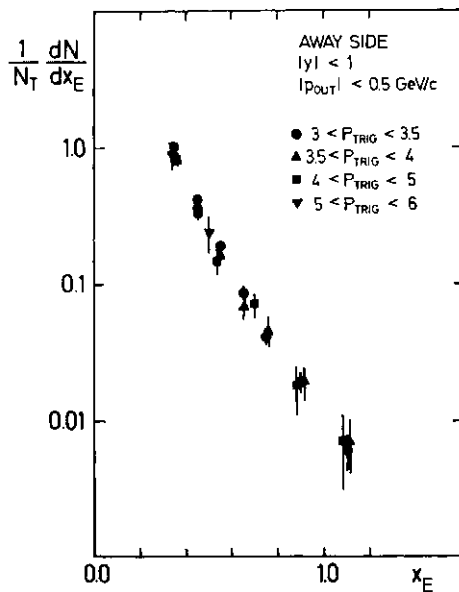


Fig. 20.

the CCOR Collaboration<sup>12</sup> for still higher trigger momenta. The BCSY Collaboration has measured the  $x_E$  distributions for neutral pions. They scale in a similar way as those for charged particles.

The CCHK Collaboration<sup>6</sup> studied the average electric charge of the fastest particle in the away jet. One would expect that it will reflect the charge of the scattered constituent. In the experiment the SFM detector was triggered by a large- $p_T$  charged particle emitted at the  $45^\circ$  polar angle. The subset of collisions with an away jet emitted with the rapidity opposite to that of the trigger was selected. The quantity  $X_j$  was defined to be a fraction of the transverse momentum of the trigger jet balanced by the charged fragments of the away jet. The average charge of the fastest away jet fragment,  $\langle q_f \rangle$  is plotted versus  $X_j$  (Fig. 21a). For  $X_j$  large enough when we

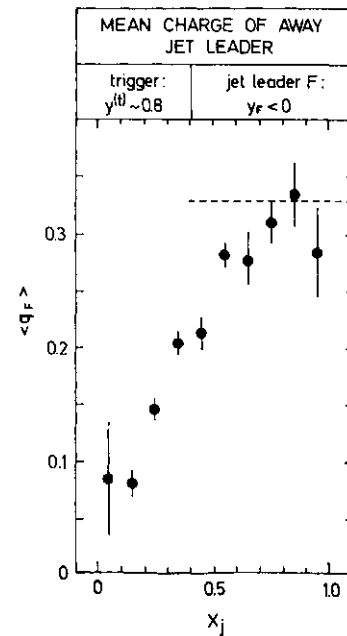


Fig. 21a.

do not expect that a neutral particle is the fastest one ( $q_f$ ) reaches the value  $1/3$  as expected from the quark-parton scattering picture.

The second subset of events was that with both trigger and away jets emitted with similar rapidities. Such a configuration occurs when a fast constituent (valence quark) scatters against a slow one (sea quark, gluon). When the trigger particle is positive the away jet originates more likely from a slow constituent and therefore  $\langle q_f \rangle$  should be close to zero. On the other hand the negative trigger should be associated with an away jet that comes from the scattered valence quark. The average charge of the leading particle should be in this case equal to  $1/3$ . Figure 21b supports

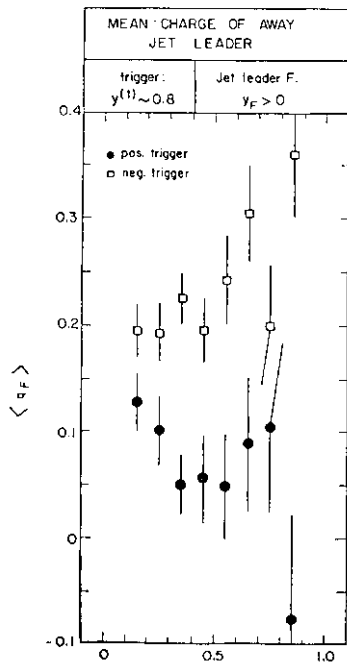


Fig. 21b.

these expectations.

The charge of particles in the away jet region was also studied by the BFS Collaboration<sup>1</sup>. The average number of positive and negative particles with  $p_T > 1.5 \text{ GeV}/c$  and  $|J| < 1$  was determined for different triggers. The results are shown in Fig. 22. For the  $K^-$

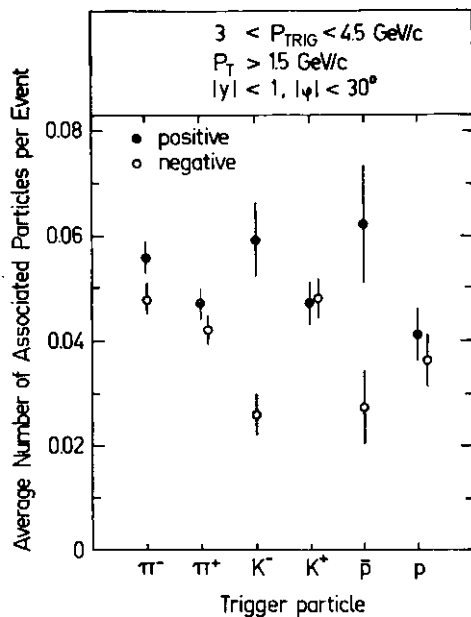


Fig. 22.

and  $p$  triggers there are twice as many positive particles as negative ones. This corresponds to the average charge of fast particles in the away jet equal to  $1/3$ . On the other hand for  $n^+$ ,  $K^+$  and  $p$  triggers the average charge of

highly away particles is close to zero. The data suggest that large- $p_T$   $K^-$ -mesons and antiprotons observed at  $90^\circ$  originate from constituents which scattered against the valence quarks of an incoming proton. Other large- $p_T$  particles do not show this behaviour. However going to much higher momenta the CERN-Saclay Collaboration<sup>11</sup> has found that a neutral-pion trigger is associated with an away jet in which the positive to negative particle ratio reaches the value 1.6 for the fastest jet fragments.

According to the hard scattering picture trigger and away jets come from a two-body scattering. We could expect therefore a rather strong correlation between polar angles (rapidities) of two jets due to energy-momentum conservation. Experimentally no clear correlation was observed for jets produced in proton-proton collisions. We can explain this as the result of the wide longitudinal momentum spectrum of hadronic constituents and their transverse motion. The correlation between two scattered constituents which has to be strong in the constituent rest system is depressed by the transformation to the laboratory system.

The situation is different for pion-proton collisions. The FLPW Collaboration<sup>7</sup> has shown that in this case both jets prefer to occur in the same hemisphere following the incoming pion. This is shown in Fig. 23 where the

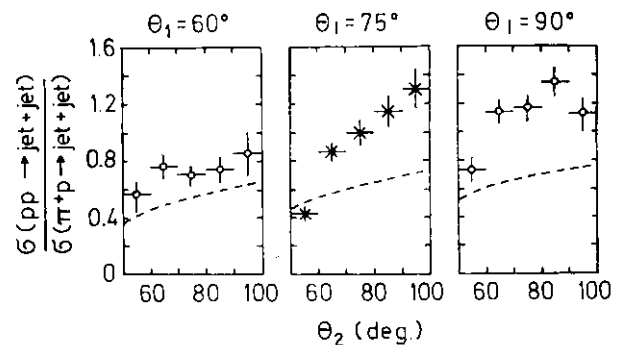


Fig. 23.

ratio of the production rate for two jets in  $p$ - $p$  collisions to that in  $n$ - $p$  collisions is plotted as a function of two jet polar angles,  $\theta_1$  and  $\theta_2$ . The angles are measured with respect to the incoming pion direction. We see that when both angles are small the two-jet production is higher in  $\pi$ - $p$  collisions than it is in  $p$ - $p$

collisions. This correlation supports the expectation that constituents of a meson carry in average a larger fraction of its momentum than it was observed for constituents of a proton. By comparing the two jet production rates in  $n$ - $p$  and  $p$ - $p$  collisions the collaboration was able to estimate the pion structure function.

Let us now summarize what we have learned about the away jet:

- It does exist. There is, however, no indication that there is more than one away jet.
- The transverse momentum of jet fragments with respect to the jet momentum,  $\langle q_{\perp} \rangle$  is equal to  $0.55 \pm 0.04$  GeV/c. This value is close to that observed for trigger jets.
- The average electric charge of leading particles,  $\langle q_{\perp} \rangle$  equals  $1/3$ . However, for the configurations of trigger and away jets for which we expect that a slow constituent recoils,  $\langle q_{\perp} \rangle \sim 0$ .
- The distribution of jet fragments (charged and neutral) versus the variable  $x_{\perp}$  scales.
- The average value of  $p_{\perp}$  increases with  $x_{\perp}$  and with  $p_{\perp}$  of the trigger. The average value of the transverse momentum of hadronic constituents,  $\langle k_{\perp} \rangle$  has to be as large as 1 GeV/c in order to explain this observation. Moreover  $\langle k_{\perp} \rangle$  should increase with the trigger  $p_{\perp}$ .
- The away jet transverse momentum does not balance that of the trigger jet. The value  $\langle k_{\perp} \rangle$  close to 1 GeV/c has to be assumed to explain this effect.

### §3. Spectator Jets

There is no doubt that two spectator jets are present in the collisions with a large transverse momentum object produced. They are clearly seen in Fig. 3. At the first sight they resemble an ordinary soft collision. However more detailed analysis shows some significant differences.

Let us look first at the transverse momentum distribution in the spectator jets. The BFS Collaboration<sup>13</sup> analyzed secondaries with  $0.2 < |x| < 0.6$  emitted perpendicularly to the trigger plane, *i.e.*, with  $\phi = \pm(90^\circ \pm 20^\circ)$ . The quantity  $x$  means here the fraction of the longitudinal cm momentum of an incoming hadron taken by a secondary particle. For

these particles the ratio  $R+1$  was plotted versus their transverse momentum (Fig. 24). The quantity  $R$  is defined as

$$R+1 = \frac{\text{particle density in large-} p_{\perp} \text{ collisions}}{\text{particle density in minimum bias collisions}}$$

We see that the ratio increases at large  $p_{\perp}$  which means that the  $p_{\perp}$  distribution in the spectator jets is wider than in the minimum bias collisions.

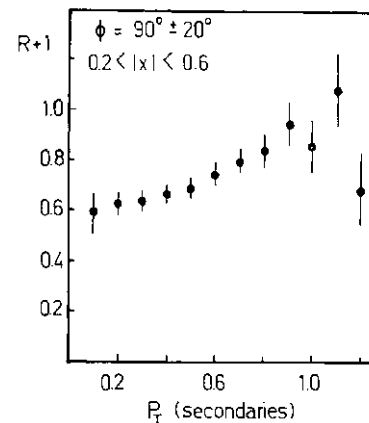


Fig. 24.

There are two reasons why transverse momenta of particles in the spectator jet are larger than those in soft collisions. The first one is that this is an intrinsic behaviour of the jet fragmentation. The similar effect we have already observed for trigger and away jets. However there exists also the possibility that spectator jet axis does not coincide with the direction of the incoming hadrons. Small deviation up or down will cause an apparent increase of the transverse momenta of jet fragments.

A similar effect has been pointed out by the CCHK Collaboration.<sup>8</sup> It has been suggested that the spectator jets should not follow exactly the line of flight of incoming hadrons but deviate slightly in the away direction. This is expected if the hadronic constituents have a transverse motion. In this case a large- $p_{\perp}$  trigger accepts more easily scatterings of constituents which move towards the trigger. Due to the momentum conservation spectator constituents undergo the recoil in the away direction.

In order to verify that, the BFS Collaboration selected forward particles with  $0.4 < |x| < 0.6$  and  $0.6 < |x| < 0.8$ . At these large  $x$  values

the admixture of particles from the away jet is small. To eliminate it further only particles with  $|p_z|$  larger than 0.4 GeV/c were taken. A  $p_z$  component is that perpendicular to the trigger plane. The average component of the transverse momentum in the trigger plane,  $p_s$ , was calculated and plotted versus the trigger  $p_t$ . A positive  $p_s$  means the away direction. It has been found (Fig. 25) that

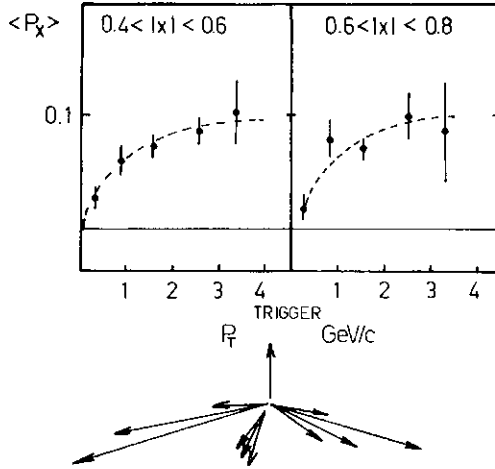


Fig. 25.

( $p_y$  increases with the  $p_t$  of a trigger at low values and then saturates. Such a behaviour is expected from the hard scattering model when constituents have a transverse motion.

According to the hard scattering picture spectator jets originate from hadronic constituents which do not take part in the hard collision. The nature of these constituents depends on the nature of the high- $p_t$  triggering particles. This has been confirmed by the analysis performed by the CCHK Collaboration.<sup>5</sup> For that, proton-proton collisions at  $\sqrt{s} = 52$  GeV with a large- $p_t$  particle emitted at  $20^\circ$  were used. It is natural to believe that the trigger jet and the spectator jet both going in the same longitudinal rapidity hemisphere come from the same incoming hadron (see the insert to Fig. 26). In this case we expect that the rapidity distribution of the left spectator jet does not depend on the nature of a high  $p_t$  trigger, contrary to the rapidity distribution in the right spectator jet. This expectation is well confirmed by Fig. 26. The ratio of the rapidity distributions associated with a large- $p_t$   $K^-$  to that associated with a large- $p_t$  negative pion is plotted for particles from spectator

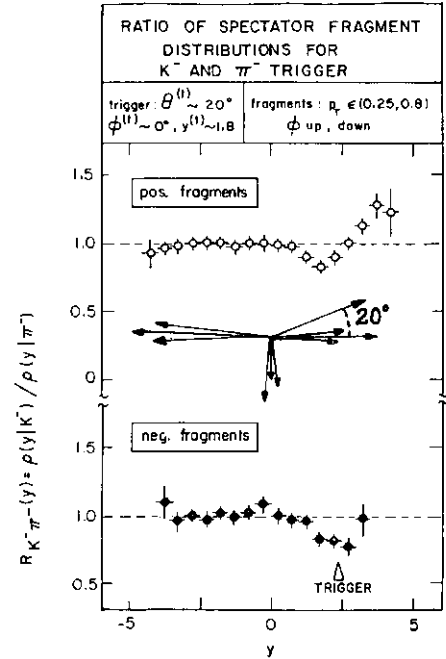


Fig. 26.

jets. As particles from spectator jets secondaries emitted roughly perpendicularly to the trigger plane were taken. The ratio of the two rapidity distributions is equal to one for negative rapidities for both positive and negative particles. The picture changes for positive rapidities where the influence of the nature of a large- $p_t$  trigger can be noticed.

The assumption that scattered constituents are quarks can be verified by looking at the longitudinal distributions of spectator jets. The counting rule predicts that the longitudinal distribution of a particle emitted from a system is of the form  $(1-x)^{2n-1}$  where  $n$  is the number of constituents remaining in the system. Here  $x$  denotes the fraction of the longitudinal momentum taken by the particle. It has been found that the counting rule describes relatively well longitudinal spectra of particles produced in soft collisions.<sup>14</sup>

The counting rule predicts, e.g., that the  $x$ -distribution of  $\bar{u}$ -mesons from a spectator system which contains a d-quark and a u-quark is of the form  $(1-x)^7$ . On the other hand, for a spectator system made of two u-quarks this distribution should be  $(1-x)^7$ . Contrary to the  $\pi$ -distributions, those predicted for  $TC$ -mesons and protons are identical for both spectator systems. In Fig. 27 the ratio of  $x$ -distributions associated with positive and negative pion triggers are plotted for spectator fragments. A good agreement with the pre-

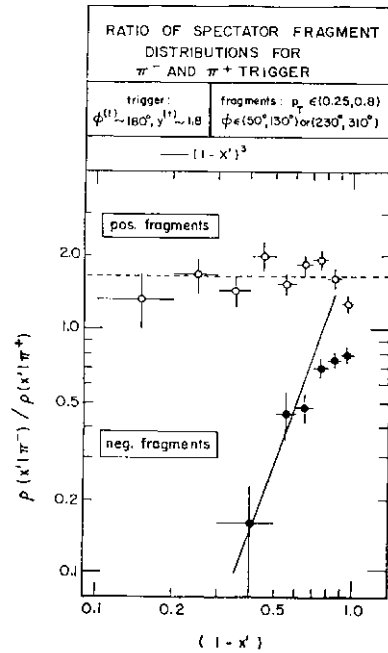


Fig. 27.

diction based on the quark-quark scattering picture is observed. Similar comparison performed for other triggers supports this picture. However, the data for the proton trigger suggest a di-quark scattering mechanism.

Studying the fragmentation of spectator jets the CCHK Collaboration has found that a short range rapidity correlation exists between jet fragments.

The correlation is, in fact, very similar to that observed for soft collisions. We conclude therefore that the spectator fragmentation occurs *via* a cluster-resonance emission.

Our knowledge on spectator jets can be summarized as follows:

- Spectator jets are not identical with the normal soft hadronic collisions although they show similar short range correlations in rapidity.
- The transverse momenta of jet fragments are larger than those of particles emitted in soft collisions. However, we have to verify whether it is the intrinsic jet behaviour or the reflection of the transverse motion of constituents.
- Spectator jets balance partially the transverse momentum of the large- $p_T$  trigger. This is probably the result of the transverse motion of hadronic constituents.
- The dependence of the longitudinal momentum distributions in spectator jets on the

nature of a trigger supports the assumption that constituents taking part in the hard scattering are quarks.

#### §4. Conclusions

- Experimental studies of large- $p_T$  phenomena in hadronic collisions have shown that a four-jet structure exists in the collisions.
  - The observed structure is consistent with the assumption that large- $p_T$  objects originate from scattered hadronic constituents.
  - Many aspects of the collisions indicate that the scattering constituents are quarks.
- We may therefore use the large transverse-momentum collisions as a tool to study the following phenomena:
- fragmentation of quark and di-quark systems,
  - dynamics of the quark-quark scattering,
  - structure functions of unstable hadrons (*it* and K mesons).

#### References

1. British-French-Scandinavian Collaboration, M. G. Albrow *et al*: "Studies of proton-proton collisions at the CERN ISR with an identified charged hadron of high transverse momentum at 90°, II On the distribution of charged particles in the central region," Paper No. 494/1 submitted to this Conference.
2. A. Clark *et al*: "Inclusive  $n^*$  production from high energy p-p collisions at very large transverse momenta," Phys. Letters **74B** (1978) 267.
3. CERN - Columbia - Oxford - Rockefeller Collaboration, A. L. S. Angelis *et al*: "A measurement of inclusive  $n^*$  production at large  $p_T$  from p-p collisions at the CERN ISR," paper No. 758 submitted to this Conference.
4. Brookhaven - CERN - Syracuse - Yale Collaboration, J. H. Cobb *et al*: "High transverse momentum  $\pi^+$  and  $y^+$  production at ISR," paper No. 677 submitted to this Conference.
5. CERN-College de France-Heidelberg-Karlsruhe Collaboration, D. Drijard *et al*: "Quantum number effects in events with a charged particle of large transverse momentum," paper No. 275 submitted to this Conference.
6. CERN-Saclay Collaboration, A. G. Clark *et al*: "Experimental study of the fragmentation of large transverse momentum jets in high-energy p-p collisions," paper No. 1085/1 submitted to this Conference.
7. Fermilab-Lehigh-Pennsylvania-Wisconsin Collaboration, M. D. Corcoran *et al*: "Results from a 2-arm calorimeter-array jet experiment," presented at Session A9 by W. Selove.

8. CERN-College de France-Heidelberg-Karlsruhe Collaboration, M. delia Negra *et al.*: Nucl. Phys. **B127** (1977) 1.
9. J. Cobb *et al.*: "Azimuthal correlations of high transverse momentum  $TT^0$  pairs at the ISR," preprint BNL-23637, OG 396.
10. P. Darriulat *et al.*: Nucl. Phys. **B107** (1976) 429 and **B110** (1976) 365.
11. CERN-Saclay Collaboration, A. G. Clark *et al.*: "Large transverse momentum jets in high-energy p-p collisions," paper No. 1085/11 submitted to this Conference.
12. CERN-Columbia-Oxford-Rockefeller Collaboration, A. L. S. Angelis *et al.*: "Results on correlations and jets in high transverse momentum p-p collisions at the CERN ISR," paper No. 758/11 submitted to this Conference.
13. British-French-Scandinavian Collaboration, M. G. Albrow *et al.*: "Studies of proton-proton collisions at the CERN ISR with an identified charged hadron of high transverse momentum at  $90^\circ$ . I: On forward particles in higher reactions," paper No. 494/11 submitted to this Conference.
14. R. E. Diebold: rapporteur talk at this Conference. Session P1b.

## P2b

# Dilepton Production in Hadron Collisions

L. M. LEDERMAN

*Columbia University, New York, N.Y. 10027*

### §1. Introduction

This subject had its inception in a critical letter published in *Il Nuovo Cimento* in 1966 by one of our hosts, Prof. Y. Yamaguchi.<sup>1</sup> In that paper, he criticized a search for  $W^+$  mesons carried out by a Columbia group.<sup>2</sup> He pointed out that the reaction we were looking at,  $pN \rightarrow W^+ + X$  would be dominated

by a background  $pN \rightarrow \gamma + X$  in which  $\gamma$  goes

to  $j\bar{j}$  pair and in which the effective mass of the virtual photon is equal to that of  $W^+$ .

This comment stung us because we had not thought about it at all. (This was also independently pointed out by Okun.<sup>3</sup>) However it also gave us an idea that massive virtual photons could be used as probes for small distance physics. In 1966-67 we designed an experiment for the 30 GeV AGS at Brookhaven,  $pN \rightarrow \ell^+ \ell^- X$ .<sup>4</sup>

In our proposal we argued that this was a good way to search for bumps and also to probe small distances.

Figure 1 is then a thumbnail ten year

Dilepton Production in Hadron Collisions  
Brief History

1968: Columbia-BNL Proposal to Probe Small Distances Using Virtual Photons and to Look for Bumps.

1978: Tokyo

Bumps Have Been Found:  $J/\psi$ ,  $\psi'$ ,  $T$ , ...

"Small Distance Probe" Has Found a Constituent (Quark-Gluon) Model Which is Completely Consistent with Lepton Scattering.

Fig. 1.

history and summary of my talk after which the reader can skip to the bibliography to see if I have referred to him properly. In 1978 at Tokyo, we have found bumps:  $J/\psi$ ,  $\psi'$  and the  $Y$  family, and what we called, "small distance probe" has become a parton model that successfully correlates all reactions involving leptons and hadrons by virtual photons and  $W$ 's. That is the optimistic argument

I will try to present. I do this grudgingly because it is clearly much more fun to confound the theorists. An outline of this talk follows:

- II. Upsilon Physics
- III. Search for New (and Old) Bumps
- IV. Dilepton Continuum Physics
  - A. Comments on Drell-Yan analysis
  - B. Experimental results
  - C. Applications of Drell-Yan analysis
  - D. Dilepton transverse momenta

Table 1a lists the groups whose data are discussed here together with the dehumanizing acronym that must be used to identify the group. Table 1b gives a resume of the respective experimental parameters.

### §11. Upsilon Physics

The CFS group (FNAL), see Fig. 2. There have been four runs:

1) There was the May-August 1977 run of about 1200 upsilons at 400 GeV where the resolution was about 2%, average intensity  $\sim 2 \times 10^8$  ppp.<sup>5a</sup>

2) September-November 1977 runs at 200 to 300 GeV to get scaling data.<sup>5d</sup> This yielded about 500 upsilons with about the same resolution.

STUDY OF SCALING IN HADRONIC PRODUCTION OF DIMUONS

J.K. Yoh, S.W. Herb, D.C. Hom, L.M. Lederman,  
J.C. Sens, and H.D. Snyder

Columbia University, New York, N.Y. 10027

and

K. Ueno, B.C. Brown, C.N. Brown, W.R. Innes,  
R.D. Kephart, and T. Yamaguchi

Fermi National Accelerator Laboratory, Batavia, Ill. 60510

and

R.J. Fisk, A.S. Ito, H. Jostlein, and D.M. Kaplan

State University of New York, Stony Brook, N.Y. 11974

Fig. 2.

3) November 1977-April 1978 high intensity ( $\sim 8 \times 10^8$  ppp) at 400 GeV, largely looking for higher mass bumps with a somewhat degraded resolution ( $J_m/m \sim 2.3\%$ ).

Table 1a. Principal contributors.

At Fermilab:	
Columbia-Fermilab-Stony Brook	CFS
Seattle-Northeastern-Michigan-Tufts	SNMT
Chicago-Illinois-Princeton	CIP
At ISR:	
CERN-Columbia-Oxford-Rockefeller	CCOR
CERN-Saclay-Zürich	CSZ
(Athens) <sup>2</sup> -CERN-BNL-Syracuse-Yale	ABCSY
CERN-Harvard-Frascati-MIT-Naples-Pisa	CHFMNP
Saclay-Imperial-Southampton-Indiana	SISI

mining the position (in the bending plane) of a point on each trajectory served to improve the resolution from 2.0 to  $\sim 1.7\%$ . In order to have this chamber survive, 60 cm of steel was added to our Be absorber and the proton intensity decreased to  $\sim 3 \times 10^6$  ppp. We also obtained some improvement from converting our PWC's to "mini" drift chambers. Figure 5 shows the results of this run with continuum subtracted and one sees the separation of  $Y$  and  $Y'$  now very clearly. As usual  $Y''$  is indicated by a shoulder on the high

Table 1b. Quality of dilepton data ( $V s > 10, m > 5$ ).

Group	Reactions	$\sqrt{s}$	$\Delta\sqrt{\tau}$	$\Delta x_F$	$\Delta m/m$	No. of events $> 5$ GeV	Assoc. particle capability
CFS (Lederman)	pN	19	0.18-0.65	+0.30→0.60	2%	180,000	No
		23.7		+0.10→0.40			
		27.3		-0.15→+0.75			
SNMT (Garelick)	pN	27.3	0.22-0.60	0.1→0.6	6%	275,000	No
ABCSY (Willis)	pp	52	0.1-0.15	$\pm 0.2$	4%	$\sim 100$	Yes
		63	0.085-0.16				
CHFMNP (Ting-Belletini)	pp	63	0.08-0.24	-0.3 → +0.9	10%	$\sim 300$	Yes
CCOR (DiLella)	pp	63	0.08-0.22	-0.2 → +0.2	5%	$\sim 60$	Yes
CP II (Pilcher-Smith)	$\pi$ N	21	0.15-0.50	$\sim 0 \rightarrow 1.0$	$\sim 5\%$	3,000	No
SISI	$\pi$ N	17	0.20-0.60	0 → 0.8	1.5%	$\sim 80$	Yes

About 7,000 upsilons were collected.

4) Finally we turned to higher resolution. Changes in the apparatus yielded a  $\Delta m/m \sim 1.5\%$ . About 500 upsilons were collected. These data will appear in various places in the talk.

The data were presented to this conference by T. Yamanouchi.

Figure 3 gives the data from run 1) and Fig. 4 is the result of the long high intensity run 3). The upsilin peak in the new data clearly shows the effects of the poorer resolution, the apparatus suffering under the very high rates ( $\sim 10-20 \times 10^6$  ppp). Nevertheless there is data out to  $\sim 20$  GeV, the upsilin is still there (the good news) but the several intriguing (1-2.5 standard deviation) peaks seen in Fig. 3 have all disappeared from Fig. 4 (see later). In order to improve resolution, we installed a specially designed PWC upstream of the spectrometer magnet<sup>5</sup> in a place where the rates normally exceeded 100 Mcps. Deter-

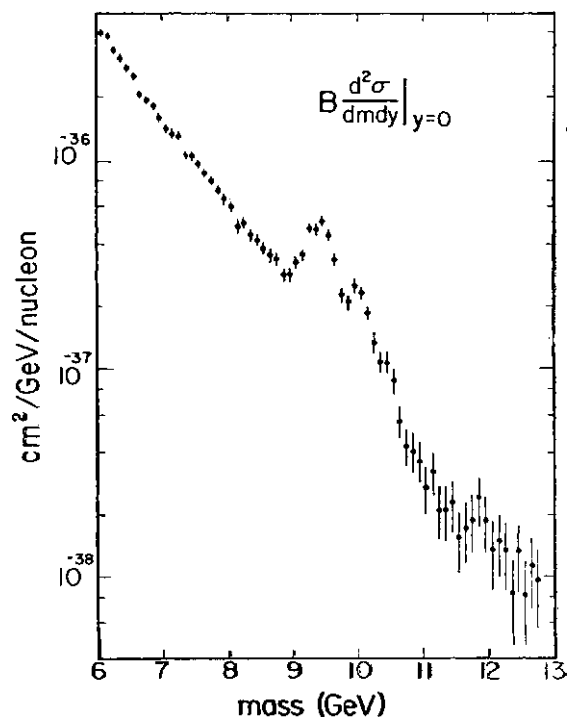


Fig. 3. CFS dimuon data, Summer '75.



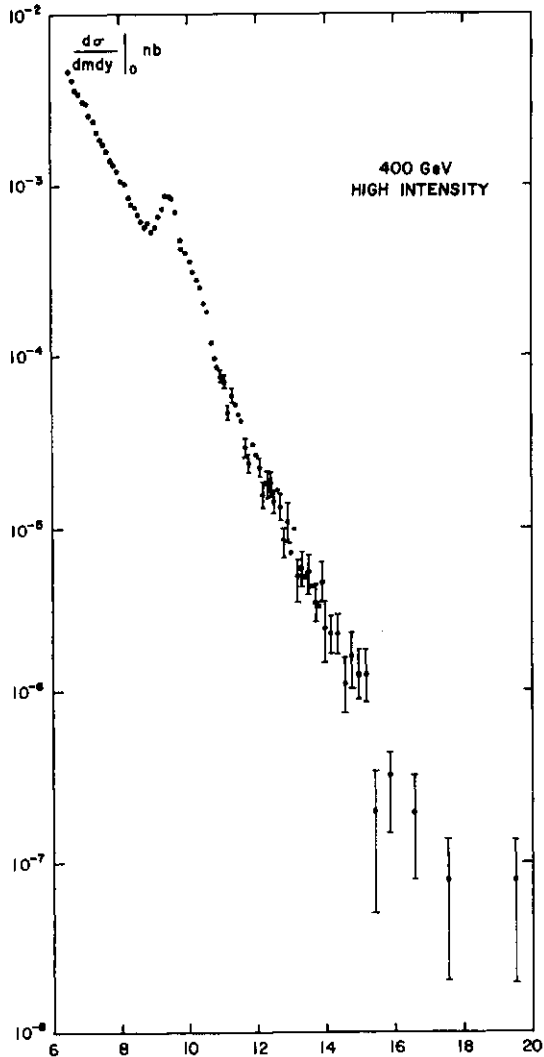


Fig. 4. CFS dimuon data, high intensity.

side of the  $Y$ . Table II shows the result of an analysis that was carried out using *all* of our data. We note that there are strong correlations between the strength of the third peak and the spacing between  $Y$  and  $Y'$ . If we insist there is *no* third peak, the fitting program increases  $\Delta m_{QT} - Y'$  from 590 MeV to 709 MeV. Note that the  $\chi^2/DOF$  increases, the  $Y''$  being favored by  $\sim 40\%$ . Several days ago, the DES Y groups reported the observation of  $Y''$  in  $e^+e^-$  collisions.<sup>6</sup> Their mass splitting is:  $555 \pm 3$  or  $557 \pm 5$  MeV.\* This splitting was imposed upon the CFS analysis program (*via* telephone) and the result is presented in Table III. Note that under *this* assumption, the  $Y''$  becomes a  $\sqrt{3} < j$  effect. So we have (at least) three narrow peaks. There is another way to designate the upsilon family, which has certain advantages in Japan:  $Y, Y', Y''$ .

\* Newer DESY data (Bienlein *et al.*, DESY 78/45) gives  $J_{\psi} = 560 \pm 10$  MeV.

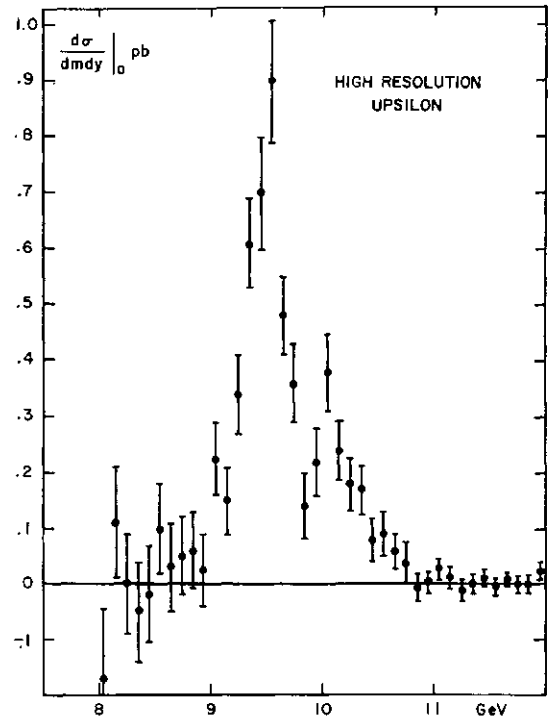


Fig. 5. CFS high resolution upsilon peak with continuum subtracted.

Table II. Upsilon analysis—All data.

	3 Peak Fit	2 Peak Fit
$m(Y)$	$9.46 \pm 0.001 \pm 0.10$	$9.47 \pm 0.006 \pm 0.10$
GeV	$0.27 \text{ pb}$	
$B(d\sigma/dy)(Y)$	$0.96 \pm 0.03$	$1.02 \pm 0.03$
$(d^2\sigma/dm \cdot dy)$ (cont.) GeV		GeV
$m(Y') - m(Y)$	$0.590 \pm 0.035$	$0.709 \pm 0.012$
GeV	$m(Y') = 10.05$	10.18
$B(d\sigma/dy)(Y')$	$0.31 \pm 0.03$	$0.35 \pm 0.015$
$m(Y'') - m(Y)$	$0.96 \pm 0.06$	—
GeV	$m(Y'') = 10.42$	
$B(d\sigma/dy)(Y'')$	$0.16 \pm 0.04$	—
$\chi^2/DF$	213/225	247/227
Comment:	$Y''$ is $\sim 4\sigma$	

The SNMT group at FNAL, see Fig. 6. This was described to us by P. Mockett as a forward spectrometer based on magnetized iron deflection of muons. It is a very high statistics experiment; with a large  $x_r$  acceptance but obtained at the expense of resolution. Figures 7a, b show their data. When one subtracts a continuum fit (7b), one sees a substantial  $Y$  peak representing the entire, unresolved  $Y$  family. The signal to continuum is in good agreement with CFS in spite of the large  $x_r$  acceptance.

Table III.  $p_T$  fit parameters.<sup>a,b</sup>

$\sqrt{s}$ (GeV)	$C$	$p_0$
19.4		
	$C$	$p_0$
$M$	(fb. GeV <sup>-2</sup> )	(GeV)
4.5	7169 ± 208	2.07 ± 0.049
5.5	1592 ± 59	2.34 ± .055
6.5	470 ± 21	2.34 ± .061
7.5	121 ± 9.9	2.19 ± .099
8.5	26.3 ± 4.4	2.01 ± .186
9.5	7.22 ± 2.07	2.29 ± .393
	23.7	
	$C$	$p_0$
4.5	9006 ± 250	2.25 ± .055
5.5	2648 ± 79	2.41 ± .044
6.5	842 ± 30	2.60 ± .055
7.5	326 ± 16	2.59 ± .068
8.5	104 ± 8.0	2.53 ± .097
9.5	70.5 ± 5.5	2.65 ± .111
10.5	19.3 ± 3.0	2.65 ± .247
	27.3	
	$C$	$p_0$
4.5	10310 ± 419	2.62 ± .095
5.5	2887 ± 55	2.70 ± .035
6.5	1058 ± 25	2.74 ± .036
7.5	386 ± 13	2.86 ± .050
8.5	163 ± 6.4	2.78 ± .058
9.5	130 ± 5.6	3.10 ± .075
10.5	41.8 ± 3.1	2.83 ± .112
11.5	10.2 ± 1.9	2.21 ± .202

\*  $E-(d^*oid)^* = -c(i+(pipy)^6$   
<sup>b</sup> Significant data extend to about 3 GeV/c in  $p_T$ .  
 See Kaplan *et al.* (réf. 5c).

A High Statistics Study  
 of Dimuon Production by 400 GeV/c Protons\*

S. Childress<sup>1</sup>, D. Garelick<sup>2</sup>, P. Gauthier<sup>2</sup>, M. Glaubman<sup>2</sup>,  
 H.R. Gustafson<sup>3</sup>, H. Johnstad<sup>2</sup>, L. Jones<sup>3</sup>, M. Longo<sup>3</sup>, M. Mallery<sup>2</sup>,  
 P. Mockett<sup>1</sup>, J. Moromisato<sup>2</sup>, W. Oliver<sup>4</sup>, T. Roberts<sup>3</sup>,  
 J. Rutherford<sup>1</sup>, S. Smith<sup>1</sup>, E. von Goeler<sup>2</sup>, M. Whalley<sup>3</sup>,  
 R. Weinstein<sup>2</sup>, and R. Williams<sup>1</sup>

Washington-Northeastern-Michigan-Tufts Collaboration

Fig. 6.

*ISR Dileptons.* We now have contributions from the ISR where the intrinsically low luminosity is compensated by the very high energy, providing an essential lever arm for studying  $\gamma$ -behavior. *The CCOR group* (Fig. 8) has a superconducting solenoid with drift chambers inside and lead glass shower spectrometer outside. They operate in the low  $\beta$  section of the ISR with twice the average luminosity. The data as presented by L. Camilleri has a hardware threshold at  $\sim 5$  GeV and is given in Fig. 9. One sees continuum events and a very clear  $Y$  peak. *The ABCSY*

RESULTS(8/13/78) MNMT COLLABORATION FERMILAB EXP. 439

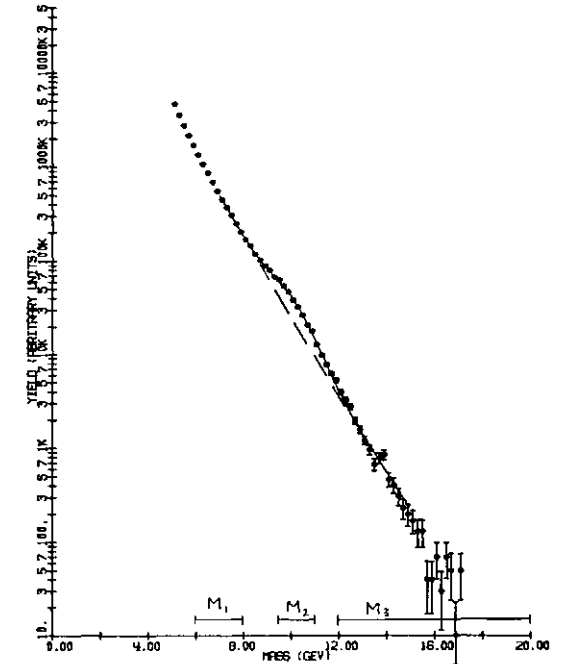


Fig. 7a. SNMT dimuon data 400 GeV protons at FNAL.

PRELIMINARY RESULTS(8/6/78) MNMT COLLABORATION FERMILAB EXPT. 439

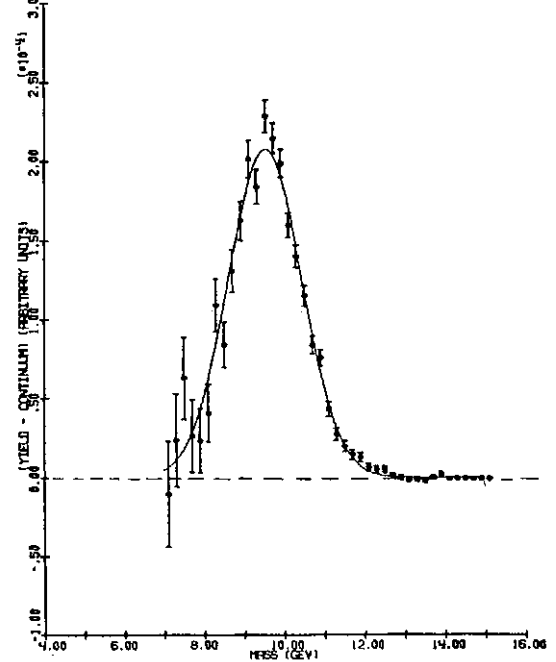


Fig. 7b. SNMT upsilon peak, continuum subtracted.

A Study of High Mass  $e^+e^-$  Pairs produced in p-p Collisions  
 at the CERN ISR

CERN<sup>1</sup>-Columbia<sup>2</sup>-Oxford<sup>3</sup>-Rockefeller<sup>4</sup> (CCOR) Collaboration  
 A.L.S. Angelis<sup>3</sup>, B.J. Blumenfeld<sup>2</sup>, L. Camilleri<sup>1</sup>, T.J. Chapin<sup>4</sup>,  
 R.L. Cool<sup>4</sup>, C. del Papa<sup>1</sup>, L. Di Lella<sup>1</sup>, Z. Dimčovski<sup>4</sup>,  
 R.J. Hollebeek<sup>2</sup>, D. Levinthal<sup>2</sup>, L.M. Lederman<sup>2</sup>, J.T. Linnemann<sup>4</sup>,  
 L. Lyons<sup>3</sup>, N. Phinney<sup>3</sup>, B.G. Pope<sup>1a</sup>, S.H. Pordes<sup>1</sup>, A.F. Rothenberg<sup>4\*\*\*</sup>,  
 A.M. Segar<sup>3</sup>, J. Singh-Sidhu<sup>1</sup>, A.M. Smith<sup>1</sup>, M.J. Tannenbaum<sup>4</sup>,  
 R.A. Vidat<sup>2\*\*\*</sup>, J. Wallace-Hadrill<sup>3</sup>, T.O. White<sup>3†</sup> and J.M. Yelton<sup>3</sup>.

Fig. 8.

(Fig. 10) data were presented by I. Mannelli as in Fig. 11. This is a detector based upon liquid argon calorimetry with transition radiation to help select electrons. What is dramatic here is the valley just before the  $T$  peak. Note

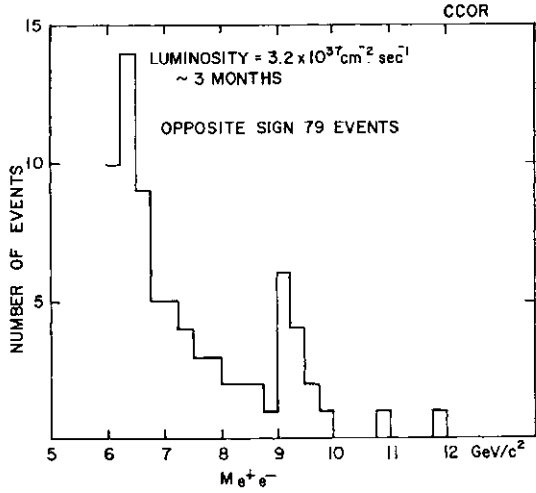


Fig. 9. CCOR electron pair data at  $V s = 62$  GeV (ISR).

ABCSY Group  
ELECTRON PAIRS PRODUCTION AT THE ISR

C. Kourkouvelis and L.K. Resvanis  
University of Athens, Athens, Greece

T.A. Filippas, E. Fokitis  
National Technical University, Athens, Greece

A.M. Cnops, J.H. Cobb<sup>6</sup>, S. Iwata<sup>1</sup>, R.B. Palmer, D.C. Rahm,  
P. Rehak, S.D. Smith and I. Stumer  
Brookhaven National Laboratory<sup>2</sup>, Upton, New York 11973, USA

C.W. Fabjan, T. Fields<sup>3</sup>, E. Fowler<sup>9</sup>, I. Mannelli<sup>4</sup>,  
P. Mouzourakis, K. Nakamura<sup>5</sup>, A. Nappi<sup>4</sup> and W.J. Willis  
CERN, Geneva, Switzerland

M. Goldberg  
Syracuse University<sup>7</sup>, Syracuse, New York 13210, USA

and

A.J. Lankford<sup>8</sup>  
Yale University, New Haven, Connecticut 06520, USA.

Fig. 10.

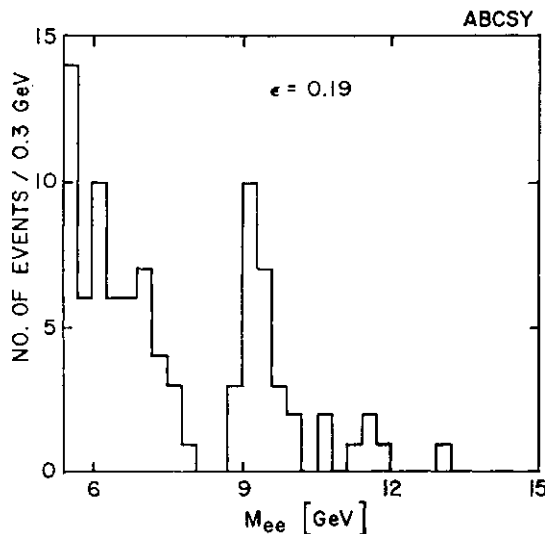


Fig. 11. ABCSY  $Y$  dielectron data at ISR.

that the previous two experiments see  $T$  in its  $e^+e^-$  mode. Comparison with CFS *via* scaling or with what follows is a (so far) crude test of  $ju\sim e$  universality in the timelike sector at  $Q^2 \sim 100$  GeV<sup>2</sup>. The CHFMNP (Fig. 12) data were presented by H. Newman (Fig. 13). This

CHFMNP Group  
MEASUREMENT OF HIGH-MASS MUON PAIRS AT VERY HIGH ENERGIES

D. Antreasyan, W. Atwood, V. Balakin, U. Becker,  
G. Bellezzini, P.L. Braccini, J.G. Branson, J. Burger,  
F. Carbonara, R. Carrara, R. Castaldi, V. Cavasinni,  
F. Cervelli, M. Chen, G. Chiofalo, T. Del Prete, E. Drago,  
M. Hodous, T. Lagerlund, P. Laurelli, O. Leistam, R. Little,  
P.D. Luckey, M.H. Massai, T. Matsuda, L. Merola,  
M. Morganti, M. Napolitano, H. Newman, D. Novikoff,  
L. Parasso, K. Reibel, J.P. Revol, R. Rinsivillo, G. Sanguinetti,  
C. Sciacca, P. Spillantini, K. Strauch, S. Sugimoto,  
S.C.C. Ting, W. Toki, M. Valdata-Nappi, C. Vannini,  
F. Vannucci, P. Visco and S.L. Wu

(CERN-Harvard-Frascati-MIT-Naples-Pisa Collaboration)

Fig. 12.

detector has large iron toroids and is sensitive to  $J/\psi$  pairs. This is the largest aperture detector (Table 1b) and has the largest number of events but with the poorest resolution resulting from coulomb scattering in iron.

We put these data together in Fig. 14 to

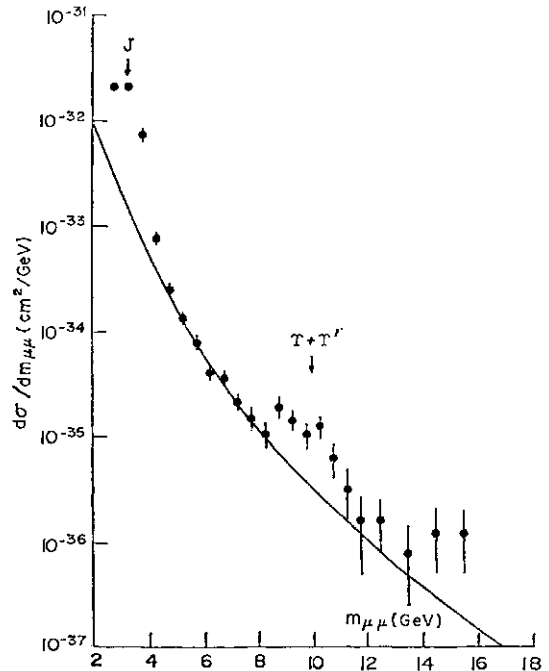


Fig. 13. CHFMNP dimuon data at ISR ( $V s = 62$  GeV).

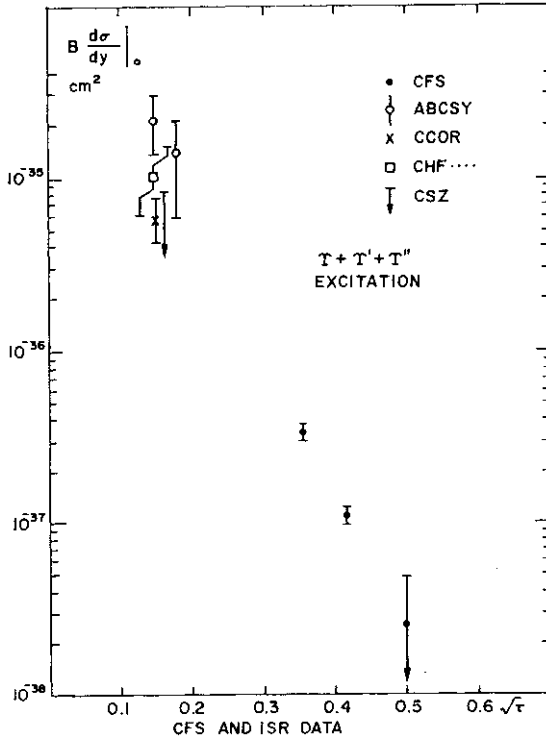


Fig. 14. Upsilon excitation curve.

obtain an excitation curve of  $Y$  production. We are plotting  $B(da/dy)|_0$ . I have added an upper limit point from CERN-Saclay-Zurich group which was presented by M. Banner. There is some mild controversy. If we overlay a continuum scaling curve (which will be discussed later), one finds that it gives a rough agreement in slope although there is evidence that the continuum levels off whereas the resonance production continues to climb as  $m_{jj}$  decreases. We now summarize up-silon physics :

1. There are three vector mesons at 9.46, 10.02, and 10.4 GeV. In hadron production at  $AJS = 27$  GeV,  $B(da/dy)|_0$  ratios are as 1: 0.3: 0.15. An early paper of Ellis *et al.*<sup>7</sup> predicted 1: 0.3: 0.12 just after the up-silon discovery. This was under the assumption that  $Y=QQ$  (bound state) and  $e_0 = -1/3$ , in agreement with the recent DESY results,<sup>6</sup> *i.e.*  $Q=b$  (beauty or bottom).

2. The up-silon excitation curve behaves roughly like  $e^{-2.0 \Lambda'}$ .

3. The  $Y$ - $Y$  splitting is sensitive to the details of the  $bb$  force but it is clear that it cannot be very different from the  $cc$  force.

4. The ratio of up-silon production to continuum at 400 GeV is 1.26 GeV. At the ISR (3800 GeV), it increases to 4-6 GeV.

5. The CFS group has also determined that the 6-quark, bound to  $u, d$  cannot be stable.<sup>7a</sup>

### §111. Search for New (and Old) Bumps

The CFS experiment, in its  $e^+e^-$  phase with  $Am/m \sim 1\%$  at 400 GeV reported<sup>8</sup> an interesting activity near 6 GeV. Now they have looked carefully at the high resolution dimuon data. See Fig. 15. The  $\langle p' \rangle$  is confirmed but every-

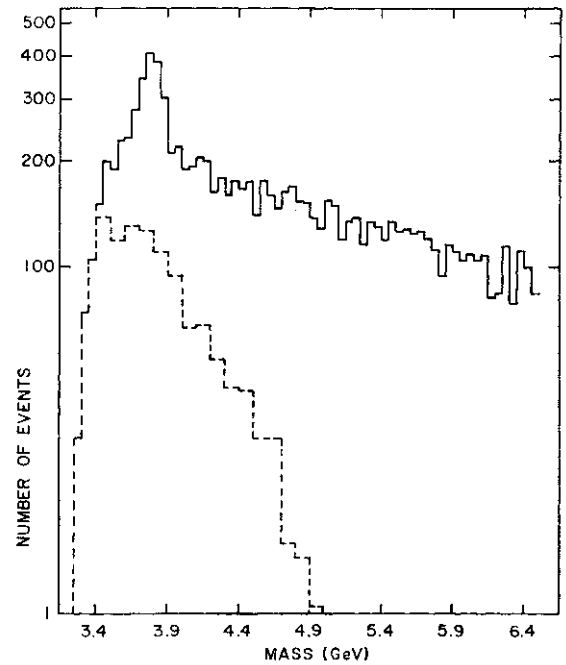


Fig. 15. CFS high resolution data with expanded low mass region. Dashed curve is like sign background.

thing else looks absolutely smooth. In the high mass region, Fig. 4 shows the CFS high intensity data with two events at 19.5 GeV. The continuum fit is also shown. We see only the traditional "bump" that universally appears at the data endpoint. See also Fig. 13. I have two comments: i) In CFS old data, our endpoint was 10 GeV and sure enough, the last data point was high! ii) A paper submitted by Mori, Muraki and Nakagawa to this Conference on logarithmic mass scaling predicts the next quarkonium level at precisely 19.5 GeV!!

Figure 16 shows a dimuon mass spectrum initiated by 225 GeV  $\pi$  reactions at Fermilab presented by Anderson for the CIP group (Fig. 17). Here again, no bumps. The failure to observe  $Y$  may very well be due to the low energy—CFS do not see up-silon at 200 GeV.

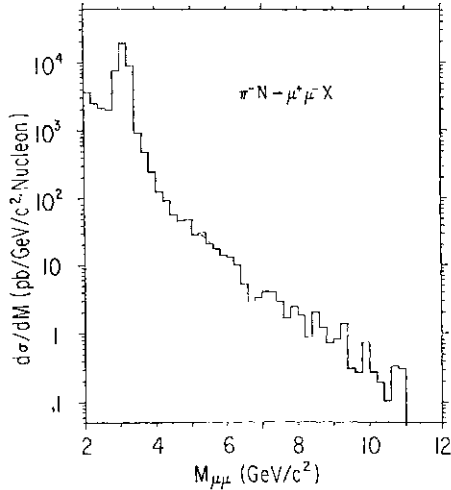


Fig. 16. CIP dimuon data using 225 GeV pions at FNAL.

CIP Group  
 Hadronic Production of High-Mass Muon Pairs and the Measurement  
 of the Pion Structure Function\*  
 K.J. Anderson, R.N. Coleman, K.P. Karhi, C.B. Newman, J.E. Pilcher,  
 and E.I. Rosenberg  
 Enrico Fermi Institute, University of Chicago, Chicago, Illinois 60637 U.S.A.  
 J. J. Thaler  
 University of Illinois, Department of Physics, Urbana, Illinois, 61801 U.S.A.  
 and  
 G. E. Hogan, K.T. McDonald, G.H. Sanders and A.O.S. Smith  
 Joseph Henry Laboratories, Princeton University, Princeton, New Jersey 08540 U.S.A.

Fig. 17.

To quantify the absence of enhancements for  $m > 11$  GeV, we use the CFS data and assume quite generally that a  $4a$  resonance would have been claimed. Thus we can set limits according to the following:

mass	14.5	15.5	17	$\geq 18$ GeV
upper limit				
$B(d\sigma/dy) _0$	10	6	4	$1 \text{ cm}^2$
$\times 10^{+40}$				

Finally we can discuss the specific case of a  $QQ$  state where  $e_q = 2/3$ , i.e.,  $u$ -quark (top or truth). Here a specific limit can be placed on the mass of the  $u$ -quark if we accept a scaling theorem, e.g., that of Gaisser, Halzen, and Paschos<sup>9</sup> or Ellis *et al.*<sup>1</sup> They propose:

$$\sigma B(t\bar{t})/\sigma B(Y) = (M_Y/M_{t\bar{t}})^3 \cdot F(\tau)_{t\bar{t}}/F(\tau)_Y$$

$\cdot \Gamma_{\mu\mu}^{t\bar{t}}/\Gamma_{\mu\mu Y}$  and  $\Gamma_{\mu\mu}/e_Q^2$  scaling,

a form that fits  $p$ ,  $\langle j \rangle$ ,  $\langle p \rangle$ ,  $T$  production. From this, we constructed the following table:

$M(t\bar{t})$	Expected $\sigma B$	90% Confidence Limit
14	$\sim 7.0 \times 10^{-39}$	$\leq 10^{-39}$
16	$1.0 \times 10^{-39}$	$\leq 5 \times 10^{-40}$

$$18 \quad 9 \times 10^{-41} \quad < 10^{-40}$$

On these assumptions, we can conclude that:

$$M_t \geq 7.5 \text{ GeV.}$$

we can also set a limit for  $qq$  state with  $e^A = 1/3$ :

$$M_q \geq 6.5 \text{ GeV.}$$

#### §IV. Dilepton Continuum Physics

##### A. Comments on Drell-Yan analysis

Early in the history of this subject, soon after the 1968 BNL data<sup>1</sup> appeared, Drell and Yan<sup>10</sup> proposed a model for the production of virtual photons: the now famous parton-antiparton annihilation model. In the very widespread application of this model, the parton is a valence quark from one of the colliding nucleons and the anti-parton was an anti-quark from the "sea." The diagram is shown in Fig. 18. Annihilation kinematics

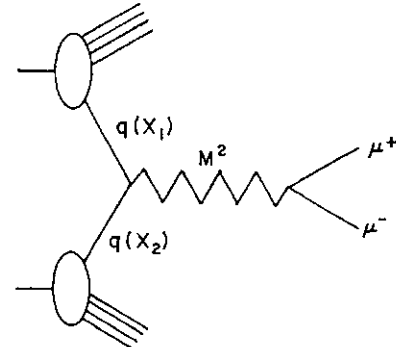


Fig. 18. Drell-Yan process.

yields:

$$x_1 x_2 = (m^2/s) \equiv \tau \quad x_1 = \sqrt{\tau} e^y$$

and

$$x_1 - x_2 = x_F \quad x_2 = \sqrt{\tau} e^{-y} \quad \text{a)}$$

The D-Y model enables one to express the dilepton spectrum as a factored product of a quark (valence) distribution and an anti-quark (sea) distribution:

$$\sigma \sim \sum q(x_1) \bar{q}(x_2) + (x_1 \leftrightarrow x_2) \quad (2)$$

e.g. in the case  $x_F \approx 0$ ,  $x_1 = x_2 \equiv x = \sqrt{\tau}$  and:

$$d^2\sigma/dm dy|_0 = 8\pi\alpha^2/3 \cdot 3m^3 \times S(x) [\nu W_2^{ep}(x) + \nu W_2^{en}(x)]. \quad (3)$$

Note that one of the factors of "3" in the denominator of the RHS comes from the color degree of freedom. Note also that in (3), we have substituted the inelastic electron proton and electron neutron structure functions for

the valence quark distributions. In the above, we have assumed an  $SU_3$  symmetric sea:

$$\bar{u}(x) = \bar{d}(x) = s(x) \equiv S(x). \quad (4)$$

The model has a logical series of necessary prerequisites:

1. The collisions must be *hard*.
2. Scaling is implied: At fixed  $y$ ,  $nf da/dm$  depends only on  $r$ .

*B. Experimental results*

We now look at the data.

1. *Hard collisions* are strongly indicated by the behavior of  $da/dm$  with the atomic number  $A$ . Figure 19 from CFS and Fig. 20 from CIP

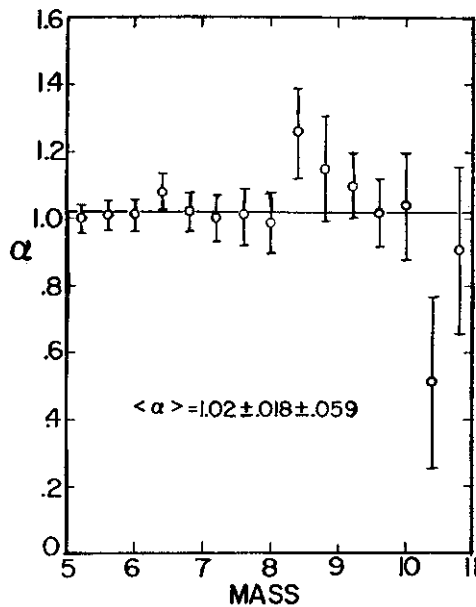


Fig. 19. CFS data on  $a$  vs where  $a \sim A$ .

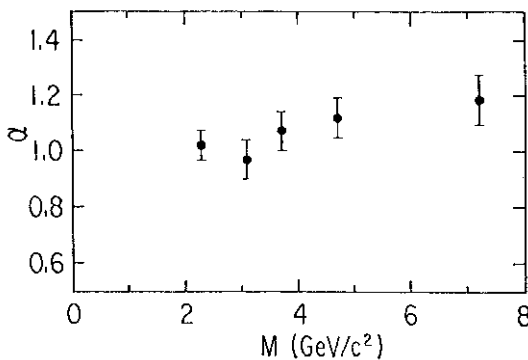


Fig. 20. CIP data on  $a$ -dependence (225 GeV pions).

show that  $a=1$  for sufficiently massive dileptons in both proton and pion-induced collisions. Here we ignore the possibility that  $a$  can exceed unity.

2. *Scaling* has recently been tested by CFS.<sup>54</sup> Their data taken at 200 GeV, 300

GeV and 400 GeV are shown in Fig. 21. When the data are plotted in dimensionless form,

$$m^3(d^2\sigma/dm dy) \text{ or } s(d^2\sigma/d\sqrt{\tau} dy),$$

we find (Fig. 22) that all three energies coalesce to a curve which depends only on  $r$ . Even the old BNL data<sup>4</sup> fit on this universal curve to better than a factor two. The crucial question is whether this form which, at FNAL, spans a small interval of  $s$  is still valid at ISR where  $\sqrt{s}=2000$  GeV,  $\sqrt{s}=62$  GeV. For earlier results, see ref. 11.

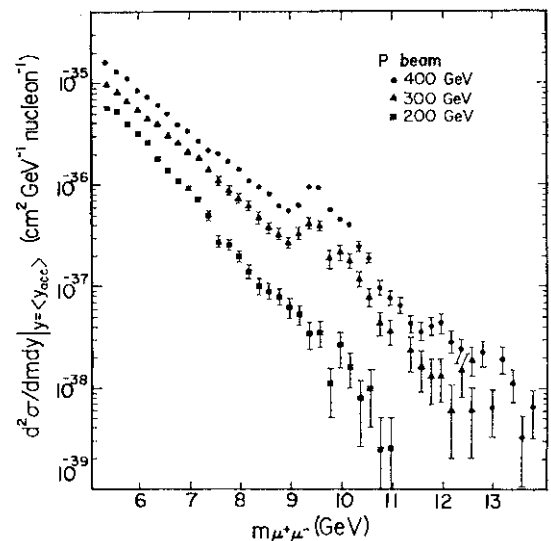


Fig. 21. CFS dimuon spectra at various energies.

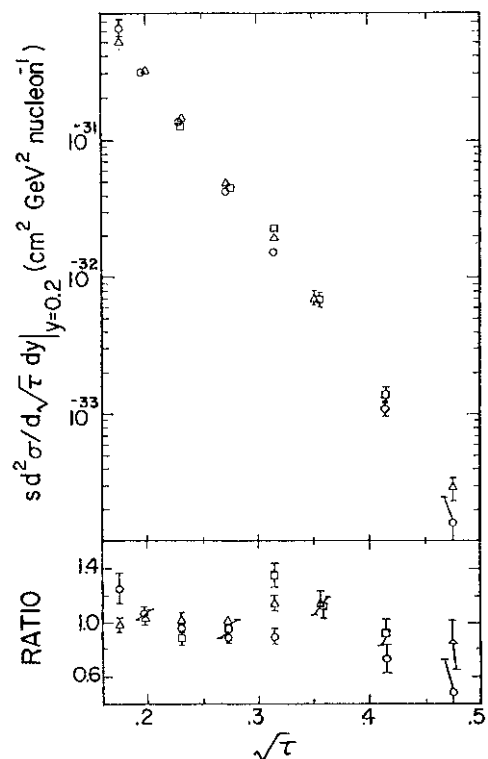


Fig. 22. CFS scaling plot.

Figure 23 presents the analytical "fit" to the CFS universal curve and the ISR data.

*Conclusions.* The scaling fit for pN collisions:

$$s(d^2\sigma/d\sqrt{\tau}dy)|_0 = 44.4e^{-26.6\sqrt{\tau}}\mu b \quad (5)$$

is valid over  $0.1 < V < 0.6$ ;  $50 < s < 3800 \text{ GeV}^2$ . The "validity" is at the level of the  $\pm 20\%$  normalization errors. These are sufficient to mask the scaling violations we now know should be there at  $y/r > 0.2$ . There is evi-

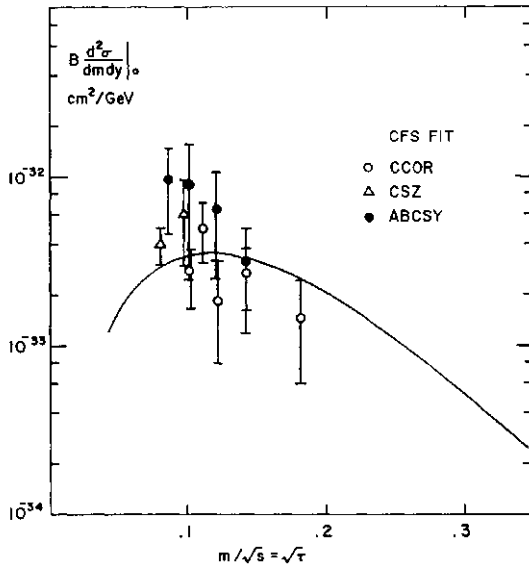


Fig. 23. Confrontation of CFS ( $V_s = 19 \rightarrow 27$ ) scaling fit with ISR electron pair data ( $\sqrt{s} = 63$ ).

dence that for  $yV < 0.1$ , the yields exceed the Drell-Yan predictions and probably indicate some other mechanisms. In the case of pion-induced data, we have contributions from CIP (225 GeV), SISI (150 GeV) and Rochester-NSF-BNL (16 and 22 GeV). These do not show scaling behavior but some of the data are preliminary and so I will not dwell on this here.

C. Applications of Drell-Yan analysis

1. Sea distributions

Having satisfied the prerequisites, we now apply the model in a "natural" way:

1. We substitute for the  $\nu W_2$  terms the data on deeply inelastic electron and muon scattering—mainly the newer results from FNAL.<sup>12</sup> Here we note that  $\nu W_2$  depends

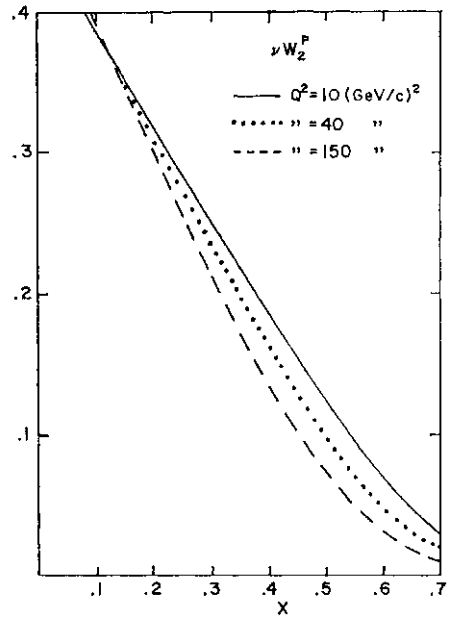


Fig. 24. Fits to FNAL muon scattering data.

on  $x$  and  $CP$  and we set  $|Q^2| = m^2$ . Figure 24 shows the input data for the valence distributions.

2. We use the CFS dimuon spectra (Figs. 16, 21) to derive a sea distribution.

3. We then compare this with  $\nu, \bar{\nu}$  scattering data (BEBC, CDHS) in order to test the overall consistency.

All of this used to be called the Drell-Yan model. Then it became the naive D-Y model. Now, I believe, it is called naive QCD theory and it may well be called naive general relativity before we are through.

In the CFS 400 GeV data<sup>5c</sup> the application of  $\nu W_2[x, g^2 - 10 (\text{GeV}/c)^2]$  to eq. (3) gave:

$$S(x) = 0.6(1-x)^{10}$$

However, when scale breaking data,  $\nu W_2(x, Q^2)$  were installed, they derived a result:

$$S(x) = 0.5(1-x)^8$$

due to the fact that, at high  $Q^2$ ,  $\nu W_2$  falls more rapidly with  $x$ . Now with most recent  $\nu W_2$  data from Fermilab<sup>12</sup> and the  $y \rightarrow 0$  data from CFS, we find the following results for the sea:

$$\begin{aligned} \text{Set } \bar{d} &= A(1-x)^n \\ \bar{u} &= \bar{d}(1-x)^\alpha \\ \bar{s} &= \bar{d}(1-x)^\beta \end{aligned}$$

Trial	A	n	α	β	χ <sup>2</sup> /DF
SU(3) (eq. 4)	0.54 ± 0.02	8.5 ± 0.1	0	0	237/181
Field-Feynman <sup>13</sup>	0.57 ± 0.02	7.4 ± 0.1	3	1	214/181
Free	0.56 ± 0.02	7.5 ± 0.15	2.6 ± 0.6	1.5 ± 4	213/179

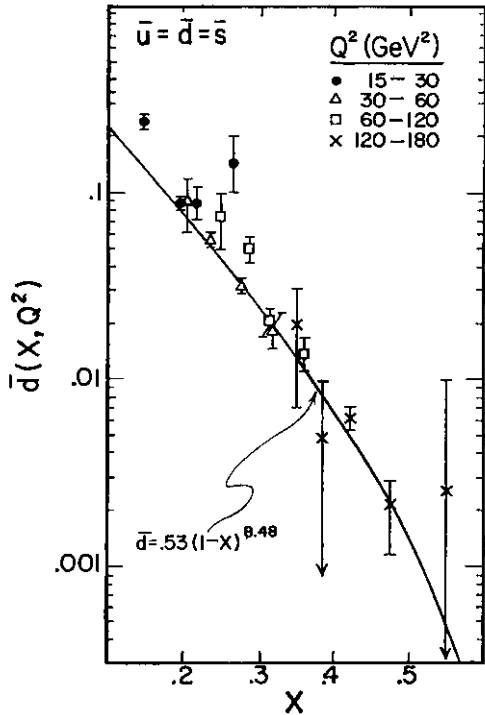


Fig. 25. Sea distribution fit from CFS data.

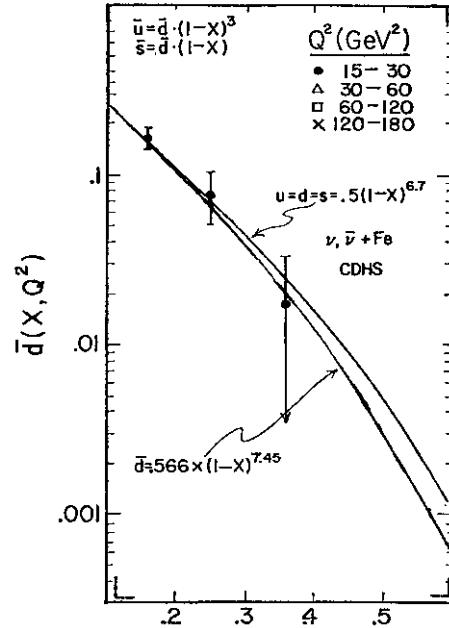


Fig. 27. Comparison of CFS dimuon sea fit with CHDS neutrino scattering fit from K. Tittel, this Conference.

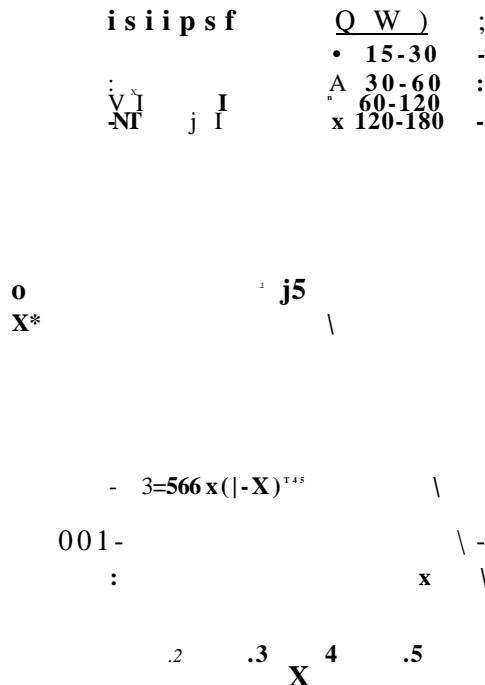


Fig. 26. Sea distribution from CFS data with  $\hat{u}^d$ .

Note that although there is no evidence for strong  $Q^2$  dependence, the large  $x$  region is dominated by high  $Q^2$  data only. Now the most exciting result at this conference, I find, is the comparison of our sea fit (Fig. 26) with the CDHS data as shown in Fig. 27. We note the agreement:

CFS (dimuons)

$$\bar{d}(x) = (0.56 \pm 0.02)(1-x)^{7.5 \pm 0.15}$$

CDHS ( $\nu, \bar{\nu}$  scattering)

$$\bar{d}(x) = 0.5(1-x)^{6.7 \pm 0.5}$$

CERN data from BEBC are consistent with these forms.

We conclude:

1. The D-Y model or its QCD version now permits a parameter free prediction of the reaction:

$$p+N \rightarrow \mu^+ \mu^- + \text{anything}$$

using as input, the data on

$$e, \nu + N \rightarrow \mu^+ + \text{anything}$$

and

$$\nu, \bar{\nu} + N \rightarrow \mu^+ + \text{anything}.$$

We believe this to be a remarkable achievement.

2. The color factor of "3" is required.

3. There is evidence that the sea is not SU(3) symmetric, a prediction by Field and Feynman.



2. Rapidity distribution

The FNAL CFS data have a rather narrow  $\wedge$ -acceptance which moves with incident energy (Fig. 28). Under the scaling hypothesis, this permits a respectable coverage in  $y$ . Figure 29 shows that the three energies combine to give a smooth picture of the  $j$ -behavior. If we calculate the slope of the  $\wedge$ -distribution at  $y=0$ , we have a new test of the D-Y model presented in Fig. 30. The solid line is the D-Y model predictions obtained from the  $y=0$  data at 400 GeV. The agreement in

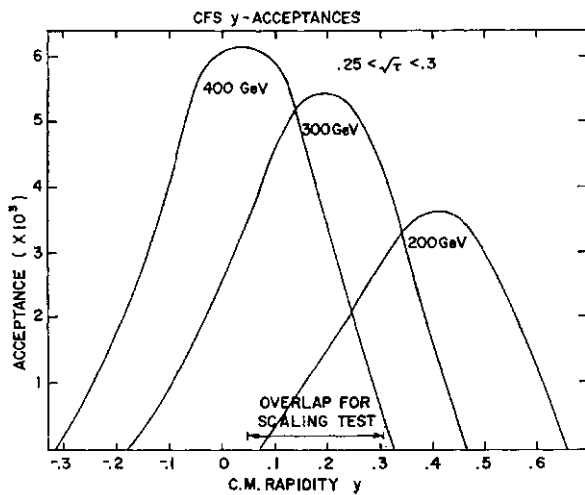


Fig. 28. CFS rapidity acceptances.

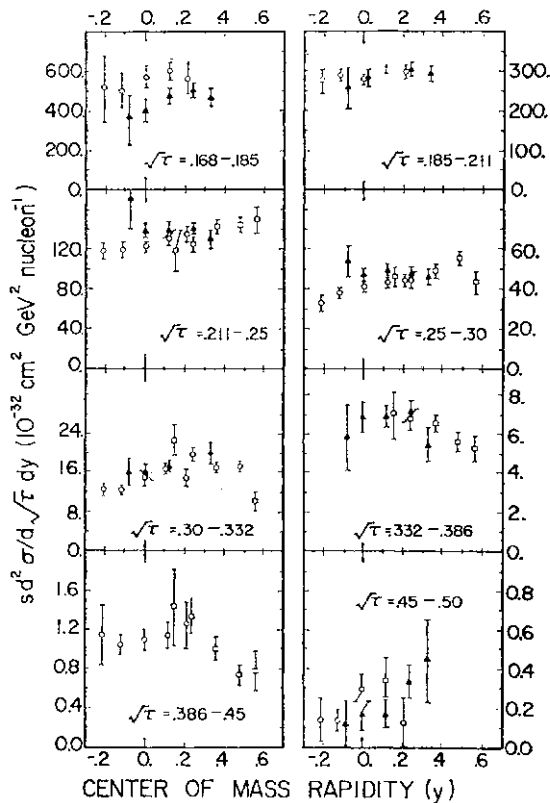


Fig. 29. CFS  $\wedge$ -behavior.

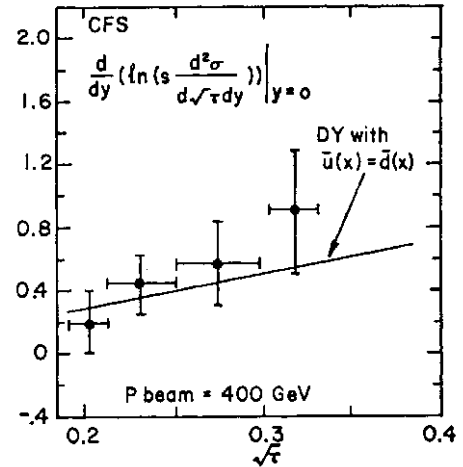


Fig. 30. Asymmetry behavior of CFS data vs  $m/Vs$ .

sign of the slope, magnitude and behavior with  $\sqrt{s}$  is another success of the model. The agreement becomes even better if we let  $d \hat{u}$ . The data of SNMT against  $x_p$  indicates the same asymmetric behavior around  $x_p=0$ .

3. Pion-induced dimuons

The CIP data (Fig. 16) have been analyzed to extract pion structure functions. This is a forward spectrometer based upon a large air magnet which was once the Chicago cyclotron.

In contrast with the proton collisions, pions bring in a valence anti-quark. High masses should be easier to make since one does not need the sea to obtain  $q(x_1)q(x_2)$  annihilations with large product  $\sqrt{s}$ . This is qualitatively seen in the mass spectrum of Fig. 16.

The 7T induced mass spectrum is written by CIP as:

$$\frac{d^2\sigma}{dmdx_F} = 8\pi\alpha^2/9m^3(1/(x_1+x_2)) f_\pi(x_1)f_N(x_2) \tag{6}$$

and if variables are changed according to eq. (1):

$$d^2\sigma/dx_1dx_2 = 4\pi\alpha^2/9 \cdot s \cdot f_\pi(x_1)f_N(x_2). \tag{7}$$

Here  $f_\pi(x) = x\bar{u}(x)$ ;  $f_N(x) = 4/9xu^N(x) + 1/9x\bar{d}^N(x)$ . Their first test is that of the factorizing prediction of the D-Y model, *i.e.*, that the cross section may be written as a function of JCI times a function of  $x_p$ . They obtain a fair  $\chi^2$  for this hypothesis and then go on to fit the two functions in eq. (7): Figs. 31, 32 give their results. A form  $(1-x)^a$  with  $a=1$  is predicted by quark counting rules of Brodsky and Farrar. However, the nucléon function derived from

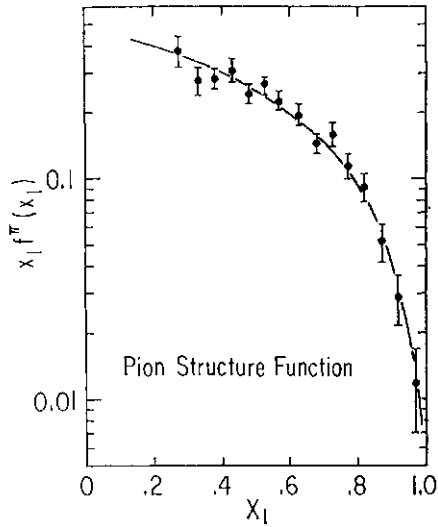


Fig. 31. CIP pion structure function from 225 GeV  $7T^-$  dimuons.

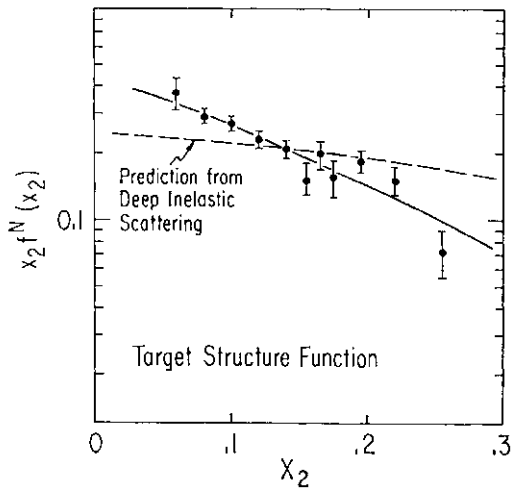


Fig. 32. CIP nucleon structure function.

CIP data is not in good agreement with muon scattering. The authors note that this *may* be related to the fact that the  $p_T$  of the muon pair has been neglected in the D-Y analysis and thus, at the least, affects the definitions of  $x_1$  and  $x_2$ . A model for including the kinematic effects of  $p_T$  of the quarks seems to be in the right direction of flattening the nucleon structure function. The analysis is continuing but it is clear that the correct nucleon structure must be acceptable if the pion structure is to be convincing.

In summary, the first data on the quark distributions in the pion are given:  $xu^2/dx = 0.27(1-x)^{0.66}$  ( $x > 0.25$ ). The data also imply that half the pion momentum is carried by gluons.

#### 4. Further Tests of the D-Y Model

##### i. $7T^+ / 7r^-$ ratio in carbon.

This is a famous test implied by the fact that a  $7r^+$  furnishes a  $d$  valence quark to a nucleon system symmetric in  $u$  and  $d$  receptors. The  $7T^-$  supplies a  $\hat{u}$  and therefore the ratio of cross sections should simply be the square of the ratio of the  $d$  to  $\hat{u}$  charges, *i.e.*, 1:4. This neglects the seas in both pions and nucleons and so one expects to approach 0.25 as the dilepton mass increases. Figure 33 shows the CIP data. More success! Earlier data from CERN confirm this result.<sup>14</sup>

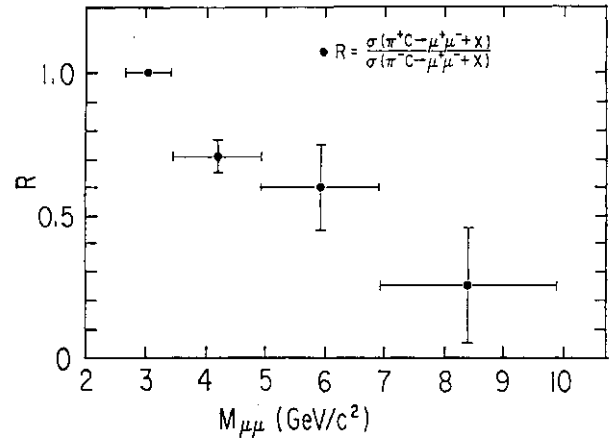


Fig. 33. CIP  $\pi^+/\pi^-$  data.

##### ii. Helicity angular distributions

The D-Y model for the annihilation of two spin 1/2 quarks into a  $1^-$  state predicts a distribution

$$f(\theta) = 1 + \alpha \cos^2 \theta^*; \quad \alpha = 1 \quad (8)$$

where  $\theta^*$  is the angle between the outgoing back-to-back muons and the collision axis in the dimuon rest frame. This picture is made vastly more complicated if the quarks have transverse momenta because then the collision axis is unknown. Figure 34 shows CIP data for  $n$  induced dimuons restricted to  $PT < \backslash \text{ GeV}/c$  and they find  $a = \backslash$  for these data and, in fact  $a > 1$  for data which include all  $p_T$ . The SNMT group can also fit their data to the form (eq. (8)) and also find strong alignment,  $a > 1$ . We view the small  $p_T$  data as being a clear success of the model and guess that the large values of  $a$  are a result of some complicated interaction between  $\theta^*$  and  $p_T$  acceptances since most effects would tend to decrease  $a$ .<sup>15</sup>

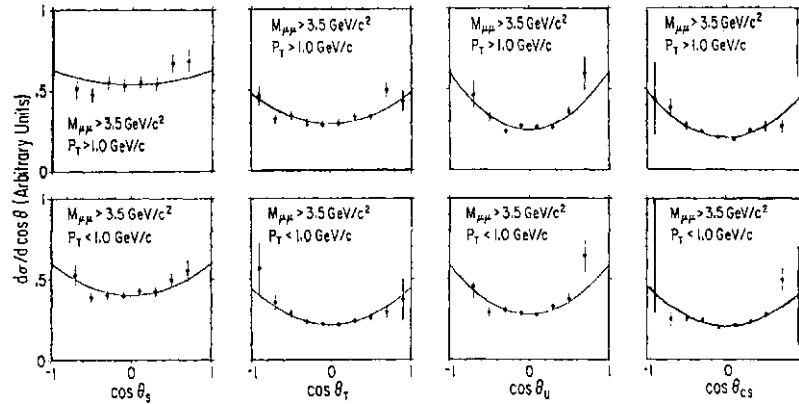


Fig. 34. CIP helicity angle data.

We summarize :

As applied by naive experimentalists, the Drell-Yan model works :

1. The nucléon sea deduced from dilepton production is the same as that deduced from neutrino scattering.
2. Color degree of freedom is observed.
3. The  $y$  distributions in  $p$ -N and TT-N are as predicted.
4. The  $K/\pi$ - production of dileptons in C approaches 0.25 as the mass increases.
5. The helicity distribution is  $1 + \cos^2 \theta^*$ .

Furthermore, we have a quantitative ( $\sim 20\%$ ) photograph of the nucleonic quark sea and the pionic valence quark cloud. This success of what appears to be the most simple model is made even more encouraging when we learn that perturbative QCD, a real theory, yields the D-Y model as we have used it, when diagrams involving quarks and gluons are summed to first order in  $a_s \log g^2$ . All of this is the good news. We now turn to a more troublesome and therefore more interesting subject.

#### D. Dilepton transverse momenta

If we integrate over  $p_T$  as we have done in the preceding (with some anxiety about the kinematic definitions, eq. (1)), we have a very successful model. Our theoretical colleagues patiently explain that what we have done is to apply QCD, summing all first order diagrams involving not only  $qq$ , but  $qG$ ,  $GG$  etc. where  $G$  are the gluons, the objects that generate the quark-quark forces. Experimentalists accept this feat modestly but then we observe that dileptons have large transverse momentum. Even the old BNL data<sup>4</sup> observed  $\langle p_T \rangle \sim 800$  MeV/c. The model neglected  $p_T$  ( $\sim 300$  MeV/

$c$  was expected). The earliest FNAL experiments<sup>8</sup> observed  $\langle p_T \rangle > 1$  GeV/c for  $m > 4$  GeV. Now the fundamental issue is that the dilepton transverse momentum  $p_T$  is related to the transverse momentum of the annihilating quarks  $\bar{q}$ :

Constituent transverse momenta are coupled to the deepest aspects of the quark theory, QCD and therefore it was not surprising that a very large number of theoretical papers addressed this issue (see talks at this Conference by Halzen, Fritzsche, Matsuda, Berger, Field, Politzer, others).

Now the data.

##### i. $p_T$ vs $m$

CFS finds that, out to  $\sim 3$  GeV/c of dilepton  $p_T$  and for  $m > 5$  GeV, there is an empirical fit (with excellent  $\chi^2$ ):

$$E(d^3\sigma/dp^3) = A(m)[1 + p_T^2/p_0^2]^{-6} \quad (9)$$

where  $p_0$  depends very little on mass but it does depend on energy. Table III lists  $p_0$ 's. The SNMT group (see Fig. 35) also find this form excellent with very similar  $p_0$ 's. The confrontation with the QCD diagrams has been made by many papers—I show in Fig. 36 the work of E. Berger presented to this Conference. Typical of these calculations is a  $7T^2$  divergence. Some of the earliest of such calculations were carried out by Politzer,<sup>16</sup> by Altarelli *et al.*<sup>17</sup> who have also tried to improve the low  $p_T$  behavior by a regularizing process. The idea is that there are two sources of dilepton  $p_T$ : One comes from the QCD gluonic diagrams (the same ones that account for the scale breaking in  $vW_2$ ), and the other from "intrinsic"  $p_T$  related by the uncertainty principle to the fact that quarks are confined in

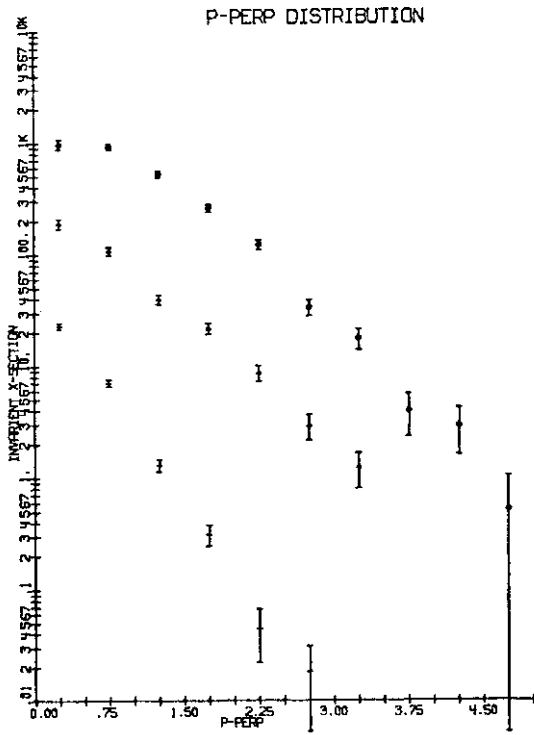


Fig. 35. SNMT dimuon  $p_T$  distributions (400 GeV protons at FNAL).

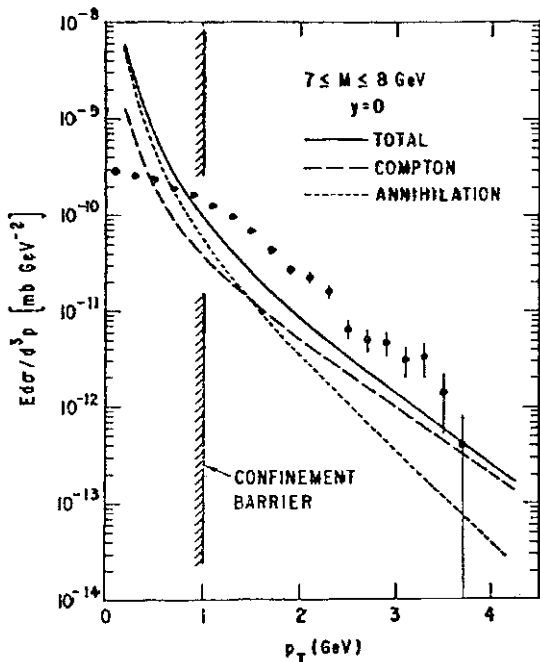


Fig. 36. QCD calculation of dilepton  $p_T$  distributions from E. Berger (this Conference).

space.

To study the behavior of  $p_T$  with mass, energy, rapidity (or  $x_T$ ), it is simplest to calculate the moments:  $\langle p_T \rangle$  or, where possible, we also calculate a bizarre  $\langle p_T \rangle$  in which we only count  $p_T > 1$  GeV (say). We can still explore the variation with  $m$ ,  $s$  etc. to see whether or not the observed behavior

is dominated by low  $p_T$ .

The CFS data are presented in Fig. 37. We see a flattening of  $\langle p_T \rangle$  vs mass for  $m > 5$  GeV (except for the Y). Figure 38 shows the

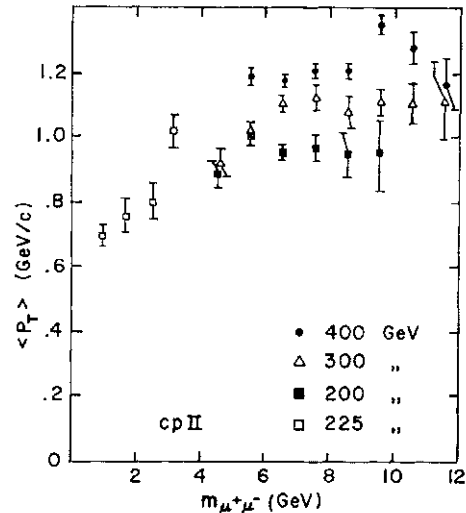


Fig. 37. CFS average  $p_T$  vs  $M_{\mu\mu}$ .

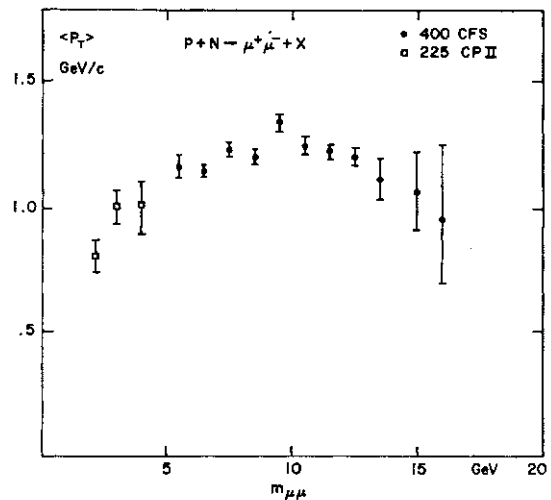


Fig. 38. High intensity CFS  $\langle p_T \rangle$  vs mass.

increased CFS data sample and a falling off at very high mass is indicated. The SNMT group agrees; this is also seen (see Fig. 39) by the CIP group for pion-induced dileptons. (The flatness persists if we neglect  $p_T < 1$  GeV). Here we have a surprise for experimentalists. ( $p_T$ ) of pions is clearly  $> \langle p_T \rangle$  of protons. Some theoretical implications: The earliest estimates (e.g., Politzer<sup>6</sup>) indicated that

$$\langle p_T \rangle \sim m^2 / \log ra^2$$

and this did not happen. The essential parameter in converting the above to the observed flat distribution is the adjustment of the gluon distribution to

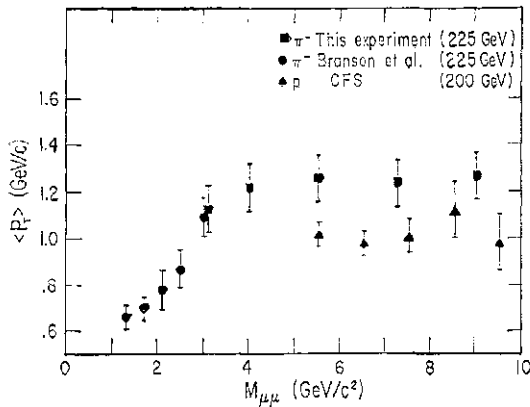


Fig. 39. Comparison of proton and pion-induced  $\langle p_T \rangle$  vs mass.

$$xG(x) \sim (1-x)^6.$$

Now if we look at the dominant gluon correction diagram for pN collisions it involves quark-gluon collisions to produce quark-virtual photon final states. In the TTN case it is quark-antiquark scattering into gluons and virtual photons which dominates. If we now appeal to the hierarchy :

- pion valence  $\sim (1-x)$ —from  $7rN \rightarrow$  dileptons
- nucléon valence  $\sim (1-x)^3$ —from  $\wedge N$  scattering
- gluons  $\sim (1-x)^6$ —from dilepton  $p_T$
- nucléon sea  $(1-x)^8$ —from dilepton spectrum. (9)

We see that  $7r(\text{valence}) N(\text{valence})$  collisions are harder than  $p(\text{valence}) G$  collisions. Since, in these diagrams,  $p_T$  arises from the conversion of longitudinal momentum, we understand the higher  $\langle p_T \rangle$  for TTN.

ii.  $p_T$  vs  $x_F$  or  $y$

The same qualitative argument given above suggests that at very large dilepton  $x_F$ , the  $\langle p_T \rangle$  must decrease since it all derives from initial parton  $x$ . The data from CFS, CIP and SNMT are given in Figs. 40 a, b, c. One sees no drop-off and this also persists if  $p_T < 1$  GeV is neglected. The predicted fall-off is moderated by the intrinsic  $p_T$  if this is independent of  $x$  but we leave this as an unsettled question.

iii.  $p_T$  vs  $s$

Figure 41 presents the CFS data and fit together with a new ISR data point from CCOR for  $6 < m < 9$  GeV. This data point has been raised from the observed  $\langle p_T \rangle = 1.65$  GeV/c to 1.9 GeV/c in order to make it fit our line but also because at ISR,  $\wedge/r \wedge 0.1$  and we

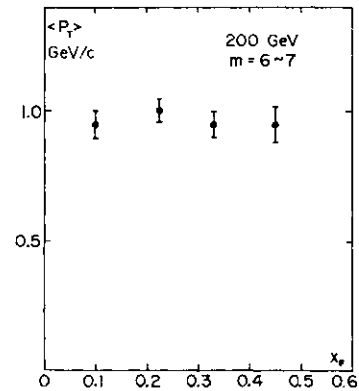


Fig. 40a. CFS  $\langle p_T \rangle$  vs  $x_F$ .

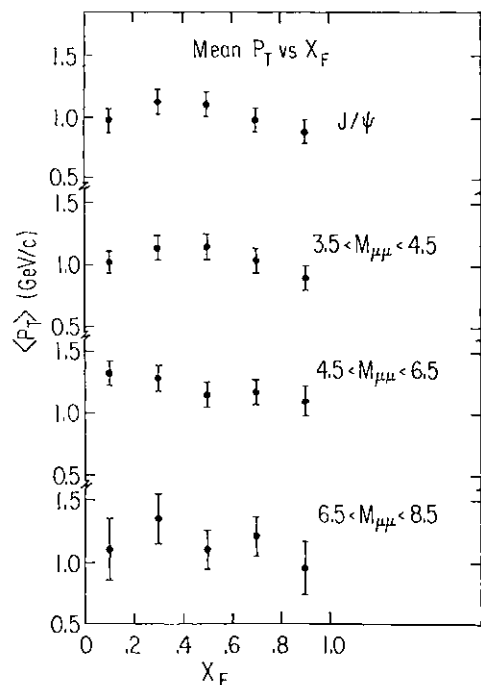


Fig. 40b.  $\langle p_T \rangle$  vs  $x_F$ .

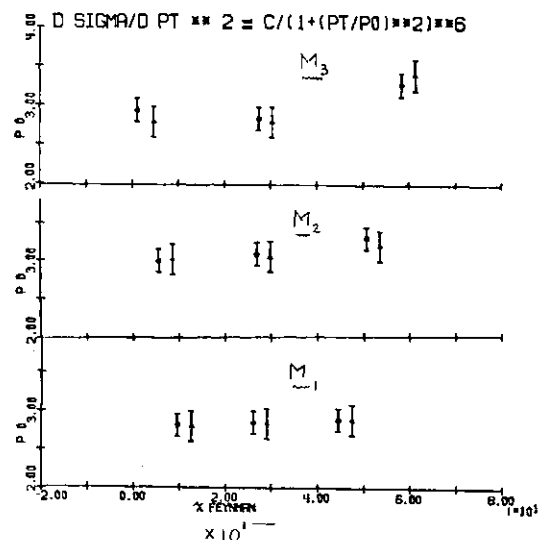


Fig. 40c. SNMT  $p_0$  parameter (eq. 9) vs  $x_F$  for 3 mass bins.

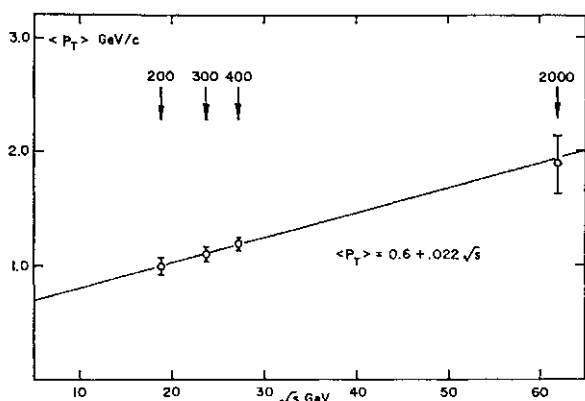


Fig. 41. CFS and CCOR  $\langle p_T \rangle$  vs  $\sqrt{s}$ .

know that  $\langle p_T \rangle$  increases with  $\sqrt{s}$  until  $\sqrt{s} \approx 0.2$ . We used the theoretical papers of Matsuda and also of Fritzsche to make this correction and so we can write

$$\langle p_T \rangle = 0.6 + 0.022 \sqrt{s} \text{ GeV/c.} \quad (10)$$

The CFS results are not changed (in slope) if we delete the  $p_T < 1$  GeV events. This behavior seems to confirm interpretation in terms of a confinement piece of parton  $k_T$  (giving rise to  $\langle p_T \rangle \sim 600$  MeV/c) and a dynamical piece which depends on  $\sqrt{s}$ . It should be pointed out that Fritzsche and Minkowski<sup>18</sup> had published a prediction:

$$\langle p_T \rangle = (0.55 + 0.023 \sqrt{s}) \text{ MeV/c.}$$

So this form is certainly consistent with QCD and clearly illustrates scale breaking. The implied quark  $k_T$  is somewhat lower than is obtained from other kinds of analysis.<sup>19</sup>

### Final Remarks

Dilepton data have produced crucial tests of the constituent theory. We can now predict the dilepton data completely from lepton-nucleon scattering with no parameters. Our theoretical colleagues have done very well because the collision of two such ugly objects as protons to produce a pair of leptons would offhand look entirely unconnected to the elegant neutrino and electron (muon) scattering. This is a major intellectual achievement (to the level of 20%! ). We have also given

shape to the pion, and the esoteric gluon cloud and sea of nucleon. They are all enumerated.

Occasionally this study of the property of the old quarks is pleasantly interrupted by a new quark. It is characteristic of the field which must now work hard to improve the precision in the familiar domain and also extend the parameters—certainly to the W with which we began this subject.

### References

1. Y. Yamaguchi: Nuovo Cimento **43** (1966) 193.
2. W. Burns *et al*: Phys. Rev. Letters **15** (1965) 830.
3. L. Okun: Sov. J. Nucl. Phys. **3** (1966) 426.
4. J. Christenson *et al*: Phys. Rev. Letters **25** (1970) 1523; Phys. Rev. **D8** (1973) 2016.
5. (a) S. Herb *et al*: Phys. Rev. Letters **39**(1977) 252; (b) W. Innés *et al*: Phys. Rev. Letters **39** (1977) 1240, 1640E; (c) D. Kaplan *et al*: Phys. Rev. Letters **40** (1978) 435; (d) J. Yoh *et al*: Phys. Rev. Letters **44** (1978) 684.
6. Bienlien *et al* (DESY-Heidelberg): this Conference; Darden *et al* (DASP II): this Conference.
7. Ellis, Gaillard, Nanopoulos and Rudaz: Nucl. Phys. **B131** (1977) 285; (a) R. Vidal *et al*: Phys. Letters **77B** (1978) 344. See also D. Cutts *et al*: Phys. Rev. Letters **41** (1978) 363.
8. D. Horn *et al*: Phys. Rev. Letters **36** (1976) 1236; Phys. Rev. Letters **37** (1976) 1374.
9. Gaisser, Halzen and Paschos: Phys. Rev. **D15** (1977) 2572.
10. S. Drell and T. M. Yan: Phys. Rev. Letters **25** (1970) 316; Ann. Phys. (N.Y.) **66** (1971) 578.
11. L. Lederman and B. G. Pope: Phys. Letters **66B** (1977) 486; Antreasyan *et al*: Phys. Rev. Letters **39** (1977) 906.
12. H. Anderson *et al*: Phys. Rev. Letters **40** (1978) 1061; T. Kirk: private communication.
13. R. Field and R. P. Feynman: Phys. Rev. **D15** (1977) 2590.
14. Cordon *et al*: Phys. Letters **76B** (1978) 226.
15. E. Berger *et al*: from ANL-HEP-PR 77-63 (1977).
16. H. D. Politzer: Nucl. Phys. **B129** (1977) 301.
17. G. Altarelli, G. Parisi and R. Petronzio: Phys. Letters **76B** (1978) 351, 356.
18. H. Fritzsche and P. Minkowski: Phys. Letters **73B** (1978) 80.
19. S. Matsuda: KUNS 467 HE(TH) 78/08, and this Conference.

### P3a: Dynamics of Hadronic Reactions

*Chairman :* **A. WROBLEWSKI**

*Speaker:* **G. VENEZIANO**

*Scientific Secretaries:* **N. SAKAI**  
**S. WADA**

### P3b: Dynamics of High Energy Reactions

*Chairman:* **L. D. SOLOVIEV**

*Speaker:* **R. FIELD**

*Scientific Secretaries:* **T. MUTA**  
**T. UEMATSU**

## P 3a

## Dynamics of Hadronic Reactions

G. VENEZIANO

CERN, Geneva

### §1. Introduction

The subject of this talk is a very wide one: I am supposed to cover the theoretical developments which have recently occurred in our understanding of hadronic processes, *i. e.*, of processes controlled by strong interactions.

Such reactions include, besides conventional low  $p_T$  hadron physics and large  $p_T$  hadron-hadron collisions, also processes with initial and/or final leptons, such as  $e^+e^- \rightarrow$  hadrons,  $l_\nu \rightarrow i, \dots$  and  $pp \rightarrow l + X$ .

In this talk I shall not be able to describe, nor even mention, all the interesting contributions in the field. Instead, and, I believe, in agreement with the guide-lines of the Program Committee, I shall try to give an over-all view of the present "state of the art," emphasizing here and there a few new results by which I have been particularly impressed.

It is perhaps the first time, at this type of Conference, that "soft" and "hard" hadron physics are discussed together in a plenary talk. I took this as a suggestion to try to present both aspects of hadron physics as one body of knowledge, stressing, as much as possible, connections, analogies and differences.

The plan of the talk will be as follows: After giving a panoramic overview of "hadron-land," and of the talk, I shall discuss, in order, hard processes, low-energy (spectroscopy), but very incidentally, intermediate to high energies at low  $p_T$ , and superasymptotic energies at low  $p_T$ . For each of these subjects, I shall refer to other speakers of parallel or plenary sessions for more details and/or complementary information. I shall conclude with a brief, tentative comparison of soft and hard hadron physics.

I will address myself, in particular, to some of the basic questions in hadron physics that have occupied our minds over the past few years. These are:

1) Is it conceivable that Quantum Chromo-

dynamics (QCD) is at the basis of hadron physics? Can we actually test QCD?

2) Does QCD conflict a priori with other successful (though incomplete) descriptions of strong interactions, such as the Regge-Mueller approach, the dual string model, Reggeon Field Theory, Regge-bootstrap schemes, or does it rather provide a unifying link among them and with the constituent (parton) models of hard processes?

3) What do hard and soft processes have in common?

Concerning the question of what is the *present* evidence for QCD, I shall rather refer you to a recent paper of Bjorken,<sup>1</sup> concluding that such evidence is far from established.

Certainly, the most convincing way to answer those questions would be to prove (or disprove!) confinement in QCD and then to compute the hadronic spectrum from few input parameters. This would be certainly convincing, but, in spite of some nice progress recently made,<sup>2</sup> it could still take a little too long.

Meanwhile, an alternative, less satisfactory, but cheaper way to answer those questions can be the following:

a) Extract from QCD as many as possible testable "predictions" (*i. e.*, results believed to be unaffected by the confinement mechanism) and check them against available data. Find "clean" tests of QCD.

b) Look at the general structure of QCD with the aim of relating it to those other (partially) successful approaches to soft hadronic phenomena.

c) See if and how soft and hard processes are related in QCD, and in nature.

Incidentally, if this less ambitious approach should disprove QCD, then we could spare ourselves from the harder task of proving confinement.

To anticipate the conclusions, what seems to come out of such an analysis is the following:

i) With a little faith in the gentle behaviour of the confinement mechanism, a lot of predic-



tions can be made for a variety of hard processes, some absolute, some relating different reactions. So far, QCD looks all right, but certainly not proven<sup>1</sup> (see also the following talk by Field). Some stringent tests are near, such as the behaviour of  $do/dp$ ? predicted by QCD (with its normalization relative to deep inelastic data) which should soon show up,<sup>3</sup> and the peculiar predictions of QCD for  $e^+e^-$  produced hadronic jets in the PETRA-PEP energy region.<sup>4</sup> The need for clean tests is certainly felt.

ii) The topological graph structure of QCD assuming, of course, confinement to hold, suggests a clear relation to dual, Gribov and even to Regge bootstrap theories (*e.g.*, the strong coupling is fixed by QCD). It looks to be just a matter of finding, in each regime, the relevant collective degrees of freedom. This may force us into QCD-inspired semi-phenomenological theories, at least for the near future.

iii) QCD points at some crucial differences between hard and soft hadronic phenomena. Progress is underway towards understanding some intermediate regimes and this should help in finding the connection, if any. It looks that a common denominator for hard and soft hadron physics may exist, as I shall explain at the end of this talk.

## §2. A Panoramic Overview of Hadronland

We have schematically represented in Fig. 1 the various regimes of hadron physics on a two-dimensional map with energy and momentum transfer (actually their logarithms) giving the co-ordinates.

First of all there is an unphysical region ( $2p_T > \sqrt{s}$ , but it actually extends in the complex planes of these variables). It is in the asymptotic part of this region (the deep Euclidean region) that improved perturbation theory (IPT) in the running coupling constant  $\alpha_s(Q^2)$  can be justified for asymptotically free theories, such as QCD.

More interesting to us is, of course, the deep physical (Minkowski) region where hard processes take place. We shall discuss in a moment the use of IPT in this region, noticing that the use of IPT is confined at present to finite (and not too small) values of  $x^2 p_T^2 \wedge s$  ( $Q^2/2Mv$ ), hence to a strip along the diagonal.

Ordinary low  $p_T$  physics also lies inside a strip, this time parallel to the energy axis with the width of such a strip shrinking if the diffraction peak does so. Asymptotically in this second strip, is where Reggeon Field Theory (RFT) is a popular theoretical framework; coming down, we encounter other interesting descriptions such as the concept of a bare Pomeron pole (ISR-Fermilab regions?), that of an exchange degenerate Reggeon and, finally, the resonance description of hadronic reactions. We shall see later how these descriptions can be linked to one another and this will also explain various arrows and words in the picture.

The resonant region is common to both strips I have mentioned. What happens there we believe to be related to what happens at larger values of  $E$  and/or  $p_T$ , either by the old Dolen-Horn-Schmit or by the Bloom-Gilman duality relations.

The most prominent (and sad) feature of Fig. 1, however, I find to be the fact that so much of our hadronland lies *outside* these two strips (about which we think we have some understanding). This is the region that should provide the link between hard and soft hadron physics, but little is known about it. There are interesting speculations, due primarily to Feynman, that valence partons are related to Reggeon exchange and sea partons and gluons to Pomeron (vacuum) exchange; but as we go to higher  $E$  and  $p_T$  ("semi-hard" processes) we are quite stuck in the dark. Nevertheless, something has been moving on in this direction during last year, and I shall try to report on it.

Before moving on, let me say that the scale of  $E$  and  $p_T$  relevant to hadrons cannot be predicted from QCD: it is a free parameter given to us by nature: it is, say, 500 MeV. Until 1974 we thought this to be the only relevant scale, but the discovery of new heavy quarks has put us into some sort of puzzle.

Turning now to Fig. 2, I am anticipating there what seems to emerge from QCD for the effective degrees of freedom relevant to the various regimes depicted in Fig. 1.

We go from a parton-like description of hard processes with quarks and gluons, colour and flavour as explicit degrees of freedom to a dual-string-type representation of the resonance

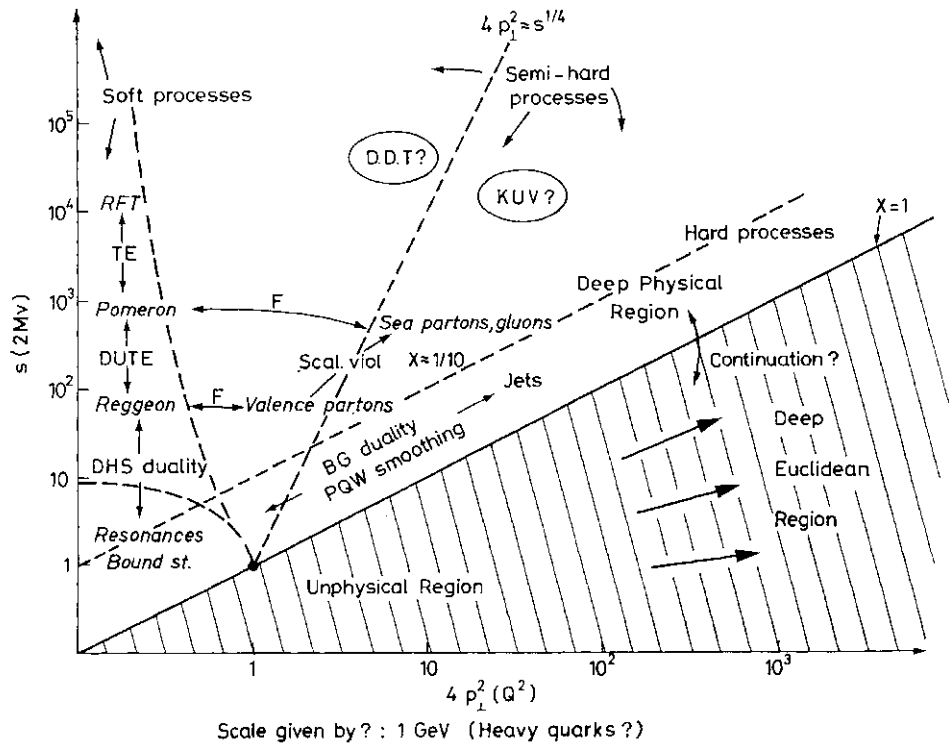


Fig. 1. An overview of "hadronland" and of its present understanding.

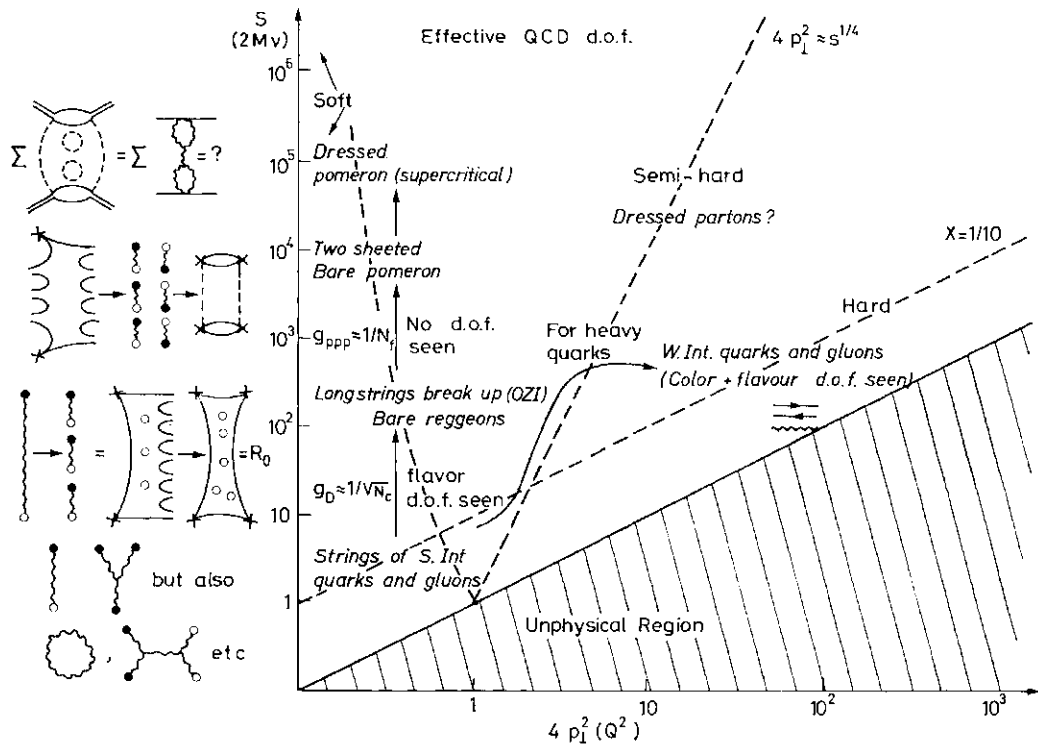


Fig. 2. Degrees of freedom appropriate to the various regions of "hadronland."

region in which colour ceases to be an explicit degree of freedom, since hadrons are supposedly colourless. Yet the existence of the underlying (hidden) colour degrees of freedom can be shown<sup>5,6</sup> to control the stability of our states  $\text{fetrong—if } N_c$  is the number of colours). As we increase the energy, the

excited, long strings break and, through multiperipheral dynamics, lead to a new degree of freedom, the exchange degenerate, ideally mixed planar Reggeon. Then, as we increase the energy further, the flavour singlet component takes over quantum number exchange and, by the time we are at Fermilab-ISR

energies, or even before, the new effective degree of freedom will be vacuum exchange, *i. e.*, the bare Pomeron  $P_0$ . Flavour degrees of freedom have also been lost at this stage, but there is a trace of them in the couplings of  $P_0$  (e.g.,  $g_{PP_0} \sim 1/N_f$  if  $N_f$  is the number of flavours<sup>6</sup>). In the end, the tube-shaped bare Pomerons interact with each other to give higher topological structures, an example of which is shown again in Fig. 2. Summing these corresponds to solving Reggeon Field Theory (RFT), presumably in the so-called supercritical region.

Finally we can ask what are the degrees of freedom in the "semi-hard" region. The authors of ref. 7 have suggested that they are still quarks and gluons, but no longer as structureless point-like objects: partons will get dressed and their predictable form factor will be measured by experiments in these kinematical regimes.

We are now ready for going down into hadronland and visit some of its most interesting sites.

### §3. Hard Processes Involving Hadrons

#### 3.1. Strictly hard processes

Under this name we mean to include both hadron and lepton initiated reactions as long as they are hard, *i. e.*, all invariants are large and of the same order. It does not look theoretically meaningful, indeed, to treat separately the reactions  $l^+l^- \rightarrow$  hadrons,  $l^+A \rightarrow$  hadrons,  $l^+Z \rightarrow$  hadrons,  $h+h+l \rightarrow$  hadrons ( $l$  for lepton,  $h$  for hadron) as long as they are all hard.

It is not an exaggeration to say that there has been a lot of progress on this subject, not only since Tbilisi, but even more within last year. Here I shall concentrate on the essential theoretical points and refer you to Politzer<sup>8</sup> for more details and to Close and Field<sup>9</sup> for the phenomenological applications, actual numbers, checks with data and so on.

In short, the trend has been towards an increased confidence in the use of improved perturbation theory (IPT) for asymptotically free (AF) theories, and in particular for QCD, outside the range of light-cone-dominated processes [*i. e.*,  $a_1(e^+e^- \rightarrow$  hadrons) and  $tf_{inc}(l^+$  hadrons)]. The way to go about it had been to deal with infra-red (IR) insensitive

quantities, *i. e.*, quantities which, perturbatively, have a smooth, finite limit as the gluon and/or the quark mass goes to zero. This is because the renormalization group (RG) equation, which is always valid, plus AF relates a large  $Q^2$  problem to a small coupling ( $tf_{inc}(\hat{O}^2) \sim \log^{-1} e^7/i^2$ ), small mass ( $m(\hat{O}^2) \sim A/Q$ ) problem. In general, the usefulness of a small  $a_s(Q^2)$  is upset by large IR logarithms of  $Q^2/m^2$ . If those are absent (IR insensitivity) an asymptotic expansion in  $oc(Q^2)$  may be all right, in the same sense as it is used in QED.

I will now sketch a general approach to this type of question, which relies heavily on the classic work<sup>10</sup> of Kinoshita and of Lee and Nauenberg (KLN). Those old results, originally obtained in QED, look to be valid for QCD or for any other renormalizable (but not super-renormalizable) field theory. They have, indeed, a very simple physical meaning which I shall now try to convey.

Consider a cross-section  $\sigma(i \rightarrow f)$  which is finite in lowest order. Then, although higher order corrections make  $\sigma(i \rightarrow f)$  IR divergent, the sum

$$\sum_{i' \sim i} \sum_{f' \sim f} \sigma(i' \rightarrow f')$$

where  $i'(f')$  are degenerate with  $i(f)$ , is completely free of divergences. There are two types of divergences to cancel and correspondingly two types of degenerate states to be considered, *i. e.*:

a) "Soft" divergences, due to  $m_{gVLo}$  or  $\wedge_{p\text{noton}} \wedge_0$  and to the possibility of emission of soft quanta by massive charged states. These are, for instance, the only divergences occurring in massive (*i. e.*,  $m \neq 0$ ) QED. In QCD they are cured by adding cross-sections to degenerate final states such as  $q, 9 + \text{soft gluon}, q, 2 \text{ soft gluons}, \text{ etc.}$

b) "Collinear" divergences, due to the decay of a massless particle (a gluon or a massless quark) into two collinear, but hard, massless particles. According to KLN these divergences, which will be our main concern here, are cured by adding cross-sections with initial and final degenerate states consisting of a collection of hard massless collinear quanta (which is also a massless system).

The reason why divergences of type (a) will not bother us is that any interesting hard cross-section will automatically sum over soft

bremstrahlung processes.

At this point, a simple classification of hard QCD processes\* follows from the KLN theorem. It looks as follows<sup>11</sup>:

1) *Processes with no initial coloured quanta* (e.g.,  $e^+e^- \rightarrow$  hadrons).

1a) If we do not detect individual hadrons in the final state, and instead limit ourselves to total or jet-inclusive cross-sections (these latter as defined by Sterman and Weinberg<sup>12</sup>), then KLN says that such processes are free of IR problems. Hence, as emphasized in ref. 12, cross-sections for producing  $n$  hadronic jets in  $e^+e^-$  collisions are completely calculable in QCD (absolute normalization included) and exhibit scaling violations only through their expansion in powers of  $a(Q^2)$ .

For further developments along these lines, see ref. 4, where a whole set of possible QCD tests at PETRA-PEP is presented.

1b) If we look instead at a single particle spectrum ( $j(e^+e^- \rightarrow \bullet / (?)$  fixing the momentum  $p$ , or better  $x=2|p|/\sqrt{Q^2}$ , will automatically include soft bremsstrahlung (which does not change  $x$ ) but will *not* include hard collinear bremsstrahlung (which brings you down in  $x$ ). Hence this process is *not* IR finite by KLN, is not absolutely calculable, and, as one can easily show, will exhibit "large" scaling violations.

2) *Processes with one initial coloured quantum* (e.g., deep inelastic scattering).

2a) If we are totally inclusive, or jet inclusive à la Sterman and Weinberg,<sup>12</sup> there are no IR problems associated with the final states. There are, however, divergences due to the initial quark state which is *not* accompanied by the full set of degenerate states demanded for cancellation by KLN. As a consequence (and as we know in this case from operator product expansion methods), the process is not absolutely calculable and exhibits "large" scaling violations (anomalous dimensions).

\* All these processes ought to be considered at the elementary constituent level. It is believed that, if a soft hadronic wave function can be defined, the results will apply to the actual world with only trivial modifications (see example below).

\*\* Here, and in the following, by "large" scaling violations we just mean  $(\log Q^2)^7$  dependences typical of an anomalous dimension  $T$ , as opposed to the asymptotically vanishing violations encountered in  $e^+e^-$  hadrons).

2b) If, on top, we are also detecting a final hadron with well defined  $x$ , new IR divergences and scaling violations occur, just as in case **i(b)**.

3) *Two incoming coloured quanta* (e.g.,  $qq \rightarrow T^+X$ ,  $qq \rightarrow qq$ ,  $q+g \rightarrow q+g$ , etc.)

3a) If we are jet-inclusive we now pick up IR divergences from both initial quanta. Since these are related to some extra hard collinear quarks and gluons in the initial state and since the two original incoming quanta are not themselves collinear, it is not surprising that we get (see below) separate IR singular factors for each incoming quantum and consequently *factorized* scaling violations.

3b) New scaling violations occur as in 1b) and 2b) if final particle inclusive spectra are looked at.

What is all this good for? Well, it looks as if it can provide, for the first time, a convincing derivation of the much used and successful parton model, or better of that particular version of it which incorporates QCD-predictable scaling violations.

This nice result came out of a large number of papers which appeared this year on the subject, but one should not forget that some of the basic points had been already laid down by the pioneering works of Gribov and Lipatov<sup>13</sup> and of Mueller.<sup>14</sup>

The new interest in the subject has been triggered by the paper of Sterman and Weinberg<sup>12</sup> and by those of Politzer.<sup>15</sup> Technically, the recognition that, by the KLN theorem,<sup>10</sup> the problem can be reduced to the study of collinear IR divergences and that those are easiest to study in physical gauges (in particular in the axial gauge, which is free of unphysically polarized gluons and of ghosts, and which has the Ward Identity relation  $Z_i = Z_1$ , as in QED), have been crucial developments.

Progress has been fast: from the one-loop calculation of some processes<sup>12,15,16</sup> to that of a general process<sup>11</sup>; from leading log calculations at higher orders in a few processes,<sup>11,17</sup> to their extension to arbitrary reactions<sup>18</sup> and, finally, to the analysis (if not the explicit calculation) of all non-leading log  $s$ .<sup>18,19</sup>

The result of all that has been to show that:

a) Soft divergences indeed cancel, reducing the singularities from double  $\log s$  for each power of  $a$ , to single  $\log s$ .

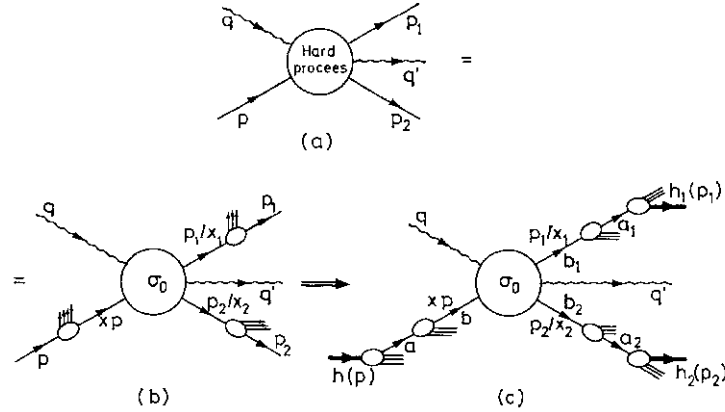


Fig. 3. QCD analysis of a typical hard process ( $r^* + \text{hadron} \rightarrow \text{hadron} + \text{hadron} + r^* + \dots$ ) in the leading  $\log Q^2$  approximation.

b) Collinear divergences are universal, *i.e.*, process independent, and factorize, *i.e.*, IR dependence factors from  $Q^2$  dependence as originally conjectured by Politzer<sup>15</sup>. Furthermore there is an independent IR divergent factor for each incoming and detected final coloured quantum.

c) The above IR divergences can be absorbed into universal  $Q^2$  independent factors to be identified with structure functions and fragmentation functions at some reference point  $Q^2$

d)  $Q^2$  dependent factors (scaling violations) are also universal and predictable by QCD.

e) Different processes can be compared by IPT because suitable ratios of hard cross-sections are IR insensitive.

f) Last, but not least, the resulting diagrammatic understanding of OPE results seems to open the way to further extensions (see below).

In order to show that the results (a)-(f) correspond to our present ideas about the QCD parton model, let me illustrate the result in an example at the leading log level.

Consider the process of Fig. 3a to be translated eventually into a hadronic process such as that of Fig. 3c, where  $q, q'$  are electromagnetic or weak currents. One finds, in accord with KLN, that large  $Q^2$  dependent factors (scaling violations) come separately from each coloured initial state and detected final state (Fig. 3b, at the parton level where the small blobs stand for collinear bremsstrahlung processes). When hadrons are added in, the final expression corresponding to Fig. 3c reads :

$$\begin{aligned} & \sigma(h(p) + \gamma^*(q) \rightarrow h_1(p_1) + h_2(p_2) + \gamma^*(q') + x) \\ &= \sum_{b_1, b_2} \int_0^1 dx_1 dx_2 G_k^b(x, Q^2) \\ & \quad \times D_{b_1}^{h_1}(x_1, Q^2) D_{b_2}^{h_2}(x_2, Q^2) \times \quad (1) \\ & \quad \times \sigma_0(b(xp) + \gamma^*(q) \rightarrow b_1(p_1/x_1) + b_2(p_2/x_2) + \gamma^*(q')) \end{aligned}$$

where  $\sigma_0$  is the lowest order hard cross-section and the structure (fragmentation) functions  $G(D)$  have a well-defined  $Q^2$  dependence, the one predicted by QCD, and are process independent (as long as the process is hard). This is exactly the QCD parton model prescription.

I will conclude this point by mentioning that the extension to non-leading log  $s$  is an important step forward, first because one is never too sure about how much trust can be put in leading log calculations and, second, because, at present values of  $g^2, p_n$ , etc., such non-leading terms appear to be important.<sup>20</sup>

The lesson here seems to be that, although for each process the computation of non-leading log  $s$  is highly complicated,<sup>21</sup> when relating different hard processes much simpler results are obtained.<sup>18</sup>

Finally, I should point out that Mueller<sup>22</sup> has recently given an OPE-like justification of the above diagrammatic results adding thus further confidence in their validity.

### 3.2. Semi-hard processes: DDT<sup>r</sup> extension

The considerations made in 3.1 hold for inclusive processes in which all invariants are large and their ratios are all of order one. We now want to consider, following ref. 7, an intermediate regime which we call "semi-hard."

Consider, for instance, the (constituent level) reactions :

- i)  $q\bar{q} \rightarrow l^+l^-(q_T) + X$
- ii)  $\gamma^* q \rightarrow q(q_T) + X$
- iii)  $\gamma^* \rightarrow q(p_1) + \bar{q}(p_2) + X; (p_1 - p_2)_T = q_T,$

where  $q_T$  is: in i), the transverse momentum of the lepton pair; in ii), the transverse momentum of the final quark relative to the direction of the "struck" quark (which can be determined); and finally, in iii),  $q$  and  $\bar{q}$  lie on opposite side jets and  $q_T$  is the transverse momentum of the slower of the two relative to the direction of the faster.

The region we would like to consider is the one in which :

$$A^2 \ll q_T^2 \ll |Q^2| \tag{2}$$

where  $Q^2$  is the virtual photon momentum and  $A$  the usual hadronic scale parameter ( $A \sim 500$  MeV). In other words, we want both  $a(Q^2)$  and  $a(q_T^2)$  to be small but, unlike the case of real hard processes, we shall not be able to neglect terms of order  $a \log G^2 / \langle r \rangle$ . As I explained in § 2, this is a very large and interesting region of phase space.

Let us consider, to be definite, the Drell-Yan process i). If, instead of fixing  $q_T$ , we would evaluate the result would be

$$\langle \# \rangle \sim \hat{O}W \langle 2^2 \rangle \sim \hat{O}71 \log Q^2 \tag{3}$$

due to the fact that  $a_i$  is dimensionless. In terms of QCD, axial gauge diagrams, the process giving rise to this large are those of Fig. 4a. Since the radiated hard gluons carry transverse momentum up to a finite fraction of  $Q$ , eq. (3) follows together with the fact that the annihilating  $q\bar{q}$  pair can be anywhere from on shell to  $O(Q^2)$  off shell.

Having instead restricted  $q_T$  to have a fixed, small value (relative to its average value) we are forcing those emitted gluons to have small transverse momenta and, consequently, we are fixing the off-shellness of the

annihilating pair to be  $O(q_T^2)$ .

DDT then claim to have obtained, within some more restricted region than (2), a very simple expression for the differential cross-section, which reads (DDT formula):

$$\frac{d\sigma}{dQ^2 dy dq_T^2} = \frac{4\pi\alpha^2}{9sQ^2} \sum_f e_f^2 \frac{\partial}{\partial q_T^2} \times [G_{h_1}^f(x_1, q_T^2) G_{h_2}^f(x_2, q_T^2) T^2(Q^2, q_T^2)]; \tag{4}$$

$$x_1 \cdot x_2 = Q^2/s; \quad x_1/x_2 = e^y,$$

where, essentially, the  $G$  structure functions, evaluated at  $q_T^2$ , can be understood as the result of the evolution of the quark density up to the  $q_T^2$  value of the annihilating pair and the  $T$  factor is the *quark form factor* associated with the electromagnetic vertex (see Fig. 4b).

DDT have estimated this form factor and found that it is related (but not identical) to the Sudakov form factor.<sup>23</sup> They find

$$T \simeq \int_1^2 dz \exp(-B/2z^2) > \exp(-B/2) \equiv S, \tag{5}$$

where  $S$  is the Sudakov form factor:

$$B = -c_F \frac{\alpha_s(q_T^2)}{\pi} \log^2 Q^2/q_T^2; \quad c_F = 4/3. \tag{6}$$

Notice that  $T$  is a more "gentle" form factor than  $S$ .

A few remarks are in order about the DDT formula, eq. (4):

1) If naively integrated in  $q_T$  from 0 to  $O(Q)$  it clearly reproduces the Drell-Yan formula (with scaling violations, of course).

2) As a result of the form factor  $T$ , the  $q_T$  distribution of the lepton pair is flatter than the naïve expectation  $(1/\#) a_i(\#)$ .

3) In a sense, one is measuring the form factor of the quark. Whereas in hard processes partons behave as point-like objects, in these semi-hard processes they behave as *dressed* particles.

4) The DDT derivation is not very simple and clear. It would seem important to have some double check of their simple final result.

5) Finally, one is dealing with a leading log approximation and some control of the non-leading terms would also be desirable.

### 3.3. Looking inside QCD jets

I would now like to describe briefly another extension of perturbative techniques for hard processes, made possible through our diagrammatic understanding of scaling violations.

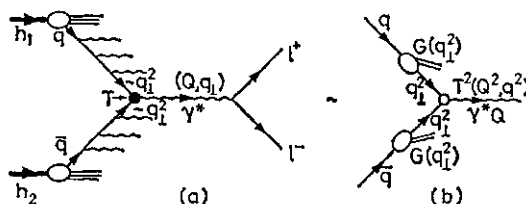


Fig. 4. Schematic understanding of the DDT formula.

This work<sup>24</sup> too goes in the direction of somewhat softer physics, because it deals with multiparton (and multiparticle) spectra inside the same (quark or gluon) jet. At first sight, it looks surprising that such quantity as a two-parton spectrum inside a jet can be computed because one thinks that the invariant mass  $(p_1 + p_2)^2$  of the system ought to be small. This, however, is not the case, and again, as in eq. (3), one knows that\*

$$\langle (p_1 + p_2)^2 \rangle \sim x_1 x_2 \cdot Q^2 / \log Q^2. \quad (7)$$

The main results are the following:

1) In the leading log approximation, multiparton spectra inside a jet can be computed in terms of the tree diagrams of an effective (non-local)  $\Lambda^3$  theory. The resulting "jet calculus" rules are very simple.

2) This prescription satisfies many consistency checks (e.g., momentum and charge conservation sum rules). In six-dimensional  $O^3$  theory ( $\zeta_{5jj}$  is also AF) it gives, as a non-trivial by-product, a recent result of Taylor.<sup>25</sup>

3) For single particle QCD spectra the main results are:

i) The ratio of the average number of gluons (quarks) in a quark jet to the average number of gluons (quarks) in a gluon jet is finite and given by:

$$\frac{\langle n_i \rangle|_q}{\langle x_i \rangle|_g} \rightarrow c_F/c_A = 4/9; \quad i=q, \bar{q}, g. \quad (8)$$

This result seems to prove a rather old conjecture of Brodski and Gunion.<sup>26</sup> Furthermore, the fact that the ratio does not depend on the type of "detected" parton makes us believe that the result simply extends to hadron multiplicities,

ii)

$$\frac{\langle x_i \rangle|_g}{\langle x_i \rangle|_q} \rightarrow c_F/c_A = 4/9; \quad i=q, \bar{q}, g, \quad (9)$$

where  $\langle x_i \rangle$  is the average  $x$  of a quark in a quark jet etc..

iii) The spectrum near  $x=l$  is softer in a gluon jet than it is in a quark jet by a factor  $(1-x)$ , up to  $\log s(l-x)$ . Properties i), ii) and iii) clearly support the general feeling<sup>9</sup> that gluon jets are softer and that they yield

higher multiplicities.

A somewhat related, interesting observation, due to Shizuya and Tye,<sup>27</sup> is that the Stermen-Weinberg opening angle<sup>12</sup> for a gluon jet,  $d_g$ , is much bigger than the corresponding one for quark jets,  $d_q$ . One finds :

$$\delta_g = (\delta_q)^{c_F/c_A} \gg \delta_q; \quad c_F/c_A = 4/9. \quad (10)$$

All these results raise the question of whether gluon jets will be easy to see experimentally [see ref. 4) for an optimistic view on this point].

4) For two parton QCD spectra the main results are:

i) For  $XIX2$  finite, various limits can be considered, e.g.,

$$(1 - X_i - x_i) < 1; \quad (1 - X_i - x_i) \mathbf{K} (1 - * i) < 1$$

etc.. Precise predictions, somewhat reminiscent of double Regge fragmentation behaviour emerge. They confirm the previous statements on gluon jets being softer than quark jets.

ii) For  $X_i \sim 0$ ,  $x_i$  finite, the two partons become essentially uncorrelated.

iii) For  $x_i, x_j \sim 0$  there are long-range (in  $\log x$ ) correlations and one finds

$$\langle n(n-1) \rangle \simeq c \langle n \rangle^2, \quad (11)$$

where  $c$  depends on the type of jet considered, and also on the observed partons, and  $c > 1$ . The constant  $c$  is also somewhat dependent on the way the IR singularities are cut off. On the other hand, all such dependence disappear when we compare quark and gluon jets. One gets, in particular

$$\begin{aligned} & [\langle n(n-1) \rangle - \langle n \rangle^2] |_{qjet} \\ &= \frac{4}{9} [\langle n(n-1) \rangle - \langle n \rangle^2] |_{gjet} \end{aligned} \quad (12)$$

independently of the observed species (hence valid for hadron?).

5) In general one finds, independently of the regularization procedures used,

$$p(z_i) |_{qjet} = c_F/c_A p(z_i) |_{gjet}; \quad c_F/c_A = 4/9, \quad (13)$$

where  $p(z)$  is the Feynman gas pressure as a function of the chemical potentials  $z_i (i=q, g)$ . Furthermore, KNO scaling follows from the general structures of the theory.

6) No phenomenon à la Cornwall-Tiktopoulos<sup>28</sup> is seen to occur. One possibility is

\* This is also why the results for parton spectra described below can be transformed into hadronic spectra using the only input of fragmentation functions (see ref. 24)).

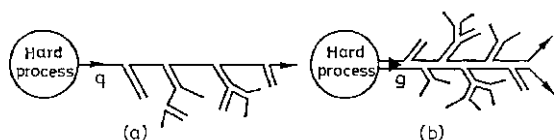


Fig. 5. Difference between a quark (a) and a gluon (b) jet in the large  $N$  limit. The graphical notation is that of refs. 5 and 6.

that things work out as in  $qjg$ , where Taylor has found<sup>25</sup> for normalized exclusive cross-sections  $\hat{\sigma}_n = \sigma_n / \sigma_T$ :

$$\hat{\sigma}_n = \hat{\sigma}_0 (1 - \hat{\sigma}_0)^n; \quad \hat{\sigma} \xrightarrow{Q^2/m^2 \rightarrow \infty} 0;$$

$$\hat{\sigma}_n / \hat{\sigma}_0 \rightarrow 1; \quad \sum_n \hat{\sigma}_n = 1. \quad (14)$$

This can be recognized as an ideal Bose gas distribution (Planck spectrum) corresponding to a black body with

$$\frac{kT}{\hbar\omega} \simeq (\log Q^2/m^2)^{1/9}$$

as can be checked from the explicit behaviour<sup>5</sup> of  $d_\sigma$ .

In a "naïve" regularization method for the QCD IR problem (which **\$1** does not have) one finds that the problem of computing the generating function of QCD jets is reduced to that of a so-called Markov branching process. This is exactly the problem encountered in studying the evolution in time of the population of competing species<sup>29</sup> (here quarks and gluons) having fixed probabilities of mutation and birth (but no death).

In this case one finds<sup>24</sup> that the gluon jet gives again a Planck spectrum (except that now  $kT/\hbar\omega$  is IR divergent) and the  $q$  jet gives the spectrum of  $C_j/C_s$  independent black bodies. Two amusing limits of this result are worth mentioning. For  $N_c \rightarrow \infty$   $C_j C_s \rightarrow j2$  and the result can be understood by the fact that, in the large  $N$  limit, only planar diagrams survive<sup>5,6</sup> giving (see Fig. 5) a "one-sided" jet for the quark (5a) as opposed to a "two-sided" jet for the gluon case (5b). The other interesting case is the QED limit, corresponding to  $C_j/C_s \rightarrow \infty$ . In such a case the quark jet is infinitely many independent black bodies: this is well known to give a Poisson distribution, the standard QED result.

I should mention, however, that, in a different (dimensional type) regularization of the IR problem, which at present looks on more solid grounds, one gets, for instance:

$$D \equiv \sqrt{\langle n(n-1) \rangle} - \langle n \rangle^2 = \gamma \langle n \rangle; \quad (15)$$

$$\gamma = 1/\sqrt{3} \text{ for } g \text{ jet}, \quad \gamma = \sqrt{3}/2 \text{ for } q \text{ jet}$$

which disagrees with the ideal gas prediction (but agrees, as usual, in the ratio of quark to gluon jet).

Amazingly, the result eq. (15) for a gluon jet is exactly the known empirical Wroblewski relation<sup>30</sup> which is seen to hold in pp hadrons at low  $p_T$ . This could support models, like the one of Pokorski and Van Hove,<sup>31</sup> in which gluons are responsible for pionization in hadronic collisions. It could also support, however, topological expansion models of the Pomeron (see below). The quark jet prediction should be checked in  $e^+e^-$  collisions.

7) Finally, it has been possible to combine the techniques of refs. 7 and 24 in order to gain some more differential information (*e. g.*,  $q_T$  spread) on final particles inside QCD jets. Interesting results appear to come out, like again a broadening of the naïve  $q_T$  spectrum, but I have no time for going into more detail here.

### 3.4. Planarity and duality in hard processes

It turns out that when QCD diagrams are computed in physical (*e.g.*, axial) gauges, the leading diagrams for collinear IR divergences are the planar ones (see, *e.g.*, refs. 7 and 18). One can then argue that non-planar contributions to hard processes are down for two reasons:

- i) Powers of  $a(Q^2)$ , *i.e.*, inverse powers of  $1^0 g Q^2$  (this is only so in the axial gauge).
- ii) Inverse powers of  $N_c$  or  $N_f$ , this being the case in any gauge.<sup>5,6</sup>

As a result planar diagrams in the axial gauge will completely dominate the dynamics of hard QCD processes.

It looks also natural to assume that, if confinement takes place at all in QCD, that should occur already at the planar level. As discussed below, this provides a very suggestive link between QCD and dual string theories. Now, by their structure, planar diagrams give, in a confining theory, resonance behaviour<sup>5</sup> (with resonance widths proportional to  $N_f/N_c$ ). In this case, a (dual) interpretation of the parton model results in terms of resonances instead of partons should be possible. We can then ask if it is true that



$$\langle \sum_{Res} \sigma_{Res} \rangle \simeq \text{Parton Model.} \quad (16)$$

When one looks into this problem for various QCD hard processes, one finds a little surprise: whereas for deep inelastic scattering and for  $e^+e^-$  annihilation one seems to be able to justify either Bloom-Gilman-type duality or Poggio-Quinn-Weinberg smoothing,<sup>32</sup> for lepton pair production a similar relation appears to be false. Without entering into details (see ref. 11), one finds that

$$\text{P. Model} \simeq \langle |A|^2 \rangle \stackrel{?}{\neq} \langle \sigma \rangle = \langle |A|^2 \rangle. \quad (17)$$

In the presence of peaks, of course,  $\langle |A|^2 \rangle > \langle \sigma \rangle$  and one predicts that narrow peaks stick out of the DY predicted background (for instance, they do not have the famous  $1/3$  suppression from colour). This is not so unexpected, perhaps, but it is nice that the theory gives automatically this difference between the dual interpretation of various processes.

In the region of broad, strongly overlapping resonances, one will again expect the parton model prediction to be valid for the average physical cross-section.

The next question is how we do go from a parton to a resonance description of hadronic reactions. Unfortunately, we can only make, at present, some qualitative guesses about this difficult question.

#### §4. Low Energy, Spectroscopy

This is not the subject of my talk<sup>33</sup> and I will then touch it only very briefly in order to make a smooth transition into high energy, low  $p_T$  processes.

When we look at strong interaction phenomena at the large scale implied by energies of a GeV or so, we do not see any more the elementary constituents, but rather that complicated, coherent superposition of quarks, antiquarks and gluons which are the hadronic resonances and bound states. This is the regime where dual resonance models have been used in the past with reasonable success.

A suggestive connection between QCD and dual (string) theory has been proposed by several people and goes more or less as follows:

i) According to presently popular ideas,<sup>34</sup> confinement is a result of the exact local gauge invariance of the vacuum (as opposed, for

instance, to a Higgs breaking situation).

ii) With a gauge invariant vacuum, only gauge invariant (colour singlet) states can propagate.

iii) The simplest gauge invariant states are formed by applying on the gauge invariant vacuum operators with a string-like structure, e.g.,

$$\bar{q}(x_1) T \exp \left( g \int_{P(x_1, x_2)} dx_\mu A^\mu(x) \right) q(x_2) \\ \sim \text{Open string, } x_1, x_2$$

$$\text{Tr} T \exp \left( g \oint_P dx_\mu A^\mu(x) \right) \sim \text{Closed string.}$$

The analogy goes a little further: if one uses the  $1/N_c$  expansion of 't Hooft<sup>5</sup> the perturbative intermediate states of the leading diagrams have the same global colour structure as the states obtained by expanding in  $g$  those gauge invariant states. It can also be argued that, if confinement takes place, such states will represent (superpositions of) infinitely narrow hadrons.<sup>5</sup>

I would also like to mention a recent paper by Nambu<sup>35</sup> where further evidence for some possible connection of this sort has been given.

In Fig. 6 we show a table of correspondence between QCD-gauge invariant operators and strings corresponding to various hadrons. One interesting development in hadron spectroscopy, which can be studied this way, extending the original scheme of Rosner, is "baryonium" for which, however, I have to refer you to other parallel and plenary<sup>33</sup> sessions.

#### §5. Intermediate to High Energies (up to ISR?)

I shall be quite short on this part and refer you to the talk of Chan.<sup>36</sup> There has not been so much news in this area last year, whereas works of the previous year have mainly concentrated on baryon and baryonium, a subject discussed elsewhere.<sup>33</sup>

I shall limit myself to a brief account of the QCD topological expansion approach to the bare Reggeons and the Pomeron, also as an introduction to the next topic: Reggeon field theory.

As we move up in energy and we go to about the 10 GeV mark, particle production at low  $p_T$  starts to become important. In the QCD inspired string picture mentioned above,

Hadron	Gauge invariant operator	String picture
$M_2 = q\bar{q}$ meson	$\bar{q}(x_1) \exp \left( g \int_{x_1}^{x_2} dx_\mu A^\mu \right) q(x_2)$	
$M_0 =$ quarkless meson	$\text{Tr} \exp \left( g \oint dx_\mu A^\mu \right)$	
$B_3 =$ qq $q$ baryon	$\epsilon_{ijk} \left[ \exp \left( g \int_x^{x_1} dx_\mu A^\mu \right) q(x_1) \right]_i \times$ $\times \left[ \exp \left( g \int_x^{x_2} dx_\mu A^\mu \right) q(x_2) \right]_j \left[ \exp \left( g \int_x^{x_3} dx_\mu A^\mu \right) q(x_3) \right]_k$	
$M_4^J =$ baryonium with qq $\bar{q}\bar{q}$ QN	$\epsilon_{ijk} \epsilon_{i'j'k'} \left[ \bar{q} \exp \left( \int_y^{y_1} \right) \right]_i \left[ \bar{q} \exp \left( \int_y^{y_2} \right) \right]_{j'} \times$ $\times \left[ \exp \left( \int_x^y \right) \right]_k^{k'} \left[ \exp \left( \int_{x_1}^x \right) q \right]^{j'}$ $\left[ \exp \left( \int_{x_2}^x \right) q \right]^{i'}$	
$M_2^J =$ baryonium with qq $\bar{q}\bar{q}$ QN	$\epsilon_{ijk} \epsilon_{i'j'k'} \left[ \bar{q} \exp \left( \int_y^{y_1} \right) \right]_i \times$ $\times \left[ \exp \left( \int_x^y \right) \right]_j^{j'} \left[ \exp \left( \int_x^y \right) \right]_k^{k'} \left[ \exp \left( \int_{x_1}^x \right) q \right]^{i'}$	
$M_0^J =$ quarkless baryonium	$\epsilon_{ijk} \epsilon_{i'j'k'} \times$ $\times \left[ \exp \left( \int_x^y \right) \right]_i^{i'} \left[ \exp \left( \int_x^y \right) \right]_j^{j'} \left[ \exp \left( \int_x^y \right) \right]_k^{k'}$	

Fig. 6. Simplest examples of correspondence between QCD gauge invariant operators and hadrons in the dual string picture.

we can say that long excited strings (heavy resonances) formed in the  $s$  channel break (decay). If the breaking up is a soft mechanism, as we believe, the fragments of the string will remember their location along the string itself, their ordering (see Fig. 7). As a result, a multiperipheral (MP) mechanism for hadronic production will follow, with approximate strong ordering, but also with cluster formation (clusters being  $qq$  resonances of a long enough lifetime).

Since the rate for string breaking (resonance decay) can be shown<sup>16</sup> to be proportional to

$N_j N_i$  (at least for small widths), this parameter is seen to control the amount of clustering in the multiperipheral chain.

In any case, the shadow (overlap functions) of the production processes discussed above builds up (see Fig. 8a) an ideally mixed, OZI conserving, exchange degenerate Regge pole, the so-called planar bare Reggeon (*e.g.*,  $p-Az-f-o$ ,  $K^*-K^{**}$ ) which is the new collective excitation (quasi particle) replacing, in the sense of the old DHS duality, individual resonances.

Because of the simple fact that cutting a sheet

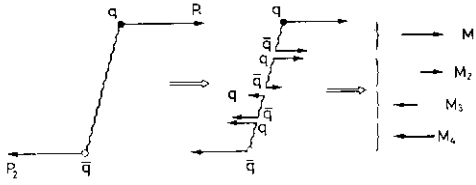


Fig. 7. Breaking of excited strings giving multiperipheral dynamics.

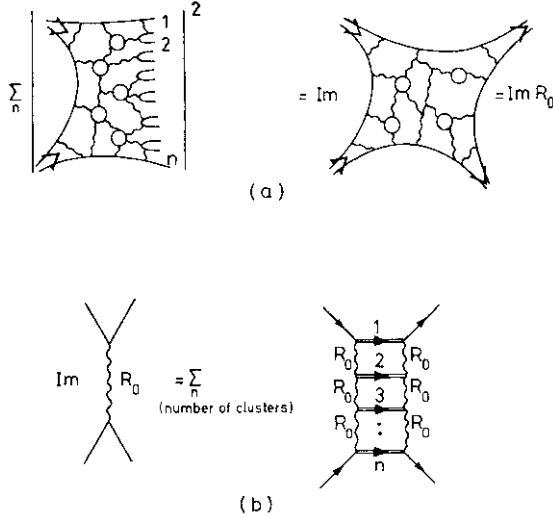


Fig. 8. (a) *s* channel content of the bare Reggeon ( $R_0$ ). (b) Planar unitarity for  $R_0$  within multiperipheral dynamics.

(plane) gives two sheets, the bare Reggeon satisfies a non-linear unitarity equation (see Fig. 8b) which is called planar unitarity. The unitarity sum is expected to be saturated in terms of the bare Reggeon itself with no AFS cut entering because of planarity.

By this kind of bootstrap, the strength of  $R_0$  can be determined to some extent. The result is roughly:

$$\frac{g_R^2 N_f}{16\pi^2} \simeq .5(1 + \bar{Y}_c/\bar{Y}_g)^{-1}, \quad (\text{is;})$$

where  $Y_c(Y_g)$  is the average cluster (gap) size in rapidity, both believed to be energy independent.

The last factor in eq. (18) is usually put to one by dual unitarization, topological expansion people, but it is actually important, both numerically and for over-all consistency with QCD.<sup>16</sup>

Numerically one gets

$$\begin{aligned} \sigma(\pi^+\pi^-) - \sigma(\pi^-\pi^-) &\simeq \frac{100}{N_f} \alpha'(\alpha's)^{-1/2} \\ &\simeq \frac{40mb}{N_f} \left( \frac{s}{1\text{Gev}^2} \right) \end{aligned} \quad (19)$$

which is quite reasonable.

More theoretically, by the arguments made on the resonance lifetime, one finds that

$$\bar{Y}_c/\bar{Y}_g \sim N_c/N_f$$

and this, for  $N_c \gg N_f$  gives

$$g_R^2 N_c/16\pi^2 \simeq O(1)$$

which is an uncontroversial QCD result.<sup>5,6</sup>

Indeed, the two extreme cases  $N/N_c < Cl$  and  $> 1$ , correspond to two opposite pictures already considered in the past:

$Nf/N_c < Cl$  gives the narrow resonance picture of the ordinary dual loop expansion, but is very far from MP behaviour (no space for rapidity gaps).

$Nf/N_c \sim 1$  corresponds to wide resonances and to direct multiperipheral production of pions, kaons, etc. It fits also with the Chew-Rosenzweig scheme of P-/identify.<sup>37</sup>

Real life has  $Nf/N_c \sim O(1)$ , and it is reassuring to find that, indeed, a model with MP production of clusters and with  $Y/Y_c \sim 1$  is more or less consistent with the data.<sup>38</sup>

Also the problem of *f-P* identity can be clarified<sup>4</sup> by varying the parameter  $NjN$ , and making contact in the relevant limits with dual perturbation theory,<sup>39</sup> which is known to give two separate vacuum trajectories.

The conclusion seems to be that it is quite easy to generate two vacuum singularities, but degeneracy of the non-leading one with the *p*, if experimentally established, will be a bit accidental in the topological expansion approach.

How does the transition to the bare Pomeron dominated regime take place? This is shown schematically in Fig. 9.

From resonance formation we go to a single multiperipheral chain with a wee valence quark being exchanged (this is also Feynman's picture explaining the behaviour of quantum

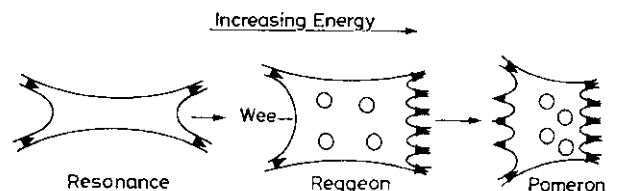


Fig. 9. Transition from the Resonance, to the Reggeon, to the Pomeron dominated regions.

number exchange cross-sections).

Increasing the energy further, it is increasingly difficult to keep the annihilating  $qq$  pair from emitting itself some mesons. When this takes place, vacuum exchange begins to be enhanced relative to quantum number exchange and this induces breakings of isospin degeneracy, ideal mixing, OZI rule, etc., in the region  $t < 0$  (*vice versa* these properties can be shown<sup>40</sup> to become better and better as  $t$  grows large and positive).

The topological organizations of QCD (or dual) graphs tell us the precise relation between  $i_0$  and the bare Pomeron  $P_0$  and allow one to define quite unambiguously the (bare) couplings of  $P_0$  to external particles, to Reggeons and to itself.

The basic picture for  $P_0$  is that of the shadow of a double MP chain (Fig. 9) with cluster production in each chain. The model is compatible with the ideas of Low and of Nussinov<sup>41</sup> on the Pomeron which also originated in QCD.

The basic properties of  $P_0$  coming from this picture (some of them are quite old results by now!) are the following:

If the two MP chains are independent:

i)  $\langle n \rangle_{P_0} \xrightarrow{E \text{ large}} 2 \langle n \rangle_{R_0}$ ; more generally, for

the Feynman gas pressure:

$$p_{P_0}(z) \xrightarrow{E \text{ large}} 2p_{R_0}(z), \quad (20)$$

which has an amusing similarity to the relation found between quark and gluon jets for large  $N$  (eq. (13) with  $C_F/C_A \rightarrow 1/2$ ).

ii)  $\alpha_{P_0}(0) = 1$  (21)

iii)  $\alpha'_{P_0}(0) = 1/2 \alpha'_{R_0}(0)$ . (22)

These three relations will be somewhat modified by correlations among the two chains and, in particular, we expect  $\alpha_{P_0}(0) > 1$  and  $\alpha_{P_0} < \alpha'_{R_0}$  to be correlated effects. In any case, the quantity  $J_0 = \alpha_{P_0}(0) - 1$  is of  $O(1)$  in the  $1/N$  expansion.

iv) One also finds that the triple Pomeron coupling at zero momentum transfer

$$\mathfrak{F} / \langle \mathbf{0} | \mathbf{W}^0 | \mathbf{0} \rangle = g_p$$

is different from zero (strong coupling RFT) and that it is of  $O(1/N)$ .

All these quantities,  $R_0$ ,  $P_0$ ,  $g_p$  belong to the  $h=0$  topology of QCD graphs (sphere).

The amusing point is that higher topologies can be related<sup>42</sup> to RFT (Gribov) diagrams in

a way consistent with  $s$  and  $t$  channel unitarity. This represents, to my knowledge, the only existing way of classifying all the diagrams of a normal field theory to obtain an RFT. The resulting RFT Lagrangian turns out to have the general structure<sup>42</sup>

$$\begin{aligned} \mathcal{L}_{\text{RFT}}^{\text{TE}} = & \bar{\psi} F(\phi/N, \bar{\psi}/N) \psi = \Delta_0 \bar{\psi} \psi + \alpha' \bar{\psi} \partial_t \psi \\ & + \frac{c}{N} \bar{\psi} (\psi + \bar{\psi}) \psi + O(1/N^2) \\ & - 4P_0 \text{ coupling} + \dots \end{aligned} \quad (23)$$

An interesting question to ask is whether we should expect this RFT to be critical, i.e. to have  $J_c = 0$ .

We know<sup>43</sup> that this happens for

$$\Delta_0 = \Delta_c = g_p^2 \times (\text{Known numbers}) \quad (24)$$

and we see therefore that, from our point of view,  $\Delta_0 = \Delta_c$  looks very accidental since  $J_0 = O(1)$  and  $J_c = O(1/N^2)$ .

For large  $N$  we certainly go in the supercritical direction  $J_0 > 1$  and in a simple but probably reliable model, Bishari has found<sup>44</sup>

$$J_c \sim 0.004 \quad (25)$$

to be compared with  $Z_f = 0.05$ . We now turn to the discussion of recent results in RFT.

### §6. Supercriticism and RFT

The first question that comes to mind is: at what energies does RFT start to be relevant? The answer depends on the input parameters of RFT because they will decide when many  $P_0$  exchanges become important.

The general feeling is that, because of the small triple Pomeron coupling  $g_p$  and of the not-so-large Pomeron intercept, triple Pomeron iterations are not important yet in the ISR region. Since, however, the Pomeron coupling to the proton looks considerably bigger than  $g_p$ , other types of iterations (*e.g.*, eikonal) could already be relevant. Finally, if the coupling of  $P_0$  to a heavy nucleus goes like  $A^{1/3} g_{pNN}$  ( $A$ =atomic number), then for scattering on nuclei, RFT could be already very relevant at present energies. This point about the coupling growing as  $A^{1/3}$  looks, however, still controversial.<sup>45</sup>

Irrespectively now of relevance to present energies the conceptually important question comes of the expected behaviour of cross-sections, in particular of  $\sigma_{tot}$  at "oo" energies,

In other words, how does a  $P_n$  above one cure its own problem with the Froissart bound?

There has been considerable progress on these questions recently, part of which has been summarized by Le Bellac<sup>46</sup> in a parallel session. The results, however, although agreed upon by the majority of people working in this area, are still being challenged by White.<sup>47</sup> Let me go just a little into the basic points of supercritical ( $A_0 > A_c$ ) RFT.

a) Case of no transverse dimensions,  $D_t = 0$ .

Even this case is controversial. It is actually believed<sup>46</sup> that settling this (apparently simple) case will also settle the dispute about the physical case  $D_t = 2$ .

The  $S$  matrix for the forward elastic amplitude is written as

$$S = \langle 0 | e^{-if a} e^{-HY} e^{-iga^+} | 0 \rangle = 1 + iT, \quad (26)$$

where  $a$  and  $a^+$  are Pomeron destruction and creation operators, the two coherent states  $\exp(-/ga^+) | 0 \rangle$ ,  $\langle 0 | \exp(-ifa)$  represent the (imaginary) couplings to the external legs of Fig. 10 and the  $\exp(-HY)$  is the propagator blob (again of Fig. 10) in rapidity (imaginary time).

Inserting a complete set of eigenstates of  $H$  in Eq. (26) we see that the vacuum reproduces 1 and possible other eigenstates of  $H$  contribute to  $T$ , a term proportional to

$$\exp(+Y\mathcal{A}) = S^{+\mathcal{A}}$$

if  $-\mathcal{A}$  is the eigenvalue.

Now  $H$  can be written down and the problem can be reduced<sup>48</sup> to the quantum mechanical problem of finding the levels of the corresponding Schrödinger equation. The potential looks quite different for  $J_0 < 0$  and  $J_0 > 0$  (see Figs. 11a and 11b).

The first case is non-controversial, but also uninteresting. For  $J_0 > 0$  the authors of ref. 48 find two low-lying levels, the vacuum and a second one which is above it by

$$-\mathcal{A} = \varepsilon \simeq \exp\left(-\frac{1}{2} \mathcal{A}_0^2 / g_\rho^2\right) \quad (27)$$

due to a tunnelling effect. A path integral formulation of such an effect, à la Polyakov, has also been obtained.<sup>49</sup>

As a result, one finds that, for  $Z_t = 0$ , there is no critical point at finite  $J_c$ . On the other hand,  $s$  goes quickly to zero at increasing  $J_c$ .

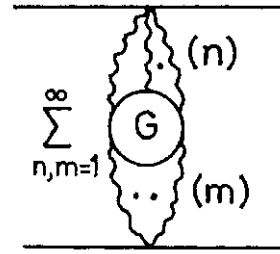


Fig. 10. RFT diagrams contributing to the elastic amplitude.

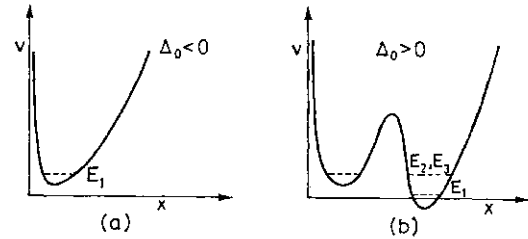


Fig. 11. Equivalent Schrödinger potential of ( $D_t=0$ ) RFT. (a)  $a_r(0) < 1$ ; (b)  $a_r(0) > 1$ .

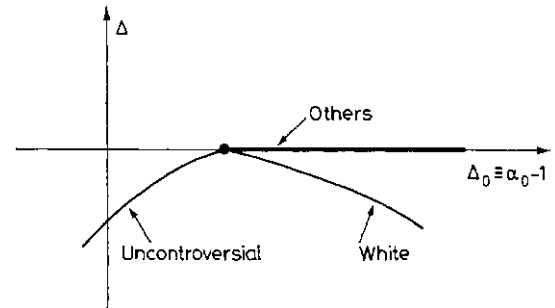


Fig. 12. Position of the output singularity (in  $E=J-1$ ) as a function of  $z/0$ . . . and of the theorist.

According to White,<sup>47</sup> instead,  $e \sim J_0$  for  $J_0$  large and positive and  $a_r$  goes to zero faster and faster. I must confess, however, that I have not been able to understand his criticism.

$A = 1, 2$

The situation is summarized in Fig. 12, where the behaviour of the output  $P$  is given as a function of the input  $J_0$ . The region below and up to  $A_0 = A_c$  (under-critical and critical) is uncontroversial, but, as we argued, the real world probably lies above it. Here White appears to disagree again with the majority of the authors, whose model I shall now briefly describe.

The idea<sup>50</sup> is to neglect at first the small slope of the Pomeron. In this way, different points in impact parameter space (of dimensions  $D_t$ ) are decoupled. Defining a lattice in such a space, we have to solve, at each lattice site, the  $D_t=0$  problem discussed above.

For  $J_0$  large, we can assume that only the two nearly degenerate states matter (the others are  $O(J_0)$  above). Hence, at each lattice site, we now have a system with two degrees of freedom, a "spin" variable which can be either up or down.

Coupling now the various lattice sites through  $a'$ , we can ask whether the resulting spin model of RFT has a zero gap state. The answer is yes according to the authors of ref. 50. They find a zero gap state  $|1\rangle$  ( $\hat{1} = 0$ ) with

$$\langle 1 | a^+(y, b) | 0 \rangle \simeq \frac{\Delta_0}{g_p} \theta(vy - b), \quad (28)$$

where  $b$  is the impact parameter,  $y$  the rapidity and  $v$  a calculable parameter. Equation (28) is equivalent to a grey expanding disc giving  $a_r \sim \log^2 s$ , as in the Froissart bound.

For  $D_r = l$  even a soliton, path integral formulation of the phenomenon can be given.<sup>51</sup>

Various authors<sup>52</sup> have been able to compute multiparticle distributions in the above spin model and have found a sort of modified geometrical scaling behaviour for the  $n$  particle density  $P^{(n)}$ :

$$\rho^{(n)}(y_i) \sim (Y^2)^n F_n(y_i/Y) \quad (29)$$

to be compared with the critical point behaviour:

$$\rho^{(n)}(y_i) \sim Y^{n\eta} \tilde{F}_n(y_i/Y). \quad (30)$$

Both eqs. (29) and (30) are compatible with KNO scaling.

Finally, exclusive and inclusive diffractive production are found<sup>53</sup> to be damped enough for  $s$  channel unitarity constraints to be fulfilled.

In conclusion, the spin model looks like a very consistent scheme for supercritical RFT and is able to predict rising cross-sections. If it will pass, as I feel it should, the further test of  $l$  channel unitarity, the remaining theoretical objections to it should probably be dismissed.

## §7. Soft vs Hard Hadron Physics

### 7.1. Phenomenological analogies

Of course the jet structure is common to both types of physics (large angle jets vs forward and backward jets). This has led to the speculation of complete jet universality between soft and hard processes.

Data suggest an approximate validity of

these predictions, *e. g.*,

a) Average multiplicities are expected to be related according to<sup>54</sup>

$$\bar{n}_{e^+e^-}(E) : \bar{n}_{\pi P}(\alpha E) : \bar{n}_{P P_{\text{anna}}}(\beta E) = 1 : 2 : 3, \quad (31)$$

where  $a, \beta$  are more or less predictable numbers<sup>55</sup> accounting for the fact that in  $e^+e^-$  all the energy goes to a single  $qq$  pair whereas in other processes it gets distributed among various  $qq$  pairs (*e.g.*, three pairs in  $pp$  annihilation).

Although the data now clearly disagree<sup>56</sup> with absolutely universal behaviour of the type predicted in ref. 26, they seem to be roughly in agreement with the prediction (31).

There are other predictions on correlations, in particular on Bose-Einstein interference,<sup>57</sup> which also look as if they have experimental support.<sup>58</sup>

b) *There have been claims*<sup>TM</sup> that fragmentation functions in  $e^+e^-$  and low  $p_r$  hadron physics scale and are roughly consistent with each other, although, in a contribution to this Conference,<sup>60</sup> the opposite statement has been made.

Notice also that the average  $\langle q_r \rangle$  relative to the jet axis has been reported<sup>61</sup> to be the same as that of low  $p_r$  physics ( $\sim 300$  MeV).

### 7.2. Theoretical QCD expectations

It looks that, in QCD, the two types of jets should differ drastically at a closer analysis. The analogy should be only superficial and/or just restricted to low values of  $Q^2$ . I shall try to argue now that this is indeed our theoretical expectation.

a) We can quote first results from two-dimensional QCD,<sup>62</sup> where one finds that, whereas fragmentation functions are universal within hard processes (as we argued to be also the case in four dimensions), they differ in soft hadron-hadron collisions.

In the actual four-dimensional case there are further reasons to doubt universality.

b) Firstly, low  $p_r$  fragmentation functions should scale, to first approximation, if QCD gives, after confinement, Regge poles interpolating its bound states. Of course there will be scaling violations associated with absorptive corrections (Regge cuts) but these are non-planar effects down at least  $O(1/N)$ .

On the contrary we have seen that, in hard

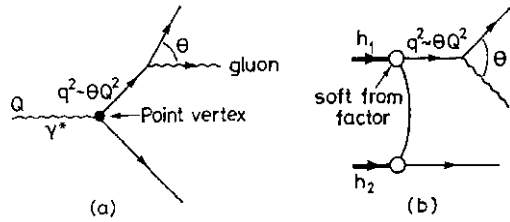


Fig. 13. Producing a large  $p_T$  in (a) hard processes (e.g.,  $e^+e^- \rightarrow$  hadrons); (b) soft processes (e.g., pions).

processes, scaling violations in fragmentation functions are there already (if not only) in the simplest planar diagrams. At some  $Q^2$  they will start being large and  $O(1)$  (in terms of a  $1/N$  expansion).

c) A very much related difference is the fact that low  $p_T$  physics is strongly damped in  $p_T$ : roughly speaking  $\langle p_T \rangle \approx 300$  MeV and constant.

In hard jet physics we expect the average  $p_T$  relative to the jet axis to increase essentially linearly with energy (same for the  $p_T$  of lepton pairs). In other words, hard jets have finite angular spread and *not* finite  $p_T$ .

As I anticipated, b) and c) have a common origin in the rather hard nature of QCD (or of any other field theory with dimensionless coupling constant). The mechanism giving a different behaviour in the two regimes is sketched in Figs. 13a and 13b. In Fig. 13a it is "easy" to send the intermediate quark line much off shell (which is necessary in order to produce a large  $p_T$  relative to the jet axis) because of the point-like coupling of the photon (a similar effect occurs also in large  $p_T$  hadron hadron collisions). On the contrary, in Fig. 13b, the same process is killed (exponentially?) by the wave function of our composite system which does not like to have partons far from the mass shell.

In other words, once a hard process is generated, it is only a little extra price ( $a(Q^2)/\pi \approx 0.1$ ) to produce an even harder one (e.g., large  $q_T$  relative to the axis of a jet of large  $p_T$ ); to do it instead the first time (z. e., large  $p_T$  relative to the beam direction) is much harder.\*

\* An interesting piece of data which seems to confirm such QCD prediction in the observation<sup>11</sup> of a larger  $\langle gv \rangle$  in the forward-backward fragments, where a large  $p_T$  trigger is used. The QCD expectation is that  $\langle q_T^2 \rangle \sim O(a(p_T^*)p_T^*)$ .

How do we then explain the apparent analogies between soft and hard hadron physics? Well, up to present values of  $s$  and  $g^2$ , very large scaling violations are neither predicted nor seen: universality could very well be an approximate and temporary property before we move to harder and harder processes.

In any case, this looks to be a distinct prediction of QCD, as opposed to softer theories like Preparata's bag model or conventional dual theories, and should be checked at the energy of next generation machines.

I would like to conclude with a speculation on what could be instead a real common denominator to soft and hard hadronic phenomena.

The guess is that such will be the concept of "order" in hadron physics be it soft or hard.

It looks now very plausible that, in the axial gauge of QCD, a small set of diagrams, having the simplest topology, describe to great accuracy both hard and soft processes, both lepton and hadron induced reactions. The manifestations of this fact would be numerous, e.g.,

a) The orderly, coherent structure of hadronic production, to be detected perhaps by sensitive interference effects of the Bose-Einstein type.

b) The simple correlation of momenta and internal quantum numbers in jets.

c) The dominance of resonance production (clusters) in low-energy channels.

d) The OZI and EXD regularities together with the pattern of their breaking.

Actually, for low  $p_T$  hadron physics, Chew and co-workers have been recently setting up an ambitious  $S$  matrix program having the concept of order as its basic starting point. This, I feel, could extend to hard processes as well and provide\* a distinctive feature of strong processes as opposed to other types of interactions.

## References

1. J. D. Bjorken: Alternatives to gauge theories, SLAC-PUB-2062, Dec. 1977.
2. B. Sakita: these Proceedings; C. G. Callan:

\* It could also provide a useful hint to confiners. For instance, instanton effects are expected to turn off in the planar limit (they are  $O(e^{-N})$ ) and, therefore, if the planar theory already confines, as we argued to be the case, instantons would have little to do with that phenomenon.

- these Proceedings; K. Kikkawa: these Proceedings.
3. For an encouraging piece of recent data, see, A. G. Clark *et al.*: "Inclusive  $n^0$  production from high energy p-p collisions at very large transverse momenta," CERN preprint (1978).
  4. A. de Rujula: these Proceedings.
  5. G. 't Hooft: Nuclear Phys. **B72** (1974) 461. For the first idea in this direction, see also H. J. Lipkin, Proc. Ecole de Physique Théorique, Les Houches (1978), eds C. de Witt and V. Gillet, p. 585.
  6. G. Veneziano: Nuclear Phys. **B117** (1976) 519.
  7. Yu. L. Dokshitser, D. I. Dyakonov and S. I. Troyan: Proc. 13th Winter School of the Leningrad B. P. Konstantinov Institute of Nuclear Physics, Leningrad (1978).
  8. H. D. Politzer: these Proceedings.
  9. R. Field: these Proceedings. F. Close: these Proceedings.
  10. T. Kinoshita: J. Math. Phys. **3** (1962) 650; T. D. Lee and M. Nauenberg: Phys. Rev. **133** (1964) 1549; See also N. Nakanishi: Progr. theor. Phys. **19** (1958) 159.
  11. D. Amati, R. Petronzio and G. Veneziano: Nuclear Phys. **B140** (1978) 54.
  12. G. Serman and S. Weinberg: Phys. Rev. Letters **39** (1977) 1436.
  13. V.N. Gribov and L.N. Lipatov: Soviet J. Nuclear Phys. **15** (1972) 438, 675.
  14. A. H. Mueller: Phys. Rev. **D9** (1974) 963; see also C. G. Callan and M. L. Goldberger: Phys. Rev. **D11** (1975) 1553.
  15. H. D. Politzer: Phys. Letters **70B** (1977) 430, and Nuclear Phys. **B129** (1977) 301.
  16. C. T. Sachrajda: Phys. Letters **73B** (1978) 185, and CERN preprint TH. 2459 (1978); C.H. Craig and C. H. Llewellyn Smith: Phys. Letters **72B** (1978) 349.
  17. C. H. Llewellyn Smith: Lectures given at Schlading, Oxford preprint 47/78 (1978). J. Frenkel, K. J. Sheiler and J. C. Taylor: Oxford preprint 25/78 (1978).
  18. D. Amati, R. Petronzio and G. Veneziano: CERN preprint TH. 2527 (1978).
  19. R. K. Ellis, H. Georgi, M. Machacek, H. D. Politzer and G. G. Ross: MIT preprint CTP No. 718 (1978) and in preparation; S. B. Libby and G. Serman: Stony Brook preprint ITP-SB-78-41 (1978).
  20. See, for example, G. Altarelli, R. K. Ellis and G. Martinelli: MIT preprint CTP No. 723 (1978), contribution No. 579.
  21. See, for example, W. A. Bardeen, A.J. Buras, D. W. Duke and T. Muta: Fermilab preprint PUB 78/42THY (1978), contribution No. 415.
  22. A. H. Mueller: Columbia preprint CU-TP 125 (1978).
  23. V.V. Sudakov: Zh. eksp. teor. Fiz. **30** (1956) 87, Sov. Phys. JETP **3** (1956) 65.
  24. K. Konishi, A. Ukawa and G. Veneziano: CERN preprint TH. 2509 (1978) and in preparation; K. Konishi: talk presented at the Symposium on Jets, NBI-Nordita, Copenhagen, Rutherford preprint RL-78-077 (1978) and these Proceedings.
  25. J.C. Taylor: Phys. Letters **73B** (1978) 85.
  26. S.J. Brodski and J. F. Gunion: Phys. Rev. Letters **37** (1976) 402.
  27. K. Shizuya and S.-H. H. Type: FNAL preprint 78/54 (1978).
  28. J. M. Cornwall and G. Tiktopoulos: Phys. Rev. **D13** (1976) 3370.
  29. S. Karlin: *A First Course in Stochastic Processes* (Academic Press, New York, 1966) Ch. II, p. 318.
  30. A. K. Wroblewski: *Proc. IVth. Int. Symp. Multiparticle Hydrodynamics (Pavia, 1973)* (eds. F. Duimio, A. Giovannini and S. Ratti) p. 625.
  31. S. Pokorski and L. Van Hove: Acta Phys. Pol. **B5** (1974) 229; Nuclear Phys. **B86** (1975) 243.
  32. E. C. Poggio, H. R. Quinn and S. Weinberg: Phys. Rev. **D13** (1976) 1958.
  33. See K. Igi, these Proceedings; Y. Hara, these Proceedings.
  34. K. Wilson: Phys. Rev. **D10** (1974) 2445; A. M. Polyakov: Phys. Letters **59B** (1975) 82.
  35. Y. Nambu: Univ. of Tokyo preprint UT-310 (1978).
  36. Chan Hong-Mo: these Proceedings.
  37. G. F. Chew and C. Rosenzweig: Phys. Letters **58B** (1975) 93.
  38. L. Caneschi: Nuclear Phys. **B108** (1976) 417; R. E. Diebold, these Proceedings.
  39. P. Aurenche and L. Gonzales Mestres: Orsay preprint LPTHE 77/33 (1977); C. B. Chiu and S. Matsuda: Nuclear Phys. **B134** (1978) 463.
  40. G. F. Chew and C. Rosenzweig: Nuclear Phys. **B104** (1976) 290; M. Bishari: Phys. Letters **59B** (1975) 461.
  41. F. E. Low: Phys. Rev. **D12** (1975) 163; S. Nussinov: Phys. Rev. Letters **34** (1975) 1286.
  42. M. Ciafaloni, G. Marchesini and G. Veneziano: Nuclear Phys. **B98** (1975) 472, 493.
  43. M. Moshe: Phys. Reports **37C** (1978) 255, and references therein.
  44. M. Bishari: Weizmann Institute preprint WIS-77/55 Ph. (1977).
  45. For a review, see, L. Caneschi and A. Schwimmer: *Proc. XII Rencontre de Moriond (Flaine, 1977)* (ed. Tran Thanh Van).
  46. M. Le Bellac: these Proceedings.
  47. A. White: CERN preprint TH. 2449 and these Proceedings.
  48. V. Alessandrini, D. Amati and R. Jengo: Nuclear Phys. **B108** (1976) 425; R. Jengo: Nuclear Phys. **B108** (1976) 447; J. Bronzan, J. Shapiro and R. Sugar: Phys. Rev. **D14** (1976) 618; M. Ciafaloni, M. Le Bellac and G. C. Rossi: Nuclear Phys. **B130** (1977) 388.
  49. M. Ciafaloni: Pisa preprint S. N. S. 5 (1978) and private communication.
  50. D. Amati, M. Ciafaloni: M. Le Bellac and G. Marchesini, Nuclear Phys. **B112** (1976) 107; D. Amati, M. Ciafaloni, G. Marchesini and G.



- Parisi: Nuclear Phys. **B114** (1976) 483; J. L. Cardy: Nuclear Phys. **B115** (1976) 141; R. C. Brower, M. A. Furman and K. Subbarao: Phys. Rev. **D15** (1977) 1756.
51. V. Alessandrini, D. Amati and M. Ciafaloni: Nuclear Phys. **B130** (1977) 429.
52. M. Ciafaloni and G. Marchesini: Nuclear Phys. **B109** (1976) 261 ; G. Marchesini and L. Trentadue: Parma preprint (1977).
53. G. Marchesini and E. Rabinovici: Nuclear Phys. **B120** (1977) 253; G. Marchesini, E. Trentadue: contribution No. 836 to the Conference.
54. G. Veneziano: in Confinement, *Proc. 9th Ecole d'Eté de Physique des Particules (Gif-sur-Yvette, September, 1977)* Vol. II, p. 23, and references therein; Similar results follow from the massive quark model, N. S. Craigie and G. Preparata: Nuclear Phys. **B102** (1976) 497.
55. B. R. Webber: private communication. J. Dias de Deus and S. Jadach: Phys. Letters **66B** (1977) 81.
56. V. Luth: SLAC Pub. 2050 (1977); J. G. Rushbrooke: private communication.
57. A. Giovannini and G. Veneziano: Nuclear Phys. **B130** (1977) 61.
58. G. Goldhaber, LBL physics notes, TG-287 (1977); M. Deutschmann *et al.*: CERN/EP/PHSY 78-1 (1978) (reviewed by R. E. Diebold).
59. B. Anderson, G. Gustafson and C. Peterson: Phys. Letters **69B** (1977) 221. F. Hayot and S. Gustafson and C. Peterson: Phys. Letters **69B** (1977) 221. F. Hayot and S. Jadach: Saclay preprint DPh-T/77/84 (1977).
60. T. Kinoshita, H. Noda, T. Tashiro and M. Mizouchi: Contr. No. 219.
61. R. Sosnowski: these Proceedings.
62. For a review and a discussion of this point, see J. H. Weis: CERN preprint TH. 2525 (1978).
63. G. F. Chew and C. Rosenzweig: Phys. Reports **41C** (1978) 5, and references therein.

## NOTE ADDED IN PROOF

Soon after the Conference, the following papers have appeared extending the analysis of QCD jets to the "semi-hard" region discussed in Section 3.2:

G. Curci and M. Greco: CERN Preprint TH-2526 (1978); R. K. Ellis and R. Petronzio: CERN Preprint TH-2571 (1978); K. Konishi, A. Ukowa and G. Veneziano: CERN Preprint TH-2577 (1978).

**P 3b**

**Dynamics of High Energy Reactions**

R. D. FIELD

*California Institute of Technology, Pasadena, California 91125*

Applications of the theory of quantum chromodynamics (QCD) with asymptotic freedom to processes involving large momentum transfers are examined. The theory describes correctly many features of the lepton initiated processes  $eN$ ,  $\bar{\nu}N$ ,  $\nu N$ ,  $\bar{\nu}N$  as well as large-mass muon-pair production *and* the production of mesons and jets at large  $p_{\pm}$  in hadron-hadron collisions. The preliminary conclusion is that QCD might well be the correct theory behind all these phenomena, although a definitive test has not yet been made.

**§1. Introduction**

During the last several years, a new framework to describe strong interaction physics has emerged: quantum chromodynamics (QCD). It is the simplest field theory which incorporates a color-dependent force among the quarks. These forces are generated by the exchange of colored vector gluons which are coupled to the quarks (and to each other) in a gauge-invariant manner. The theory is closely related to the most successful quantum field theory: QED. The only (but very important) difference is the gauge group involved. QED is an Abelian gauge theory (the photons do not couple to each other); QCD is a non-Abelian gauge theory—gauge group  $SU_3$  (color). The gluons carry color and thus couple to each other.

Although the theory is well defined, precisely what it predicts is not yet clearly known. For example, it is not known if the theory actually confines quarks and gluons within hadrons nor has the spectrum of hadron states been calculated. At present, the mathematical complexities are still too great. However, at very high energy or momentum transfer  $g$ , the theory is asymptotically free; the effective coupling between quarks and gluons decreases toward zero with increasing  $Q^2$ . As emphasized by Politzer,<sup>1,2</sup> this permits calculation of those parts of a process involving high  $Q^2$  by the use of perturbation theory. Yet most real processes involve both high *and* low  $Q^2$  together and precisely how to separate these parts is just becoming understood.

In this talk, I will examine many of the present day applications of QCD to processes

involving large momentum transfers. Some of these applications are rather crude and involve ideas that are somewhat phenomenological in nature. Nevertheless, comparisons with data are quite encouraging, although many of the most dramatic (and definitive) tests are yet to come. The theory describes correctly many features of the lepton initiated processes  $eN$ ,  $\bar{\nu}N$ ,  $\nu N$ ,  $\bar{\nu}N$  as well as large-mass muon-pair production *and* the production of mesons and jets at large  $p_{\pm}$  in hadron-hadron collisions. The preliminary conclusion is that quantum chromodynamics might well be the correct theory behind all these phenomena.

**§11. The Effective Coupling  $a_s(Q^2)$**

The theory of QCD does not produce inclusive cross sections that "scale." One cannot use dimensional counting arguments to determine the behavior of cross sections (at intermediate values of  $Q^2$ ). This is because the theory has an intrinsic "scale" or mass parameter  $\Lambda$  that is generated as a result of the *interaction* between quarks and gluons. These interactions result in an effective strong interaction coupling,  $a_s(Q^2)$ , that decreases logarithmically with increasing  $g^2$ , where  $Q$  is some characteristic momentum in a collision.

In the theory of QED, it is well known that the physical coupling  $e$ , defined by the large distance (small  $Q^2$ ) behavior, is smaller than the effective coupling  $e_{eff}$  one would measure at small distances (large  $Q^2$ ). This is due to vacuum polarization effects that shield the bare charge. In lowest order perturbation theory, the vacuum polarization contribution shown in Fig. 1a gives

$$\alpha_{\text{QED}}(Q^2) \equiv e_{\text{eff}}^2/4\pi = \alpha_0 \left[ 1 + \frac{\alpha_0}{3\pi} \log Q^2/m_e^2 \right] \quad (2.1)$$

In higher orders, a whole series of the type  $(\text{to } \log Q^2/m_e^2)^n$  appears and summing the leading logarithms yields

$$\alpha_{\text{QED}}(Q^2) = \frac{1}{1/\alpha_0 - (1/3\pi) \log Q^2/m_e^2} \quad (2.2)$$

No matter how small  $\alpha_0$  is, one can always increase  $Q^2$  to a point where  $\alpha_{\text{QED}}(\hat{\delta}^2)$  becomes infinite (see Fig. 2). This means that perturbation theory breaks down at high  $Q^2$  in QED. One needs to include higher and higher orders in  $\alpha_{\text{QED}}$  as  $Q^2$  increases. At low  $g^2$ , on the other hand,  $\alpha_{\text{QED}}(Q^2)$  is small ( $\alpha_0 = 1/137$ ) and perturbation theory works well.

An important difference between QED and QCD lies in the behavior of the renormalized

charge. The reason for the difference is the new feature of QCD, that the gluons carry charge (color) and interact with each other. The lowest order contributions to the effective charge shown in Figs. 1b, c, d give

$$\alpha_s(Q^2) = \alpha_s(\mu^2) [1 + \bar{a} \alpha_s(\mu^2) \log Q^2/\mu^2], \quad (2.3)$$

where

$$\bar{a} = (2/3n_f + 5 - 16)/4\pi. \quad (2.4)$$

In the coulomb gauge, the  $+2/3 n_f$  and the  $+5$  in (2.4) come from the quark loops (one for each flavor  $n_f$ ) and the transverse gluon loop in Figs. 1b and 1c, respectively. These contributions are of the same sign as the QED case. They produce "charge shielding." The  $-16$  comes from the diagram with one transverse and one "coulomb" gluon in the gluon bubble (Fig. 1d). If  $2/3 n_f < 11$ , this "anti-shielding" contribution dominates and after summing the infinite series of bubbles one has

$$\alpha_s(Q^2) = \frac{1}{1/\alpha_s(\mu^2) - \bar{a} \log Q^2/\mu^2} \quad (2.5)$$

which approaches zero as  $Q^2$  increases ("asymptotic freedom") since now  $\bar{a} < 0$ .

In QED it is easy to define what one means by the charge of an electron  $e$ . It is defined by the large distance behavior of the electric potential (Thomson limit). One cannot do this for QCD since the  $Q^2 \rightarrow 0$  limit of  $\alpha_s(Q^2)$  cannot be calculated by perturbation theory. Neither can one define the strong coupling as the  $Q^2 \rightarrow \infty$  limit since in this limit it is zero. Instead one must define some arbitrary point  $\mu^2$  (the renormalization point) at which the coupling is  $\alpha_s(\mu^2) = g^2/4\pi c$ . It, however, does not matter which point  $\mu^2$  one chooses. If one chooses instead the point  $M^2$ , then the couplings are related (to lowest order) by

$$1/g_\mu^2 + (\bar{a}/4\pi) \log \mu^2 = 1/g_M^2 + (\bar{a}/4\pi) \log M^2. \quad (2.6)$$

Thus the "real" parameter in the theory is not  $g$  or  $1/a^2$  but rather a mass scale  $A$  that is independent of  $\mu^2$  and is given to this order by

$$\log A^2 = 4\pi/(\bar{a}g_\mu^2) + \log \mu^2, \quad (2.7)$$

which when inserted into (2.5) yields

$$\alpha_s(Q^2) = \frac{12\pi}{(33 - 2n_f) \log Q^2/A^2}. \quad (2.8)$$

At present, the mass scale  $A$  must be determined

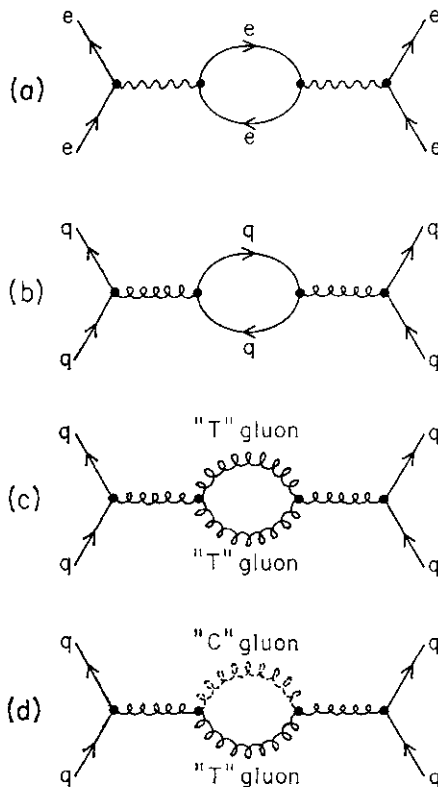


Fig. 1. (a) Lowest order vacuum polarization correction to the electric charge. (b) Lowest order correction to the quark-gluon coupling due to a virtual quark-antiquark pair. (c) Lowest order correction to the quark-gluon coupling due to a virtual pair of transverse ("JT") gluons in the coulomb gauge. (d) Lowest order correction to the quark-gluon coupling due to a virtual pair of gluons one transverse ("JT") and one "coulomb" ("C") in the coulomb gauge.

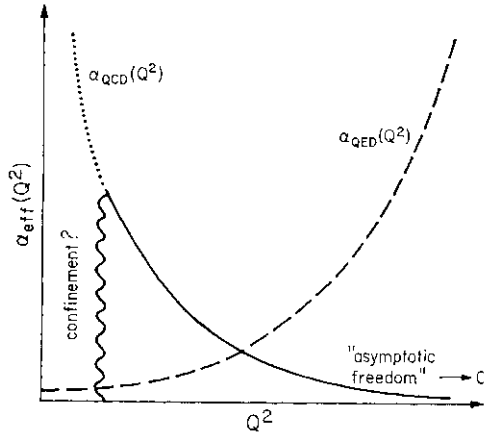


Fig. 2. Illustration of the behavior of the effective coupling calculated in perturbation theory in QED and QCD. In QED the effective coupling,  $\alpha_{QED}(Q^2)$ , is small at small  $Q^2$ , but becomes large at large  $Q^2$  (small distances). In QCD, on the other hand, the effective coupling is large at small  $Q^2$  (large distances) where confinement may occur, but decreases toward zero as  $Q^2$  increases ("asymptotic freedom"). Perturbation theory should work well for QCD (QED) at large  $Q^2$  (small  $Q^2$ ).

experimentally. It governs the point where  $\alpha_s(Q^2)$  becomes large which hopefully (?) results in the confinement of quarks within hadrons. (It is interesting to notice that eq. (2.8) becomes infinite at  $Q^2=A^2$  which corresponds to a distance of about 0.5 Fermi for  $A=500$  MeV.)

The effective couplings of QED and QCD are sketched in Fig. 2. For QCD, perturbation theory works well at large  $Q^2$  (short distances) but breaks down at small  $Q^2$  (large distances).

**§11. Scale Violations in Deep Inelastic Lepton Scattering**

*A. The Quark and Gluon Distributions:*  
 $G_i(x, \hat{O}^2)$

In calculating the rate for the deep inelastic process  $\nu l \rightarrow \nu' X$  ( $l = \text{lepton}, N = \text{nucléon}$ ), one must correct the naive parton model by including the possibility that the quark in Fig. 3a can radiate a gluon before or after it has interacted with the virtual photon  $\gamma^*$ , for example, as shown in Fig. 3b. One might, at first sight, think that since the strong interaction coupling between quarks and gluons,  $\alpha_s(Q^2)$ , decreases with increasing  $g^2$ , that one could go to sufficiently high  $Q^2$  so that all corrections due to gluon emission are negligible and thereby regain the naive parton

model. This is, however, not the case for  $\nu W_2(x, Q^2)$ . Since the transverse momentum within the proton is no longer bounded (as it was for the naive parton model approach), the QCD predictions deviate more and more from the naive parton model as  $Q^2$  increases.

If we define, for the purpose of discussion, a quark distribution  $G_q(x, A)$  as the probability of finding a quark with fractional momentum  $x$  and transverse momentum less than some fixed  $\hat{a}$  (let  $A$  be the usual naive parton model value of 300-500 MeV), then if the gluon radiation in Fig. 3b is soft, it is already included in  $G(x, A)$ . Hard gluon corrections must be included explicitly when calculating any specific process. For example, for  $ep \rightarrow e + X$ , we would have (symbolically)

$$\sigma(ep \rightarrow e + X) = \sum_i \int dy G_{p \rightarrow q_i}(y, \Delta) \{ \hat{\sigma}_0(eq_i \rightarrow eq_i) + \hat{\sigma}_1(eq_i \rightarrow eq_i g, \Delta) + \hat{\sigma}_2(eq_i \rightarrow eq_i gg, \Delta) + \dots \}, \quad (3.1)$$

where  $\hat{\sigma}_0(eq \rightarrow eq)$  is just the usual elementary electron-quark cross section (Fig. 3a) and  $\hat{\sigma}_1$  is the two-to-three subprocess  $eq \rightarrow eq + \text{gluon}$

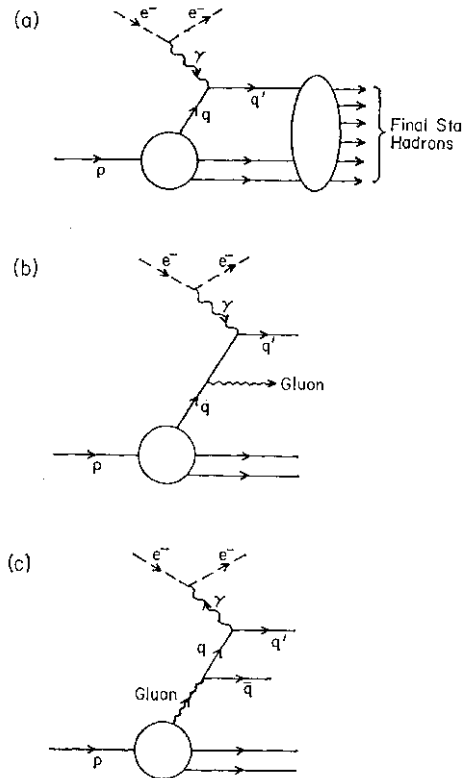


Fig. 3. (a) Inelastic electron scattering in the naive parton model approximation. (b) A typical gluon Bremsstrahlung correction to (a). (c) A correction to (a) that involves the gluon distribution inside the proton.

(Fig. 3b) where the quark-gluon invariant mass is greater than  $A$ . The usual theory of Bremsstrahlung gives

$$\hat{\sigma}_1(eq \rightarrow eqg, A) \propto \alpha_s(Q^2) \log^2(Q^2/A^2), \quad (3.2)$$

and since  $a_s(Q^2)$  only decreases like  $1/\log g^2$ , the overall probability of gluon radiation outside  $A$  increases like  $\log g^2$ . As  $Q^2$  increases, it becomes more and more likely that the quarks radiate hard gluons and so higher and higher order subprocesses,  $\hat{\sigma}_i(A)$ ,  $\hat{\sigma}_i(Q)$ , etc., must be included in (3.1). It appears that the hope of using perturbation theory is lost, since higher order terms are proportional to  $(\alpha_s(Q^2) \log^2 Q^2)^n$  which is not small even though  $a_s(Q^2)$  may be.

The utility of perturbation theory can be restored in a clever manner.<sup>3</sup> Since the results of any calculation cannot depend on the choice of  $A$  in (3.1), one chooses  $A^2=Q^2$ . Now  $d_i$  behaves like  $a_s(Q^2) \log^2(Q^2/Q^2)=a_s(Q^2)$  and can be neglected at sufficiently high  $Q^2$  whereupon (3.1) becomes

The utility of perturbation theory can be restored in a clever manner.<sup>3</sup> Since the results of any calculation cannot depend on the choice of  $A$  in (3.1), one chooses  $A^2=Q^2$ . Now  $d_i$  behaves like  $a_s(Q^2) \log^2(Q^2/Q^2)=a_s(Q^2)$  and can be neglected at sufficiently high  $Q^2$  whereupon (3.1) becomes

$$\sigma(ep \rightarrow e + X) = \sum_i \int dy G_{p \rightarrow q_i}(y, Q^2) \hat{\sigma}_0(eq_i \rightarrow eq_i). \quad (3.3)$$

The photon now "sees" an "effective" parton distribution  $G_p^{\wedge}(x, g^2)$  that depends on  $g^2$ . As  $Q^2$  increases, more and more of the incoming quarks' energy will radiate away and the photon will find less and less high  $x$  quarks in the proton.<sup>4</sup>

At any particular value of  $g^2$ , say  $g^2$ , one cannot, at present, calculate the quark and gluon distributions,  $G(x, g^2)$ . This is because these distributions have developed over a long time scale (many quark and gluon interactions) and involve low  $Q^2$  where perturbation theory is not applicable. However, if the distributions are given at  $g^2$ , then the renormalization group (a consequence of the arbitrariness of  $Q^2$ ) can be used to calculate them at any other  $Q^2$  as long as both ( $Q^2$  and  $Q^2$ ) are large enough so that  $a_s$  is small.<sup>5,6</sup>

One defines a non-singlet distribution by

$$q^{NS}(x, \tau) \equiv q(x, \tau) - \bar{q}(x, \tau), \quad (3.4)$$

where  $t = \log Q^2/Q^2$ . The QCD theory predicts<sup>1,2</sup> that the moments of this distribution

$$M_n^{NS}(\tau) = \int_0^1 x^{n-1} q^{NS}(x, \tau) dx \quad (3.5)$$

are related at two different  $g^2$ 's by

$$M_n^{NS}(\tau) = M_n^{NS}(0) [\alpha(0)/\alpha(\tau)]^{B_n^{NS}} \quad (3.6a)$$

$$= M_n^{NS}(0) [\log(Q^2/A^2)/\log(Q_0^2/A^2)]^{B_n^{NS}}, \quad (3.6b)$$

where according to (2.8)

$$\alpha(0)/\alpha(\tau) = 1 + b\alpha(0)\tau, \quad (3.7a)$$

with

$$b = (33 - 2n_f)/12\pi. \quad (3.7b)$$

The quantities  $B_n^{NS}$  are simple numbers (called "anomalous dimensions") that are calculated from the theory. In particular

$$A_n^{NS} \equiv 2\pi b B_n^{NS} = \left(\frac{4}{3}\right) \left[ -\frac{1}{2} + \frac{1}{n(n+1)} - 2 \sum_{j=2}^n \frac{1}{j} \right] \quad (3.8)$$

Equation (3.6) is equivalent to the following differential equation

$$dM_n^{NS}(\tau)/d\tau = (\alpha(\tau)/2\pi) A_n^{NS} M_n^{NS}(\tau), \quad (3.9)$$

with the condition that  $M_n^{NS}(t=0) = M_n^{NS}(0)$ , which is equivalent to the following convolution equation

$$\frac{dq^{NS}(x, \tau)}{d\tau} = \frac{\alpha(\tau)}{2\pi} \int_x^1 \frac{dy}{y} q^{NS}(y, \tau) P_{q \leftarrow q} \left(\frac{x}{y}\right), \quad (3.10)$$

provided

$$A_n^{NS} = \int_0^1 z^{n-1} P_{q \leftarrow q}(z) dz. \quad (3.11)$$

Thus following Altarelli and Parisi,<sup>7</sup> we can interpret the change in the quark distribution  $q^{NS}(x, r)$  w.r.t.  $r$  (or  $\log g^2$ ) as being due to the Bremsstrahlung radiation of a gluon from an initial quark with fraction longitudinal momentum  $y$  resulting in a quark of momentum  $x$  (see Fig. 4a). The quantity  $(\alpha(z)/2\pi) P_{q \leftarrow q}(z) dz$  is interpreted as the probability density of finding, inside a quark, another quark with fractional longitudinal momentum  $z$  of the parent quark. The change with  $r$  of this probability density produces the variation of the quark distributions.

In general,

$$\frac{dq_i(x, \tau)}{d\tau} = \frac{\alpha(\tau)}{2\pi} \int_x^1 \frac{dy}{y} \left[ q_i(y, \tau) P_{q \leftarrow q} \left(\frac{x}{y}\right) + g(y, \tau) P_{g \leftarrow q} \left(\frac{x}{y}\right) \right], \quad (3.12a)$$

$$\frac{dg(x, \tau)}{d\tau} = \frac{\alpha(\tau)}{2\pi} \int_x^1 \frac{dy}{y} \left[ \sum_{j=1}^{2n_f} q_j(y, \tau) P_{g \leftarrow q} \left(\frac{x}{y}\right) \right]$$

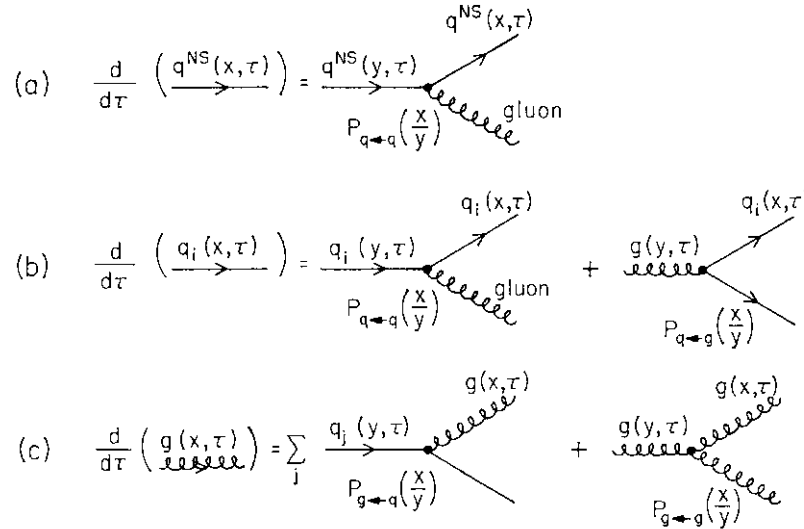


Fig. 4. (a) Illustrates that the change of the non-singlet quark distribution,  $q^{NS}(x, r)$ , w.r.t.  $r = \log(Q^2/Go^2)$  is due to the radiation of a gluon with  $P_{q \leftarrow q}(z)$  being the probability of finding a quark with momentum fraction  $z$  "within" a quark. (b) Illustrates that the change of a quark distribution,  $q^A(x, r)$ , w.r.t.  $r$  is due to the Bremsstrahlung radiation of a gluon,  $P_{q \leftarrow q}(z)$ , and the production of quark-antiquark pairs from a gluon,  $P_{q \leftarrow g}(z)$ . (c) Illustrates that the change of the gluon distribution,  $g(x, T)$ , w.r.t.  $r$  is due to the Bremsstrahlung radiation of gluons from incident quarks,  $P_{g \leftarrow q}(z)$ , and from incident gluons,  $P_{g \leftarrow g}(z)$ .

$$+ g(y, \tau) P_{g \leftarrow g} \left( \frac{x}{y} \right) \Big], \quad (3.12b)$$

$$M_i(n, Q^2) = \int_0^1 x^{n-1} G_i(x, Q^2) dx \quad (3.13a)$$

where  $q^A(x, r)$  and  $g(x, r)$  are the individual quark and gluon distributions, respectively, and where the probabilities  $P_{a \leftarrow b}(z)$  are calculated by perturbation theory from the Feynman rules for the vertices shown in Fig. 4. As illustrated in Fig. 4, the change in the quark distribution  $q_i(x, T)$  w.r.t.  $T$  arises from the radiation of gluons from an incoming quark,  $P_{q \leftarrow q}$  and from the production of quark-antiquark pairs from an initial gluon,  $P_{q \leftarrow g}$ . Similarly, the change w.r.t.  $T$  of the gluon distribution,  $g(x, r)$  arises from gluons radiated from an initial quark,  $P_{g \leftarrow q}$ , and from gluons radiated from an initial gluon,  $P_{g \leftarrow g}$ . These equations are not diagonal; the change of the quark distribution  $q_i(x, r)$  depends on both the quark distribution  $q^A(y, r)$  and on the gluon distribution  $g(y, r)$ . On the other hand, the change w.r.t.  $r$  of non-singlet distribution defined by (3.4) does depend only on the non-singlet distribution,  $q^{NS}(y, r)$ , as given by (3.10). This is because gluons produce quarks and antiquarks with equal likelihood and thus the term proportional to  $g(y, r)$  in (3.12a) drops out when one forms  $q^A(x, T) - q^B(x, T)$ .

In terms of the moments of the quark and gluon distributions

one has, in general,

$$M_j(n, Q^2) = \sum_{i=1}^9 M_i(n, Q_0^2) R_{ij}(n, Q^2, Q_0^2, A^2), \quad (3.13b)$$

where  $R^A(n, g^2, Q, A^2)$  is a known matrix (depending on  $A^2$ ) and  $i$  corresponds to the constituent types (w, d, s, c,  $\hat{u}$ , d, s, c, gluon). The distributions at  $Q^2$  are calculated in terms of these at  $Q_0$  by diagonalizing (3.13b) and inverting (3.13a) by an inverse Mellin transform (eq. (13) of ref. 8).

Figure 5a shows the expected behavior of  $vW_2(x, Q^2)$  resulting from an analysis of  $ep$  and  $fip$  data by Fox.<sup>8</sup> The  $x$  dependence of the parton distributions at the reference momentum,  $\hat{Q}_0 = 4(\text{GeV}/c)^2$ , was chosen to agree with experiment. An analysis of  $ep$  and  $fip$  data is sensitive to the gluon distribution through diagrams like that of Fig. 3c. The gluon distribution  $xG_{-+}(x, \hat{Q}_0) \approx (1+9x)(1-x)^4$  at the reference momentum, but the analysis of  $ep$  and  $fip$  is not sensitive to this precise choice. The resulting  $Q^2$  dependence of  $G_{p \leftarrow g}(x > Q^*) = g(x, Q^2)$  is shown in Fig. 5b. Both  $vW_2(x, Q^2)$  and  $xg(x, Q^2)$  exhibit a rise at small  $x$  and a decrease at large  $x$  as  $Q^2$  increases.

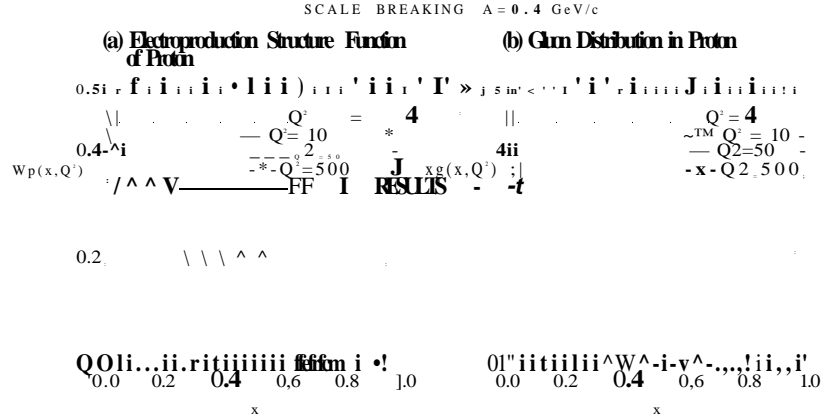


Fig. 5. (a) Shows the predicted  $Q^2$  dependence (scale breaking) of the electroproduction structure function for the proton,  $\nu W_2(x, <Q^2)$ , arising from the constituent (quarks, antiquarks and gluons) distributions  $G_i(x, Q^2)$  used in this analysis. The distributions at high  $Q^2$  are calculated from the distributions at the reference momentum  $<Q^2=4 \text{ GeV}^2$  using a QCD moment analysis with  $A=0.4 \text{ GeV}/c$ . In asymptotically free theories, one expects a decrease in the number of high  $x$  constituents and an increase in the number of low  $x$  constituents as  $Q^2$  increases. Also shown is the value of  $\nu W_2(x)$  (independent of  $Q^2$ ) used in the quark-quark "black-box" model of FFF.<sup>43</sup>

(b) Shows the predicted  $Q^2$  dependence of the distribution of gluons within the proton  $xG_{g,+}(x, Q^2)$  used in this analysis. The distribution at high  $Q^2$  is calculated in terms of a distribution at the reference momentum  $Q_0^2=4 \text{ GeV}^2$  given by  $xg(x, Q_0^2) = (1-9x)(1-x)$

**B. Comparison with the ep and jup Data**

Figure 6 shows the fits to the existing ep and jup data.<sup>8</sup> The data show a decrease at large x and an increase at small x as  $Q^2$  increase in precisely the manner expected from QCD. The amount of the scale breaking indicates that A in (2.8) is in the range 0.4-0.6 GeV/c.

**C. Comparison with Neutrino and Antineutrino Data**

(1) "Scale-breaking" of the distribution  $F_2(x, Q^2)$  and  $xF_3(x, Q^2)$

The neutrino and antineutrino differential cross sections can be written in terms of the structure function,  $F_1$ ,  $F_2$  and  $F_3$  as follows:

$$\frac{d^2\sigma^{\nu, \bar{\nu}}}{dx dy} = \frac{G^2 ME}{\pi} \left[ \left( 1 - y - \frac{Mxy}{2E} \right) F_2(x, Q^2) + y^2 x F_1(x, Q^2) \pm y \left( 1 - \frac{y}{2} \right) x F_3(x, Q^2) \right], \quad (3.14)$$

where  $x=Q^2/2M\nu$ ,  $y=\nu/E$ , and  $\nu=E-E'$  ( $E$  and  $E'$  are the initial neutrino and final muon energy, respectively). In terms of the quark and antiquark distribution, one has

$$F_2(x, Q^2) = x[q(x, Q^2) + \bar{q}(x, Q^2)] \quad (3.15a)$$

$$xF_3(x, Q^2) = x[q(x, Q^2) - \bar{q}(x, Q^2)] \quad (3.15b)$$

or

$$\frac{d^2\sigma^{\nu}}{dx dy} \simeq \frac{2G^2 ME}{\pi} \left\{ xq(x, Q^2) + x\bar{q}(x, Q^2)(1-y)^2 - \frac{y^2 Rx}{2} (q(x, Q^2) + \bar{q}(x, Q^2)) \right\} \quad (3.16a)$$

$$\frac{d^2\sigma^{\bar{\nu}}}{dx dy} \simeq \frac{2G^2 ME}{\pi} \left\{ xq(x, Q^2)(1-y)^2 + x\bar{q}(x, Q^2) - \frac{y^2 Rx}{2} (q(x, Q^2) + \bar{q}(x, Q^2)) \right\} \quad (3.16b)$$

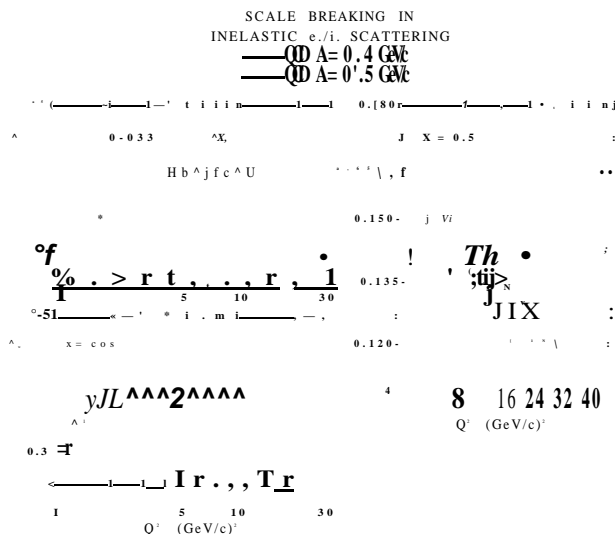


Fig. 6. Comparison of the scale breaking effects ( $Q^2$  dependence) expected from an asymptotically free theory with data on ep and jup inelastic scattering at  $x \sim 0.033, 0.08$  and  $0.5$ . The theory comes from the analysis of ref. 8 using  $y_1=0.4 \text{ GeV}/c$  (solid curve) and  $A=0.5 \text{ GeV}/c$  (dashed curve).

where the quark distributions,  $q(x, Q^2)$ , and antiquark distributions,  $\bar{q}(x, Q^2)$ , to be used are as follows:

Reaction	Final state	Quark distributions
$\nu p \rightarrow \mu^- + X$	Non-charm	$\bar{u}, d \cos^2 \theta_c + s \sin^2 \theta_c$
	Charm	$d \sin^2 \theta_c + s \cos^2 \theta_c$
$\bar{\nu} p \rightarrow \mu^+ + X$	Non-charm	$u, \bar{d} \cos^2 \theta_c + \bar{s} \sin^2 \theta_c$
	Charm	$\bar{d} \sin^2 \theta_c + \bar{s} \cos^2 \theta_c$

(3.17)

where  $\theta_c$  is the Cabibbo angle and the charm content in the nucleon has been neglected. The effects of  $R=(F_2 - 2xF_1)/F_2 = a_1/m(3A - 6)$  are small. The QCD perturbative contribution (of order  $a_s(Q^2)$ ) is about 5% integrated over all  $x$  and  $y$  for antineutrino scattering and about 2.5% for the neutrino case.<sup>9,11</sup> The data from the BEBC analysis<sup>12</sup> yield  $J_f = 0.11 \pm 0.12$  for  $\hat{Q}^2 > 1.0 \text{ GeV}^2$  while the CDHS data<sup>13</sup> imply  $i < 0.05$  with a 90% confidence level  $\langle g^2 \rangle \sim 2.2 \text{ GeV}^2$ .

In comparing with the neutrino and antineutrino data, one must separate the quark and antiquark distributions (the  $ep$  and  $\bar{\nu}p$  analysis was sensitive only to  $\#^* + \langle ?^* \rangle$ ). We have taken<sup>9,11,14,16</sup>

$$x\bar{u}(x, Q_0^2) = x\bar{d}(x, Q_0^2) = 0.25(1-x)^7 \quad (3.18)$$

at the reference momentum  $Q_0 = 4 \text{ GeV}^2$ , which yield,

$$\int_0^1 x(\bar{u} + \bar{d}) dx / \int_0^1 x(u + d) dx \simeq 0.1 \quad (3.19)$$

at  $Q_0$ ; however, this ratio increases with increasing  $Q^2$ . In the SU(3) limit, the amount of strange quarks in the proton would equal the amount of  $\bar{u}$  or  $\bar{d}$  quarks. It is, however, expected that since strange quarks are more massive, that they occur at less than the SU(3) value. We take

$$s(x, Q_0^2) = \bar{s}(x, Q_0^2) = \frac{1}{2} \bar{u}(x, Q_0^2). \quad (3.20)$$

In the naive parton model, one expects  $F_2$  and  $xF_3$  to "scale" (i.e., be only functions of  $x$ ). On the other hand, QCD predicts that these functions should be functions of both  $x$  and  $Q^2$ . Figures 7 and 8 show a comparison of the data on  $F_2$  and  $xF_3$  from the BEBC analysis with the QCD predictions.<sup>9</sup> The theory is calculated at energies where  $y < 0.5$  so that the effect of  $R$  in (3.16) is small. The agreement between theory and experiment

is quite good. Remember that the normalization and shape of the curves come from the electroproduction analysis. The  $\nu$  and  $\bar{\nu}$  data

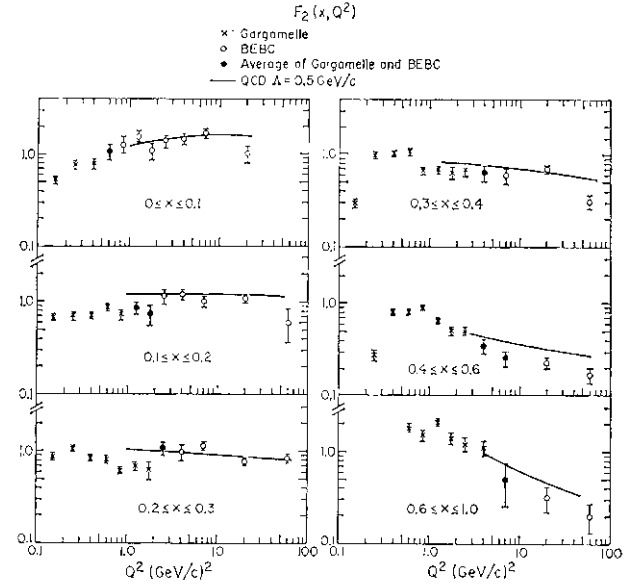


Fig. 7. The values of  $F_2(x, Q^2)$  from the BEBC Gargamelle collaboration.<sup>12</sup> They are compared with the QCD calculations with  $\Lambda = 0.5 \text{ GeV}/c$  and the strange quark at one half its SU<sub>3</sub> value. The effect of using an SU<sub>3</sub> symmetric sea is to raise the prediction by 15% in the lowest  $x$  bin 0 to 0.1 with smaller effects at higher  $x$ . Further, the nonzero value of  $R = G_2/G_1$  (at small  $x$ ) in the theory makes " $F_2(x, Q^2)$ " a function of energy. This is again about a 20% effect with the lower energy, high  $y$ , point falling below the higher energy value at the same  $Q^2 = 2mExy$ . These two small effects are not shown on figure. (This figure is taken from ref. 9.)

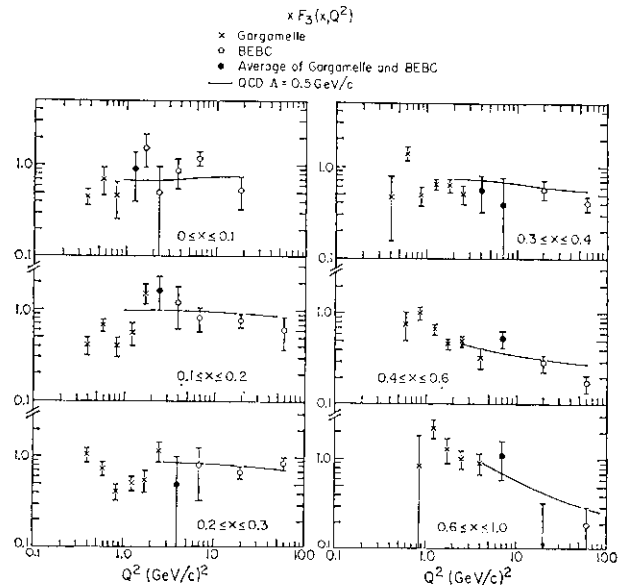


Fig. 8. Same as Fig. 7 except for  $x F_3(x, Q^2)$  instead of  $F_2(x, Q^2)$ . The results are not sensitive to either  $R$  or the strange sea.



have not been used in the determination of the quark distributions or in the determination of  $A$ . It is interesting to note that the Gargamelle data, which gave some of the early support for the quark parton picture, has  $\langle g^2 \rangle \sim 1.0 \text{ GeV}^2$  where even a believer in QCD would expect sizable  $1/Q^2$  corrections. Nevertheless, these data join on quite smoothly to the larger  $g^2$  BEBC data.

(2) *Moment analysis*

In neutrino scattering,  $x F_3$  is proportional to  $q - \bar{q}$  (eq. 3.15b) which is the non-singlet combination defined by (3.4). The non-singlet distributions (or moments) do not mix with gluon distributions and have a  $Q^2$  evolution given simply by (3.6). Namely

$$M_3(n, Q^2) = M_3(n, Q_0^2) [\log(Q^2/A^2) / \log(Q_0^2/A^2)]^{B_n^{NS}}, \quad (3.21a)$$

where  $B_n^{NS}$  is given by (3.8). The moments of the structure function  $F_3$  are defined by

$$M_3(n, Q^2) = \int_0^1 x^{n-1} F_3(x, Q^2) dx. \quad (3.21b)$$

In practice, one actually defines Nachtmann moments using the variable  $\xi = 2x / (1 + \sqrt{1 + 4x^2 M^2 / Q^2})$  instead of  $x$ . This variable approaches  $x$  at high  $Q^2$  (i.e.,  $\xi \sim x - M^2 x / Q^2$ ) and at low  $Q^2$  removes some of the target mass corrections that are of order  $M^2 / Q^2$ .

Taking the log of both sides of eq. (3.21a) gives

$$(1/B_n^{NS}) \log M_3(n, Q^2) = C(n) + \log \log Q^2 / A^2, \quad (3.22)$$

where  $C(n)$  is independent of  $Q^2$ . This means that a plot of  $\log M_3(n, Q^2)$  vs  $\log M_3(n', Q^2)$  is a straight line,

$$\log M_3(n, Q^2) = (B_n^{NS} / B_{n'}^{NS}) \log M_3(n', Q^2) + B_n^{NS} (C(n) - C(n')) \quad (3.23)$$

with slope given by

$$\begin{aligned} B_n^{NS} / B_{n'}^{NS} &= A_n^{NS} / A_{n'}^{NS} \\ &= \left[ -\frac{1}{2} + \frac{1}{n(n+1)} - 2 \sum_{j=2}^n \frac{1}{j} \right] / \\ &\quad \left[ -\frac{1}{2} + \frac{1}{n'(n'+1)} - 2 \sum_{j=2}^{n'} \frac{1}{j} \right]. \end{aligned} \quad (3.24)$$

In addition, this slope is independent of  $A$  and the number of quark flavors  $n$ . Figure 9 shows log-log plots for some of the moments of  $x F_3$  for  $g^2 > 1$  ( $\text{GeV}/c$ )<sup>2</sup> from the BEBC

analysis.<sup>12</sup> The anomalous dimensions,  $A_n^{NS}$ , predicted by QCD are in agreement with the data at about the 10% level. This is one of the most impressive tests of QCD to date. Remember the naive parton model would predict that all the data along the lines in Fig. 9 should lie at one point (i.e., no  $Q^2$  dependence).

The skeptic may, however, worry that the data in Fig. 9 go down to  $Q^2 \approx 1$  ( $\text{GeV}/c$ )<sup>2</sup> where the quantitative validity of the asymptotic predictions of QCD are not so obvious. Undoubtedly,  $1/Q^2$  effects and higher order perturbative effects are important at these low  $Q^2$  values.<sup>6</sup> To be on the safe side, we have, in our analysis of electroproduction data,<sup>8</sup> restricted ourselves to the region  $Q^2 > 4$  ( $\text{GeV}/c$ )<sup>2</sup>. This means that we should only be comparing with the last three points along each line in Fig. 9 (square points). These last three points are certainly consistent with the QCD predictions although one cannot use them to prove the QCD solution is correct. Nevertheless, the qualitative agreement with the theory and the data shown in Figs. 6, 7, 8 and 9 provides substantial support for the QCD approach.

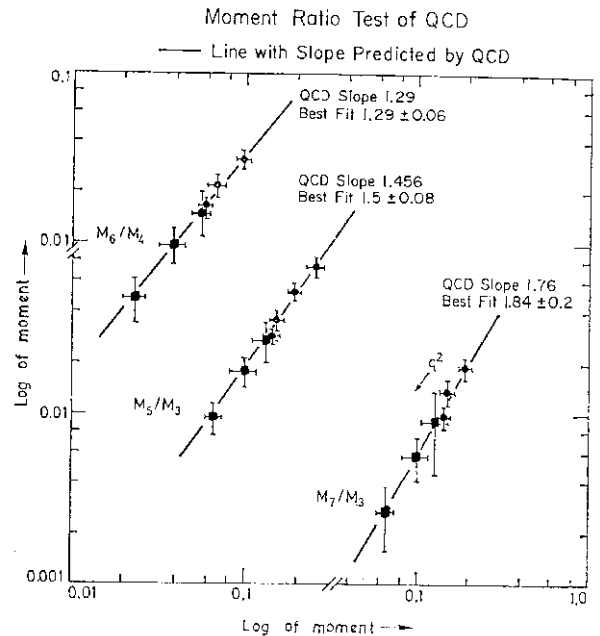


Fig. 9. Plot of  $\log M_3(\ll, Q^2)$  vs  $\log M_3(\gg, Q^2)$ , where  $M_3(n, Q^2)$  are moments of  $x F_3$  from the BEBC analysis of neutrino and antineutrino interactions.<sup>12</sup> According to QCD, the data should lie along straight lines with a slope given by the theory. The data are plotted for  $Q^2 > 1$  ( $\text{GeV}/c$ )<sup>2</sup> with the square points having  $Q^2 > 4$  ( $\text{GeV}/c$ )<sup>2</sup>.

§IV. Large Mass Muon Pair Production

A. QCD Factorization and the Total Muon Pair Rate

The quark and gluon distributions,  $G(x, Q^2)$ , defined and determined in Section IIIA and IIIB, respectively, are most useful if they are in some sense process independent. It would be nice if parton distributions determined from one process (like  $ep \rightarrow eX$ ) could be used to make predictions elsewhere (like for  $pp \rightarrow \mu^+ \mu^- + X$  or  $pp \rightarrow \tau^+ \tau^- + X$ ). Recently several groups<sup>17-20</sup> have shown that all the divergent perturbative contributions to these processes can be summed and absorbed into *universal* quark and gluon distributions.<sup>21</sup> These divergences arise from, for example, the parallel emission of a massless gluon by a massless incoming or outgoing quark. (The "soft" divergences that arise as the gluon energy becomes small are cancelled by other diagrams containing virtual gluon corrections.) These "parallel" divergences are a property of the incoming (or outgoing) quark line and can be "factored" out from the basic hard subprocess (this hard subprocess is, of course, different for different reactions). They are precisely the terms in Fig. 3 that are responsible for the  $Q^2$  dependence of the parton distributions.

The total muon pair cross section (integrated over all muon pair  $p_\perp$ ) is given to leading order in  $a_s(Q^2) \log Q^2$  by<sup>22,23</sup>

$$\sigma_{\text{tot}}(s, M^2, y) \equiv \frac{d\sigma}{dM^2 dy}(s, M^2, y) = \frac{4\pi\alpha^2}{3sM^2} \left( \frac{1}{3} \right) \sum_i e_i^2 \{ G_{p \rightarrow q_i}(x_a, Q^2) G_{p \rightarrow \bar{q}_i}(x_b, Q^2) + (q_i \leftrightarrow \bar{q}_i) \}, \quad (4.1)$$

where  $y$  is the rapidity of the muon pair of mass  $M$  and

$$x_a = \sqrt{\tau} \exp(y), \quad x_b = \sqrt{\tau} \exp(-y), \quad (4.2)$$

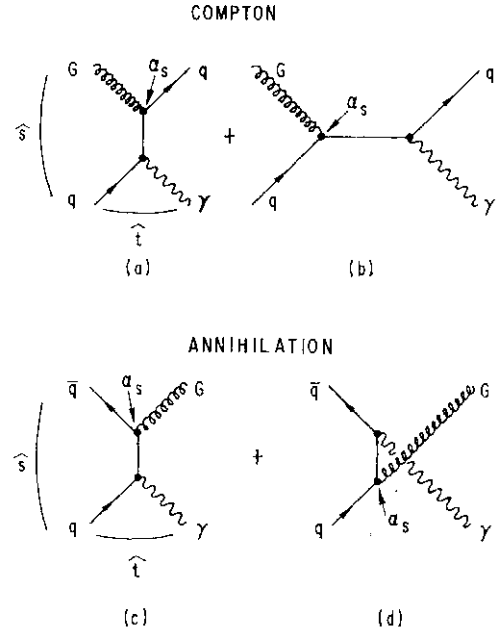


Fig. 10. QCD processes to first order in the strong coupling constant  $a_s$ . Diagrams (a) and (b) represent quark-gluon "Compton" scattering to yield a quark and a virtual photon. Diagrams (c) and (d) represent quark-antiquark annihilation into a gluon and a virtual photon.

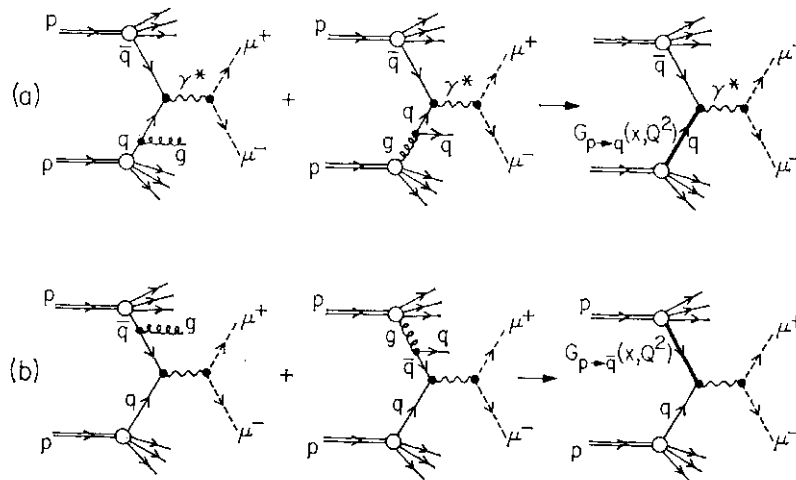


Fig. 11. (a) Illustration of two diagrams for  $pp \rightarrow \mu^+ \mu^- + X$  which are included (divergent parts) in the "renormalization group" improved quark distributions,  $G_{p \rightarrow q}(x, Q^2)$ , when one calculates the contribution from the subprocess  $q\bar{q} \rightarrow \gamma^* \rightarrow \mu^+ \mu^-$ . (b) Illustration of two diagrams which are included (divergent parts) in the "renormalization group" improved antiquark distributions,  $G_{p \rightarrow \bar{q}}(x, Q^2)$ .

and where the parton distributions  $G(x, Q^2 = M^2)$  are the "renormalization group improved" functions given in Section III. One does not see the "Compton" term,  $g+q^*q+r^*$  (see Fig. 10a, b), explicitly in (4.1) since to leading order in  $a_s(Q^2) \log Q^2$  it is included in the probability of finding an antiquark in the proton. As illustrated in Fig. 11, the divergent pieces (behaving like  $a_s(Q^2) \log Q^2$ ) of gluon Bremsstrahlung from the incoming antiquark and incoming gluon quark-antiquark pair production are absorbed into and generate the  $Q^2$  dependence of  $G_r^A(x, g^2)^{21, 24}$ . Figure 12 shows the data on  $da/dMdy$  for  $pN \rightarrow p\bar{p} + X$  at  $W=27.4$  GeV and  $y=0$  together with the predictions from eq. (4.1) using the parton distributions  $G_i(x, Q^2)$  determined in Section III. The agreement is quite satisfactory.

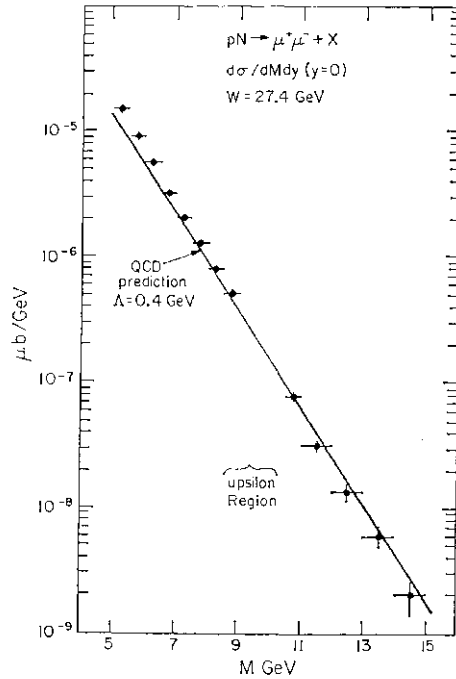


Fig. 12. Leading order QCD prediction from Eq. (4.1) of the dimuon mass spectrum at  $y=0$  and  $W=V_s=27.4$  GeV using the "renormalization group" improved quark and antiquark distributions  $G^A(x, g^2)$  from eq. (3.13a) and (3.13b). The data are from ref. 34.

### B. Muon Pairs Produced at Large Mass and Large $p_t$

Effects due to the transverse momentum,  $k_\perp$ , of quarks and gluons within hadrons can

sometimes be very important. In QCD, transverse momentum of partons can arise in two ways. Firstly, in, for example, a proton beam, quarks are confined in the transverse direction to within the proton radius. Therefore, from the uncertainty principle, they must have some transverse momentum. This momentum, called primordial, is intrinsic to the basic parton wave function inside the proton. It involves small  $Q^2$  values and thus cannot be calculated using perturbation theory. At present, it must be viewed as unknown but bounded (falling off like an exponential or gaussian in  $k_j$ ). Secondly, in QCD, one expects to receive an "effective"  $k_\perp$  of quarks in protons due to the hard Bremsstrahlung of gluons which can be calculated perturbatively if the momentum transfers are large.

A particularly nice place to study the interplay between these two components of transverse momentum is in the production of large mass muon pairs in  $pp$  collisions,  $pp \rightarrow j\mu^+\mu^- + X$ . Many people have analyzed this process in terms of QCD.<sup>23, 29</sup> The analysis presented here follows closely the work of Altarelli, Parisi and Petronzio.<sup>24</sup>

The perturbative component of the transverse momentum of muon pairs is generated by the two-to-two constituent subprocess  $qq \rightarrow j^* + \text{gluon}$  and  $\text{gluon} + \# \rightarrow j^* + g$  shown in Fig. 10, where the virtual photon,  $y^*$ , then decays into a  $j\mu^+j\mu^-$  pair. Other graphs are higher order in  $a_s$  and have been neglected.<sup>30</sup> The cross sections for these processes are given by

$$\frac{d\sigma_A}{dM^2 d\hat{t}} = \left(\frac{8}{27}\right) \left(\frac{\alpha^2 \alpha_s e_q^2}{M^2 \hat{s}^2}\right) \left(\frac{2M^2 \hat{s} + \hat{u}^2 + \hat{t}^2}{\hat{t}\hat{u}}\right) \quad (4.3a)$$

$$\frac{d\sigma_C}{dM^2 d\hat{t}} = \left(\frac{1}{9}\right) \left(\frac{\alpha^2 \alpha_s e_q^2}{M^2 \hat{s}^2}\right) \left(\frac{2M^2 \hat{u} + \hat{s}^2 + \hat{t}^2}{-\hat{t}\hat{s}}\right), \quad (4.3b)$$

where  $s$ ,  $t$ , and  $u$  are the usual Mandelstam invariants and  $M^2$  is the invariant mass squared of the muon pair and where A and C refer to annihilation and compton, respectively. The cross section for producing muon pairs of mass  $M^2$ , rapidity  $y$ , and transverse momentum  $p_\perp$  at a center of mass energy squared  $s$  is then given by

$$\begin{aligned} \sigma_P(s, M^2, y, p_\perp) &\equiv \frac{d\sigma_P}{dM^2 dy d^2p_\perp}(s, M^2, y, p_\perp) \\ &= \sum_{q=u, d, s} \int_{x_a^{\min}}^{1.0} dx_a \{G_{p \rightarrow q}(x_a, M^2) G_{p \rightarrow \bar{q}}(x_b, M^2) + (\bar{q} \leftrightarrow q)\} \frac{x_a x_b}{(x_a - x_1)} \left( \frac{1}{\pi} \frac{d\sigma_A}{dM^2 d\hat{t}} \right) \\ &\quad + \sum_{q=u, d, s, \bar{u}, \bar{d}, \bar{s}} \int_{x_a^{\min}}^{1.0} dx_a \{G_{p \rightarrow q}(x_a, M^2) G_{p \rightarrow q}(x_b, M^2) + (g \leftrightarrow q)\} \frac{x_a x_b}{(x_a - x_1)} \left( \frac{1}{\pi} \frac{d\sigma_G}{dM^2 d\hat{t}} \right), \end{aligned} \quad (4.4)$$

where  $x_a^{\min} = (x_1 - \tau)/(1 - x_2)$  and  $x_b = (x_a x_2 - \tau)/(x_a - x_1)$ . The quantities  $x_1$  and  $x_2$  are given by

$$x_1 = \frac{1}{2} (x_\perp^2 + 4\tau)^{1/2} e^y \quad (4.5a)$$

$$x_2 = \frac{1}{2} (x_\perp^2 + 4\tau)^{1/2} e^{-y}, \quad (4.5b)$$

where  $x_\perp = 2p_\perp/\sqrt{s}$  and  $\tau = M^2/s$ .<sup>31</sup> The subprocess invariants are given by

$$\hat{s} = x_a x_b s \quad (4.6a)$$

$$\hat{t} = -x_a s x_2 + M^2 \quad (4.6b)$$

$$\hat{u} = -x_b s x_1 + M^2. \quad (4.6c)$$

In (4.4), the label  $P$  refers to "perturbative contribution" and where the "renormalization improved" parton distributions  $G(x, Q^2 = M)$  from (3.13) and the running coupling constant  $a(Q^2)$  from (2.8) are used. It is clear from the work of Politzer<sup>22</sup> and Sachrajda<sup>33</sup> that here one should use the "renormalization improved"  $G(x, Q^2)$  and  $a(Q^2)$  functions. However, here there are two large invariants  $M^2$  and  $p_\perp$  and it is *not* clear whether the  $Q^2$  dependence evolves according to  $G(x, Q^2 = M)$  or  $G(x, Q^2 = p_\perp^2)$  or some other combination. It, of course, does not matter in leading order and at very large values of  $M^2$  and  $p_\perp$  but it certainly matters for the phenomenology at existing  $M^2$  and  $p_\perp$  values. Using  $Q^2 = M^2$  in (4.4) is an assumption that is probably not precisely correct.<sup>33</sup>

The perturbative contributions in (4.4) are shown in Fig. 13. They are absolutely normalized and agree roughly with the data at large  $p_\perp$ . They, however, have the wrong shape at small  $p_\perp$  and diverge at  $p_\perp = 0$ . This infrared difficulty besets other QCD perturbative calculations. (The gluon Bremsstrahlung in Fig. 3b also produces divergences as  $A$  in (3.2) goes to zero.) One expects that non-perturbative phenomena at small  $p_\perp$  will regularize this singularity leaving a smooth  $p_\perp$  distribution.

The soft, non-perturbative, component of

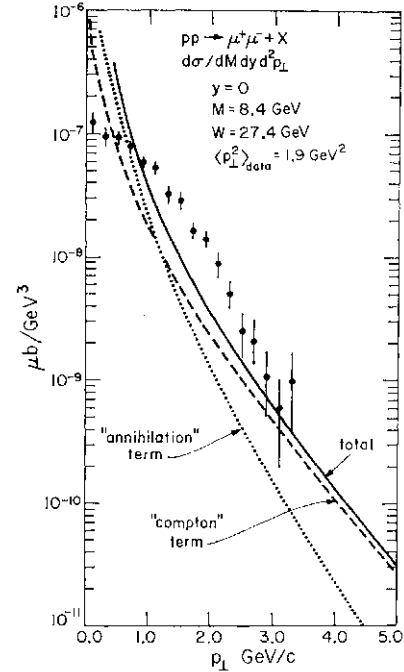


Fig. 13. The distribution in transverse momentum,  $p_\perp$  of the  $\mu\mu$ - pair produced in  $pp$  collisions at  $W=21A$  GeV together with the QCD perturbative predictions. The "Compton" (Fig. 10 a, b) and "annihilation" (Fig. 10 c, d) are given by the dashed and dotted curves, respectively.

$k_\perp$  (the primordial  $k_\perp$ ) can be used to regularize  $\langle j_P(s, M, y, p_\perp) \rangle$  and produce a finite distribution in  $p_\perp$  at all  $p_\perp$ . This is done by convoluting  $\langle j_P(p_\pm) \rangle$  with a quark primordial motion given, for instance, by

$$f(k_\perp^2) = \exp(-k_\perp^2/(4\sigma_q^2))/(4\pi\sigma_q^2) \quad (4.7)$$

where for a single constituent in a proton, one has

$$\langle k_\perp^2 \rangle_{\text{primordial}} = 2\sigma_q^2. \quad (4.8)$$

The result is

$$\begin{aligned} \sigma(s, M^2, y, p_\perp^2) &= \int d^2k_\perp \sigma_P(s, M^2, y, (p_\perp - k_\perp)^2) f(k_\perp^2) \\ &= \int d^2k_\perp \sigma_P(s, M^2, y, (p_\perp - k_\perp)^2) [f(k_\perp^2) - f(p_\perp^2)] \\ &\quad + f(p_\perp^2) \int d^2k_\perp \sigma_P(s, M^2, y, (p_\perp - k_\perp)^2), \end{aligned} \quad (4.9)$$

where I have added and subtracted the second term in (4.9). Actually, in doing this convolution, I should have added to  $a_s$  a contribution of order  $\langle x \rangle$  arising from the vertex correction to the subprocess  $qq \rightarrow j^*$ . This contribution also diverges but only contributes at  $p_{\perp} = 0$  (i.e., has a  $d(p_j)$ ). It does not contribute to the first term in (4.9) since  $[f(k_{\perp}) - f(p_{\perp})] \delta(q_{\perp})$  is zero, but when added to the second term yields

$$\begin{aligned} \sigma(s, M^2, y, p_{\perp}^2) &= \int d^2 q_{\perp} \sigma_P(s, M^2, y, q_{\perp}^2) [f((p_{\perp} - q_{\perp})^2) - f(p_{\perp}^2)] \\ &+ f(p_{\perp}^2) \sigma_{tot}(s, M^2, y), \end{aligned} \quad (4.10)$$

where I have defined  $q_{\perp} = P_{\pm} - k_{\pm}$  (keep track of the vector direction) and where  $\sigma_{tot}(s, M^2, y)$  is given by definition by (4.1).

Both terms in (4.10) are now finite at all  $p_{\perp}$  and one is left with one additional parameter, the primordial  $\langle k_{\perp}^2 \rangle$  in (4.8), to be adjusted to fit the data. The fit to the data is shown in Fig. 14 and yields  $\langle k_{\perp}^2 \rangle_{\text{primordial}} = 0.48 \text{ GeV}^2$  or

$$\langle k_{\perp} \rangle_{\text{primordial}} = \sqrt{\pi/2} \sigma_q \approx 600 \text{ MeV}. \quad (4.11)$$

This means that the mean  $p_{\perp}$  of the  $u\bar{u}$  data, which at this energy and  $y=0$  is about 1.9

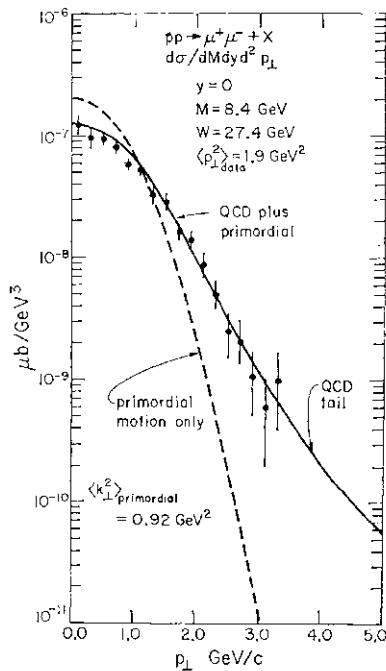


Fig. 14. The same data as Fig. 13 together with the perturbative QCD contributions of Fig. 10 folded with a Gaussian momentum spectrum with  $\langle k_{\perp} \rangle = \langle p_{\perp} \rangle = 600 \text{ MeV}$  (solid curve). The dashed curve results from the primordial motion only with no perturbative QCD terms.

$\text{GeV}^2$ , results from about  $0.9 \text{ GeV}^2$  due to primordial motion and about  $1.0 \text{ GeV}^2$  due to the hard QCD subprocesses. Figure 14 shows also the second term in (4.10) which would be the prediction if only primordial motion (with  $\langle k_{\perp}^2 \rangle = 0.48 \text{ GeV}^2$ ) were present.

Clearly, this smearing procedure which is used to regulate the divergences is a bit *ad hoc* and the fit to the shape of the  $p_{\perp}$  spectrum shown in Fig. 14 can not be viewed as a success of QCD. One could have fit the same data with a Gaussian with  $\langle k_{\perp}^2 \rangle = 0.611 \text{ GeV}^2$ . The real test of the presence of the QCD component to the effective  $k_{\perp}$  of partons comes from examining the energy dependence of the muon pair  $p_{\perp}$  spectrum. Predictions for this are shown in Fig. 15. One expects

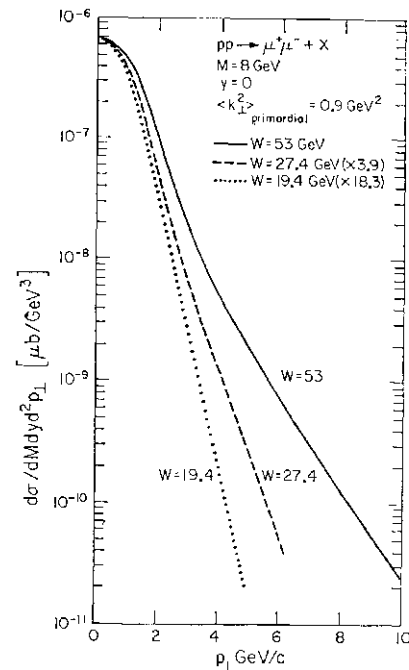


Fig. 15. Energy dependence of the large  $p_{\perp}$  tail expected for  $pp \rightarrow V + X$  from the QCD perturbative contributions shown in Fig. 10 folded with a primordial transverse momentum with  $\langle k_{\perp}^2 \rangle = 600 \text{ MeV}$  for each parton.

to see a flatter  $p_{\perp}$  spectra as the energy increases (and  $M^2$  is fixed). Recent data on  $pN \rightarrow p + \mu + \mu + X$  at 200, 300 and 400  $\text{GeV}^2$  do show a mean  $p_{\perp}$  that increases with increasing energy (Fig. 16) in agreement with the QCD expectations.

### C. "Scale" Breaking in $pp \rightarrow u\bar{u} + X$

It is interesting to look at the "scale-breaking" expected in QCD for observables in

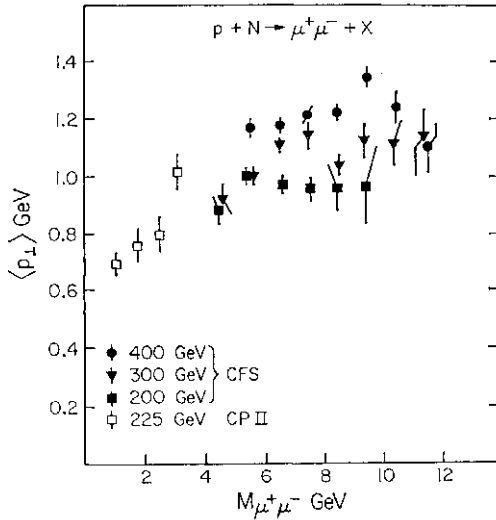


Fig. 16. Data from ref. 34 on the energy dependence of the  $\langle p_{\perp} \rangle$  of the  $\mu^+\mu^-$  pair in proton-nucleon collisions which indicate that the  $p_{\perp}$  distribution is becoming broader as the energy increases. This is in agreement with the QCD predictions in Fig. 15.

$pp \rightarrow \mu^+\mu^- + X$ . In the old parton model, one expected

$$M^4 \frac{d\sigma}{dM^2 dy}(s, M^2, y) = f(\tau, y), \quad (4.12)$$

to be only a function of  $T=M^2/s$  and  $y$  and not to depend separately on  $W=\sqrt{s}$ . As

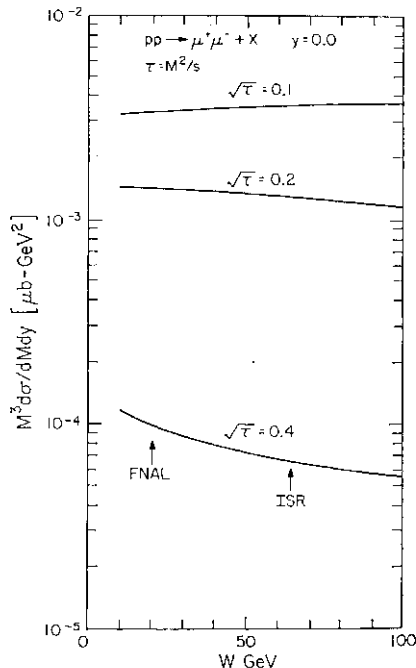


Fig. 17. Expected "scale breaking" of the quantity  $M^4 d\sigma/dM^2 dy$  for  $pp \rightarrow \mu^+\mu^- + X$  at  $y=0$  from the QCD non-scaling structure functions with  $A=0.4$  GeV/c. Scaling would predict this quantity to be independent of  $W$  at fixed  $r$ .

shown in Fig. 17, one now expects small scale breaking effects. At small  $r$  one sees a slight rise with increasing  $W$  and at large  $r$  a decrease with increasing  $W$ . The effects are small. They are comparable to the breaking of  $vW_{\nu}(x, Q^2)$  in Fig. 6 and will probably not be seen experimentally for quite some time.

Other muon pair observables show larger scale breaking effects. For example, for the subprocesses in Fig. 10 dimensional counting yields

$$M^4 p_{\perp}^2 \frac{d\sigma}{dM^2 dy d^2 p_{\perp}} = F(\tau, y, x_{\perp}), \quad (4.13a)$$

where  $x_{\perp} = 2p_{\perp}/W$  or

$$W^5 \frac{d\sigma}{dM^2 dy d^2 p_{\perp}} = \tilde{F}(\tau, y, x_{\perp}). \quad (4.13b)$$

For asymptotically free theories, (4.13) does not scale. Figure 18 shows that for fixed  $x_{\perp}$  and  $r$ ,  $W d\sigma/dM^2 dy d^2 p_{\perp}$  decreases as  $W$  increases and approaches a constant ("scaling" result) asymptotically.<sup>24</sup> As can be seen in this figure, the primordial motion produces

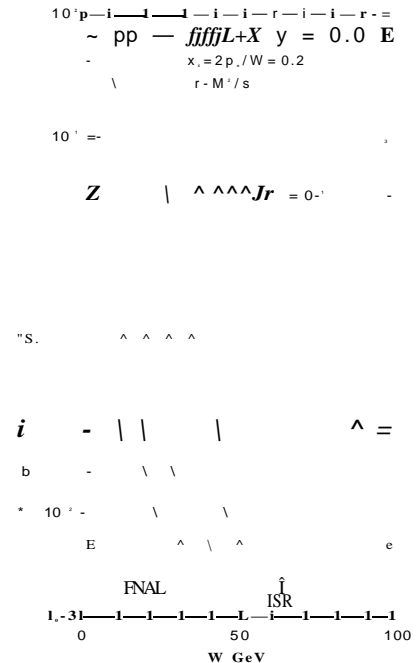


Fig. 18. Expected "scale breaking" of the quantity  $W d\sigma/dM^2 dy d^2 p_{\perp}$  for  $pp \rightarrow \mu^+\mu^- + X$  at  $y=0$  and  $x_{\perp}=0.2$  from the QCD diagrams in Fig. 10 with  $A=0.4$  GeV/c. The solid (dashed) curves are the results after (before) smearing with a primordial parton transverse momentum with  $\langle p_{\perp} \rangle = 600$  MeV for each parton. The dotted curves would be expected if primordial motion alone were responsible for the muon pair  $p_{\perp}$ . Scaling would predict this quantity to be independent of  $W$  at fixed  $r$  and

an additional "scale breaking" term. (If there were only primordial motion, then  $W da/dM dy dp_x$  would go to zero at increasing  $W$  (fixed  $T$  and  $x_j$  like  $l/W$ .) If one could observe experimentally this decrease and approach to a constant for  $F$  in (4.13b), it would certainly be support for QCD. However, such measurements are a long way off. They require, for example, at  $x_i=0.2$  and  $V r =0.2$ , comparing a point at FNAL  $W=19A$ ,  $M=3.9$  GeV and  $\Lambda = 1.94$  GeV/c with a point at ISR  $1\Lambda =53$  GeV,  $M=10.6$  GeV, and  $p_x = 5.3$  GeV/c

D. *Away-Side Jet in  $A+B^N u p C \rightarrow X$*

Several authors<sup>25-27,529</sup> have pointed out the usefulness of observing the "awayside" jet of hadrons that balances the momentum of a large  $p_x$  muon pair in  $\Lambda^+ + 5 \rightarrow \mu^+ p r + X$ . For  $pp$  collisions, large  $p_x$  muon pairs occur predominantly by the "Compton" subprocess,  $q+g \rightarrow q+Y^*$  as seen in Fig. 13. This means that for  $pp$  collisions, the "away-side" jet is predominantly a quarkjet. On the other hand, for  $7up \rightarrow i+j u \rightarrow +X$  (or  $pp \rightarrow u/u \rightarrow -X$ ) the "annihilation" term,  $qq \rightarrow j^* \rightarrow -g$ , is the dominant subprocess for producing large  $p_x$  muon pairs. This means that for these processes, the away jet is more likely initiated by a gluon rather than a quark. By comparing the away-side distributions of hadrons in large  $p_x$  muon production in  $pp \rightarrow j u \rightarrow +X$  and  $np \rightarrow p/u \rightarrow +X$ , one can in principle elucidate the differences between gluon and quark fragmentation.

**§V. Quark and Gluon Fragmentation Functions**

Gluon radiation from an outgoing quark results in scale breaking of the quark fragmentation function  $D^h(z)$ . As in (3.2), the probability of radiating a hard gluon goes as  $a_s(Q^2) \log^2(g^2/J^2)$  where  $A$  is, say, the invariant mass of the resulting quark-gluon pair. If  $A$  is large enough then this quark and gluon will appear as two distinct jets (each of which may radiate hard gluons and split again). If  $A$  is small then it will merely "appear" as if the original quark jet is becoming fatter as  $Q^2$  increases. If one chooses to describe this in terms of a single fragmentation function of the original quark,  $D(z, Q^2)$ , (which may not be the best way to handle this), then clearly as  $Q^2$  increases, the probability of finding a

large  $z$  hadron decreases. As  $Q^2$  increases, the momentum of the original quark is shared among the radiated gluon jets.<sup>35</sup>

One can analyze the  $Q^2$  dependence of the fragmentation functions,  $D(z, g^2)$ , by the methods developed by Altarelli and Parisi<sup>7</sup> for the quark distributions.<sup>35,37</sup> One defines "non-singlet" function for partons to fragment into a specific hadron  $h$  as follows

$$D_{NS}^h(z, Q^2) = D_{q_i}^h(z, Q^2) - D_{\bar{q}_i}^h(z, Q^2). \tag{5.1}$$

The change of these functions w.r.t.  $r$  is then given in an analogous manner to (3.10). Namely,

$$\frac{dD_{NS}^h(z, \tau)}{d\tau} = \frac{\alpha(\tau)}{2\pi} \int_z^1 \frac{dy}{y} P_{q \rightarrow q}(y) D_{NS}^h\left(\frac{z}{y}, \tau\right) \tag{5.2}$$

In general, there is mixing of the gluon fragmentation functions  $D^*(z, r)$  and the quark fragmentation functions  $D^\wedge(z, r)$ , since, for example, an observed hadron  $h$  could come from an outgoing quark or from a hard gluon that was radiated by the initial quark. Thus, in general,

$$\frac{dD_{q_i}^h(z, \tau)}{d\tau} = \frac{\alpha(\tau)}{2\pi} \int_z^1 \frac{dy}{y} \left[ P_{q \rightarrow q}(y) D_{q_i}^h\left(\frac{z}{y}, \tau\right) + P_{g \rightarrow q}(y) D_g^h\left(\frac{z}{y}, \tau\right) \right], \tag{5.3a}$$

$$\frac{dD_g^h(z, \tau)}{d\tau} = \frac{\alpha(\tau)}{2\pi} \int_z^1 \frac{dy}{y} \left[ \sum_{j=1}^{2n_f} P_{q_j \rightarrow g}(y) D_{q_j}^h\left(\frac{z}{y}, \tau\right) + P_{g \rightarrow g}(y) D_g^h\left(\frac{z}{y}, \tau\right) \right], \tag{5.3b}$$

where the probabilities  $F_{q_i}^\wedge(z)$  are the same as in (3.12). The moments of the fragmentation function for a constituent of type  $i$  to a given hadron,  $A$ , given by

$$\bar{M}_i^h(n, Q^2) = \int_0^1 z^{n-1} D_i^h(z, Q^2) dz \tag{5.4a}$$

are given in terms of the moments at some reference momentum  $Q_0$  by an equation similar to (3.13b). Namely,

$$\bar{M}_i^h(n, Q^2) = \sum_{i=1}^9 \bar{M}_i^h(n, Q_0^2) \bar{R}_{ij}(n, Q^2, Q_0^2, A^2), \tag{5.4b}$$

where the matrix  $R_0$  is simply related to  $R_g$ .

Care must be taken in choosing  $D(z, Q)$  since one must use in (5.3) the distribution of "primary" mesons before decay. In addition, one must guess at the distribution of hadrons

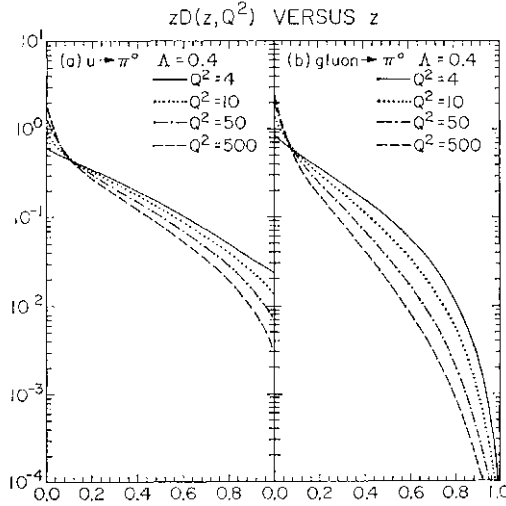


Fig. 19. (a) The  $Q^2$  dependence of the fragmentation function for a  $u$ -quark to a  $\pi^0$ ,  $D^u(z, Q^2)$ , expected from QCD. The distributions at high  $Q^2$  are calculated from the distribution at the reference momentum  $Q_0^2 = 4 \text{ GeV}^2$  using  $\Lambda = 0.4 \text{ GeV}/c$ , where  $D(z, Q_0^2)$  is taken from the analysis in ref. 60.

(b) Same as (a) but for the gluon fragmentation function  $D^g(z, Q^2)$ .

in a gluon jet,  $D^g(z, Q^2)$ . Figure 19 shows the resulting  $Q^2$  dependence of  $D^u(z, Q^2)$  and  $D^g(z, Q^2)$  for the particular reference momentum choices discussed in ref. 16. (The gluon fragmentation function at  $Q_0^2$  has been chosen to be steeper than the quark fragmentation function. That is, it is assumed that gluons fragment into fewer high  $z$  hadrons and into a larger multiplicity of hadrons than quarks.<sup>35,38</sup> Notice that although  $D^g(z, Q^2)$  decreases a large  $z$  as  $Q^2$  increases, the amount of "scaling breaking" is not predicted to be as great as for  $D^u(z, Q^2)$ . This is because the shape of the  $z$  distribution of  $D^g(z, Q^2)$  at  $Q_0^2$  is not as steep at large  $z$  as the  $x$  distribution of  $D^u(x, Q_0^2)$  is at large  $x$ .

## §VI. Large $p_\perp$ Meson and "Jet" Production in Hadron-Hadron Collisions

### A. The QCD Approach

In the naive parton model, the large  $p_\perp$  production of hadrons in the process  $A+B \rightarrow h_1+h_2+X$  is described by the diagram in Fig. 20b. The large-transverse-momentum reaction is assumed to occur as the result of a single large-angle scattering  $a+b \rightarrow c+d$ , followed by the decay or fragmentation of constituent  $c$  into the trigger hadron  $h_1$  and constituent  $d$  into the "away-

side" hadrons,  $h_2$ . This results in the four jet structure in Fig. 20a. The invariant cross section for the process  $A+B \rightarrow h_1+h_2+X$  is given by

$$E \frac{d\sigma}{d^3P}(s, p_\perp, \theta_{cm}) = \sum_{a,b} \int dx_a \times \int dx_b G_{A \rightarrow a}(x_a) G_{B \rightarrow b}(x_b) D_c^h(z_c) \frac{1}{z_c} \frac{1}{\pi} \frac{d\hat{\sigma}}{d\hat{t}}(\hat{s}, \hat{t}), \quad (6.1)$$

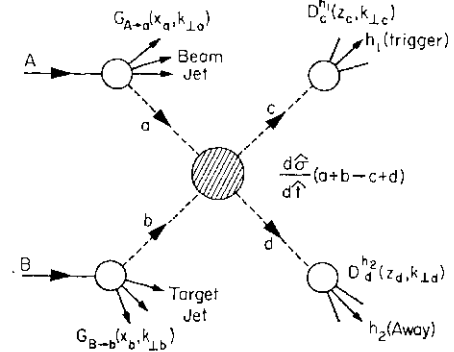
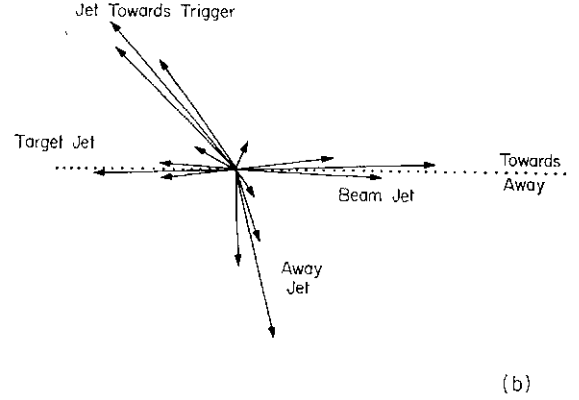


Fig. 20. (a) Illustration of the four jet structure resulting from a beam hadron (entering at left along dotted line) colliding with a target hadron (entering at right along dotted line) in the CM frame: two jets with large  $p_\perp$  (collection of particles moving roughly in the same direction), one called the "toward" (trigger) side and one on the "away" side; and two jets with small  $p_\perp$  that result from the break up of the beam and target hadrons (usually referred to as the "soft hadronic" background).

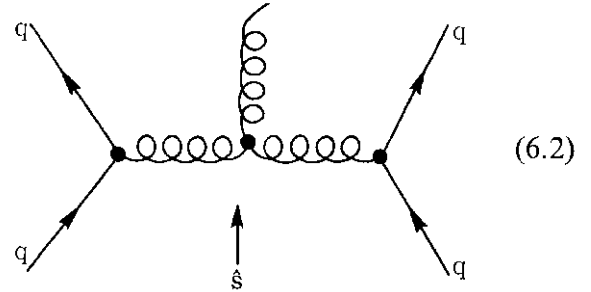
(b) Illustration of the underlying structure of the large  $p_\perp$  process  $A+B \rightarrow h_1+h_2+X$ . The large  $p_\perp$  trigger hadron  $h_1$  occurs as the result of a large angle scattering of constituents  $(q_a+q_b \rightarrow q_c+q_d)$ , followed by the decay or fragmentation of constituent  $c$  into a towards side jet of hadrons (one being the trigger  $h_1$ ) and constituent  $d$  into an away side jet of hadrons (one being  $h_2$ ). The quantities  $x_a, x_b, k_{\perp a}, k_{\perp b}$  are the longitudinal fraction of the incoming hadrons  $A, B$  momentum and perpendicular momentum of constituents  $a, b$  and  $z_c, z_d, k_{\perp c}, k_{\perp d}$  are the fraction of the outgoing constituents longitudinal momentum and perpendicular momentum carried by the detected hadrons  $h_1$  and  $h_2$ .



where  $s, t$  are the usual invariants but for the constituent two-to-two subprocess  $d\hat{o}/dt$  ( $a+b \rightarrow c+d$ ). The quantities  $x_a$  and  $x_b$  are the fractional momentum carried by the constituents  $a$  and  $b$ , respectively, and  $z_c$  is the fraction of the outgoing constituent momentum that appears in the hadron,  $h$ .

In the theory of QCD, the constituent subprocess,  $a+b \rightarrow c+d$ , must be corrected for the emission of gluons. That is one must include the higher order subprocesses  $a+b \rightarrow c+d+g$ ,  $a+b \rightarrow c+d+g+g$ , etc., where  $g$  is a gluon. As discussed by C. Sachrajda,<sup>39</sup> to leading order these processes modify (5.1) in the manner illustrated in Fig. 21.<sup>40</sup> For example, summing all the (divergent) gluon radiation from the outgoing quark in  $q+q \rightarrow q+q$  generates the "renormalization group improved" scale breaking fragmentation function  $D_q(z, Q^2)$  (Fig. 21a). Summing over all the (divergent) gluon radiation from the incoming quarks generates the "renormalization group improved" scale breaking quark dis-

tributions  $G_r^A(x, Q^2)$  (Fig. 21b). The divergent piece of the diagram



is contained in the "renormalization improved" gluon distribution  $G_r^A(x, Q^2)$  (Fig. 21c), where the constituent subprocess is now  $g+q \rightarrow g+q$ . Other higher order corrections to the gluon propagators and to the vertices generate the "renormalized" coupling  $a(Q^2)$  as discussed in Section II. Thus to leading order in QCD, eq. (6.1) becomes

$$E \frac{d\sigma}{d^3P}(s, p_\perp, \theta_{cm}) = \sum_{a,b} \int dx_a \times \int dx_b G_{A \rightarrow a}(x_a, Q^2) G_{B \rightarrow b}(x_b, Q^2) D_c^h(z_c, Q^2) \times \frac{1}{z_c} \frac{1}{\pi} \frac{d\hat{o}}{d\hat{t}}(\hat{s}, \hat{t}), \tag{6.3}$$

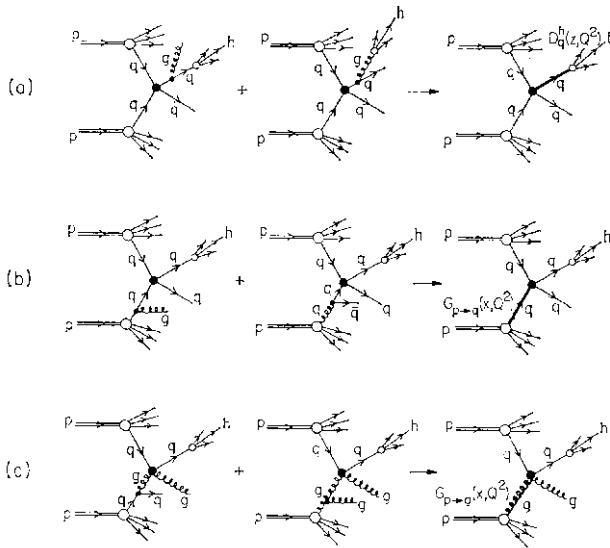


Fig. 21. (a) Illustration of two diagrams for  $pp \rightarrow h+X$  which are included (divergent parts) in the "renormalization group" improved quark fragmentation function,  $D_c^h(z, Q^2)$ , when one calculates the contribution from the subprocess  $qq \rightarrow qq$ .

(b) Illustration of two diagrams for  $pp \rightarrow h+X$  which are included (divergent parts) in the "renormalization group" improved quark distribution,  $G_{r \rightarrow a}(x, Q^2)$ , when one calculates the contribution from the subprocess  $qq \rightarrow qq$ .

(c) Illustration of two diagrams for  $pp \rightarrow h+X$  which are included (divergent parts) in the "renormalization group" improved gluon distribution,  $G_r^A(x, Q^2)$ , when one calculates the contribution from the subprocess  $qg \rightarrow qg$ .

where  $G(x, Q^2)$  and  $D(z, Q^2)$  are the "renormalization group improved" parton distributions and fragmentation functions, respectively, and where one includes all eight subprocesses:  $qq \rightarrow qq$ ,  $qq \rightarrow qq$ ,  $qq \rightarrow qq$ ,  $gq \rightarrow gq$ ,  $gq \rightarrow gq$ ,  $gg \rightarrow qq$ ,  $qq \rightarrow gg$ , and  $gg \rightarrow gg$ . Each  $2 \rightarrow 2$  differential cross section,  $dd/dt$ , is calculated to lowest order in perturbation theory with an effective coupling constant  $a(Q^2)$  as in (2.8). These cross sections have been calculated previously by Cutler and Sivers<sup>41</sup> and by Cornbridge, Kripfganz, and Ranft<sup>42</sup> and all behave as  $s^{-2}$  at fixed  $t/s$  (and for constant  $a$ ).

For  $ep$  collisions,  $Q$  is the 4-momentum transfer from the electron to the quark and for  $pp \rightarrow \mu^+ \mu^- + X$ , it is the mass of the muon pair. On the other hand, the correct kinematic quantity to use for  $Q^2$  in the constituent subprocesses contributing to large  $p_\perp$  meson production in  $pp$  collisions is not at present known. For our analyses of high  $p_\perp$  we take for definiteness

$$Q^2 = 2\hat{s}\hat{t}\hat{u}/(\hat{s}^2 + \hat{t}^2 + \hat{u}^2), \tag{6.4}$$

where  $\hat{s}, \hat{t}$ , and  $\hat{u}$  are the usual Mandelstam

invariants but for the constituent subprocesses. This uncertainty in the form for  $Q^2$  makes predictions at low  $Q^2$  (*i.e.*, low  $p_t$ ) in hadron-hadron collisions uncertain.

B. Smearing

There is considerable experimental evidence that the constituents inside the proton have a large internal transverse momentum.<sup>43,45</sup> Effects due to the transverse momentum of quarks within hadrons,  $(k_t)_h^{\Lambda_{op}}$  and of hadrons within the outgoing jets,  $(k_t)_j^{\Lambda_{op}}$ , called "smearing" effects are particularly important for large  $p_t$  calculations. This is due to the "trigger bias" which selects the configuration in which the initial quarks (or gluons) are

already moving toward the trigger. As for the muon pairs, in QCD, this transverse momentum of the partons can arise from two sources (illustrated in Fig. 22).

Firstly, in a proton beam, quarks are confined in the transverse direction to within the proton radius. Therefore, from the uncertainty principle, they must have some transverse momentum. This "primordial" momentum is intrinsic to the basic parton "wave function" inside the proton. As illustrated in Fig. 22a, one might expect the wave function to have a term where the trigger parton  $k_t$  is balanced by another constituent (or constituents) which has the opposite  $k_t$  and most of the remaining longitudinal momentum. Consider now the plane formed by the beam, target and a 90° trigger hadron (called the  $x$ - $z$  plane in Fig. 22). Typically, the trigger arises from the fragmentation of a constituent with  $k_t > 0$  which is balanced by the remaining constituents having  $k_t < 0$ . One expects to see this negative  $k_t$  as a shift in the beam and target jets at large  $|x_{11}|$ . This shift (*i.e.*, nonzero  $(k_{t,y})$  of the beam jet as one increases the  $\Lambda$  of a 90° trigger has recently been observed by the BFS group at ISR<sup>46</sup> (see Fig. 14 of ref. 15).

Secondly, in QCD, one expects to receive an "effective"  $k_t$  of quarks in protons due to the Bremsstrahlung of gluons. This perturbative term, which arises from diagrams like those in Fig. 21, is illustrated in Fig. 22b. It corresponds to including two particle to three or more particle processes (2->3) rather than just the two particle to two particle 2->2 scatterings. For such subprocesses, the  $k_t$  of the quark  $q_a$  is balanced by a gluon jet on the away-side which subsequently fragments into many low momentum hadrons. In addition, the mean value of the effective  $k_t$  is expected to depend on the  $x$  value of quark  $q_a$  and on the  $Q^2$  for the processes. Separating the origin of the transverse momenta into Type I and Type II as seen in Fig. 22 is, of course, a bit artificial since both mechanisms occur simultaneously.

The analysis of large  $p_t$  meson production is not as complete as the discussion of  $pp \rightarrow f\bar{f}j\bar{j}u\bar{u} + X$  presented in Section IV. We have not separated the "effective"  $k_t$  of the quarks and gluons in the initial hadrons in the "pri-

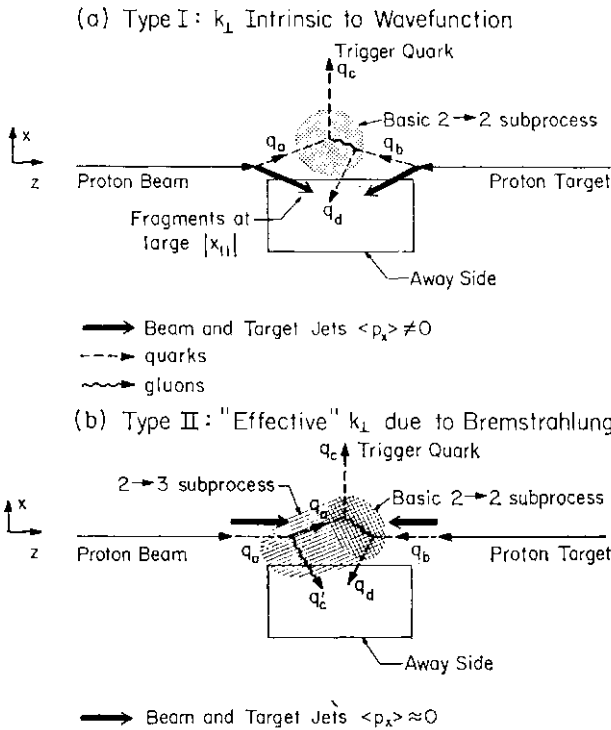


Fig. 22. (a) Illustration of the non-perturbative ("primordial") component of the transverse momentum of quarks within proton that is intrinsic to the wave function of the proton. One expects this transverse momentum to be balanced by the remaining constituents in the proton which can, in turn, fragment into particles at high  $|x_{11}|$ . The away-side consists of the recoiling quark,  $q_b$ , and two slightly shifted jets, one from the beam and one from the target.

(b) Illustration of a perturbative component to the transverse momentum of a quark with a hadron which is due to the Bremsstrahlung of a gluon before the basic 2->2 scattering occurs. In this case, the trigger quark is balanced by two away-side jets, one from the quark  $q_d$  and one from the radiated gluon  $q_c$ .

mordial" and "perturbative" components. For the present, we parameterize the transverse momentum of the partons (quarks and gluons) by a Gaussian with  $\langle f_{c_{\perp}} \rangle = 848$  MeV which produces for  $pp \rightarrow u\bar{u}j\bar{u} + X$  a mean  $p_{\perp}$  of 1.9 GeV<sup>2</sup> in agreement with the data in Fig. 14. We take this distribution to be independent of  $x$  and  $Q^2$  and to be the same for quarks, antiquarks, and gluons in the proton.<sup>47</sup> In so doing, we are *not* handling properly the  $x$  and  $Q^2$  dependence of the high  $k_{\perp}$  tails expected from QCD Bremsstrahlung. The next step would, of course, be to calculate and include explicitly the 2- $\rightarrow$ 3 subprocess expected by QCD (like  $qq \rightarrow qqg$ , etc.) and smear the results with the "primordial"  $k_{\perp}$  only (which is presumably smaller than the effective 848 MeV we now use). Care would have to be taken since one would include only the non-divergent parts of the 2- $\rightarrow$ 3 subprocesses.<sup>40</sup> The divergent parts have already been included by the use of the "renormalization improved" distributions  $G(x, Q^2)$  and fragmentation functions  $D(z, Q^2)$ . For the present, however, we merely use the data in Fig. 14 to give an "effective"  $k_{\perp}$  distribution and include explicitly only 2- $\rightarrow$ 2 subprocesses.

The emission of gluons after the hard scattering (2- $\rightarrow$ 2) subprocesses induces an "effective"  $k_{\perp}$  of the hadrons that fragment from the outgoing quarks because one is sometimes really seeing two jets rather than one. As for the quark distributions in the proton, we do not include these effects (we also neglect the interferences that arise between the amplitude for emitting gluon before and after the hard 2- $\rightarrow$ 2 process) and for the present take the transverse momentum distribution of hadrons from outgoing quarks (and gluons) to be a Gaussian with  $\langle f_{c_{\perp}} \rangle = 439$  MeV independent of  $z$  or  $Q^2$ . Again, this is not precisely correct and should be improved upon in later work.

### C. The Single Particle Cross Section

Figure 23 shows the final results for  $p_{\perp}^4 Edo/d^3p$  for  $pp \rightarrow n^0 + X$  at  $\theta_{c.m.} = 90^\circ$  and  $x_{\perp} = Q^2$  where now all eight subprocesses discussed in Section VL4 are included. The dash-dot and solid curves are the results before and after the additional scale breaking due to the transverse momentum of the quarks and gluons within the initial protons (smearing) have been

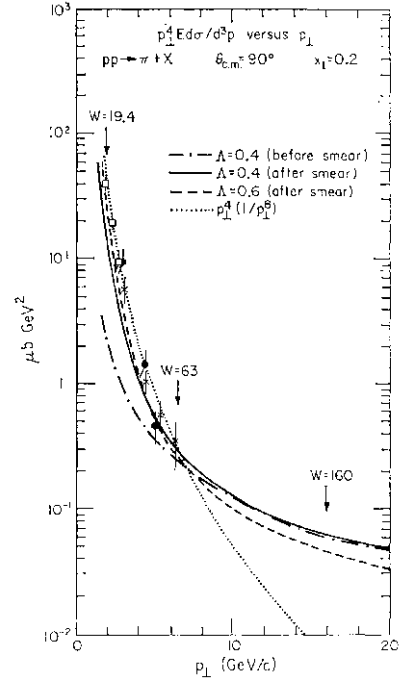


Fig. 23. The data on  $p_{\perp}^4$  times  $Edo/d^3p$  for large  $p_{\perp}$  pion production at  $\theta_{c.m.} = 90^\circ$  and fixed  $x_{\perp} = 0.2$  versus  $p_{\perp}$  (open squares=ref. 82, solid dots=ref. 83, crosses=ref. 84) compared with the predictions (with absolute normalization) of a model that incorporates all the features expected from QCD. The dot-dashed and solid curves are the results before and after smearing with  $\langle f_{c_{\perp}} \rangle = 848$  MeV, respectively, using  $A=0.4$  GeV/c and the dashed curves are the results using  $A=0.6$  GeV/c (after smearing). The dotted curve is  $p_{\perp}^2 \sim (1/W)$ .

included with  $\langle f_{c_{\perp}} \rangle = 848$  MeV and  $A=0A$  GeV. The dashed curve is the final result (after smearing) with  $A=0.6$  GeV and the dotted curve shows a  $p_{\perp}^2$  behavior. The final result exhibits a rough  $p_{\perp}^2$  behavior over the range  $2 < p_{\perp} < 6$  with an approach to  $p_{\perp}^{\pm}$  at very high  $p_{\perp}$  ( $p_{\perp} > 12$  GeV/c).

The QCD results for  $p_{\perp}^4 Edo/d^3p$  for  $pp \rightarrow 7T^0 + X$  in Fig. 23 can be compared to the prediction for  $W^0 dojdMdydk_{\perp}$  for  $pp \rightarrow f\bar{f}j\bar{u} + X$  in Fig. 18. The nature of the expected scale breaking is similar except the "breaking" is somewhat larger in the  $pp \rightarrow X^0 - X$  case. This is due to the additional "scale breaking" from the fragmentation functions and from a trigger bias effect which makes  $pp \rightarrow X^0 - X$  more sensitive to transverse momentum effects. When one performs a high  $p_{\perp}$  experiment, one sits at large  $p_{\perp}$  and waits for an event. This biases one in favor of the configuration where the initial partons are already moving toward the trigger and so smearing makes a large effect in these experiments.

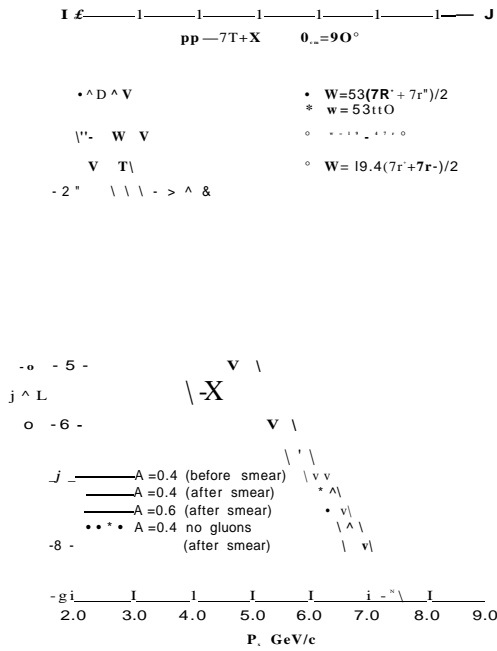


Fig. 24. Comparison of a QCD model (normalized absolutely) with data on large  $p_{\pm}$  pion production in proton proton collisions at  $W=V\sqrt{s}=19A$  and  $53 \text{ GeV}/c$  with  $\theta_{cm}=90^{\circ}$  (open squares=ref. 82, solid dots=ref. 83, crosses=ref. 84, solid triangles^ ref. 85, open circles=ref. 86). The dot-dashed and solid curves are the results before and after smearing, respectively, using  $A=0A \text{ GeV}/c$  and  $\langle \xi_{LX} \rangle_{\theta_{cm}=90^{\circ}}=838 \text{ MeV}$  and the dashed curves for  $A=0.6 \text{ GeV}/c$  (after smearing). The contribution arising from quark-quark, quark-antiquark, and antiquark-antiquark scattering (*i.e.*, no gluons) is shown by the dotted curves (after smearing).

The data on  $E d^3\sigma/d^3p$  at fixed  $W=19A$  and  $53 \text{ GeV}$  versus  $p_{\pm}$  are compared with the theory in Fig. 24. The agreement is quite good. The results before smearing are shown by the dot-dashed curves. Smearing has little effect for  $p_{\pm} > 4.0 \text{ GeV}/c$  at  $W=53 \text{ GeV}$  but has a sizable effect (even at  $p_{\pm}=6.0 \text{ GeV}/c$ ) at  $W=19.4 \text{ GeV}$  due to the steepness of the cross section at this low energy. At  $p_{\pm}=2.0$  and  $W=19A \text{ GeV}$ , smearing increases the cross section by about a factor of 10. The contributions to the total invariant cross section from quark-quark elastic scattering (plus  $qq \rightarrow qq$  and  $qq \rightarrow qq$ ) are shown by the dotted curves. As noted by several authors, gluons make important contributions to the cross section at small  $x_{\pm}$  ( $x_{\pm} < 0.4$ ).<sup>41,42</sup>

The disagreement in the normalization of the theory seen in Figs. 23 and 24 at low  $x_{\pm}$  (the  $A=0A \text{ GeV}/c$  solution is about a factor of 2 low at  $p_{\pm}=2 \text{ GeV}/c$  and  $W=53 \text{ GeV}$ ) is not significant. The  $f=0.6 \text{ GeV}$  solution

agrees better at low  $p_{\pm}$  but the theory at present cannot be calculated precisely at these low  $p_{\pm}$  values. At low  $p_{\pm}$  the results depend too sensitively on things like the unknown gluon distributions, the precise shape of the transverse momentum distributions, the low  $s$  and  $t$  cut-off employed,<sup>48-50</sup> the choice for  $Q^2$ , and also higher order QCD corrections may be important. (For  $a(Q^2) > 0.3$  non-perturbative effects may begin to play a role.<sup>51</sup>) It may well be that the scattering of quarks and gluons as described by QCD is responsible for all the cross section down to  $p_{\pm}s$  as low as 1.0 or  $2.0 \text{ GeV}/c$ ; one simply cannot say at present. On the other hand, it may be that other non-leading CIM constituent subprocesses like the ones discussed by Blankenbecler, Brodsky, and Gunion<sup>52</sup> play a role at low  $p_{\pm}$  with the leading processes dominating for  $j^{\wedge} S.O \text{ GeV}/c$ .

Figure 25 shows a comparison of the pre-

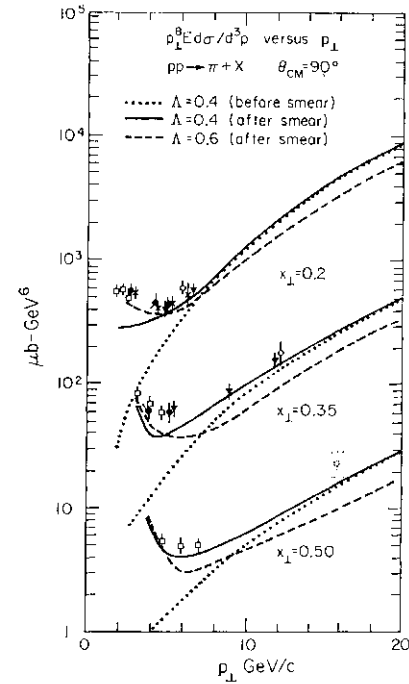


Fig. 25. The data on  $p_{\pm}$  times  $E d^3\sigma/d^3p$  for large  $p_{\pm}$  pion production at  $\theta_{cm}=90^{\circ}$  and fixed  $x_{j1}=0.2, 0.35,$  and  $0.5$  vs.  $p_{\pm}$  (open squares=ref. 82, solid dots=ref. 83, crosses=ref. 84) compared with the predictions (with absolute normalization) of a model that incorporates all the features expected from QCD. The dot-dashed and solid curves are the results before and after smearing, respectively, using  $A=0A \text{ GeV}/c$  and the dashed curves are the results using  $A=0.6 \text{ GeV}/c$  (after smearing). Recent data (triangles=ref. 54, open circles=ref. 53) from the ISR do show a deviation from a straight line ( $1/p_{\pm}^2$ ) behavior as expected from QCD.

dieted and experimental behavior of  $p \setminus$  times  $E d\sigma/d^3p$  for  $pp \rightarrow h_1 + h_2 + X$  at  $\theta_{cm} = 90^\circ$  and  $x_\pm = 0.2, 0.35$  and  $0.5$ . The dot-dashed and solid curves are the final results before and after smearing, respectively, with  $A=0.4$ . The dashed curves are the results (after smearing) using  $A=0.6$ . For the range  $2.0 < p_\pm < 6.0$  GeV/c at  $x_\pm = 0.2$ , and  $4.0 < p_\pm < 10.0$  GeV/c at  $x_\pm = 0.5$ , the results are roughly independent of  $p_\pm$  (when multiplied by  $p_\pm^*$ ). However, this  $p_\pm^*$  behavior is only a "local" effect. It holds only over a small range of  $p_\pm$  (at low  $p_\pm$ ); the region depending somewhat on  $x_\pm$ . As  $p_\pm$  increases, the predictions approach the expected  $p_\pm^{-1}$  behavior. The new data from ISR (triangles<sup>54</sup> and open circles<sup>55</sup>) shown in Fig. 25 do show an increase from the flat ( $1/p_\pm$ ) behavior at large  $p_\pm$  in agreement with the QCD expectations.

*D. Scaling of the Back-to-Back  $pp \rightarrow h_1 + h_2 + X$  Cross Section*

As seen in Fig. 23 and Fig. 25, the basic QCD subprocesses (before smearing) behave roughly like  $1/p_\pm$  at fixed  $x_\pm$  for  $2 < p_\pm < 10$  GeV/c. To get a  $1/p_\pm$  behavior, one must include large smearing effects that raise the small  $p_\pm$  prediction considerably while leaving the large  $p_\pm$  region essentially unchanged. There is considerable controversy over the question of whether smearing really produces enough scale breaking to change  $1/p_\pm^*$  to  $1/p_\pm$ .<sup>49,50</sup> Fortunately, the question can be answered experimentally. The increase at small  $p_\pm$  due to the "trigger bias" effect can be removed by triggering on events with equally large  $p_\pm$ 's on the toward and away-side.<sup>55</sup> Thus we expect the  $p_\pm$  dependence of the back-to-back cross section  $E d\sigma/d^3p d\zeta dy_2$  ( $pp \rightarrow h_1 + h_2 + X$ ) to differ (in the region where smearing is an important effect) from that of the single particle cross section, where  $\xi = p_\pm$  (away)/ $p_\pm$  (trig)  $\sim 1$  and  $y_2 = 0$ . The back-to-back cross section should reflect more closely the  $1/p_\pm$  behavior of the basic QCD subprocess.

New data submitted to this conference from a Columbia, Fermilab, Stony Brook collaboration<sup>56</sup> at FNAL yield

$$E d\sigma/d^3p(pp \rightarrow \pi + X) \propto p_\pm^{-8.2 \pm 0.2} \quad (6.5a)$$

at fixed  $x_\pm$  for a single particle trigger and

$$E_1 d\sigma_1/d^3p d\xi dy_2(pp \rightarrow h_1 + h_2$$

$$+ X) \Big|_{\substack{\xi \approx 1 \\ y_2 = 0}} \propto p_\pm^{-6.4 \pm 0.2} \quad (6.5b)$$

at fixed  $x_\pm$  ( $x_\pm > 0.25$ ) for the back-to-back trigger. This is an important result. It means that even at FNAL energies and  $p_\pm$  values, one is seeing a basic subprocess behaving like  $1/p_\pm$  (after the scale breaking due to smearing has been removed) which is easily explained by a basic  $1/p_\pm$  subprocess plus the scale breaking due to  $a(Q^2)$ ,  $G(x_\pm, Q^2)$  and  $D(z_\pm, Q^2)$  in the amount expected by QCD.

*E. Away-Side Correlations*

An important consequence of the QCD approach is that the number of away-side hadrons with large  $p_\pm$  (or  $-p_\pm$  as in Fig. 26) is pre-

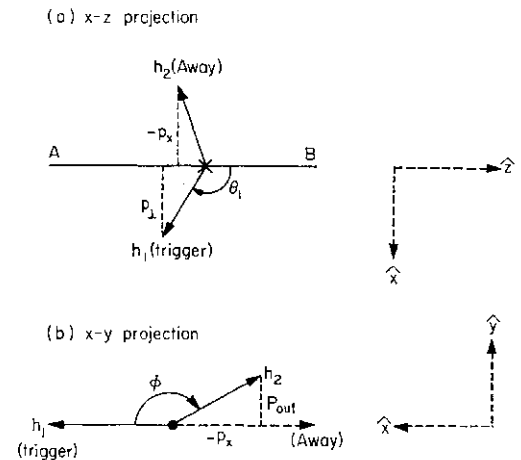


Fig. 26. Definition of kinematic variables used in describing the process  $A+B \rightarrow h_1+h_2+X$ : (a)  $x-z$  projection, where the beam, target and trigger hadron  $h_1$  form this plane; (b)  $x-y$  projection.

dicted to be considerably smaller than in the quark-quark scattering approach. Figure 27 shows that the number of away hadrons carrying a certain fraction,  $z_{tr}$ , of the trigger momentum is predicted to be 3 to 4 times less than the FFF results,<sup>43</sup> and now agree quite well with experiment. This reduction in the away-side multiplicity for large  $z_{tr}$  is due to three factors. First,  $\langle fc \rangle_{\Lambda_{tr}}$  has been increased from 500 MeV to 848 MeV. Second, the fragmentation functions  $D(z_\pm, Q^2)$  decrease at large  $z$  as  $Q^2$  increases (see Fig. 19). Finally, in the QCD approach, the away-side constituent is quite often a gluon which produces on the average fewer hadrons at large  $z$  than do the quarks.

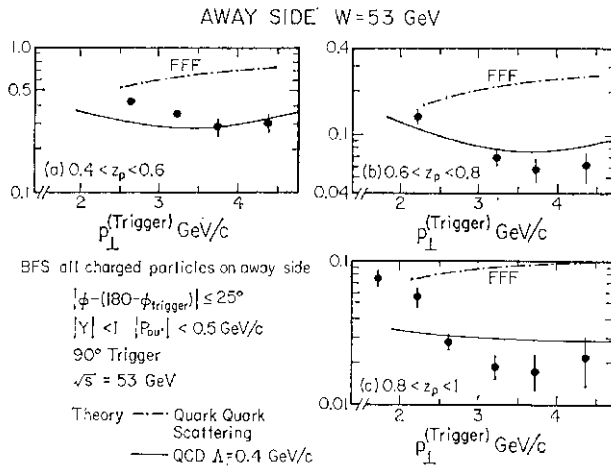


Fig. 27. The dependence on the trigger  $p_{\pm}$  of the away-side hadron multiplicity  $n(z_{\pm}) = (1/a) \int da dz_{\pm}$  where  $z_{\pm} = -p_{\pm}(\text{away})/p_{\pm}(\text{trig})$  from the British-French-Scandinavian collaboration<sup>57</sup> on  $pp \rightarrow h^+ h^- X$  at  $W=53$  GeV,  $\theta_{cm}=90^\circ$  and with an away-side acceptance of  $25^\circ$  in  $\phi$  and  $|Y_{\pm}| < 1$ ,  $1^{\text{away}} < 0.5$  GeV/c. The predictions from the QCD approach with  $A=0.4$  GeV/c (solid curves) and the results of the quark-quark "black-box" model of FFF<sup>43</sup> (dash-dot curves) are shown. Background contributions from the fragmentation of the beam and target (see Fig. 20) which might be important for low  $p_{\pm}$  triggers have not been included in either the QCD or FFF predictions.

Demanding a high  $p_{\pm}$  trigger means that the toward-side constituent is predominantly a quark (72% of the time at  $W=53$  GeV,  $p_{\pm}=4.0$  GeV/c,  $\theta_{cm}=90^\circ$ ) whereas the recoiling away-side constituent will quite often be a gluon (62% at the above energy). This is illustrated in Fig. 28 for  $pp \rightarrow 7v^0 + X$  at  $W=53$  GeV,  $p_{\pm}=4.0$  GeV/c and  $\theta_{cm}=90^\circ$ . These away-side gluons produce equal numbers of positives and negatives so that the away-side plus to minus ratio is, at the ISR (low  $x_{\pm}$ ), predicted to be considerably smaller than in FFF where all away-side partons were quarks. Figure 29 shows that the QCD approach yields almost equal numbers of positives and negatives for  $p_{\pm}$  (away)=1.5 GeV/c at  $W=51$  GeV and  $3.0 < p_{\pm}(\text{trig}) < 4.0$  GeV/c in agreement with recent ISR data.<sup>57</sup> In FFF,<sup>43</sup> this ratio was predicted to be about 1.5 in gross disagreement with the experiment. At present, neither the QCD approach nor the FFF model can explain the apparently large increase in the away-side positive to negative ratio when triggering on  $K^-$  as observed by R-413<sup>57</sup> (Fig. 29).

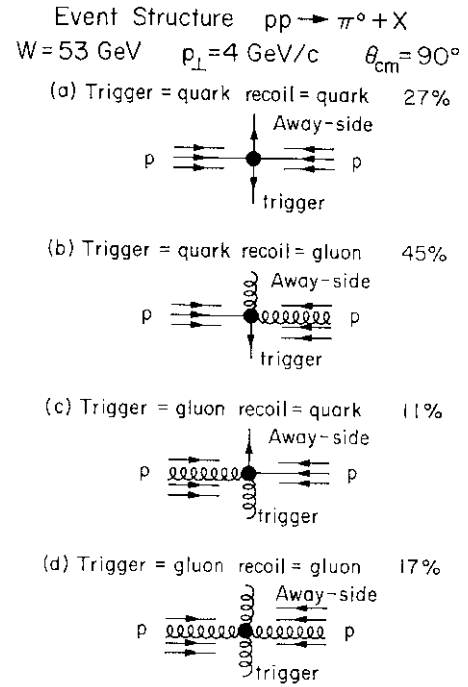


Fig. 28. Illustration of the underlying event structure expected from QCD at  $W=53$  GeV,  $p_{\perp}=4$  GeV/c, and  $\theta_{cm}=90^\circ$  for the process  $pp \rightarrow 7v^0 + X$ .

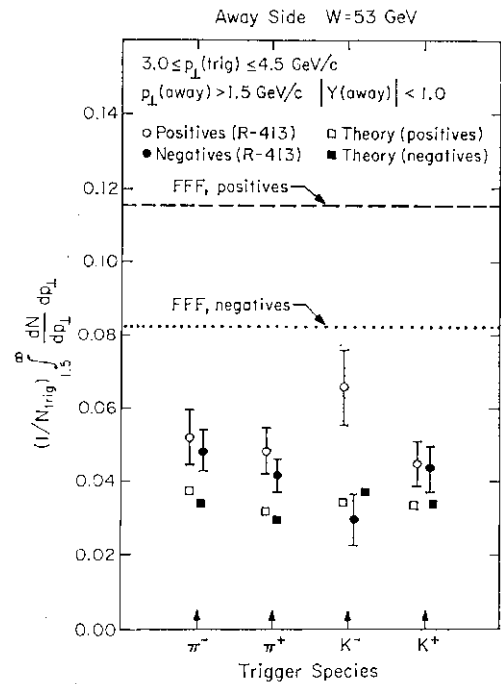


Fig. 29. The number of away-side positive and negative hadrons with  $p_{\pm}$  (away)  $> 1.5$  GeV/c per trigger with  $3.0 < p_{\pm}(\text{trig}) < 4.5$  GeV/c from the BFS collaboration (R-413)<sup>57</sup> on  $pp \rightarrow h^+ h^- X$  where  $W=53$  GeV/c and  $d_{\perp}=90^\circ$  and  $|Y_{\pm}| < 1.0$ . The results for  $7T^-, 7T^+, K^-$  and  $K^+$  triggers are shown and compared to the predictions of the quark-quark "black-box" model of FFF<sup>43</sup> and the QCD approach with  $A=0.4$  GeV/c (open and solid squares). Background contributions from the beam and target jets (see Fig. 20) have not been included in either the QCD or FFF predictions.

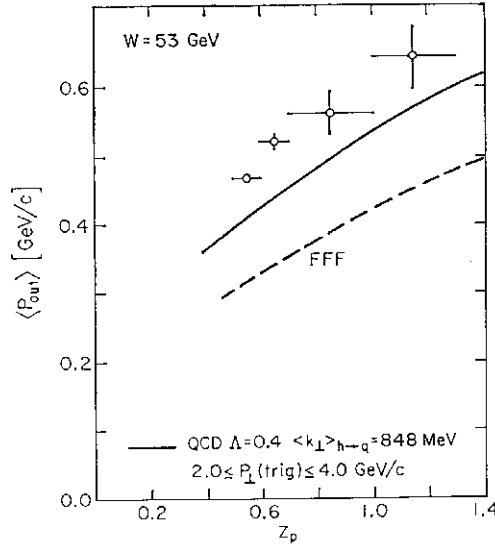


Fig. 30. The dependence on  $z_p$  of the mean value of the  $\langle P_{out} \rangle$  of away-side charged hadrons at  $W=53$  GeV and  $2.0 < P_{\perp}(trig) < 4.0$  GeV/c with  $\theta_x$  averaged over  $45^\circ$  and  $20^\circ$  from the CCHK collaboration on  $pp \rightarrow h_1^+ h_2^+ X$ , where  $z_p = \langle p_{\perp}(away) \rangle / \langle p_{\perp}(trig) \rangle$  (see Fig. 26). The predictions from the QCD approach at  $\theta = 45^\circ$  with  $A = 0.4$  GeV/c, and  $\langle k_{\perp} \rangle_{h \rightarrow q} = 848$  MeV, and  $\langle k_{\perp} \rangle_{g \rightarrow q} = 439$  MeV (solid curve) and the results of FFF<sup>43</sup> (dashed curve) curve are shown.

F. P-out Distributions

The use of an effective transverse momentum of  $\langle k_{\perp} \rangle = 848$  MeV as determined from the muon pair data results in mean P-out values that are considerably larger than the FFF results where  $\langle k_{\perp} \rangle$  was 500 MeV. (P-out is defined in Fig. 26.) As can be seen in Fig. 30, the new results are in much better agreement with the hadron data, although the predicted  $\langle P-out \rangle$  is still a bit too small. Some of the discrepancy may be due to contributions from the beam and target jets which have not been included. Also, it may be that one should be using a slightly larger  $\langle k_{\perp} \rangle$  in the ISR range  $W=53$  MoV since the effective  $\langle k_{\perp} \rangle$  distribution should increase slightly with increasing energy as seen in Fig. 15.

We have not really done a proper analysis of the P-out distribution. What one should do (and many are undoubtedly working on this) is to include 2-3 process explicitly in the large  $p_{\perp}$  analysis similar to what was done for  $pp \rightarrow j u + j u + X$ . The primordial motion could then be set at the value determined from  $pp \rightarrow f x f A + X$  (i.e.,  $\langle k_{\perp} \rangle_{ord} \approx 600$  MeV or perhaps less). One would then predict a

large momentum tail to the P-out distribution. It would not be expected to be bounded (like a Gaussian) and the tail would increase at increasing energies. There is, at present, no experimental evidence for a large momentum tail to the P-out distribution, although ( $J$ -out) is large. As Fig. 31 shows, it looks Gaussian, but so does the  $\langle j u \rangle$  spectrum in Fig. 14.

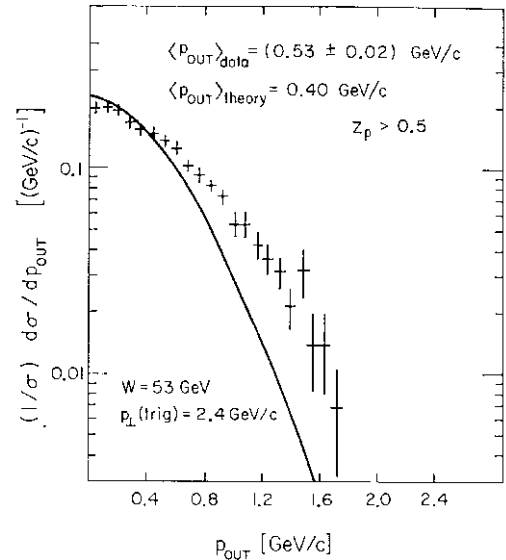


Fig. 31. The P-out spectrum (see Fig. 26) for away-side charged hadrons with  $z_p > 0.5$  at  $W=53$ ,  $2.0 < P_{\perp}(trig) < 4.0$  GeV/c with  $\theta_x$  averaged over  $45^\circ$  and  $20^\circ$  from the CCHK collaboration on  $pp \rightarrow h_1^+ h_2^+ X$ . The prediction from the QCD approach at  $\theta = 45^\circ$  with  $A = 0.4$  GeV/c,  $\langle k_{\perp} \rangle_{h \rightarrow q} = 848$  MeV and  $\langle k_{\perp} \rangle_{g \rightarrow q} = 439$  MeV is shown by the solid curve.

G. The "Jet" Cross Section

A dramatic prediction of the QCD parton approach is the size of the cross section for producing a jet (parton=quark, antiquark, or gluon) of momentum  $p_{\perp}$  compared to that for producing a single particle at the same  $p_{\perp}$ . In this approach, the single particle trigger always comes from a parton carrying more  $p_{\perp}$  (typically about 15 % more for quarks and greater for gluons) than the trigger particle. Furthermore, the chance of a parton fragmenting into hadrons in such a way that one particle carries almost all the momentum is small (only a few percent) as can be seen in Fig. 19. These two effects combine to give the large  $\sigma(pp \rightarrow jet + X) / \sigma(pp \rightarrow X + X)$  ratio shown in Fig. 32.<sup>44</sup> In the QCD approach, this ratio does not scale (i.e., it is a function of

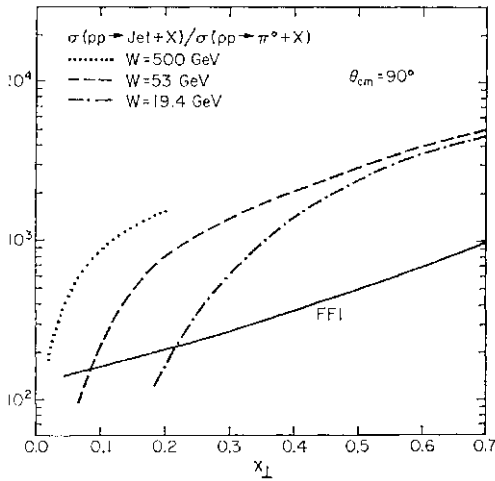


Fig. 32. Prediction of the jet to single  $\pi^0$  ratio at  $\theta_{cm} = 90^\circ$  vs  $x_{\perp}$  for  $W = 500, 53,$  and  $19.4$  GeV from the QCD approach using  $A = 0A \text{ GeV}/c$ . The jet cross section is defined as the cross section for producing a parton (quark, antiquark and glue) with the given  $x_{\perp}$ . Also shown is the prediction from the quark scattering model of FFF which is independent of  $W$  at fixed  $x_{\perp}$  and  $d_{\text{cut}}$ .

$x_{\perp}$ ,  $b_{cm}$  and  $W$ ).

The cross section for producing a "jet" of particles whose transverse momentum sum to give  $p_{\perp}$  has been measured now by two groups<sup>45,159</sup> and is shown in Fig. 33. The measured jet rate is several orders of magnitude greater than the  $\pi^0$  rate and is in qualitative agreement with the QCD predictions.

It is extremely difficult to make precise quantitative comparisons with the jet data in Fig. 33. Theoretically what is shown in Fig. 32 and Fig. 33 is the cross section for producing a quark (or gluon) with a given momentum (in Fig. 32 it is divided by the  $K^0$  cross section at the same momentum). However, as discussed in ref. 60, quarks of a given momentum (equal to their energy) cannot produce jets with the momentum of all particles equal to the energy of all particles. Our jet model<sup>60</sup> gives  $E_{\text{jet}} = p_{\text{jet}} \wedge 1.2 \text{ GeV}$  for quark jets. Since the cross section for producing jets falls so steeply, the cross section for producing a jet with a given  $p_{\text{jet}}$  is considerably smaller than that for producing one with a given  $E_{\text{jet}}$ . As explained in ref. 61, it is the former that is more closely connected to what is measured experimentally. At  $W = 19A \text{ GeV}/c$ , the cross section to produce a jet where  $p_{\text{jet}} = 5 \text{ GeV}/c$  at  $90^\circ$  is about 8 times smaller than the cross section to produce a jet whose  $E_{\text{jet}} = 5 \text{ GeV}/c$ .

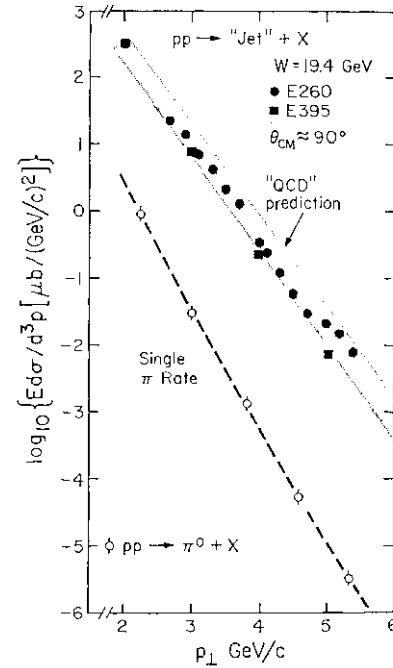


Fig. 33. Comparison of the jet and single  $\pi^0$  cross sections measured at  $200 \text{ GeV}/c$  ( $W = 19A \text{ GeV}$ ) and  $\theta_{cm} \sim 90^\circ$ . The jet data are from two FNAL experiments, E260<sup>59</sup> and E395,<sup>45</sup> where a jet is defined as the sum of all particles into their respective detectors. Also shown is the QCD prediction for the cross section of producing a parton (quark, antiquark or gluon) at  $\theta_{cm} = 90^\circ$  and  $W = 19A \text{ GeV}$  with a given  $p_{\perp}$ .

The difference between  $E_{\text{jet}}$  and  $p_{\text{jet}}$  of a jet arises, of course, from low momentum particles that have energy due to their mass (or  $k_{\perp}$ ) but have little momentum  $p_{\perp}$ . This is tangled with the experimental uncertainty in all hadron jet experiments concerning low  $p_{\perp}$  particles. One cannot be sure that one is not losing the low  $p_{\perp}$  jet particles that are not well collimated or gaining low  $p_{\perp}$  background from the beam and target jets in Fig. 20. Only by doing a very careful analysis, including the precise acceptances of a given experiment, can one make any quantitative statements.

The "bias" in favor of toward-side quarks, discussed in Section VI E and illustrated in Fig. 28, does not occur when one triggers on jets rather than on single particles and thus gluons make up a sizable fraction of the jet cross section. With our guesses for the gluon distributions, gluons are responsible for 73% of the jet triggers at  $p_{\perp} = 4 \text{ GeV}/c$ ,  $W = 52 \text{ GeV}$  and  $\theta_{cm} = 90^\circ$ . Even at higher  $x_{\perp}$  values like  $p_{\perp} = 6.0 \text{ GeV}/c$ ,  $W = 19A \text{ GeV}$ ,  $\theta_{cm} = 90^\circ$ , gluons still make up 45% of the jets. One might hope someday to distinguish experi-



mentally between gluon and quark jets, the gluon jets are assumed to have a higher multiplicity of particles each with lower momentum on the average. In addition, unlike the quark jets discussed in ref. 60, gluon jets will carry on the average no net charge (or strangeness, etc.).

H. Very High Energy Expectations

Figure 25 shows that the QCD predictions begin to deviate from a  $ljp$  behavior (at fixed  $x_+$ ) as  $p_+$  increases yielding a much larger cross section than expected from a  $pj^*$  model. This is also seen in Fig. 34 where the QCD predictions for  $p$  times  $E d\sigma/d^3p$  versus  $p_+$  at  $x_+=0.05$  and  $\theta_{cm}=90^\circ$  are plotted. At  $W=500$  GeV, the QCD results are a factor of 100 greater than a straight  $(1/p)$  extrapolation and show a factor of 1000 increase at  $W=1000$  GeV. Figure 35 shows the predictions for  $90^\circ \pi^0$  and jet production at  $\sqrt{s}=53, 500$  and  $1000$  GeV vs  $p_+$ . The  $p_+=30$  GeV/c  $90^\circ \pi^0$  cross section at  $\sqrt{s}=500$  GeV is predicted in the QCD approach to be about the same magnitude as that measured at  $p_+=6.0$  GeV/c at Fermilab ( $W=19A$  GeV)!

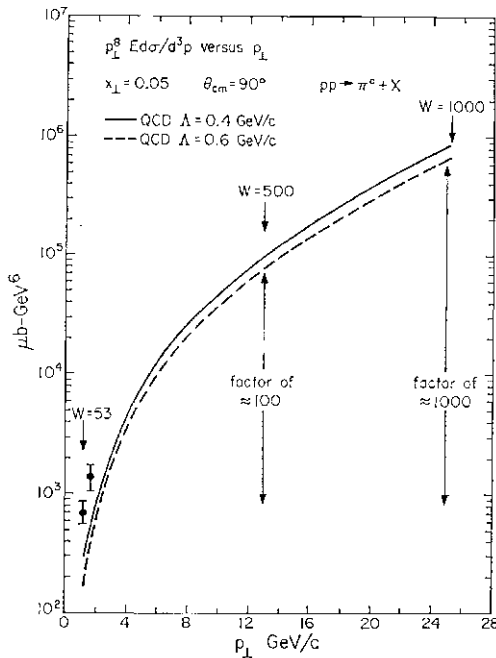


Fig. 34. The behavior of  $p_+$  times the  $90^\circ$  single  $tt^0$  cross section,  $E d\sigma/d^3p$ , at  $x_+=0.05$   $p_+$  calculated from the QCD approach with  $\Lambda=0.4$  GeV/c (solid curve) and  $\Lambda=0.6$  GeV/c (dashed curve). The two low  $p_+$  data points are at  $W=53$  and  $63$  GeV.<sup>83</sup> The predictions are a factor of 100 (1000) times larger than the flat ( $p_+^{-1}$ ) extrapolation to  $W=500$  (1000 GeV).

It is not clear yet precisely what the quark and gluon jets will look like at very high  $p_+$  (like  $p_+=30$  GeV/c). If QCD is correct, they will certainly not look like the well collimated  $(k_+)^{\Lambda}=430$  MeV objects used in this analysis. At  $p_+=30$  GeV/c, they should "appear" to be fatter. This is because as the  $p_+$  of the outgoing quark increases, it becomes increasingly likely that it radiate a hard gluon and become two jets (one quark and one gluon). Then, this quark or gluon might radiate producing still more subjects. This is the same mechanism that is responsible for the scale breaking of the fragmentation functions  $Z(z, Q)$  discussed in Section V. The net result is that most of the time it will look as if there is one somewhat fatter jet (with the fatness increasing with increasing momentum); however,

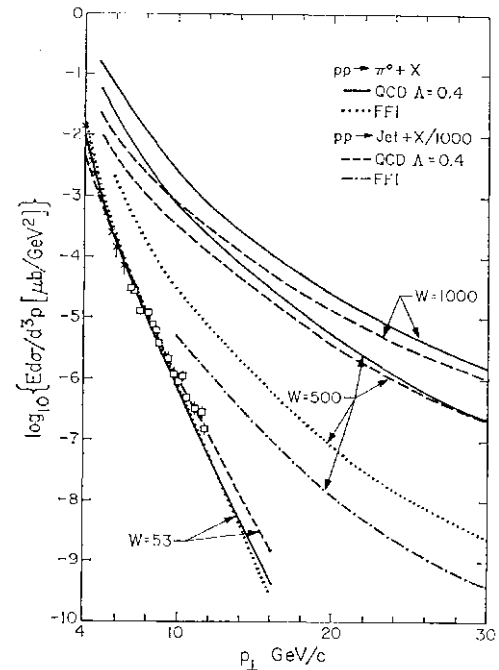


Fig. 35. Comparison of the results on the  $90^\circ \pi^0$  cross section,  $E d\sigma/d^3p$ , from the QCD approach with  $\Lambda=0.4$  GeV/c (solid curve) and the quark-quark "black-box" model of FFF (dotted curves). Both models agree with the data at  $W=53$  GeV (crosses=ref. 84) where the open squares are the "preliminary" data from the CCOR collaboration<sup>84</sup> normalized to agree with the lower  $p_+$  experiments. The QCD approach results in much larger cross sections than the FFF model at  $\sqrt{s}=500$  and  $1000$  GeV. The FFF results at  $1000$  GeV (not shown) are only slightly larger than the results at  $500$  GeV. Also shown are the cross sections for producing a jet at  $90^\circ$  (divided by 1000) as predicted by the QCD approach (dashed curves) and the FFF model (dot-dashed curve).

occasionally when the radiation is hard enough, one will see two or three subjects. I will discuss this more in a later section.

/. Charm Production at Large  $p_{\pm}$

An interesting consequence of the presence of gluons within the proton is that one can now produce heavy quarks (like charm) at large  $p_{\pm}$  by the process  $gg \rightarrow cc$  as illustrated in Fig. 36a. This subprocess is somewhat analogous to  $e^+e^- \rightarrow qq$  that results in heavy quark production in  $e^+e^-$  collisions. Figure 37 shows the estimated total cross section for producing a charm quark,  $c$ , with  $p_{\pm}(c) > 2.0$  GeV/c in proton-proton collisions. Since each charm quark must fragment into at least one charmed hadron (these hadrons won't necessarily have  $p_{\pm} > 2.0$  GeV/c), this can be viewed as the total cross section for charm that arises from charm quarks having  $p_{\pm} > 2.0$  GeV/c. The large  $p_{\pm}$  charm production is not negligible. It reaches about 10 *fib* at the highest ISR energies.

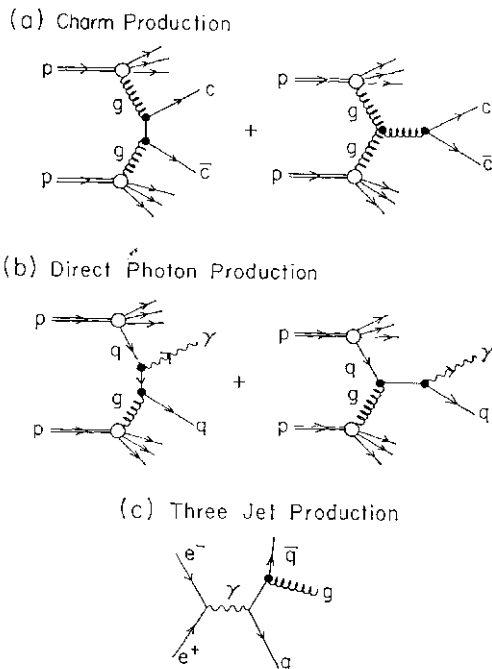


Fig. 36. (a) Two diagrams for the production of charm at large  $p_{\pm}$  in  $pp$  collisions from the subprocess  $gg \rightarrow cc$ , where  $g$  is a gluon. (b) Two diagrams for the production of direct photons,  $\gamma$ , at large  $p_{\pm}$  in  $pp$  collisions from the "Compton" subprocess  $gq \rightarrow Tq$ . (c) Illustration of three jet production in  $e^+e^-$  annihilations due to the Bremsstrahlung radiation of a hard gluon.

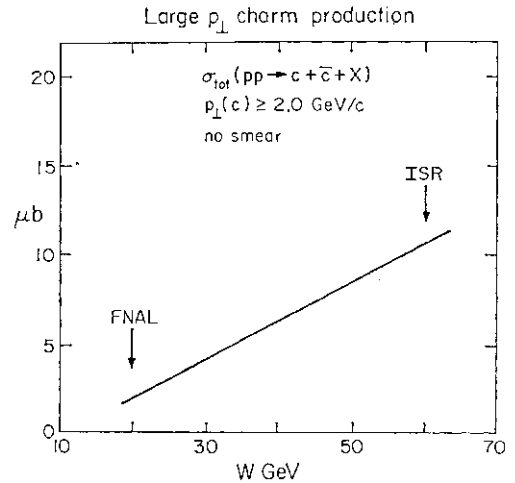


Fig. 37. Estimate of the total cross section for producing a charm quark,  $c$ , with  $p_{\pm}(c) > 2$  GeV/c in  $pp$  collisions from the  $gg \rightarrow cc$  subprocess illustrated in Fig. 36a.

/. Direct Photons at Large  $p_{\pm}$

As shown in Fig. 24, gluons are responsible for a sizable portion of the large  $p_{\pm}$   $n^{\circ}$  cross section. In fact, Fig. 28 indicates that the dominant subprocess at  $W=53$  GeV,  $p_{\pm}=4$  GeV/c,  $\theta_{cm}=90^{\circ}$  is quark-gluon scattering,  $g+q \rightarrow g+q$ . If gluons participate in this subprocess, then necessarily they must produce direct large  $p_{\pm}$  photons by the process,  $g+q \rightarrow \gamma+q$ , as illustrated in Fig. 36b. Even though the process  $g+q \rightarrow \gamma+q$  is down by  $\alpha_{em}/\alpha_s$  relative to  $g+q \rightarrow g+q$ , when comparing the rate for large  $p_{\pm}$  photons to that for producing, say,  $n^{\circ}$ s it is enhanced since this latter must proceed via a quark or gluon fragmentation function.

Figure 38 shows the ratio of photons produced by the subprocess  $g+q \rightarrow \gamma+q$  to the total QCD  $n^{\circ}$  rate.<sup>69</sup> At  $p_{\pm}=14$  GeV/c,  $d_{cm}=90^{\circ}$ , and  $W=53$  GeV, one expects about as many direct photons as  $n^{\circ}$ s! These photon events are quite distinctive. They occur with a photon at large  $p_{\pm}$  on the trigger side with no accompanying to ward-side hadrons. The away-side hadrons come from the fragmentation of a quark. On the other hand, the production of photons due to Bremsstrahlung from, say,  $q+q \rightarrow q+q$  results in events where the photon is produced in association with other trigger-side hadrons. In addition, the  $JTT$  rate for photons produced via Bremsstrahlung is only about 2-5% as shown in Fig. 38.<sup>64,67</sup>

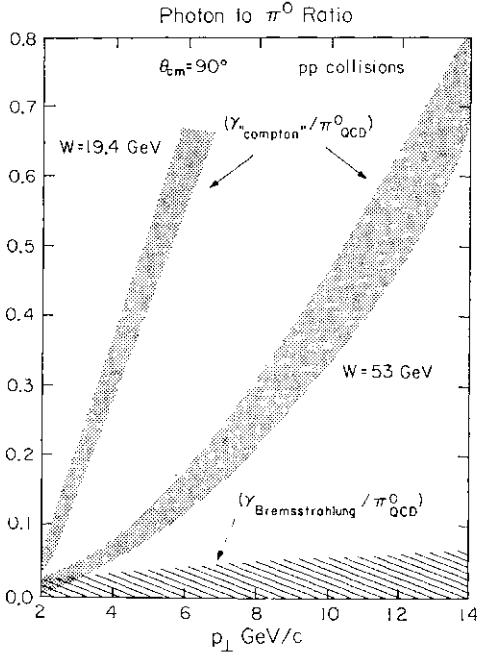


Fig. 38. Estimate of the rate of large  $p_{\perp}$  direct photon production at  $\theta_{cm}=90^\circ$  to the rate for producing  $n^\circ$  at  $W=19.4$  and  $53$  GeV, where the photons are produced by the "Compton" subprocess  $gq \rightarrow Tq$  illustrated in Fig. 36b and the  $\pi^0$  rate is given by the QCD predictions in Fig. 24 ( $A=0.4$  GeV/c). Also shown is the estimate for  $T_s$  produced by Bremsstrahlung from quark-quark and quark-gluon scattering.

It is interesting that in  $ep$  collisions one probes the quark distributions with an incoming virtual photon, while studying large  $p_{\perp}$  real photons in  $pp \rightarrow j+X$ , one can probe the distribution of gluons within the proton through the subprocess  $g+q \rightarrow T+q$ . If one does not find a reasonable rate for producing  $fs$  at large  $p_{\perp}$ , the QCD approach will be in trouble.

## §VII The Search for Three-Jet Events

### A. Analysis of Event Shapes in $e^+e^-$ Annihilation

Experiments have shown that the final states in  $e^+e^-$  hadrons consist predominantly of two jets of hadrons presumably resulting from the process  $e^+e^- \rightarrow qq$ . The theory of QCD expects this basic two-jet structure, but predicts that occasionally one of the outgoing quarks should emit a hard gluon,  $g$ , resulting in a three-jet final state (see Fig. 36c).<sup>70,71</sup> As discussed in Section IIIA and Section V (see eq. (3.2)), the probability of emitting a hard gluon is proportional to  $\alpha_s(Q^2) \log^2(\mathcal{E}^2/\Lambda^2)$  and thus increases logarithmically with increasing  $g^2$ . The observation of such

"three-jet" events would provide strong support for QCD.

Unfortunately, two-jet events can from time to time fragment into a configuration of final state hadrons that looks like a three-jet configuration; so the question is one of *rate*. One looks for observables to describe event structure that can be calculated to order  $\alpha_s^2(\hat{O}^2)$  in QCD and are "infrared finite." Presumably observables that do not discriminate between final states differing by the inclusion of a very low energy particle or by the replacement of one particle by two collinear particles with the same total momentum are infrared finite in QCD perturbation theory.

Two such observables recently examined by De Rujula, Ellis, Floratos and Gaillard<sup>72</sup> are the "thrust" defined by

$$T = 2 \max \frac{\sum_i \mathbf{p}_i^z}{\sum_i |\mathbf{p}_i|} \quad (7.1)$$

and the "sphericity"

$$S = \left(\frac{4}{\pi}\right)^2 \min \left( \frac{\sum_i |\mathbf{p}_i^z|}{\sum_i |\mathbf{p}_i|} \right)^2, \quad (7.2)$$

where the sum in the denominator runs over all observed particles and the sum  $\mathbf{2}$  in (7.1) runs over all particles in a hemisphere. The momenta  $p_i$  are parallel to a "jet" axis, normal to the plane defining the hemispheres, and chosen to maximize  $T$ . The thrust and sphericity lie in the range  $1 > T > 0.5$  and  $0 < S < 1$ , respectively. One expects the number of events with  $S$  or  $1-T$  large to be considerably different if the QCD perturbative  $e^+e^- \rightarrow qqg$  state exists than if it does not. This is shown in Fig. 39a, b. The perturbative QCD  $qqg$  contribution results in a large  $S$  and large  $1-T$  tail to the  $da/dS$  and  $doj/dT$  distributions, respectively, that are considerably larger (at  $\sqrt{s} = 18$  GeV) than the expected background from the two-jet  $qq$  contribution. However, as these distributions indicate, the great majority of events still have small  $S$  and small  $1-T$  and look like two jets.<sup>73</sup>

Since there is no natural axis defined for the final states in  $e^+e^-$  annihilation, it would be convenient to have a set of observables that characterizes the shape of each event that are rotationally invariant. Recently Fox and

Wolfram<sup>74</sup> have come up with just such a set of observables. They define

$$\langle H_i \rangle = \frac{1}{4\pi} \int d\Omega \sum_{\text{hadrons}} |Y_l(Q)|^2 \quad (7.3)$$

where the inner sum is over all the hadrons which are produced in the event and  $Y_l(Q)$  are the usual spherical harmonics. One must choose a particular set of axes to evaluate the angles  $Q_i$  but the values of  $H_i$  deduced will be independent of the choice. These observables can be calculated to order  $\alpha_s(Q)$  in QCD and have the advantage that one need not find any "jet-axis" by minimization.

Energy and momentum conservation requires  $\sum H_i = \sqrt{s}$  and  $\sum H_i \mathbf{t}_i = 0$ . In principle, all the other  $H_i$  carry independent information. A convenient measure of the event shape is provided by the mean value of  $H_i$ . For example, the processes  $e^+e^- \rightarrow qq$  and  $e^+e^- \rightarrow qqg$  calculated to lowest order in  $\alpha_s$  give

$$\langle H_2 \rangle = 1 + \frac{2\alpha_s}{3\pi} (33 - 4\pi^2). \quad (7.4)$$

Figures 39c and 39d show the distribution  $da/dH_2$  and  $da/dH_1$  respectively, for the pro-

cess  $e^+e^- \rightarrow qq$  and for the final sum of this term plus the first order QCD  $e^+e^- \rightarrow qqg$  contribution at  $\sqrt{s} = 20$  GeV. The fragmentation of quarks into hadrons results in a large modification of the idealized two-jet productions (i.e.,  $y_i = 1$ ). Nevertheless, one could clearly establish (at  $\sqrt{s} > 10$  GeV) whether  $e^+e^- \rightarrow qqg$  events exist by observing the rate at which small  $H_2$  (or large  $H_1$ ) events occur. (Fox and Wolfram use the jet model of ref 60 to "smear" their idealized perturbative results and make predictions concerning the outgoing hadrons. The  $qqg$  contributions in Fig. 39a, b have not been "smeared" over the final state quark and gluon fragmentations.)

### B. Three Large $p_{\perp}$ Jets in $pp$ Collisions

#### (1) Measurements of P-out

In the QCD approach, one expects a broad P-out distribution for mesons produced out of the production plane in  $pp$  collisions like that observed in Fig. 31. This lack of coplanarity is due to the presence of two-to-three subprocess like  $qq \rightarrow qqg$  as illustrated in Figs. 21 and 22. One expects a large momentum tail of the P-out distribution due, for example, to the Bremsstrahlung radiation of a hard gluon from an outgoing quark in  $qq \rightarrow qq$ . The tail should increase with increasing trigger

There is some evidence for an increasing  $\langle P\text{-out} \rangle$  with increasing trigger  $p_{\perp}$  from the CCOR ISR experimental results shown in Fig. 40.<sup>54</sup> In this figure,  $\langle P\text{-out} \rangle$  is plotted

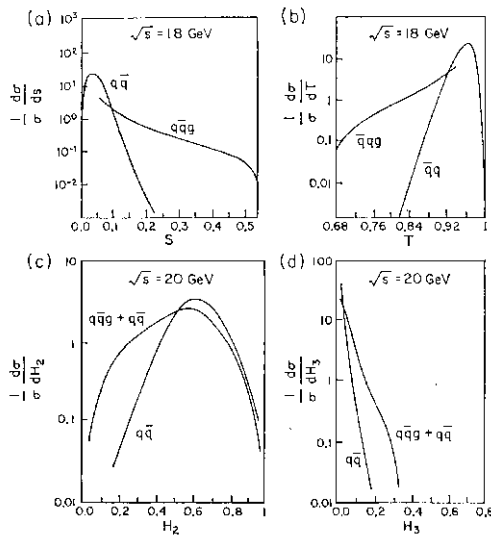


Fig. 39 (a) Distribution of spherocity  $S$ , defined by eq. (7.2) for the process  $e^+e^- \rightarrow$  hadrons at  $\sqrt{s} = 18$  GeV from ref. 72. The curves are the "two jet"  $qq$  and the QCD perturbative "three jet"  $qqg$  contributions.

(b) Same as Fig. (a) but for the thrust  $T$ , defined by eq. (7.1).

(c) Distribution of the quantity  $H_2$ , defined by eq. (7.3), for the process  $e^+e^- \rightarrow$  hadrons at  $\sqrt{s} = 20$  GeV from ref. 74. The curves are the "two jet"  $qq$  contribution and the total ( $qq$  plus the QCD perturbative "three jet"  $qqg$ ) result.

(d) Same as (c) but for the quantity  $H_1$ .

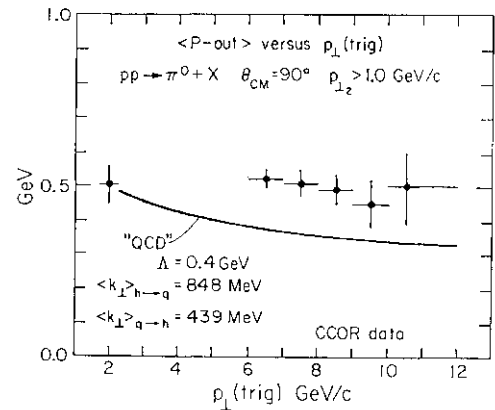


Fig. 40. Data on the mean value of P-out (see Fig. 26 for definition) of the away-side hadrons in  $pp$  collisions with  $p_{\perp}(\text{away}) > 1.0$  GeV/c versus  $p_{\perp}(\text{trigger})$  from the CCOR collaboration.<sup>54</sup> The curve is the prediction of the QCD approach with  $\langle k_{\perp} \rangle_{h \rightarrow q} = 848$  MeV and  $\langle k_{\perp} \rangle_{q \rightarrow h} = 439$  MeV, where  $\langle k_{\perp} \rangle_{q \rightarrow h}$  and  $\langle k_{\perp} \rangle_{h \rightarrow q}$  are taken to be independent of  $Q^2$ .

for all away particles with  $p_{\perp}(\text{away}) > 1.0 \text{ MeV}/c$  so that  $z_p = p_{\perp}(\text{away})/p_{\perp}(\text{trig})$  is decreasing as  $p_{\perp}(\text{trig})$  increases. A model with fixed  $\langle k_{\perp} \rangle$  and  $\langle k_{\parallel} \rangle$  yields a decreasing  $\langle P_{\text{out}} \rangle$  with increasing  $p_{\perp}(\text{trig})$  for  $p_{\perp}(\text{away}) > 1.0 \text{ GeV}/c$  as seen in the figure. The large values of  $\langle P_{\text{out}} \rangle$  at large triggers seen in the data indicate that either  $\langle k_{\perp} \rangle$  or  $\langle k_{\parallel} \rangle$  has increased slightly in going from  $p_{\perp}(\text{trig}) = 2$  to  $10 \text{ GeV}/c$ .

### (2) Measurements of the Three Particle Cross Section

One way to test for three jet events is to simply measure the rate for simultaneously producing three large  $p_{\perp}$  particles all at large angles to each other.<sup>75</sup> For example, one could measure the rate for producing three particles all with  $p_{\perp} > 3 \text{ GeV}/c$  and all at  $90^\circ$  to the beam and all  $120^\circ$  degrees apart. The rate will, of course, be small, but it will be orders of magnitude larger if three jet events exist than if they don't. Efforts to estimate these rates are in progress.

### (3) Measuring Events Shapes in Large $p_{\perp}$ Jet Production

Fox and Wolfram<sup>74</sup> have suggested that one can analyze large  $p_{\perp}$  events in a manner analogous to  $e^+e^- \rightarrow \text{hadrons}$  by defining (now in two dimensions)

$$C_i = \left| \sum_{\perp} p_{\perp i} \exp(i l \phi_i) \right|^2, \quad (7.5)$$

where  $p_{\perp i}$  are the perpendicular momenta of the resulting hadrons and  $\phi_i$  is measured relative to an arbitrary f-axis chosen in the plane perpendicular to the beam direction (the x-y plane in Fig. 26). The choice of the f-axis does not matter since the  $C_i$  are rotationally invariant. Again these observables are infrared finite and can be calculated in QCD perturbation theory. They are distinctly different for two and three-jet processes. (For idealized two jet events  $C_i/C_0 = 1$  for  $i = \text{even}$  and  $C_i/C_0 = 0$  for  $i = \text{odd}$ . For three jet events  $C_2/C_0 < 1$ ,  $i = \text{even}$ .) Future measurements of these observables will establish if, as expected by QCD, three jet events really exist.

## §VIII. Summary and Conclusions

The calculations discussed here should be considered as first "crude" phenomenological

attempts to examine experimental consequences of QCD. The theory of QCD is, however, more than a phenomenological model. It is a precise and complete theory purporting to be an ultimate explanation of all hadronic experiments at all energies, high and low. There are many reasons to hope and expect it to be right. The question is, is it indeed right? Mathematical complexity has, so far, prevented quantitative testing its correctness. The theory itself is remarkably simple and beautiful; however, what it predicts is not clearly known. Nevertheless, its property of asymptotic freedom leads one to expect that phenomena of high momentum transfer should be analyzable (by perturbation) and some applications of the theory have been examined here.<sup>76</sup> Unfortunately, most processes involve both low and high energy aspects and ways of separating the low energy (or  $Q^2$ ) pieces that cannot be calculated by perturbation from the high  $Q^2$  perturbative corrections are just now becoming understood.

One reason to view many of the present day applications of QCD as a bit preliminary is because calculations to leading order are only meaningful if one shows that the next order corrections are indeed small. For example, although to leading order the antiquark distributions as measured in neutrino and antineutrino interactions are the same as the antiquark distribution one should use in the Drell-Yan calculation (4.1), there are higher order corrections that vitiate this direct connection. There is a contribution to the total muon pair rate,  $da/dMdy$ , from the non-divergent part (of order  $\alpha$ ) of the Compton term,  $qg^*qj^*$  in Fig. 10 that is not included in eq. (4.1).<sup>77-80</sup> Since there are many more gluons than antiquarks within the proton, this term can be important. However, one cannot include order  $\alpha$  corrections to the Drell-Yan formula without also including corrections of the same order to the analysis of the neutrino data. To order  $\alpha$ , the structure function  $F_2 \sim xF_1$  in eq. (3.15) receives contributions from the gluon and quark distributions as well as from the antiquark distributions. This means that to this order  $F_2 \sim xF_1$  is not a direct measure of the antiquark content within the proton.<sup>78</sup> No one has done a consistent analysis of all the processes  $ep$ ,

$jp$ ,  $vp$ ,  $vp$  and  $pp \rightarrow fi + X$  beyond leading order. Some of the phenomenology may change slightly when all the order  $\alpha_s$  corrections are included.<sup>78, 80</sup>

Recent data from  $ep$ ,  $fp$ , and  $vp$  experiments do show clearly the "scale" breaking effects expected from QCD. However, since most of the data are at relatively low  $q^2$ , the results are sensitive to  $1/Q^2$  contributions that are difficult, if not impossible, to calculate (they involve knowledge of, for example, the primordial transverse momentum).

The transverse momentum of muon pairs is certainly larger than one would have expected from the naive parton model; however, the experiments have not really seen the high  $p_{\perp}$  tail predicted by QCD. There is some evidence to suggest that  $\langle p_{\perp}^2 \rangle$  does increase with increasing energy (fixed  $M^2$ ) as expected. But, there is no data to check the approach to a constant of  $W^2 \ln M^2 / k_{\perp}^2$  as  $W$  increases, shown in Fig. 18. Finally, there is the question of why the primordial transverse momentum still comes out as large as 600 MeV even after one includes the first order QCD perturbative corrections.

At one time it was thought that the experimentally observed  $p_{\perp}^2$  behavior of large  $p_{\perp}$  meson production in hadron-hadron collisions might pose a problem for QCD. However, we see that there is no problem.<sup>81</sup> The energy ( $p_{\perp}$ ) of existing experiments is too low and there are too many non-asymptotic effects acting. All the scale breaking effects act in the *same* direction to produce an effective apparent  $p_{\perp}$  power that is roughly eight at low  $p_{\perp}$ . In addition, the predicted size of the invariant cross section is just about right. Results closer to a  $p_{\perp}^2$  fall off should appear only at much higher  $p_{\perp}$  (see Fig. 23). Furthermore, one has indirect evidence from large  $p_{\perp}$  correlations that gluons as well as quarks must be included in a description of the data.

We conclude that there is no evidence from  $eN$ ,  $juN$ ,  $\nu N$ , interactions  $orpp \rightarrow p'p'' + X$ , or large  $p_{\perp}$  production in hadron-hadron experiments against QCD. On the contrary, the overall picture favors a QCD approach. However, most of the conclusive and exciting predictions of the theory have not yet been seen. The next generation proton-proton

machines should see hundreds or even thousands of times more mesons at large  $p_{\perp}$  than expected from extrapolations of existing data. One should occasionally see three distinct jets in  $e^+e^-$  collisions and at large  $p_{\perp}$  in  $pp$  collisions. One should see gluon jets as well as quark jets.

QCD is not just "another theory." If it is not the correct description of nature then it will be quite some time before another candidate theory emerges.

### Acknowledgements

It is a pleasure to thank my collaborators R. P. Feynman and G. C. Fox without whom this work could not have been performed. In addition, I would like to acknowledge useful discussions with G. Altarelli, E. L. Berger, S. Brodsky, H. Georgi, M. Jacob, J. F. Owens, H. D. Politzer, R. Raitio, C. T. Sachrajda and S. Wolfram.

### Footnotes and References

1. H. D. Politzer: Phys. Reports **14C** (1974).
2. Also see, D. Gross and F. Wilczek: Phys. Rev. **D8** (1973) 3633; Phys. Rev. **D9** (1974) 980.
3. This is explained in a clear way by H. Georgi in "The Use and Misuse of the Parton Model," Harvard preprint HUTP-78/A003.
4. H. D. Politzer: Phys. Letters **70B** (1977) 430; H. Georgi and H. D. Politzer: Phys. Rev. Letters **40** (1978) 3.
5. H. Georgi and H. D. Politzer: Phys. Rev. **D14** (1976) 1829; A. De Rújula, H. Georgi and H. D. Politzer: Ann. Phys. (N. Y.) **103** (1977) 351.
6. A. J. Buras, E. G. Floratos, D. A. Ross and G. T. Sachrajda: Nucl. Phys. **B131** (1977) 308; A. J. Buras and K. J. F. Gaemers: Nucl. Phys. **B132** (1978) 249.
7. G. Altarelli and G. Parisi: Nucl. Phys. **B126** (1977) 298.
8. G. C. Fox: Nucl. Phys. **B131** (1977) 107.
9. G. C. Fox: "The Physics of Inclusive Charged Current Neutrino Reactions," CALT-68-658, invited talk at the International Conference on Neutrino Physics, Purdue University 1978.
10. H. Anderson, H. S. Matis and L. C. Myriantopoulos: submitted paper No. 764.
11. G. C. Fox: Nucl. Phys. **B134** (1978) 269.
12. Aachen-Bonn-CERN-London-Oxford-Saclay Collaboration: "Analysis of Nucléon Structure Functions in CERN Bubble Chamber Neutrino Experiments," Oxford preprint 16/78 (1978).
13. H. Wahl: Invited talk presented at the International Conference on Neutrino Physics, Purdue University (1978); K. Tittel: plenary session talk (P7a) at this Conference.
14. R. D. Field: Phys. Rev. Letters **40** (1978) 997.

15. G. C. Fox: "Application of Quantum Chromodynamics to High Transverse Momentum Hadron Production" invited talk at the Orbis Scientiae 1978 (Coral Gables) CALT-68-643.
16. R.P. Feynman, R. D. Field and G. C. Fox: "A Quantum Chromodynamic Approach for the Large Transverse Momentum Production of Particles and Jets; CALT-68-651 (to be published in Phys. Rev.).
17. R. K. Ellis, H. Georgi, M. Machacek, H. D. Politzer and G. Ross: "Factorization and the Parton Model in QCD," MIT preprint No. 718 (1978); Caltech preprint CALT-68-684.
18. D. Amati, R. Petronzio and G. Veneziano: CERN preprint TH-2470, submitted paper No. 882.
19. S. Libby and G. Sterman: ITP Stony Brook preprint ITP-SB-78-42.
20. A. V. Efremov and A. V. Radyushkin: submitted papers No. 175 and No. 215.
21. See the talks by H. D. Politzer (session A12) and G. Veneziano (session P3a) at this Conference.
22. H. D. Politzer: Nucl. Phys. **B129** (1977) 301 and CALT-68-628 (1977).
23. C. T. Sachrajda: Phys. Letters **73B** (1978) 185.
24. G. Altarelli, G. Parisi and R. Petronzio: Phys. Letters **76B** (1978) 351; Phys. Letters **76B** (1978) 356; R. Petronzio: CERN preprint TH-2495 (1978).
25. H. Fritzsche and P. Minkowski: Phys. Letters **73B** (1978) 80.
26. C. Michael and T. Weiler: Contribution to the XH1th Rencontre de Moriond, Les Arcs, France (1978).
27. K. Kajantie and R. Raitio: Helsinki report HU-TFT-77-21; K. Kajantie, J. Lindfors and R. Raitio: Helsinki report HU-TFT-78-18.
28. F. Halzen and D. Scott: University of Wisconsin report COO-881-21 (1978).
29. E. L. Berger: "Massive Lepton Pair Production in Hadronic Collisions," invited talk at the International Conference at Vanderbilt University (1978), ANL-HEP-PR-78-12; E. L. Berger: "Tests of QCD in the Hadronproduction of Massive Lepton Pairs," ANL-HEP-PR-78-18.
30. It is a bit dangerous to neglect the processes  $q+q \rightarrow q+q+T^*$ , for although this subprocess is down by  $\alpha_s$  from  $g+q \rightarrow q+g$  and  $q'rq \rightarrow q'rg$ , there are many more quarks at high  $x$  in a proton than there are gluons or antiquarks. Until this process is properly included, any analysis on muon pair production must be viewed as preliminary.
31. The region of integration in eq. (4.4) is discussed in detail in ref. 27.
32. This smearing of the final  $o(s, M^2, y, p^\pm)$  is not the same method of smearing as we used in refs. 14-16. In these papers, the initial quarks were assigned a perpendicular and parallel component of momentum and the  $s$  and  $t$  invariants were then constructed. Thus both  $s$  and  $t$  were affected by the smearing.
33. Y. L. Dokshitzer, D. I. D'Yakonov and S. L. Troyan: "Inelastic Processes in Quantum Chromodynamics," from the XH1th Winter School of Leningrad B. P. Konstantinov Institute of Nuclear Physics (1978), SLAC translation No. 183.
34. D. C. Horn *et al.*: Phys. Rev. Letters **36** (1976) 1239 and **37** (1976) 1374; S. W. Herb *et al.*: Phys. Rev. Letters **39** (1977) 252; W. R. Innes *et al.*: Phys. Rev. Letters **39** (1977) 1240; also see, the talk by L. Lederman (session P2b) at this Conference.
35. See, K. Konishi, A. Ukawa and G. Veneziano: "A Simple Algorithm for QCD Jets," CERN preprint TH2509 (1978).
36. J. F. Owens: Phys. Letters **76B** (1978) 85.
37. T. Uematsu: Phys. Letters **79B** (1978) 97.
38. S. Brodsky and J. Gunion: Phys. Rev. Letters **37** (1976) 402; S. Brodsky, invited talk at the XII Rencontre de Moriond (1977), (SLAC-PUB-1937).
39. C. T. Sachrajda: Phys. Letters **76B** (1978) 100.
40. See also, W. Furmanski: "Large  $p_\pm$  Jet Cross-Section from QCD," Jagellonian University preprints TPJU-10/78, TPJU-11/78, and TPJU-12/78 (1978).
41. R. Cutler and D. Sivers: Phys. Rev. **D16** (1977) 679; Phys. Rev. **D17** (1978) 196.
42. B. L. Combridge, J. Kripfganz and J. Ranft: Phys. Letters **234** (1977).
43. (FFF) R.P. Feynman, R. D. Field and G. C. Fox: Nucl. Phys. **B128** (1977) 1; (FF1) R. D. Field and R.P. Feynman: Phys. Rev. **D15** (1977) 2590.
44. M. Delia Negra *et al.* (CCHK Collaboration): Nucl. Phys. **B127** (1977) 1.
45. Fermilab-Lehigh-Pennsylvania-Wisconsin Collaboration: talk given by W. Selove in Session A9 at this Conference.
46. M.G. Albrow *et al.*: Nucl. Phys. **B135** (1978) 461.
47. It is quite possible that quarks, antiquarks and gluons do not all have the same "effective"  $k_x$  spectra. For example, the larger mean  $k_\pm$  of the Upsilon compared with the non-resonant background might be interpreted by saying that gluons have a larger effective  $\langle k_\pm \rangle$  than do quarks. This approach has been adapted by the Florida State group; J. F. Owens, E. Reya and M. Gluck: FSU preprint 77-09-07 (1978); J. F. Owens and J. D. Kimel: FSU HEP 78-03-30 (1978).
48. F. Halzen, G. A. Ringland and R. G. Roberts: Phys. Rev. Letters **40** (1978) 991.
49. J. F. Gunion: "The Interrelationship of the Constituent Interchange Model and Quantum Chromodynamics," presented at the discussion meeting on Large Transverse Momentum Phenomena, SLAC, January 1978; R. Horgan, W. Caswell and S. J. Brodsky: SLAC-PUB
50. K. Kinoshita and Y. Kinoshita: "Effects of Parton Transverse Momenta on Hadronic Large  $p_\pm$  Reactions," submitted paper No. 535.
51. See, for example, the talk by D. Gross in Session CI at this Conference.

52. R. Blankenbecler, S. J. Brodsky and J. F. Gunion: "The Magnitudes of Large Transverse Momentum Cross Sections," SLAC-PUB-2057 (1977).
53. A. G. Clark *et al.*: Phys. Letters **74B** (1978) 267; A. G. Clark: talk presented in Session A9 at this Conference.
54. CERN-Columbia-Oxford-Rockefeller Experiment: Reported by L. Di Leila in the Workshop on Future ISR Physics, Sept. 14-21, 1977, edited by M. Jacob; and the talk by R. Cool in Session A9 at this Conference.
55. B. Combridge: in ISR Discussion Meeting Between Theorists and Experimentalists Number 21, March 1977, edited by M. Jacob.
56. R. McCarthy: talk given in Session A9; R.J. Fisk: Ph.D. thesis, State University of New York at Stony Brook (1978).
57. H. Boggild (British-French-Scandinavian Collaboration): invited talk at the Eighth Symposium on Multiparticle Dynamics, Kaysersberg, France (1977); R. Moller: invited talk at the Moriond Conference (1977). Also see the talk by K. Hansen in Session A9 at this Conference.
58. This was also predicted in a less model dependent way by S. D. Ellis, M. Jacob and P. V. Landshoff: Nucl. Phys. **B108** (1976) 93; M. Jacob and P. V. Landshoff: Nucl. Phys. **B113** (1976) 395.
59. C. Bromberg *et al.*: Phys. Rev. Letters **38** (1977) 1447; C. Bromberg *et al.*: CALT-68-613 (to be published in Nucl. Phys.).
60. R. D. Field and R. P. Feynman: Nucl. Phys. **B136** (1978) 1.
61. G. C. Fox: "Recent Experimental Results on High Transverse Momentum Scattering from Fermilab," invited talk given at the Argonne APS Meeting (1977).
62. J. Babcock, D. Sivers and S. Wolfram: "QCD Estimate for Heavy Particle Production," Argonne preprint ANL-HEP-PR-77-68.
63. B. Combridge: invited talk presented at the symposium on "Jets in High Energy Collisions," Niels Bohr Institute-Nordita, July 1978.
64. G. Farrar and S. Frautschi: Phys. Rev. Letters **36** (1976) 1017; G. R. Farrar, Phys. Letters **67B** (1977) 337.
65. F. Halzen and D. M. Scott: Phys. Rev. Letters **40** (1978) 1117; University of Wisconsin preprint COO-881-21 (1978).
66. C. O. Eschobar: Nucl. Phys. **B98** (1975) 173; Phys. Rev. **D15** (1977) 355.
67. R. Ruckl, S. J. Brodsky and J. F. Gunion: "The Production of Real Photons at Large Transverse Momentum in  $pp$  Collisions," UCLA preprint (1978).
68. H. Fritzsche and P. Minkowski: CERN preprint TH2320 (submitted paper No. 68).
69. There is, of course, also a contribution to direct photon production from the annihilation subprocess,  $q+q \rightarrow g+T$ , which I have neglected since the gluon content within the proton is considerably larger than the antiquark content.
70. G. Sterman and S. Weinberg: Phys. Rev. Letters **39** (1977) 1436.
71. J. Ellis, M. K. Gaillard and G. G. Ross: Nucl. Phys. **B111** (1976) 253.
72. A. De Rujula, J. Ellis, E. G. Floratos and M. K. Gaillard: "QCD Predictions for Hadronic Final States in  $e^+e^-$  Annihilation," CERN preprint TH-2455 (1978); also, see the talk by A. De Rujula in Session A12 at this Conference.
73. See also, C. Bashram, L. Brown, S. D. Ellis and S. T. Love: "Energy Correlations in  $e^+e^-$  Annihilations: Testing QCD," University of Washington preprint RLO-1388-759 (1978).
74. G. C. Fox and S. Wolfram: "Observables for the Analysis of Event Shapes in  $e^+e^-$  Annihilation and Other Processes," CALT-68-680 and CALT-68-678.
75. J. Kripfganz and A. Schiller: "QCD Three-Jet Production in Large  $p_{\pm}$  Processes," Leipzig preprint KMU-HEP-78-10 (1978).
76. Due to lack of time, I have not been able to cover all applications of QCD. For example, there are interesting applications of QCD to the production of jets in photon-photon collisions. See S. J. Brodsky, T. A. De Grand, J. F. Gunion and J.H. Weis: SLAC-PUB-7102 (1978); and W. Frazer and J. F. Gunion: UCSD preprint UCSD-10P10-194 (1978).
77. H. Georgi: "The Use and Misuse of the Drell-Yan Formalism," Harvard preprint HUTP-77/A090.
78. G. Altarelli, R. K. Ellis and G. Martinelli: "Leptonproduction and Drell-Yan Processes Beyond the Leading Approximation in Chromodynamics," MIT preprint CTP No. 723 (1978), submitted paper No. 579.
79. W. Bardeen, A.J. Buras, D.W. Duke and T. Muta: "Deep Inelastic Scattering Beyond Leading Order in Asymptotically Free Gauge Theories," Fermilab-PUB-78/42 THY, submitted paper No. 415. Also see the talk by T. Muta in Session A12 at this Conference.
80. A. Humbert, submitted papers No. 1119, No. 1120, No. 1121.
81. See also, A. P. Contogouris, R. Gaskell and S. Papadopoulos: submitted papers No. 34 and 1115; A. P. Contogouris, submitted paper No. 35; J. Ranft and G. Ranft: submitted paper No. 486; R. Raitio and R. Sosnowski: University of Helsinki preprint HU-TFT-77-22, invited talk given at the Workshop on Large  $p_x$  Phenomena, University of Bielefeld, Sept. 5-8, 1977.
82. J. W. Cronin *et al.* (CP Collaboration): Phys. Rev. **D11** (1975) 2105; D. Antreasyan *et al.*: Phys. Rev. Letters **38** (1977) 112; Phys. Rev. Letters **38** (1977) 115.
83. B. Alper *et al.* (BS Collaboration): Nucl. Phys. **B100** (1975) 237.
84. F. W. Busser *et al.*: Nucl. Phys. **B106** (1976) 1.
85. G. Donaldson *et al.*: Phys. Rev. Letters **36** (1976) 1110.
86. D. C. Carey *et al.*: Fermilab Report No. FNAL-PUB-75120-EXP. (1975).



P4 :  $e^+e^-$  Reactions

*Chairman:* **H. SCHOPPER**

*Speaker:* **G. J. FELDMAN**

*Scientific Secretaries:* **H. SUDA**  
**T. TSURU**

G. J. FELDMAN

Stanford Linear Accelerator Center, Stanford University, Stanford, California 94305

§1. Introduction

In principle this talk is supposed to review all the work that has been done in  $e^+e^-$  annihilation in the past year or two. It won't for two reasons. First, in the next talk on particle spectroscopy, Günter Flügge will cover recent work on charmonium, F mesons, the Y family, and related studies of jet structure at high energy. Second, even eliminating these topics, there is too much to cover in the time allotted. Thus, I have decided to break this talk into two segments. The first will briefly cover three topics: the status of resonances below 3 GeV, total cross sections, and inclusive D spectra at high energy. The second segment, comprising the bulk of the talk, will be a comprehensive review of the properties of the T lepton.

There are several reasons for singling out the T for a detailed review at this time. First, it is one of only three charged leptons of which we have any knowledge. Clearly, our conception of the elementary particles and their interactions depends critically on the properties of this particle. Second, new results from five experiments have been presented to this conference or have become available in the past few months. And third, because of these results, there is now appearing a rather clear picture of the r as a sequential lepton. It thus appears to be an opportune time for this review.

§II. Resonances below 3 GeV

Isospin 1 resonances will appear in states with even numbers of pions. Data for  $e^+e^- \rightarrow 4\pi^+$  and  $2\pi^+2\pi^0$  are shown in Fig. 1.<sup>1,2</sup> In the  $4\pi^+$  state there is a broad enhancement centered around 1550 MeV/c<sup>2</sup>. The  $2\pi^+2\pi^0$  cross sections are similar to those for  $4\pi^+$ , but perhaps less peaked. The experimenters have made a variety of fits to the hypotheses that one or two resonances are present in these data,<sup>1,2</sup> but they should not be taken too

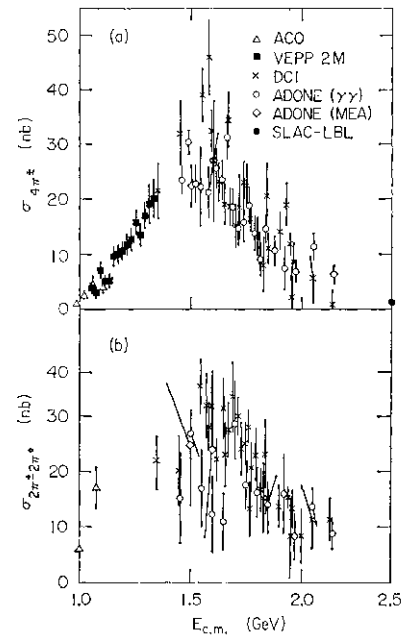


Fig. 1. Cross sections for the production of (a)  $4\pi^+$  and (b)  $2\pi^+2\pi^0$  final states.

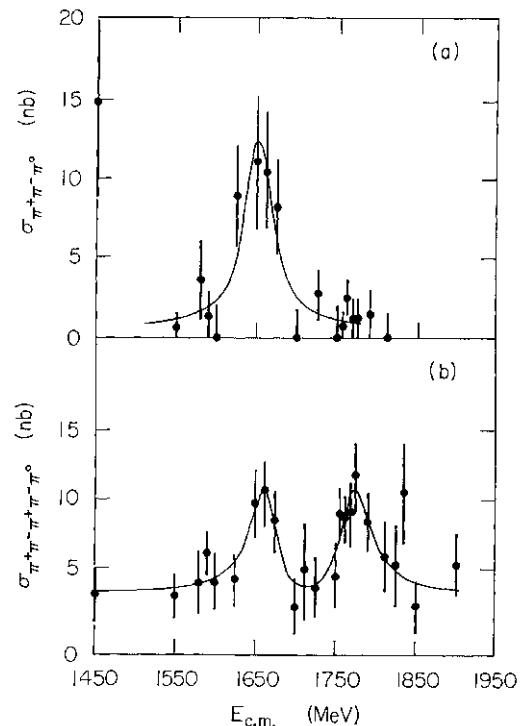


Fig. 2. Cross sections for the production of (a)  $I^0 T^0$  and (b)  $4\pi^0$  final states measured at DCI.<sup>2</sup>

seriously given the current statistical precision. The situation for isospin 0 resonances is

somewhat clearer. The DCI experiment has seen evidence for a  $40 \text{ MeV}/c^2$  wide resonance near  $1660 \text{ MeV}/c^2$  in  $3\pi$  and  $5\pi\pi$  states and a  $50 \text{ MeV}/c^2$  wide resonance near  $1770 \text{ MeV}/c^2$  in the  $5\pi\pi$  state.<sup>1</sup> These are shown in Fig. 2. The two peaks near  $1660 \text{ MeV}/c^2$  each have a statistical significance greater than 3 standard deviations, and the peak near  $1770 \text{ MeV}/c^2$  has a significance of about 5 standard deviations. These enhancements are narrower than one might expect for  $\text{a}\gamma'$  states.

Last year at the Hamburg conference, groups from ADONE presented evidence for three narrow resonances around 2130, 1820, and  $1500 \text{ MeV}/c^2$ . There is no new information on the two higher mass resonances, but the region around  $1500 \text{ MeV}/c^2$  has been restudied. Figure 3(a) shows new data from the  $\gamma\gamma$  group

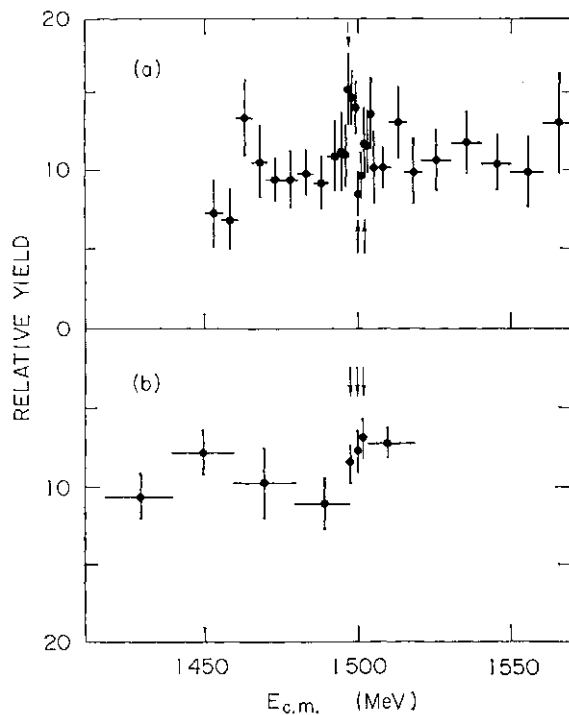


Fig. 3. Relative total cross sections versus energy near  $1500 \text{ MeV}$  measured by the  $\gamma\gamma$  group at ADONE.<sup>2</sup> (b) shows higher statistics data taken to study possible structure seen in (a). The arrows indicate corresponding points.

which shows some weak evidence for an enhancement in this region.<sup>2</sup> In order to study this further a higher statistics run was performed on the three data points indicated by arrows. The results, shown in Fig. 3(b), do not show any evidence for the enhancement.

### §111. Total Cross Sections

At this conference we have several new

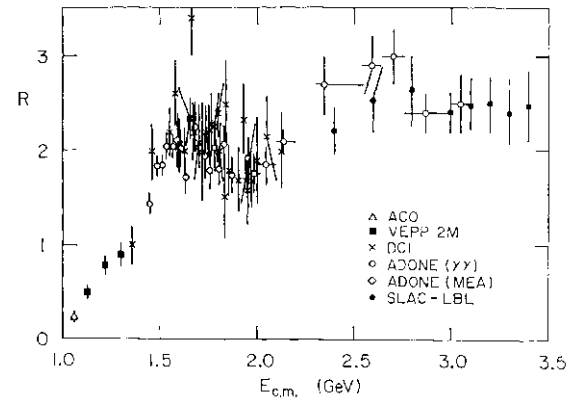


Fig. 4.  $R$  versus energy.

measurements of the ratio,  $R$ , of the total hadronic cross section to the muon pair production cross section. Figure 4 shows the lower energy data.<sup>1,2,4,7,8</sup> The results from

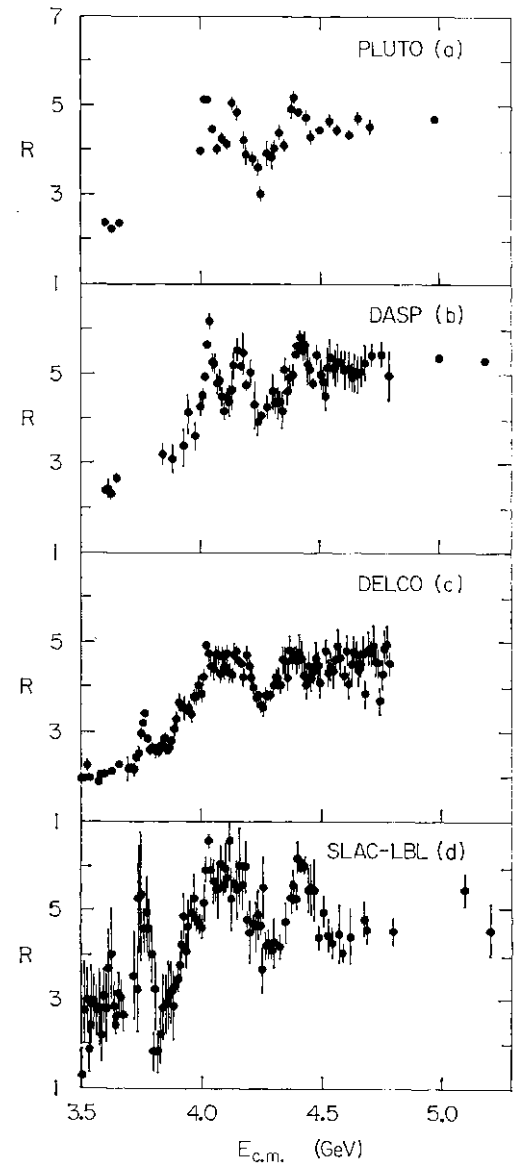


Fig. 5.  $R$  versus energy. The  $R$  values have been radiatively corrected in (a), (b), and (d), but not in (c).  $T$  pair production is included in  $R$ .

DCI and ADONE agree well and it is interesting to note that the scaling value of approximately 2 sets in as low as 1.5 GeV.

The values of R around the threshold region for charmed particle production from four experiments are shown in Fig. 5.<sup>9-12</sup> These values of R include the contribution of *r* pair production. The DELCO results are presented without any radiative corrections; the other three experiments have made an attempt to correct for radiative effects. We will return to this thorny problem shortly.

There is rather good agreement among the experiments for the general structure of the cross sections: there is a resonance-like peak at 3.77 GeV ( $\langle p^0 \rangle$ ), a shoulder at 3.95 GeV, a peak at 4.05 GeV, a broad dip near 4.25 GeV, and a peak in the vicinity of 4.4 GeV. There is, however, some disagreement over details of the structure. For example there is a factor of 1.9 difference in the ( $p^0$ ) leptonic width measured by the DELCO<sup>13</sup> and lead glass wall (LGW) experiments.<sup>14</sup> The main disagreement between experiments on the existence of structure is the extent to which there is a dip at 4.10 GeV. The PLUTO and DASP results show a deep dip, while the DELCO and SLAC-LBL results show little evidence for one.

The four experiments agree surprisingly well on the general level of R. For example at the highest energy at which all of the experiments have reported measurements, 4.7 GeV, the values of R range from only 4.5 (PLUTO) to 5.0 (DASP) in spite of the fact that all the experiments have systematic uncertainties of around 15%.

The most vexing problem in these measurements is that of radiative corrections. Radiative effects always smooth out structure. Thus the application of corrections for radiative effects will always make observed peaks higher and observed dips deeper. One cannot apply radiative corrections on a point to point basis because this would greatly enhance fluctuations. In practice one has to have a perception of what structure exists before one can apply the corrections. If two experiments perceive different structure in their raw data, they will greatly enhance the difference in applying the corrections. A comparison of the SLAC-LBL and DASP data provides a

good example. The two sets of data agree quite well everywhere except near 4.10 GeV where they apparently disagree by many standard deviations. Although I have not seen the raw DASP data, I am fairly sure that any disagreement in the raw data is within reasonable bounds of statistical uncertainty. Even though radiative corrections are slightly apparatus dependent, it would be very useful for experimenters to publish their data both with and without these corrections.

**§IV. Inclusive D Meson Spectra at High Energy**

The measurement of D meson energy spectra above the charmonium resonance region is important both because it is useful for predicting or unfolding secondary spectra from D decays and because it is interesting in its own right. There has recently been considerable theoretical speculation on how heavy quarks fragment into hadrons, and whether in particular the hadron containing the heavy quark would be unusually energetic.<sup>15</sup>

A measurement of this type by the SLAC-LBL and LGW experiments has been presented to this conference at an average energy of 7 GeV.<sup>16,17</sup> The technique is simply to plot  $K^+n^+n^*$  invariant mass spectra in several momentum bins and to extract the D

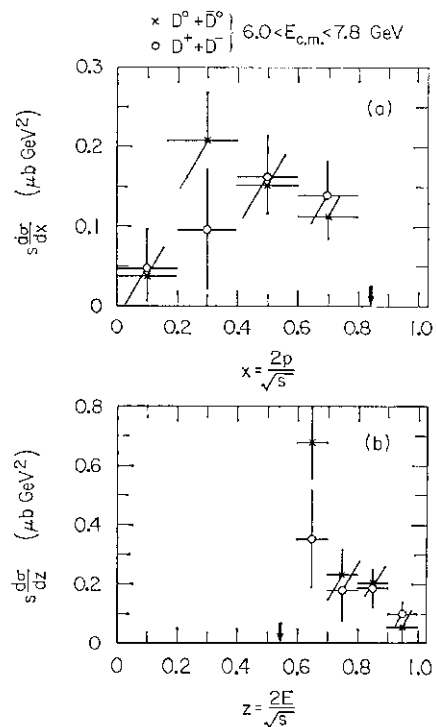


Fig. 6. Inclusive D production at 7 GeV versus (a)  $x=2p/E_{c.m.}$  and (b)  $z=2E/E_{c.m.}$

cross sections by fitting to a D peak plus background. Even at 7 GeV the D mass severely restricts the kinematic range over which this measurement can be made. Using the variable  $x=2p_n/2?_{o,m}$ , the allowed kinematic range is  $0 < x < 0.84$ ; for  $z=2E/E_{c.m.}$  the allowed range is  $0.54 < z < 1$ . The spectra in these two variables are shown in Fig. 6. Figure 7 shows a comparison between D spectra and  $n$  and K spectra. Within the limited kinematic range available the D spectra

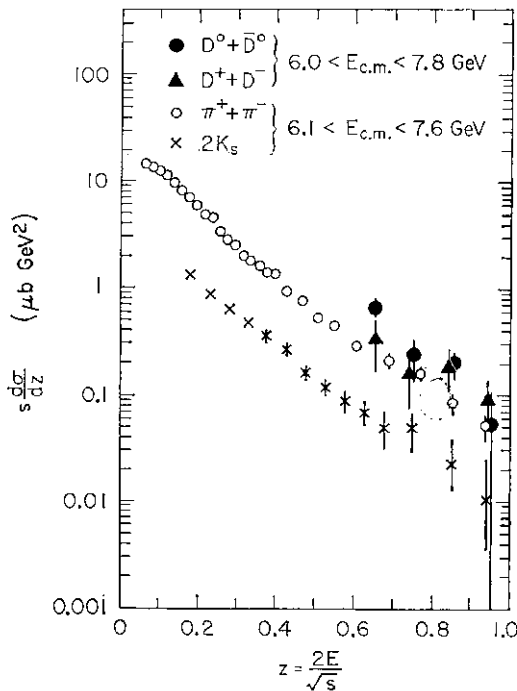


Fig. 7. Inclusive D production at 7 (SeV versus  $z$  compared to inclusive  $\pi$  and K production.

seem to be consistent with having the same slope as those of other mesons. The data give good fits to either

$$(d\sigma/dz) \propto (1/z)(1-z)^{(0.7 \pm 0.4)}$$

or

$$(d\sigma/dz) \propto e^{-(5.5 \pm 1.5)z}$$

## §V. Review of $r$ Properties

### A. History

Although this talk will not be organized in a chronological manner, I think it is useful to spend a minute or two putting the present situation into its historical perspective.

The history of the  $r$  began in 1975 with the observation by the SLAC-LBL group of 24 events which contained an electron and a muon but no other visible charged or neutral

particles.<sup>18</sup> These events could not be explained by any known processes. Possible hypotheses which could explain these data included the decay of a new lepton or a weakly-decaying spin one boson.

The SLAC-LBL group collected additional data and studied the momentum spectrum of the leptons and the presence or absence of other particles in these events. It concluded that the lepton momentum spectrum was characteristic of a three-body decay and that, by elimination, the missing particles had to be neutrinos. In a paper published in 1976, the SLAC-LBL group stated.

'The simplest hypothesis compatible with all the data is that these events come from the production of a pair of heavy leptons...'<sup>19</sup>

This was the state of the  $\nu$  at the last conference in this series. All of the evidence for a new lepton came from a single experiment and one that admittedly had poor lepton identification. Independent confirmation was badly needed. It came during the following year from the PLUTO<sup>20,21</sup> and DASP<sup>22</sup> experiments.

It is clear that at this conference we are entering a new stage in the history of the  $r$ . Its existence and general identification are accepted and we are beginning the detailed measurements of its properties.

It is in this spirit that I have prepared this review. In the next section we shall review the measurements of  $r$  branching fractions, first the general modes, then a more detailed look at the semi-hadronic modes, and finally, a review of upper limits for rare modes. In sections C through G we shall briefly review measurements of the  $T$  mass, the  $T$  spin, the  $\nu$  lifetime, the  $T \sim V_r$  coupling and the  $\nu_r$  mass. We shall conclude in section H with a discussion of the type of lepton the  $r$  could be.

### B. Branching fractions

Figure 8 illustrates the three possible  $r$  decay modes in the standard model. In each case the  $T$  decays to its own neutrino,  $\nu_r$ , and the charged weak current, which can materialize as an  $e\nu_e$ , a  $p\hat{u}_p$ , or a  $d\hat{u}$  pair. The  $du$  quark pair (or more precisely the  $d'u$  pair, where  $d' = d \cos^2 \theta_c - s \sin^2 \theta_c$ ) forms a hadronic system such as a charged  $\mathbf{TT}$ ,  $p$ , or  $A_1$ . There are three general observations that we can make from Fig. 8:

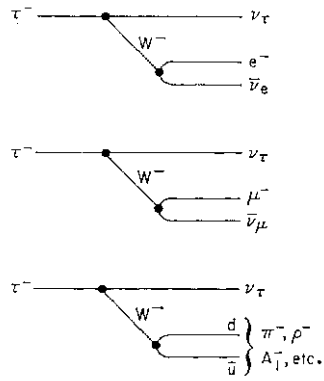


Fig. 8.  $\tau^-$  decay modes.

(1) Each of the diagrams has equal weight since all of the couplings to the weak current are equal, with the proviso that the last diagram stands for three diagrams corresponding to the three colors of quarks. Thus, there are five equivalent diagrams and so the electronic branching fraction should be 20%. QCD corrections give an enhancement to the

semihadronic final states and reduce the prediction for the electronic branching fraction to 18%.<sup>23</sup>

(2) Many of the branching fractions for the semi-hadronic modes are precisely predicted. For example, the coupling of the  $T^-$  to the weak current is known from the measurements of their lifetimes. Thus, the ratio of branching fractions for  $T^- \rightarrow K^- \nu$  to that for  $T^- \rightarrow \pi^- \nu$  is precisely predicted. We shall return to a discussion of the predictions for the semi-hadronic modes below.

(3) Most  $\nu$  decays will contain only one charged particle. Clearly the decays to  $e$ 's,  $ju$ 's,  $7r$ 's, and  $p$ 's contain only one charged particle, and it will turn out that about half of the semi-hadronic modes contain only one charged particle. Thus production will be most prominent in events with only two charged particles.

Table I. Experiments which have measured  $T^- T^-$  production, the method of electron identification (if relevant), and the modes measured.

Experiment	Institutions	Laboratory	$e^-$ ident.	Modes				
				$e\mu$	$ee$	$\mu\mu$	$ex$	$\mu x$
SLAC-LBL	LBL	SPEAR	Lead-scintillation	✓	✓	✓		✓
PLUTO	SLAC	(West pit)	counters					
	DESY	DORIS	Lead-proportional	✓				✓
DASP	Hamburg		chambers					
	Siegen							
	Wuppertal							
	Aachen	DORIS	Cerenkov	✓			✓	✓
LGW	DESY		counters					
	Hamburg		(ex) or lead					
	München		proportional					
MPP	Tokyo		chambers ( $e\mu$ )					
	Hawaii	SPEAR	Lead-glass	✓			✓	
	LBL	(West pit)	counters					
Iron Ball	Northwestern							
	SLAC							
DELCO	Maryland	SPEAR	—					✓
	Pavia	(East pit)						
DESY-Heidelberg	princeton							
	Colorado	SPEAR	—				✓	
	Pennsylvania	(East pit)						
Mark II	Wisconsin							
	Irvine	SPEAR	Cerenkov	✓			✓	
	Los Angeles	(East pit)	counters					
	Stanford							
Mark II	Stony Brook							
	DESY	DORIS	NaI and					
Mark II	Heidelberg		lead-glass					
	Heidelberg		counters					
Mark II	LBL	SPEAR	Lead-liquid					
	SLAC	(West pit)	argon					
			counters					

Table II. Measurements of  $B_e$ ,  $B_\mu$ ,  $B_{3h}$ , and  $B_{3h}$ .

Mode	Measurement	Experiment	Result	Reference
$e\mu$	$\sqrt{B_e B_\mu}$	SLAC-LBL	$.186 \pm .030$	24
$e\mu$	$\sqrt{B_e B_\mu}$	PLUTO	$.145 \pm .040$	20
$e\mu$	$\sqrt{B_e B_\mu}$	DASP	$.182 \pm .031$	25
$e\mu$	$\sqrt{B_e B_\mu}$	LGW	$.224 \pm .055$	26
$e\mu$	$\sqrt{B_e B_\mu}$	DELCO	$.183 \pm .039$	11
$ee$	$B_e/B_\mu$	SLAC-LBL	$1.12 \pm 0.48$	27
$\mu\mu$	$B_\mu/B_e$	SLAC-LBL	$1.40 \pm 0.48$	27
$\mu\mu$	$B_\mu$	Iron Ball	$.22 \pm .08$	28
$ex$	$B_e(B_\mu + B_{3h})$	DASP	$.086 \pm .012$	25
$ex$	$B_e(B_\mu + B_{3h})$	LGW	$.151 \pm .064$	26
$ex$	$B_e(B_\mu + B_{3h})$	DELCO	$.084 \pm .013$	29
$\mu x$	$B_\mu(1 - B_{3h})$	SLAC-LBL	$.149 \pm .034$	24
$\mu x$	$B_\mu(1 - B_{3h})$	PLUTO	$.109 \pm .025$	21
$\mu x$	$B_\mu(1 - B_{3h})$	MPP	$.170 \pm .085$	30
$\mu x$	$B_\mu/B_e$	DASP	$.92 \pm .32$	25
$e$ -any	$B_{3h}$	DELCO	$.32 \pm .05$	29, 34
$e$ -any	$B_e B_{3h}$	DELCO	$.045 \pm .010$	33, 34
$\mu$ -any	$B_{3h}$	PLUTO	$.30 \pm .12$	21

### General modes

From the preceding discussion it is clear that  $T^+ T^-$  production can be most easily measured by studying  $e^+e^-$  annihilation events with two charged particles in which at least one is a lepton. There are five possibilities:  $e/u$ ,  $ee$ ,  $f\bar{f}i\bar{i}$ ,  $ex$ , and  $l/x$ , where  $x$  stands for any charged particle. Seven experiments have measured one or more of these modes,<sup>20-30</sup> and two other experiments have measured other modes or properties.<sup>31,32</sup> Table I gives a list of these experiments and the modes which each measured.

From these measurements we want to derive the branching fractions for  $\tau$  decay into  $e\nu\nu$  ( $B_e$ ),  $j\nu\nu$  ( $B_j$ ), one charged hadron plus neutrals ( $B_{1h}$ ), and three or more charged hadrons plus neutrals ( $B_{3h}$ ), subject to the constraint that the sum of these four modes is unity. Table II gives the results of the 15 measurements listed in Table I. An attempt has been made here to determine precisely the quantity that each experiment measured. In general, experiments measure products or combinations of products of these four basic branching fractions, and then use either theoretical assumptions or other experimental measurements to derive the branching fractions quoted in their papers. Thus the values quoted in Table II are derived from the results given in the reference papers, but in some cases may not be explicitly found there. Table II

also includes three measurements of  $2\gamma_{3h}$  which were determined by studying the multiplicity accompanying a single lepton in regions in which charmed particle production is unimportant.<sup>21,29,33</sup>

The results of constrained fits to the 18 measurements in Table II are given in Table III. One fit has been done leaving  $B_e$  and  $B_\mu$  free and the other has constrained  $B_\mu = 0.973 B_e$ , its theoretical value. Both fits are extremely good and, in fact, all 18 measurements agree with the fit results within one standard deviation of the experimental errors. Al-

Table III. Results of constrained fits to the measurements listed in Table II.

	$B_e$ and $B_\mu$ free	$B_\mu = 0.973 B_e$
$B_e$ (%)	$16.5 \pm 1.5$	$17.5 \pm 1.2$
$B_\mu$ (%)	$18.6 \pm 1.9$	$17.1 \pm 1.2$
$B_{1h}$ (%)	$34.3 \pm 4.2$	$35.0 \pm 4.0$
$B_{3h}$ (%)	$30.6 \pm 3.0$	$30.4 \pm 2.9$
$B_\mu/B_e$	$1.13 \pm 0.16$	

though no single experiment has done a particularly sensitive job of testing  $c$ - $j$  universality in  $T$  decays, the result of all measurements taken together provides a reasonably stringent limit on its violation. Also, it is impressive that there is excellent agreement between the theoretical prediction for the electronic mode, 18%, and the results of the fits.

### Semi-hadronic modes

Many details of the semi-hadronic decays

are predicted in the standard model.<sup>35,36</sup> As we mentioned previously, the ratio between the leptonic decays and the  $\rho\nu$  mode is precisely predicted from the pion lifetime. The vector decays, which are decays to even numbers of pions plus a neutrino, are precisely predicted from measurements of  $e^+e^-$  annihilation *via* the conserved vector current hypothesis<sup>37</sup>. The decay to  $\rho\nu$  is the largest component of this class. For the axial-vector decays, the  $A_1$  plays the same role as the  $\rho$  does for vector decays. For this reason, it is hoped that  $\rho$  decays will provide a convenient way to study the  $A_1$ , which has proved so difficult to isolate in hadronic interactions.<sup>38</sup> The  $A_1 \nu$  branching fraction can be calculated from the  $\rho\nu$  branching fraction with the aid of Weinberg's sum rules.<sup>39</sup>  $\rho$  decays involving kaons will be suppressed by  $\tan^2\theta_c$  in the standard model. A summary of these predictions is given in Table IV under the assumption that  $B_c=B^+$  18%.

The  $\rho\nu$  decay mode has been measured by the DASP group<sup>40</sup> to have a branching fraction of  $(24\pm 9)\%$  in good agreement with the theoretical expectation of 20% from Table IV.

Table IV. Predictions for  $\rho$  branching fractions under the assumption that  $B_c=B^+$  18%.

Mode	Branching fraction (%)	Input
$e\nu$	18	Measurement
$\mu\nu$	18	Measurement
$\pi^-\nu$	10	$\pi$ decay
$\rho^-\nu$	20	CVC + $e^+e^-$ annihilation
$(4\pi)^-\nu$	10	CVC + $e^+e^-$ annihilation
$A_1\nu$	9	Weinberg sum rules
$(K+n\pi)^-\nu$	4	$\tan^2\theta_c$
$(3 \text{ or } 5\pi)^-\nu$	11	Remainder

The Mark II experiment has also presented preliminary data on the  $\rho\nu$  decay mode to this conference.<sup>32</sup> Although no quantitative branching fraction was quoted, it was stated that the result was consistent with the expected theoretical result.

The DASP group has studied  $T$  decays to strange particles by measuring the fraction of ex events in which the x is a kaon. The result is  $(7\pm 6)\%$  in agreement with the prediction in Table IV.

We shall now review in more detail the measurements on two interesting classes of semi-hadronic decay modes:  $iZ\nu$  and  $(3TT)\nu$ .

*The TTV mode*

Last summer at the Hamburg Photon-Lepton Symposium, the DASP group reported that the  $\rho \rightarrow 7r\nu$  branching fraction was substantially smaller than expected.<sup>40</sup> This was rather surprising since, as we have already discussed, the  $T\nu$  mode is completely predicted and a failure of this prediction would imply, at the least, that different weak currents were important in  $T$  and  $xr$  decays. The DASP group searched for a high momentum pion ( $> 1$  GeV/c) with an electron or any charged particle and no detected photons. Nine events were expected but only four were seen. When any charged particle plus a pion was required only 17 events were found and 34 were expected. Above 4.52 GeV center-of-mass energy only four events were found and 13 were expected.<sup>41</sup>

As of this conference four experiments have repeated the DASP measurement in either the  $e7r$  or  $xx$  modes.<sup>32,42,43,44</sup> All four experiments are in good agreement with the theoretical prediction. In each case the pion momentum spectrum is close to constant, which is expected for the  $\nu \rightarrow +m>$  decay mode but would be rather unlikely for possible background sources. Table V summarizes the results of these experiments. The weighted average of these four measurements is a branching fraction of  $(8.3\pm 1.4)\%$  in good agreement with the theoretical prediction. The  $r^*K\nu$  mode requires more detailed study, but given the results of these experiments, there is no longer good reason to suspect that it is anomalous.

*(3TC)V and (4TT)V modes*

The PLUTO<sup>45,46</sup> and SLAC-LBL<sup>47</sup> groups have studied  $\rho$  decays to three charged pions plus a neutrino. These decays are of particular interest since the long-sought  $A_1$  meson is expected to be prominent in the three pion mass spectrum.

The SLAC-LBL group studied events with a muon, three charged pions, and any number of photons. The three pion mass spectrum after background subtractions is shown in Fig. 9 for cases in which no photons, one or two photons, and more than two photons are observed. In the first two cases there is a



Table Y. Results on the  $r \rightarrow \pi \nu$  decay mode. The first error is statistical, the second systematic.

Experiment	Mode	Events	Background	$B(\tau \rightarrow \pi \nu)(\%)$	Reference
SLAC-LBL	$\chi\pi$	$\sim 200$	$\sim 70$	$9.3 \pm 1.0 \pm 3.8$	42
PLUTO	$\chi\pi$	32	9	$9.0 \pm 2.9 \pm 2.5$	43
DELCO	$e\pi$	18	7	$8.0 \pm 3.2 \pm 1.3$	44
Mark II	$\chi\pi$	142	46	$8.0 \pm 1.1 \pm 1.5$	32
	$e\pi$	27	10	$8.2 \pm 2.0 \pm 1.5$	
Average				$8.3 \pm 1.4$	

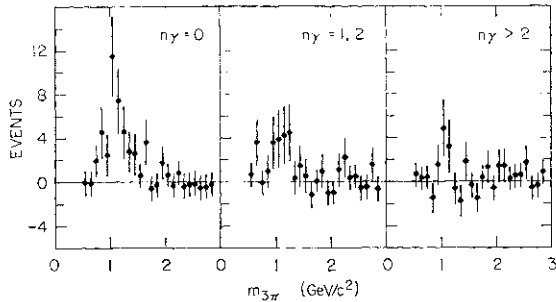


Fig. 9. Invariant mass distributions of three pions in events in which they are detected along with a muon and zero, one or two, or more than two photons. The distributions have been corrected for hadron misidentification as a muon. The data are from the SLAC-LBL and LGW experiments.<sup>47</sup>

significant signal in the vicinity of  $1.1 \text{ GeV}/c^2$ . The momentum spectra of the muon and the three charged pions in this mass region agree with hypothesis of pair production, as seen in Fig. 10. Figure 11 shows fits to the three pion mass spectrum with no detected photons under three hypotheses: (a) that all the events are due to  $T \rightarrow K^* \pi^+ \pi^- \pi^0 \nu$ , where the  $K^*$  is not

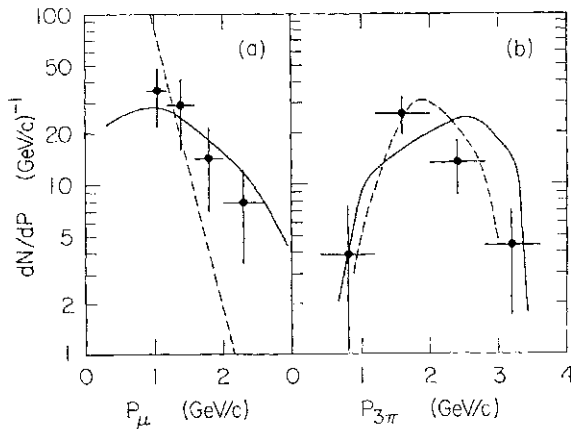


Fig. 10. (a) Momentum distribution of muons in events in the  $0.95 < m_{3\pi} < 1.25 \text{ GeV}/c^2$  region of Fig. 9(a) and (b). The solid and dashed curves are the expected spectra from  $e$  decays and charmed particle decays. (b) Momentum distribution of the three pion system in these events. The solid and dashed curves are the spectra expected for  $r \rightarrow 3\pi \nu$  and  $r \rightarrow 47ri$  decays.

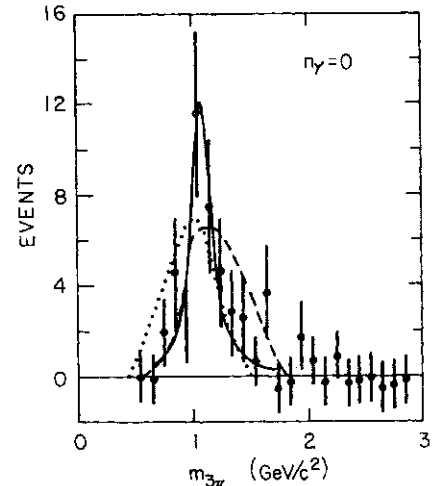


Fig. 11. Data from Fig. 9(a) with fits to different hypotheses. The dotted line represents  $r \rightarrow 7i 7i K - 7i \nu$  decays, the dashed line represents non-resonant  $r \rightarrow 7r 7r 7r - \gamma$  decays, and the solid line represents  $T \rightarrow A_i V$  decays where the  $A_i$  has a mass of  $1.1 \text{ GeV}/c^2$  and width of  $200 \text{ MeV}/c^2$ .

detected, (b) that all the events are due to  $T \rightarrow p^0 \nu$ , where the  $\Lambda^0$  is non-resonant, and (c) that all the events are due to  $T \rightarrow A_1 \rightarrow H^+ \pi^- \pi^0 \nu$ . Fits to the first two hypotheses have only a few percent confidence level but cannot be excluded. The resonance hypothesis is a good fit with  $A_1$  mass of  $1.1 \text{ GeV}/c^2$  and full width of  $200 \text{ MeV}/c^2$ .

The SLAC-LBL group obtains an  $(18 \pm 6.5)\%$  branching fraction for  $r \rightarrow 7r^+ 7r^- 7r^0 + n 7r^0 \nu$ . By using the number of observed photons, in principle it is possible to unfold this branching fraction for the number of  $r$ 's produced. In practice the statistical accuracy is rather poor. The results are  $(7 \pm 5)\%$  for  $r \rightarrow 7r^+ 7r^- 7r^0 \nu$  and  $(11 \pm 7)\%$  for  $r \rightarrow 7r^+ 7r^- 7r^0 \nu$ . All these results are consistent with the theoretical predictions given in Table IV.

The PLUTO group has studied events with an electron or muon, three charged pions, and no photons. Since PLUTO has more efficient photon detection than the SLAC-LBL detector, the background from the  $4\nu$  decay

to the  $3\pi\pi$  signal is small. This has allowed the PLUTO group to go beyond the SLAC-LBL analysis in two significant aspects. First, a study of dipion masses showed that the entire signal was consistent with two of the pions forming a  $p^0$ . The higher mass dipion combination for each event is shown in Fig. 12. Second, an analysis of the three pion Dalitz plot has shown that the three pion state is consistent with the expected spin-parity assignment of  $1^-$ , but not  $0^-$  or  $1^+$ . The normalized distance to the Dalitz plot boundary is shown in Fig. 13. The axial-vector hypothesis fits the data with a 10% confidence level. The hypotheses that the  $3\pi$  system is a pure pseudoscalar or vector state are excluded at the

0.01% and 0.3% confidence levels. A vector  $3\pi\pi$  system would require second class currents.

The  $3\pi\pi$  mass spectrum from the PLUTO experiment is shown in Fig. 14 along with a

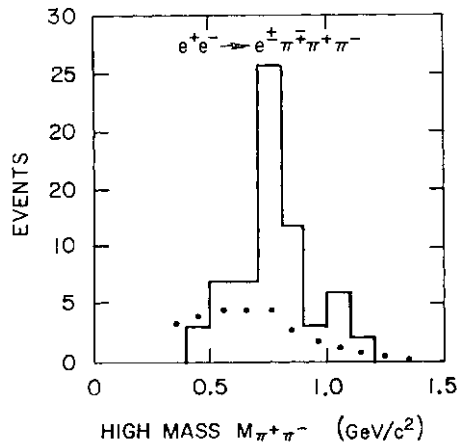


Fig. 12. Invariant mass of the higher mass  $\pi^+\pi^-$  pair from events with a lepton and three charged detected which are compatible with  $T^+T^-$  decays. The dotted curve represents an estimate of the background. The data are from the PLUTO experiment.<sup>451160</sup>

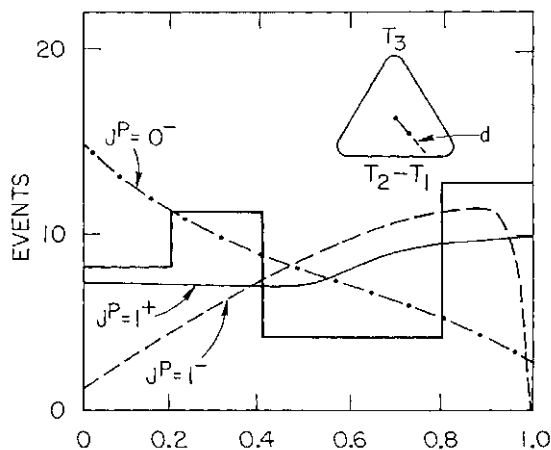


Fig. 13. The normalized distance to the boundary of the  $3n$  Dalitz plot for  $p^0\pi^0$  data described in Fig. 12. The curves show the expected distributions for  $0^-$ ,  $1^-$ , and  $1^+$  spin-parity  $3^A$  states.

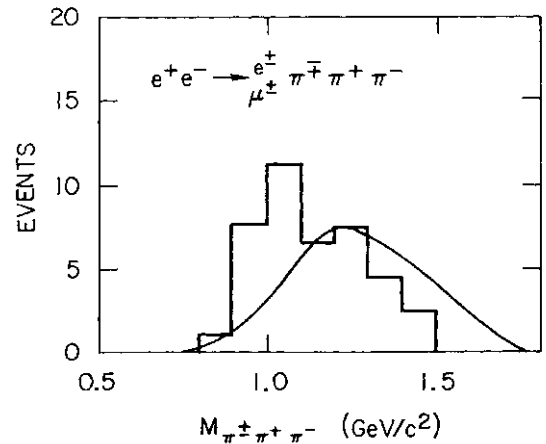


Fig. 14. Invariant mass distribution of  $P\bar{K}$  combinations for events described in Fig. 12. The curve represents a non-resonant  $p^0n$  spectrum from  $r$  decay.

curve representing  $pit$  non-resonant phase space. This appears to be an enhancement near 1.0 GeV over the phase space curve. The branching fraction for  $T \rightarrow p\bar{t}\pi$  from the PLUTO experiment is  $(10.4 \pm 2.4)\%$  where the result includes both the  $p^*\bar{t}$  and  $p+n$  final states.

Finally, what can we say about the  $A_i$  given the results from these two experiments? There are at least three statements which can be made without serious fear of contradiction:

- (1) It is significant that both experiments see an enhancement near 1.1 GeV.
- (2) The present data are statistically insufficient to pin down the  $A_i$  parameters.
- (3) In the future  $r$  decays will be crucial in understanding the  $A_i$ .

*Rare decay modes*

There have been numerous searches for  $r$  decay modes which should not exist in the standard model.<sup>20,48149</sup> There is no evidence for any of these modes and the upper limits are given in Table VI.

*C. r Mass*

DASP was the first experiment to use the energy dependence of the  $r$  production cross section to deduce a precise value for the  $r$  mass.<sup>25</sup> The result was  $1807 \pm 20$  MeV/c<sup>2</sup> and the data are shown in Fig. 15.

Table VI. Upper limits on rare  $r$  decay modes, stands for any charged particle and  $\gamma$  stands for any charged lepton.

Mode	Experiment	Upper limit (%)	Confidence level (%)	Reference
$3x$	PLUTO	1.0	95	48
$3l$	SLAC-LBL	0.6	90	49
$l + \text{charged particles}$	PLUTO	4.0	90	20
$l + \text{photons}$	PLUTO	12.0	90	20
$e^- + \gamma$	SLAC-LBL	2.6	90	49
$\mu^- + \gamma$	SLAC-LBL	1.3	90	49

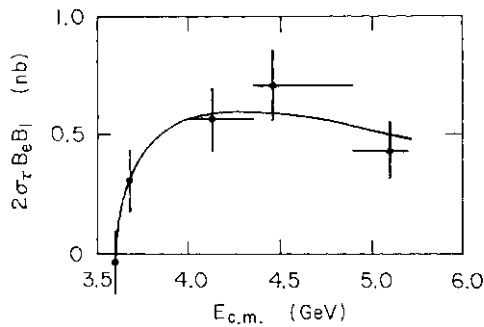


Fig. 15. Cross sections for  $ex$  events measured by DASP experiment. The curve is a fit to the production cross section for point-like spin 1/2 particles.

Later measurements by DESY-Heidelberg<sup>31</sup> and DELCO<sup>11,19</sup> are shown in Figs. 16 and 17,

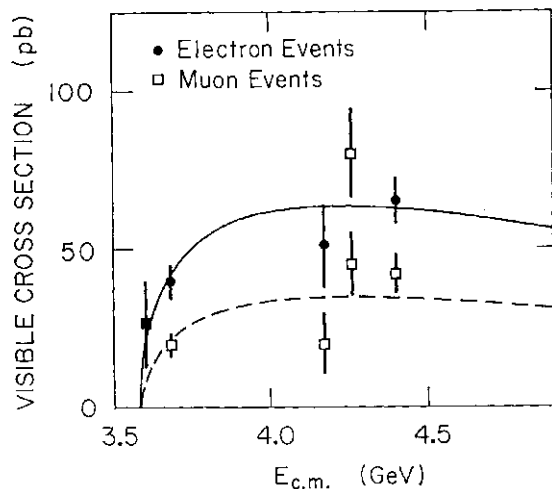


Fig. 16. Observed cross sections for  $ex$  and  $\mu x$  events measured by the DESY-Heidelberg experiment. The curves are fits to the production cross sections for point-like spin 1/2 particles.

with results of  $1790 \pm 10$  and  $1782 \pm 10$  MeV/c<sup>2</sup>, respectively. The DELCO data beautifully delineate the  $r$  threshold by having points just above and just below it. The high precision of the DELCO mass determination is primarily due to the data point at 3,570 MeV which

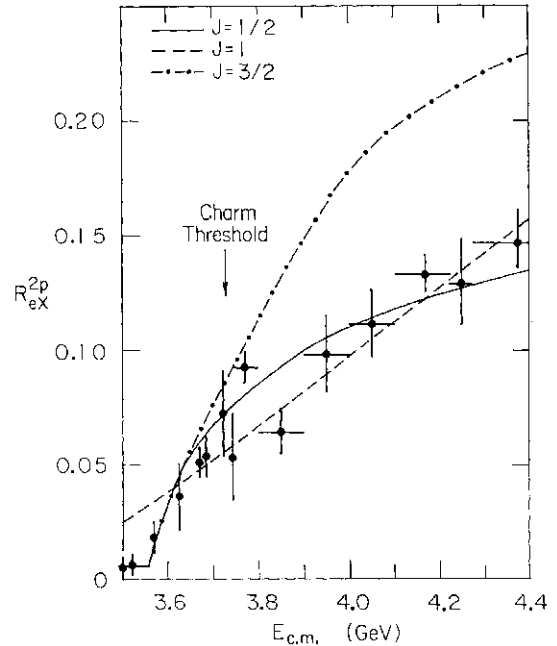


Fig. 17. The ratio of  $ex$  events to  $\sqrt{s}$  pair production as a function of center-of-mass energy. The solid curve is a best fit to the spin 1/2  $r$  pair production cross section. The dashed and dot-dashed curves represent typical cross sections for spin 1 and spin 3/2 particle production. The data are from the DELCO experiment.<sup>11</sup>

observed 8  $ex$  events with 1.6 expected from backgrounds. Although there is no reason to suspect this point, it is worth noting that if it were removed from the fit, the remaining data points would pull the  $r$  mass to  $\approx 1900$  MeV/c<sup>2</sup> as can be seen from the existence of a second minimum in the  $f$  versus mass plot, Fig. 18.

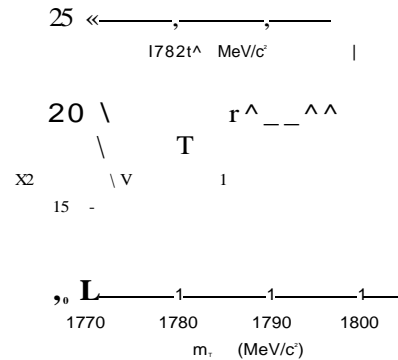


Fig. 18.  $\chi^2$  for 17 degrees of freedom for the fit to the  $T$  mass from the data in Fig. 17.

### D, $T$ Spin

As long as we assume that the  $z$  does not have a form factor which varies rapidly over the range of a few GeV, all spin assignments except 1/2 are excluded. All integer spins

will require a  $/3^3$  threshold dependence and half-integer spins greater than  $1/2$  will lead to much too large a cross section above 4 GeV when normalized to fit the threshold region.<sup>50</sup> These points are illustrated in Fig. 17 by the spin 1 and  $3/2$  curves.

*E.  $z$  Lifetime*

The  $r$  lifetime has been studied by examining the closest distance of approach to the interaction region of leptons from  $z$  decays. The best upper limits are  $3.5 \times 10^{-12}$  sec from the PLUTO experiment<sup>46</sup> and  $3.0 \times 10^{-12}$  sec from the DELCO experiment<sup>11</sup> both at the 95% confidence level. For a full strength  $z$ - $\nu_r$  coupling to the weak current and assuming the  $\nu_r$  is massless, the  $z$  lifetime,  $\tau_z$ , is given by

$$\tau_z = B_0(m_\mu/m_\tau)\tau_\mu = (2.8 \pm 0.2) \times 10^{-13} \text{ sec,}$$

where the error is primarily from the uncertainty in the electronic branching fraction,  $B_e$ . Thus the  $z$ - $\nu_r$  coupling has to be at least 9% of full strength.

*F.  $z$ - $\nu_r$  Coupling*

The lepton momentum spectrum can be used to determine the F, A structure of the  $z$ - $\nu_r$  coupling.  $V-A$  gives the hardest spectrum,  $V+A$  gives the softest, and pure  $V$  or  $A$  is halfway in between. The PLUTO experiment favored  $V-A$  over  $V+A$  slightly.<sup>21</sup> The SLAC-LBL experiment strongly disfavored  $V+A$ , giving it a statistical confidence level of at most a few percent.<sup>24</sup>

The most conclusive data on the  $z$ - $\nu_r$  coupling were reported to this conference by the DELCO experiment.<sup>11</sup> They have extracted a Michel parameter,  $p$ , of  $0.83 \pm 0.19$  from the electron momentum spectrum of  $e^+e^-$  events, shown in Fig. 19. The radiatively corrected Michel parameters for  $V-A$  is 0.53, for  $V+A$  is -0.15, and for either  $V$  or  $A$  is 0.91.<sup>51</sup> The confidence level for  $V-A$  is 4%, while the confidence level for  $V+A$  is infinitesimal. Thus the DELCO data completely exclude  $V+A$  and strongly disfavor pure  $V$  or  $A$ .

*G.  $\nu_r$  Mass*

If the  $\nu_r$  had a mass, it would soften the charged lepton momentum spectrum. All experimental measurements are consistent with a massless  $\nu_r$ .<sup>11, 21, 24, 52</sup> The upper limits on

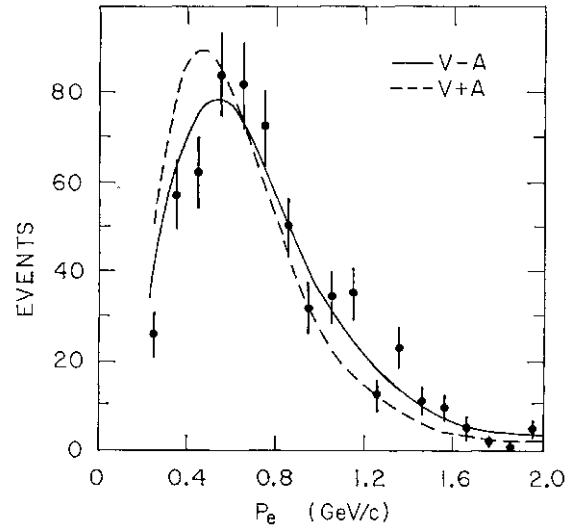


Fig. 19. Electron momentum spectrum for  $e^+e^-$  events at energies between 3.57 and 7.4 GeV. The solid and dashed curves represent the spectra expected for  $V-A$  and  $V+A$   $r$ - $\nu_r$  couplings. The data are from the DELCO experiment.<sup>11</sup>

Table VII. Upper limits on  $\nu_r$ .

Experiment	Upper limit (MeV/c <sup>2</sup> )	Confidence level (%)	Reference
SLAC-LBL	600	95	24
PLUTO	540	90	52
DELCO	250	95	11

Table VIII. Summary of selected  $r$  properties

Parameter	Experimental findings
Mass	$1782^{+3}_{-4} \text{ MeV}/c^2$
Neutrino mass	$< 250 \text{ MeV}/c^2$ at 95% confidence level
Spin	$1/2$
Lifetime	$< 3 \pm 10^{-12} \text{ sec}$
$\tau$ - $\nu_r$ coupling	Consistent with $V-A$ , $V+A$ excluded
$B_0$	$0.175 \pm 0.012$ (assuming $B_\mu = .973 B_0$ )
$B_\mu/B_0$	$1.13 \pm 0.16$

the  $\nu_r$  mass are given in Table VII.

*H. What Type of Lepton is the  $r$ ?*

All of the evidence, summarized in Table VIII, is consistent with the  $z$  being a sequential lepton decaying to its own massless neutrino with a  $V-A$  coupling.

One can ask, however, what other possibilities could exist.<sup>53</sup> The simplest case would be to have the  $r$ , but no  $\nu_r$  in an  $SU(2) \times U(1)$  gauge theory. The  $z$  would then decay into a mixture of  $\nu_r$  and  $\nu_\tau$ . An analysis of this case shows that it is excluded by several of the measured  $z$  properties. For example, the  $z$  would have to decay into 3 charged leptons

at a rate an order of magnitude above the experimental upper limit,<sup>54,55</sup> and  $B_e/B_\nu$  would have to be close to 0.5 or 2.0.<sup>55</sup>

Another possibility is that the  $\nu_x$  exists, but is more massive than the  $\nu_e$ . This is also excluded.<sup>56</sup> The argument is that the sum of couplings to  $p$ , and  $n$  must be greater than 0.09 of full strength from the  $\nu_e$  life-time measurement. But the  $\nu_x$  coupling is limited to 0.025 by the absence of  $r$  production by  $\nu_e$  beams,<sup>57</sup> and the  $\nu_x$  coupling is limited to be less than 0.006 more than the  $\nu_e$  coupling by the  $n^+/\nu_e/r/r^-\wedge\zeta\nu$  ratio.<sup>58</sup>

Dropping the requirement of an  $SU(2)\times U(1)$  gauge theory, one can ask more generally whether it is possible that the  $r$  has the same lepton number as either the  $e^-$ ,  $e^+$ , or  $\mu$ ; that is, whether it couples to the  $\nu_e$ ,  $\nu_\mu$ , or  $\nu_\tau$ . The  $r$  cannot have the lepton number of either the  $\nu_\mu$  or  $\nu_\tau$  it would be produced in  $\nu_e$  interactions. The  $r$  cannot have the lepton number of either the  $e^+$  or  $\mu^+$ . If it did there would be two identical neutrinos in the final state and  $B_e/B_\nu$  would be either .5 or 2.

The one possibility which cannot be excluded at present is that the  $r$  has the same quantum number as the  $e^-$ . Detailed measurements of  $\nu_e$  interactions, possibly from beam dump or tagged decay experiments, may be able to address this question in the future.

Of course, there are many more possibilities than the simple ones we have discussed here, and, in general, one must simply compare the predictions of a given model to the range of parameters allowed by the data. It is remarkable, in the three years since the  $r$  discovery, how tight the constraints have become.

### References

1. J. Perez-y-Jorba: these proceedings.
2. G. P. Murtas: these proceedings.
3. J. LeFrancois: in *Proceedings of the 1971 International Symposium on Electron and Photon Interactions at High Energy, Cornell University, Ithaca, New York, August 23-27, 1971*, edited by N.B. Mistry, p. 51.
4. V. A. Siderov in *Proceedings of the XVIII International Conference on High Energy Physics, July 1976, Tbilisi, USSR*, edited by N. N. Bogolyubov *et al*, p. B13.
5. B. Jean-Marie *et al.*: Stanford Linear Accelerator Center preprint SLAC-PUB-1711 (1976, unpublished).
6. C. Bemporad: in *Proceedings of the 1977 International Symposium on Lepton and Photon Interactions at High Energies, Hamburg, August 25-31, 1977*, edited by F. Gutbrod (DESY, Hamburg, 1977), p. 165.
7. See K. Strauch: in *Proceedings of the 6th International Symposium on Electron and Photon Interactions at High Energies, August 27-31, 1973, Bonn, Federal Republic of Germany*, edited by H. Rollnik and W. Pfeil (North Holland, Amsterdam, 1973), p. 1.
8. J.-E. Augustin *et al.*: Phys. Rev. Letters **34** (1975) 764.
9. J. Burmester *et al.*: Phys. Letters **66B** (1977) 395.
10. R. Brandelik *et al.*: DES Y report 78/18 (1978).
11. J. Kirz: these proceedings.
12. J. Siegrist: private communication.
13. W. Bacino *et al.*: Phys. Rev. Letters **40** (1978) 671.
14. P. A. Rapidis *et al.*: Phys. Rev. Letters **39** (1977) 526; corrected in I. Peruzzi *et al.*: Phys. Rev. Letters **39** (1977) 1301, footnote 11. These data are not shown in Fig. 5, but are similar to the "older" SLAC-LBL data which are shown.
15. V. Barger, T. Gottschalk and R.J.N. Phillips: Phys. Letters **70B** (1977) 51; R. Odorico: Phys. Letters **71B** (1977) 121; A. Seiden: Phys. Letters **68B** (1977) 157; M. Suzuki: Phys. Letters **68B** (1977) 164; **71B** (1977) 139; J. D. Bjorken: Phys. Rev. **D17** (1978) 171.
16. R. R. Ross: these proceedings.
17. P. A. Rapidis *et al.*: to be published.
18. M. L. Perl: in *Proceedings of the SLAC Summer Institute on Particle Physics, July 21-31, 1975*, edited by M. C. Zipf, Stanford Linear Accelerator Center report SLAC-191 (1975); M. L. Perl *et al.*: Phys. Rev. Letters **35** (1975) 1489.
19. M. L. Perl *et al.*: Phys. Letters **63B** (1976) 466.
20. J. Burmester *et al.*: Phys. Letters **68B** (1977) 301.
21. J. Burmester *et al.*: Phys. Letters **68B** (1977) 297.
22. R. Brandelik *et al.*: Phys. Letters **70B** (1977) 125.
23. T. Appelquist: in *Particles and Fields* (Proceedings of the Banff Summer Institute on Particles and Fields, Banff, Alberta, August 25-September 3, 1977), edited by D. H. Boal and A. N. Kamal (Plenum, New York, 1978), p. 33.
24. M. L. Perl *et al.*: Phys. Letters **70B** (1977) 487.
25. R. Brandelik *et al.*: Phys. Letters **73B** (1978) 109.
26. A. Barbaro-Galtieri *et al.*: Phys. Rev. Letters **39** (1977) 1058.
27. F. B. Heile *et al.*: Nucl. Phys. **B138** (1978) 189.
28. J. G. Smith *et al.*: Phys. Rev. **D18** (1978) 1.
29. W. Bacino *et al.*: Phys. Rev. Letters **41** (1978) 13.
30. H. F. W. Sadrozinski: in *Proceedings of the 1977*

- International Symposium on Lepton and Photon Interactions at High Energies, Hamburg, August 25-31, 1977*, edited by F. Gutbrod (DESY, Hamburg, 1977), p. 47.
31. W. Barrel *et al.*: DESY report DESY 78/24 (1978).
  32. D. Hitlin: these proceedings.
  33. J. Kirkby: talk given at the 1978 SLAG Summer Institute on Particle Physics, July 9-21, 1978 (to be published).
  34. The two measurements of  $B_{\mu}$  by the DELCO experiment are independent. The former is made by studying the ratio of three-or-more prong electron events to two prong electron events as the function of the electron momentum. At high momentum the contribution from charmed particle decays becomes small and the ratio becomes a measure of  $B_{\mu}$ . The latter measurement is from a cross section measurement of three-or-more prong electron events below charmed particle threshold.
  35. H. B. Thacker and J.J. Sakurai: Phys. Letters **36B** (1971) 103.
  36. Y. S. Tsai: Phys. Rev. **D4** (1971) 2821.
  37. F. J. Gilman and D. H. Miller: Phys. Rev. **D17** (1978) 1846.
  38. J. J. Sakurai: in *Proceedings of the 1977 International Symposium on Lepton and Photon Interactions at High Energies*, edited by W. T. Kirk (Stanford Linear Accelerator Center, Stanford University, Stanford, California, 1976), p. 353.
  39. S. Weinberg: Phys. Rev. Letters **18** (1967) 507.
  40. S. Yamada: in *Proceedings of the 1977 International Symposium on Lepton and Photon Interactions at High Energies, Hamburg, August 25-31, 1977*, edited by F. Gutbrod (DESY, Hamburg, 1977), p. 69.
  41. The expected numbers of events reported in ref. 40 were higher because a value of 0.20 was used for  $B_c$  rather than the value of 0.175 from Table III used here. The expected numbers vary proportionally as the square of  $B_c$ .
  42. G.J. Feldman: talk given at the International Conference on Neutrino Physics—Neutrinos '78, Purdue University, April 28-May 2, 1978, Stanford Linear Accelerator Center preprint SLAC-PUB-2138 (1978).
  43. G. Alexander *et al.*: Phys. Letters **78B** (1978) 162.
  44. W. Bacino *et al.*: Stanford Linear Accelerator Center preprint SLAC-PUB-2223 (1978). The value "quoted here is from a revised analysis and differs from the value presented at the conference.
  45. G. Alexander *et al.*: Phys. Letters **73B** (1978) 99.
  46. H. Spitzer: these proceedings.
  47. J. Jaros *et al.*: Phys. Rev. Letters **40** (1978) 1120.
  48. G. Flugge: in *Proceedings of the Fifth International Conference on Experimental Meson Spectroscopy 1977, Northeastern University, April 29-30, 1977*, edited by E. von Goeler and R. Weinstein (Northeastern University Press, Boston, 1977), p. 132.
  49. M. L. Perl: in *Proceedings of the 1977 International Symposium on Lepton and Photon Interactions at High Energies, Hamburg, August 25-31, 1977*, edited by F. Gutbrod (DESY, Hamburg, 1977), p. 145.
  50. Y. S. Tsai: Stanford Linear Accelerator Center preprint SLAC-PUB-2105 (1978).
  51. A. Ali and Z. Z. Aydin: Nuovo Cimento **43** (1978) 270.
  52. G. Knies: in *Proceedings of the 1977 International Symposium on Lepton and Photon Interactions at High Energies, Hamburg, August 25-31, 1977*, edited by F. Gutbrod (DESY, Hamburg, 1977), p. 93.
  53. I am indebted to F. J. Gilman for useful discussions on this question.
  54. D. Horn and G. G. Ross: Phys. Letters **67B** (1977) 460.
  55. G. Altarelli, N. Cabibbo, L. Maiani and R. Petronzio: Phys. Letters **67B** (1977) 463.
  56. G. Altarelli: these proceedings.
  57. A. M. Cnops *et al.*: Phys. Rev. Letters **40** (1978) 144.
  58. D. A. Bryman and C. Picciotto: Phys. Rev. **D11** (1975) 1337; E. DiCapua, R. Garland, L. Pondrom and A. Strelzoff: Phys. Rev. **133B** (1964) 1333.

## P5a: Particle Spectroscopy, Experimental. I

*Chairman :* G. H. STAFFORD

*Speaker:* G. FLÜGGE

*Scientific Secretaries:* Y. SUMI  
R. SUGAHARA

## P5a': Particle Spectroscopy, Experimental. II

*Chairman:* G. H. STAFFORD

*Speaker:* R. J. CASHMORE

*Scientific Secretaries:* Y. SUMI  
R. SUGAHARA

## P5b: Particle Spectroscopy, Theoretical

*Chairman:* L. V. CHUVILO

*Speaker:* Y. HARA

*Scientific Secretaries:* J. ARAFUNE  
T. KURODA

P5a

Particle Spectroscopy

G. FLÜGGE

DESY

§1. Introduction

During the last years particle spectroscopy has evolved into a spectroscopy of leptons and quarks. This era was initiated in 1974 by the discovery of the  $J/\psi$  mesons,<sup>1</sup> quickly followed by the new lepton<sup>2</sup>  $r$  and finally the Ypsilon meson.<sup>3</sup> One is therefore tempted to outline this talk following the common prejudice that high energy physics can be described by leptons, quarks and their mutual interactions (Fig. 1).

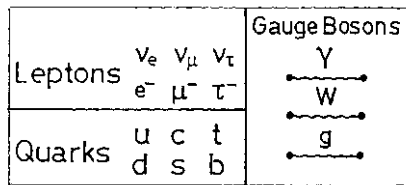


Fig. 1. Common belief on quarks, leptons and their mutual interactions.

Let me first say a few words about the subjects I am not going to cover. I will not talk about leptons. You just heard a beautiful review of the new lepton  $r$  by Gary Feldman in the previous talk.<sup>4</sup> I will be brief also on the old quarks  $u$ ,  $d$  and  $s$  since the old hadron spectroscopy will be covered in the next talk by Cashmore.<sup>5</sup> In my talk I will just concentrate on one specific aspect of

old hadrons, namely exotics. The main part of my report will then be devoted to the new quarks charm and beauty. Being inspired by Sosnowsky's talk,<sup>6</sup> I will also try to offer you a jet tour, starting with 2 jets in  $e^+e^-$  reactions and leading eventually to a glimpse of three gluon jets at the Ypsilon.

§11. Exotics

The possible existence of exotic particles has mainly been discussed in the context of two hypothetical quark compounds, dibaryons<sup>7</sup> and baryonium.<sup>8</sup> Dibaryons are constructed from the old baryons by doubling the quark content of the particle from 3 to 6 quarks. Similarly baryonium evolves from the concept of mesons  $qq$  by doubling the quark content giving  $qqqq$  states.

II. 1 Baryonium—broad states

Experimentally baryonium is readily defined as mesonic states with strong coupling to an antibaryon-baryon ( $BB$ ) system. First observations of this kind of phenomena were made in the famous  $S$ ,  $T$  and  $U$  states, which reveal themselves as a resonance in the elastic, total and annihilation cross sections of nucleon-antinucleon ( $NN$ ) systems with a large elasticity.<sup>9,10</sup>

Table I summarizes the situation encountered in 1977. The  $S$ ,  $T$  and  $U$  states were seen

Table I. Broad baryonium candidates. Masses and widths are given in MeV, the latter in brackets. Quantum numbers are indicated as far as they are known.

1974		New		
$\bar{p}p$ total <sup>8,13,14</sup>	$\bar{p}p \rightarrow \pi^+\pi^-$ <sup>9</sup>	$\bar{p}p \rightarrow K^+K^-$ <sup>10</sup>	$\bar{p}p \rightarrow \pi^0\pi^0$ <sup>11</sup>	$\pi^-p \rightarrow \bar{p}pn$ <sup>12</sup>
	$1480 \pm 30$ ( $280 \pm 25$ ) $J^{PC} = 5^{--}, I=1$	also $I=0$		
' $U$ ': $2350 \pm 15$ ( $160 \pm 20$ ) $I=0, 1$	$1310 \pm 30$ ( $210 \pm 25$ ) $J^{PC} = 4^{++}, I=0$			$\sim 2300$ ( $200-300$ ) $J^P = 4^+$
' $T$ ': $2190 \pm 10$ ( $90 \pm 20$ ) $I=1$	$2150 \pm 30$ ( $200 \pm 25$ ) $J^{PC} = 3^{--}, I=1$	also $I=0$	$2150 \pm 10$ ( $250 \pm 10$ ) $J^P = 2^+$	$\sim 2100$ ( $200-300$ ) $J^P = 3^-$ ( $\sim 2000$ ( $\sim 150$ )) $J^P = 2^+$
' $S$ ': $1936 \pm 1$ ( $\leq 10$ ) $I=1, (0)$				$\sim 1950$ ( $200-300$ ) $J^P = 1^-$



in many experiments on  $NN$  cross sections. In particular an analysis of the reaction  $pp \rightarrow T:7Z\sim$  by Carter *et al* gave clear evidence for the existence of  $J^{PC}=3\sim\sim$  ( $I=1$ ),  $J^{PC}=4^{++}$  ( $I=0$ ), and  $J^{PC}=5\sim\sim$  ( $I=1$ ) states.<sup>9</sup> In 1978 Carter *et al.* extended their analysis to the reaction  $pp \rightarrow K^+K\sim$  and established the presence of  $I=0$  components with  $J^{PC}=3\sim\sim$  and  $5^{++}$  as well.<sup>10</sup> Dulude *et al* analysed the reaction  $pp \rightarrow \pi^+ \pi^0 n^0$  and found a state with  $J^{PC}=2^{++}$  ( $I=0$ ) at 2.1 GeV.<sup>11</sup> Further data became available from a measurement of  $iz\sim p \rightarrow ppn$  by the Bari-Bonn-CERN-Daresbury-Glasgow-Liverpool-Milano-Vienna-Collaboration at the Omega spectrometer at CERN.<sup>12</sup> They found evidence for at least three broad resonances at 1950, 2100 and 2300 MeV with  $J^P = l\sim, 3\sim$  and  $4^+$ , respectively and may be an additional  $2^+$  state at 2000 MeV.<sup>12</sup>

In summary there is good and increasing evidence for the existence of broad  $NN$  states and in the  $S$ ,  $T$  and  $U$  range. However, the situation seems to be rather complex since  $I=0$  and 1 Regge recurrences with  $J=\backslash 4$  and 5, and maybe also  $J=l$  and 2 are encountered. The best established state is certainly the  $S$  resonance<sup>13</sup> (new evidence became available from the Tokyo-Massachusetts Collaboration at this Conference<sup>14</sup>). However, there is no  $J^P$  determination of this state so far, and it may even have two  $J^P$  components.<sup>15</sup>

### 77.2 Baryonium—narrow states

We have good evidence for the existence of broad states coupled to the  $BB$  system. Of course, it is by no means clear that this has something to do with exotics. A possible description of these states would for instance be to view them as  $BB$  bound states. The narrow width of the  $S$  state could be explained due to its vicinity to the  $BB$  threshold. However, in 1977 narrow high mass states coupled to  $BB$  were discovered. There seemed to be no possible explanation for these states in the

usual framework of meson spectroscopy. They could indeed be viewed as good candidates for baryonium states.

The existence of such  $qqqq$  compounds was first predicted by Rosner from duality arguments.<sup>16</sup> For such meson states a strong coupling to  $BB$  and the apparent reluctance to decay into usual mesons can be explained by an OZI rule analogue<sup>17</sup> (Fig. 2).

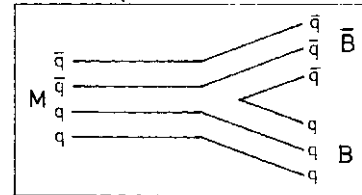


Fig. 2. Baryonium decay.

The elaboration of these ideas does explain both narrow and broad states in the  $BB$  system at least qualitatively.<sup>18</sup> The three best candidates for narrow  $BB$  states are compiled in Table II together with the  $S$  state.

The first one, a narrow state at 2.95 GeV with a width of less than 15 MeV, was first seen in 1977 at the CERN-Omega spectrometer by the Bari-Bonn-CERN-Daresbury-Glasgow-Liverpool-Milano-Purdue-Vienna Collaboration in the reaction  $iz\sim p \rightarrow pp \pi^+ \pi^0 +$  something. It showed up as a spike in the  $ppn^0$  mass distribution.<sup>19</sup> Since then this experiment has been repeated with 10 times more statistics. As we heard on this Conference there are no definite new results yet. An analysis of part of the data did not confirm the effect.<sup>20</sup> Consequently, the existence of this resonance seems to be questionable.

The other two candidates were seen in the reaction  $\pi^+ p \rightarrow \pi^+ p p p$ . Imposing the condition that the forward proton and the  $\pi^+$  form an  $N^*$  or a  $J$ , the remaining  $pp$  system exhibits two spikes at 2.02 and 2.2 GeV (Fig. 3). They can be viewed as resonances in the off shell  $pp$  scattering of the baryon exchange

Table II. Narrow baryonium candidates.

Mass (MeV)	Width (MeV)	Seen in reaction	Ref.	Status
$2950 \pm 10$	$\lesssim 15$	$\pi^+ p \rightarrow \pi^+ p_f p + X$	19, 20	?
$2204 \pm 5$	$16^{+20}_{-16}$	$\pi^+ p \rightarrow \pi^+ p_f p \bar{p}$	21, 22, 23, 24	Confirmed, although with low statistical significance
$2020 \pm 3$	$24 \pm 12$			
$1936 \pm 1$	$\lesssim 10$	$\bar{p} p$ : 'S' resonance	13, 14	Well established

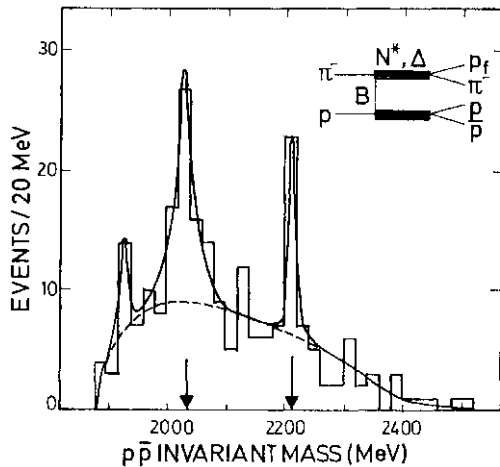


Fig. 3. CERN-College de France-Ecole Polytechnique-Orsay Collaboration: Backward ( $pp$ ) mass distribution in the reaction  $\pi^- p \rightarrow \pi^- pp$  exhibiting two narrow peaks at 2.02 and 2.20 GeV, 9 and 12 GeV data with selection on  $\hat{a}$  and  $\cos \theta^*(p,p) < 0$  are shown.

reaction. The experiment was repeated by the Toronto-York-Purdue Collaboration with positive pions.<sup>22</sup> They find some indication for a 2.2 GeV state with a statistical significance of 2 standard deviations. The experiment does not confirm the 2.95 state. The Pittsburgh-Massachusetts Collaboration has looked into the reaction  $\pi^- p \rightarrow \pi^- p p$ .<sup>23</sup> They see an indication for the existence of the 2.2 GeV state in the  $\pi^- p$  system with a statistical significance of 4 to 5 standard deviations. If this were confirmed it would mean that the 2.2 state is an isovector state. As we have heard in P. Soding's talk there is also evidence for the 2.02 state being seen in the virtual photon production reaction  $\gamma p \rightarrow p p p$  at Cornell.<sup>24</sup> The statistical significance of this effect is 3 standard deviations. To summarize: There seems to be evidence confirming the existence of two narrow states at 2.02 and 2.20 GeV from several different experiments.

### II. 3 Dibaryons

Let us see whether even higher combinations do exist, for example a 6 quark combination like the dibaryon states mentioned above.

We all know at least one candidate for dibaryons, the deuteron. We know also that this is a nuclear force bound state and not the type of exotics we are looking for. Real exotic dibaryon states were for instance predicted in the MIT bag model by Jaffe in 1977.<sup>25</sup> I will only summarize the three best

candidates and refer for all details to the parallel session.

The first candidate is a  $pp$  resonance at 2.26 GeV first seen in the Argonne total cross section experiment with polarized targets and beams.<sup>26</sup> The resonance known as the  ${}^3F_3$  has a width of 200 MeV and the quantum numbers  $J^P = 3^-(I=1)$ .<sup>\*</sup> The possible existence of further  $pp$  states was discussed on this Conference.<sup>27</sup>

The second candidate comes from the Tokyo-KEK measurements on the photodisintegration of deuterons.<sup>28</sup> The analysis of these data reveals the possible existence of a  $z/J$ -resonance at the mass of 2.38 GeV with a width of 200 MeV, and  $J^P = 3^+(7=0)$ .  $J^P = 1^+$  cannot be ruled out.

The third candidate, a strange dibaryon state, has been seen in many experiments.<sup>29,30</sup> A recent analysis was carried out by the CERN-Heidelberg-München Collaboration.<sup>30</sup> In the reaction  $K^- p \rightarrow \Lambda p n$  they find a narrow bound state in the  $\Lambda p$  system with a mass of 2.129 GeV, a width of less than 10 MeV, and  $S=-1$ .

### IIA Exotic quantum numbers

Although there are several candidates for baryonium and dibaryon states, the only convincing argument in favour of exotic states would be the discovery of states with exotic quantum numbers.

Two searches for such states have been reported at this Conference. The first one by the Indiana-Purdue-SLAC-Vanderbilt Collaboration, does not show any evidence.<sup>31</sup> The second one, however, from the CERN-Omega spectrometer by the Glasgow-DESY Collaboration, does indeed show an effect in the reaction  $K^- p \rightarrow \Lambda p n$ .<sup>32</sup> Applying a fit to this reaction and constraining the  $Jp_x$  system to

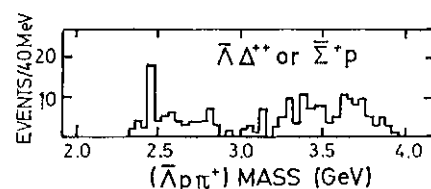


Fig. 4. Glasgow-DESY Collaboration: ( $\Lambda p n$ ) mass distribution in the reaction  $K^- p \rightarrow \Lambda p n$  with an indication of a peak at 2.46 GeV.

\* Details were also given in V. A. Tsarev's talk at this Conference.

either  $\hat{A}J^+$  or  $2LP$  they see a spike in the mass distribution of the  $\hat{A}pic^+$  system (Fig. 4). It has a statistical significance of 3 to 5 standard deviations and certainly needs experimental confirmation.

### II.5 Summary

To conclude this part there is no firm evidence for exotic quantum numbers so far. There have been many sightings of baryonium, narrow and wide, and dibaryon candidates. Qualitative arguments favour the exotic nature of the baryonium states. However, the high mass narrow states still need experimental confirmation. Convincing evidence for the exotic nature of these states is certainly yet missing. Consequently both experiments and theory have to be improved.

### §111. New Quark Spectroscopy

The rest of my talk will be devoted to the discussion of the two new flavours of quark, charm and beauty. Since new results on the D meson were already discussed in the previous talk by Feldman<sup>4</sup> I will concentrate on charmonium and the F meson in the context of charm. Concerning beauty I will show the experimental evidence for Ypsilon and Ypsilon Prime in  $e^+e^-$  reactions; I shall also talk about the event topology in the Ypsilon region discussing evidence for a 2 jet structure outside the resonance and the search for 3 gluon jets.

### III A Quark charge

Before I go into a detailed discussion of the two new quarks let me briefly ask whether there is any experimental evidence supporting our common belief that quarks are fractionally charged. Two quantities might be used as a test for the quark charge.

The first one is the radiative width  $r(r) \sim \Lambda_{jj}$ . Since the  $rj'$  is dominated by the SU(3) singlet amplitude there is a strong dependence of this quantity on the charge of the quarks. For fractional charge quarks (Gell-Mann quarks) a width of  $\Lambda = 6.0$  keV is calculated whereas for integer charge quarks (Han-Nambu quarks) the width is  $r = 25.6$  keV.<sup>33</sup> Experimental results on this quantity have become available now from the Bonanza group at DES Y.<sup>34</sup> They look for the two photon process  $e^+e^- \rightarrow$

$e^+e^- + \text{hadrons}$  with the two electrons tagged in the forward direction. The reaction was monitored by the two photon QED reaction  $e^+e^- \rightarrow e^+e^- e^+e^-$  which was found to be in good agreement with predictions. From the fact that no final states of the type  $e^+e^- + \text{hadrons}$  were found they could infer an upper limit  $r(\gamma\gamma) < 11.5$  KeV (95% confidence level). Previous results had been obtained by ADONE ( $T < 33$  KeV) and Imperial College ( $r_{tot} < 8$  MeV) groups.<sup>35</sup>

The other test quantity is the width  $F(J)$

Again the coupling depends on the quark charge and the predictions are 2.6 eV for fractional charge quarks and 13 eV for integer charge quarks.<sup>36</sup> DASP has measured an upper limit of this  $Jj(p)$  decay width giving  $r < 5.1$  eV (95% confidence level).<sup>37</sup> Thus an integer charge of the quarks is ruled out by both experiments.

### III.B Charm

#### III. B. 1 Charmonium

The  $cc$  system exhibits a series of bound states known as charmonium. The situation we faced one year ago is summarized in Fig. 5.<sup>38</sup> We have a rather firm knowledge

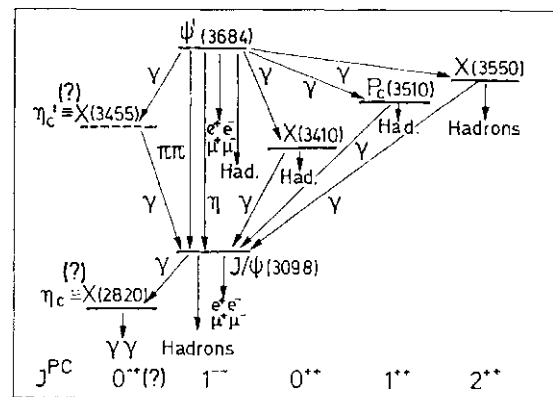


Fig. 5. The experimental knowledge on the charmonium states (1977).

of the existence and even the spin assignment of the  $^3P$  states. The situation is much worse on the  $^1S$  states. Although the X(2820) was firmly established by the DASP collaboration<sup>37</sup> and the existence of this state was confirmed in the reaction  $np \rightarrow \gamma jn$  by the IHEP-CERN-Karlsruhe-Pisa-Vienna Collaboration,<sup>39</sup> nothing—except its even C parity—is known about its quantum numbers. In particular its identity as  $rj_c$  is certainly still questionable. The

situation is even worse on the other state, the  $\psi(3455)$  which was only seen in the 77 cascade decay of  $\psi(3700)$ . It is statistically significant only when the results from three different experiments are combined. This situation has not changed since about 1.1/2 years except for some new results of the DESY-Heidelberg Collaboration which I am going to describe now.

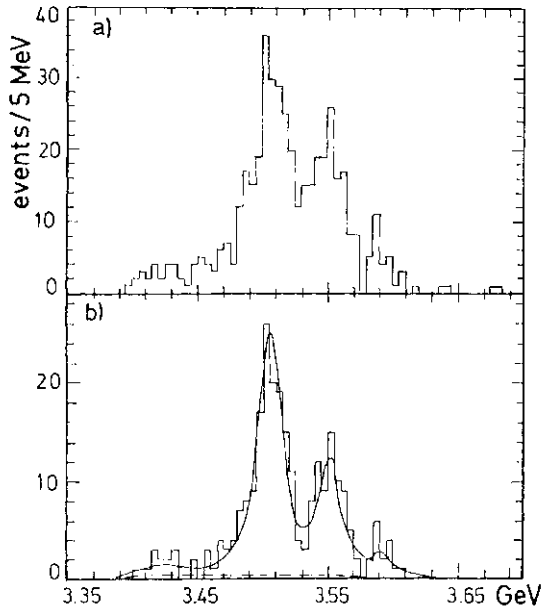


Fig. 6. DESY-Heidelberg Collaboration: High mass solution of the  $(J/\psi)$  system in the decay  $\psi' \rightarrow T7J/\psi$ . Note the excess of events at 3.6 GeV. (a) Two photon mass less than 520 MeV. (b) In addition, photon angular error less than 200 mrad.

Figure 6 shows the results of this group on the reaction  $\psi' \rightarrow \gamma\gamma \psi$  with the directions  $\downarrow \rightarrow \mu\mu$  measured for both photons and the muons. Constraining the two charged particles to the  $J/\psi$  mass they obtain the mass distribution displayed in Fig. 6 for the high mass solution of the  $J/\psi$  system. The two  $\psi$  states at 3.5 and 3.55 GeV are clearly visible. Let me draw your attention to the excess of events above 3.55 GeV. It can not be explained by the TTV background (indicated by the dashed line) nor by tails of the 3.55 peak. This situation was known at the Hamburg Conference one year ago.<sup>40</sup> Since then the DESY-Heidelberg group improved their mass resolution by taking only those events where the photons were converted in the inner detector.<sup>41</sup> This allowed a more precise determination of the angle of photon emission. Thus, with in-

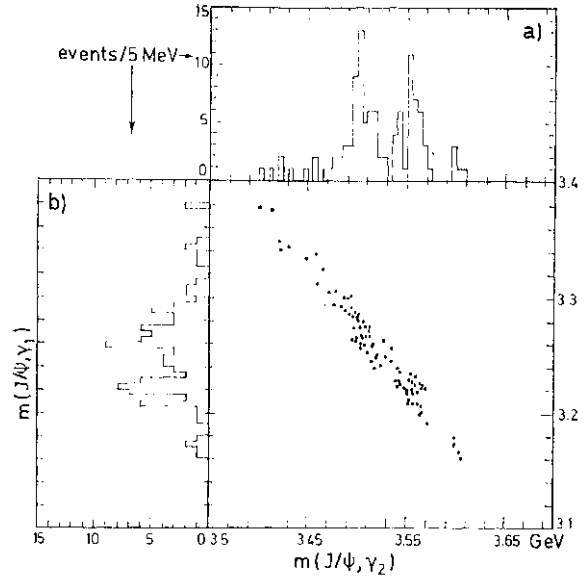


Fig. 7. DESY-Heidelberg Collaboration: High vs low mass solution of the  $(J/\psi)$  system in the decay  $\psi' \rightarrow \gamma\gamma J/\psi$ . Only events with converted photons.

(a) High mass solution; (b) Low mass solution.

creased mass resolution but of course less statistics the group got the result displayed in Fig. 7a which indicates a clearly separated excess of events at 3.6 GeV. From these 5 events above no background the group concludes the possible existence of a state at 3.59 GeV with a branching ratio product

$$BR(\psi' \rightarrow \chi(3.6)\gamma) \cdot BR(\chi \rightarrow \gamma J/\psi) = (1.8 \pm 0.6) \cdot 10^{-3}.$$

The scatter plot (Fig. 7) of the low mass against the high mass solution of their data shows however, that the high mass solution is not unique. A low mass state at 3.18 GeV could be equally possible. Table III summarizes the situation on the branching ratios of the  $P/x$  states in the charmonium system. Note that the new limit from the DESY-Heidelberg group for the  $\chi(3.45)$  state is about a factor of 3 lower than the average value of about 0.7% known so far. This casts new suspicion on the existence of this state.

To summarize, the situation on the charmonium  $^*S$  states has not been cleared up during the last year. New data from the DESY-Heidelberg group rather question the existence of the  $\psi(3455)$  at 3.45 GeV, and instead point to the possible existence of another state at 3.6 GeV. Certainly more data are needed to clarify the situation.

Table III. Branching ratios of  $PJx$  states.  $BR(\langle p' + Tx \rangle - BR(i \sim *iJ \langle p \rangle)$  in %. Upper limits 95% C.L.

	Status	DASP <sup>45</sup>	DESY-HD <sup>41</sup> new values	MPPSSSD <sup>42</sup>	SLAC-LBL <sup>43</sup>	PLUTO <sup>44</sup>
$\chi(3.41)$	O.K.	$0.3 \pm 0.2$	$< 0.25$	$3.3 \pm 1.7$	$0.2 \pm 0.2$	$1.2 \pm \begin{smallmatrix} 0.9 \\ 0.6 \end{smallmatrix}$
$\chi(3.45)$	?	$< 0.5$	$< 0.2$	$< 2.5$	$0.8 \pm 0.4$	$0.7 \pm \begin{smallmatrix} 0.8 \\ 0.5 \end{smallmatrix}$
$\chi(3.51)$	O.K.	$2.1 \pm 0.4$	$2.5 \pm 0.4$	$5.0 \pm 1.5$	$2.4 \pm 0.8$	$1.2 \pm \begin{smallmatrix} 1.0 \\ 0.6 \end{smallmatrix}$
$\chi(3.55)$	O.K.	$1.6 \pm 0.4$	$1.0 \pm 0.2$	$2.2 \pm 1.0$	$1.0 \pm 0.6$	$0.9 \pm \begin{smallmatrix} 1.0 \\ 0.5 \end{smallmatrix}$
(3.59)	?		$0.18 \pm 0.06$			

### III.B.2 Charm particles

You all know the exciting story of the discovery of the D meson at SLAC<sup>38,45</sup> and you just heard a review of the situation by Feldman in the previous talk. Let me therefore only add some information on the particle which was still missing in the multiplet of pseudoscalar mesons of SU(4) shown in Fig. 8. Evidence for the existence of this pseudoscalar meson F and its vector counterpart F\* came from the DASP detector at DESY.<sup>46</sup> I am going to describe their new data in some detail.<sup>47</sup>

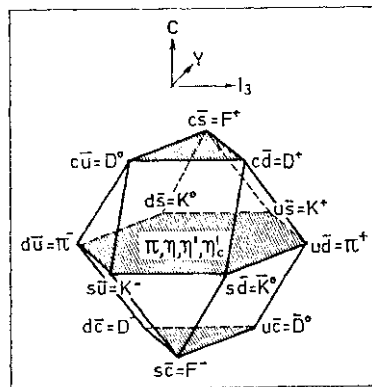


Fig. 8. The multiplet of pseudoscalar mesons in SU(4).

### III.B.3 F Meson

If we assume that the mass of the F meson is smaller than the sum of the masses of the D and the K meson, the particle can only decay weakly into an  $ss$  system in the final state. Consequently we expect  $KK$ ,  $\langle f\bar{i}, r \rangle$  or  $TJ'$  in the debris of this decay. Since K's are difficult to spot in the heavy background of other charm particle production the DASP group looked for the inclusive production of  $rfs$  in the reaction

$$e^+e^- \rightarrow \eta + X$$

$$\quad \quad \quad \rightarrow \gamma\gamma$$

The experimental problem is of course the high combinatorial background of photons from 2 to 3  $\pi\pi$ 's produced per event at these energies. The DASP group could, however, overcome this problem with a relatively good detection efficiency for photons (95% above an energy of 140 MeV) and an angular and energy resolutions which combine to give a mass resolution of about 80 MeV at the  $rj$ . They select events with two charged particles and least 2 photons with an energy of more than 140 MeV, an opening angle of more than  $11.5^\circ$  and a momentum vector sum of more than 300 MeV. With these cuts the  $\pi\pi$  efficiency is relatively low.

Figure 9 shows the result of these measurements for 6 different energy intervals. The full curves indicate fits to the  $iz^\circ$  and  $7J$  mass peaks on a background obtained by combining  $fs$  from different events. The dashed curves indicate the background below the  $rj$  signal.

Note that there is no  $rj$  signal at 4.03 GeV whereas there is a clear signal at 4.16 GeV, a very strong signal at 4.42 GeV and maybe an indication of  $rj$  production in the other energy regions. Figure 9(b) summarizes the data in terms of the inclusive cross section for  $rj$  production over the whole energy range from 4 to 5 GeV. For comparison the trend of the total cross section is indicated below the figure. The figure shows the presence of  $rj$  production above about 4.1 GeV. Strong signals are present at 4.16 and 4.42 GeV. At both energies a resonance-like structure is visible in the total cross section. As mentioned by Feldman in the previous talk<sup>4</sup> the detailed structure of the 4.16 GeV region is however controversial comparing SLAC<sup>4,48</sup> and DESY<sup>49,50</sup> data.

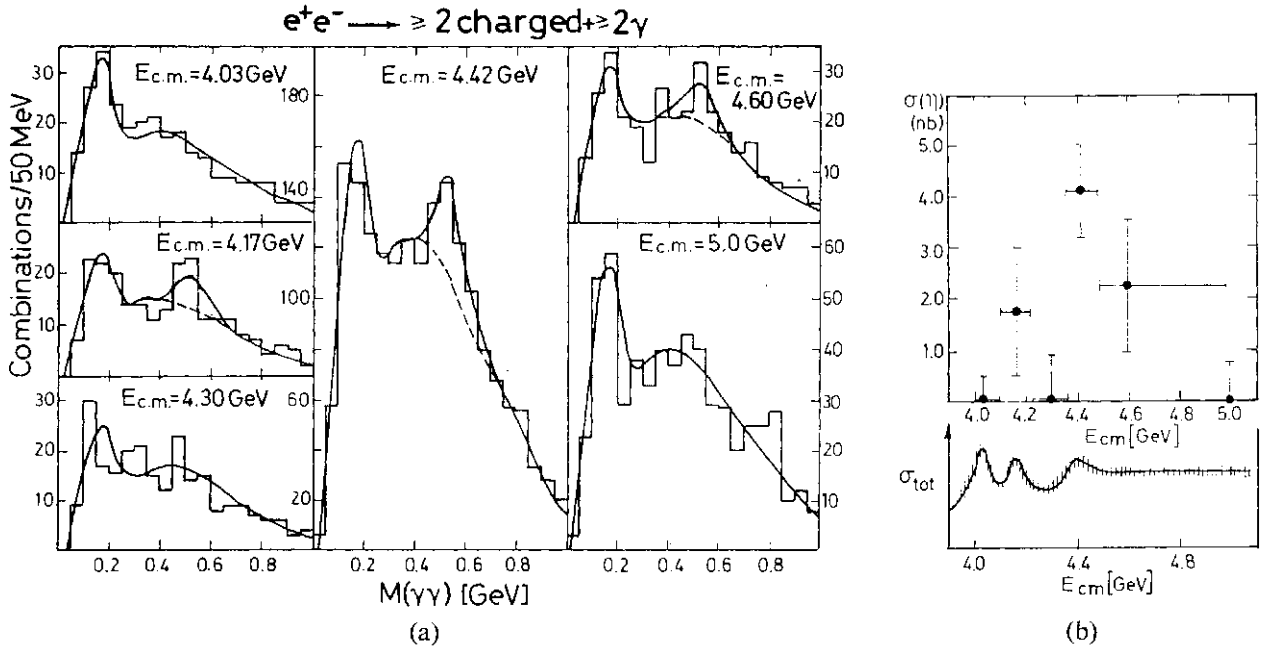


Fig. 9. DASP Collaboration: Inclusive  $rj$  production in  $e^+e^-$  annihilation in the 4 to 5 GeV energy range. (a) Two photon mass distribution in different energy intervals. The full curve is the sum of the combinatorial background (photons taken from different events) and a fit to the  $n^0$  and  $rj$  production. The dashed curve represents the background without  $rj$  production. (b) Inclusive cross section for  $rj$  production as a function of energy. The trend of the total cross section is given for comparison.

Let me draw your attention again to the fact that no  $rj$  production is present at 4.03 MeV. This is a crucial point in the whole argument since the spike at 4.03 GeV is known for abundant D production.<sup>45</sup> Consequently the lack of an  $rj$  signal at this point indicates that the  $\gamma\gamma$  production can not be explained by any known source including D production and decay.

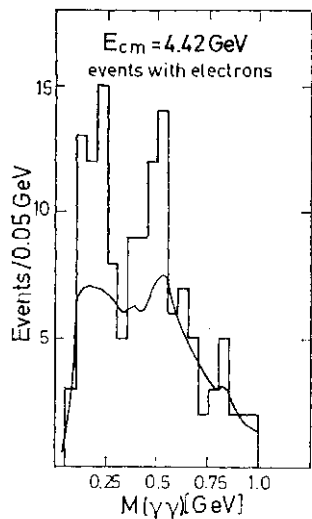


Fig. 10. DASP Collaboration: Two photon mass distribution of events including electrons in the 4.42 GeV energy region. The full curve indicates the background from misidentified electrons.

The next point to be checked is whether the  $rj$ 's really originate from a weakly decaying particle. To check this all events were scanned for the presence of electrons. Figure 10 shows e.g., the result for the 4.4 GeV region, where the  $rj$  signal was strongest. Electron events are plotted against the  $\gamma\gamma$  mass. The background due to misidentified electrons is indicated by a full line. The figure shows that a strong signal above background is present in the region of the  $n^0$  and the  $rj$  mass. This indicates in particular that  $rj$  production is correlated with the emission of electrons indicating the presence of a weak decay. If

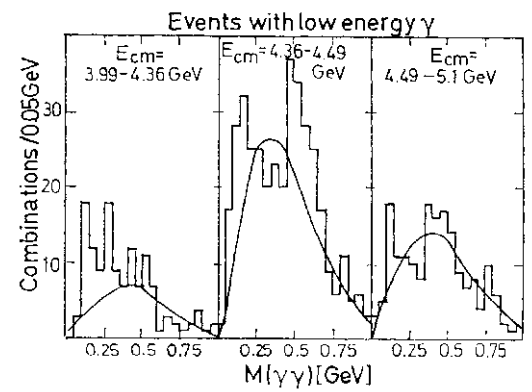


Fig. 11. DASP Collaboration: Two photon mass distribution of events including an additional low energy photon in three different energy intervals.

we assume now that the  $rj$  production at 4.16 and 4.42 GeV is due to F production one might suspect that at 4.42 GeV at least  $F^*$  production is also involved. For the further argument let us therefore consider possible signatures for an  $F^*$ . Assume F and  $F^*$  are both  $ci, \sim sc$  states, the  $F^*$  being a spin excitation. In this case both F and  $F^*$  are ( $I=0$ ) states and the  $F^*$  can only decay into the F emitting an ( $I=0$ ) system. We further assume that the mass difference in the  $FF^*$  system is about equal to the mass difference in the  $DD^*$  system namely less than two times the pion mass. The only possible decay mode for the  $F^*$  will then be the decay

$$F^* \rightarrow F\gamma.$$

These considerations led the DASP group to look for the associated production of  $rj$  with a soft photon possibly originating from the decay of  $F^*$  into  $F\gamma$ . Figure 11 shows the result of this search displaying again the mass of the  $rj$  system at 3 different energy intervals. It shows again a strong  $rj$  signal at 4.42 GeV. No such signal is present above and below this energy range. This proves that at 4.42

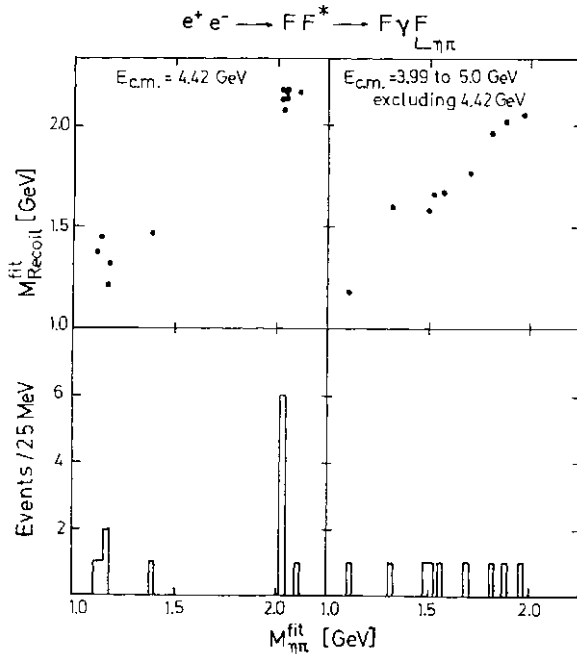


Fig. 12. DASP Collaboration: Events from the reaction  $e^+e^- \rightarrow FF^* \rightarrow F\gamma F$ . A fit assuming  $e^+e^- \rightarrow FF^*$ ;  $F^* \rightarrow rF$ , one  $F \rightarrow \gamma n$  is applied. The figure shows biplots of the fitted mass distribution against the recoil mass and  $rj$  distributions for events with  $X^2 < 8$  and a  $rj$  mass difference  $|M_{fit} - M_{recoil}| < 250$  MeV.

GeV  $rj$  production is strongly correlated with low energy photons. One is therefore urged to look for direct evidence for  $FF^*$  or  $F^*F^*$  production at 4.42 GeV. One assumes again that the  $F^*$  is cascading down to the F by emitting a soft photon and that one of the F particles decays into  $rj$  and  $\pi\pi$ . Therefore the DASP group looked into the reaction

$$e^+e^- \rightarrow F + \text{soft photon} + X.$$

43 events of this type were found. The events were fitted to the hypothesis of  $F^*F^*$  or  $FF^*$  production. Figure 12 shows the result for the case of  $FF^*$  production. The mass of the  $rj\pi\pi$  system is plotted against the recoil mass. A clustering of 6 events can be seen at an  $rj\pi\pi$  mass value of  $2.03 \pm 0.06$  GeV. The background is of the order of less than 0.5 events.

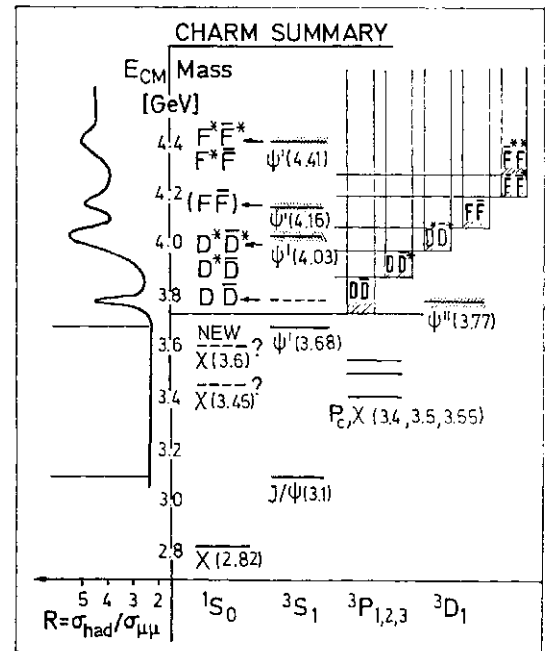


Fig. 13. Schematic summary of the experimental situation on charm.

Since the  $rj\pi\pi$  system cannot unambiguously be associated to the F or the  $F^*$  and since also no clear distinction can be made between the  $FF^*$  and the  $F^*F^*$  hypothesis the recoil mass is not very suitable to determine the mass of the  $F^*$ . One can however infer the mass difference between  $F^*$  and F from the energy distribution of soft photons. The result is

$$M_{F^*} - M_F = 110 \pm 46 \text{ MeV.}$$

Taking into account all efficiencies the DASP group determined a relative branching ratio

$$BR(F \rightarrow \eta\pi) / (BR(F \rightarrow \eta X)) = 0.09 \pm 0.04.$$

The SLAG-LB L group also looked for possible F production in the reaction

$$e^+e^- \rightarrow K^+K^-\pi^+\pi^-\pi^0 + X, \quad K^+K_s^0 + X, \\ K^+K^-\pi^+\pi^-\pi^0 + X.$$

Constraining these data to the hypothesis that they originated from the process  $e^+e^- \rightarrow FF$  with a subsequent decay of one of the F to one of the above (KKJ $\pi$ ) systems they got a signal of about 4 standard deviations at a mass of  $2039.5 \pm 1.0$  MeV<sup>51</sup> at 4.16 GeV CM energy. The signal was not present in the equal sign KK systems. However, a repetition of the search in the Mark II detector could not confirm this result although it collected about the same statistics.<sup>52</sup>

Hitlin reported at this Conference that the Mark II detector did not see any  $rj$  signal at 4.16 GeV.<sup>53</sup> However, both Mark II and the DASP group agreed that due to the different experimental cuts this does not contradict the DASP result.<sup>53,54</sup>

To summarize,  $rj$  production has been observed by the DASP Collaboration above  $E_{cm} = 4.1$  GeV. No  $y$  signal is seen at  $E_{cm} = 4.03$  GeV. Strong  $rj$  signals are present at 4.16 and 4.42 GeV, the latter being associated with soft photon production. The observed  $y$  production is correlated with electrons, which is indicative for the weak decay origin of these particles.

From a study of  $rjx$  events with soft photons the masses of F and F\* could be determined as  $M_F = 2.03 \pm 0.06$  GeV,  $M_{F^*} = 2.14 \pm 0.06$  GeV. The relative branching ratio  $BR(F \rightarrow \eta\pi) / BR(F \rightarrow \eta X)$  is  $0.09 \pm 0.04$ . These results are neither confirmed nor contradicted by any other experiment.

#### III.B.4 Summary

Our experimental knowledge on charm is schematically summarized in Fig. 13. The odd C-parity  $^3S$  state  $J/\psi$ , its radial excitations  $\psi'$  and the  $^3D$  state  $\psi''$  (3.77) show up in the total  $e^+e^-$  cross section, the latter due to its mixing with the nearby  $^3S$  state. The existence of the  $\psi'$  (4.16) is somewhat controversial.

The  $^3P$  states are established, although their quantum number assignment is not rigorously proven.

Whereas there is firm evidence for the

$X(2.82)$ , the existence of the states  $\psi(3.45)$  and  $\psi(3.59)$  is not established. The quantum numbers of all three states are unknown, except for their even C-parity.

The upper part of Fig. 13 indicates, how the production of D, D\*, F and F\* mesons comes in with increasing energy: DD at the  $\psi''$  (3.77),  $D^*\bar{D}$  and  $D^*\bar{D}^*$  at  $\psi'$  (4.03),  $F\bar{F}$  at  $\psi'$  (4.15) and  $F^*\bar{F}$  and/or  $F^*\bar{F}^*$  at  $\psi'$  (4.42). The evidence for FF production at the  $\psi'$  (4.16) is suggestive but not compelling, since it is only based on the inclusive  $rj$  signal of the DASP group. No clear distinction between  $F^*\bar{F}^*$  and  $F^*\bar{F}$  production at the  $\psi'$  (4.42) can be made.

#### III.C Beauty

Since the discovery of the Ypsilon meson by the Columbia-Fermilab-Stony Brook Collaboration at FNAL in 1977<sup>55</sup> the new particle has been produced in various hadron experiments<sup>56</sup> and the discoverers themselves improved both the statistics and the resolution of their experiment.<sup>57</sup> As Lederman outlined in his talk there is firm evidence for the existence of at least two T states and some indications of even a third one.<sup>56</sup> The challenge for  $e^+e^-$  physics was of course to search for these new states as narrow resonances in  $e^+e^-$  collisions and thereby reveals their potential nature as bound states of new quarks. Therefore after the announcement of the discovery in June 1977 the PLUTO Collaboration proposed in July 1977 to upgrade DORIS to reach the 10 GeV region. On April 12, 1978, the preparations were finished to start the search. Already on May 2, 1978, thanks also to the precise determination of the mass by the

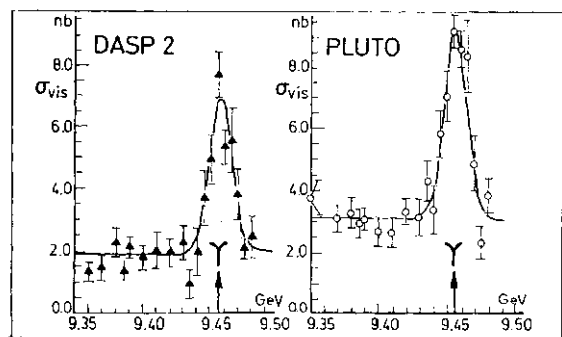


Fig. 14. PLUTO and DASP 2 Collaborations: The original evidence for T production in  $e^+e^-$  annihilation.



Columbia-Fermilab-Stony Brook Collaboration, the  $Y$  was found at DORIS by the PLUTO<sup>58</sup> and DASP2<sup>59</sup> Collaborations simultaneously. The original data of this search are shown in Fig. 14 which displays the visible cross section in both detectors as a function of energy. A clear signal at 9.46 GeV is seen in both experiments.

From these original data both groups agreed on a mass value of  $M_Y = 9.46 \pm 0.01$  GeV, an electronic width of  $\Gamma_{ee} = 1.3 \pm 0.4$  keV and a total width of the resonance  $\Gamma_{tot} < 18$  MeV. Note that the error in the mass is due to the DORIS calibration uncertainty and the width corresponds to the DORIS energy spread. These values already strongly favoured an interpretation of the  $Y$  being a bound state of a new quark-antiquark pair with a charge of  $1/3$ .<sup>58</sup>

### III. C. 1 Ypsilon parameters

The immediate issue of  $e^+e^-$  physics of the  $Y$  is of course a determination of the leptonic and the total width of the resonance. The leptonic width  $\Gamma_{ee}$  can be inferred directly by integrating the hadronic cross section of the resonance according to the formula

$$\frac{M^2}{6\pi^2} \int \sigma_{had} dE = \frac{\Gamma_{ee} \Gamma_{had}}{\Gamma_{tot}} \approx \Gamma_{ee}.$$

The integral extends to infinitely high energies which in practice means that radiative corrections have to be applied properly. The absolutely normalized results of the PLUTO group are shown in Fig. 15. Outside the resonance the cross section ratio is  $R = a_{tot}/a_{pt} = 5.2 \pm 1.0$  in good agreement with the value of  $4.7 \pm 1.0$  measured at 5 GeV. Note that both values include contributions from the heavy lepton  $\tau$ . The 9.4 GeV value is not radiatively

corrected. The results of two other experiments, the DASP2 group<sup>61</sup> and the DESY-Heidelberg 2 detector, which replaced the

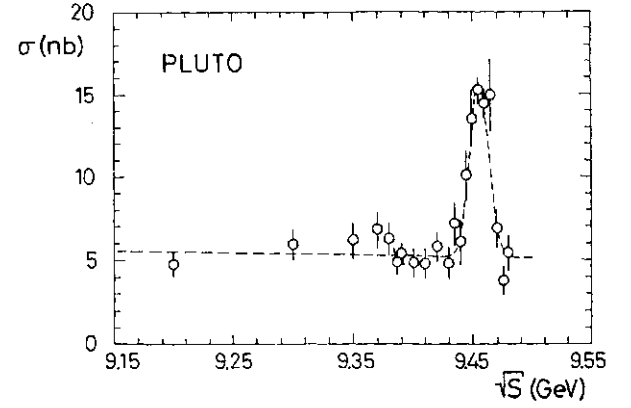


Fig. 15. PLUTO Collaboration: Absolutely normalized hadronic cross section in the  $T$  region.

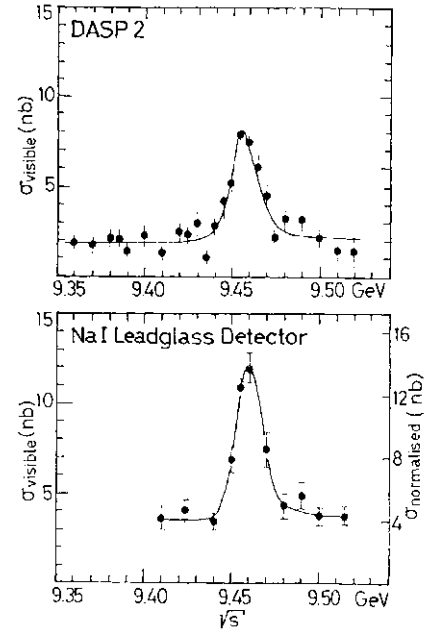


Fig. 16. DASP 2 and DESY-Hamburg-Heidelberg-Munchen Collaborations: Visible cross section for  $e^+e^- \rightarrow \text{hadrons}$  in the  $T$  region.

Table IV. Results on  $Y(9.46)$ .

	$M(Y)$ (GeV)	Exp. width (MeV)	$\Gamma_{ee}(Y)$ (keV)	$B_{\mu\mu}$ (%)	$\Gamma_{tot}$ (keV)
PLUTO	$9.46 \pm 0.01$	$18 \pm 2$	$1.3 \pm 0.4$	$2.7 \pm 2.0$	$> 20$ (2s.d.)
DASP II	$9.46 \pm 0.01$	$18 \pm 2$	$1.5 \pm 0.4$	$2.5 \pm 2.1$	$> 20$ (2s.d.)
D-H II	$9.46 \pm 0.01$	$17 \pm 2$	$1.04 \pm 0.28$	$1.0 \pm 3.4$ $-1.0$	$> 15$ (2s.d.)

#### Mean values

$$\begin{aligned} \Gamma &= (1.2 \pm 0.2) \text{ keV} \\ B_{\mu\mu} &= (2.6 \pm 1.4) \% \\ \Gamma_{tot} &> 25 \text{ keV (95\% c.l.)} \end{aligned}$$

(Best value  $\Gamma_{tot} = 50$  keV)

PLUTO detector after its removal to PETRA, are shown in Fig. 16. (The latter detector was operated by a DESY-Hamburg-Heidelberg-Munich Collaboration.) Their values are not absolutely normalized. For the determination of the leptonic width  $\Gamma_{ee}$ , both detectors used the PLUTO value of  $R$ . The results of the three experiments are summarized in Table IV.

An attempt was made by the three groups to determine the total width of the resonance. The procedure is to determine the  $JU$  pair branching ratio  $B^{\wedge}$  on the resonance. Assuming  $f_{xt}$  universality, the total width can then be obtained as  $\Gamma^{\wedge} = \Gamma_j B^{\wedge}$ . In all three experiments the determination of  $B^{\wedge}$  suffers from very low statistics. For example the PLUTO group found 60  $ju$  pairs off resonance and 74  $ju$  pairs on resonance.<sup>63</sup> The angular distribution of these events is shown in Fig. 17. The data are in good agreement with the expectation of  $1 + \cos^2\theta$ . The values of  $B^{\wedge}$  obtained from the three experiments are summarized again in Table IV.

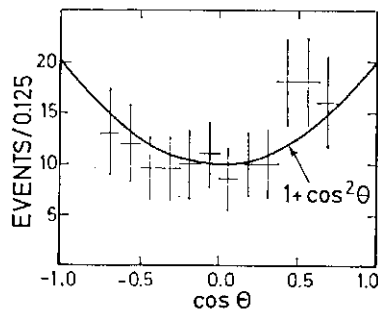


Fig. 17. PLUTO Collaboration: Angular distribution of muon pairs produced in the  $Y$  region. Data on and off resonance are combined.

Due to the large error on  $\Gamma_{ee}$  only lower limits can be given on the total width of the resonance. Even if all values are combined the error is still too large to obtain a two standard-deviation upper limit of the total width. Again one can only obtain a lower limit of 25 keV at a 95% confidence level. If we take however  $\Delta\Gamma_{ee} = 2.6\%$  at face value we find the 'best' value of

$$\Gamma_{\text{tot}} = 50 \text{ keV.}$$

### III.C.2 Event topology

According to common prejudice the topology of events should change drastically in the resonance region. The continuum is expected

to be governed by the production of quark jets with a characteristic angular distribution of  $1 + \cos^2\theta$  due to the  $1/2$  spin of the quarks. The resonance itself is expected to decay into gluons which then fragment into 3 jets in a disc-like configuration.<sup>64</sup>

To test these theoretical conjectures we have analyzed our events in terms of sphericity. This quantity which was introduced by Brodsky and Bjorken<sup>65</sup> and later used successfully in the analysis of the SLAC-LBL data<sup>66</sup> is defined by

$$S = \min\left(3/2 \frac{1}{\sum p_{\perp}^2} \cdot \sum p_{\perp}^2\right),$$

$p_{\perp}$  = momentum perpendicular to the  $z$ -axis.

The limiting values of  $S$  are 0 in the limit of two infinitely narrow jets and 1 in the limit of an isotropic event.

Also another quantity, thrust,<sup>64</sup> which was first introduced by Brandt *et al.*<sup>67</sup> will be used. This quantity is defined as

$$T = \max\left(\frac{1}{\sum |p_{\parallel}|} \cdot \sum |p_{\parallel}|\right),$$

$p_{\parallel}$  = momentum parallel to the  $T$ -axis.

$T$  varies between the values of 1 for two line jets and  $1/2$  for isotropic events. Since it turns out that the features of the data in terms of thrust and sphericity are very similar<sup>68</sup> I will not discuss all aspects of both quantities. I will mostly concentrate on the sphericity, although sometimes the thrust axis will be used for convenience, because its definition is technically very simple. A word of caution should be said in this context: Although the mean angle between the jet axis defined by either  $S$  or  $T$  is zero, the distribution has a width of about  $15^\circ$ . This reflects the uncertainty inherent in defining the real jet axis.<sup>68</sup>

### III.C.3 Quark jets

The existence of jets in  $e^+e^-$  annihilation was first demonstrated by the SLAC-LBL group.<sup>66</sup> Their results are shown again in Fig. 18. Their data are in good agreement with the prediction of a jet model (full curve) whereas the phase space Monte-Carlo (dashed curved) is completely ruled out at large energies. The PLUTO Collaboration has made a very similar analysis.<sup>68</sup> The result is presented in Fig. 19. It shows the mean observed sphericity as a function of energy over the energy range from 3 to 10 GeV. The figure

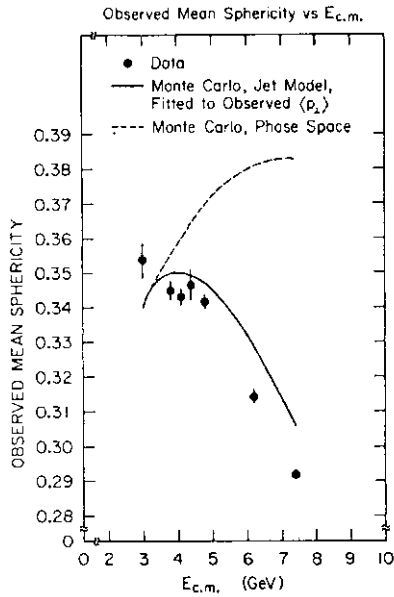


Fig. 18. SLAC-LBL Collaboration: First evidence for jets in  $e^+e^-$  annihilation. Observed mean sphericity as a function of energy. The full and dashed lines show Monte-Carlo simulations of a jet and phase space model, respectively.

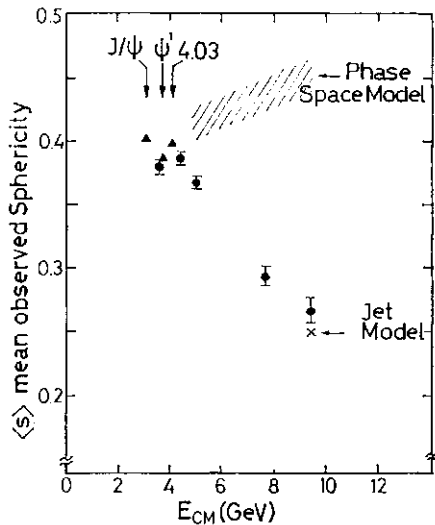


Fig. 19. PLUTO Collaboration: Observed mean sphericity of charged particles ( $>4$  prongs) as a function of energy. The shaded region represents the phase-space prediction, the crossed one for two jets.

shows again a dramatic fall over this energy range in good agreement with a two jet Monte-Carlo<sup>69</sup> and in complete disagreement with phase space predictions.

Note the small but significant change in sphericity at the charm threshold around 4 GeV.

The angular distribution of the jet axis is shown in Fig. 20. Data are in good agreement with the theoretical expectation for spin 1/2

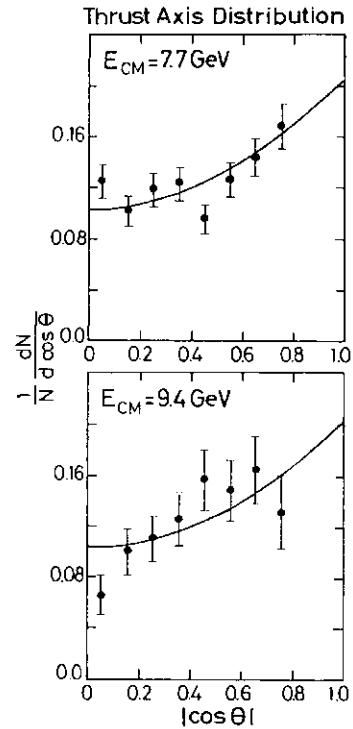


Fig. 20. PLUTO Collaboration: Angular distribution of the jet axis as defined by thrust for two energies.

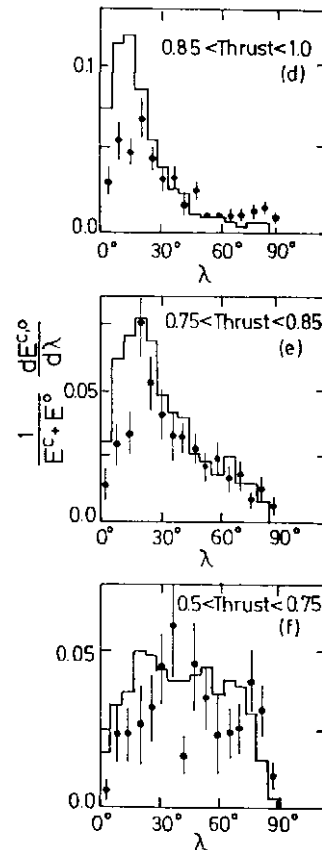


Fig. 21. PLUTO Collaboration: Angular distribution  $1/E dE/d\lambda$  of neutral (data points) and charged (histogram) energy with respect to the thrust axis for three different thrust intervals.  $\lambda$  is the angle between the momentum vector and the thrust axis.

quark jets. A fit to the data with  $1+a\cos^2\theta$  gives the values of  $a=0.76\pm 0.3$  at 7.7 GeV and  $1.63\pm 0.6$  at 9.4 GeV. Two other interesting properties of these jets can be read from Fig. 21. It shows the energy distribution of both charged and neutral energy with respect to the thrust axis for three different thrust intervals. The first observation is that the neutral energy flow follows almost exactly the energy flow of the charged particles. The relative partition of neutral to charged energy can be determined from this figure to be about 0.8. Furthermore the half opening angle of the jets turns out to be of the order of  $30^\circ$ . A similar result is obtained, if one compares the mean momenta perpendicular and parallel to the jet axis.

Many observations on jets are best demonstrated by looking at a typical event shown in Fig. 22. To summarize, there is clear (confirming) evidence for two jets in  $e^+e^-$  annihilation, the sphericity decreasing with increasing energy. The angular distribution of these jets is compatible with the quark spin being  $1/2$ . Neutral and charged energy in these jets are strongly correlated and subtend a half opening angle of about  $30^\circ$ .

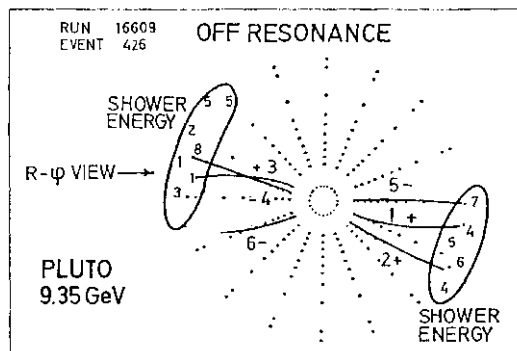


Fig. 22. PLUTO Collaboration: A typical two jet event at 9.35 GeV CM. energy.

*ILCA Change of topology at the Ypsilon*

Whereas off resonance only quark pair production is at work, the on-resonance cross section is composed of three different processes, as shown in Fig. 23. Since we are interested in the direct decay mechanism, the off resonance and the vacuum polarization terms have to be subtracted in all distributions. The latter, which is proportional to  $R\hat{B}^A$  represents about 13% of the resonance cross section. Figure 24 shows again the mean observed sphericity over the full energy range including

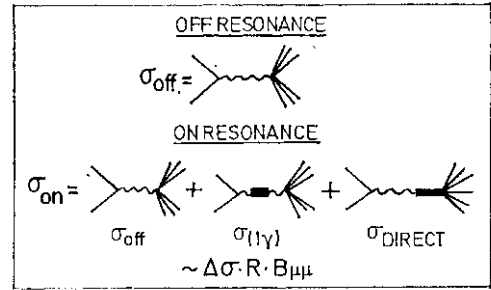


Fig. 23. Off and on resonance contributions to the annihilation cross section.

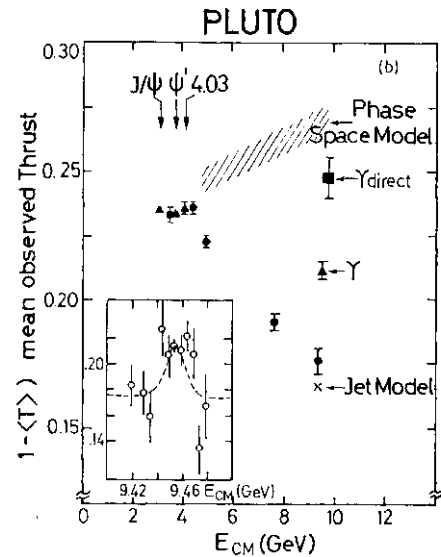


Fig. 24. PLUTO Collaboration: Observed mean sphericity of charged particles (>4 prongs) including the Y region. Values without (Y) and with (Y direct) subtraction of nondirect terms.

now the  $T$  region. We notice a strong rise of the sphericity as we go across the resonance (inset of the figure). This increase gets even more pronounced if we extract the direct decay terms as indicated above.

This value comes in fact very near to the value predicted by Hagiwara assuming a three gluon jet decay of the Ypsilon ('QCD' prediction).<sup>70</sup> Note however that in terms of sphericity there is only very little difference between the phase space and the QCD prediction.

The features of these data change very little if we take thrust instead of sphericity. Figure 25 shows a distribution of  $(1 - \text{the mean observed thrust})$  over the same energy range. Again there is a dramatic change of topology in the  $T$  region and the direct term gets very close to the QCD prediction by Koller, Walsh and Krasemann<sup>71</sup> of  $\langle T \rangle = 0.75$ . However,

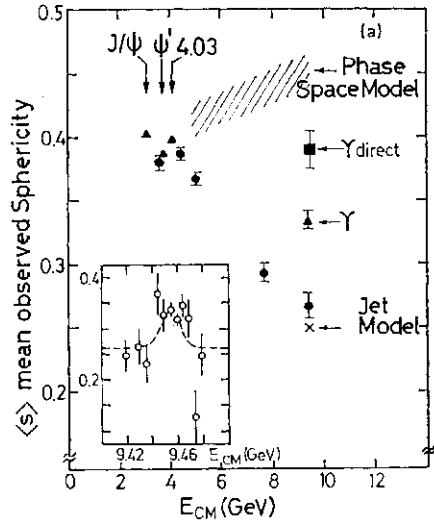


Fig. 25. PLUTO Collaboration: (1-observed mean thrust) of charged particles ( $>4$  prongs) including the  $Y$  region. Values without ( $Y$ ) and with ( $Y$  direct) subtraction of nondirect terms.

the value is again very close to the phase space prediction.

The fact that the QCD and phase space predictions are so similar may be surprising at first sight, since one expects isotropic events in phase space and disc-like events in QCD. However, at the low multiplicities encountered here phase space is not at all isotropic and the definition of sphericity and thrust always tends to find a planar structure in the events. On the other hand we are dealing with 3 GeV gluon jets in QCD which may be very broad jets and hence the disc structure is smeared out. These features have been discussed in detail by G. Alexander in the parallel session.<sup>68</sup> Note also that the sphericity and thrust values are

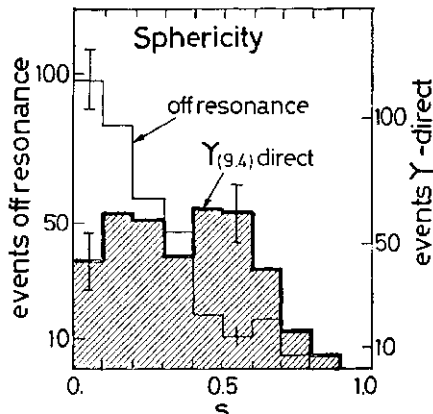


Fig. 26. DESY-Hamburg-Heidelberg-Munchen Collaboration: Observed sphericity distribution for events on and off resonance in the  $Y$  region. The sphericity is defined from the measured shower energies.

not corrected for acceptance and one has to be cautious in comparing them directly with the prediction. Acceptance corrections are however not expected to be very large.

The previous two figures showed a strong change of events topology in the charged energy flow. Figure 26 shows a complementary observation of the DESY-Heidelberg 2 group who have measured the distribution of the neutral sphericity and compared the differential sphericity off and on resonance.<sup>62</sup> A striking difference is seen in the two distributions, the mean value changing from  $\langle S \rangle = 0.19$  to  $\langle S \rangle = 0.37$  with an error of 0.02 which is again very close to the QCD prediction of  $\langle s \rangle = 0.4$ .<sup>70</sup>

*ILLC.5 Other properties of events in the Ypsilon region*

A surprising observation<sup>72</sup> which all three groups agree on is the relatively small change in mean multiplicity as one passes from the continuum to the resonance. Figure 27 shows the distribution of observed charged multiplicity on and off resonance for the DESY-Heidelberg 2 detector. The mean charged multiplicity changes from 6.4 off resonance to 7.3 on resonance (error 0.2) including the correction for non direct terms.<sup>62</sup> A very similar increase of about one unit is also found by the PLUTO<sup>63</sup> and the DASP 2 Collaborations.<sup>61</sup>

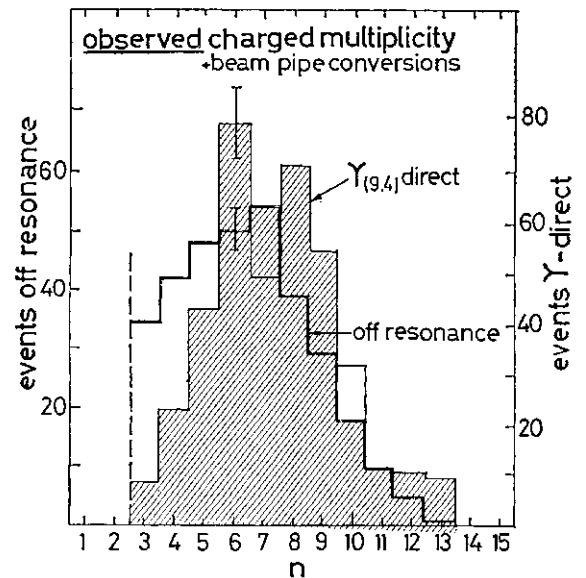


Fig. 27. DESY-Hamburg-Heidelberg-Munchen Collaboration: Observed charged multiplicity (including beam pipe conversion) on and off resonance in the  $Y$  region.

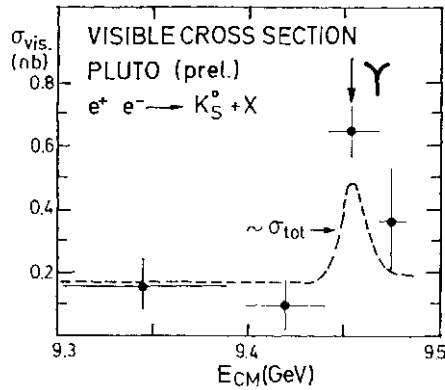


Fig. 28. PLUTO Collaboration: Visible cross section for inclusive  $K_S^0$  production in the  $Y$  region. The trend of the total cross section is indicated by a dashed line.

The last piece of information I want to mention is from the PLUTO group who measured the inclusive  $K^0$  production in the 9.5 GeV energy region.<sup>63</sup> Their result for the visible cross section is displayed in Fig. 28 as a function of energy. For comparison the total cross section is indicated by a dashed curve in the same figure with arbitrary normalization.

The comparison shows that the  $Kg$  production follows about the trend of the total cross section. Quantitatively the comparison of on and off resonance cross sections yields a ratio of  $4.0 \pm 1.7$  for  $K^0$  production, whereas it is about 2.5 for the total cross section. They conclude therefore that there is no significant change of  $Ks$ 's produced per event if one goes through the resonance region.

### III.C.6 Ypsilon summary

In summary we have seen that the  $T$  is produced in  $e^+e^-$  annihilation with a mass of  $9.46 \pm 0.01$  GeV, a leptonic width of  $r_{ee} = 1.2 \pm 0.2$  keV, a branching ratio  $\mathcal{B} = 2.6 \pm 1.4\%$  and a total width of more than 25 keV (best value 50 keV). These parameters strongly suggest that the Ypsilon is a quark-antiquark bound state with a quark charge of  $-1/3$ . Further observations in the resonance region are:

a considerable change of topology from a 2 jet structure outside the resonance to a more isotropic structure at the  $T$ , a small increase of the charged multiplicity by about 1 unit as one goes from off to on resonance and no large change of the  $Ks$  content per event. A quantitative analysis of the change of topology in terms of thrust and sphericity shows that the change in the  $T$  region is about as expected from QCD (change from a 2 quark jet to a 3 gluon jet structure). However, the proximity of phase space does not yet allow a firm conclusion on the existence of gluon jets.

### III.C.7 Ypsilon prime

During the last weeks before the Conference the DASP 2<sup>81,73</sup> and the DESY-Heidelberg 262,74 groups proceeded into the region of 10 GeV to search for the first excitation in the  $T$  family ( $Y'$ ) suggested by the data of the Columbia-Fermilab-Stony Brook Collabora-

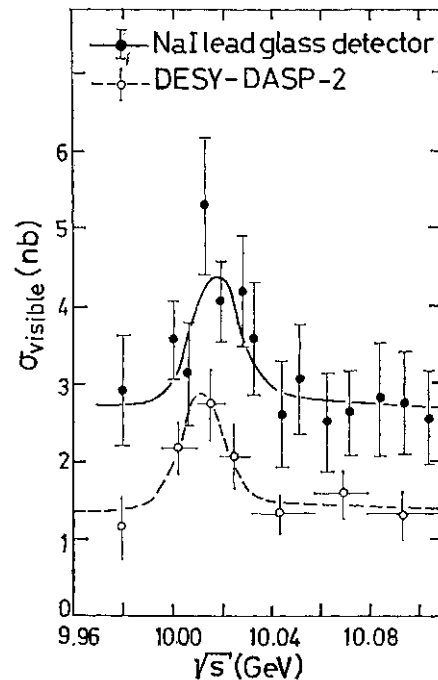


Fig. 29. DASP 2 and DESY-Hamburg-Heidelberg-Munich Collaborations: Evidence for the  $Y'$  in  $e^+e^-$  annihilation.

Table V. Results on  $Y$  (10.02)

	$M(Y')$ (GeV)	$M(Y') - M(Y)$ (MeV)	$\Gamma_{ee}(Y')$ (keV)	$\frac{\Gamma_{ee}(Y')}{\Gamma_{ee}(Y)}$
DASP II	$10.012 \pm 0.020$	$555 \pm 11$	$0.35 \pm 0.14$	$4.3 \pm 1.5$
D-H II	$10.02 \pm 0.02$	$560 \pm 10$	$0.32 \pm 0.13$	$3.3 \pm 0.9$
Mean	$10.016 \pm 0.020$	$558 \pm 10$	$0.33 \pm 0.10$	$3.6 \pm 0.8$

$$M(Y') - M(Y) < M(\phi') - M(J/\psi)$$

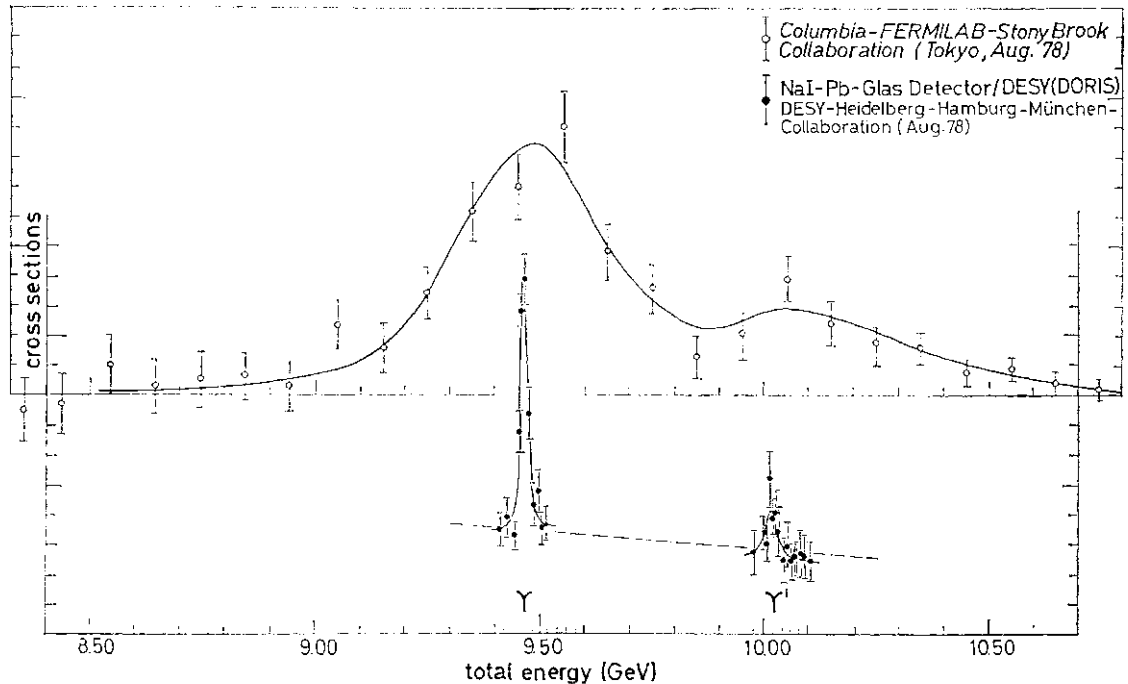


Fig. 30. Columbia-Fermilab-Stony Brook and DESY-Hamburg-Heidelberg-München Collaborations: The  $T$  family in hadronic and  $e^+e^-$  reactions.

tion. Figure 29 shows their result. There is a resonance structure around 10.02 GeV with a width compatible with the resolution of the  $e^+e^-$  machine DORIS. In Table V the parameters of the  $Y'$  as found by the two groups are compiled together with the mean values. The first surprising feature of these data is the relatively low mass difference between  $Y$  and  $Y'$ . Figure 30 compares the FNAL and DESY data. The value is lower than the one suggested by the Columbia-Fermilab-Stony Brook Collaboration and in particular  $M(Y') - M(Y) = 558 \pm 10$  MeV is smaller than  $\Delta M(\langle p \rangle) = 590 \pm 10$  MeV. This value for the mass difference gives increasing evidence for the existence of a second existed state ( $QT''$ ) below threshold.<sup>56,57</sup> As we heard in J. Rosner's talk the low value of  $r_{cc}$  at the  $Y'$  eliminates the last doubt about the identity of the component quark.<sup>75</sup> It is the 'beauty' quark with a charge of  $-1/3$ .

#### IV. Conclusion

To conclude let me return to Fig. 1. We heard in the preceding talk that there is overwhelming evidence now for the existence of a new heavy lepton and most probably also for its own neutrino. If we look into the quark sector symmetry seems to prevail. In addition to the charm quark there is now

ample evidence for the existence of a new heavy quark which is most probably of the 'beauty' type. To answer the question whether a 6th quark  $t$  would constitute perfect symmetry between leptons and quarks again our answer can now only be:

PETRA works and CESR and PEP will follow soon!

#### Acknowledgement

I am indebted to L. Montanet, V. Hepp, B. French, J. Six, B. Pietrzyk, D. Treille, Chan Houg-Mo, H. Hogaasen, and V. Hungerbühler for many discussions and hints on the subjects of chapter II. I also want to express my gratitude to G. Feldman, G. Alexander, J. Bienlein, R. Devenish, G. Heinzelmann, K. Koller, H. Meyer, G. Mikenberg, H. Rubinstein, W. Schmidt-Parzefall, B. Stella, H. Spitzer, T. Walsh, G. Wolf, and all my colleagues at DESY who helped me in the preparation of this talk. I am particularly grateful to my scientific secretaries Y. Sumi and H. Suda for their continuous support during the Conference.

#### References

1. J. J. Aubert *et al.*: Phys. Rev. Letters **33** (1974) 1404; J.-E. Augustin *et al.*: Phys. Rev. Letters **33** (1974) 1406.

2. M. L. Perl *et al.*: Phys. Rev. Letters 35 (1975) 1489; M. L. Perl *et al.*: Phys. Rev. Letters 38 (1976) 117; PLUTO Collaboration, J. Burmester *et al.*: Phys. Letters 68B (1977) 297 and 301.
3. S. W. Herb *et al.*: Phys. Rev. Letters 39 (1977) 252; W. R. Innés *et al.*, Phys. Rev. Letters 39 (1977) 1240.
4. G. Feldman: this Conference.
5. R.J. Cashmore: this Conference.
6. R. Sosnowski: this Conference.
7. Recent reviews, V. Hepp: Frühjahrstagung der DPG, Heidelberg (unpublished); K. Hidaka: ANL-HEP-CP-78-15 (March 1978).
8. Recent reviews, L. Montanet: *Proc. Vth Int. Conf. Exp. Meson Spectroscopy (Boston, April 1977)* and *XIII Rencontre de Moriond, (Les Arcs, 1978)*; C. Rosenzweig: APS Meeting, Argonne (October 1977), also issued as preprint COO-3533-106; K. Kilian and B. Pietrzyk: *7th Int. Conf. High Energy Physics and Nuclear Structure (Zurich, 1977)*.
9. A. A. Carter *et al.*: Phys. Letters 67B (1977) 117 and 122.
10. A. A. Carter: Rutherford Lab. report RL-78 032 (1978).
11. R. S. Dulude *et al.*: submitted to Phys. Letters.
12. C. Evangelista *et al.*: Contribution to this Conference (No. 521).
13. A. S. Carroll *et al.*: Phys. Rev. Letters 32 (1974) 247.  
V. Chaloupka *et al.*: Phys. Letters 61B (1976) 487.  
W. Brückner *et al.*: Phys. Letters 67B (1977) 222.
14. S. Sakamoto *et al.*: Contribution to this Conference (No. 1058).
15. L. Montanet: *loc cit.* (réf. 8).
16. J. L. Rosner: Phys. Rev. Letters 21 (1968) 950.
17. P. G. O. Freund, R. Waltz and J. L. Rosner: Nucl. Phys. B13 (1969) 237.
18. Y. Hara: this Conference.
19. C. Evangelista *et al.*: Phys. Letters 70B (1977) 373, 72B (1977) 139.
20. J. Six: this Conference.
21. P. Benkheiri *et al.*: Phys. Letters 68B (1977) 483.
22. A. W. Key *et al.*: Contribution to this Conference (No. 220).
23. D. R. Green *et al.*: Contribution to this Conference (No. 810).
24. P. Söding: this Conference.
25. R. L. Jaffe: Phys. Rev. Letters 38 (1977) 195.
26. I. P. Auer *et al.*: Contribution to this Conference (No. 447).
27. A. Yokosawa: this Conference.
28. H. Ikeda *et al.*: Contribution to this Conference (No. 625).
29. B. A. Shabazian *et al.*: Contribution to this Conference (No. 143).
30. O. Braun *et al.*: Nucl. Phys. B124 (1977) 45 with further references.
31. M.S. Alam *et al.*: Contribution to this Conference (No. 554 and 1067).
32. T. A. Armstrong *et al.*: Contribution to this Conference (No. 608).
33. H. Suura, T. F. Walsh and B. L. Young: Lettere Nuovo Cimento 4 (1972) 505.
34. H. J. Besch *et al.*: submitted to Phys. Letters.
35. L. Paoluzzi *et al.*: Lettere Nuovo Cimento 10 (1974) 435; A. Duane *et al.*: Phys. Rev. Letters 32 (1974), 425.
36. H. Fritzsche and P. Minkowski: Nuovo Cimento 30A (1975) 393; E. Pelaguier and F. M. Renard: Nuovo Cimento 32A (1976) 421.
37. DASP Collaboration, W. Braunschweig *et al.*: Phys. Letters 67B (1977) 243 and 249; S. Yamada: Hamburg Conference (1977).
38. Recent reviews, G. Goldhaber: Budapest Conference (1977); G. Feldman: Banff Summer Institute, Alberta (CA) (Sept. 1977); H. Schopper: DESY-report 77/79 (1977); B. H. Wiik and G. Wolf: DESY-report 78/23 (1978).
39. W. D. Apel *et al.*: Phys. Letters 72B (1978) 500.
40. J. Olsson: Hamburg Conference (1977).
41. W. Bartel *et al.*: DESY 78/49 (1978), submitted to Phys. Letters.
42. C. J. Biddiek *et al.*: Phys. Rev. 38 (1977) 1324; see also H. F. W. Sadrozinsky: Hamburg Conference (1977).
43. W. Tannenbaum *et al.*: Phys. Rev. Letters 35 (1975) 1323.
44. PLUTO Collaboration, V. Blobel: XII Rencontre de Moriond, Flaine, 1977 and V. Blobel: private communication.
45. DASP Collaboration, W. Braunschweig *et al.*: Phys. Letters 57B (1975) 407; S. Yamada: Hamburg Conference (1977).
46. DASP Collaboration, R. Brandelik *et al.*: Phys. Letters 70B (1977) 132.
47. G. Mikenberg: this Conference; DASP Collaboration, R. Brandelik *et al.*: submitted to Phys. Letters.
48. J. Kirz: this Conference.
49. DASP Collaboration, R. Brandelik *et al.*: Phys. Letters 76B (1978) 361.
50. PLUTO Collaboration, J. Burmester *et al.*: Phys. Letters 66B (1977) 395.
51. D. Luke: Meeting of the APS, Argonne, October, 1977; also issued as SLAC-PUB-2086 (Febr. 1978).
52. G. Feldman and D. Hitlin: private communication.
53. D. Hitlin: this Conference.
54. G. Mikenberg and D. Hitlin: private communication.
55. S. W. Herb *et al.*: Phys. Rev. Letters 39 (1977) 252. W. R. Innés *et al.*: Phys. Rev. Letters 39 (1977) x240.
56. L. Lederman: this Conference.
57. T. Yamanouchi: this Conference.
58. PLUTO Collaboration, Ch. Berger *et al.*: Phys. Letters 76B (1978) 243.
59. C. W. Darden *et al.*: Phys. Letters 76B (1978) 246.
60. e.g., K. Gottfried: Hamburg Conference (1977).
61. W. Schmidt-Parzefall: this Conference.
62. G. Heinzelmann: this Conference.



63. H. Spitzer: this Conference.
64. *e.g.*, A. de Rujula, J. Ellis, E. G. Floratos and M. K. Gaillard: Nucl. Phys. **B138** (1978) 387.
65. J. D. Bjorken and S. J. Brodsky: Phys. Rev. D1 (1970) 1416.
66. G. Hanson *et al.*: Phys. Rev. Letters **35** (1975) 1609; G. Hanson: XIII Rencontre de Moriond, Les Arcs (1978) and SLAC-PUB 2118 (1978).
67. S. Brandt, Ch. Peyrou, R. Sosnowski and A. Wroblewski: Phys. Letters **12** (1964) 57; E. Fahri: Phys. Rev. Letters **39** (1977) 1587.
68. PLUTO Collaboration, Ch. Berger *et al.*: DESY 78/39 (1978) to be published in Phys. Letters; G. Alexander: this Conference.
69. R. D. Field and R. P. Feynman: Nucl. Phys. **B136**(1978)1.
70. K. Hagiwara: Nucl. Phys. **B137** (1978) 164.
71. K. Roller, H. Krasemann and T. F. Walsh: DESY 78/37 (1978); K. Roller: this Conference.
72. S. J. Brodsky, D. G. Coyne, T. A. de Grand and R. R. Horgan: Phys. Letters **73B** (1978) 203.
73. C. W. Darden *et al.*: DESY 78/44 (1978), submitted to Phys. Letters.
74. J.K. Bienlein *et al.*: DESY 78/45 (1978; submitted to Phys. Letters.
75. J. L. Rosner, C. Quigg and H. B. Thacker: Phys. Letters **74B** (1978) 350; J. L. Rosner: this Conference.

R. J. CASHMORE

Department of Nuclear Physics, University of Oxford, Keble Road, Oxford

§1. Introduction

In this review I will deal with the hadronic states of the light (u, d and s) quarks. I will not deal with baryonium or dibaryon systems<sup>1</sup> but will concentrate on the  $B=0$  and  $B=1$  states, the conventional mesons and baryons.

In order to put the mass of information in perspective some framework is required. This will be the simple SU(6) quark model.<sup>2</sup> The status of accepted supermultiplets will be reviewed first and then evidence for new multiplets discussed. Wherever possible attempts will be made to emphasize the physical insights that can be obtained from light quark hadrons and which are relatively inaccessible in the heavy quark hadrons, e.g., glueballs<sup>3</sup> and multi-quark states.<sup>4</sup>

§2. The Mesons

(i) The quark-antiquark model

The mesons are obtained from a qq system where the quarks are spin 1/2 fermions. We obtain 36 states which have the SU(6) structure

$$6 \times 6 - 1 + 35$$

where each SU(6) multiplet can be broken down to give the following SU(2) x SU(3) multiplets:

$$1 = {}^0 1, \\ 35 = {}^0 8; \quad {}^1 8, \quad {}^1 3$$

where the notation is <sup>s</sup>[SU(3) multiplet] and S is the spin of the qq system, i.e., we have a nonet of spin 0 mesons and a nonet of spin 1 mesons.

If we now give the qq system an internal orbital angular momentum L we arrive at states with the following quantum numbers:

$$J = L + S, \\ P = (-1)^{L+1}, \\ C = (-1)^{L+S}.$$

In general there will be 4 nonets associated with each L value (except for L=0 where we have only 2).

Finally we can also give the quarks some

degree of radial excitation so that we expect multiplets to be repeated at higher masses. If a particular potential is assumed, i.e., simple harmonic oscillator, then we have the following prediction for multiple masses

$$M_{oc}(2n+L)K = NK$$

where n is the radial degree of excitation. A different potential would lead to different mass values.

This situation is summarized in Fig. 1 where the  $J^PC$  values are noted for each multiplet and the well known states are included.

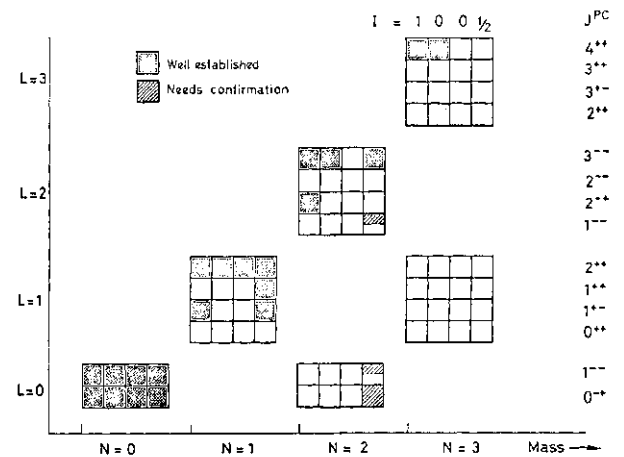


Fig. 1. The expected meson spectrum containing observed states.

(ii) N=0 states

In this multiplet all of the states are well known and the only new information is concerned with the electromagnetic properties of the vector mesons. A new measurement of

$$\rho \rightarrow \pi\gamma$$

has been made<sup>5</sup> giving a width of 50+10 keV which is in better agreement with the theoretical result of >60keV<sup>6</sup> (the previous experimental value was 35+10keV). Also new values have been presented for the  $K^{*0}$  and  $K^{*+}$  masses<sup>7</sup> which are different from the values compiled by the PDG.<sup>8</sup> In the case of the  $K^{*0}$ , the biggest change, the difference is 5-6 standard deviations. This results in a  $K^{*}$

electromagnetic mass difference of

$$\Delta M = M_{K^{*0}} - M_{K^{*-}} = 1.5 \pm 1.5 \text{ MeV}$$

which is consistent with theoretical calculations<sup>9</sup> of

$$\Delta M \leq 1.9 \text{ MeV.}$$

This result is in conflict with recent high statistics spectrometer data<sup>10</sup> and needs corroboration.

(hi)  $N=l$  states

$2^{++}$  mesons:

These are all well identified and the only new information at this Conference is an upper limit for the electromagnetic decay of the

$$\Gamma(A_2^- \rightarrow \pi\gamma) \leq 60 \text{ keV}$$

which is in conflict with theoretical estimates of 300-1000 keV obtained by VDM methods from the decay  $A \rightarrow \rho n$

$7^{++}$  mesons \

There is now good evidence for the existence of a strange meson ( $Q_s$ ) belonging to this nonet<sup>11,12</sup> and the situation is becoming clearer as concerns the other states, the A1, D and E.

$I=1$ , AL There are now many independent analyses<sup>13-15</sup> of the diffractively produced  $3n$  system, which all require a resonance in order to fit the mass spectrum. However there is no agreement on the mass and width of the state due, presumably, to the different theoretical approaches taken:

$$M_{A1} \sim 1200-1400 \text{ MeV,}$$

$$\Gamma \sim 300 \text{ MeV.}$$

Furthermore there is evidence<sup>16</sup> for the production of a 3% enhancement with  $J=l^+$  in the reaction

$$K^- p \rightarrow \Sigma^- (\pi\pi\pi)^+$$

at small momentum transfers from K to 2- If interpreted as a resonance the following mass and width are obtained

$$M_{A1} \sim 1040 \text{ MeV,}$$

$$\Gamma \sim 230 \text{ MeV.}$$

$\tau$  decay is a further source of information on the axial  $3TZ$  system and Feldman<sup>17</sup> has shown evidence that in the decay

$$\tau^- \rightarrow \nu\pi^- \pi^+ \pi^-,$$

the  $3TZ$  system is predominantly  $Ttp$  in the state  $J^P=l^+$ . Again if interpreted simply as a

Breit-Wigner resonance this gives

$$M \sim 1100 \text{ MeV}$$

$$\Gamma \sim 400 \text{ MeV}$$

but analyses of such data by Basdevant and Berger<sup>18</sup> give a mass and width consistent with the results from the diffractive  $3TT$  states.<sup>14</sup>

Finally the SU(3) analyses of the decay couplings of the  $B$ ,  $Q_s$ ,  $Q_2$  and A1<sup>19,20</sup> present a coherent picture.

Thus in summary the evidence for the A1 is now strong and the only problem seems to be a precise measurement of the mass and width. The true picture will, however, only become apparent when all available data are analysed within the same framework.

$I=0$  D meson. Very clear evidence<sup>21</sup> for the observation of this state in the reaction

$$\pi^- p \rightarrow \pi^+ \pi^- \eta n$$

is shown in Fig. 2. A partial wave analysis<sup>22</sup> of the  $\pi\eta\eta$  state has been made leading to the decomposition of the  $J^P=l^+$  wave shown in

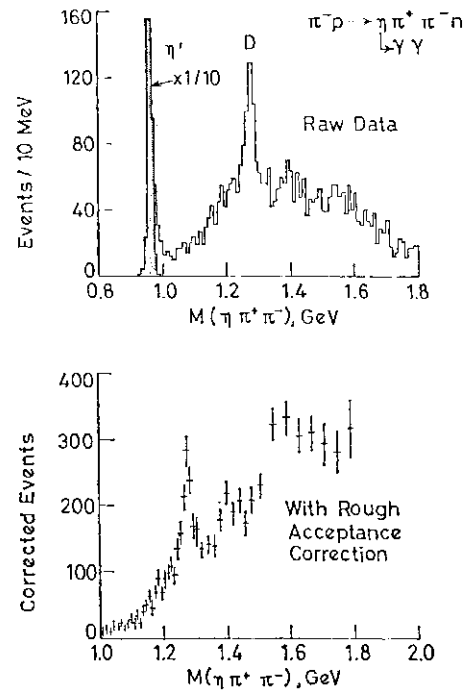


Fig. 2. The D meson in  $D \rightarrow \pi\pi\eta$ .

Fig. 3. The amplitude and phase variation of the  $I=0$ ,  $J^P=l^+$   $7i8$  wave are unambiguous evidence for the assignment of the D meson. (The possible assignment of this state as a  $2^{++}$  glueball is clearly ruled out<sup>23</sup>). The mass and width of the D are

$$M_D = 1276 \pm 3 \text{ MeV}$$

$$\Gamma_D = 15-30 \text{ MeV}$$

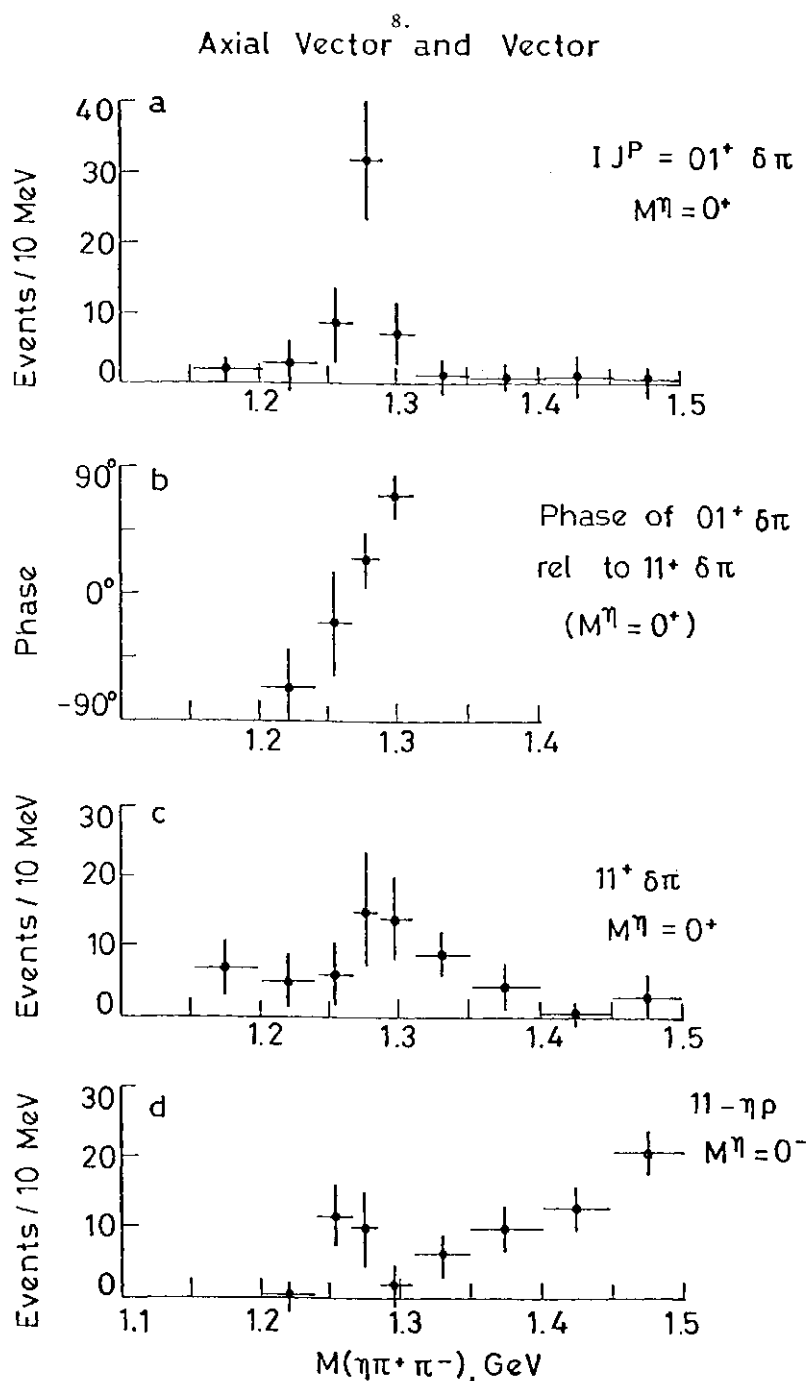


Fig. 3. The axial vector and vector partial wave amplitudes in the  $n\pi$  system.

$I=0$   $E$  meson. The evidence<sup>24</sup> of Fig. 4 demonstrates that this state is now well established and we require an unambiguous spin parity measurement. This is relevant as it could be located either in this  $1^+$  multiplet or possibly in a  $0^-$  multiplet. (This will be discussed later.) The mass and width are

$$M_E = 1431 \pm 3 \text{ MeV}$$

$$\Gamma_E = 26 \pm 8 \text{ MeV}$$

This latter value is rather small when compared with SU(3) predictions for a  $1^{++}$  state

but as it is rather near  $KK^*$  threshold it would be premature to regard this as evidence against a  $1^{++}$  assignment.

*mesons.* The  $B$  and  $Q_B^{n\pi 2}$  are comparatively well established but there are still no candidates for the  $I=0$  members which should lie in the region of 1000-1300 MeV.

$0^+$  scalar mesons. These are of particular interest because it is in this  $J^{PC}$  state that we might expect the first evidence for glueballs<sup>3</sup> or multiquark states<sup>4</sup> and hence a good identification of the  $qq$  states is essential. As we

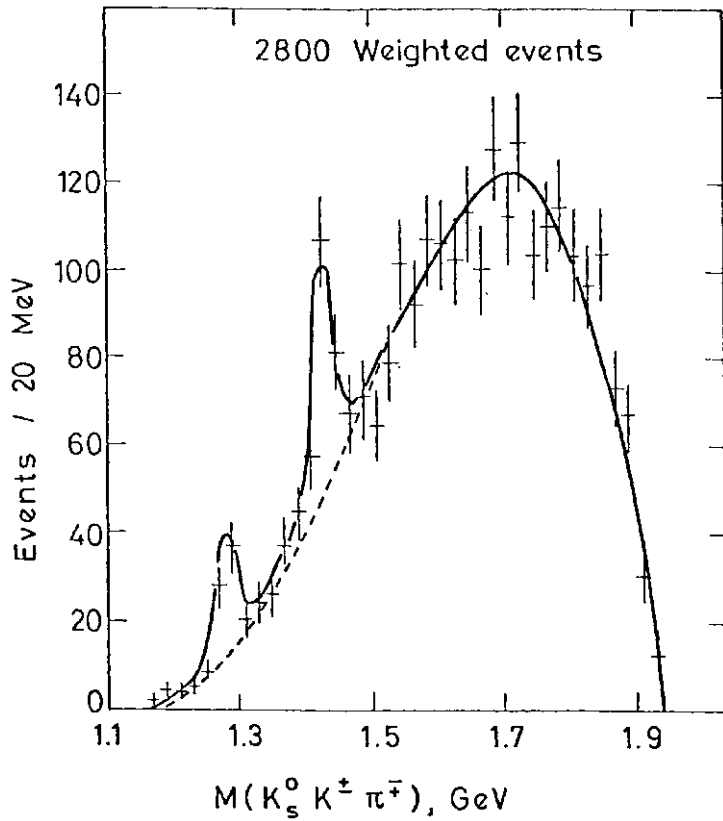


Fig. 4. The observation of the E-meson at 1420 MeV.

shall see no clear picture emerges at present.

The first problem encountered is exactly what states exist.

$I=1/2$   $S=\pm 1$ . Partial wave analysis<sup>25</sup> of high statistics  $KTT$  data together with K-matrix fits<sup>26</sup> to the S-wave amplitude indicate that only one resonance is required with a mass and width

$$M \sim 1500 \text{ MeV,}$$

$$\Gamma \sim 260 \text{ MeV.}$$

In particular there is no need for a low mass  $KTT$  S-wave resonance although presumably a very wide state cannot be ruled out.

$I=1$ : The  $d$  (980) is well known and recent analyses<sup>27</sup> of  $\pi^- p \rightarrow K^0 K^- n$  indicate a possible S-wave resonance at  $\sim 1300$  MeV. However further support for such a state is needed and will only come from joint fits to  $KK$  and  $Tr$  final states.

$I=0$  Here the situation is most confused with data and amplitude analyses available from the reactions<sup>28-32</sup>

- $\pi^- p \rightarrow \pi^+ \pi^- n,$
- $\pi^- p \rightarrow K^+ K^- n,$
- $\pi^- p \rightarrow K_s^0 K_s^0 n,$
- $\pi^+ n \rightarrow K^+ K^- p,$

$$\pi^- p \rightarrow \pi^0 \pi^0 n.$$

There is no question of the existence of the  $S^*$  (998) and a large S-wave amplitude in the region of 1300 MeV (see Fig. 5) which is most probably  $\eta=0^{29}$  in nature rather than  $\eta=1^{30}$ .

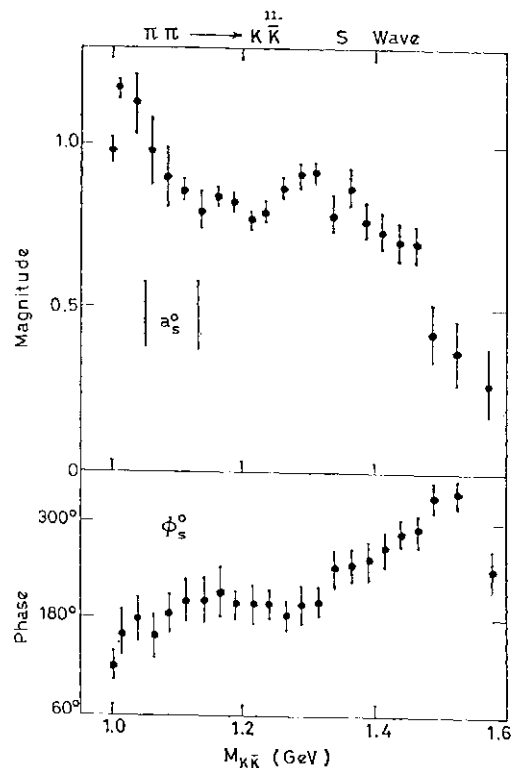


Fig. 5. The  $\pi^- p \rightarrow KK$  S-wave scattering amplitude.

Estabrooks<sup>26</sup> has fitted both  $nn^{\text{TM}}$  and  $KK^{29}$  S-waves and requires the existence of 3 poles

$$\begin{aligned} M_\epsilon &\sim 800 \text{ MeV} & \Gamma_\epsilon &\sim 1000 \text{ MeV}, \\ M_{S^*} &= 1005 \text{ MeV} & \Gamma_{S^*} &\sim 8 \text{ MeV}, \\ M_{\epsilon'} &= 1550 \text{ MeV} & \Gamma_{\epsilon'} &\sim 250 \text{ MeV}. \end{aligned}$$

The  $\epsilon'$  appears at a larger mass than one might expect from studying the  $KK$  S-wave alone and a low mass  $\epsilon$  is also required.

In summary the observed states would appear to be

$$\begin{aligned} I=1/2: & \quad \kappa(1510), \\ I=1: & \quad \delta(980), \quad \delta'(\sim 1300), \\ I=0: & \quad \epsilon(800), \quad S^*(998), \quad \epsilon'(1540), \end{aligned}$$

with the  $\epsilon$  and  $\delta'$  being the most dubious.

*SU(3) assignments.* Since we have more  $0^{++}$  candidates than are required for a nonet we have to investigate various possible assignment schemes for these states in terms of  $qq$ ,  $qqqq$  and glueball states<sup>26</sup>

(a)  $\epsilon$ ,  $\epsilon'$ , 3 and  $tc$  as  $qq$  nonet states

These can be accommodated<sup>26</sup> in a nonet with a mixing angle of  $-21^\circ$ . However there remain two unsatisfactory features;

- (1)  $M_\kappa - M_\delta \sim 4$  ( $M_{\kappa^*} - M_\rho$ ) which is inconsistent with our prejudices.
- (2) the couplings of the  $S^*$  are not consistent with an  $SU(3)$  singlet assignment<sup>26</sup> (as we would expect for a glueball) e.g.,  $g_{\kappa\kappa}/g_{\rho\rho} = 2$  rather than  $\mathbf{A}/2/3$  of an  $SU(3)$  singlet.

(b)  $\delta$ ,  $S^*$  and  $\epsilon$  as  $qqqq$  states

This is the identification argued for by Jaffe<sup>1</sup> and indicated in Table I. Once again this scheme has unsatisfactory features.

Table I. The  $qqqq$   $0^{++}$  Nonet.

Isospin	State	Quark content
0	$\epsilon(800)$	$u\bar{d} \, d\bar{u}$
0	$S^*(998)$	$1/\sqrt{2} \, s\bar{s}(u\bar{u} + d\bar{d})$
1	$\delta$	$u\bar{d} \, s\bar{s}$
1/2	—	$u\bar{s} \, d\bar{d}$

- (1) There is no positive identification of a  $K$  state in the vicinity of 900 MeV.
- (2) We would have to associate the  $\epsilon$  |  $tc$  and  $\delta'$  in an  $SU(3)$   $qq$  nonet predicting another isoscalar in the vicinity of 1350 MeV (having a large width). This would then imply that the  $0^{++}$  states

would have masses larger than the  $1^{++}$ ,  $1^{+}$  and  $2^{++}$  mesons, a feature hard to produce in  $qq$  models.

*Summary.* At present there is no completely successful scheme for the allocation of the scalar mesons and further data on  $Krj$ ,  $nrj$  etc. are of vital importance. The existence of only one  $tc$  state at high masses will continue to present a problem in any scheme. Thus at present there is no compelling evidence for multiquark states or glueballs and the whole situation may well be further confused if the radially excited states ( $N=3$  level) are found at lower masses than might initially be expected (see discussion of  $N=2$  level).

(iv)  $N=2$  states

In this level we are dealing with both the  $L=2$  excitation and the first radial excitation of the  $L=0$  mesons. The well known resonances are the  $3^-$  states:  $g(1680)$ ,  $\omega(1670)$  and  $K^*(1780)$  and the  $2^-$  state:  $A_3(1640)$ . These have to be allocated to the  $L=2$  multiplet. There is evidence for a  $1^-$   $K^*$  at 1700 MeV which can be assigned to either the  $L=0$  or  $L=2$  supermultiplet and analyses of  $K_7T_7T^{\text{TM}}$  indicate the existence of a pseudoscalar state at  $\sim 1400$  MeV which must belong to the radially excited  $L=0$  system. New information has been presented on vector and pseudoscalar mesons at this Conference.

*$1^-$  mesons.* Recent results from DCI and ADONE have been summarized by Feldman.<sup>17</sup> There are indications of two  $J=1$  vector mesons at -1500 and -1650 MeV, and two  $I=0$  states at  $\sim 1660$  and -1750 MeV. The latter do not show any preference for  $K$ 's in the final states and so are assumed to be  $\omega$  like states rather than  $\langle f \rangle$ . While these states are desperately in need of confirmation (the  $I=0$  states appear to be somewhat narrow) they are all required at the  $N=2$  level.

*$0^-$  mesons.* The partial wave analysis of the  $\{Tm\}$  system<sup>22</sup> also shows tentative evidence (see Fig. 6) for a resonance in the  $0^{++} TT\bar{O}$  system, both in amplitude and phase variation

$$M \sim 1260 \text{ MeV},$$

$$\Gamma \sim 100 \text{ MeV}.$$

Clearly this needs thorough investigation and further confirmation but it would have to be assigned as a radial excitation ( $37'$ ) joining the

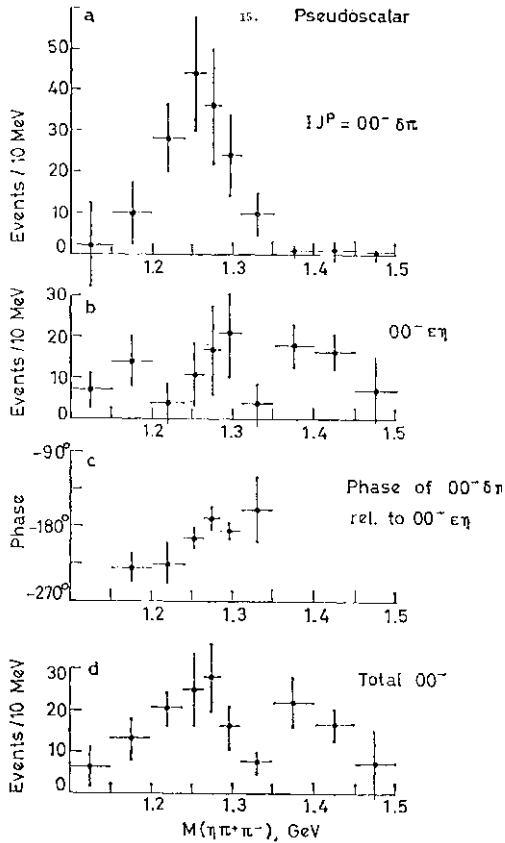


Fig. 6. The pseudoscalar partial wave amplitude in the  $K\pi\pi\pi$  system.

$K\pi\pi\pi$  state of mass 1400 MeV.<sup>33</sup>

*Summary.* There remain a lot of states to be identified at this level but there appears to be an improvement particularly in the radial excitations. The pseudosalar states need confirmation and the existence of an  $I=1$   $0^-$  will only be revealed by careful analyses of the  $0^-$   $3K$  system similar to those applied in the case of the  $1^+$  system. The question of the spin parity of the E meson is also relevant as this could be the remaining  $I=0$  pseudoscalar. Finally if the radial excitations have been identified then they appear at a somewhat lower mass than the  $L=2$  states (cf., the Roper P11 (1470) baryon resonance which also appears at lower masses). This would of course be consistent with potentials (e.g., Coulomb) other than simple harmonic oscillator.

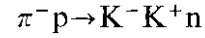
(v)  $N=3$  level

At this level only the  $I=0$  h(2040) and  $I=1$  (1950) resonances have been observed and there is a debate over the existence of an A4 resonance (analogous to the A1, A3 situations). Confirmation of the  $I=1$  state has been presented to this Conference,<sup>34</sup> although

higher statistics would be desirable.

(vi)  $N=4$  level

Analysis of the reaction<sup>35</sup>



seems to indicate an excess of events at high KK mass as shown in Fig. 7. If this excess is interpreted as a resonance it would have

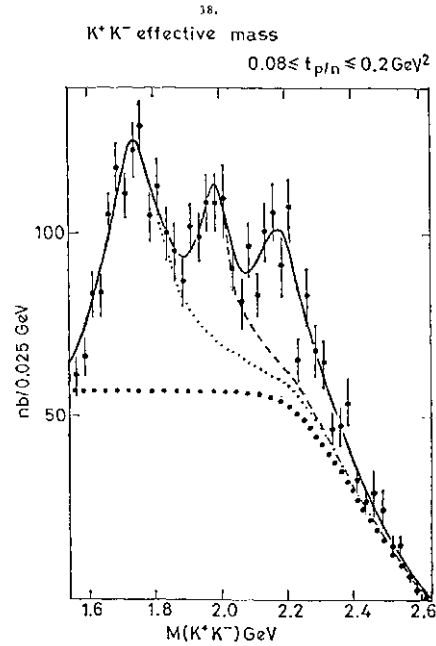


Fig. 7. The observation of a new meson at 2.21 GeV in the KK system (in addition to the g and h mesons).

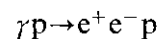
$$M \sim 2210 \text{ MeV,}$$

$$\Gamma \sim 280 \text{ MeV.}$$

Unfortunately no reliable spin measurement exists but if it is assumed to be spin 5 (the most conspicuous) it would have to belong to the  $N=4$  level.

(vii) *Conclusions*

In Fig. 8 I show the spectrum of observed states at the time of this Conference and we see that the  $N=0, 1$  and  $2$  levels are beginning to be filled out (although the scalars are not clearly assigned I have included them in this figure). The scalar mesons still present a problem and remain the most likely candidates for multiquark states although the evidence for them or glueballs is not compelling. There remains a possible vector state  $\sim 1100 \text{ MeV}$ <sup>36</sup> seen in



by interference with the Bethe-Heitler produc

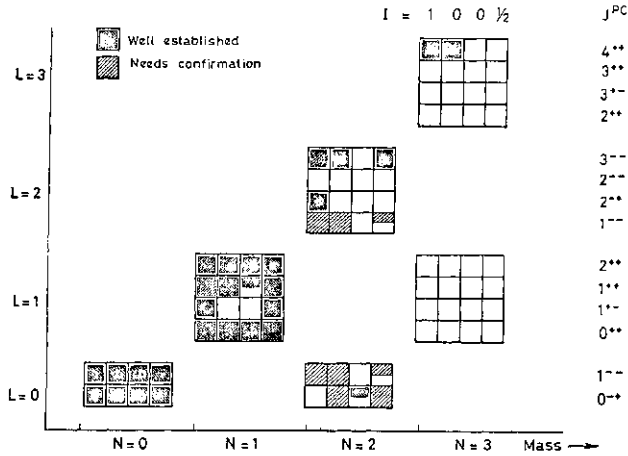


Fig. 8. The meson spectrum containing well established and tentative studies.

tion. No sensible assignment of this state exists.

Finally the improvements in our knowledge of the meson spectrum are due to the analysis of high statistics experiments and we can look forward to a similar improvement with the advent of new high statistics experiments at high energies from the SPS.<sup>34,37</sup>

§3. The Baryons

(i) The qq̄q model

The baryons are obtained from a three quark system requiring the wave function to

be symmetric<sup>38,39</sup> (correct antisymmetric wave functions are then obtained via the colour degree of freedom). Thus in SU(6) we expect

$$6 \times 6 \times 6 = 20 + 70 + 70 + 56$$

and the SU(6) multiplets of interest have the following SU(3) X SU(2) decomposition.

$$\begin{matrix} \underline{70} & {}^2 1, {}^2 8, {}^4 8, {}^2 10 \\ \underline{56} & {}^2 8, {}^4 10. \end{matrix}$$

[The 20 is ignored as it does not couple to N, KN systems and hence is not expected to be observed. Furthermore there is no evidence for the existence of states belonging to such a multiplet].

Finally the physical states are obtained by introducing internal degrees of excitation in the three quark system, either radial or orbital in nature, and are denoted by

$$[SU(6), L^*]$$

where L is the orbital angular momentum and P the parity of the system. Table II and III contain the states of positive and negative parity that might be expected in each supermultiplet together with the number of N, J, A and I states. These are included as the most significant data in baryon spectroscopy is obtained using TTN (S=0) and KN (S=-1)

Table II. Even parity supermultiplets.

Super-multiplets	SU(3)	J <sup>P</sup>	N	A	A	Σ
[56, 0 <sup>+</sup> ]	8	1/2 <sup>+</sup>	1		1	1
	10	3/2 <sup>+</sup>		1		1
			1	1	1	2
[70, 0 <sup>+</sup> ]	1	1/2 <sup>+</sup>			1	
	8	1/2 <sup>+</sup> , 3/2 <sup>+</sup>	2		2	2
	10	1/2 <sup>+</sup>		1		1
			2	1	3	3
[70, 2 <sup>+</sup> ]	1	3/2 <sup>+</sup> 5/2 <sup>+</sup>			2	
	8	3/2 <sup>+</sup> 5/2 <sup>+</sup> ; 1/2 <sup>+</sup> , 3/2 <sup>+</sup> , 5/2 <sup>+</sup> , 7/2 <sup>+</sup>	6		6	6
	10	3/2 <sup>+</sup> 5/2 <sup>+</sup>		2		2
			6	2	8	8
[56, 2 <sup>+</sup> ]	8	3/2 <sup>+</sup> 5/2 <sup>+</sup>	2		2	2
	10	1/2 <sup>+</sup> 3/2 <sup>+</sup> 5/2 <sup>+</sup> 7/2 <sup>+</sup>		4		4
			2	4	2	6
[56, 4 <sup>+</sup> ]	8	7/2 <sup>+</sup> 9/2 <sup>+</sup>	2		2	2
	10	5/2 <sup>+</sup> , 7/2 <sup>+</sup> , 9/2 <sup>+</sup> , 11/2 <sup>+</sup>		4		4
			2	4	2	6



Table III. Odd parity supermultiplets.

Super-multiplet	SU(3)	$J^P$	N	$\Delta$	$\Lambda$	$\Sigma$
[70, 1 <sup>-</sup> ]	1	1/2 <sup>-</sup> , 3/2 <sup>-</sup>			2	
	8	1/2 <sup>-</sup> 3/2 <sup>-</sup> ; 1/2 <sup>-</sup> 3/2 <sup>-</sup> 3/2 <sup>-</sup> 5/2 <sup>-</sup>	5		5	5
	10	1/2 <sup>-</sup> 3/2 <sup>-</sup>		2		2
			5	2	7	7
[56, 1 <sup>-</sup> ]	8	1/2 <sup>-</sup> , 3/2 <sup>-</sup>	2		2	2
	10	1/2 <sup>-</sup> 3/2 <sup>-</sup> 5/2 <sup>-</sup>		3		3
			2	3	2	5
[70, 3 <sup>-</sup> ]	1	5/2 <sup>-</sup> 7/2 <sup>-</sup>			2	
	8	5/2 <sup>-</sup> 7/2 <sup>-</sup> ; 3/2 <sup>-</sup> 5/2 <sup>-</sup> 7/2 <sup>-</sup> 9/2 <sup>-</sup>	6		6	6
	10	5/2 <sup>-</sup> 7/2 <sup>-</sup>		2		2
			6	2	8	8

systems coupling to resonances in the S-channel. We will concentrate on reactions of the type

$$\pi N \rightarrow N^*, \Delta \rightarrow \pi N, \pi \Delta, K \Lambda, \eta N$$

$$\bar{K} N \rightarrow A^*, \Sigma^* \rightarrow \bar{K} N, \pi \Lambda, \pi \Sigma, \pi \Sigma^*(1385),$$

$$\pi A^*(1520),$$

in studying these resonances.

The first observation that can be made from these tables is that an enormous number of states are in principle expected and, furthermore, within any supermultiplet we identify a number of states of the same quantum numbers which implies the possibility of mixing.

The use of a specific quark model (*e.g.*, with SHO forces) gives a specific ordering in mass of these multiplets. Such an ordering is given in Table IV and we see that at the

Table IV. Mass ordering of supermultiplets.

$N$	Supermultiplet
0	[56, 0 <sup>+</sup> ]
1	[70, 1 <sup>-</sup> ]
2	[56, 2 <sup>+</sup> ], [70, 0 <sup>+</sup> ], [70, 2 <sup>+</sup> ], [56, 0 <sup>+</sup> ]'
3	[70, 3 <sup>-</sup> ], [56, 1 <sup>-</sup> ], [70, 1 <sup>-</sup> ]'
4	[56, 4 <sup>+</sup> ], [56, 2 <sup>+</sup> ], [70, 0 <sup>+</sup> ]', [70, 2 <sup>+</sup> ]', [56, 0 <sup>+</sup> ]'
⋮	

$N=2$  level we obtain a large number of supermultiplets. Indeed all quark models will give a low lying [56, 0<sup>+</sup>] and a [70, 1<sup>-</sup>] and it is only at this  $N=2$  level where the details of the interaction really become apparent leading, perhaps, to the absence of multiplets or different mass values. Inspection of Table II also indicates that at this  $N=2$  level the

scope for mixing is immense with states of the same  $J$  appearing in different supermultiplets.

Clearly the observation of a state of specific  $J^P$  is not enough to demonstrate in which multiplet it lies, although there might be some bias from knowing its mass value. Some other means is needed in order to assign states to multiplets or account for the mixing between states. This other means is by measurement of the coupling strengths and relative signs in different reactions

$$\pi N \rightarrow \pi N, \pi \Delta,$$

$$\bar{K} N \rightarrow \bar{K} N, \pi \Lambda, \pi \Sigma, \pi \Sigma^*(1385).$$

These will in general differ from state to state within a supermultiplet and from supermultiplet to supermultiplet. However a specific model is necessary to make predictions and the current most popular model is to use  $SU(6)_w$  and the Melosh transformation.<sup>40</sup> The validity of this approach has been tested for states in the [70, 1<sup>-</sup>] and [56, 2<sup>+</sup>] where approximately 80 coupling strengths in reactions

$$7rN \rightarrow 7rN, \quad 5N, \quad AK, \quad \%A,$$

$$KN \rightarrow KN, \quad TCA, \quad ni, \quad 7^\wedge(1385),$$

have been successfully described.<sup>41</sup> Thus we can conclude that this model is a useful tool in placing states in  $SU(6)$  supermultiplets. However one should always treat this scheme with some degree of skepticism as it might not be correct.<sup>42</sup>

This represents a brief summary of the

standard model of baryons.

(ii) *Exotic baryons*

The standard model does not allow the existence of  $S=+1$  baryon resonances ( $Z^*$ 's). These would have to be obtained as five quark (qqqqq) states. Hence considerable effort has been, and is still, expended in the search for such states.

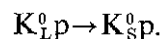
$I=1$   $S=+1$  system. A new partial wave analysis of the  $K^+p$  system has been presented to this Conference.<sup>43</sup> Many of the partial wave amplitudes contain poles, in general rather a long way from the real axis. The best candidate for a resonance is in the  $P13$  ( $J=3/2^+$ ) partial wave with a pole position of

$$(1798-115 \text{ } 0 \text{ MeV})$$

Unfortunately no information is given on the residues and furthermore this resonance would be very inelastic. Analyses of the most prominent inelastic channel<sup>44</sup> do not clearly demonstrate a resonance.

Thus we must await further partial wave analyses which incorporate all of the new data which are currently available.<sup>45</sup>

$I=0$   $S=+/-$  system. Partial wave analyses<sup>46</sup> of  $K^+n$  and  $K^0p$  data have indicated the possible existence of a resonance in the  $P01$  ( $J=1/2^+$ ) partial wave around 1780 MeV. The partial wave solution containing such a resonance was supported by analysis<sup>47</sup> of



New data on this reaction<sup>48</sup> were presented at this Conference, which again support the solution containing a resonance. The true picture will only become apparent when a new partial wave analysis is completed using all the available data.

*Summary.* We are still in the position where the  $Z^*$ 's are struggling for life. Hopefully new partial wave analyses incorporating all new data will allow some resolution of this problem.

(iii) *The present status of [56, 0<sup>+</sup>], [70, 1<sup>-</sup>], [56, 0<sup>+</sup>Y], [56, 2<sup>+</sup>].*

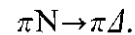
These multiplets are well established and the decays of their states well studied.<sup>41</sup> In Table V are listed the numbers of  $N$ ,  $J$ ,  $A$  and  $I$  states which are known. We immediately see that all the  $N$ ,  $\hat{a}$  states are now known and

Table Y.  $N$ ,  $A$ ,  $A$  and  $I$  states in low lying multiplets.

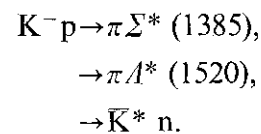
Multiplet	$N, A$	$A$	$\Sigma$
[56, 0 <sup>+</sup> ]	2/2	1/1	2/2
[70, 1 <sup>-</sup> ]	7/7	6/7	5/7
[56, 2 <sup>+</sup> ]	6/6	1/2	2/6
[56, 0 <sup>+</sup> ']	2/2	1?/1	1/2

Notation: Observed/expected.

only the [56, 2<sup>+</sup>] is poorly represented in  $A$  and  $I$  states. The situation has been helped by the unambiguous need for 2 high mass P33 resonances in  $7rN$  partial wave analyses<sup>49,50</sup> of mass -1600 MeV and -1900 MeV. These states are assigned respectively to the [56, 0<sup>+</sup>'] and [56, 2<sup>+</sup>], the former because of the sign of the amplitude in the reaction

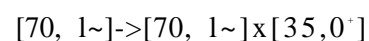


*Decays.* There now exists<sup>51-53</sup> substantial information on the reactions



The first of these reactions is predicted from earlier analyses<sup>41</sup> and the results and comparison shown in Table VI. Some comments are in order. In general the agreement is good. However the prediction for the D05 ( $A, 5/2^-$ ) results from a decoupling of<sup>48</sup> states from  $KN$  (within  $SU(6)$ ) and demonstrates the limitations of the  $SU(6)_w$  scheme (there are no other states with which to mix). Thus we should be wary of arguments that rest heavily on such decoupling theorems. There is a total disagreement for the P03 (1900) ( $A, 3/2^+$ ) which in the spirit of the model has to be accounted for by placing this state in some other multiplet than the [56, 2<sup>+</sup>].

The observation of the decays to  $\chi A^*$  (1520) is examples of



and no analysis of these at present exists.

In summary there has been a large increase in the available data on decays, broadly in agreement with present phenomenology<sup>41</sup> but clearly a rescrutiny of the data and model is required.

**3\*** The information on  $B^*$ 's is meagre and I include here two new results,

(a) A measurement<sup>54</sup> of the spin of the  $B^*$

Table VI. Observed  $K\pi p^* n l^*(1385)$  resonance couplings together with predictions.

Resonance	Status	Elasticity ( $x$ )	Outgoing wave	$t_{\pi\Sigma(1385)}$	Predictions of $t_{\pi\Sigma(1385)}$ from $SU(6)_w \times O(3)$ fits	Branching fraction into $\pi\Sigma(1385)$
S01(1825)	Possible	0.37 $\pm .05$	D	-0.056 $\pm .028$	-0.128	0.008
P03(1900)	Established	0.18 $\pm .02$	P	<0.030	+0.05	—
			F	+0.126 +0.055	-0.100	0.088
D13(1920)	Possible	<0.04	S	-0.068 $\pm .025$	-0.177	<0.109
			D	—	+0.018	—
D05(1830)	Established	0.04 $\pm .03$	D	-0.141 $\pm .014$	0.	0.497
			G	<0.030	0.	—
D15(1775)	Established	0.41 $\pm .03$	D	+0.184 $\pm .011$	+0.115	0.083
			G	<0.030	—	—
F05(1820)	Established	0.57 $\pm .02$	P	+0.167 $\pm .054$	+0.215	0.049
			F	-0.065 $\pm .029$	-0.091	0.007
F05(2100)	Possible	0.07 $\pm .03$	P	-0.071 $\pm .025$	—	0.072
			F	<0.03	—	—
F15(1906)	Established	0.05 $\pm .03$	P	<0.01	-0.035	—
			F	-0.039 $\pm .009$	+0.021	0.030
F17(2040)	Established	0.24 $\pm .02$	F	-0.153 $\pm .026$	-0.127	0.098
			H	—	—	—

(1830) has been made demonstrating  $J=3/2$  as shown in Fig. 9. Unfortunately it is impossible to identify the parity. This result is in agreement with the expected spin parity of  $3/2^-$  estimated from its branching fractions.<sup>41</sup>

- (b) Some tentative evidence<sup>55</sup> for a  $3^*(1680)$  at  $UK$  threshold which also couples to  $AK$ . Unfortunately it is difficult to demonstrate such a resonance unambiguously.

*Summary.* The picture of these multiplets at present appears to be in good shape but more  $A$  and  $I$  states are necessary (a new  $Z^*$  state at  $\sim 1550$  has been presented to this Conference<sup>56</sup> but no spin parity measurement exists). A re-analysis of the decay couplings is clearly needed.

(iv) *Existence of higher spin multiplets*

In Table VIII listed the evidence for higher spin multiplets using only 'good' resonances.

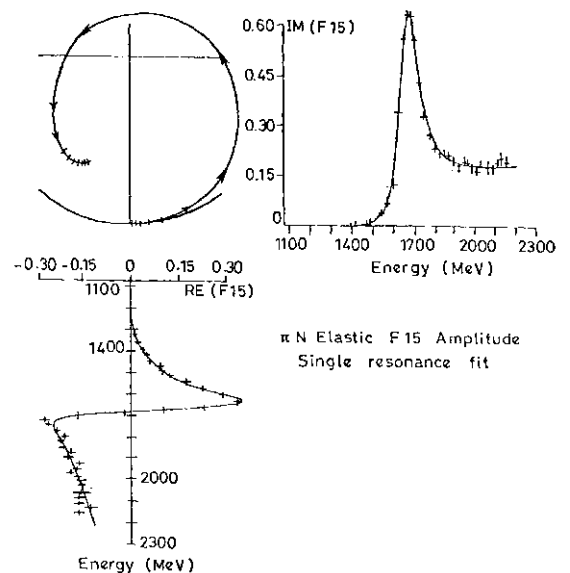


Fig. 9. The moments analysis of  $f^*(1820)$  decay indicating a spin of  $3/2$ .

The information is sparse and mainly from  $N$  and  $A$  states. Also included are states which can be associated with these multiplets but which do have alternative assignments.

Table VII. High spin multiplets.

Multiplet		States	Possible states (with alternative assignments)
[70, 3 <sup>-</sup> ]	N*	7/2 <sup>-</sup> (2190) 9/2 <sup>-</sup> (2200)	5/2 <sup>-</sup> (2230) [70, 1 <sup>-</sup> ]'
	A	7/2 <sup>-</sup> (2215)	5/2 <sup>-</sup> (1900) [56, 1 <sup>-</sup> ]
	A	7/2 <sup>-</sup> (2100)	
[56, 4 <sup>+</sup> ]	N*	9/2 <sup>+</sup> (2200)	7/2 <sup>+</sup> (1970) [70, 2 <sup>+</sup> ]
	A	11/2 <sup>+</sup> (2420)	
[56, 6 <sup>+</sup> ]	N*	13/2 <sup>+</sup> (2612)	
	A	15/2 <sup>+</sup> (2990)	
[70, 5 <sup>-</sup> ]	N*	11/2 <sup>-</sup> (2577)	
[70, 7 <sup>-</sup> ]	A	13/2 <sup>-</sup> (2794)	

The assignment of the A (1900) 5/2<sup>-</sup> to a [70, 3<sup>-</sup>] might be regarded as rather unreliable since its mass is rather low when compared with the other states (a similar argument is true for the N\* (1970) 7/2<sup>+</sup>).

These higher multiplets exist and inspection on Tables II and III indicates that we should expect an enormous number of states above 2 GeV in mass, which will only be unravelled by high statistics precision data in many channels.

(v) *Existence of lower spin multiplets [70, 0<sup>+</sup>], [70, 2<sup>+</sup>], [56, 1<sup>-</sup>] etc.*

In this section I want to critically discuss the evidence for multiplets of the type [70, 0<sup>+</sup>], [70, 2<sup>+</sup>] and [56, 1<sup>-</sup>]. Again I will restrict myself to only 'good' resonances (2<sup>+</sup> in PDG). In particular I will ignore all second resonance fits of the CMU group<sup>44</sup> to their partial wave amplitudes, as Figs. 10 and 11 seem to indicate little qualitative improvement is achieved (the F15 wave is representative of these types of fits). I also use coupling signs and decoupling theorems of SU(6) e.g.,

$$8 \wedge KN,$$

in assigning states. In view of the discussion of 3(iii) concerning the D05 (1830) some skepticism is needed.

7V\*(2100) 3/2<sup>-</sup>. This can be accommodated in a [56, 1<sup>-</sup>] or a radial excitation of the [70, 1<sup>-</sup>], i.e., a [70, 1<sup>-</sup>]'.

The observation of the decay into AK<sup>07</sup> forbids it from lying in a [70, 3<sup>-</sup>].

J(1850) 1/2<sup>+</sup>. This state is the weakest considered but could be assigned

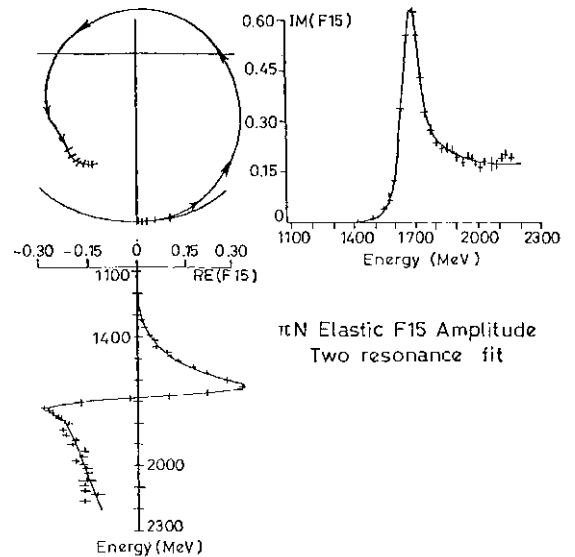


Fig. 10. A single resonance fit to the F15 (S=0) T1N partial wave.

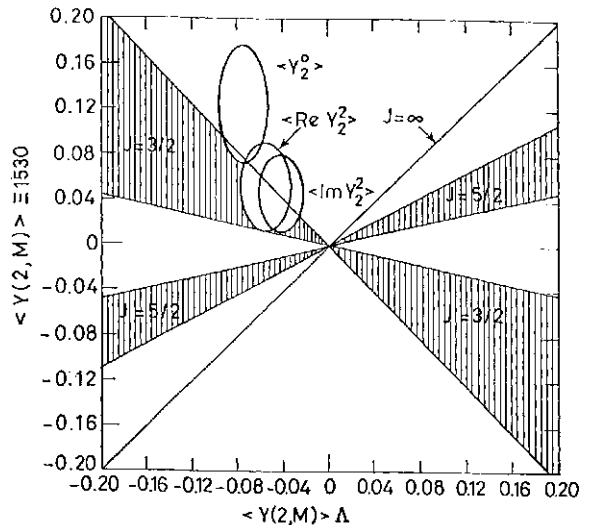


Fig. 11. A two resonance fit to the F15 (S=0) 7rN partial wave.

to a [56, 1<sup>-</sup>] or a [70, 1<sup>-</sup>].

N\*(1750) 1/2<sup>-</sup>. This can be assigned to either a [56, 0<sup>+</sup>] or a [70, 0<sup>+</sup>]. The observation<sup>57</sup> of the decay to

$AK$  forbids its assignment to a  $[70, 2^+]$ . Weak evidence<sup>41</sup> from photoproduction would favour the  $[56, 0^+]$  assignment while the evidence for the coupling sign in

$$7rN \rightarrow 7rJ$$

is conflicting<sup>41</sup> and would imply either multiplet.

$4(1900) 3/2^+$ . This state was discussed in 3 (iii) and possesses the wrong sign in  $K \sim p \rightarrow nZ^*$  (1385) to be assigned to a  $[56, 2^+]$ . A  $[70, 0^+]$  would decouple from KN and hence the most likely assignment is to a  $[70, 2^+]$ .

$\Lambda(2100) 5/2^+$ . In this case the observed

$$KN \rightarrow \pi n$$

coupling sign rules out its association with a  $[56, 2^+]$  and we are only left with a  $[70, 2^+]$  possibility.

*Summary.* It is clear that the best evidence exists for a  $[70, 2^+]$  with some very tentative evidence for a  $[56, 1^-]$ ,  $[70, 1^-]$  and  $[70, 0^+]$ . However there is at present no compulsion to invoke a  $[56, 1^-]$  or a  $[70, 0^+]$ . The consequences of finding these multiplets are horrifying. We would have to address the following questions:

- (a) Where are all the states? An escape might be possible if many of the  $A$ 's and  $2$ 's are decoupled from KN as suggested in some models.<sup>58</sup>
- (b) Why did the previous  $SU(6)_w$  analyses work so well in view of all the mixing that could well have occurred?

Only further experiments and analyses of this  $\sim 2$  GeV region will reveal the true nature of the baryon spectrum at the  $N=2$  level.

#### (iv) Conclusions.

It would appear that the  $[56, 0^+]$ ,  $[70, 1^-]$ ,  $[56, 2^+]$ ,  $[56, 0^+]$  multiplets are in good shape as is the analysis of their decay couplings via  $SU(6)_w$  and Melosh transformations. However a re-analysis is clearly needed, perhaps along the lines of Isgur and Karl.<sup>58</sup>

Higher multiplets exist ( $[70, 3^-]$ ,  $[56, 4^+]$  . . .) and there may be tentative evidence for some lower spin multiplets ( $[70, 2^+]$  . . .). The con-

sequences of definite observation of these would be alarming but possibly unavoidable. A tremendous investment of experiment and analysis would then be essential in unravelling the situation.

## §4. Conclusions

The last few years has seen a tremendous increase in the information on light quark mesons and baryons and we are now able to study the multiplet structure in detail above the ground states. It is only by looking at such information (*i.e.*, the overall structure) than we will be able to understand exactly how hadrons are made from their constituent quarks. A lot of work remains to be done but the reward will be great.

## References

1. G. Flügge: Experimental Particle Spectroscopy I, Review at this Conference.
2. O. W. Greenberg: P. RL **13** (1964) 598; R. H. Dalitz: *Les Houches Lectures 1965* (Gordon and Breach, New York, 1965) p. 253; H.J. Lipkin: Phys. Reports **8** (1973) 175; J. L. Rosner: Phys. Reports **11** (1974) 189.
3. R. L. Jaffe and K. Johnson: P. L. **60B** (1975) 201.
4. R. L. Jaffe: P.R. **D15** (1977) 267.
5. D. Berg *et al*: Paper 609.
6. F. Gilman and I. Karliner: P.R. **D10** (1974) 2194.
7. W. Cameron *et al*: Paper 416.
8. Particle Data Group Tables, April 1978.
9. A. De Rujula *et al*: P.R. **D12** (1975) 147.
10. P. Estabrooks *et al*: SLAC-PUB-2004. A. Wicklund *et al*: ANL-PR-77-58.
11. G. W. Brandenburg *et al*: PRL **36** (1976) 703.
12. R. K. Carnegie *et al*: N.P. **B127** (1977) 509. M. G. Bowler: J. Phys. **G3** (1977) 775. E. Berger *et al*: Paper 1092, ANL-HEP-PR-78 28.
13. M. G. Bowler *et al*: NP **B97** (1975) 227.
14. E. Berger *et al*: P.R. **D16** (1977) 657.
15. R. Aaron *et al*: PRL **38** (1977) 1509.
16. P. Gavillet *et al*: to be published in P.L.B.
17. G. Feldman,  $e^+e^-$  Reactions, Review at this Conference.
18. J. L. Basdevant *et al*: PRL **40** (1978) 994.
19. R. K. Carnegie *et al*: PL **68B** (1977) 287.
20. M. Mazzucato *et al*: CERN/EP/PHYS 78-18, Paper 623.
21. K. W. Edwards *et al*: Paper 120.
22. K. W. Edwards *et al*: Paper 119 (II)
23. D. Robson: Liverpool preprint LTH 33.
24. GDionisi<sup>^</sup>tf/.: CERN/EP/PHYS 78-23, Paper 620.
25. P. Estabrooks *et al*: SLAC-PUB-2004,

26. P. Estabrooks: Paper 1051.
27. A. D. Martin *et al.*: NP **B121** (1977) 514.
28. G. Grayer *et al.*: N.P. **B75** (1974) 189; P. Estabrooks and A. D. Martin: NP **B79** (1974) 301; NP **B95** (1975) 322.
29. D. Cohen *et al.*: ANL-HEP-PR-78-22, Paper 939.
30. N. M. Cason *et al.*: PRL **36** (1976) 1485.
31. V. P. Kenney *et al.*: Papers 503, 504.
32. V. P. Kenney *et al.*: Paper 502. W. D. Apei *et al.*: Paper 585.
33. G. W. Brandenburg *et al.*: PRL **36** (1976) 1239.
34. W. Cleland *et al.*: Paper 1082.
35. C. Evangelista *et al.*: Paper 710.
36. S. Bartalucci *et al.*: NC **39** (1977) 374.
37. B. Alper *et al.*: Paper 693 and 696.
38. R. H. Dalitz: *Pion Nuclear Scattering*, eds. G. L. Shaw & D. Y. Wong (Wiley, New York, 1969).
39. O. W. Greenberg: *Proc. 5th Int. Conf. Elementary Particles* (Lund, Sweden, 1969) p. 398.
40. H. J. Melosh: PR **D9** (1974) 1095; D. Fairnan and D. E. Plane: N.P. **B50** (1972) 379; F. Gilman *et al.*: P.R. **D9** (1974) 715; J. Weyers: CERN TH-1743.
41. A. J. G. Hey, P. J. Litchfield and R. J. Cashmore: NP **B95** (1975) 516; NP **B98** (1975) 237; RL-76-111.
42. J. Babcock *et al.*: NP **B126** (1977) 87.
43. R. A. Arndt *et al.*: VPI and State University preprint, Paper 1105.
44. G. Gaicomelli *et al.*: N.P. **B110** (1976) 67.
45. R.L. Kelly: LBL-7976.
46. G. Giacomelli *et al.*: N.P. **B71** (1974) 138; B. R. Martin: N.P. **B94** (1975) 413.
47. W. Cameron *et al.*: N.P. **B110** (1976) 25.
48. M. J. Corden *et al.*: Paper 709.
49. R. E. Cutkosky *et al.*: Carnegie Mellon & LBL preprint.
50. G. Hohler *et al.*: Karlsruhe preprint TKP 78-11, Paper 969.
51. W. Cameron *et al.*: RL/IC preprint, Paper 417.
52. W. Cameron *et al.*: N.P. **B131** (1977) 399.
53. W. Cameron *et al.*: RI/IC preprint, Paper 416.
54. D. Teodoro *et al.*: CERN/EP/PHYS 78-11, Paper 895.
55. C. Dionisi *et al.*: CERN/EP/PHYS 78-20, Paper 617.
56. C. Dionisi *et al.*: CERN/EP/PHYS 78-17, Paper 619.
57. R. D. Baker *et al.*: Rutherford Lab. preprints RL-78-041, RL-78-050, Papers 38, 39, 40.
58. N. Isgur and G. Karl: PL **72B** (1977) 109; PL (1978) 353; RL-78-045.

P5b

Particle Spectroscopy, Theoretical

Y. HARA

Institute of Physics, University of Tsukuba,  
Ibaraki 300-31

§ 1. Introduction

There were only five particles on the list of the elementary particles, when Professor Yukawa, the President of this Conference, invented the pions forty four years ago.<sup>1</sup>

At that time the proton, neutron and electron were considered to be the basic constituents of matter, and nuclear forces were proposed to be mediated by pions.

Since then, an enormous number of particles have been discovered. For example, there were an exciting discovery of the *Y* particle last summer and confirmation of *Y'* we have just heard at this Conference.

Now the colored quarks with flavors are considered to be the basic constituents of hadrons, and we have quantum chromodynamics (QCD) as a promising candidate of the dynamics of the strong interaction.

Today I will try to report on the progress of particle spectroscopy from this point of view.

I will speak about  
charmonium,

*R*,

spectroscopy of old hadrons and QCD,  
charmed hadrons,

baryonium,

and

dibaryons.

§ 2. Charmonium

At first let us discuss charmonium. We show the levels and branching ratios of the known charmonium in Fig. 2. I.<sup>2,13</sup>

Qualitatively the level structure of the *Jj(p)* family of new particles can be explained as charmonium, *i.e.*, as a charmed quark-antiquark (*cc*) system bound nonrelativistically by a potential suggested by the idea of QCD. However, there are still two serious problems in this model, the hyperfine splittings of 1*S* and 2*S* states and the magnitudes of the

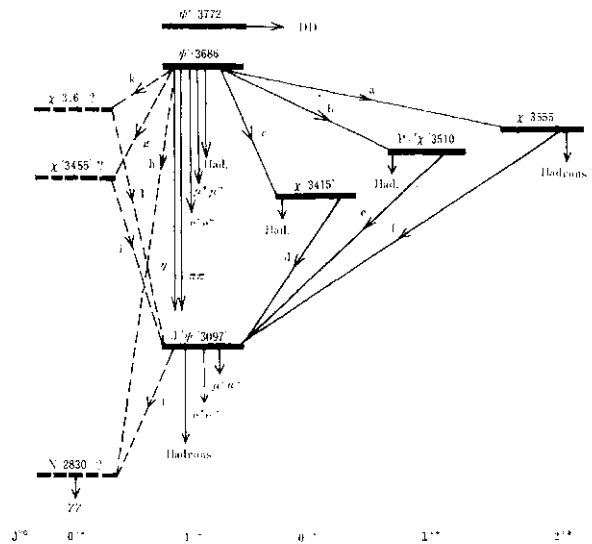


Fig. 2. 1. Charmonium.

Branching ratios of *γ*-decays; *a* = 7 ± 2%, *b* = 7 ± 2%, *c* = 7 ± 2%, *d* = 16 ± 3%, *e* = 23.4 ± 0.8%, *f* = 3.3 ± 1.0%, *g* < 2.5%, *h* < 1.0%, *ig* ≈ 0.5%, *j* < 1.7%, *kl* = 0.28 ± 0.12%. Data are taken from refs. 2, 3 and particle data group, Phys. Lett. 75B (1978) i.

M1 transition rates if JST(2.83) and ψ(3.455) are to be identified with the 1*S*<sub>0</sub> and 2*S*<sub>0</sub> state.

The contribution of the spin-spin interaction,<sup>4</sup> (327ca,19m<sup>2</sup>)*s*<sub>1</sub>*S*<sub>2</sub>δ(*r*), arising from the exchange of a single color-gluon to the hyperfine splitting is given by

$$\Delta M = \frac{32\pi\alpha_s}{9m_c^2} |\phi(0)|^2 \approx \begin{cases} 36 \text{ MeV for } 1S \\ 15 \text{ MeV for } 2S, \end{cases} \quad (2.1)$$

for  $\alpha_s \approx 1.65$  GeV and  $\alpha_s = 0.19$ . Here,  $a_s(m) = 0.09$  was obtained by applying the formula<sup>5</sup>  $T_{ij}(\text{hadrons}) \ll R(V \rightarrow ggg) = (160/81)(7r^2 - 9)(a^3/M^2)|\phi(0)|^2$  to  $f(1/1 \text{ hadrons})$ . Here, we used the magnitudes of  $|\phi(0)|^2$  determined from<sup>6</sup>  $\Gamma(F \rightarrow p^+p^-) = 16a^2 e^2 |\phi(0)|^2 / M^2$ . The predicted mass differences (2.1) should be compared with the experimental values of 270 and 230 MeV, respectively.

In the nonrelativistic approximation, the decay width of the M1 transition  $Jjcp \rightarrow XA-j$  is predicted to be 29 keV, while experimentally it is < 1 keV.

Let us discuss these problems.

The potential suggested by the idea of QCD consists of spin independent part and spin dependent part,

$$U(r) + U_{\text{spin}}(r). \tag{2.2}$$

Traditionally spin independent potential  $U(r)$  is a sum of a phenomenological long-range confining potential assumed to vary linearly with distance and a short-range Coulomb type potential arising from the exchange of a single color-gluon between the quarks,<sup>7</sup>

$$U(r) = ar - \frac{4}{3} \frac{\alpha_s}{r}. \tag{2.3}$$

Since the confining potential is considered to arise from multiple-gluon-exchanges, it consists of Lorentz-vector part  $j^{\mu} \otimes 7 \rightarrow \dots$  and scalar part  $1(x)$  (and pseudoscalar part  $y \wedge j^{\mu} s$  etc.<sup>8</sup>)

This spin independent potential  $U(r)$  yields the following generalized Breit-Fermi potential for fine and hyperfine splittings,<sup>9-13</sup>

$$\begin{aligned} U_{\text{spin}} = & \frac{1}{3m_c^2} \left( \frac{d^2 V}{dr^2} - \frac{1}{r} \frac{dV}{dr} \right) [s_1 \cdot s_2 \\ & - 3(s_1 \cdot \hat{r})(s_2 \cdot \hat{r})] + \frac{2}{3m_c^2} s_1 \cdot s_2 \nabla^2 V(r) \\ & + \frac{1}{2m_c^2 r} \left( 3 \frac{dV}{dr} - \frac{dS}{dr} \right) (\mathbf{r} \times \mathbf{p}) \cdot (s_1 + s_2), \end{aligned} \tag{2.4}$$

where  $V$  and  $S$  denote Lorentz-vector and scalar part<sup>14</sup> of  $U(r)$ ,

$$\begin{aligned} U(r) &= V(r) + S(r), \\ V(r) &= -\frac{4}{3} \frac{\alpha_s}{r} + far, \\ S(r) &= (1-f)ar. \end{aligned} \tag{2.5}$$

The contribution of pseudoscalar part, 7-5(8)7-5, due to multiple-gluon-exchanges to spin dependent potential is neglected for simplicity.

In order to explain the observed  $^3P_j$  splittings the fraction of Lorentz-vector vertices  $V=1$ . For  $f=1$ ,  $|A^{\wedge} M \zeta P J - M \zeta P i| / [M m - i M \zeta P o J \wedge O \hat{a}]$  while the experimental value of this ratio is about 0.42.

Quantitatively it is impossible to reproduce the hyperfine structure of the charmonium by this potential. The splitting of the  $1S$  states,  $M(1^3S_1) - M(1^1S_0)$ , is found to be less than about 100 MeV, which should be compared with the experimental value,  $M(J < p) - M(X) = 270$  MeV.

One proposal to avoid this difficulty is to

introduce an anomalous color "magnetic" term<sup>12</sup>  $K$  to the vector part of the linear confining potential  $far$ .<sup>15-18</sup> Then, the term  $far$  in the tensor and spin-spin interactions in (2.4) are multiplied by a factor  $(1+r)^2$  and that in the LS interaction is multiplied by a factor  $(1+A)$ . This hypothesis provides an extra parameter and can reproduce all of  $1S_V$ ,  $2S_j$  and  $^3P_j$  splittings simultaneously<sup>19</sup> for  $f \approx 4 \sim 5$ ,  $f \ll 0.1$  and  $A \approx 0.45$ .

According to another proposal, instantons are responsible to the splitting of  $J_j < p$  and  $r_j$ . Unfortunately there is no quantitatively reliable calculation of the contributions of instantons to the splitting. According to Wilczek and Zee,<sup>20</sup>

$$M(J < p) - M(\chi) \sim 37 r^4 v^4 / m^2 c \sim 450 \text{ MeV}, \tag{2.6}$$

where  $u$  is the usual renormalization scale and taken to be about 200 MeV. However, the numerical result is very sensitive to the cutoff in the size of the instantons.<sup>21</sup>

Next let us discuss electromagnetic transitions of the charmonium.

The E1 transition rates have been reproduced fairly well in the charmonium model.<sup>22,23</sup>

In the nonrelativistic quark model the M1 transition rates are expressed as<sup>22,23</sup>

$$\begin{aligned} \Gamma(M1) &= \frac{4}{3\pi} (2J_f + 1) k^3 \mu_c^2 \\ &\times | \langle f | -1 + \frac{k^2 r^2}{24} | i \rangle |^2. \end{aligned} \tag{2.7}$$

Therefore,

$$\Gamma_{\text{allowed}}(M1) = \frac{4}{3\pi} (2J_f + 1) k^3 \mu_c^2, \tag{2.8}$$

and

$$\Gamma_{\text{forbidden}}(M1) = \frac{1}{72\pi} \frac{k^7}{m_c^2 \omega^2} (2J_f + 1) \mu_c^3, \tag{2.9}$$

where  $ix_c = e_c e / 2m_c c$  and for simplicity we have used the wave functions of the harmonic oscillator potential in evaluating  $\langle 1S | r^2 | 2S \rangle$ .

If we identify  $X(2.83)$  with  $y_c(1^3S_1)$  and  $\chi(3.45)$  with  $r_j(2^1S_0)$ , we obtain the following predictions from (2.8) and (2.9),

$$\Gamma(J/\psi \rightarrow X\gamma) = 29 \text{ keV} \rightarrow Br(J/\psi \rightarrow X\gamma) = 40\%, \tag{2.10a}$$

$$\Gamma(\psi' \rightarrow X\gamma) = 8.5 \text{ keV} \rightarrow Br(\psi' \rightarrow X\gamma) = 4\%, \tag{2.10b}$$

$$\Gamma(\chi(3.45) \rightarrow J/\psi \gamma) = 0.13 \text{ keV}, \tag{2.10c}$$



$$\Gamma(\psi' \rightarrow \chi(3.45)\gamma) = 21 \text{ keV} \rightarrow Br(\psi' \rightarrow \chi(3.45)\gamma) = 9\%, \quad (2.10d)$$

where  $m_{\psi'} = 1650 \text{ MeV}$  and  $m_{\chi(3.45)} = 330 \text{ MeV}$  determined from  $M(\langle p' \rangle) - M(J/\psi)$  and  $e^+e^- \rightarrow \psi' \rightarrow \chi(3.45)\gamma$  are used. (See, Fig. 2.2.) All of these predictions are sources of troubles. Experimental results,  $Br(J/\psi \rightarrow \chi(3.45)\gamma) < 0.5\%$  and  $Br(\psi' \rightarrow \chi(3.45)\gamma) < 2.5\%$ , are not compatible with the above theoretical values, and (2.10c) and the experimental results<sup>24</sup>  $Br(\psi' \rightarrow \chi(3.45)\gamma) > 20\%$  predict  $P(\chi(3.45)) < 0.1 \text{ keV}$ , which seems too small.

However, forbidden transition rates are not reliable since the matrix elements depend sensitively on the choice of the confining potential. For example, if we include spin-spin interaction in the unperturbed Hamiltonian,  $\langle 1^1S^0 | S^i S^j | 1^1S^0 \rangle$  and  $\langle 1^3S_1 | S^i S^j | 1^3S_1 \rangle$  are no longer zero and the forbidden MI transition rates increase considerably.<sup>23</sup> There are also relativistic correction terms<sup>25</sup>  $\langle 1^1S^0 | \frac{1}{2} \frac{d^2}{dr^2} | 1^1S^0 \rangle + \langle 1^3S_1 | \frac{1}{2} \frac{d^2}{dr^2} | 1^3S_1 \rangle$  to be added to the radial matrix element  $\langle 1^1S^0 | -1 + (\mathbf{p}^2/24) | 1^1S^0 \rangle$ .

One proposed solution to the MI troubles is as follows.  $X(2.83)$  and  $\chi(3.45)$  are not  $rj_c$  and  $rj_s$ . Instead there are real  $rj_c$  and  $rj_s$  with  $100 \text{ MeV} > M(\langle p' \rangle) - M(O^?) > 0$  and  $50 \text{ MeV} > M(O^?) - M(O^?) > 0$ . Then, what is  $X(2.83)$  and  $\chi(3.45)$ ? Lipkin has suggested<sup>26</sup> that  $X(2.83)$  and  $\chi(3.45)$  are  $ccqq$  states ( $q=u$  and/or  $d$ ) and that

there are two  $0^+$  mesons, one with  $J=0$  and another with  $J=1$ . He has also suggested that  $\chi(3.45)$  is a cress state with  $J=0$ . In order to test Lipkin's conjecture one should search for the transition  $\langle p' \rangle + Xp$  since its observation indicates that  $X$  is not a  $cc$  state.

Now let me mention that the assignment of  $X(2.83)$  to  $YJ_c$  has another problem; If we use the formula,  $F(TJ_c \rightarrow \gamma\gamma) = 48 \pi^2 V_0 \langle p(0) | 7 M(r) | YJ_c \text{ hadrons} \rangle \gg F(rj_c \rightarrow \gamma\gamma) = (32/3) a^2 |O(O)|^2 / M(O)^2$ , we find

$$Br(\gamma_c \rightarrow \gamma\gamma) \approx 10^{-3}, \quad (2.11)$$

while we obtain

$$Br(X \rightarrow \gamma\gamma) \geq 0.008 \quad (2.12)$$

from experimental results  $Br(J/\psi \rightarrow \chi(3.45)\gamma) Br(X \rightarrow \gamma\gamma) = \{A \pm 0A\} \times 10^{-4}$  and  $Br(J/\psi \rightarrow \chi(3.45)\gamma) < 0.7\%$

The large branching ratio  $Br(X \rightarrow \gamma\gamma) > 0.008$  indicates that hadronic decays of  $X$  are forbidden, for example, by flavor selection rules.

Finally let us discuss the candidate of a new charmonium level at 3.6 GeV observed in the  $S^1 + YJ_c \rightarrow p$  decay and reported at this Conference.<sup>27,28</sup> If we identify this resonance with  $rj'_c$ , the allowed MI transition rate is predicted to be

$$\Gamma(\psi' \rightarrow \chi(3.6)\gamma) = 1.1 \text{ keV} \rightarrow Br(\psi' \rightarrow \chi(3.6)\gamma) = 0.5\%, \quad (2.13)$$

and the forbidden MI transition rate is predicted to be

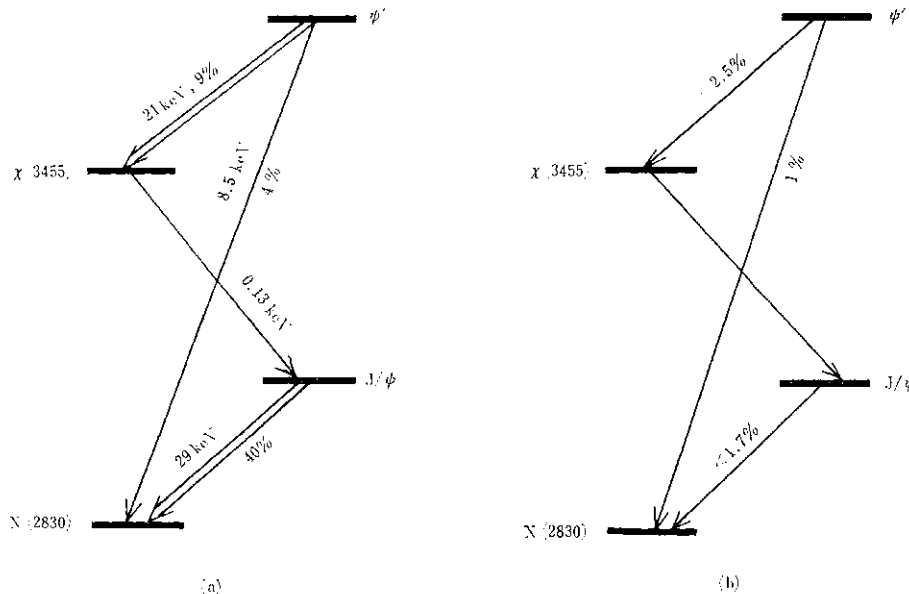


Fig. 2.2. MI transitions, (a) Theory; (b) Experiment.

$$\Gamma(\chi(3.6) \rightarrow J/\psi\gamma) = 10 \text{ keV}. \quad (2.14)$$

Since experimentally<sup>3</sup>

$$\begin{aligned} Br(\psi' \rightarrow \chi(3.6)\gamma) Br(\chi(3.6) \rightarrow J/\psi\gamma) \\ = (2.8 \pm 1.2) \times 10^{-3}, \end{aligned} \quad (2.15)$$

the branching ratio of the forbidden M1 transition is predicted to be

$$Br(\chi(3.6) \rightarrow J/\psi\gamma) \approx 60\%, \quad (2.16)$$

which is too large to be acceptable, it seems that the experimental result (2.15) is possible only if both radiative transitions are E1 transitions. This means that the spin-parity of the new resonance is  $0^+$ ,  $1^+$  or  $2^+$ .

### §3. $\Gamma$

$Y$  was observed last summer as a strong enhancement at 9.5 GeV in the mass spectrum of dimuons produced in 400 GeV proton-nucleus collisions,<sup>29</sup>

$$p + (\text{Cu, Pt}) \rightarrow \mu^+ + \mu^- + \text{anything},$$

at Fermilab. Later they found two peaks whose widths are consistent with their resolution and evidence for the possible existence of a third peak.<sup>30</sup>

Three months ago  $Y$  was confirmed by using the PLUTO and DASP detectors at DORIS in the reaction,<sup>31</sup>

$$e^+ + e^- \rightarrow \text{hadrons}.$$

According to their latest results<sup>31</sup>

$$\begin{aligned} M(Y) &= 9.46 \pm 0.01 \text{ GeV}, \\ \Gamma_s(Y) &> 25 \text{ keV (95\% CL)} \\ &\quad \text{(best value 50 keV)}, \\ \Gamma_{ee}(Y) &= 1.3 \pm 0.2 \text{ keV}. \end{aligned}$$

At this Conference the confirmation of  $Y'$  at DORIS has been reported. According to their results,<sup>3</sup>

$$\begin{aligned} M(Y') - M(Y) &\approx 556 \text{ MeV}, \\ \Gamma_{ee}(Y') / \Gamma_{ee}(Y) &\approx 3. \end{aligned}$$

It is quite natural to regard the T-particle as a bound state of a new heavy quark and its

antiparticle. While the existence of the charmed quark was predicted based on the lepton-hadron symmetry<sup>32</sup> and the absence of the strangeness changing weak neutral current,<sup>33</sup> a six-quark model was proposed by Kobayashi and Maskawa<sup>34</sup> in 1973 in order to explain CP nonconservation in the gauge model.<sup>35</sup> Properties of the six quarks, u, d, s, c, t and b, are summarized in Table I.

In Table I  $T$  and  $B$  are new quantum numbers conserved in both strong and electromagnetic interactions. The charges of hadrons are expressed as

$$Q = I_3 + \frac{1}{2}(B + S + C + T + B).$$

Let us determine the charge of the new heavy quark  $e_0$  from the leptonic decay width of  $Y$  by making use of the nonrelativistic relation,<sup>6</sup>

$$\Gamma(V \rightarrow e^+e^-) = 16\pi\alpha^2 e_q^2 |\phi_q(0)|^2 / M_v^2, \quad (3.1)$$

where  $|\phi_q(0)|$  is the magnitude of the  $qq$  wavefunction of the vector-meson  $V$  at the origin.

From the leptonic decay widths of  $p$ ,  $a$ ,  $\langle f \rangle$  and  $J/\psi$  Jackson derived an empirical formula,<sup>22</sup>

$$|\phi_q(0)|^2 \propto M_v^{1.89 \pm 0.15}. \quad (3.2)$$

Therefore,  $r(V \rightarrow e^+e^-) / e_0^2$  should be nearly independent on the mass of the vector-meson<sup>36</sup>  $M_v$ , and we find

$$e_0^2 \approx \frac{1}{9} \text{ but } \neq \frac{4}{9} \quad (3.3)$$

as we can clearly see in Fig. 3. 1, in which  $r(V \rightarrow e^+e^-) / e_0^2$  vs  $M$  is plotted.

The conclusion (3.3) is also reached by comparing the lower bounds

$$\Gamma(Y \rightarrow e^+e^-) / e_0^2 > 2.6 \text{ keV}$$

and

$$r(X \rightarrow e^+e^-) / e_0^2 > |A| \text{ keV}, \quad (3.4)$$

with the experimental results from DORIS. The lower bounds (3.4) were derived by Rosner, Quigg and Thacker<sup>37</sup> for potentials which are

Table I. Properties of six quarks.

Quark	$Q$	$B$	$I$	$I_3$	$S$	$C$	$T$	$B$
u	2/3	1/3	1/2	1/2	0	0	0	0
d	-1/3	1/3	1/2	-1/2	0	0	0	0
s	-1/3	1/3	0	0	-1	0	0	0
c	2/3	1/3	0	0	0	1	0	0
t	2/3	1/3	0	0	0	0	1	0
b	-1/3	1/3	0	0	0	0	0	-1

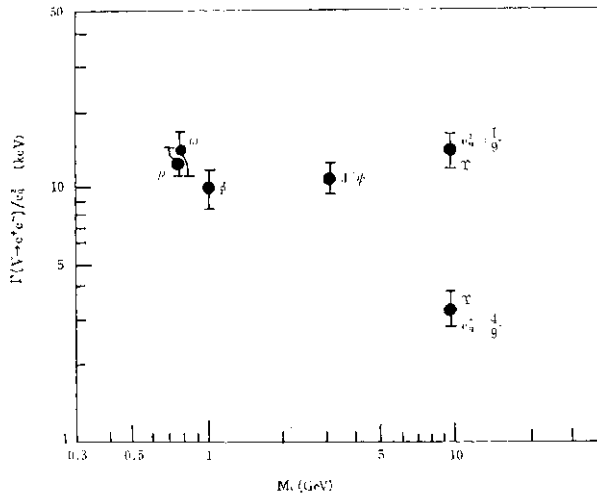


Fig. 3. 1.  $\Gamma(Y \rightarrow e^+e^-)/\alpha_s^2$  vs  $M_q$ .

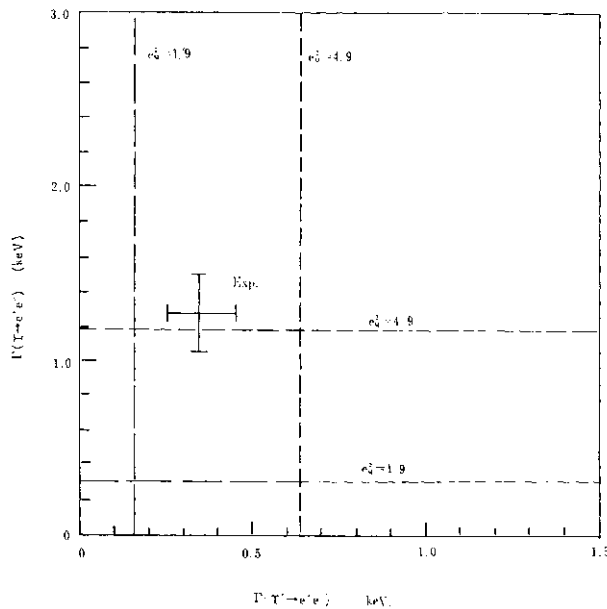


Fig. 3. 2.  $\Gamma(Y' \rightarrow e^+e^-)$  vs  $\Gamma(Y \rightarrow e^+e^-)$ .

Lower bounds on these leptonic decay widths for  $e_s^2=4/9$  and  $1/9$  are shown (broken lines). The observed value of  $\Gamma(Y' \rightarrow e^+e^-)$  is incompatible with the lower bound if  $e_s^2=4/9$ . This figure is taken from ref. 37.

concave-downward,  $d^2F/dr^2 < 0$ . In deriving these lower bounds they have assumed that  $m_b/m_c > 2.6$  and made use of the experimental results  $\Gamma(J/\psi \rightarrow e^+e^-) = (4.5 \pm 0.6) \text{ keV}$  and  $\Gamma(\psi' \rightarrow e^+e^-) = (2A \pm 0.3) \text{ keV}$ . We find that the experimental value of  $\Gamma(\psi' \rightarrow e^+e^-)$  is incompatible with the lower bound (3.4) in the case of  $e_s^2 = 4/9$ . (See Fig. 3.2.)

Of course, the best way to prove that  $Y$  is a bound state of  $b$  and  $\bar{b}$  is to find an isodoublet of "beautiful" ("bottom") mesons,  $B^0 = (b\bar{d})$  and  $B^- = (b\bar{u})$ .

The dominant decay modes of these mesons

involve charmed mesons,

$$5^0, 2^? \sim \rightarrow a \text{ charmed meson} + \text{wr.}$$

Last year several papers on the bound states of a new heavy quark and its antiparticle were published. For example, before the discovery of  $Y$  Eichten and Gottfried<sup>38</sup> calculated the energy levels to be expected from the potential model used in charmonium. Their potential

$$U(r) = -\frac{4}{3} \alpha_s(m_c^2)/r + r/a^2 \quad (3.5)$$

( $a_s(r) = 0.19$  and  $a = 2.22 \text{ GeV}^{-1}$ ) predicts  $M(\psi') - M(\psi) = 420 \text{ MeV}$ , which should be compared with the experimental result,  $556 \text{ MeV}$ .

The difference of the predicted and experimental level spacing  $M(Y') - M(Y)$  suggests that the shape of the above potential must be modified, and it has been noticed<sup>39</sup> that the apparent equal spacing,

$$M(Y') - M(Y) \approx M(\psi') - M(J/\psi); \quad 556 \text{ MeV}$$

vs  $588 \text{ MeV}$ , is realized in the nonrelativistic limit if a logarithmic potential<sup>40</sup>

$$U(r) = C \ln(r/r_0), \quad C \approx 0.75 \quad (3.6)$$

is used instead of (3.5).

Though  $U(r) = C \ln(r/r_0)$  is unique in giving level spacing independent of the quark mass, the equal spacing,  $M(Y') - M(Y) \approx M(\psi') - M(J/\psi)$ , is reproduced by the modified Coulomb Potential<sup>39,41</sup>

$$U(r) = -\frac{4}{3} \alpha_s/r + r/a^2 \quad (3.7)$$

with  $a_s = 0.45$  and  $a = 2.48 \text{ GeV}^{-1}$ . It is interesting to notice that the value  $a_s = 0.45$  is the value used in order to reproduce the  $1S$ ,  $2S$  and  $3P_j$  splittings of charmonium.

Now let us consider the magnitude of the quark-gluon fine structure constant,  $a_s(q^2)$ . In QCD

$$\alpha_s(q^2) \approx [12\pi/(33 - 2F)]/\ln(q^2/\Lambda^2), \quad (3.8)$$

where  $F$  is the number of quark flavors. Various experimental data, e.g., scaling violations in deep inelastic reaction indicates<sup>42</sup>  $4 = 0.3 \sim 0.7 \text{ GeV}$ . If we use (3.8) with  $4 = 0.5 \text{ GeV}$ , we find  $a_s(m_l) = 0.63$ ; and if we choose  $A = 0.3 \text{ GeV}$ , we find  $a_s(m_l) = 0M$ . These results are by a factor of three or two bigger than the value  $a_s(m^2) = 0.19$  obtained at time-like  $q^2 \sim m^2$ .

However, we have to notice that the running

constant  $a(q^2)$  evaluated at time-like  $q^2=-m_c^2$ , and that evaluated at space-like  $q^2=m_c^2$ , are different in general since  $q^2$  is finite.<sup>43</sup>

Now let us discuss one-gluon-exchange potential. Because of the  $q^2$  dependence of  $a_s$ , which is expressed in (3.8), the  $1/r$  behavior of the Coulomb type potential is modulated by an inverse log factor. The asymptotic form of the Fourier transform of  $oc(q^2)/q^2$  as  $r \rightarrow 0$  is given by<sup>44</sup>

$$[87r/(33-2F)]/(r \ln r). \quad (3.9)$$

However, traditionally this effect has been ignored by taking an average value of  $a_s$  at  $q^2=m_c^2$ . I consider that it is more appropriate to evaluate  $a_s$  at  $q^2=(l/r)^2$ . The average of  $1/r$ ,  $(\sqrt{r})^{1/2+3\alpha}$  for power-law confining potential  $U(r)=kr^A/A$ , where  $M$  is the reduced mass of the system. For the charmonium in the harmonic oscillator potential  $\langle 1/r \rangle \approx 0.6$  GeV.

Of course we can use the Fourier transform of  $a_s(q^2)/q^2$  as the one-gluon-exchange potential.<sup>44+45</sup>

Next let us discuss the hadronic decay width of  $T$ . According to QCD,<sup>5</sup>

$$\begin{aligned} \Gamma_h(Y) &\approx \Gamma(Y \rightarrow ggg) \\ &= (160/81)(\pi^2 - 9)(\alpha_s^3/M(Y)^2)|\phi(0)|^2 \end{aligned} \quad (3.10)$$

and<sup>6</sup>

$$\Gamma_{ee}(Y) = 16\pi\alpha^2 e_b^2 |\phi(0)|^2 / M(Y)^2. \quad (3.11)$$

Therefore,

$$\begin{aligned} \Gamma_h(Y)/\Gamma_{ee}(Y) &\approx (10/81\pi)(\pi^2 - 9)(\alpha_s^3/\alpha^2 e_b^2) \\ &= 19.5 \end{aligned} \quad (3.12)$$

for  $\alpha_s = 0.15$ , which is derived from

$$\alpha_s(s) = \alpha_s(\mu^2) [1 + (23/12\pi)\alpha_s(\mu^2) \ln(s/\mu^2)]^{-1}, \quad (3.13)$$

and  $\alpha_s = 0.19$  for  $J/\psi$ . In (3.12)  $e_b$  stands for the charge of the b-quark.

The QCD prediction (3.12) seems somewhat smaller than the experimental result,<sup>3</sup>

$$\begin{aligned} r_h(r)/r_h(T) &= (>25 \text{ keV}; \text{ best value } 50 \text{ keV}) \\ &\times (1.3 \pm 0.2 \text{ keV}^{-1}). \end{aligned} \quad (3.14)$$

But, they are compatible if we make a correction for second order electromagnetic decays to the hadronic decay width of  $T$ .

There is an inequality on the mass of the b-quark,

$$m_b - m_c > 3.29 \text{ GeV} \quad (3.15)$$

derived by Grosse and Martin<sup>46</sup> for potentials which satisfy the conditions,

$$-\infty < \lim_{r \rightarrow \infty} [rV(r)] \leq 0 \quad (3.16)$$

and

$$(\Delta)W_0(r) > 0$$

and by making use of the experimental values of the masses of  $T$ ,  $T'$  and  $J/\psi$ .

#### §4. Spectroscopy of Old Hadrons and QCD

Effective quark-quark interaction suggested by QCD, which has been applied to charmonium and  $T$  in the previous sections has been applied to the spectroscopy of old hadrons.

A long-range Lorentz-scalar confining force, together with a short-range Coulomb-like vector exchange has been applied to meson spectroscopy by Schnitzer.<sup>18</sup> This interaction gives an excellent overall account of the spin structure of ordinary mesons, if  $a_s(M)$  is sufficiently large as has been suggested by the violation of scaling in deep inelastic processes,

$$\alpha_s(M^2) = (12\pi/25)(\ln M^2/A^2)^{-1}$$

with  $A=0.5$  GeV. Here,  $M$  is taken to be the mass of the bound state.

This model predicts the inverted  $^*P$  multiplets for  $D$  and  $F$  charmed mesons and bottom mesons,<sup>1\*147</sup>

$$M(^3P_0) > M(^3P_1) > M(^3P_2).$$

The hyperfine interaction arising from a short-range Coulomb-like vector exchange with  $a_s \sim 1$  together with flavor independent long-range confining force has been applied to the spectrum and mixing angles of baryons by Isgur and Karl.<sup>48,49</sup> They have found a good agreement in the  $S=0$  and  $S=-1$  sector (except for  $4(1405) \text{ } ^1P=1/2-$ ). They have discarded the spin-orbit interaction from the vector-exchange since they may be cancelled by the spin-orbit interaction from the long-range Lorentz-scalar confining force.

#### §5. Charmed Hadrons

The observation of the  $D$  and  $Z^*$  mesons were reported at the last conference. Last year candidates of the  $F$  and  $F^*$  mesons have been discovered at DESY with the following masses<sup>50,3</sup>

$$M(F) = (2.03 \pm 0.06) \text{ GeV}$$

and (5.1)

$$M(F^*) - M(F) = (110 \pm 46) \text{ MeV.}$$

Some branching ratios of the  $D$  mesons have been measured. The observed branching ratio of the inclusive semileptonic decay is<sup>51</sup>

$$Br(D \rightarrow e\nu X) \approx 10\%. \quad (5.2)$$

If the nonleptonic decays of the  $D$ -mesons are not enhanced, we expect

$$Br(D \rightarrow e\nu X) \approx 20\%. \quad (5.3)$$

Thus the nonleptonic decays of the  $D$ -mesons are enhanced by a factor of about 8/3. Therefore, we do not have a serious problem such as the origin of the  $|J|=1/2$  rule in the hyperon decays and  $7\mathcal{L}$ -meson decays. In these decays  $|A_1| = |j_2|$  part is enhanced by a factor of about 20.

Main part of the difference between (5.2) and (5.3) may be explained by QCD, in which nonleptonic decays are enhanced by a factor,<sup>52</sup>

$$(2c_+^2 + c_-^2)/3 \approx 5/3, \quad (5.4)$$

and semileptonic decays are suppressed as much as 35%,<sup>53</sup> where

$$c_- = \{1 - [(33 - 2F)/12\pi] \alpha_s(m_c^2) \times \ln(m_W^2/m_c^2)\}^{1/2/(33-2F)}$$

and (5.5)

$$c_+ = (c_-)^{-1/3}.$$

In (5.4) we have used  $c_- = 2.0$  and  $c_+ = 0.7$  assuming  $\alpha_s(m_f) = 0.7$ .

Because of the large masses, the charmed mesons decay into various channels and through the study of these decays we can test various models of weak nonleptonic decays. For example, by making use of the bounds<sup>54</sup>

$$0 < r(D^+)/r(D^0) < 3, \quad (5.6)$$

which are imposed by the  $|J|=1$  rule, and the measured branching ratios of  $D^+ \rightarrow K^- 7r^+ 7r^+$  and  $J^{5^0-} \rightarrow K^- 7r^+ 7r^0$ ,<sup>55</sup> it has been shown that the matrix elements of some of  $D \rightarrow K n 7t$  decays cannot be uniform over the Dalitz plot<sup>56,57,59</sup>. It has been suggested that  $D^+ K^- 7t x^0$  decay is dominated by  $K \sim p^+$  states.<sup>57</sup>

§6.  $\nu$

All observed properties of  $r$  are consistent with those of a new sequential heavy lepton.<sup>61,60</sup> (See, Table II.)

Table II.  $r$  decays

Decay mode	Experiment	Theory <sup>61</sup>
$e\nu\bar{\nu}$	$16.9 \pm 1.9\%$	$\sim 18\%$
$\mu\nu\bar{\nu}$	$18.3 \pm 1.9\%$	$\sim 18\%$
$\pi\nu$	$7.7 \pm 1.3\%$	$\sim 10\%$
$\rho\nu$	$24 \pm 9\%$	$\sim 22\%$

If  $T$  is a bound state of a  $b$ -quark and its antiparticle, and if the  $b$ -quark and the  $t$ -quark belong to a doublet of the weak  $SU(2)$  group, we find a beautiful correspondence between

$(w, d), (c, s)$  and  $(t, b)$ ,

and

$(e, \nu), (p, \quad)$  and  $(r, \nu_r)$ .

§7. Baryonium

In the nonrelativistic quark model a baryon is a bound state of three quarks, and a meson is a bound state of a quark and an antiquark.

However, there are some indications that there might be other types of mesons.

For example, several narrow peaks have been observed in  $pp$  system<sup>3</sup>

Name	Mass (MeV)	Width (MeV)	Remarks
S	$1936 \pm 1$	$< 4 \sim 8$	$\bar{p}p$ formation experiment, <sup>62</sup>
—	$2020 \pm 3$	$\lesssim 10 - 20$	baryon exchange reaction, <sup>63</sup>
—	$2204 \pm 5$	$\lesssim 10 - 20$	

Here S(1936) is a narrow resonance with a large elasticity. There are additional indications of narrow resonances with  $i^P = 0$ .<sup>64</sup>

It is difficult to regard the narrow resonances observed in  $PP$  system, such as S(1936), as mesons which consist of a quark and an antiquark. These resonances have narrow widths of about 10 MeV in spite of their high masses. They are characterized by their reluctance for decaying into meson states, as inferred either from the measured branching ratios, or from their small total widths. That is, their couplings with mesons are weak. Therefore, they are popularly called "baryonium".<sup>56,5</sup>

Necessity of such resonances was advocated by Rosner when duality was applied to baryon-antibaryon reactions<sup>66,67</sup>. In order to draw duality diagrams for  $BB \rightarrow BB$  we have to introduce resonances which consist of two quarks and two antiquarks ( $iqqq$ ) (Fig. 7.1). If the  $qqqq$  resonances couple strongly with

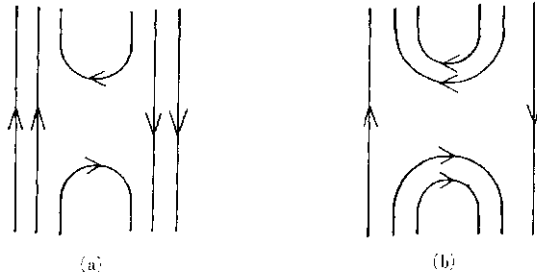


Fig. 7. 1. Duality diagrams for  $B\bar{B} \rightarrow B\bar{B}$ .

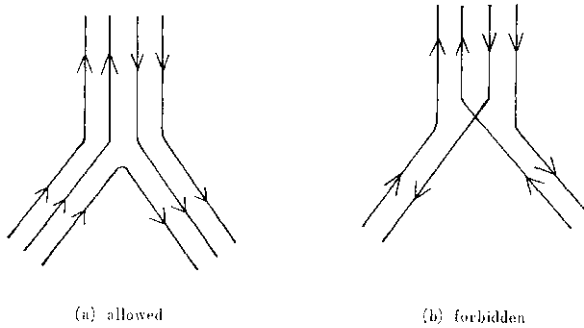


Fig. 7. 2. Freund-Waltz-Rosner rules, (a) allowed; (b) forbidden.

two-meson states, we cannot expect that the vector and tensor trajectories are exchange degenerate. Therefore, the  $qqqq$  resonances are not allowed to couple strongly with meson states in dual models.

Thus, the following selection rules for the vertices were proposed by Freund, Waltz and Rosner<sup>68</sup>;

(1) Every quark-line connects two different hadrons. (OZI rule)

(2) Every pair of the hadrons must be connected by at least one quark-line.

According to these rules, the decays of the  $qqqq$  resonance into  $BB$  states are allowed but the decays into meson states are forbidden. (See Fig. 7.2.)

If the baryonium is a  $qqqq$  resonance, we have to explain how two quarks and two antiquarks are bound together and why it cannot decay into mesons strongly. In order to answer these questions we have to know how a quark-antiquark pair and three quarks are confined to the interior of mesons and baryons, respectively.

There are several models of hadrons. As examples let us consider the junction model<sup>69,71</sup> and the bag model.<sup>72-74</sup>

7.7 Exotic mesons in the junction model

In the junction model mesons are bound

states of a colored quark and a colored anti-quark bound by a colored oriented string (Fig. 7.3 (a)). Baryons consist of three colored quarks, each of which is tied at the end of three colored oriented strings, and the three strings are joined at a point called the string "junction"<sup>69,70</sup> (Fig. 7.3(b)).<sup>75,76</sup>

The meson and baryon in this model shown in Fig. 7.3 correspond to the following color gauge invariant operators,<sup>71</sup>

$$\bar{\psi}^i(x)[G(P(x, y))]_i^j \psi_j(y) \tag{7.1}$$

and

$$e^{*} \gg [G(P(x, y)W(y)MG(P(x, z))^\wedge(z)], \tag{7.2}$$

respectively, where

$$[G(P(x, y))]_i^j = \left[ T \exp \int_{P(x, y)} A_\mu(x) dx^\mu \right]_i^j, \tag{7.3}$$

and  $ij$  and  $k$  are color SU(3) indices.

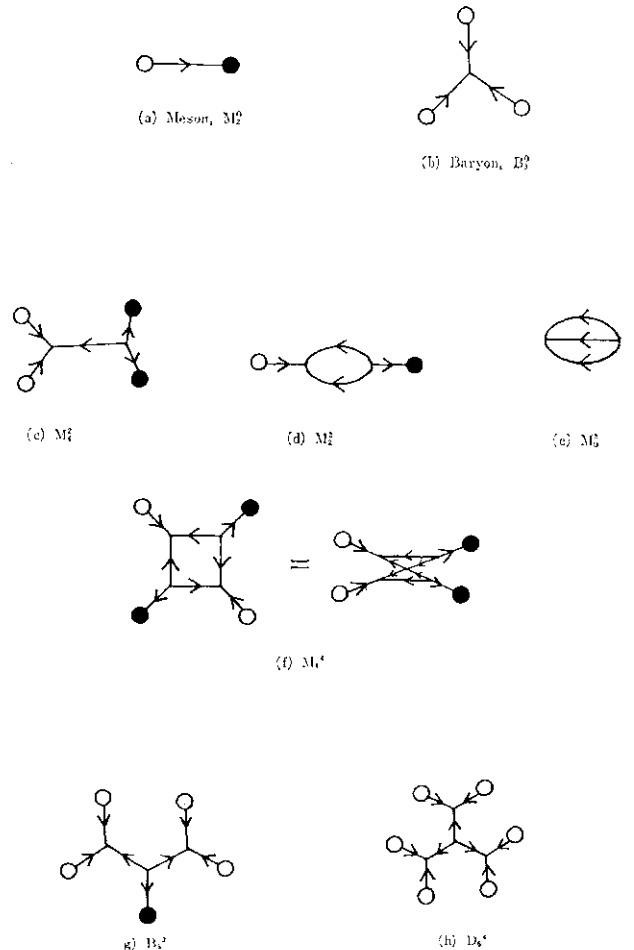


Fig. 7. 3. Various types of hadrons in the junction model.

(a) Meson,  $M_2^0$ ; (b) Baryon,  $B_3^0$ ; (c)  $M_4^2$ ; (d)  $M_2^2$ ; (e)  $M_0^2$ ; (f)  $M_4^4$ ; (g)  $B_3^2$ ; (h)  $D_3^*$ .

In the junction model baryons consist of three colored quarks (tied at the ends of three strings) and a junction. Hence, we draw junction lines (broken lines) as well as quark lines (solid lines) in duality diagrams.

Various hadrons of new types can be constructed of quarks and junctions. In Fig. 7.3 some of possible types of hadrons in this model,  $M_l$ ,  $M_l$ ,  $M_l$ ,  $M_i$ ,  $B_l$  and  $D_l$  are also shown. Here, the superscripts are the numbers of the junctions,  $N_j$ , and the subscripts are the numbers of the quarks and antiquarks,  $N_q$ .

Since hadrons are regarded to consist of quarks and junctions, Freund-Waltz-Rosner rules for vertices are enlarged as follows<sup>77</sup>:

- (1) Every quark-line and every junction-line connect two different hadrons.
- (2) Every pair of hadrons must be connected by at least one quark-line or one junction-line.

These rules are called covalence rules by Imachi and Otsuki.<sup>77</sup>

Then, the following decays into meson states are forbidden by the rules (1) and/or (2), (Fig. 7.4)

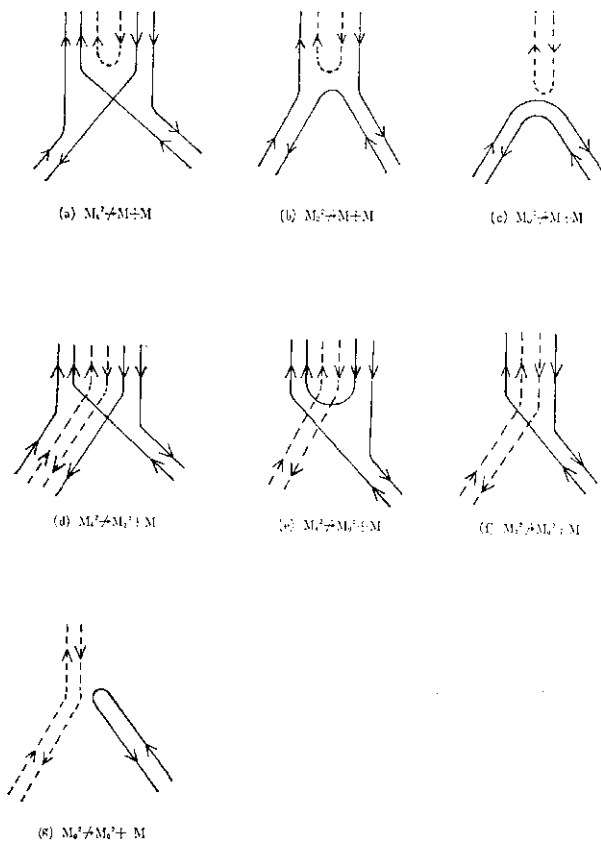


Fig. 7.4. Forbidden decays of baryonium.  
 (a)  $M_4^2 \rightarrow M+M$ ; (b)  $M_2^2 \rightarrow M+M$ ; (c)  $M_0^2 \rightarrow M+M$ ;  
 (d)  $M_4^2 \rightarrow M_2^2+M$ ; (e)  $M_4^2 \rightarrow M_0^2+M$ ; (f)  $M_2^2 \rightarrow M_0^2+M$ ;  
 (g)  $M_0^2 \rightarrow M_0^2+M$ .

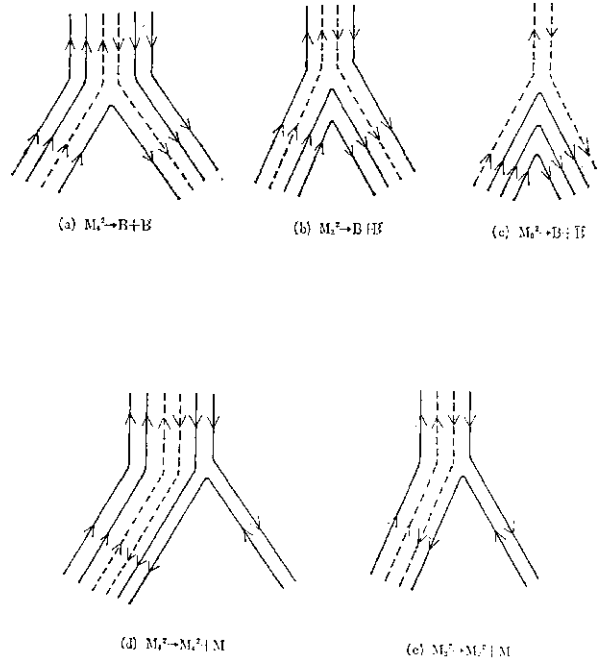


Fig. 7.5. Allowed decays of baryonium.  
 (a)  $M_4^2 \rightarrow B+B$ ; (b)  $M_2^2 \rightarrow B+B$ ; (c)  $M_0^2 \rightarrow B+B$ ;  
 (d)  $M_4^2 \rightarrow M_4^2+M$ ; (e)  $M_2^2 \rightarrow M_2^2+M$ .

$$\begin{aligned}
 &M_4^2 \leftrightarrow MM, M_2^2 \leftrightarrow MM, M_0^2 \leftrightarrow MM, \\
 &M_4^2 \leftrightarrow M_2^2 M, M_4^2 \leftrightarrow M_0^2 M, M_2^2 \leftrightarrow M_0^2 M, \\
 &M_0^2 \leftrightarrow M_0^2 M,
 \end{aligned} \tag{7.4}$$

but the following decays into  $BB$  states are allowed, (Fig. 7.5)

$$M_4^2 \rightarrow B\bar{B}, M_2^2 \rightarrow B\bar{B}, M_0^2 \rightarrow B\bar{B}. \tag{7.5a}$$

Therefore, we may call  $M_l$ ,  $M_l$  and  $M_l$  baryonium. The mesonic decays of baryonium,  $M_l$  and  $M_l$ , into the baryonium of the same type  $\bar{B}$  are also allowed, (Fig. 7.5).

$$M_4^2 \rightarrow M_4^2 M, M_2^2 \rightarrow M_2^2 M. \tag{7.5b}$$

The allowed decays of baryonium occur through string breaking and fusion of "active" quarks created by the breaking.

There are several attempts to justify the covalence rules from the exchange degeneracies of baryons.<sup>75, 78, 79</sup>

In Fig. 7.6 we show some of the duality diagrams in this model. From the duality diagrams, we find that the Regge trajectories  $a'_q$  of the baryonium  $M'_q$ ,  $a(s)$ ,  $a(s)$  and  $a(s)$  are dual with ordinary meson trajectory  $a_n(s)(=a(s))$ , two-meson ( $MM$ ) cut and three-meson ( $MMM$ ) cut, respectively. The effective slopes of  $MM$ -cut and  $MMM$ -cut are  $(1/2)a'$  and  $(1/3)a'$ , respectively. Therefore, we obtain

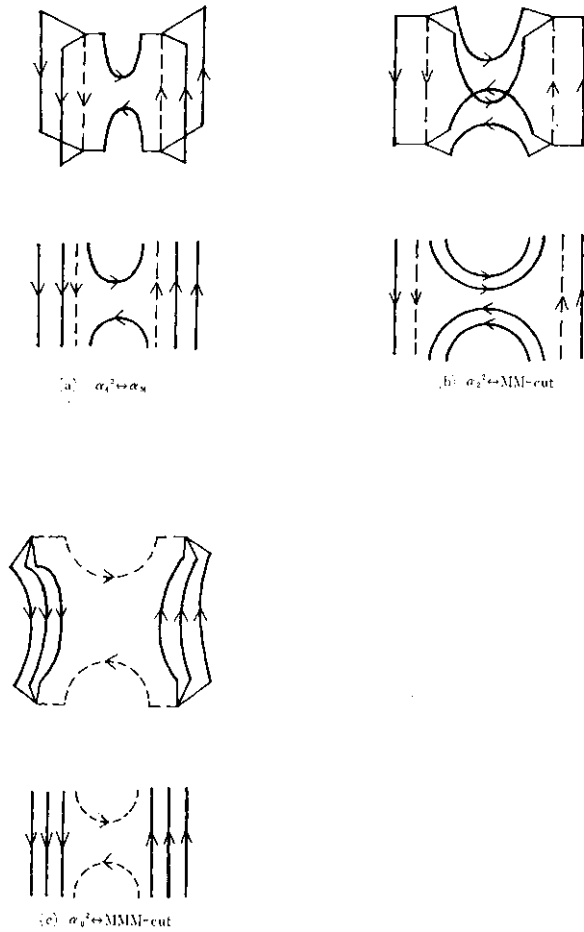


Fig. 7. 6. Duality diagrams in the junction model. (a)  $\alpha_4^2 \leftrightarrow \alpha_M$ ; (b)  $\alpha_2^2 \leftrightarrow MM$ -cut; (c)  $\alpha_0^2 \leftrightarrow MMM$ -cut.

$$\alpha_4^{2'} \approx \alpha', \alpha_2^{2'} \approx (1/2)\alpha', \text{ and } \alpha_0^{2'} \approx (1/3)\alpha' \quad (7.6)$$

from semilocal duality.<sup>7179</sup>

According to the dual unitarization scheme,<sup>80</sup> we find the following rule for the zero-intercepts,<sup>81</sup>

$$\alpha_{N_q}^{N_f}(0) \approx 1 - (1/4)N_q - (1/4)N_f - (1/4)N_s, \quad (7.7)$$

where  $N_i$  is the total number of  $i$ -quark and  $\bar{i}$ -quark.

Therefore, assuming linear trajectories for the baryonium, we obtain

$$\begin{aligned} \alpha_4^2(s) &\approx -0.5 + \alpha's, \\ \alpha_2^2(s) &\approx (1/2)\alpha's, \\ \alpha_0^2(s) &\approx 0.5 + (1/3)\alpha's. \end{aligned} \quad (7.8)$$

(See, Fig. 7.7.)

I will not try to assign observed narrow resonances to some of  $M^2$  states in this talk.<sup>79, 82</sup> Of course, it is possible to assign some of them to  $M^{**}$ .<sup>81</sup>

### 7.2 $qqqq$ states in the bag model

In the bag model colored quarks and anti-quarks are confined to the interior of a finite domain called a bag. In this model long-range confining forces are replaced by the bag pressure,  $B$ . There are the following contributions to a hadron mass in the model<sup>72-74</sup>; 1) the quark mass and kinetic energy; 2) the energy stored in the confining forces (bag energy); 3) the finite energy associated with zero-point energies of the fields confined to the bag; (We have to include this energy since it is dependent on the radius of the bag,  $R$ .) and 4) the spin-spin interaction arising from one-gluon exchange;

$$M = \sum_i \frac{\alpha_i(R)}{R} + \frac{4\pi}{3} R^3 B - \frac{Z_0}{R} + \sum_{ij} V_{ij}(R). \quad (7.9)$$

The bag model has been successful in describing the spectrum of light hadrons ( $1/2^+$  and  $3/2^+$  baryons,  $0^-$  and  $1^-$  mesons),<sup>74</sup> and can be applied to  $qqqq$  states without introducing new parameters.<sup>85</sup> In the bag model  $L=C$   $qqqq$  states are constructed by populating quark modes in a bag. Jaffe and Johnson<sup>85</sup> found the lowest mass  $qqqq$  states to be an  $SU(3)$  nonet of scalar mesons with masses ranging from 645 to 1120 MeV,

$E_K^+$ ; $ud\bar{s}\bar{d}$ , $E_K^0$ ; $ud\bar{s}\bar{u}$ ,	$\sim 880$ MeV,
$E_K^0$ ; $us\bar{u}\bar{d}$ , $E_K^-$ ; $ds\bar{u}\bar{d}$ ,	$\sim 880$ MeV,
$E^+$ ; $us\bar{d}\bar{s}$ , $E^0$ ; $(us\bar{u}\bar{s} - ds\bar{d}\bar{s})/\sqrt{2}$ ,	
$E^-$ ; $ds\bar{u}\bar{s}$ ,	$\sim 1120$ MeV,
$E_2^0$ ; $(us\bar{u}\bar{s} + ds\bar{d}\bar{s})/\sqrt{2}$ ,	$\sim 1120$ MeV,
$E_1^0$ ; $ud\bar{u}\bar{d}$ ,	$\sim 645$ MeV,

by making use of the parameters used in describing the spectrum of the light hadrons.

They have suggested that the scalar nonet [ $e(700)?$ ,  $S^*(993)$ ,  $3(980)$ ,  $4800-1100$ ] <sup>86</sup> should be identified with the above scalar  $qqqq$  nonet than with the  $^3P_0$  nonet of the conventional nonrelativistic quark model.

In the bag model  $L=0$   $qqqq$  states are expected to be broad. A broad  $qqqq$  state can simply fall apart into two  $qq$  mesons.

Higher orbital angular momentum states are obtained by rotating the bag with a diquark in one side and an antiquark in another side of an elongate bag. There are two quark configurations.<sup>87</sup> In one con-



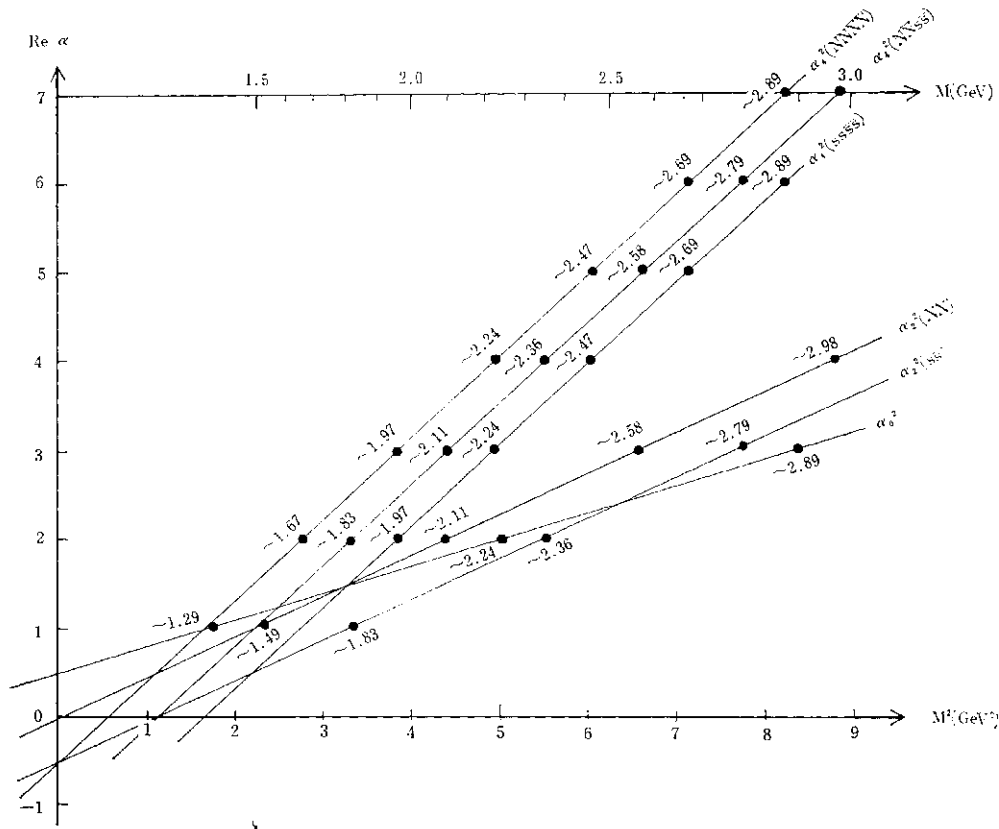


Fig. 7.7. Regge trajectories of baryonium (for  $\alpha' = 0.9 \text{ GeV}^{-2}$ ). Here, leading trajectories  $\alpha_4^2 (NNNN)$ ,  $\alpha_4^2 (NN\bar{s}s)$ ,  $\alpha_4^2 (ss\bar{s}\bar{s})$ ,  $\alpha_2^2 (NN)$ ,  $\alpha_2^2 (s\bar{s})$  and  $\alpha_0^2$  are shown, where  $N$  stands for  $u$  and/or  $d$ .

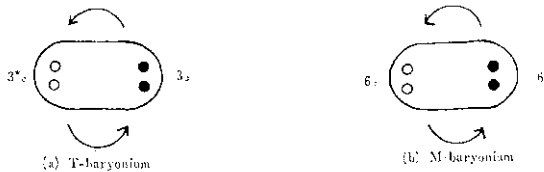


Fig. 7.8.  $qq\bar{q}\bar{q}$  states with high spin in the bag model. (a) T-baryonium; (b) M-baryonium.

figuration both the diquark and the antiquark are color-triplets (T-baryonium) and in another configuration both are color-sextets (M-baryonium),<sup>88</sup> *i. e.*,

$$(qq)_{3^*} - (\bar{q}\bar{q})_3, \quad (\text{T-baryonium})$$

and

$$(qq)_6 - (\bar{q}\bar{q})_{6^*}, \quad (\text{M-baryonium}).$$

(Fig. 7.8)

Two types of the  $qq\bar{q}\bar{q}$  states lie on Regge trajectories with different slopes. Let us discuss the slopes of the Regge trajectories. Asymptotically for large mass, we expect the trajectories to be linear in  $M^2$ . In the bag model the slope is proportional to  $(\delta^2) \sim 1/2$ , where  $Q^2$  is the quadratic Casimir for the color SU(3) representation inside the bag,<sup>89</sup>

$$Q^2 = 16/3 \quad \text{for } 3, \\ = 40/3 \quad \text{for } 6. \quad (7.10)$$

Therefore, the T-baryonium slope  $\alpha'_T$  is the same as that for ordinary  $qq$  mesons,

$$\alpha'_T = \alpha' \approx 1 \text{ GeV}^{-2} \quad (7.11a)$$

and the M-baryonium slope is given by

$$\alpha'_M = \sqrt{2/5} \alpha'_T \approx 0.63 \text{ GeV}^{-2}. \quad (7.11b)$$

The T-baryonium and M-baryonium have very different physical properties.<sup>88</sup> Although both are expected to have inhibited decays into pions because of the angular momentum barrier, they have different couplings to  $BB$ . The diquark in a T-baryonium state, being in a  $3^*$  representation, can combine with another quark in a 3 representation to form a color singlet baryon. (Fig. 7.9(a).) Therefore, the T-baryonium couples strongly with  $BB$  channel and is expected to have a decay width of  $\sim 100$  MeV. Whereas M-baryonium<sup>90</sup> cannot decay in this manner, since the diquark in a 6-representation when combined with another quark in 3 does not give a color singlet ( $6 \times 3 = 10 + 8$ ). They are, therefore, weakly coupled both to meson and  $BB$  channels (Fig. 7.9(b)-(e)), and prefer to decay by cascade into a

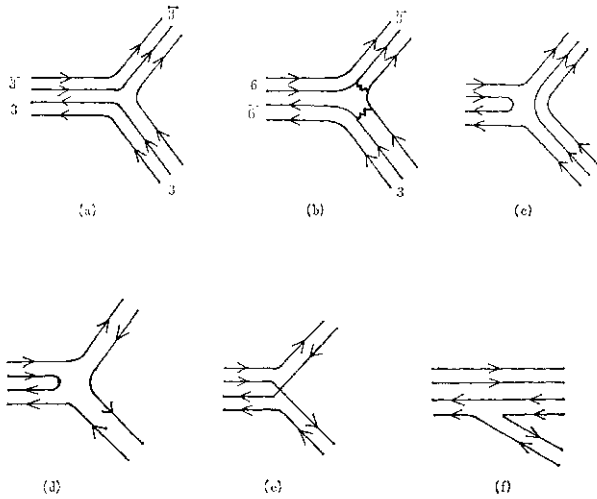


Fig. 7.9. Decays of T-baryonium and M-baryonium

resonance of the same type<sup>88</sup> (Fig. 7.9(f)).

Observed narrow resonances have been assigned to baryonium states by Chan and Hogaasen.<sup>88,84</sup>

Finally let us discuss the stability of the baryonium.<sup>91</sup>

The mass of T- and M-baryonium have been estimated by Barbour and Ponting<sup>92</sup> in variational method by making use of a model Hamiltonian. According to their results, in the T-baryonium case the two  $q\bar{q}$ -meson states, through which baryonium may decay into meson final states, are generally found to be more massive than the baryonium state itself, but in the M-baryonium case they are lighter than the baryonium state.

However, asymptotically for large mass, the M-baryonium with spin  $J$  is lighter than the two  $g$   $\Lambda$ -mesons with spin  $J/2$  since<sup>93</sup>  $2a'_m > a'$ ; Since the mass ( $M$ ) of the M-baryonium with spin  $J$  is  $\ll j\bar{j}\bar{a} = (j5j2J/ay^2)$  ( $\sim a'_m M$ ) and since the mass ( $m$ ) of the  $qq$ -meson with spin  $J/2$  is  $\ll j/2a'$  ( $J/2 \sim a'm^2$ ),  $2m \ll \sqrt{2J/a'} \sim (5/2)^{1/4} \sqrt{J} a' M$ . Notice, however, this argument is applicable only when  $|\sigma(\mathbf{0})| < 1$ .

### §8. Dibaryons

Once pp total cross sections were considered

to be roughly energy independent.<sup>94</sup> If they are independent of energy, there should be no hadrons with baryon number two in dual models.

Recently a remarkable energy dependence has been discovered in measurements of pp total cross sections with a polarized beam and target,<sup>95</sup> and several evidences on the existence of the hadrons with baryon number two listed in Table III have been reported.<sup>95-101</sup>

$5^2(2.14)$  and  $B(2.22)$  are characterized by their small elasticity.

The deuteron is not listed in the table since it is not a hadron, but a nucleus, *i. e.*, a bound state of a proton and a neutron bound by nuclear force. To regard the deuteron as a six-quark state is not adequate.<sup>103</sup> In the terminology of the quark model it is a molecular state of two clusters of three-quarks bound by colorless interaction.

Then, are  $5^2(2.14)$  and  $5^2(2.22)$  the subject of this conference, *i. e.*, are they nuclei or hadrons? I would like to regard them as hadrons because of their small elasticity and their small sizes.

The bag model has been applied to dibaryon resonances.<sup>104,105</sup> In the bag model  $L=0$  six-quark states are constructed by populating quark levels in a bag. The predicted energy levels are

$$I=1; \quad {}^1S_0 (M=2.24 \text{ GeV}),$$

$${}^1D_2 (M=2.36 \text{ GeV})$$

$$I=0; \quad {}^3S_1 (M=2.16 \text{ GeV}),$$

$${}^3D_3 (M=2.36 \text{ GeV}).$$

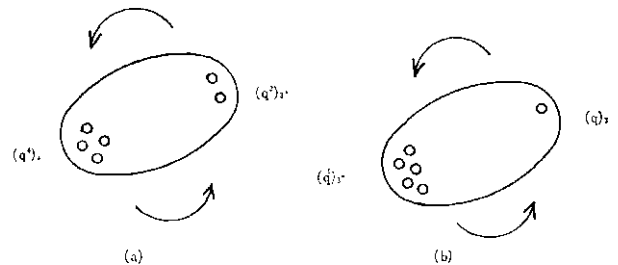


Fig. 8.1. Dibaryon resonances in the bag model ( $a^*o$ )..

Table III. Dibaryon resonances.

Name <sup>102</sup>	Mass (GeV)	Width (MeV)	$I$	NN-state	Elasticity	Remarks
$B^2(2.14)$	2.14-2.17	50-100	1	${}^1D_2$	0.1	$\Delta\sigma_L, \Delta\sigma_T$ etc. <sup>95-98</sup>
$B^2(2.22)$	2.20-2.26	100-150	1	${}^3F_3$	0.2	$\Delta\sigma_L$ etc. <sup>95,96,99</sup>
$B^2(2.43)$	2.43-2.50	150	1	${}^1S_0$ or ${}^1G_4$		$\Delta\sigma_L, \Delta\sigma_T, C_{LL}$ etc. <sup>96</sup>
$B^2(2.38)$	2.38	?	0?	?		$\gamma d \rightarrow np$ <sub>1<sup>100,101</sup></sub>

$L=l$  negative parity resonances are obtained by rotating the bags with the following clusters of quarks in two ends,

$$(q^4)_3 - (q^2)_3^*, (q^5)_3^* - (q)_3 \text{ etc.}$$

(See, Fig. 8.1.) Mulders, Aerts and de Swart have estimated the masses of dibaryon states in the bag model.<sup>105</sup> Some states occur with quantum numbers foreign to NN states, which they refer to as extraneous states.

## §9. Concluding Remarks

Any talk on particle spectroscopy is incomplete unless something is mentioned about the quarks.

An expert on English literature told me that there were four seagulls in a dence fog when Tristan and Isolde heard three quarks.<sup>106</sup>

Now we have already found five seagulls and it seems that there is at least one more seagull in a fog. Let me speculate that this sixth seagull will be discovered before next Conference.

## Acknowledgments

I would like to thank Dr. T. Kobayashi, Dr. S. Sakai, Dr. T. Inami, Prof. Y. Iwasaki, Prof. H. Miyazawa and Prof. M. Uehara for fruitful discussion. I would like to express my sincere gratitude to Prof. J. D. Jackson for his valuable advices and comments. It is a great pleasure to acknowledge the help I have received from Prof. J. Arafune, the scientific secretary.

## References

1. H. Yukawa: Proc. Phys.-Math. Soc. Japan, **17** (1934) 48.
2. G. Feldman and M. L. Perl: Phys. Reports, **33** (1977) 285.
3. G. Flugge: rapporteur talk at this Conference.
4. A. DeRújula, H. Georgi and S. L. Glashow: Phys. Rev. **D 12** (1975) 147.
5. T. Appelquist and H. D. Politzer: Phys. Rev. Letters **34** (1975) 43; Phys. Rev. **D 12** (1975) 1404.
6. R. Van Royen and V. F. Weisskopf: Nuovo Cimento, **50A** (1967) 617.
- 7) E. Eichten, K. Gottfried, T. Kinoshita, J. Kogut, K. D. Lane and T. M. Yan: Phys. Rev. Letters **34** (1975) 369.
8. The contributions from multiple-gluon-exchange to  $Of\hat{a}Oi$  with  $i=P, T$  and  $A$  have no spin independent component in the static limit.
9. J. Pumplin, W. Repko and A. Sato: Phys. Rev. Letters **35** (1975) 1538.
10. H. J. Schnitzer: Phys. Rev. Letters **35** (1975) 1540.
11. H. J. Schnitzer: Phys. Rev. **D 13** (1976) 74.
12. H. J. Schnitzer: Phys. Letters **65B** (1976) 239.
13. See, also, J. S. Kang and H.J. Schnitzer: Phys. Rev. **D 12** (1975) 841; J. G. Wills, D. B. Lichtenberg and J. T. Kiehl: Phys. Rev. **D 15** (1977) 3358; K. Hirata, T. Kobayashi and N. Nakamaru: Phys. Rev. **D 18** (1978) 834; W. Celemaster, H. Georgi and M. Machacek: HUTP-771A051; D. B. Lichtenberg and J. G. Wills: IUHET-27.
14. A. B. Henriques, B. H. Kellett and R. G. Moorhouse: Phys. Letters **64B** (1976) 85.
15. X. Y. Pham and J. M. Richards: Phys. Letters **70B**(1977) 370.
16. L. H. Chan: Phys. Letters **71B** (1977) 422, Paper No. 6 submitted to this Conference.
17. C.E. Carlson and F. Gross: Phys. Letters **74B** (1978) 404.
18. H.J. Schnitzer: Paper No. 46 submitted to this Conference.
19. In this model
 
$$M(^3S_1) - M(^1S_0) = \frac{32\pi}{9m_c^2} \alpha_s |\psi(0)|^2 + \frac{4}{3} \frac{fa(1+\kappa)^2}{m_c^2} \langle r^{-1} \rangle_{S\text{-wave}}$$
20. F. Wilczek and A. Zee: Phys. Rev. Letters **40** (1978) 83.
21. See, also, M. Suzuki: Phys. Letters **76B** (1978) 466; C. G. Callan, R. Dashen, D.J. Gross, F. Wilczek and A. Zee: Princeton preprint, COO-2220-132; According to Suzuki (private communication),  $V_s(0) < 36\text{MeV}$   $SX'S$ .
22. J. D. Jackson: Proc. Summer Inst. Particle Physics SLAC Report No. 198 (1976) p. 147.
23. J. Arafune, M. Fukugita and Y. Oyanagi: Phys. Rev. **D 16** (1977) 772.
24. The lower bound  $\sim 20\%$  is derived by making use of the experimental results,  $2\pi(0 \rightarrow \mathbf{x}(3.45)0) \approx 2\pi X(\mathbf{x}(3.45) \rightarrow \mathbf{r}) \approx 0.5\%$  and  $\mathcal{E}r(0 \rightarrow \mathbf{z}(3.45)\mathbf{r}) < 2.5\%$ .
25. G. Feinberg and J. Sucher: Phys. Rev. Letters **35** (1975) 1740; J. S. Kang and J. Sucher: Paper No. 659 submitted to this Conference.
26. H. Lipkin: Fermilab Conf. 77/93 THY (1977).
27. R. Barbieri, R. Gatto and R. Kôgerler: Phys. Letters **60B** (1976) 183.
28. At present the mass of the possible new resonance can be  $-3.17$  GeV instead of  $-3.6$  GeV.<sup>3</sup>
29. S. W. Herb, et al: Phys. Rev. Letters **39** (1977) 252.
30. W. R. Innés, et al.: Phys. Rev. Letters **39** (1977) 1240.
31. Ch. Berger, et al.: Phys. Letters **76B** (1978) 243; C. W. Darden, et al.: Phys. Letters **76B** (1978) 246.
32. Y. Hara: Phys. Rev. **B 134**, (1964) 701; Z. Maki: Progr. theor. Phys. **31** (1964) 331.
33. S. L. Glashow, J. Iliopoulos and L. Maiani: Phys. Rev. **D2** (1970) 1285.
34. M. Kobayashi and K. Maskawa: Progr. theor. Phys. **49** (1973) 652.
35. See, also, H. Harari: Phys. Letters **57B** (1975)

- 265; Ann. Phys. (N. Y.) **94** (1975) 391; L. Maiani: Phys. Letters **62B** (1976) 183; S. Pakvasa and H. Sugawara: Phys. Rev. **D14** (1976) 305; J. Ellis, M. K. Gaillard and D. V. Nanopoulos: Nucl. Phys. **B109** (1976) 213.
36. D. R. Yennie: Phys. Rev. Letters **34** (1975) 239; See, also, J. J. Sakurai: Paper No. 111 submitted to this Conference (to be published in Priysica A); K. Ishikawa and J.J. Sakurai: Paper No. 1110 submitted to this Conference.
37. J. L. Rosner, C. Quigg and H. B. Thacker: Paper No. 879 submitted to this Conference.
38. E. Eichten and K. Gottfried: Phys. Letters **66B** (1977) 286.
39. C. Quigg and J. L. Rosner: Phys. Letters **71B** (1977) 153; **72B** (1978) 462.
40. See, also, Y. Muraki: Progr. theor. Phys. **41**, (1969) 473; K. Mori, Y. Muraki and M. Nakagawa: Paper No. 471 submitted to this Conference.
41. D. Pignon and C. A. Piketty: Phys. Letters **74B** (1978) 108.
42. See, for example, O. Nachtmann: *Proc. Int. Symp. Photon and Lepton Physics, Hamburg, Aug. 1977*; A. De Rújula, H. Georgi and H. D. Politzer: Ann. Phys. (N. Y.) **103** (1977) 315; W. A. Bardeen, A. J. Buras, D. W. Duke and T. Muta: Fermi-Lab-Pub-78/42 THY.
43. R. G. Moorhouse, *et al.*: Nucl. Phys. **B124** (1977) 285.
44. W. Celemaster, H. Georgi and M. Machacek: Phys. Rev. **D17** (1978) 879; W. Celemaster and F. Henyey: UCSD-10P10-191 (1978).
45. R. Levine and Y. Tomozawa: UMHE 78-41 (1978). These authors derived a potential which interpolates the  $r \rightarrow 0$  limit (3.9) and  $r \rightarrow \infty$  limit  $r \ln r$ , by solving a renormalization group equation in QCD.
46. H. Grosse and A. Martin: Réf. TH. 2513-CERN (1978).
47. H. J. Schnitzer: Paper No. 47 submitted to this Conference.
48. N. Isgur and G. Karl: Paper No. 13, 14 and 16 (Phys. Letters **72B** (1977) 109) submitted to this Conference.
49. There is also an interesting application of a rotating stringlike bag model, in which the quarks reside at the ends, to both  $q^*$  and  $q^*q$  baryons. See, P. J. G. Mulders, A. Th. M. Aerts and J. J. de Swart: Paper No. 386 submitted to this Conference.
50. R. Brandelik, *et al.*: Phys. Letters **70B** (1977) 132.
51. G. Feldman: rapporteur talk at this Conference.
52. J. Ellis, M. K. Gaillard and D. V. Nanopoulos: Nucl. Phys. **B100** (1975) 313. See, also, G. Altarelli, N. Cabibbo and L. Maiani: Phys. Rev. Letters **35** (1975) 635, N. Cabibbo and L. Maiani: Phys. Letters **73B** (1978) 418.
53. M. Suzuki: LBL Report, LBL-7948 (1978).
54. M. Peshkin and J. L. Rosner: Nucl. Phys. **B122** (1977) 144, A. Pais and S. B. Treiman: Phys. Rev. **D15** (1977) 2529.
55. P. Rapidis, *et al.*: Phys. Rev. Letters **39** (1977) 526; D. L. Scharre, *et al.*: Phys. Rev. Letters **40** (1978) 74.
56. M. Matsuda, N. Nakagawa, K. Odaka, S. Ogawa and M. Shin-Mura: Progr. theor. Phys. **59** (1978) 1396.
57. M. Matsuda, T. Matsushita, K. Odaka and S. Ogawa: Paper No. 351 submitted to this Conference.
58. S. P. Rosen: Paper No. 125 submitted to this Conference and Phys. Rev. Letters **41** (1978) 3.
59. See, also, Y. Hara: talk given at the Symposium on New Particles at Research Inst, for Fundamental Physics, Kyoto University, Feb. 1978.
60. Observed value of Michel parameter,  $\lambda = 0.83 \pm 0.12 \pm 0.15$  is incompatible with  $V+A$  ( $\rho = -0.15$ ), but compatible with  $V-A$  ( $\rho = 0.53$ ). (See ref. 51.)
61. N. Kawamoto and A. I. Sanda: Phys. Letters **76B** (1978) 446; F. Gilman and D. Miller: Phys. Rev. **D17** (1978) 1846.
62. A. S. Carroll, *et al.*: Phys. Rev. Letters **32** (1974) 247; V. Chaloupka, *et al.*: Phys. Letters **61B** (1976) 487; W. Bruckner, *et al.*: Phys. Letters **67B** (1977) 222; S. Sakamoto, *et al.*: Paper No. 1058 submitted to this Conference.
63. P. BenkheirL *et al.*: Phys. Letters **78B** (1977) 483.
64. H. Braun, *et al.*: Phys. Letters **60B** (1976) 481; C. Evangelista, *et al.*: Phys. Letters **72B** (1977) 139; P. Pavlopoulos, *et al.*: Phys. Letters **72B** (1978) 415; A. A. Carter, *et al.*: Phys. Letters **67B** (1977) 117; S. Bartalucci, *et al.*: DESY 77/59 (1977); G. Bemporad: Hamburg International Conference on Lepton and Photon Interactions, Aug. 1977; C. Cosme, *et al.*: presented by F. Laplanche, Hamburg International Conference on Lepton and Photon Interactions, Aug. 1977; G. Cosme, *et al.*: Phys. Letters **67B** (1977) 231; B. Esposito, *et al.*: Phys. Letters **68B** (1977) 389; C. Bacci, *et al.*: Phys. Letters **68B** (1977) 393; G. Barbiellini, *et al.*: Phys. Letters **68B** (1977) 397.
65. G. F. Chew: *Proc. Third Europ. Symp. NN Interaction, Stockholm, 1976* (Pergamon Press) p. 515.
66. J. L. Rosner: Phys. Rev. Letters **21** (1968) 950, 1422 (E); J. L. Rosner: Phys. Reports **11C** (1976) 189.
67. See, also, Y. Hara, Progr. theor. Phys. **47** (1972) 1624.
68. P. G. O. Freund, R. Waltz and J. L. Rosner: Nucl. Phys. **B13** (1969) 237.
69. M. Imachi, S. Otsuki and F. Toyoda: Progr. theor. Phys. **55** (1976) 551; **57** (1977) 517.
70. X. Artru: Nucl. Phys. **B85** (1975) 442.
71. G. C. Rossi and G. Veneziano: Nucl. Phys. **B123** (1977) 507.
72. A. Chodos, R. L. Jaffe, K. Johnson, C. B. Thorn and V. F. Weisskopf: Phys. Rev. **D9** (1974) 3471.
73. A. Chodos, R. L. Jaffe, K. Johnson and C. B. Thorn: Phys. Rev. **D10**, (1974) 2594.
74. T. A. DeGrand, R. L. Jaffe, K. Johnson and K. Kiskis: Phys. Rev. **D12** (1975) 2060.

75. Linear baryons have been proposed by T. Inami, K. Kawarabayashi and S. Kitakado in Paper No. 284 submitted to this Conference.
76. Baryons and exotic hadrons in the quark-string model have been studied in a semi-classical approach by looking for classical rigid rotator solutions by K. Kikkawa, T. Kotani, M. Sato and M. Kenmoku in Paper No. 356 submitted to this Conference.
77. M. Imachi and S. Otsuki: *Progr. theor. Phys.* **58** (1977) 1657, 1660; **59** (1978) 1290.
78. F. Toyoda and M. Uehara: *Progr. theor. Phys.* **58** (1977) 1456; T. Inami, K. Kawarabayashi and S. Kitakado: *Phys. Letters* **72B** (1977) 127.
79. M. Uehara: *Progr. theor. Phys.* **59** (1978) 587.
80. Y. Eylon and H. Harari: *Nucl. Phys.* **B80** (1974) 349.
81. Upper and lower bounds of  $a_1^i(0)$ ,  $a_1^i(0)$  and  $a_1^i(0)$  have been derived by K. Igi and S. Yazaki in Paper No. 365 submitted to this Conference.
82. M. Imachi, S. Itoh and S. Otsuki: Paper No. 538 submitted to this Conference.
83. M. Uehara: SAGA 78/2 (1978).
84. See, also, A. W. Hendry and I. Hinchliffe: Paper No. 253 submitted to this Conference.
85. R. L. Jaffe and K. Johnson: *Phys. Letters* **60B** (1976) 201; R. L. Jaffe: *Phys. Rev.* **D15** (1977) 267, 281.
86. As to the present experimental status of the scalar nonet, see, Cashmore, rapporteur talk at this Conference.
87. These two types of states do not mix when the orbital angular momentum  $L$  (of the diquark about the antiquark) is large because of the following reason. From one-gluon-exchange we obtain a spin-spin interaction between the two quarks of the following form,

$$a = 1$$

where  $C$  is proportional to the quark-gluon coupling  $a$ , and depends on the overlap of the quark spacial wave functions with the potential. Two quarks may couple to a  $3^*$  or  $6$  of color SU(3) and a spin singlet or triplet. The diquark system can thus be in the following representations with the eigenvalue  $AE$  of the spin-spin interaction

(color, spin)	Flavor	$\Delta E$
$(3^*, 1)$	$3^*$	$-8C$
$(6, 3)$	$3^*$	$-(4/3)C$
$(3^*, 3)$	$6$	$(8/3)C$
$(6, 1)$	$6$	$4C$

Since the color magnetic forces between the quarks and the antiquarks are short-ranged, their effect should decrease rapidly with  $L$ . At high  $L$ , therefore, there are no interaction which mixes the color-triplet diquark and the colorsextet diquark. For detail see ref. 88.

88. Chan H. M. and H. Hogaasen: *Phys. Letters* **72B** (1977) 121; (1978) 400; *Nucl. Phys.* **B136** (1978) 401. See, also, R. L. Jaffe: *Phys. Rev.* **D17** (1978) 1444.
89. K. Johnson and C.B. Thorn: *Phys. Rev.* D13 (1977) 1934.
90. The M-baryonium may correspond to the  $M_i^+$  meson in the junction model shown in Fig. 7.3 (f). The decays of  $M_i^+$  into  $M_i^+ + M$ ,  $B+B_s$ ,  $B+B+B+B$  etc. are allowed, but the decay of  $M_i^+$  into  $B+B$  is forbidden. There is also a possibility that there may be a new type of strings, at the ends of which diquarks and antidiquarks in color sextets are tied. The allowed decay of the new  $qqqq$  state tied with the new string  $M_i^+$  is  $M_i^+ \rightarrow M_i^+ + M$ .
91. Quantitative calculation of  $qqqq$  states has been carried out in (3+1) dimensional lattice gauge theory by Sakai and Hikosaka, and they have obtained the result,  $M(qqqq)/M(N) = 2.8$ ; S. Sakai and K. Hikosaka: Paper No. 250 submitted to this Conference. In this model the results,  $M(\hat{u}O \ll M(\hat{O}) \ll 0.82Af(N)$ , have already been obtained by Banks, *et al.*; T. Banks, *et al.*: *Phys. Rev.* D15 (1977) 1111.
92. I. M. Barbour and D. K. Ponting: Paper No. 258 submitted to this Conference.
93. H. M. Chan: private communication.
94. See, however, B. Schrempp and F. Schrempp: *Phys. Letters* 55B (1975) 303.
95. L.P. Auer, *et al.*: *Phys. Letters* 67B (1977) 113; 70B (1977) 475; *Phys. Rev. Letters* 41 (1978) 354; Paper No. 447 submitted to this Conference.
96. N. Hoshizaki: *Progr. theor. Phys.* 57 (1977) 1099; 58 (1977) 716; Paper No. 520 submitted to this Conference.
97. See, also, S. Furuichi, M. Matsuda and W. Watari: *Nuovo Cimento* 23A (1974) 375.
98. R. A. Arndt: *Phys. Rev.* 165 (1968) 1834; Los Alamos Nucleon-Nucleon Workshop (June, 1978), H. Suzuki: *Progr. theor. Phys.* 54 (1975) 143.
99. K. Hidaka, *et al.*: *Phys. Letters* 70B (1977) 497.
100. T. Kamae, *et al.*: *Phys. Rev. Letters* 38 (1977) 468.
101. T. Kamae and T. Fujita: *Phys. Rev. Letters* 38 (1977) 471.
102. The symbol  $B^2$  for dibaryon resonances has been invented by A. Yokosawa at this Conference.
103. However, a model where a deuteron is considered as the two nucléon bound state with a small mixture of the six-quark bound state has been proposed. It has been shown that this six-quark state determines the deuteron form factors when  $\#^2 > 1(\text{GeV}/c)^2$ . See, A. P. Kobushkin: Paper No. 994 submitted to this Conference; Y. Kizukuri, M. Namiki and K. Okano: Waseda Univ. preprint (1978).
104. R. L. Jaffe: *Phys. Rev. Letters* 38 (1977) 195 and 617(E).
105. P. J. G. Mulders, A. Th. M. Aerts and J. J. de Swart: Paper No. 386 submitted to this Conference. See, also, P. J. G. Mulders, A. Th. M. Aerts and J. J. de Swart: *Phys. Rev. Letters* 40 (1978) 1543.
106. K. Fujii: *Butsuri* 28 (1973) 989.

P6:  $eN$ ,  $fiN$ ,  $rN$  Reactions

*Chairman:* W. PAUL

*Speaker:* E. GABATHULER

*Scientific Secretaries:* K. KONDO  
T. SATO

## P 6 Experimental Review of Electron, Muon and Photon Physics

E. GABATHULER

CERN

### Introduction

In order to review in a one-hour talk the work of many experiments in the field of photon, electron and muon physics, it has been necessary to be selective and to apologise to all those groups whose work is not reported in this plenary review. However, there have been many excellent mini-reviews in the parallel sessions of this Conference and much more detailed information can be found there as well as in previous Conference reports.<sup>1</sup>

For the study of hadronic final states, the photon can be considered as a real or virtual probe, and there is now considerable evidence that the dual role of the real photon in terms of its hadronic (long-range) and non-hadronic (point-like) behaviour can be reasonably well extrapolated into the  $g^2$ -domain of the virtual photon interaction. In fact the success of the quark-parton model in explaining many features of the hadronic final states in low  $Q^2$  electron and muon scattering and the vector dominance model in explaining photo-production strongly point towards a single unified explanation of all photon interactions within the framework provided by the quark-parton model together with Quantum Chromodynamics. The ability to carry out experiments at higher energies has in general simplified both the experimental and theoretical understanding.

### §1. Total Photon Cross-Sections

#### 1.1. Hydrogen

The measurement of real photon cross-sections has been carried out by a U.C.S.B.-Toronto-F.N.A.L. (U.T.F.) group<sup>2</sup> in a high precision experiment (systematic error  $\sim 0.7\%$ ) using tagged photons up to an energy of 185 GeV. The main source of difficulty in achieving such precision is caused by the electromagnetic pairs whose cross-section is  $\sim 200$  greater than the hadronic cross-section. The photon energy range has been extended down

to 18 GeV to provide a comparison with lower energy data.<sup>3</sup> The results, illustrated in Fig. 1, show that the photon behaves very much like a hadron in that the cross-section has a broad minimum around a photon energy of 40 GeV and rises by  $\sim 4/ub$  over the measured energy range. A straight line fit to the data for  $E_\gamma > 35$  GeV gives:

$$a_\tau(\gamma p) = (112.76 \pm 0.41) + (0.0272 \pm 0.00050) E_\gamma$$

which is very similar to that obtained in hadron-induced total cross-sections. This comparison can be made qualitative using vector dominance which relates

$$\sigma_T(\gamma p) = \alpha \sum_V (4\pi/\gamma_V^2) \sigma_T(Vp)$$

and the quark model which relates  $\sigma(Vp)$  to the measured hadronic cross-sections. The curves given in Fig. 1 show that if the energy dependences of all the  $p, \pi^0$  and  $j^+$  cross-sections are representative of all the components of  $a_\tau$  for the higher vector mesons then it is difficult to fit the data. It has been suggested by the U.T.F. group that this excess of  $2.6/ub$  cross-section could be due to the charm cross-section. This assumption relies heavily on the normalization to the previous lower energy data and it is doubtful to use the Vector Dominance Model to explain small differences at the 5% level.

#### 1.2. Complex nuclei

The U.T.F. group have also measured the total photon cross-section in different nuclei which is of interest mainly due to the concept of shadowing. Shadowing has been observed at lower energies,<sup>4</sup> and is caused by the "hadronic" part of the photon being absorbed by nucleons on the front surface of the nucleus. The main interest in going to higher energies is to measure the amount of shadowing since there have been conflicting results as to the amount at lower energies.<sup>5</sup> In addition, vector dominance arguments can be

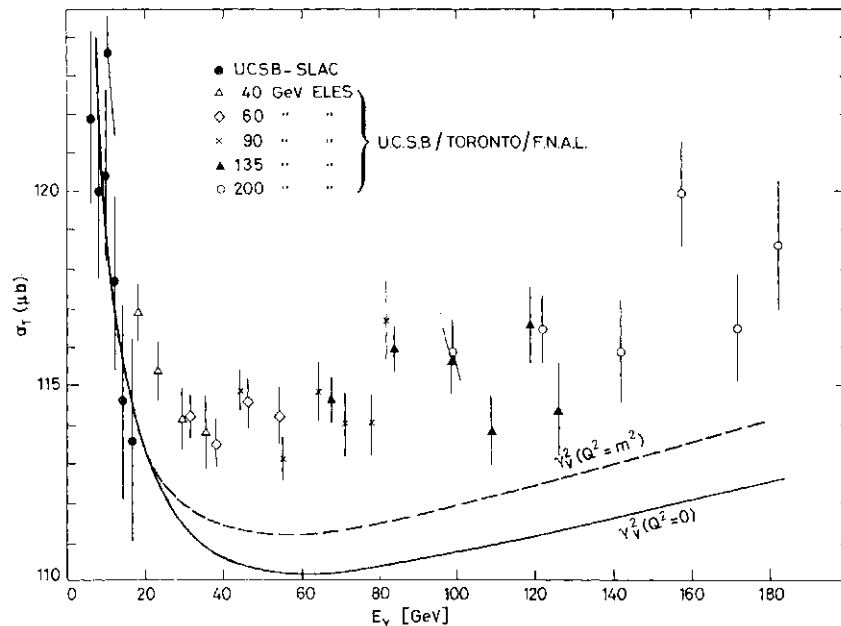


Fig. 1.  $\sigma(\gamma p)$  total photon cross-section versus  $E_\gamma$  for U.T.F. experiment. Curves are fits to the energy dependence given by  $p$ ,  $\langle o \rangle$  and  $\langle f \rangle$  cross-sections using  $\gamma - V$  couplings given by photons ( $Q^2=0$ ) and  $e^+e^-$  ( $Q^2=m^2$ ).

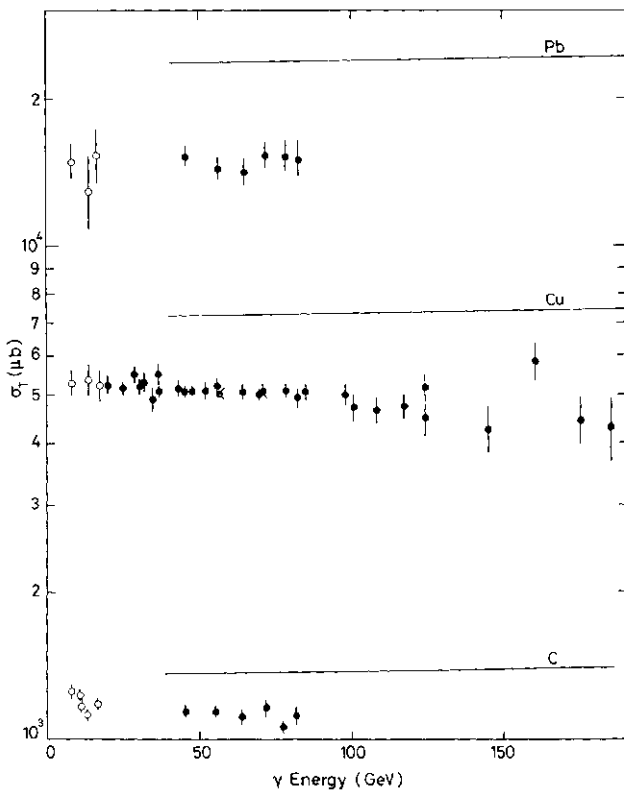


Fig. 2.  $G(JA)$  total cross-section versus  $E_\gamma$  for C, Cu and Pb targets. The solid lines are  $A$  times the energy-dependent fit to the  $H_2$  data.  $\$$ , U.C.S.B.;  $+$ , U.T.F.

used to show that higher mass vector mesons should increase the amount of shadowing since the distance travelled by the meson in the nucleus  $\sim 2E/M_V$ -

The results are presented in Fig. 2 for Carbon, Copper and Lead, where the solid line is  $A$  times the energy dependent fit from  $H_2$  for  $E_\gamma < 35$  GeV, i.e., neglecting small effects due to proton-neutron differences. There is clear evidence for shadowing, and the results on Copper are in good agreement with the lower energy data of the previous measurements of the U.C.S.B. group at SLAC.<sup>6</sup> There is little energy dependence of the Copper data by itself, but in order to show the effect of shadowing it is simpler to compare the nuclear cross-section with that for free nucleons in terms of the effective nucleon number defined as

$$\frac{A_{\text{eff}}}{A} = \frac{\sigma(\gamma A)}{Z\sigma(\gamma p) + (A-Z)\sigma(\gamma n)}$$

This quantity is plotted in Fig. 3, and shows that there is indeed increased shadowing with photon energy. When more complete data are available, it will be useful to study the behaviour of the cross-section on different nuclei around the region of the broad minimum around 50 GeV in order to obtain a better understanding of the shadowing process. In this region the real part of the scattering amplitude off a single nucleon presumably goes through zero, which will minimise many of the corrections brought about by the real part.



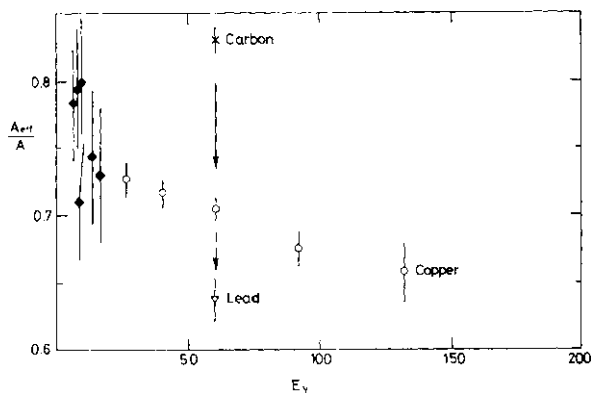


Fig. 3.  $A_{\text{eft}}/A$  versus  $E_\gamma$  for U.T.F. experiment on different targets.  $\square$ , U.C.S.B. (Cu);  $+$ , Cornell (Cu).

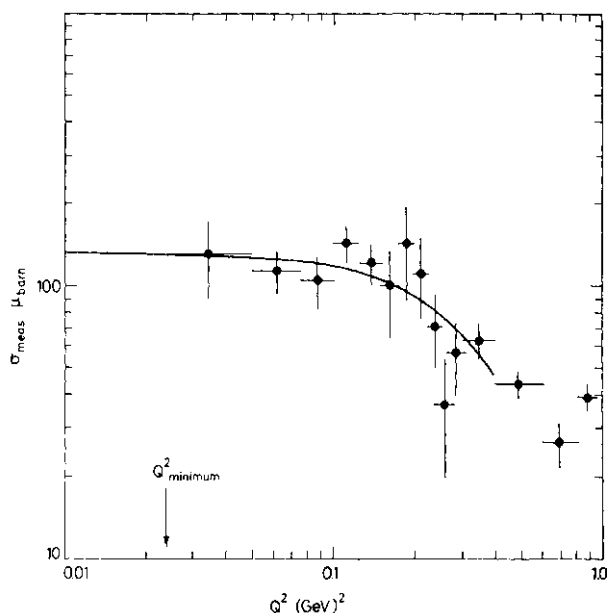


Fig. 4. The total inelastic cross-section on  $H_2$  versus  $Q^2$  in the  $\nu$  range 170-200 GeV using data from C.H.I.O. Fit given in text.

## §2. Inelastic Structure Functions Including Determination of $R$

### 2.1. Comments on $R$

The study of inelastic lepton scattering enables the photon to be taken off the mass shell and introduces two cross-sections for longitudinal and transverse photons whose ratio  $R$  is related to the structure functions  $W_1$  and  $W_2$  or  $F_1$  and  $F_2$ . The  $Q^2$  dependence of the inelastic cross-section has been measured by the Chicago-Harvard-Illinois-Oxford (CHIO) collaboration<sup>7</sup> at very small  $Q^2$  in the energy range 170-200 GeV and the results are presented in Fig. 4. A fit has been made to the data of the form

$$\sigma_{\text{meas}}(UQ^2) = \sigma(UQ^2=0) [A^2/(q^2+A^2)]$$

giving

$$A = 0.09 \pm 0.03 \text{ GeV}.$$

In order to relate this cross-section to photoproduction it is necessary to know  $i?$ , since  $R=0$  gives  $\sigma_{\text{meas}} = 132 \pm 13 \text{ } \mu\text{b}$  and  $R=0.5$  gives  $\langle 7y \rangle = 113 \pm 13 \text{ fib}$ .

The importance of  $R$  can also be understood in terms of the quark-parton model where  $R$ , which is a function of  $x=Q^2/2M\nu$  can be written as

$$\begin{aligned} R(x)_{\text{prim}} &= \sigma_L/\sigma_T = 4(M_q^2 + p_\perp^2)/Q^2 \\ &= 4p_\perp^2/Q^2 \quad (\text{Quark mass}=0) \end{aligned}$$

where  $p_\perp$  is the transverse momentum of the valence quark inside the nucleon and is now known from Drell-Yan type measurements to be as large as  $\sim 800 \text{ MeV}/c$ . In addition to the primordial contribution (related only to the target nucleon at rest) there is an additional contribution from the dynamics of the interaction which is given by Q.C.D. and is a slowly varying function of  $Q^2$ . For reasons of simplicity, since both contributions are related,  $R$  can be expressed as

$$\begin{aligned} R(x) &= R(x)_{\text{prim}} + R(x)_{\text{dyn}} \\ &= 4p_\perp^2/Q^2 + 1/\log(Q^2/A^2). \end{aligned}$$

The most precise range of data on  $R$  comes from the different SLAC experiments and the results of this compilation presented at the Conference<sup>8</sup> are presented in Fig. 5, where the values of  $R$  obtained for each  $Q^2$  and  $W^2$  region have been derived from a large set of kinematic data points which are all very consistent. There is no obvious strong dependence on  $Q^2$  or  $W^2$  and the average value of  $R$  is  $\langle i? \rangle_{\text{w.r. ave}} = 0.21 \pm 0.1$  which is somewhat smaller than that given a year ago of  $0.25 \pm 0.1$ .

In order to study the dependence of  $R$  on  $x$ , this has been plotted in Fig. 6 for different values of  $Q^2$ , together with the theoretical Q.C.D. predictions.<sup>10</sup> The data are in good agreement at low  $Q^2$ , but generally lie above the theoretical predictions for larger  $Q^2$ . It is clearly important, but difficult to measure, to have more precise data on  $R$  as a function of  $x$  and  $Q^2$ , since the quantity is related to the transverse momentum of the quarks within the nucleon. A determination of  $R$  from neutrino experiments in the range  $q^2 > \backslash \text{GeV}^2$  gives smaller values.<sup>11</sup> However, the uncer-

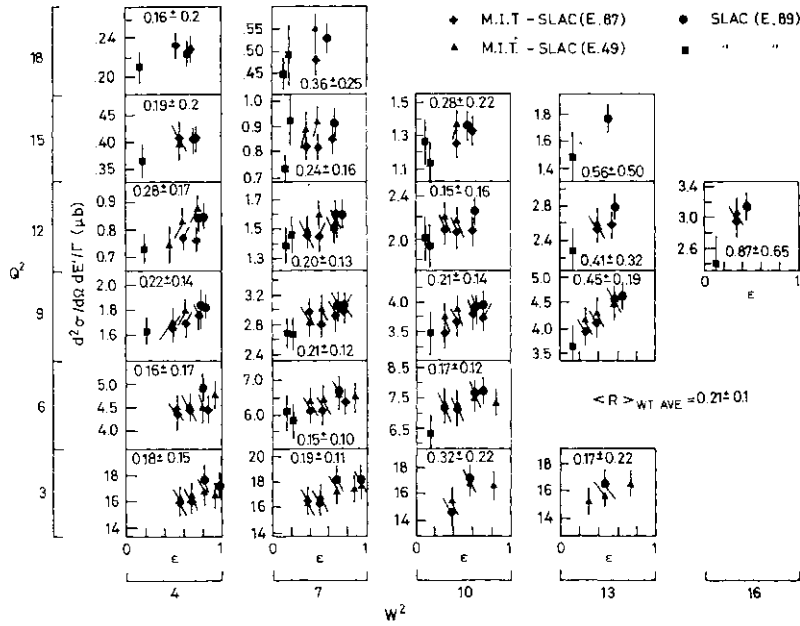


Fig. 5. Value of  $R$  obtained from measurements at each value of  $g^2$  and  $W$  from SLAC-MIT data.

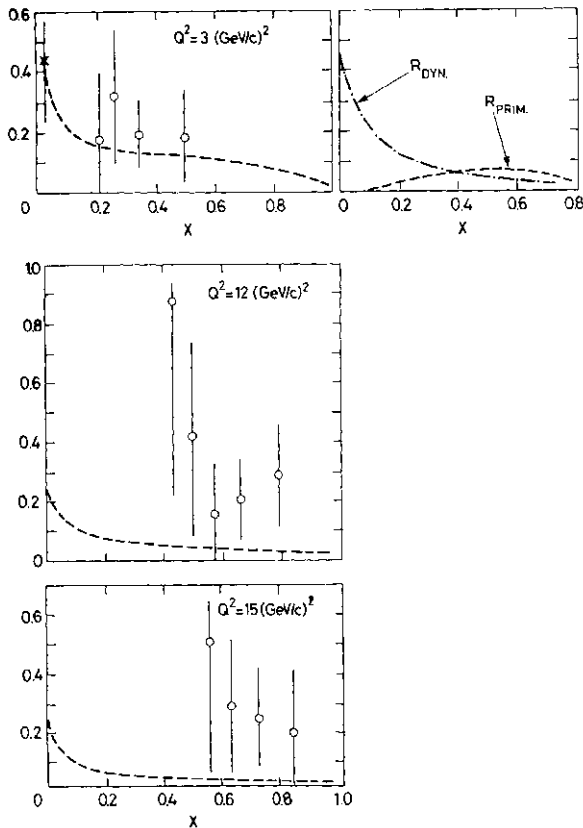


Fig. 6. The variation of  $R$  with  $x$  at fixed  $Q^2$ . The dotted curve is the Q.C.D. prediction.  $\odot$ , SLAC-MIT;  $\times$ , C.H.I.O.

tainty in  $R$  does not have much effect on the determination of  $\nu W_2$ , as will be seen below.

2.2.  $\nu W_2$  structure function from  $H_2$

The most recent data on the structure function  $\nu W_2$  (or  $F_2$ ) have been obtained

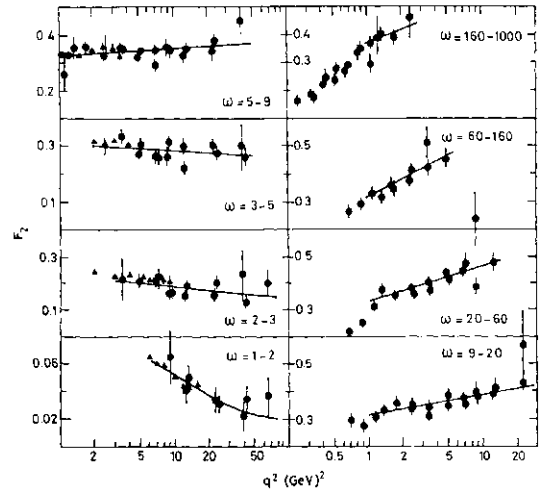


Fig. 7. Variation of  $F_2$  with  $Q^2$  for different  $\alpha$  regions.  $+$ , C.H.I.O.;  $I$ , SLAC. Solid line is fit given in text.

by the CHIO Collaboration<sup>12</sup> and extend their previous  $H_2$  measurements down to smaller  $x$  (larger  $a=l/x$ ) values, using 219 GeV muons. The  $q^2$  dependence of the structure function  $\nu W_2$  is plotted in Fig. 7 together with the older SLAC data and shows the familiar pattern of scaling violations. The indicated errors are statistical and the overall systematic error has been estimated to be 5%. The solid line is a fit to the data using a  $q^2$  power law dependence of the form

$$F_2(x, Q^2) = F_2(x, Q_0^2) [Q^2/Q_0^2]^b$$

where  $Q_0$  has been chosen as  $3(\text{GeV}/c)^2$ . The value of  $R$  used in the extraction of  $F_2$  was

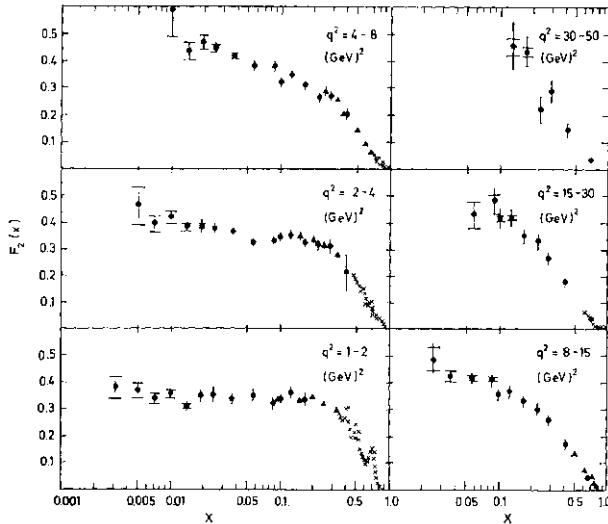


Fig. 8. Variation of  $F_2$  with  $x$  for different  $Q^2$ . Large horizontal bars indicate a total change in  $R$  of 0.5. 4, C.H.I.O.; |, ^ (resonance region), SLAC.

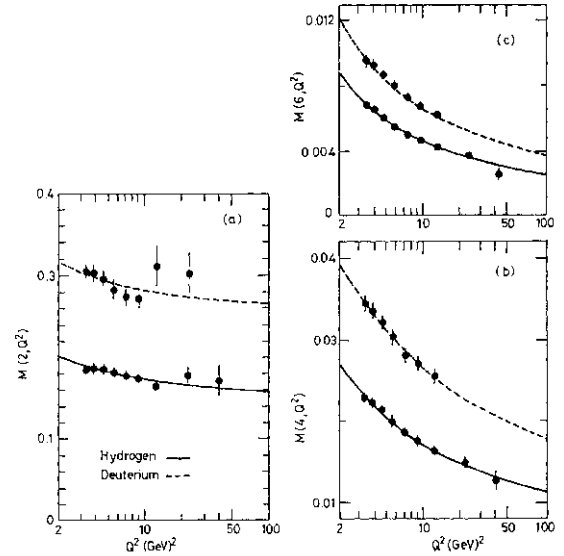


Fig. 9. Nachtmann moments versus  $Q^2$  for  $H_2$  and  $D_2$  C.H.I.O. data.

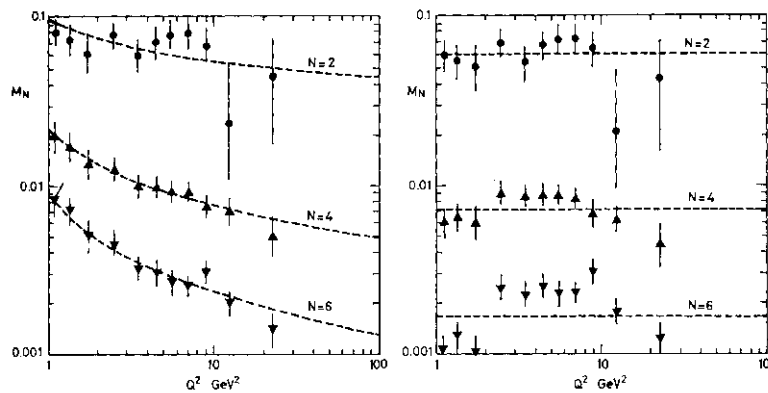


Fig. 10. Moments of  $F^A - F_2^N$  versus  $Q^2$  for C.H.I.O. data and SLAC data. The L.H.S. differs from R.H.S. by the inclusion of the elastic channel.

$i=0.44$  based on measurements at 96, 147 and 219 GeV. The change in  $F_2$  due to a change in  $R$  can be seen in Fig. 8 where the horizontal upper and lower bars indicate a change in  $R$  by  $\pm 0.25$ . This clearly shows that the rise in  $F_2$  with  $Q^2$  at small  $x$  cannot be removed by reducing  $R$ . It is interesting to note that for fixed  $Q^2$  in the region 1-2(GeV/cf there is no evidence of any decrease in  $F_2$  down to the smallest  $x$ .

Scaling variations can at present be explained in terms of the theory of Q.C.D., which is an extension of the Quark-Parton model to include gluon emission. In analogy with Q.E.D., it is necessary to measure

$$\alpha_s = \left[ \frac{12\pi}{33 - 2N_{f1}} \right] \frac{1}{\log(Q^2/A^2)}$$

where  $N_f$  is the number of flavours. The

theory is most rigorously tested through a determination of the ratio of the moments of the structure functions, given by

$$M_i(Q^2) = \int_0^1 dx [x^{N-2}] F_i(x, Q^2)$$

The Nachtmann moments are usually plotted, where  $x$  is replaced by the Nachtmann variable  $\xi = 2x / \{1 + \sqrt{1 + (4M^2 x^2 / Q^2)}\}$ , since these take into account mass effects. However, in order to show the comparison with the experimental data, the Nachtmann moments are plotted for  $H_2$  and  $D_2$  data versus  $Q^2$  in Fig. 9 and a value extracted of

$$A = 0.66 \pm 0.08 \text{ GeV.}$$

In general, the moments analyses give a larger value for  $A$  than that obtained by fitting the structure function directly. All these analyses involve three terms with different  $Q^2$  varia-

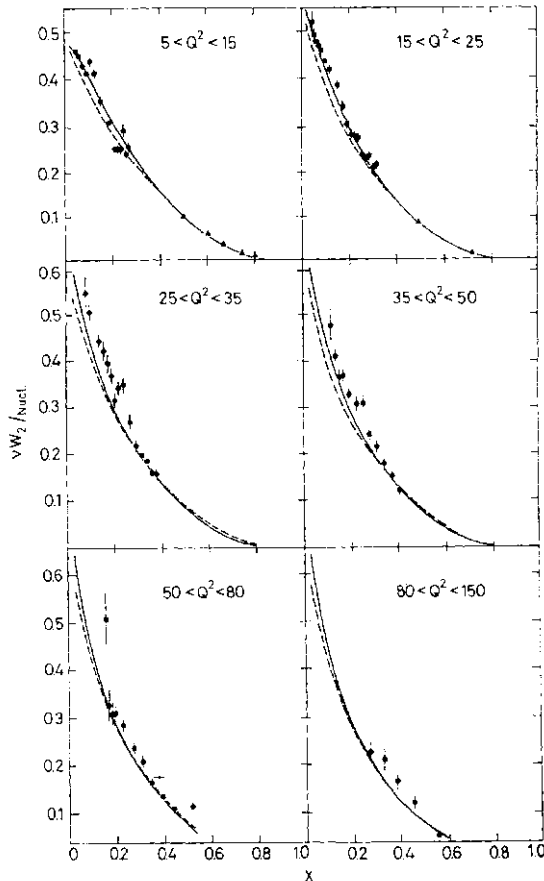


Fig. 11.  $\nu W_2 / \text{nuclon}$  versus  $x$  at fixed  $Q^2$  for M.S.F. data (+). The solid and dashed lines are Q.C.D. fits, i, SLAC-MIT (Z).

tions, whereas an analysis of  $F_2 \sim F_1$  involves only one term—the flavour non-singlet term. The results of this analysis by the CHIO Collaboration are plotted in Fig. 10, and an excellent fit is achieved using  $1/\lambda = 0.675 \pm 0.100$  GeV. The necessity of including the elastic channels is seen in the fits to the higher moments, which are weighted by the contribution at large  $x$ . At present all results from deep inelastic scattering from  $H_2$  and  $D_2$  targets are in excellent agreement with the Q.C.D. predictions, but much more precise data will be required to see the effect of higher order corrections.

### 2.3. Structure functions from complex targets

New high precision data have been reported to this conference by the Michigan State-F.N.A.L. (M.S.F.) collaboration,<sup>14</sup> who have extended their previous measurements on  $\nu W_2$  up to  $q^2 = 150$  (GeV/c)<sup>2</sup> and  $W = 2 \sqrt{150}$  GeV. The target consisted of a 7.4 m long iron-scintillator calorimeter (4.260 g/cm<sup>2</sup>) and recorded  $10^6$  events ( $Q^2 > 5$  (GeV/c)<sup>2</sup> using  $3.10^{10}$

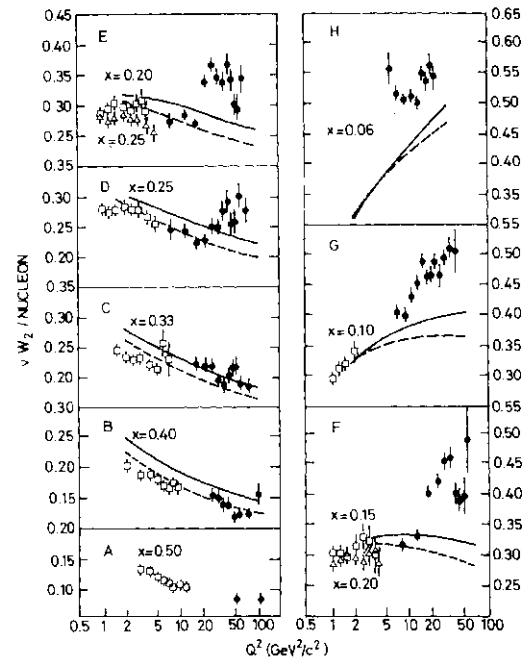


Fig. 12.  $\nu W_2 / \text{nuclon}$  versus  $Q^2$  for different  $x$  ranges. Curves are Q.C.D. predictions. 4, SLAC-MIT.

incident muons of 270 GeV. The overall systematic and normalization uncertainties were 10%. Figure 11 shows  $\nu W_2 / \text{nuclon}$  as a function of  $x$  for different values of  $Q^2$  where the solid ( $A=0.5$ ) and dashed ( $A=0A$ ) are Q.C.D. predictions.<sup>15</sup> The data are in good agreement with the predictions and therefore the existing data in the lower  $Q^2$  range up to  $Q^2 = 25$  (GeV/c)<sup>2</sup>, but a systematic difference appears at higher  $Q^2$ . This difference is seen more clearly in Fig. 12, where the structure functions are plotted versus  $Q^2$  for different values of  $x$ , and the same Q.C.D. predictions are illustrated. The increase in  $\nu W_2$  at small  $x$  and the decrease at large  $x$  with increasing  $Q^2$  is apparent, together with a strong enhancement in the region of  $Q^2 = 50$  (GeV/c)<sup>2</sup>. The possibility of this enhancement having  $W$  dependence has been studied by the M.S.F. group using the  $H_2$  data from C.H.I.O. and SLAC-MIT experiments. Figure 13a shows all this data plotted in the form  $b(x)$  against  $\log(1-x)$  where  $b$  is given by the power law  $Q^2$  dependence given previously. Figure 13b shows the M.S.F. data for two different ranges of  $W$  and indicates that the enhancement has a threshold at  $W = 10$  GeV.

It is difficult to explain this effect in any obvious way with the  $Y$  meson, since even

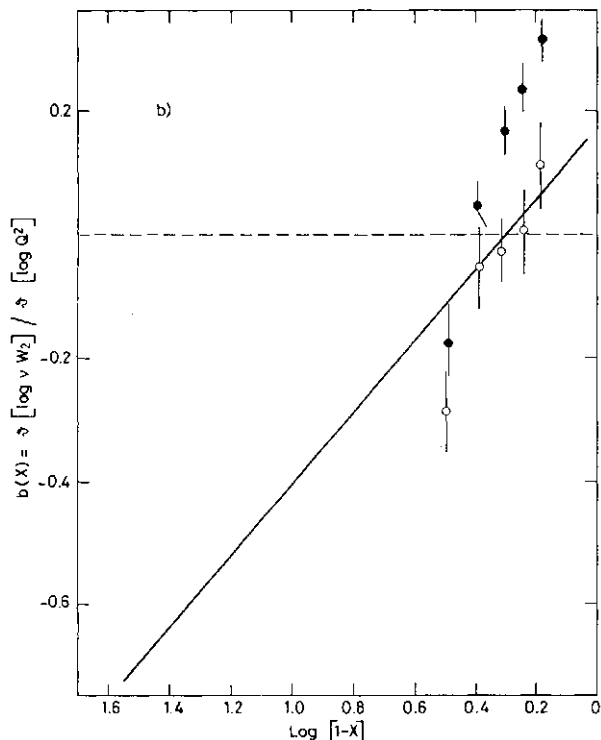
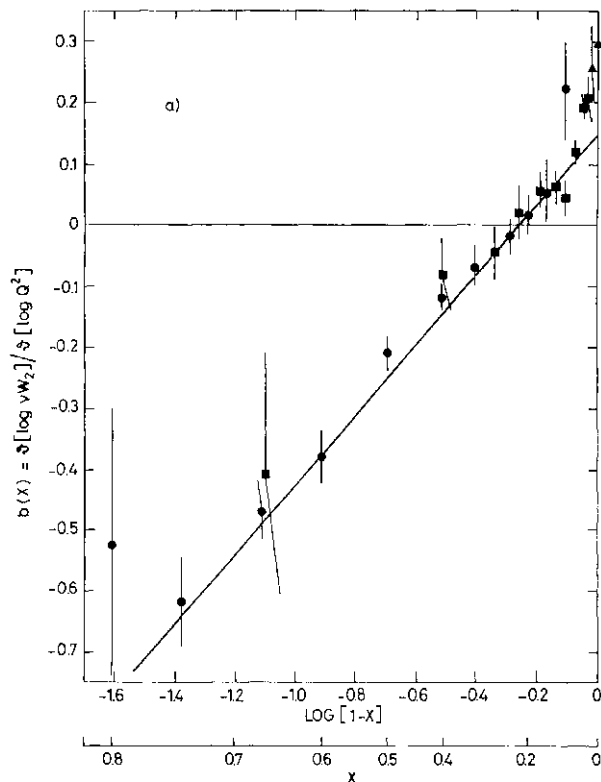


Fig. 13. (a) Slope parameter  $b(x)$  versus  $\log(1-x)$ . Straight line is fit to  $\bullet$  CH.I.O. ( $\#^2 < 40$  ( $\text{GeV}/c^2$ ));  $+$  SLAC-MIT ( $\Lambda^2 < 16$  ( $\text{GeV}/c^2$ ));  $|$  CH.I.O. 219 GeV only. (b) M.S.F. ( $\text{PF} < 10 \text{ GeV}$ );  $+$ , M.S.F. (no HP cut). Fit is that given in (a).

allowing for propagator effects, the photoproduction cross-section should be much too small.<sup>16</sup> Results from new experiments at

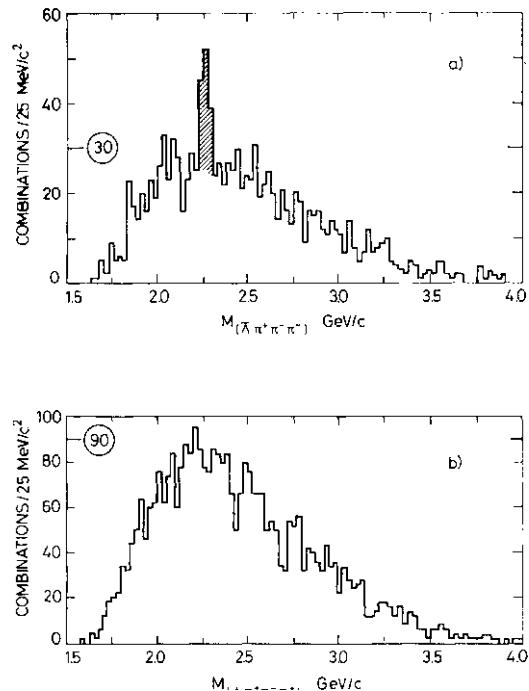


Fig. 14. (a)  $\text{Air } 7r-7c$  mass spectrum, (b)  $A7r-7r 7c$  mass spectrum for previous C.I.F. photoproduction experiment.

F.N.A.L.<sup>17</sup> and CERN<sup>18</sup> will be important in verifying these results which violate Q.C.D. predictions, since data from neutrino experiments have not yet attained the necessary precision in this  $Q^2$  range.

### §3. Evidence for Charm in Photoproduction

Photoproduction has always been considered as a likely reaction in which to see charmed hadrons. The coupling of the  $cc$  state to the photon is identical to that of the  $u\bar{u}$  state and estimates using different models<sup>19</sup> indicate that the charm cross-section should be  $\sim 1\%$  of the total cross-section, *i.e.*,  $\sim 1/\mu\text{b}$ . Indeed, the first evidence for charm outside  $e^+e^-$  reactions came from the Columbia-Illinois-FNAL (C.I.F.) Collaboration<sup>20</sup> who found a peak at 2.26 GeV in the  $A_{t\bar{c}+i\bar{z}\bar{t}\bar{z}}$  anti-baryon mass spectrum but not in the  $A_{t\bar{z}+t\bar{z}+t\bar{z}'}$  baryon mass spectrum. The results of that experiment are illustrated in Fig. 14. Results from three experiments have been presented to the Conference using photons to search for charm, but so far there are no results on charm or  $\langle p \rangle$  production using virtual photons where it should be possible to tune the signal to background using the  $Q^2$  dependence of the propagator.

The first experiment has been carried out

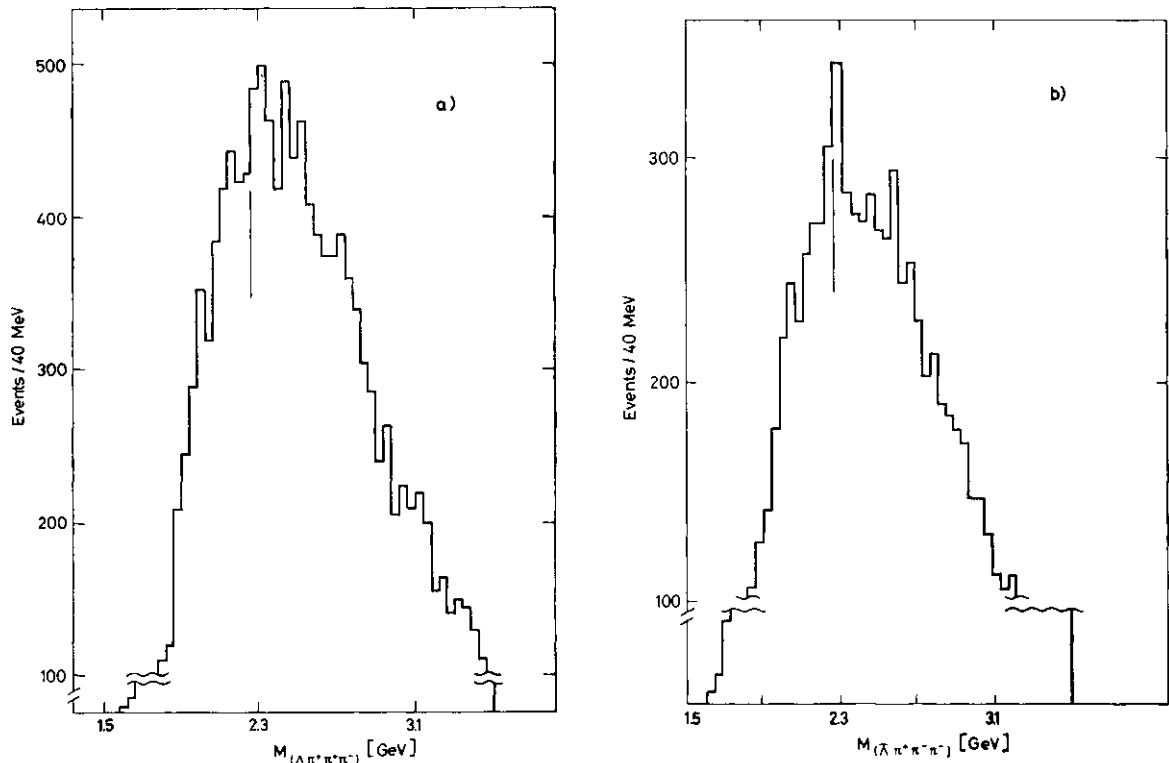


Fig. 15. (a)  $An+iz+n'$  mass spectrum.  
 (b)  $AIZ\sim IZ\sim TZ+$  mass spectrum in new C.I.F. experiment. Vertical line occurs at 2.26 GeV.

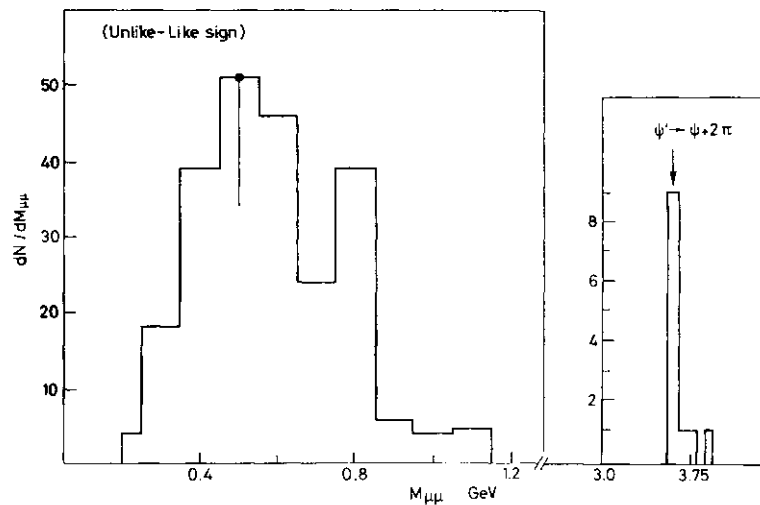


Fig. 16.  $Ni^{\wedge}-Ni^{\wedge}$  muon pair mass spectrum in new C.I.F. experiment.  
 Also indicated  $\langle p^{\wedge}+iz^*n\sim p$  where  $\langle p\sim ff; pL\sim$ .

by the C.I.F. Collaboration<sup>21</sup> using a wide-band photon beam of maximum energy 300 GeV. The apparatus consisted of a forward magnetic spectrometer containing Cerenkov counters for particle identification, and used a solid CH target. The sensitivity of the experiment was 200 events/nanob. Preliminary results from this experiment are presented in Figs. 15a and b for the  $ATZ+TI+TZ-$  and  $AK+K\sim TI-$  mass spectra. The peak is again visible at 2.26 GeV, but there is some evidence of

structure in the neighbourhood of the 2.26 GeV region in the mass spectra. Special runs have been performed to study the effects of  $\wedge$ -induced reactions, since these are contained in the broad band beam. Preliminary results also show structure in the region around 2.26 GeV,<sup>22</sup> and further detailed analyses of these backgrounds are under way.

A search has been made by the same group for  $DD$  production through the  $JUJU\sim$  pair mass spectrum by the decay  $D\sim \wedge f x^{\wedge} X$  ( $\sim 10\%$ ).

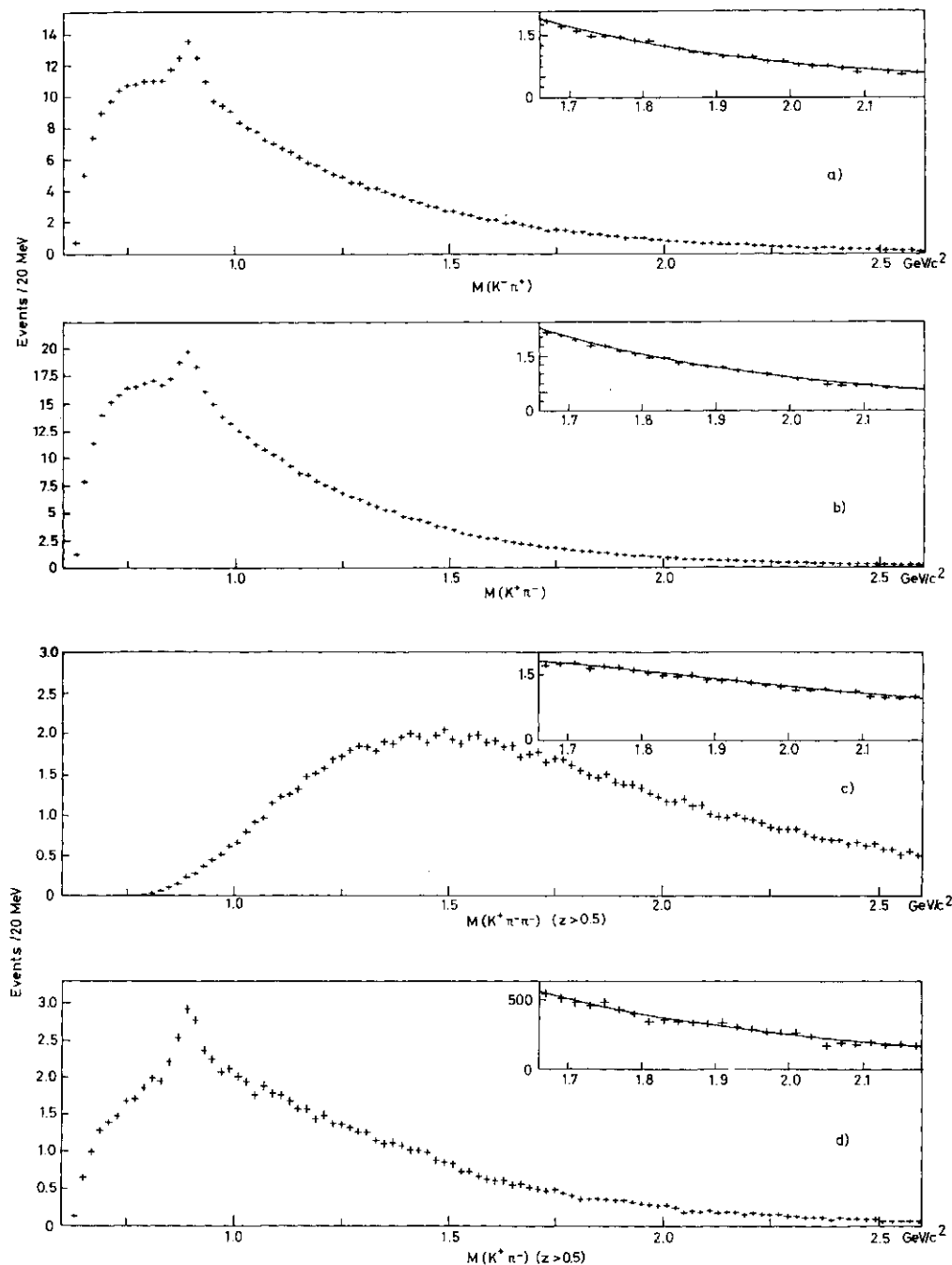


Fig. 17. (a)  $K\bar{r}$  mass spectrum.  
 (b)  $K\bar{r}$  mass spectrum.  
 (c)  $K\bar{r}T\bar{r}C\bar{r}$  mass spectrum ( $z > 0.5$ ).  
 (d)  $K\bar{n}$  mass spectrum in WA4 CERN-Omega experiment.

The lepton spectrum from  $D$  decay at rest is known to peak around 300-400 MeV/c, therefore the mass spectrum for  $N(u^+ / u^-) - N(b\bar{v}^{+/-})$  should show an enhancement in the low mass region if all backgrounds are properly taken into account. Figure 16 contains the results of the resulting subtracted muon-pair spectrum and there is an enhancement in this preliminary data at low mass. However, it will be necessary to determine the production of  $p, \rho \rightarrow \pi\pi$  (including the mass region below

the  $p^0$ ) and possible Dalitz decays of the  $w$  and  $r$  mesons into muon pairs in order to determine the shape of the background mass spectrum. Also indicated in Fig. 16 is the mass spectrum of the  $\langle p \rangle (juJU^-) + 7T7U^-$  where the muon pairs in the  $\langle p$  mass region were assumed to have the  $\langle p$  mass. This is the first indication of  $\langle p' \rangle$  production in photoproduction and underlines the analysis power of the spectrometer.

The second experiment has been made by

Table I. Properties of trident-like events

Event	Decay path ( $\mu$ )	$E_\gamma$	Tracks charge/momentum (GeV/c)	Angular aperture (deg)	Invariant mass (GeV/c <sup>2</sup> )	Decay time (sec)
(a)	$16 \pm 4$	64.1	1) +23.913 2) + 7.759 3) - 7.899	$3.4 \pm 0.2$	$E_{vis}$ 39.6 $\pi$ $\pi \sim 1.1 \pm .2$ $\pi$	$0.2 \cdot 10^{-14}$
(b)	$30 \pm 2$	65.1	1) +37.452 2) - 0.800 3) - 0.100 : 0.500	$6 \pm 0.2$	$K$ $\pi \sim 1.2$ $e$	$0.46 \cdot 10^{-14}$

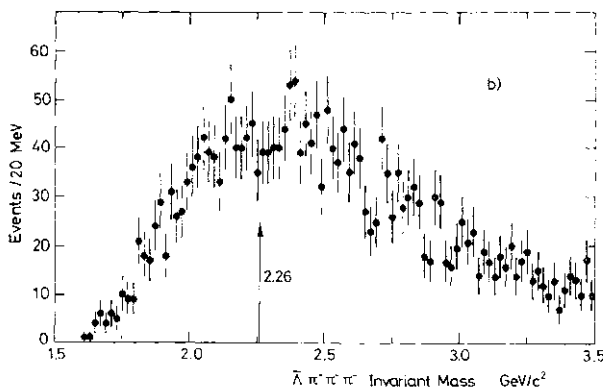
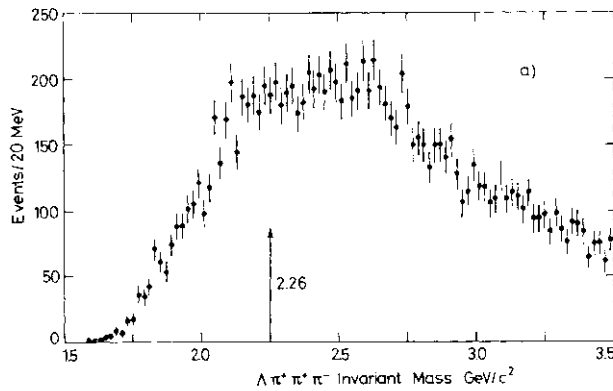


Fig. 18. (a)  $A7iK n^-$  mass spectrum.  
(b)  $An-iz+Tz^*$  mass spectrum in WA4 CERN-Omega experiment.

the WA4 CERN-Omega Collaboration<sup>23</sup> using the large multi-particle spectrometer in conjunction with a  $H_2$  target. The incident beam was tagged in the energy interval between 20 and 70 GeV and the experiment had a sensitivity of 60 events/nanob. The results of this experiment are illustrated in Fig. 17 (a-d) for the  $K^* i c^* i i^*$  mass spectrum expected from  $DD$  meson decays. There is no evidence of any peak in the  $D$  meson mass region, even after demanding that the  $D$  mesons have large longitudinal momenta. This highlights one of the major difficulties in all these experiments where multi-combinatorial backgrounds arise from the strange-particle cross-section, which is at least ten times that of the charm-particle cross-section and where the  $D \rightarrow KTZ$  is  $\sim 1\%$ .

Table II. Summary of results from three charm experiments.

Experiment	Channel	Comment	$\sigma_c$
COL/ILL/ FNAL	$\bar{A} 3\pi$	Peak at same mass	$0.1-1 \mu b$
	$K\pi, K2\pi$	Not seen	
	$\mu^+ \mu^-$	Not proven	
CERN SPS ( $\Omega$ ) WA4	$K\pi, K3\pi$	Not seen	$\leq 0.5 \mu b$
	$3\pi, 3\pi$	Not seen	Model dependent
EMULSION GP+WA4	2 $D$ events seen		$\geq 0.5 \mu b$

The WA4 Collaboration have also studied the  $A7iK n^-$  and  $A7iZ^* T Z^*$  mass spectrum where a forward kaon or proton was demanded in the trigger. The results are plotted in Figs. 18a and b, and no enhancement is visible in the region of 2.26 GeV.

The third experiment has been performed by an emulsion group in association with the WA4 Collaboration,<sup>24</sup> using the CERN-Omega spectrometer and nuclear emulsions as targets. The group have been able to locate 482 hadronic vertices in the emulsion and from these events two candidates have been found which satisfy their criterion of short-lived trident-type events. Their properties are listed in Table I.

The life-time of these two candidates is very short compared with the theoretical predictions of  $6 \times 10^{-13}$  s,<sup>25</sup> but if accepted as charm candidates, then a lower limit can be set of  $0.5 \mu b$  for the charm cross-section at the 90% confidence level, when all the correction factors and efficiencies are included.

Table II is an attempt to summarise the results of all three preliminary experiments from which the following conclusions can be drawn:

- Charm particle production should be seen at the level of  $\sim 0.5 \mu b$ .
- The production of a charmed antibaryon is seen, but it is difficult to understand



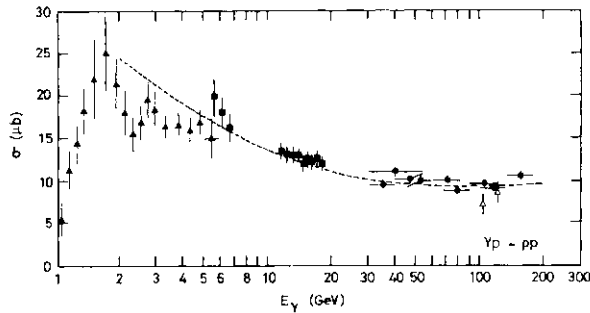


Fig. 19.  $\sigma(\gamma p \rightarrow p p)$  versus  $E_\gamma$ . The dotted curve is fit to V.M.D. relationship using hadronic  $o_r$  values. +, DESY; +, SLAC; U.T.F.; 4, C.H.L.O.

why there is no charmed baryon signal. The fact that no signal is seen at lower energies suggests a strong energy dependence which is not apparent in photoproduction of  $pp$  pairs. The possibility of  $\Lambda$ -induced production has to be resolved.

#### §4. Vector Mesons of Mass <3 GeV

##### 4.1. Production of $p, \rho, \omega$ mesons by real photons

The reaction  $j+p \rightarrow \Lambda^0+p$  has been measured at high energies by the U.T.F. Collaboration<sup>26</sup> using a tagged photon beam in the energy range up to 200 GeV. The energy dependence of the cross-section is plotted in Fig. 19 where the dotted curve is obtained from the relationship given by (V.M.D. + Additive Quark Model):

$$\begin{aligned} \sigma(\gamma p \rightarrow \rho^0 p) \\ = (\alpha\pi/\gamma_\rho^2) \frac{1}{2} [\sigma(\pi^+ p \rightarrow \pi^+ p) + \sigma(\pi^- p \rightarrow \pi^- p)] \end{aligned}$$

using experimental data from pion elastic scattering measurements<sup>27</sup> and  $\gamma^*/4t = 0.64$ , which is the value extracted from  $p^0$  studies in complex targets. Clearly at higher energies  $\langle j(jp \rightarrow P^0 p) \rangle$  would be expected to show the same increase with energy as that seen in pion total cross-sections and  $o_i(jp)$ . No new results have been presented in  $\rho^0$  photoproduction.

The reaction  $j+p \rightarrow \langle f \rangle + p$  is of interest since it cannot have any meson or baryon exchange in the  $s$  and  $t$  channels through the OZI rules<sup>28</sup> and therefore this reaction has a high-energy Pomeron-type behaviour from very low energy ( $\sim 2$  GeV). Three results have been presented to this conference covering three widely different energy regions.

A high-precision experiment has been performed by a Daresbury-Lancaster-Sheffield

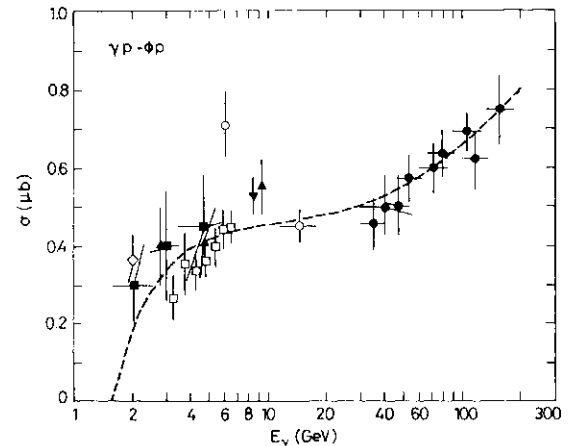


Fig. 20.  $\sigma(\gamma p \rightarrow \phi p)$  versus  $E_\gamma$ . The dotted curve is a fit to V.M.D. relationship using hadronic  $a_r$  values. DESY; !, LBL/SLAC; f, BONNN; SLAC;  $\pm$ , U.T.F.

Collaboration<sup>29</sup> in the photon energy range 3-5 GeV, extending the  $\sqrt{s}$ -range out to 1.3 (GeV/c)<sup>2</sup>. The results show that there is a distinct break in the  $\ln$ -slope around  $\sqrt{s} = 0.4$  (GeV/c)<sup>2</sup> and are consistent with  $\Lambda$ -channel helicity conservation throughout the entire  $t$ -range. Results have been presented by the WA4 CERN-Omega Collaboration<sup>30</sup> in the energy range 20-35 GeV which are consistent with a constant cross-section. Finally high-energy measurements have been performed by the U.T.F. group<sup>31</sup> in the photon energy range up to 150 GeV. The results are shown in Fig. 20 and again give very beautiful evidence of the success of (V.D.M.+Additive Quark Model) using the relationship linking the  $\gamma I/4T I$  with the measured values of the  $K, K^*$  and  $T C^*$  total cross-sections. The spectacular increase in the total cross-section comes from the fall and rise in the  $K^*p$  cross-section superimposed on the continually rising  $Kp$  cross-section. Similar effects should be present in the  $\langle f i \rangle$  total cross-sectional behaviour at high energies which could be used to shed light on the behaviour of  $Dp$  total cross-sections.

##### 4.2. Production of $p, a_1, \langle j \rangle$ mesons by virtual photons

The production of  $p, \rho$  and  $\langle p \rangle$  mesons by virtual photons requires the separation of longitudinal and transverse cross-sections in order to compare with the V.D.M. model which predicts that the transverse cross-section should fall like the square of the propagator term

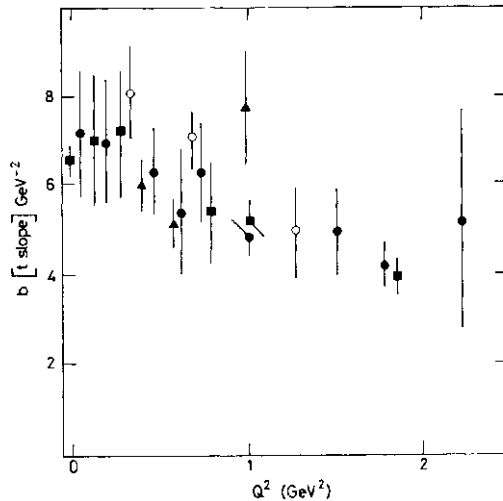


Fig. 21. The slope parameter  $b$  for  $\gamma_V + p \rightarrow \rho^0 + p$  as a function of  $Q^2$ .  $\bullet$ , Cornell  $\langle W \rangle = 2.5$  GeV;  $\blacksquare$ , Cornell  $\langle W \rangle = 3.2$  GeV;  $\circ$ , UCSC/SLAC;  $\blacktriangle$ , SLAC.

$$m_{\tilde{V}}^2/[Q^2 + M_{\tilde{V}}^2].$$

The results of experiments on  $p''$  production, where the broad skewed  $\pi\pi + \pi\pi'$  mass spectrum makes separations difficult to perform, are in reasonable agreement with this picture. Results presented to this Conference from the Cornell group<sup>32</sup> and the SLAC-U.S.S.C group<sup>33</sup> however indicate that in general the data points lie below the V.D.M. predictions in the  $Q^2$  range up to  $2.5$   $(\text{GeV}/c)^2$  and  $2 < W < 5$  GeV. Results from the same two groups on  $\rho^0$  production indicate that the ratio  $a^{\Delta j}$  ( $T\rho^0$  is constant in the same  $Q^2$  and Grange.

An interesting question, first raised at the 1971 Electron Photon Conference<sup>34</sup> was the possibility that the radius of the photon would shrink with  $Q^2$ . This would manifest itself via the optical model in a decrease of  $b$  with  $g^2$ , where  $\tilde{e}$ , the slope parameter, measures the radius of the interaction and reflects the combined size of the photon and proton. An experiment has been carried out by the Cornell group<sup>35</sup> and the results are sufficiently precise to show that  $b$  does decrease with  $Q^2$  as illustrated in Fig. 21. However, published data exist on  $\rho^0$  electro-production measurements<sup>36</sup> which show no evidence of shrinkage. Further experiments are required at high energy in order to resolve this question completely.

#### 43. Higher mass mesons beyond $p$ , $\omega$ and $\langle f \rangle$

The search for higher mass vector mesons in the region between 1 and 3 GeV is important to look for new vector mesons containing

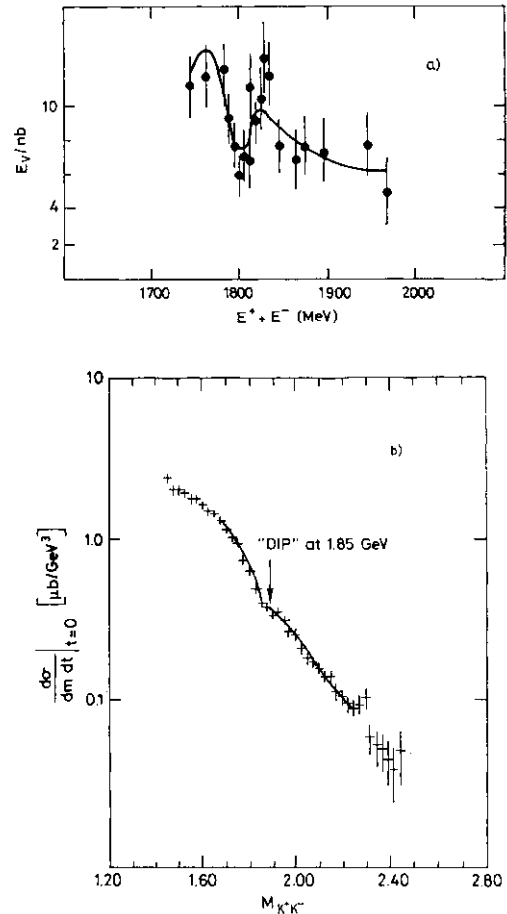


Fig. 22. (a) Cross-section ( $n > 3$  charged tracks) for  $BB$  group (Frascati).

(b) The photoproduction cross-section versus  $K\bar{K}$  pair mass in Cornell-Harvard experiment.

( $w$ ,  $d$ ,  $X$ ) quarks, multiquark states etc, since there are many confusing results in this mass range both from photoproduction and  $e^+e^-$  storage rings.<sup>37</sup> The  $p'$  ( $\sim 1260$  MeV) has been obtained from fitting interference spectrum in the process  $\gamma'rp \rightarrow e^+e^-rp$  by a DESY-Frascati-Pisa group,<sup>38</sup> but this state has not been established elsewhere. The  $p''$  ( $1500$ - $1600$  MeV) has been seen as a broad 300 MeV resonance in  $\gamma\gamma\gamma\gamma\gamma\gamma\gamma\gamma$  mass spectrum, and also determined in the  $TCK$  final state from a phase-shift analysis in the reaction  $K\bar{p} \rightarrow$

A study has been made of the reaction  $\gamma p \rightarrow K^+ + K^- + p$  (assumed) by a Cornell group<sup>39</sup> using a spectrometer to select the two charged kaons. The investigation concentrated on the region around 1800 MeV where various dip structures have been observed in the Frascati storage ring measurements.<sup>40</sup> The results of one of these measurements is indicated in Fig. 22a giving the cross-section as a func-

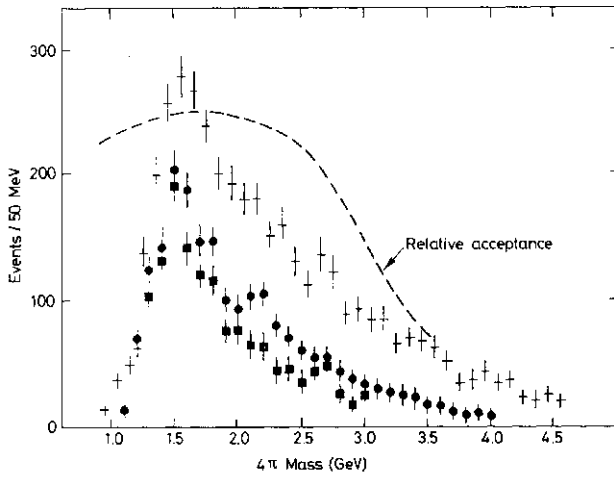


Fig. 23. The  $T: n \sim n \bar{n} \sim$  mass spectrum in WA4 CERN-Omega experiment + all / values; + 0 < / < 0.3 GeV<sup>2</sup>; fritting A<sup>+</sup> in 1<sup>-</sup> state.

tion of beam energy into >3 charged particles. The experimental technique was checked using pion pairs where  $p^0$ ,  $f^0$  and  $g^0$  signals were established and the resulting  $K\bar{K}$  invariant mass plot is shown in Fig. 22b, where a pronounced dip is seen at a mass of 1.8 GeV. A mass of  $1.83 \pm 0.013$  GeV and a width  $\Gamma = 111 \pm 23$  MeV are determined for this resonance by fitting the mass spectrum with a combination of resonance, coherent and incoherent background. However the parameters obtained for this resonance are sensitive to the phase and form of the background.

The WA4 CERN-Omega Collaboration<sup>41</sup> have studied the reaction  $\gamma + p \rightarrow n + \pi^+ \pi^+ \pi^- + p$  and have observed a broad enhancement in the region of 1.5 GeV with a F.W.H.M. of 0.5 GeV as seen in Fig. 23. An investigation of the sub-structure of the 4-pion spectrum shows a very strong  $p^0$  signal, and the  $K^* \pi$  opposite to the  $p^0$  region has the features of a broad threshold enhancement peaking around 0.5 GeV. A spin-parity analysis indicates that the  $p^0$  decays predominantly into  $\rho^0 \pi^0$  with  $J = l = 0$ , but there is a lot of structure in the higher mass region. Preliminary results from the electroproduction experiment at Cornell<sup>42</sup> in the range  $Q^2 > 0.1$  GeV<sup>2</sup>,  $W > 2$  GeV show a broad enhancement peaking in the region of 1.8 GeV as illustrated in Fig. 24. Again 50% of the  $\pi^+ \pi^-$  events occur in the  $p^0$  region.

The WA4 CERN-Omega Collaboration<sup>43</sup> have also studied the reaction  $f + p \rightarrow K^+ K^- \pi^+ \pi^- + p$ . The resulting mass spectrum

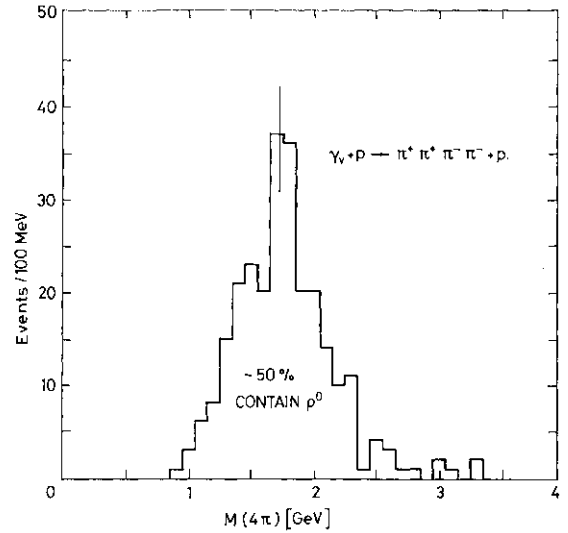


Fig. 24. The  $\pi K \sim \pi$  mass spectrum in the Cornell electroproduction experiment.

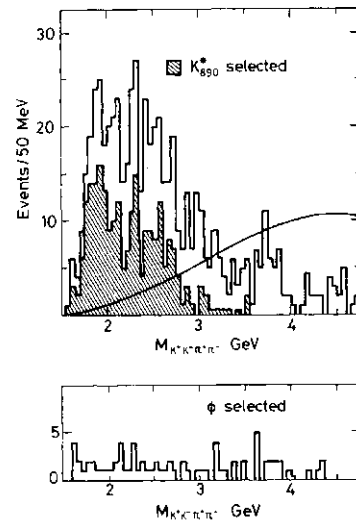


Fig. 25. The  $K^+ K^- \pi^+ \pi^-$  mass spectrum in the WA4 CERN-Omega experiment. The solid line is predicted mass spectrum for peripheral  $K^* K^0 \rho$  production.

illustrated in Fig. 25 shows a broad threshold enhancement which has strong  $K^*$  (890 MeV) and  $\phi$  signals in the  $K^* \pi$  and  $K\bar{K}$  states respectively. There is no evidence for any enhancement in the  $\pi^+ \pi^- \pi^+ \pi^-$  mass spectrum, predominantly in  $K^* K n$ . Figure 26 shows the excellent agreement between the  $K^* K \sim n^*$  mass spectrum measured in the electroproduction Cornell experiment and that from photo-production.

These broad enhancements in the  $p \pi^+ \pi^- + K^0$  and  $K^+ K^- + \pi^+ \pi^-$  channels are similar in that the decay is predominantly  $V^* \rightarrow V + K T \sim (K T C)$  where the two pseudoscalar mesons are presumably an  $\gamma$ -wave enhancement. This is

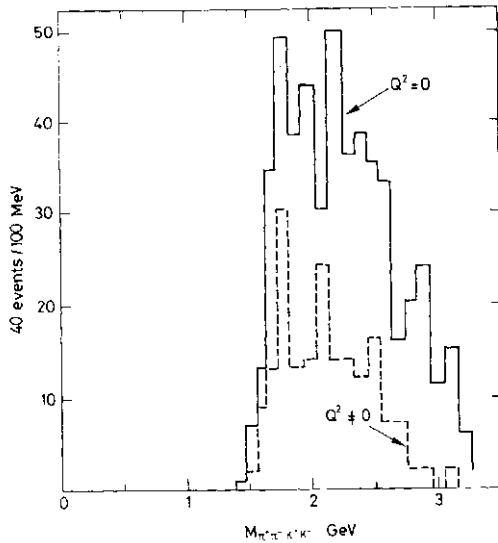


Fig. 26. The  $KK-nrr$  mass spectrum in the photoproduction ( $Q^2=0$ ) and electroproduction ( $Q^2 \neq 0$ ) experiments.

similar to what is seen in the decay of  $\rho \rightarrow \pi^+ \pi^- + \pi^0$  (s-wave).

In the higher mass region  $>2$  GeV, there are indications in data from photoproduction and electroproduction by the previous groups for threshold enhancements in  $pp$  mass spectra. It is not possible to draw any conclusions on possible baryonium states at this time due to the small number of events. There is a need for much more detailed work to untangle the whole mass region between 1 and 3 GeV, which is clearly rich in spectroscopy but requires special techniques, e.g., polarised photons, decay channels etc., in order to isolate states of different quantum numbers.

**§5. Inclusive Final States Involving Hadrons**

The inclusive final states involving hadrons in inelastic lepton scattering have been used to test ideas on the simple quark parton model. In general, the inclusive hadron distributions behave very much like those produced from incident hadrons in terms of multiplicity,  $x_F = 2p^*/V s$  and  $p_L$  distributions. There are certain areas where the deep inelastic process can be used to advantage to simplify the reaction process using the following assumptions (quark-parton model):

- (1) Photon interacts only with one valence quark of fractional momentum  $x$
- (2) Struck quark with fractional momentum  $z=Ev/v$  decays into hadron
- (3) Factorisation of two processes enabling

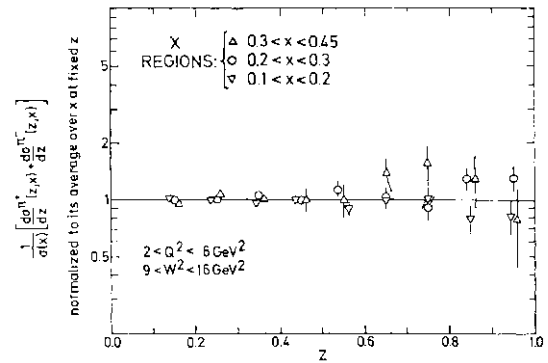


Fig. 27. The sum of  $7r^+$  and  $n^-$  cross-sections plotted versus  $z$  for different  $x$  regions in the DESY-Cornell experiment.

determination of fragmentation function  $D^h Q$

An experiment has been carried out by a Cornell-DESY group<sup>44</sup> using a streamer chamber and has provided a determination of the fragmentation function for  $T^* \pi^+$ , since the contribution due to protons and kaons has been excluded. The data from this experiment ( $W^2 > 20$  GeV<sup>2</sup>) has been compared with data from the C.H.I.O. Collaboration ( $J^2 > 150$  GeV<sup>2</sup>), and shows no evidence for  $W$  dependence in the quantity

$$\frac{1}{\sigma_{tot}} \left\{ \frac{d\sigma^{\pi^+}}{dz}(x, z) + \frac{d\sigma^{\pi^-}}{dz}(x, z) \right\} = D_u^{\pi^+}(z) + D_u^{\pi^-}(z)$$

which is independent of  $x$  due to isospin invariance and charge conjugation (neglecting strange quarks). There is no evidence of any  $W$  dependence to within 20%. Figure 27 gives the above invariant cross-section versus  $z$  for different  $x$  regions and indicates that the factorisation works reasonably well.

The results of this experiment are compared with those of other experiments in Fig. 28, and show that the agreement is very good as expected from the quark-parton model. The comparison of  $e^+e^-$  hadron distributions with those from deep inelastic scattering is clearly seen in the data and is an indication that target effects have to be considered more carefully. The comparison with predictions of different jet models<sup>45</sup> for hadronic production is also included. The separation of the  $D_u^{\pi^+}$  and  $D_u^{\pi^-}$  has been made using the quark parametrisation of Feynman and Field, and the results are illustrated in Fig. 29 together with the results of neutrino experiments. The

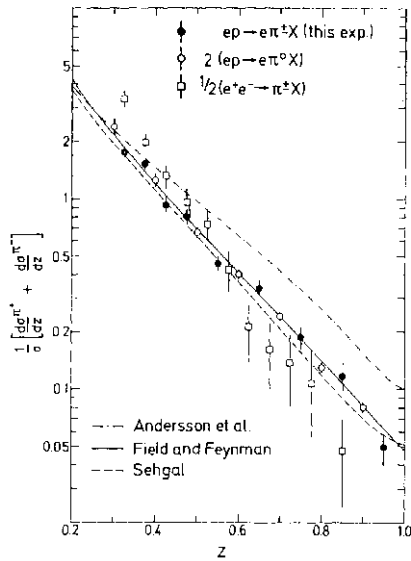


Fig. 28. The sum of  $n^*$  and  $n^-$  cross-sections plotted against  $z$  for Cornell-DESY electroproduction experiment § Aachen-DESY electroproduction experiment and § DASP  $e^+e^-$  experiment.

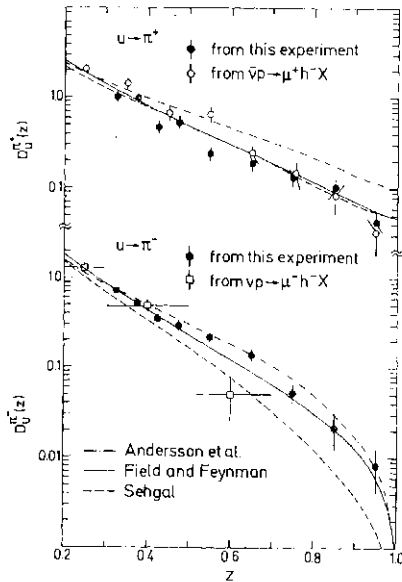


Fig. 29. Fragmentation functions for  $u$  quark into  $T^+$  and  $7t^-$  from Cornell-DESY experiment (+). Also indicated are those for neutrino ( $\wedge$ ) and anti-neutrino C6\

difference between the favoured and unfavoured fragmentation function as  $z \rightarrow 1$  is clearly seen from the experimental results.

The same collaboration has also measured the net electric charge of the forward-going hadrons for  $x_f > 0$ , which according to the ideas of the  $Q$ - $P$  model should reflect the charge of the parent quark. In the case of the proton this would be the  $w$ -quark ( $+2/3$  charge) for increasing  $x$ . The mean hadron charge for  $x_f > 0$  is plotted in Fig. 30 as a function of

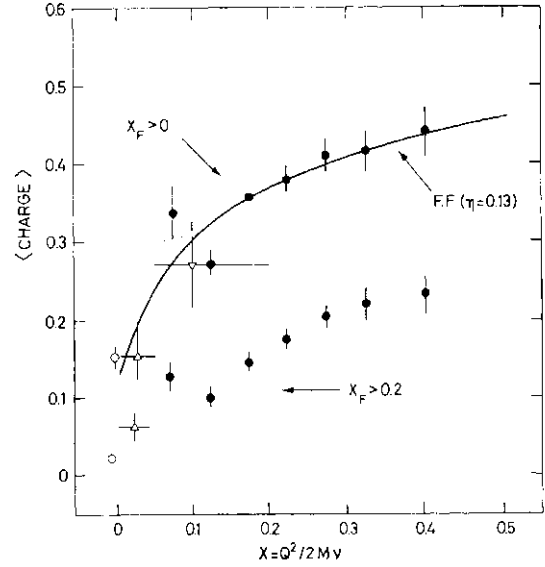


Fig. 30. Mean hadron charge for  $x_f > 0, 0.2$  versus  $x$  from Cornell-DESY electroproduction experiment.

$x (=Q^2/2Mv)$  and shows that there is a net rise with  $x$ . The curve is given by the relation

$$\langle \text{charge} \rangle = \frac{\sum l_j^2 [l_j \mp \eta] Q_j(x)}{\sum l_j^2 Q_j(x)}$$

where the summation is over all quark flavours with charge  $l_j$  and quark distributions  $Q_j(x)$  given by Field and Feynman,<sup>46</sup>  $r_j$  is the mean quark charge and the experimentally-determined value  $\eta = 0.13$  was used, in agreement with  $\eta = 1/6$ , the prediction for an SU(2) symmetric sea.

Many other results have been presented to this Conference on the hadronic final states of deep inelastic scattering which have been reviewed in other sessions.<sup>47</sup> The results are in qualitative agreement with present ideas on the quark-parton model. However the  $p_z$  dependence of the hadrons should reflect the  $p_z$  of the quarks which "undress" from the nucleon and subsequently, by the inverse process, "dress" to produce the final state hadron. At present there is no clear evidence emerging from the data on what are the important parameters among  $q^2, x, x_p, W, z$  in determining the  $p_z$  distributions, but preliminary attempts have been made by the C.H.I.O. group.<sup>48</sup>

It is clear that inclusive final states will provide sensitive measurements for future tests of Q.C.D. in the region of large  $Q^2$  and  $W$ .

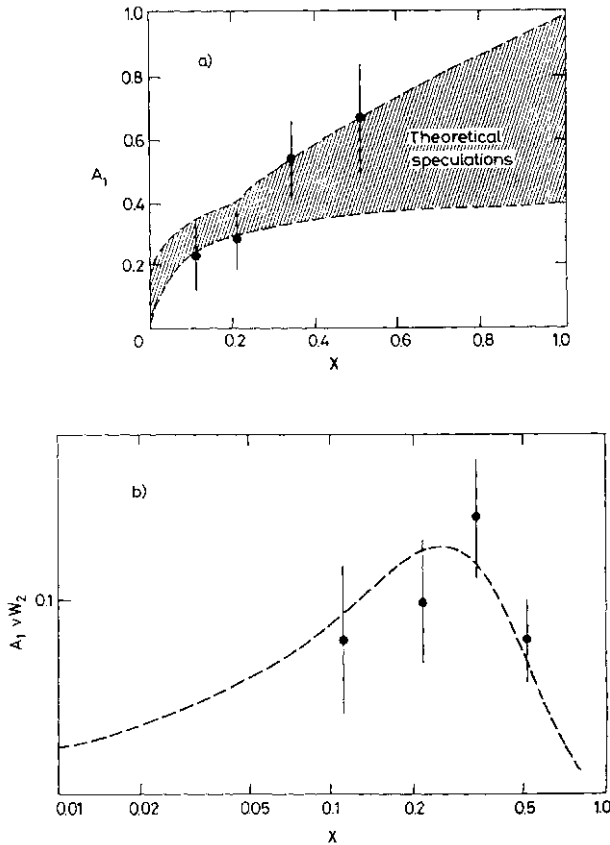


Fig. 31. (a) Asymmetry in scattering polarised electrons off polarised protons from B.S.T.Y. collaboration at SLAC.  
 (b)  $A_1 \nu W_2$  versus  $x$  as test of Bjorken sum rule.

## §6. Spin Dependent Structure Functions

The study of polarised electrons off polarised protons is according to the simple Quark Parton picture a method of scattering polarised electrons off polarised quarks, and provides information on the additional spin dependent structure functions. The asymmetry for the longitudinal polarisation is given by

$$A = \frac{d\sigma(\uparrow\downarrow) - d\sigma(\uparrow\uparrow)}{d\sigma(\uparrow\downarrow) + d\sigma(\uparrow\uparrow)} \\ \approx K\{A_1 + \eta A_2\}$$

where  $A_1$  is related to the difference between the spin 1/2 and spin 3/2 photoabsorption cross-sections and  $A_2$  is related to the transverse longitudinal interference,  $\eta$  is a small kinematic factor and  $K$  is a depolarisation factor. The asymmetry is essentially a measure of  $A_1$ , which is predicted by the Quark Parton Model to be +5/9 for the proton, whereas for  $g^2 = 0$  the asymmetry is negative.<sup>49</sup>

An experiment has been performed by a Bielefeld-SLAC-Tsukuba-Yale Collaboration<sup>50</sup> using a beam of  $10^9$  e<sup>-</sup>/sec with a polariza-

sation of 50%. In order to understand all the systematic errors, an experiment was first made on elastic scattering where the asymmetry is related to the form factors  $G_E$  and  $G_M$  and can be predicted. The measured asymmetry was  $A_{xp} = 0.103 \pm 0.015$  ( $A_M = 0.12 \pm 0.001$ ) and the relative sign of  $G_E/G_M$  was found to be positive. The asymmetry was then measured for inelastic scattering and the results are illustrated in Fig. 31a as a function of  $x$  in the range  $1 < Q^2 < 4$  (GeV/c)<sup>2</sup> and  $2 < W < 4$  GeV in agreement with the Quark Parton Model. The data are in agreement with a very wide range of theoretical quark-type predictions.<sup>51</sup>

The Bjorken sum rule states

$$\int_0^1 \frac{dx}{x} (A_1^p \nu W_2^p - A_1^N \nu W_2^N) = \frac{1}{3} \frac{g_A}{g_V} = 0.417$$

Assuming the  $A^2=0$  (Q-P Model), it is possible to check this sum rule approximately from the proton data using a simple scaling extrapolation. The results are illustrated in Fig. 31b and give  $\int_0^1 \frac{dx}{x} A_1 \nu W_2 = 0.41 \pm 0.05$  in good agreement with the predicted value considering the uncertainty in the extrapolation. Data have also been obtained in the resonance region and are consistent with the predicted asymmetry for the different resonance transitions. Future high precision data for deep inelastic scattering should provide very sensitive tests of Q.C.D. effects, in particular at small and large value of  $x$ .

## §7. Pion and Kaon Form Factors

A determination of the pion and kaon form factors is of interest since it is possible to compare the sizes of the electromagnetic structure of the mesons, and there are many different theoretical predictions based on geometrical models, analyticity and vector dominance. Experimental interest has been stimulated in this field recently by the availability of high-energy high-intensity beams of pions, kaons and even anti-protons using target electrons since the maximum  $q^2$  attainable even for 300 GeV pion and kaon beams is  $0.29$  (GeV/c)<sup>2</sup> and  $0.17$  (GeV/c)<sup>2</sup> respectively.

### 7.1. Pion form factors

The form factors of the pion can be determined by three different methods using space-like and time-like  $q^2$  photons. The precise

measurement of the  $\pi\pi$  mass spectrum in  $e^+e^-$  storage rings from threshold through the  $p^0$  mass region has been made by an Orsay group.<sup>52</sup> Since the two-pion mass spectrum is dominated by the  $p^0$  meson close to threshold, they have derived a value of the mean charge radius of the pion which is essentially model-independent of

$$\langle r^2 \rangle^{1/2} = 0.678 \pm 0.004 \text{ (stat)} \\ \pm 0.008 \text{ (model) fm.}$$

The electroproduction process  $e^-N \rightarrow e^-itN$  has also been used to determine the pion form factor. It has the advantage that it is possible to cover a large range in  $Q^2$  ( $\sim 10$  (GeV/c)<sup>2</sup>), but the results are very dependent on the model used to extract the amplitude for the  $t$ -channel pion pole term for longitudinally-polarised photons. The following values have been reported for  $\langle r^2 \rangle^{1/2}$  which are in reasonable agreement with the storage ring determination:

- 1973 Inverse Electroproduction<sup>53</sup>  
0.73±0.13
- 1976 Electroproduction above Resonance<sup>54</sup>  
0.704±0.025
- 1977 Electroproduction on Resonance<sup>55</sup>  
0.74±8:ii
- 1978 Electroproduction above Resonance<sup>56</sup>  
0.711±0.018

It is not clear that given much more precise data on longitudinal and transverse polarisation measurements on pion electroproduction, it will be possible to improve on the uncertainty in the extraction of the form factor from this process.

In principle the measurement of the elastic process  $n+e^- \rightarrow n+e^-$  provides the most direct method of measuring the pion form factor since

$$\left[ \frac{d\sigma}{dq^2} \right]_{\text{el}} = \left[ \frac{d\sigma}{dq^2} \right]_{\text{point}} |F_\pi(Q^2)|^2$$

The experiments are difficult to perform since the measurements are made in Hydrogen producing very large hadronic backgrounds and the main uncertainty arises from the systematic errors in the experiment.

Measurements have been made using 50 GeV pions at Serpukhov<sup>57</sup> and 100 GeV pions at F.N.A.L.<sup>58</sup> The results of these experiments give for  $\langle r_\pi^2 \rangle^{1/2}$

- 1974  $E_\pi = 50$  GeV                      0.78±0.10
- 1977  $E_\pi = 100$  GeV                    0.56±0.04

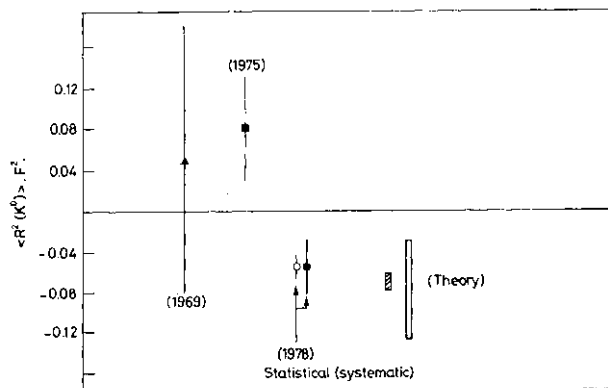


Fig. 32. The  $K^0$  charge radius compared with other experiments. |, Foeth *et al.* (1969);  $\circ$ , Dydak *et al.* (1975); +, Gsponer *et al.* (1978). The rectangular bars are the theoretical predictions—see text.

An alternative analysis of the first result performed by different authors<sup>59</sup> gave  $\langle r^2 \rangle = 0.71 \pm 0.05$ . It is somewhat disturbing to see such a large difference in these measurements and clearly further measurements are necessary. Theoretical predictions of the mean charge radius in fm are 0.58—0.69 F (V.M.D.),<sup>60</sup>  $0.7 \pm 0.15$  (analyticity)<sup>61</sup> and  $0.561 \pm 0.16$  or  $0.657 \pm 0.15$  (geometrical model).<sup>62</sup>

### 7.2. Kaon form factor

The first measurement of the charged kaon form factor has been reported at this conference by the U.C.L.A.-F.N.A.L.-Notre Dame-Pittsburgh group,<sup>63</sup> who have used a 250 GeV  $K^-$  beam. Preliminary results from this experiment give  $\langle r \rangle^{1/2} = 0.51 \pm 0.07$ , but at present a comparison with the pion radius is not possible. A theoretical prediction for the kaon radius has been given<sup>62</sup> of  $0.520 \pm 0.081$  or  $0.622 \pm 0.068$  using the geometrical model and different determinations of the proton radius.

An experiment has been carried out by the Chicago-Wisconsin-SIN group<sup>64</sup> to measure the charge radius of the  $K^0$  meson. This charge can be visualised in the simple non-relativistic quark model, where the  $s$  and  $d$  quarks orbit about their centre of mass with the lighter  $d$  negative quark further out producing a finite negative charge radius. The amplitude of  $\Lambda$ -regeneration was determined by comparing the rates of coherent regeneration and of diffraction regeneration at  $Q^2=0$  using two lead regenerators of very different thicknesses to maximise the coherent signal

and to reduce the correction due to multiple scattering. The results of this very beautiful experiment give

$$\langle i^?(\wedge^\circ) \rangle = -(0.054 \pm 0.010) \text{ fm}^2$$

Previous measurements<sup>65</sup> of  $(R^2(K^0))$  including this new measurement are illustrated in Fig. 32 together with theoretical predictions.<sup>66</sup>

A precise comparison of the charged kaon and pion form factors will require new experimental determinations in the same apparatus where the systematic errors are well understood.

### §8. Resonance Production

There are many experimental results in the field of electroproduction and photoproduction in the resonance region  $1 < W < 2.5 \text{ GeV}$ .<sup>67</sup> The object of this work is to determine the  $Q^2$  dependence of the electromagnetic couplings of the nucleon resonances in  $\gamma\text{-AW}^*$ , where many detailed tests of radiative decays of quarks can be tested.

In photoproduction, it is necessary to measure seven quantities in order to determine unambiguously four complex amplitudes (photon  $\pm 1 \rightarrow$  target  $\pm 1/2$ ). These consist of the unpolarised differential cross-sections  $da_0$  together with six different kinds of polarisation, *i.e.*, six different asymmetries arising from single and double polarisation measurements  $I, P, T, G, H$  together with recoil proton polarisation from polarised beam on target.

The most complete set of measurements in this energy range has been made by the Glasgow-Liverpool-Sheffield group at Daresbury,<sup>68</sup> who have measured  $da_0, 2, P, T, G$  and  $H$ , *le.*, six out of the seven required. Many new measurements on these quantities have been submitted to this conference,<sup>69</sup> as can be seen from Table III on various pion processes, mainly from the different Japanese groups using the Tokyo synchrotron. The major new contribution in electroproduction comes from the total cross-section measurements for polarised beam on polarised target, but other data are now available of various channels. A large amount of new data is available at present and therefore it is important to attempt a complete analysis of all these data from photoproduction and electroproduction in order to

Table III. Experiments (resonance region).

1. $\sigma_T$ (pol. proton-pol. target)			Bielefeld/SLAC/ Tsukuba/Yale
$W=1200-2000,$			
$Q^2=0.5, 1.5$			
2. $\gamma p \rightarrow p\pi^0$			
$\Sigma$	0.75-1.31	40°, 50°	Yerevan
$T$	0.42-1.0	30°, 80°, 105°, 120°	Nagoya/Osaka/Kyoto
$P$	0.3-1.15	100°, 130°	INS/Tokyo/Sendai/ Kyoto
$P$	0.83-1.45	60°	Yerevan
$P$	0.5-0.8	100°, 120°, 140°	Karkov
$d\sigma/d\Omega$	0.6-0.83	130°	INS/Tokyo/Sendai/ Kyoto
$d\sigma/d\Omega$	0.6-1.8	170°	Bonn
3. $\gamma + p \rightarrow \pi^+ + n$			
$\Sigma$	1.3-1.7	40°, 60°	Yerevan
4. $\gamma + n \rightarrow \pi^- + p$			
$p$	0.7-1.2	60°-100°	Tokyo/KEK/INS
$\Sigma$	0.9-1.5	30°-60°	Yerevan
5. <i>Electroprod</i> $\pi^0, \gamma^0$			
	0°-40°	$Q^2=.15$	Bonn
		$Q^2=0.3$	

determine the  $Q^2$  dependence of the various  $\gamma NN^*$  couplings. Following this, it should then be possible to decide which experiments are important and necessary to be carried out.

### §9. The Next Step

The next step will come from experiments which are either approved or have already taken a lot of data, but there are obvious areas of physics where progress should occur.

In photoproduction, charm must surely be seen from the existing large amounts of data which are presently under analysis at the level of  $\sim 1/\text{nb}$ . The emulsion technique works well in what appears to be at first sight a very hostile environment, and with ten times the statistics already available to be measured, tens of charmed events should be found. Once charm has been well proven, then photoproduction is a good process in which to study charmed baryons.

The possibility of studying quark jets through quark pair production in comparison with  $e^+e^-$  data should provide important information on the photon structure. In this connection, the use of the nucleus as a "quarkfilter" where the  $u, d, X$  quarks are absorbed preferentially compared with  $c, b, t$  quarks is an application where high mass states can be enhanced relative to low mass



states. The measurement of Compton scattering and Compton inelastic scattering at high energies becomes easier and should be able to provide useful information on quark and gluon effects similar to inelastic scattering.

At lower energies, the study of mesons in the 1-3 GeV mass region is still an area of physics which is largely unexplored, but requires special probes, e.g., polarised photons etc. to separate out the complex resonance structures. In the resonance region, the time has surely been reached in both photoproduction and low  $Q^2$  lepton production when only specific experiments should be done which are necessary to remove ambiguities in the extraction of the amplitudes. In inelastic lepton scattering, the obvious need is for high precision data over the whole  $(x, Q^2)$  plane and its extension to large  $Q^2$ , including the separation of proton and neutron structure functions to prove or disprove the very successful Q.C.D. theory. The study of electrons, muons and photons in the final state has very interesting applications in our understanding of different flavours in the small  $x$  sea, including a test of quark mass scales through  $Q^2$  dependences. If the present Q.C.D. picture continues to work well, then the study of final states in deep inelastic scattering will provide many interesting tests on the role of the quark in the nucleon and how the quarks dress to form hadrons in comparison with other processes like  $e^+e^-$ , Drell-Yan etc. The study of quark and gluon jets will be difficult in the present accelerator energy range, and new techniques for analysing the data will be required.

The study of lepton-quark scattering where the lepton is either charged or neutral ( $\nu$ ) is a very basic process in which to make explicit tests of any model which explains the role of the basic constituents within the nucleon. At this conference, it is now known that through interference certain hadronic final states produced by photon and  $Z^0$  exchange are the same. High precision experiments can therefore be made using charged lepton and neutrino beams in order to see what, if any, are the differences in the behaviour of the final states, and therefore in the weak and electromagnetic interaction of the quarks. Perhaps

by the next Rochester Conference in two years' time there will be one review of all inelastic lepton scattering processes!

### Acknowledgements

I would like to thank Professor K. Kondo for his help in preparing this review, Professor M. Konuma and his colleagues of the University of Kyoto and Professor Y. Yamaguchi and his colleagues of the University of Tokyo for their assistance.

### References

1. L.N. Hand and R. Marshall: *Proc. 1977 Int. Symp. Lepton and Photon Interactions, (DESY, Hamburg, 1977)*.
2. Contributed paper 647, D. O. Caldwell *et al* (1978).
3. D. O. Caldwell *et al*: *Phys. Rev. Letters* **23** (1969) 1256.
4. E. Gabathuler: *Proc. 6th Int. Symp. Electron and Photon Interactions at High Energies, (Bonn, 1973)*, p. 299.
5. S. Michalowski *et al*: *Phys. Rev. Letters* **39** (1977) 737.
6. D. O. Caldwell *et al*: *Phys. Rev.* **D7** (1973) 1362.
7. CH.I.O. Collaboration: T. W. Quirk (private communication) (1978).
8. R. E. Taylor: session B3E (1978).
9. L. N. Hand: *Proc. 1977 Int. Symp. Lepton and Photon Interactions, (DESY, Hamburg, 1977)*, p. 426.
10. E. Reya: private communication.
11. Aachen-Bonn-CERN-London-Oxford-Saclay Collaboration: Oxford University preprint (1978).
12. Contributed paper 763, H. L. Anderson *et al* (1978).
13. O. Nachtmann: *Nucl. Phys.* **B63** (1973) 237; **B78** (1974) 455.
14. Contributed paper 837, R. C. Bail *et al* (1978).
15. A. J. Buras: F.N.A.L. (unpublished).
16. J. Ellis and M. K. Gaillard: *Nucl. Phys.* **B131** (1977) 285.
17. Berkeley-F.N.A.L.-Princeton Collaboration.
18. European Muon Collaboration (NA2) and CERN-Dubna-Munich-Saclay Collaboration (NA4).
19. D. Sivers *et al*: *Phys. Rev.* **D13** (1976) 1234.
20. W. Y. Lee: *Proc. 1977 Int. Symp. Lepton and Photon Interactions, (DESY, Hamburg, 1977)*, p. 555.
21. Contributed paper, M. Binkley *et al* (1978).
22. W. Y. Lee: Session B4E (1978).
23. Contributed paper 805, Bonn etc. (1978).
24. Contributed paper 974, Bologna etc. (1978).
25. N. Cabibbo and L. Maiani: *PAR-LP THE* 78/12 (1978).
26. Contributed paper 439, R. M. Eglyoff *et al* (1978).

27. C. W. Akerlof *et al.*: Phys. Rev. **D 14** (1976) 2864.
28. The decay  $(j \rightarrow \bar{n} n \sim \bar{\tau} \tau^0)$  indicates small admixture of non-strange quarks.
29. Contributed paper 778, D. P. Barber *et al.* (1978).
30. Contributed paper 809, Bonn etc. (1978).
31. Contributed paper 439, R. M. Egloff *et al.* (1978).
32. Contributed paper 297, L. A. Aherhs *et al.* (1978).
33. Contributed paper 1079, K. Bunnell *et al.* (1978).
34. H. Cheng and T. T. Wu: *Proc. 1971 Int. Symp. Electron and Photon Interactions at High Energies (Cornell University, 1971)*.
35. Contributed paper 297, L. A. Ahrens *et al.* (1978).
36. R. Dixon *et al.*: Phys. Rev. Letters **39** (1977) 516.
37. G. P. Murtas: session B2E (1978).
38. S. Bartalucci *et al.*: DESY 77/59 (1977).
39. Contributed paper 1069, D. Peterson *et al.* (1978).
40. C. Bemporad: *Proc. 1977 Int. Symp. Lepton and Photon Interactions (DESY, Hamburg, 1977)*, p. 165.
41. Contributed paper 808, Bonn etc. (1978).
42. Contributed paper 297, L. A. Ahrens *et al.* (1978).
43. Contributed paper 806, Bonn etc. (1978).
44. Contributed paper 1095, G. Drews *et al.* (1978).
45. B. Andersson *et al.*: Nucl. Phys. **B 135** (1978) 273; R. D. Field and R. P. Feynman: CALT-68-618 (1977); L. M. Seghal: *Proc. 1977 Int. Symp. Lepton and Photon Interactions (DESY, Hamburg, 1977)*, p. 837.
46. R. D. Field and R. P. Feynman: Phys. Rev. **D 15** (1977) 2590.
47. P. Söding: session B3E (1978).
48. R. Wilson: session B3E (1978).
49. S. D. Drell and A. C. Hearn: Phys. Rev. Letters **16** (1966) 908.
50. Contributed paper 686 M. J. Alguard *et al.* (1978).
51. M. J. Alguard *et al.*: SLAC-PUB-2110 (1978) and references therein.
52. J. C. Bizot: private communication.
53. S. F. Bereznev *et al.*: Sov. J. Nucl. Phys. **16** (1973) 99.
54. C. J. Bebek *et al.*: Phys. Rev. **D 13** (1976) 25.
55. G. Bardin *et al.*: Nucl. Phys. **B 120** (1977) 45.
56. Contributed paper 383, C. J. Bebek *et al.* (1978).
57. G. T. Adylov *et al.*: Phys. Letters **53 B** (1974) 285.
58. E. B. Daily *et al.*: Phys. Rev. Letters **39** (1977) 1176.
59. S. Dubnicka and O. V. Dumbrajs: Phys. Letters **53 B** (1974) 285.
60. C. F. Cho and J. J. Sakurai: Lett. Nuovo Cimento **2** (1971) 7.
61. V. Baluni: Phys. Letters **38 B** (1972) 535.
62. Contributed paper 1171, T. T. Chou (1978).
63. Contributed paper 857, A. Berevtas *et al.* (1978).
64. Contributed paper 899, A. Gsponer *et al.* (1978).
65. H. Foeth *et al.*: Phys. Letters **30 B** (1969) 276; F. Dydak *et al.*: Nucl. Phys. **B 102** (1976) 253.
66. N. M. Kroll, T. D. Lee and B. Zumino: Phys. Rev. **157** (1967) 1376; O. W. Greenberg *et al.*: Phys. Letters **70 B** (1977) 464 and reference therein.
67. R. Marshall: *Proc. 1977 Int. Symp. Lepton and Photon Interactions (DESY, Hamburg, 1977)* p. 489 and references therein.
68. J. R. Holt: private communication.
69. R. Kajikawa: session A4E.

**P7a: Neutrino Reactions I—Charged Current Interactions  
and Multilepton Production**

*Chairman:* M. CONVERSI

*Speaker:* K. TITTEL

*Scientific Secretaries:* Y. NAGASHIMA  
Y. KOBAYASHI

**P7b: Neutrino Reactions II—Neutral Current Interactions  
and Charm Production**

*Chairman:* D. C. COLLEY

*Speaker:* C. BALTAY

*Scientific Secretaries:* H. YUTA  
S. KABE

## P 7a Neutrino Reactions I: Charged Current Interactions and Multilepton Production

K. TITTEL

*Institute für Hochenergiephysik der Universität Heidelberg, Heidelberg*

### §0. Introduction

Neutrino physics is one of the fields which in the last years has attracted the interest of many people. Not only the study of the structure of the weak interaction was the object of various experiments, but soon it became also evident that the neutrino is as well an ideal probe to study the internal structure of the nucléon. Neutrino reactions offer furthermore the possibility to search for and to investigate new phenomena such as charm, righthanded quarks and heavy leptons. In the preceding years many interesting results had been presented, some of which gave rise to quite an excitement or even to controversial discussions.

Since the last conference a lot more data has been collected and many experiments have contributed to a much better understanding of all these questions. Some of the exciting new results have been confirmed, others were found wrong.

The earlier situation in neutrino physics has been reviewed in a number of excellent articles.<sup>1-4</sup> In this report however a summary of the latest results on three specific subjects will be presented. At first the new development in inclusive charged current scattering will be discussed rather extensively. Many new results have been presented at this conference. Of particular interest here is the question of scaling violation.

In a second chapter a brief resume will be given on the status of hadron production in charged current interactions. Most data in this field are still of preliminary nature and it is probably too early to draw firm conclusions.

And finally the multilepton production will be the subject of our discussion. The main-point here will be to understand the origin of the in the meanwhile copiously observed trimuon events and to see whether indications

can be given for the existence of new particles. The other large subject in this domain, the dilepton production, will be discussed by Prof. Baltay in his plenary talk,<sup>5</sup> as well as the still remaining field of neutral currents.

### §1. Inclusive Charged Current Scattering

#### 1. Outline of phenomenology

Before starting the discussion on the latest results of neutrino interactions a brief introduction to the formalism, usually used in this context, should be given. For a more detailed discussion the reader is referred to one of the excellent review articles.<sup>6,7</sup>

The process we are dealing with is the following :

$$\nu + N \rightarrow \mu^- + X$$

The kinematics of the interaction can be described by three variables :

the neutrino energy  $E$

the momentum transfer squared  $-q^2 = Q^2 = 4E \cdot E' \sin^2 \theta/2$

and the energy transfer  $\nu = E - M \cdot E_n$

$E_p$  is the muon energy,  $E_n$  the energy of the outgoing hadrons,  $M$  the nucléon mass and  $\theta$  the scattering angle of the muon. Alternatively the scaling variables

$$x = \frac{Q^2}{2M\nu} \text{ and } y = \frac{\nu}{E} \text{ are used.}$$

The differential cross section for inclusive neutrino scattering is then given by:

$$\frac{d^2\sigma}{dx dy} = \frac{G^2 M E}{\pi} \left[ \left( 1 - y - xy \frac{M}{2E} \right) F_2(x, Q^2) + \frac{y^2}{2} \cdot 2x F_1(x, Q^2) \pm \left( y - \frac{y^2}{2} \right) \cdot x F_3(x, Q^2) \right] \quad (1)$$

where the upper sign stands for neutrinos, the lower for antineutrinos. The structure functions are in general different for the two cases.

Let us now for the moment neglect strangeness and charm changing currents and let us

assume charge symmetry which means  $F_1=F_2$  for an isoscalar target, and validity of the Callan-Gross relation:  $2xF_1=F_2$ .

The cross sections reduces then to a simpler form in the high energy limit ( $Q^2 \gg Af$ ):

$$\frac{d^2\sigma}{dx dy} = \frac{G^2 ME}{\pi} \left\{ \frac{1}{2}(1+(1-y)^2)F_2(x, Q^2) \pm \frac{1}{2}(1-(1-y)^2)x F_3(x, Q^2) \right\} \quad (2)$$

where the structure functions now are the same for neutrinos and antineutrinos.

All the dynamics of the process is contained in the structure functions  $F_i(x, Q^2)$  which can be extracted from the data in the following way:

$$\begin{aligned} F_2(x, Q^2) &\propto \frac{d^2\sigma^\nu}{dx dy} + \frac{d^2\sigma^{\bar{\nu}}}{dx dy} \\ \text{or } F_2(x, Q^2) &= \left. \frac{d\sigma^{\nu, \bar{\nu}}}{dx dy} \right|_{y=0} \\ xF_3(x, Q^2) &\propto \frac{d^2\sigma^\nu}{dx dy} - \frac{d^2\sigma^{\bar{\nu}}}{dx dy} \end{aligned} \quad (3)$$

In the concept of Bjorken scaling (for  $Q^2$  and  $\nu \rightarrow \infty$  at fixed  $x$ ) these functions do not depend on  $Q^2$ . We know from many experiments that this hypothesis is good only to a level in the order of 10%. In neutrino experiments highest values of  $Q^2$  are attainable so that significant tests should be possible.

A dynamical model for the structure functions which can explain scaling, is the quark-parton model. Scattering of the neutrino as well as of the electron in deep inelastic electron scattering takes place at quarks, the pointlike constituents of the nucléon. The angular distribution of the scattering of two spin 1/2 particles of same or opposite helicity reflects in the  $j$ -distribution: flat or  $(1-y)^2$  respectively. The differential cross section in this picture is then given by:

$$\frac{d^2\sigma^\nu}{dx dy} = \frac{G^2 ME}{\pi} \cdot x \cdot [(q(x) + s(x)) + (\bar{q}(x) - \bar{s}(x))(1-y)^2] \quad (4)$$

$$\frac{d^2\sigma^{\bar{\nu}}}{dx dy} = \frac{G^2 ME}{\pi} \cdot x \cdot [(\bar{q}(x) + \bar{s}(x)) + (q(x) - s(x))(1-y)^2] \quad (5)$$

with  $q(x) = u(x) + r(d(x) + s(x))$  being the quark density distribution of the proton. Strange quarks are now included, but charmed quarks in the quark-antiquark sea are still ignored.

To relate the earlier defined structure func-

tions to the quark density distributions we rearrange relation (2):

$$\frac{d^2\sigma^{\nu, \bar{\nu}}}{dx dy} = \frac{G^2 ME}{\pi} \left[ \frac{1}{2}(F_2 \pm xF_3) + \frac{1}{2}(F_2 \mp xF_3)(1-y)^2 \right] \quad (6)$$

By comparing (6) with (4) and (5) we find:

$F_2(x) = x(q(x) + \bar{q}(x))$ , is the momentum distribution of all partons, and  $xF_3(x) = x(q(x) - \bar{q}(x) \pm s(x)) = x(q_v(x) \pm s(x))$ , is the momentum distribution of the valence quarks, when the contribution of  $s(x)$  is neglected.

We see  $F_2(x)$  is the same for neutrino and antineutrino scattering whereas  $xF_3(x)$  is different.

The quark distribution function must not be seen only in the framework of scaling: they can, of course, as well be dependent on  $g^2$ , as it is for the structure functions. The  $F_i(x)$  are more general, but the  $q(x)$  are certainly handier for our imagination.

## 2. Integral quantities

The phenomenological framework has been prepared in the preceding chapter, and it shall be used as a guideline for understanding experimental results. To have an easy access to the various aspects of inclusive neutrino scattering the total cross section and similar quantities, which are integrated over the kinematical variables  $x$  and  $y$  should be discussed first. In the simplest picture, the scaling hypothesis,  $a_{tot}$  will rise linearly with the energy at least as long as propagator effects due to the heavy boson can be neglected, which is certainly true at presently available energies. Other quantities, like average  $y$  or the integral over the structure functions should be entirely energy independent. Deviations from scaling are however expected from opening up of new thresholds as charm or others.

In Fig. 1 the slopes of the *total cross sections* for neutrino and antineutrino scattering are presented as a function of energy. In this figure only published data are given. The data are flat or eventually falling in the case of neutrinos and rising for antineutrinos. For illustration a QCD calculation by Buras & Gaemers<sup>11</sup> is indicated. New data have been presented to this conference by three

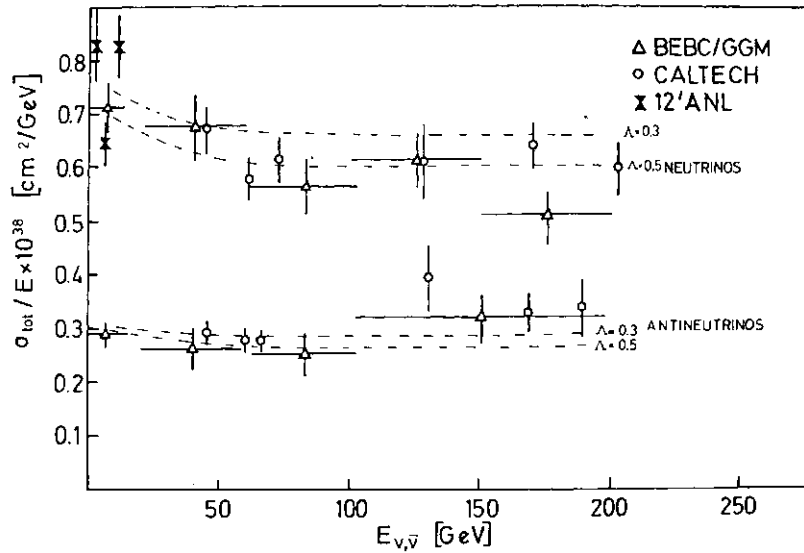


Fig. 1. Slope of total cross section of charged current interactions (published data [refs. 8, 9 and 10]). The lines represent QCD-calculations of Buras+Gaemers [ref. 11].

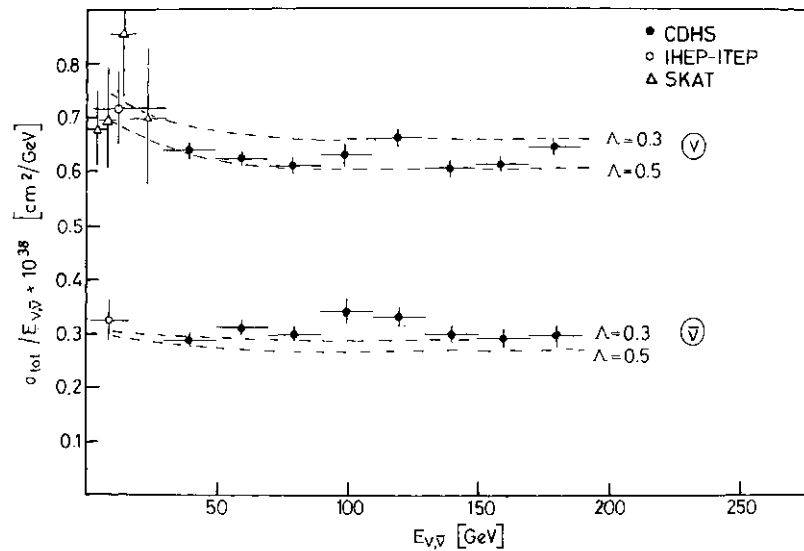


Fig. 2. Slope of total cross section (data presented to this Conference [refs. 12, 13 and 14]).

groups: IHEP-ITEP<sup>12</sup> and SKAT<sup>13</sup> from Serpukhov at lower energies and CDHS<sup>14</sup> at the CERN-SPS in the high energy range (see Fig. 2). The data of the CDHS-group show no energy dependence but are in the case of neutrinos definitely below the low energy points. Errors are statistical only, and an overall flux error of  $\pm 5\%$  at 30-90 GeV and  $\pm 10\%$  at 90-190 GeV should be added.

In Table 1 the values of the slopes and their ratios are listed for the various experiments. Whereas the slopes in the high energy range are compatible with each other within the errors, disagreement is found on their energy dependence as stated above. This is even more evident in the cross section ratios.

But the errors are large and no firm conclusion is possible. The data are compatible both with being flat or with a modest rise. Significant only is the increase of  $a^*/a''$  from 0.38 (GGM) at very low energies to 0.48 (CDHS) at high energies. The QCD predictions as indicated in the figures describe quite well the data.

Average  $y$  is a global measure for the shape of the  $\Lambda$ -distribution which should not vary with energy if scaling is valid. The CDHS-data<sup>14</sup> shown in Fig. 3 are well energy independent, whereas the CITFR-data<sup>10</sup> seem to indicate a slight rise for antineutrinos. In any case, no apparent threshold is visible

Table 1. Slopes of neutrino and antineutrino cross sections (in units of  $10^{-38} \text{ cm}^2 \text{ nucléon}^{-1} \text{ GeV}^{-1}$ ) and cross section ratios.

	Energy (GeV)	IHEP-ITEP	CITFR	GGM/BEBC	CDHS
$\sigma^\nu/E_\nu$	2-10			$0.72 \pm 0.05$	
	10-30	$0.72 \pm 0.07$			
	30-90		$0.61 \pm 0.02$	$0.62 \pm 0.04$	$0.62 \pm 0.04$
	90-190		$0.62 \pm 0.03$	$0.57 \pm 0.04$	$0.63 \pm 0.05$
$\sigma^{\bar{\nu}}/E_{\bar{\nu}}$	2-10			$0.29 \pm 0.02$	
	10-30	$0.32 \pm 0.03$			
	30-90		$0.28 \pm 0.01$	$0.26 \pm 0.02$	$0.30 \pm 0.02$
	90-190		$0.34 \pm 0.03$	$0.32 \pm 0.04$	$0.31 \pm 0.04$
$\sigma^{\bar{\nu}}/\sigma^\nu$	2-10			$0.38 \pm 0.02$	
	10-30	$0.44 \pm 0.05$			
	30-90		$0.46 \pm 0.02$	$0.42 \pm 0.08$	$0.48 \pm 0.025$
	90-190		$0.55 \pm 0.05$	$0.56 \pm 0.07$	$0.49 \pm 0.05$

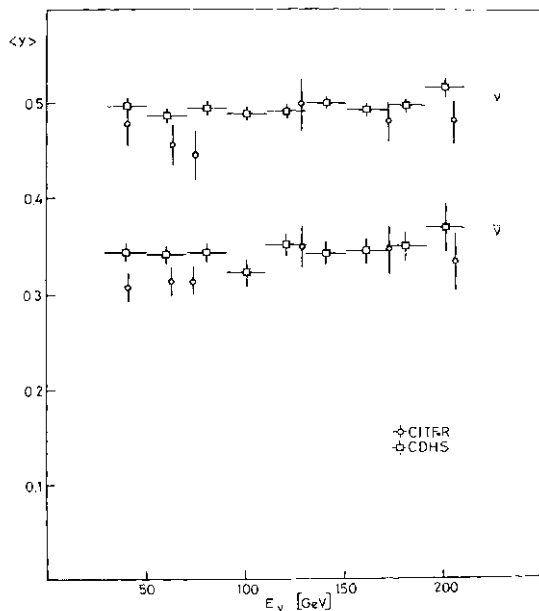


Fig. 3. Average  $y$  as function of energy [refs. 10 and 14].

The average slope of  $Q^2$  is given in Fig. 4. Quite some energy dependence is seen here, but again in the low energy range only. For  $E > 50 \text{ GeV}$  the CDHS data in particular are flat with energy. Since  $Q^2 = 2MExy$ ,  $(Q^2)/E$  will reflect the shrinkage of  $\langle y \rangle$  predicted by QCD as can be seen from the straight lines in Fig. 4.

The  $B$ -value as given in Fig. 5 is related to the antiquark content of the nucléon. It is:

$$B^{\bar{\nu}} = \int x F_3^{\bar{\nu}} dx / \int F_2 dx = 1 - 2 \cdot \frac{\bar{Q}_f}{Q + \bar{Q}}$$

with  $Q_f = \int x(q(x) + \bar{s}(x)) dx$  = fractional momentum carried by antiquarks.

The data show a significant decrease of  $B$  from  $\sim 0.85$  to  $\sim 0.7$  going from 0 to  $\sim 60 \text{ GeV}$ . At higher energies all is consistent with flat. This does certainly not

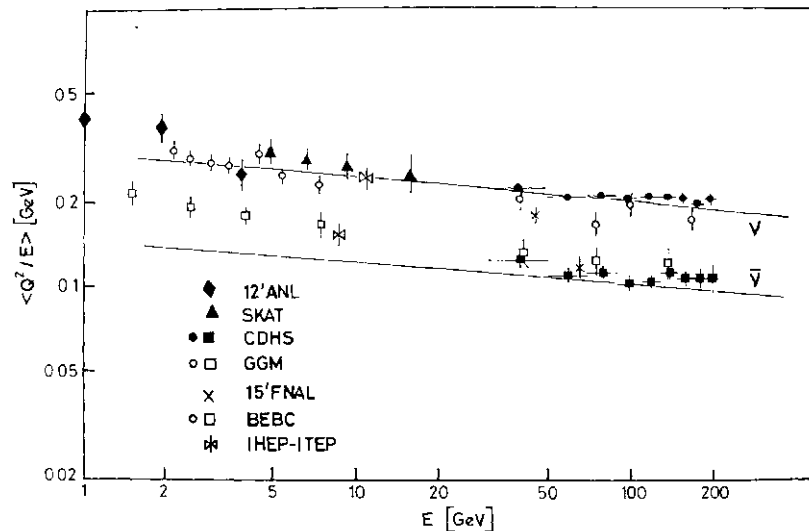


Fig. 4. Average slope of  $Q^2$  as function of energy.

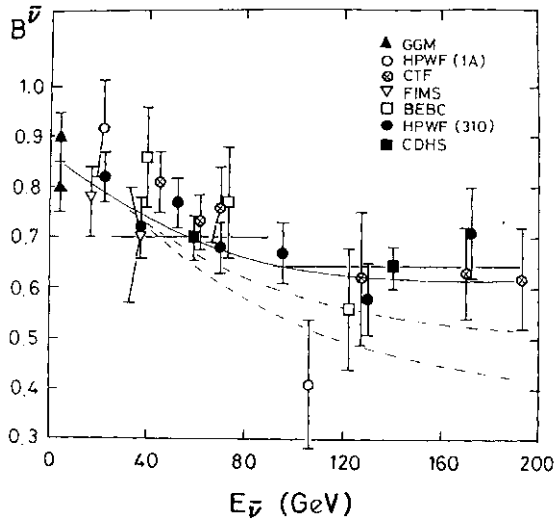


Fig. 5.  $B$ -values for antineutrinos as function of energy. The upper line represents a QCD-calculation of Barnett. The lower lines include righthanded currents with  $[\sin^2 \theta_W]_{e=0.1}$  and  $0.2$ . [ref. 15].

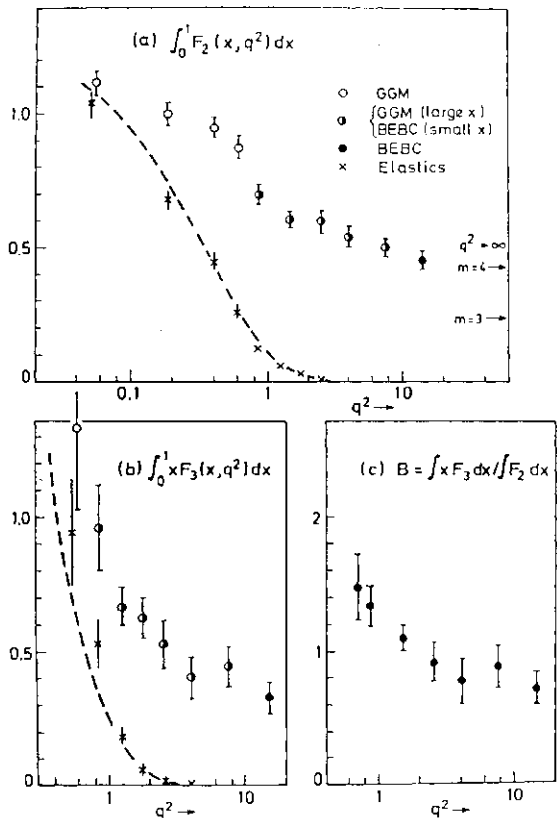


Fig. 6. The integrals of  $F_2$  and  $xF_3$  and their ratio as function of  $Q^2$ . [ref. 16].

favour righthanded currents as can be seen from the dotted lines which represent QCD calculations including righthanded currents with coupling strength of  $0.1$  and  $0.2$  respectively. QCD alone describes well the data.

The  $\int F_2(x) dx$  measures the fractional mo-

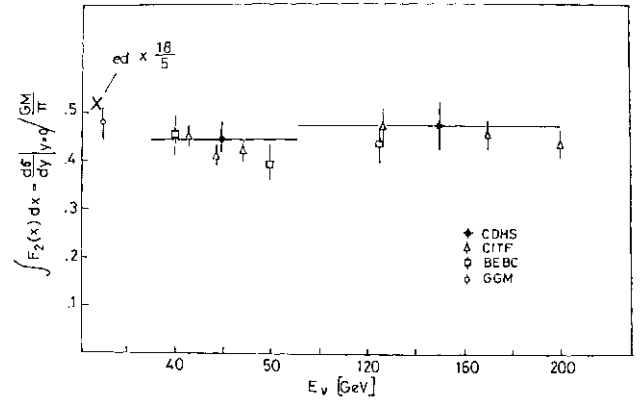


Fig. 7. Integral of  $F_2$  as function of energy [refs. 14, 10, 9, 18].

mentum carried by all partons. Figure 6a shows the  $Q^2$  dependence of this integral as measured by BEBC and GGM.<sup>16</sup> The limiting values for  $Q^2 \rightarrow \infty$  are indicated for 3 and 4 flavours. In Fig. 7  $\int F_2 dx$  is plotted as function of  $E$ . Again no energy dependence is seen for  $E > 40$  GeV or even not for lower energies.  $(18/5) \int F_2 dx$  from ed-scattering<sup>17</sup> compares well with the neutrino data. But care should be taken by comparing different results, since the experimentors use different methods to extract this quantity.

**Conclusion:** Integral quantities show variation with energy only for  $E < 50$  GeV. At higher energies no significant energy dependence could be found. This of course implies no significant ( $\Lambda$ -dependence as well. If data are looked at as function of energy, a  $g^2$ -dependence however is smeared out, since a data point at a given energy is integrated over all  $Q^2$  from 0 to  $e_{max} = 2 M \xi$ .

Summarizing it can be stated, for high energy experiment scaling is still a good working hypothesis. Deviations from it are small.

### 3. Differential distributions

Since scaling is found to be an acceptable approach one might study differential distributions averaged over a large energy range as covered by the high energy experiments at CERN-SPS and FNAL. In the following data from 30 to 200 GeV are combined in the analysis of single differential distributions.

#### i) $y$ -distribution

The  $j$ -distribution as measured in the high statistics counter experiment of the CDHS-



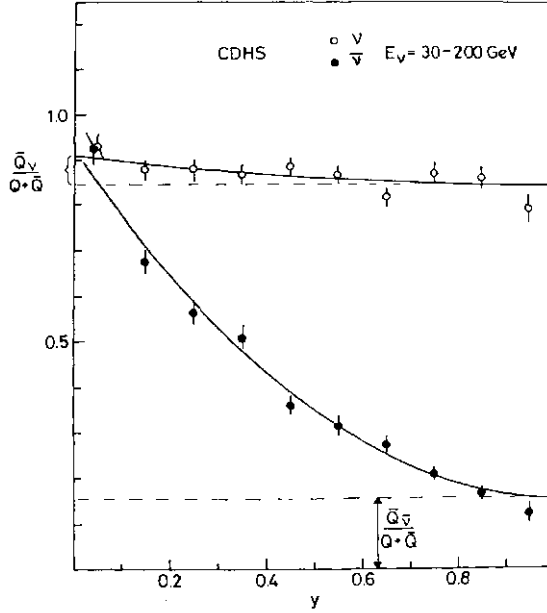


Fig. 8.  $\hat{\Lambda}$ -distribution for neutrinos and antineutrinos [ref. 14].

group<sup>14</sup> is shown in Fig. 8 as an example. The data points are apparently well parametrized as a sum of a flat and an  $(1-j)^2$ -term, as expected from the simple phenomenological formalism outlined earlier. The amount of antiquarks, contained in the nucléon, can easily be extracted. But before doing so two assumptions used in the phenomenology should be tested: charge symmetry and the Callan-Gross-relation.

*Charge symmetry* means in the case of an isoscalar target, that the structure functions  $jp_2$  are the same for scattering of neutrinos and of antineutrinos. This is tested experimentally by comparing  $da/\hat{\alpha}y|_{y=0}$  for the two cases.

The following results have been obtained.

$$\frac{d\sigma^\nu}{dy} \Big|_{y=0} / \frac{d\sigma^{\bar{\nu}}}{dy} \Big|_{y=0} = \begin{cases} 1.05 \pm 0.07 & \text{CDHS}^{14} \\ 0.9 \pm 0.2 & \text{BEBC}^{16} \end{cases}$$

and CITFR<sup>10</sup> presented a plot of  $da/\hat{\alpha}y|_{y=0}$  for neutrinos and antineutrinos as a function of energy (Fig. 9) from which the authors extract a confirmation of charge symmetry to about 5%.

All three experiments are clearly in line with the validity of charge symmetry. The level to which this assumption is tested is in the order of 5%.

The second assumption which is used in the phenomenological frame is the *Callan-Gross relation*:

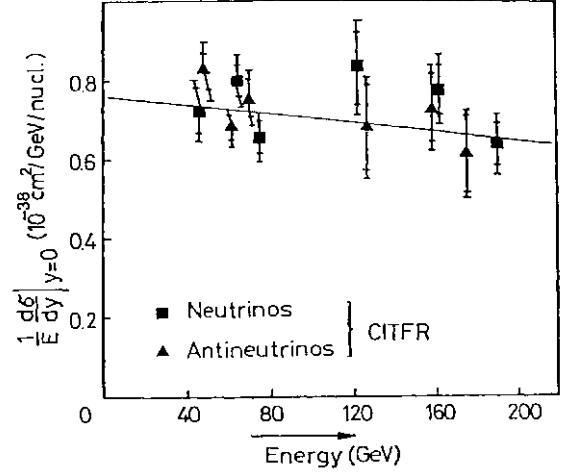


Fig. 9. Differential cross section at  $y=0$  for neutrinos and antineutrinos as function of energy, [ref. 10].

$$2xF_1 = F_2.$$

In the quark-parton model this relation is a consequence of the partons having spin 1/2 and no transverse momentum. It is related to the ratio of longitudinal to transversal cross section  $R=G_L/G_T$ , as measured in electron scattering in the following way:

$$R = \frac{1}{A} \left[ (1-A) + \frac{4M^2 x^2}{Q^2} \right]$$

with

$$A = \frac{\int 2xF_1 dx}{\int F_2 dx}$$

In neutrino scattering a violation of this relation gives rise to an additional  $(1-j)$ -term in the differential cross section. Several groups have extracted a value or a limit for A from their data:

$$\begin{array}{l} \text{GGM}^{16}: \\ \text{BEBC}^{16}: \\ \text{CITFR}^{10}: \\ \text{CDHS}^{14}: \end{array} \quad (1-A) \begin{cases} = 0.32 \pm 0.10 \\ \text{for } Q^2 < 1 \text{ GeV}^2 \\ = 0.11 \pm 0.12 \\ \text{for } Q^2 > 1 \text{ GeV}^2 \\ = 0.17 \pm 0.09 \\ \leq 0.05 \text{ (90\% CL)} \\ \langle Q^2 \rangle \approx 22 \text{ GeV}^2 \end{cases}$$

One should however be cautious by using these figures. Radiative corrections have not been applied, and the Callan-Gross term is certainly sensitive to such corrections.

The high energy experiments show no really significant violation of Callan-Gross, they are furthermore well compatible with the result  $\hat{\alpha} = 0.24 \pm 0.12$ <sup>19</sup> of deep inelastic

electron scattering at SLAC. But it would be difficult to accommodate the high value of  $i^? = 0.45 \pm 0.25$  from the FNAL muon experiment<sup>20</sup>. To understand the high value for  $(I-A)$  in the low energy GGM-experiment, one has to realize that at low  $Q^2, R$  is dominated by contributions from the primordial transverse momentum of the partons. This term goes with  $1/Q^2$  and may become large at small

In the present situation it is certainly justified to assume the Callan-Gross relation to be valid for our further analysis.

Finally one can extract from the  $\hat{\Lambda}$ -distribution some information on the amount and the composition of the sea in the nucléon. As can be seen from Fig. 8 the  $\hat{\Lambda}$ -distribution of antineutrinos provides us at high  $y$  with a measure of the anti-quark content as seen by antineutrinos. The difference of the cross section at low and high  $y$  for neutrino scattering tells us about the sea content as seen by neutrinos. The two are different. The CDHS-experiment<sup>14</sup> gives the following two numbers:

$$\frac{\bar{Q}_\nu}{Q + \bar{Q}} = \frac{\bar{Q} - \bar{S}}{Q + \bar{Q}} = 0.08 \pm 0.04$$

$$\frac{\bar{Q}_\bar{\nu}}{Q + \bar{Q}} = \frac{\bar{Q} + \bar{S}}{Q + \bar{Q}} = 0.16 \pm 0.02$$

with

$$\bar{Q} = \int x \bar{q}(x) dx.$$

The difference then gives the amount of strange quarks in the sea. But this quantity is extracted also from the rate of opposite sign dimuons in neutrino and antineutrino scattering, here even with better precision. The method will be explained by Prof. Baltay in the next talk.<sup>5</sup> The presently available results are summarized in Table 2.

Table 2. Amount of total and of strange sea.

Group	Method	$\bar{Q}/(Q + \bar{Q})$	$\bar{S}/(Q + \bar{Q})$
CDHS	$y$ -distr.	$0.12 \pm 0.02$	$0.04 \pm 0.02$
CDHS	$\mu^+ \mu^-$	—	$0.02 \pm 0.01$
BEBC	Structure	$0.11 \pm 0.03$	
	fct.		
HPWFOR	$\mu^+ \mu^-$	$0.14 \pm 0.03$	$0.04 \pm 0.02$
Col.-Brookh.	$\mu^+ \mu^-$	—	$0.015 \pm 0.01$
Average		$0.12 \pm 0.02$	$0.02 \pm 0.01$

At high energies 12% of the momentum of all partons is carried by antiquarks. Strange

quarks contribute probably only less than half of the  $SU_3$ -symmetric value,

ii)  $x$ -distributions

The structure functions or in the QPM the quark densities depend on  $x$ , the fractional momentum. Since for different values by  $y$  the relative amount of antiquarks is different, the  $x$ -distributions are expected to depend on  $y$ . In particular at large  $y$  one will find quarks only (valence and sea quarks!) in the case of neutrino scattering, and antiquarks only in antineutrino scattering. Figure 10 shows the distribution of the fractional momentum of quarks and of antiquarks as measured in the CDHS-experiment.<sup>14</sup> The distribution of antiquarks is concentrated at small  $x$ , whereas

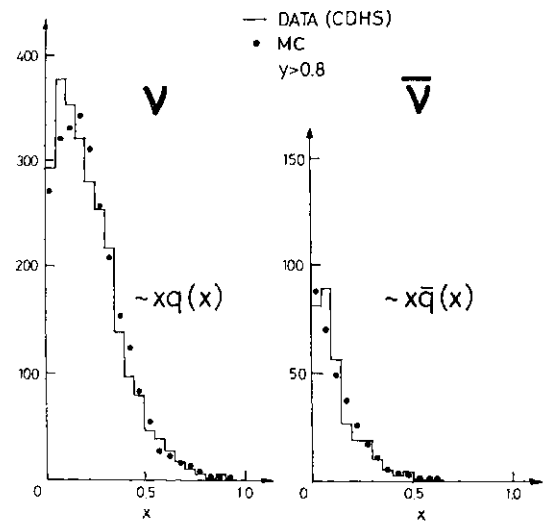


Fig. 10.  $\hat{\Lambda}$ -distributions at  $y=0.8$  for neutrinos and antineutrinos [ref. 14].

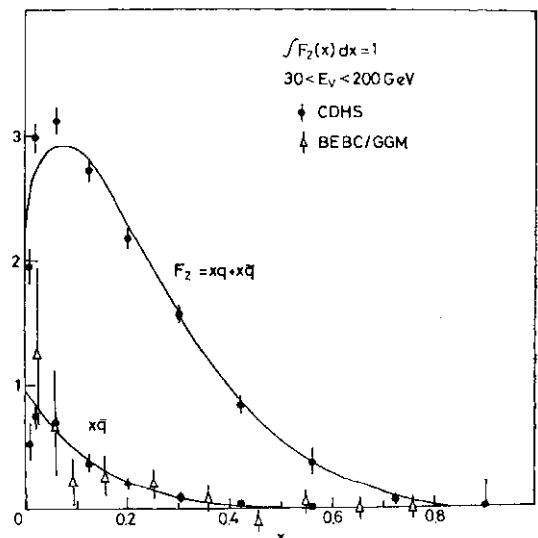


Fig. 11. Structure functions  $F_2(x)$  and  $xq(x)$  as function of  $x$  [ref. 14].

the quark distribution is rather wide. The average  $x$  is  $\sim .10$  for the sea compared to  $\sim 0.26$  for the valence quarks.

The structure functions  $F_2(x)$  and  $xq(x)$  are calculated less directly but using the impact of the full data sample according to the relation (3) given in I. The result of the CDHS group<sup>14</sup> is presented in Fig. 11. The BEBC<sup>16</sup> points for  $xq(x)$  are added. The BEBC group has presented as well results for  $x\bar{F}_2$ .

Both groups have given a parametrization of the curves :

$$x(\bar{q}x) \propto (1-x)^n \quad \text{with } n=6.7 \pm 0.5$$

CDHS

$$\text{with } n=4.9^{+2.4}_{-1.7}$$

BEBC

$$xq_v(x) \propto \sqrt{x}(1-x)^n \quad \text{with } n=3.5 \pm 0.5$$

CDHS

$$\propto (1-x)^n \text{ for } x > 0.3, \text{ with } n \approx 3$$

BEBC.

Simple counting rules predict  $n=l$  for antiquarks and  $n=3$  for valence quarks in good agreement with the data.

Figure 12 finally shows the relative fraction of antiquark momentum. It decreases rapidly with  $x$ . Qualitatively the same is shown in

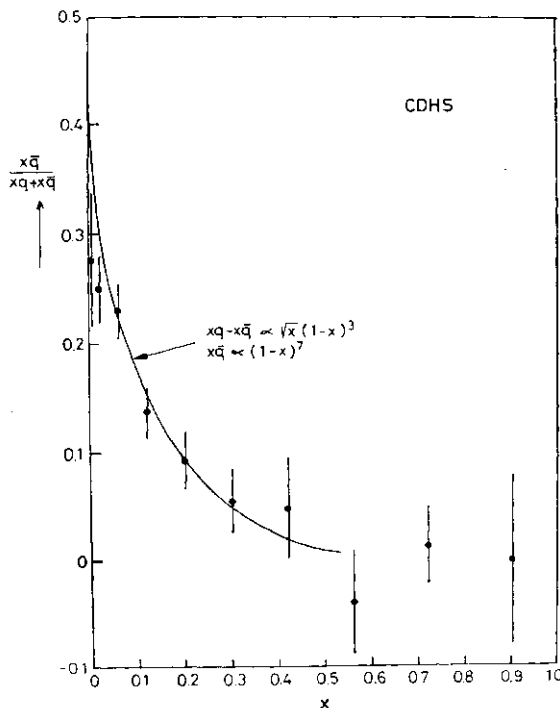


Fig. 12. Ratio of fractional momentum carried by antiquaries over fractional momentum of all partons as function of  $x$  [ref. 14].

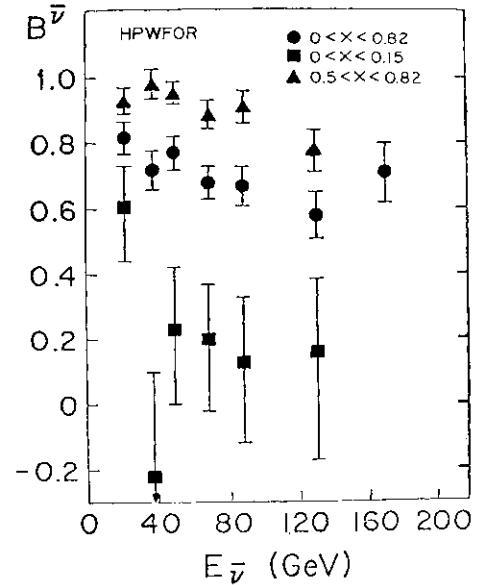


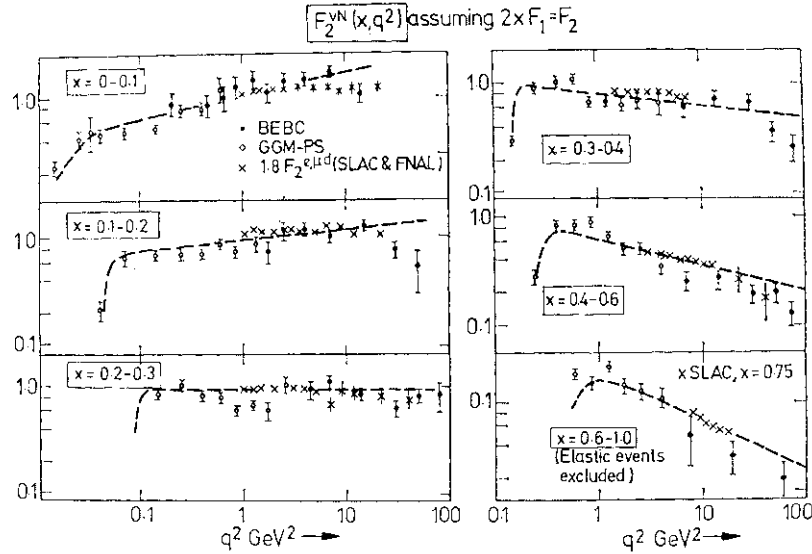
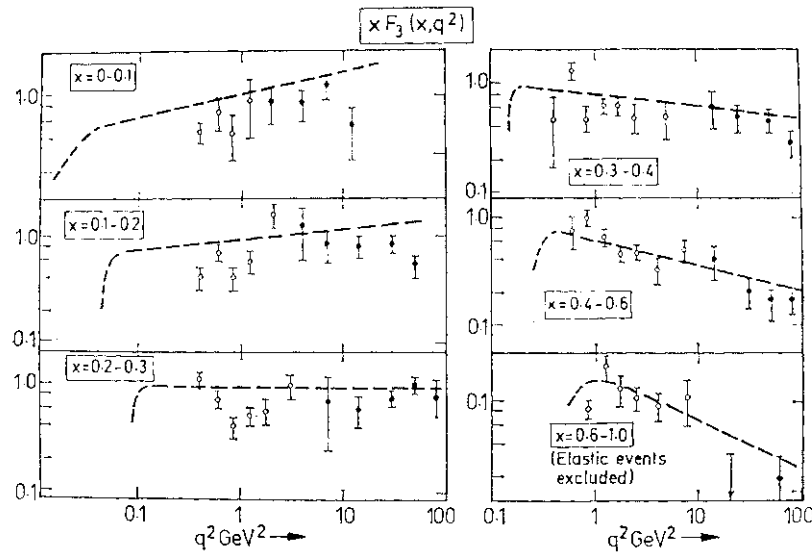
Fig. 13.  $2^2$ -value for antineutrinos in different  $x$ -ranges as function of energy [ref. 15].

Fig. 13 by the HPWFOR group,<sup>15</sup> where low  $5$ -values at small  $x$  indicate a high antiquark fraction.

#### 4. Scaling violations

##### i) $Q^2$ -dependence of structure functions

The results discussed so far have given very little evidence for scaling violations at least at higher energies. In electron<sup>17</sup> and muon<sup>21</sup> scattering experiments on the other side significant variations of the structure functions with  $Q^2$  have been observed. These deviations from scaling can not be explained to be entirely due to threshold and target mass effects. Asymptotically free gauge theories (AFGT) like the Quantum Chromo Dynamics (QCD) predict deviations from exact Bjorken scaling as consequence of the dynamics of the strong interaction. In 1977 results have been reported from BEBC<sup>22</sup> which give indication of scaling violations also in neutrino interactions. The structure functions  $F_2(x, Q^2)$  and  $xF_3(x, Q^2)$  as presented in Figs. 14 and 15 in different  $x$ -bins show a clear  $<2^2$ -dependence. The data are well described by an empirical fit<sup>23</sup> to the  $ed$ - and  $\bar{\nu}d$ -data of SLAC and FNAL. It should be noted however that the  $\bar{\nu}$ -dependence can be seen only by combining the high energy BEBC data with the low energy GGM data alone, indicated by full circles in the figures, show no significant scaling violation. QCD calculations however can be reliably performed only for large  $Q^2$  where large


 Fig. 14. Structure function  $F_2(x, Q^2)$  in different  $x$ -bins as function of  $Q^2$  [ref. 16].

 Fig. 15. Structure function  $xF_3(x, Q^2)$  in different  $x$ -bins as function of  $Q^2$  [ref. 16].

means a few  $\text{GeV}^2$ . The GGM data are at low  $Q^2$ , therefore not very useful to test QCD.

To this conference new data have been presented on this subject by a high statistics experiment, the CDHS-experiment.<sup>14</sup> The datasample of this group as well as that of BEBC/GGM is given in Table 3.

The structure function  $F_2(x, Q^2)$  as measured by the CDHS-collaboration is shown in Fig. 16 as function of  $Q^2$  in different  $x$ -bins. This data show definitely a significant  $g$ -dependence. The ed-data<sup>17</sup> which are predominantly at low  $Q^2$  are given as well. In the overlapping region they agree well with the CDHS-data, they furthermore follow the same trend in  $Q^2$ . One should however be cautious by comparing the two data samples since radiative corrections

 Table 3. Datasamples of the CERN  $e$  xperiments.

Group	$\nu$ -Events	$\bar{\nu}$ -Events	Energy range
GGM	3.000	2.000	2–12 GeV
BEBC	1.120	270	20–200 GeV
CDHS	23.000	6.200	30–200 GeV

have not been applied to the neutrino events. The structure function  $F_2$  increases with  $Q^2$  for  $x < 0.2$  and decreases for  $x > 0.2$ . This behaviour is predicted by QCD as indicated by the lines in Fig. 16 which represent a QCD-fit to the ed-data by Reya and Gluck<sup>24</sup>. The agreement is excellent. Another way to demonstrate the  $g^2$ -dependence of the structure functions is to plot  $F_2$  and  $x \cdot q$  as function of  $x$  for different values of  $Q^2$  or what is almost equivalent in different energy bins. The  $g^2$ -

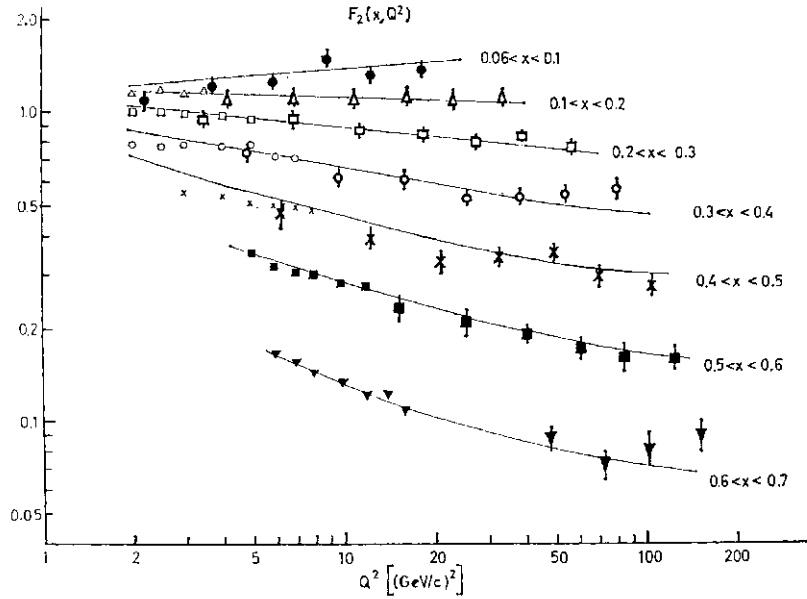


Fig. 16. Structure function  $F_2(x, Q^2)$  in different  $x$ -bins as function of  $Q^2$ . Heavy symbols: CDHS-data [ref. 14], light symbols: SLAC  $\nu$ -scattering [ref. 17], lines; QCD-calculations by Gluck and Reva [Ref. 241].

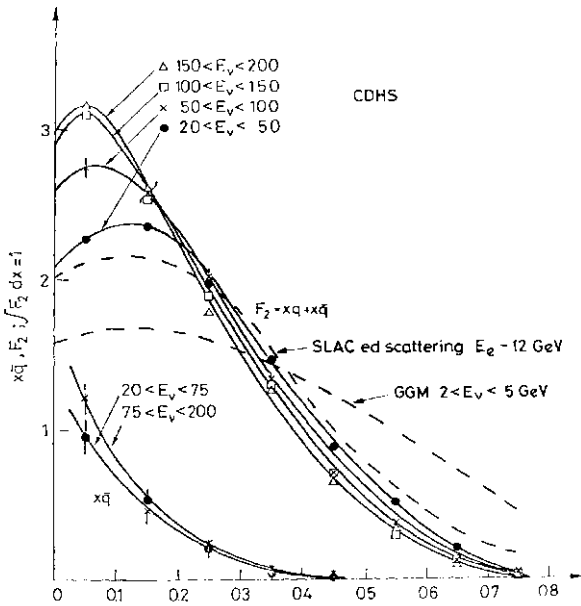


Fig. 17. Structure functions  $F_2(x)$  and  $xq(x)$  in different  $\nu E^\wedge$ -bins as function of  $x$ .

dependence observed in Fig. 16 is then translated into a shrinkage of the structure functions with increasing energy. Results are presented in this form by the CDHS-collaboration in Fig. 17. The SLAC- and GGM-results at lower energies are indicated as well. The shrinkage of  $F_2(x)$  is clearly visible, for  $xq(x)$  however less significant,

ii) Moments

In the preceding chapter a significant  $g^2$ -dependence of the structure function  $F_2(x, Q^2)$

has been demonstrated. To test QCD it is however more adequate to calculate the moments of the structure functions and to compare them to theory. QCD makes definite predictions for the moments whereas the structure functions themselves are not as directly calculable. The moments in the simplest form are defined as follows :

$$M_i(N, Q^2) = \int_0^1 x^{(N-1)} F_i(x, Q^2) dx \quad (7)$$

where  $F_i(x, Q^2)$  stands for  $F_2$  or  $xF_3$ .

In practice one has however to face a serious experimental difficulty: An experiment at least at presently attainable energies, covers only a limited domain in the  $Q^2$ - $x$ -plane as seen in Fig. 18. At high  $Q^2$  low  $x$  values can not be reached due to the limited neutrino

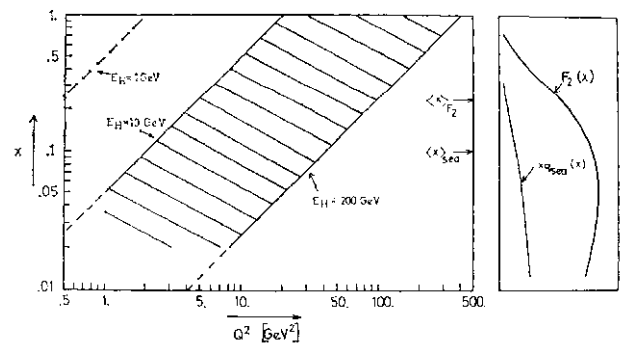


Fig. 18. Domain in  $g^2$ - $x$ -plane covered by high energy experiments (hatched area). On the right the structure functions are indicated.

energy and at low  $Q^2$  a natural limit is set to large  $x$ -values due to the finite hadron energy resolution which becomes large at small  $E_{\nu}$ , that means at large  $x$  for a given  $Q^2$ . The line with  $E_{\nu} = 0$  GeV in Fig. 18 corresponds to a 30% error on  $E_{\nu}$  as it is true for counter experiments. Bubble chamber experiments are slightly better. As a result there is no  $Q^2$ -value where the integral can be evaluated over the complete  $x$ -range.

The BEBC-collaboration is the first group presenting an analysis of neutrino data in the frame of AFGT.<sup>16</sup> They overcome the above mentioned problem by using low energy GGM-data in the low  $Q^2$ - $x$  corner. At high  $Q^2$  and low  $x$  extrapolations into the unseen region has to be made. This may lead to a significant uncertainty only for moments of low order. This analysis is performed for the Nachtmann-moments where instead of  $x$  the variable  $\xi$  is used which is given as:

$$\xi = \frac{2x}{1 + \sqrt{1 + 4M^2 x^2 / Q^2}}$$

This variable absorbs target mass corrections, and QCD effects should therefore manifest themselves more clearly. The moments are then written as:

$$\begin{aligned} M_2(N, Q^2) &= \int_0^1 -\xi \frac{N+1}{x^3} \cdot F_2(x, Q^2) \\ &\quad \times f(N, 4M^2 x^2 / Q^2) dx \\ M_3(N, Q^2) &= \int_0^1 -\xi \frac{N+1}{x^3} \cdot x F_3(x, Q^2) \\ &\quad \times \hat{f}(N, 4M^2 x^2 / Q^2) dx \end{aligned} \quad (8)$$

where  $f$  and  $\hat{f}$  are well defined functions of  $N$  and  $4M^2 x^2 / Q^2$ .  $M_2$  is defined for  $N$  even and  $M_3$  for  $N$  odd.

In Fig. 19 the Nachtmann moments of  $F_2$  and  $x F_3$  as evaluated by the BEBC-group are given as function of  $Q^2$ . All moments clearly decrease with  $Q^2$ . A QCD prediction with  $\Lambda = 0.75$  GeV describes well the data for  $x F_3$ , at least for  $Q^2 > 1$  GeV<sup>2</sup>.

A more direct and quantitative test of AFGT can be done by comparing the moments to explicit expressions given by theory. The moments of the valence quark distribution  $x F_3$  are independent of the gluon distribution and have therefore a simple  $g^2$ -dependence of the following form:

$$M_3(N, Q^2) = \text{const} \cdot (\ln Q^2 / \Lambda^2)^{-d^{NS}} \quad (9)$$

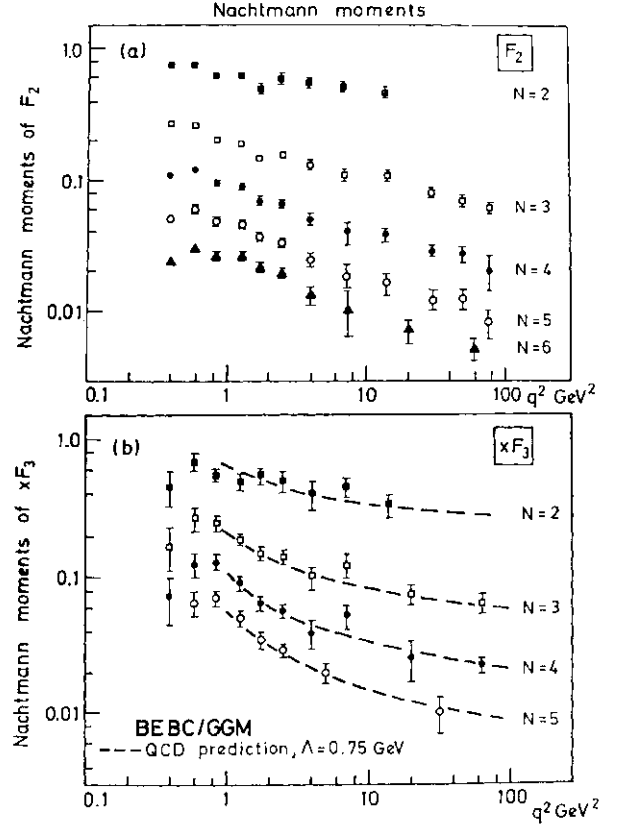


Fig. 19. Nachtmann-moments for  $F_2(x, Q^2)$  and  $x F_3(x, Q^2)$  [ref. 16].

The "anomalous dimension"  $d^{NS}$  is given by:

$$d^{NS} = \frac{4}{33 - 2m} \left( 1 - \frac{2}{N(N+1)} + 4 \sum_{j=2}^N \frac{1}{j} \right) \quad (10)$$

where  $m$  is the number of flavours. This formula assumes that  $Q^2$  is large compared with  $\Lambda^2$  and with any quark masses or transverse momenta. Data with  $Q^2 > 1$  are used in the analysis. This low cut might not always be adequate.

Relation (9) suggests that a simple power law should exist between different moments of  $x F_3$ . Figure 20 gives log-log plots of pairs of moments demonstrating this kind of relation. The lines represent the predictions of QCD. The slopes are given by the ratios of the anomalous dimensions. In Table 4 the observed slopes are compared to the ones predicted by QCD:

Table 4.  $x F_3$  moment ratios.

$N_1$	$N_2$	Observed slope	Predicted slope
6	4	$1.29 \pm 0.06$	1.290
5	3	$1.50 \pm 0.08$	1.456
7	3	$1.84 \pm 0.20$	1.760

Within the experimental errors the agreement

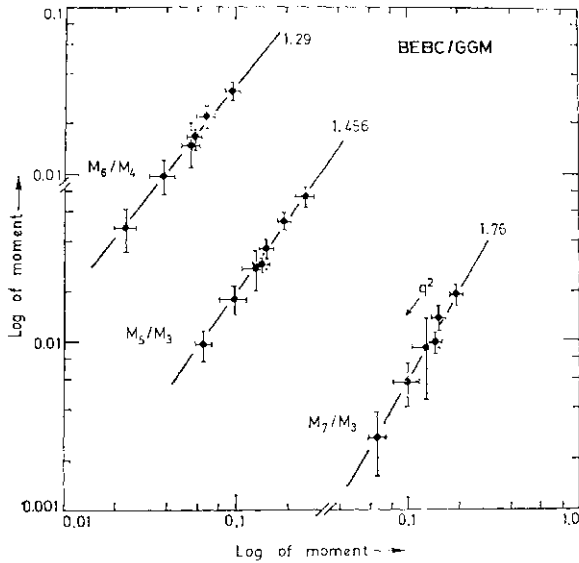


Fig. 20. Log-log plots of various moments of  $x F_3$ . The straight lines indicate the predicted slopes of the power law relations amongst the different moments [ref. 16].

is good. This result proves that the gluons emitted in the bremsstrahlung of quarks are vectorparticles as expected in QCD. No other field theory could reproduce these numbers. The test is independent of the numbers of flavours and colours and of the value of  $A$ .

Another obvious relation is given by

$$M_3^{-1/d^{NS}}(N, Q^2) = \text{const} \cdot (\ln Q^2 - \ln A^2) \quad (11)$$

to first order in  $a_s$ , the strong coupling constant. This equation can be used to determine the cut-off parameter  $A$ . The data are pre-

sented in Fig. 21. Lines using the anomalous dimensions as given by QCD are fitted to the data points for  $Q^2 > 1 \text{ GeV}^2$ . The values of  $A$  so obtained are all compatible with each other. In summary the following results have been obtained:

$$\text{for } Q^2 > 1 \text{ GeV}^2 \text{ and 1}^{\text{st}} \text{ order in } \alpha_s: \\ = 0.74 \pm 0.05$$

$$\text{including 2}^{\text{nd}} \text{ order in } \alpha_s: \\ = 0.45 \pm 0.05$$

$$\text{for } Q^2 > 2 \text{ GeV}^2 \text{ and 1}^{\text{st}} \text{ order in } \alpha_s: \\ = 0.83 \pm 0.10$$

The errors are statistical only.

A few remarks should be made here: It is evident that higher order corrections in  $a_s$  are large. Is it then appropriate to use points at  $Q^2$  values as low as 1-2  $\text{GeV}^2$ ? A higher cut in  $Q^2$  however would certainly diminish the significance of the result drastically. It is furthermore not clear what contribution will come from higher twist corrections. These corrections should be different for different  $N$ . No such effect is seen. They might therefore be small.

In concluding it seems certainly too early to take these results for  $A$  as a final answer. A firm result of the data presented in this chapter is however the definite observation of scaling violations in neutrino physics in particular as it is presented by the CDHS-collaboration at high  $Q^2$ . A very nice analysis of the moments

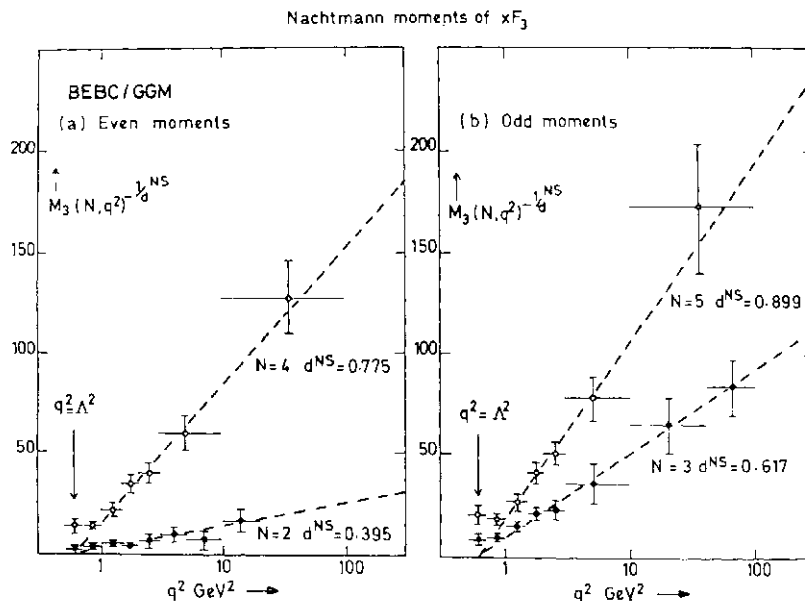


Fig. 21. Values of the moments  $x F_3$ , raised to the power  $|j|d^{NS}$  as function of  $\ln Q^2$ . The intercept with the x-axis gives  $\ln A^2$  with  $A = 0.75 \text{ GeV}$  [ref. 16].

of the structure functions has been presented by the BEBC-group. This analysis has provided a quantitative test of QCD-predictions.

**§11. Hadron Production by Charged Currents**

In bubble chamber exposures the hadron energy is not observed as global quantity as in counter experiments. The particles of the hadron shower are observed individually. The additional information obtained in this way gives the possibility to study not only the inclusive behaviour of the charged current as discussed before, but also the physics of the hadron fragmentation of the current jet and other hadronic properties of the interaction.

This field will however be summarized only very briefly since data at present are not yet very conclusive. It can be hoped that interesting result may come out in the near future.

*1. Inclusive hadron distributions*

Several groups at FNAL and CERN have presented data on inclusive hadron distributions on charged hadrons as well as on  $7r^{0+}$ s.<sup>25,26,27</sup> Results for the fragmentation functions  $D(z)$  have been given. All groups basically confirm earlier observations that the distributions are essentially independent of  $E$ ,  $Q^2$  and  $x$ . Great similarities with the hadron production in pion and electron scattering have been observed. No striking effects were found.

*2. QCD-effects*

Several effects are predicted by QCD to happen in the hadron jet. The average transverse momentum for example is expected to rise with  $Q^2$  and a azimuthal asymmetry in the plane perpendicular to the current direction should be observed. Gluon-jets furthermore should be emitted by the quark which was struck by the neutrino. Variables like sphericity and thrust would give a handle to investigate such processes.

BEBC-groups<sup>27,28</sup> have presented data on this subject, and first indications of an effect might be seen. This is certainly an interesting field, but more data and more work is needed to get meaningful results.

*3. Exclusive channels*

Production of  $\pi^+$ ,  $p$  and  $A_x$  has been studied by a BEBC-group.<sup>28</sup> The cross sec-

tions of these channels as well as those of other 3C-multibody final states have been found to be flat with neutrino energy in contrast to the rising total cross section. The investigation of these processes should lead to some better understanding of diffractive or coherent production of resonances in neutrino interactions.

**§11.1. Multilepton Production**

$juju^-$  events have been discovered by the HPWF-collaboration at FNAL in 1974. They have soon been explained as production of charmed particles with a subsequent semileptonic decay as for example :

This process however is not the subject of the present discussion. It will be treated in the talk of Prof. Baltay<sup>9</sup> at this Conference.

The observation of neutrino interactions with several leptons is of particular interest since these events represent an excellent signature for the production of new particles such as top or bottom quarks or heavy leptons. The observation of  $3/\Lambda^-$ -events soon after the discovery of the  $2/\Lambda^-$ -events has consequently lead to quite some excitement.

*1. Trimuon events*

Events containing  $3/\Lambda^-$ s have first been seen 1976 by the CITFR-group at FNAL, soon later also by HPWF and last year then by the CDHS-collaboration at CERN. These events were first considered as possible evidence for the production of heavy leptons in neutrino interactions. Now large data samples from two experiments, CDHS<sup>29,30</sup> at CERN and HPWFOR<sup>15</sup> at FNAL are existing as presented in Table 5 :

Table 5. Samples of  $3/\Lambda^-$ -events.

	$\mu^- \mu^- \mu^+$	$\mu^+ \mu^+ \mu^-$	
CDHS $\nu$ WBB	76	4	} $p_\mu > 4.5 \text{ GeV}$
$\bar{\nu}$ "	—	6	
HPWFOR	49*	2	$p_\mu > 2 \text{ GeV}$

\* 24 events where the charges of only two muons are known, are assigned as  $ii^- \rightarrow \sim \Lambda^-$ .

A detailed analysis of the origin of these events is now possible. This has first been done and published by the CDHS-collabora-



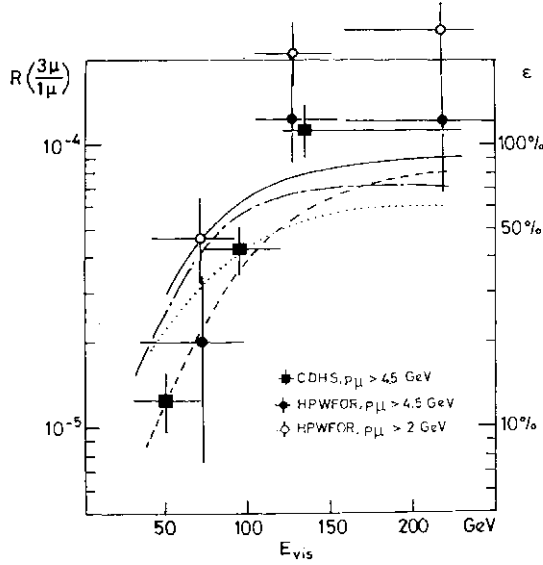


Fig. 22. Ratio of 3//-event rate over charged current rate as function of visible energy. The lines indicate the detection efficiencies for the different production mechanism:—, electromagnetic (EMP);---, hadronic (HMP);....., heavy leptons (HLC);-·-·-, heavy quarks (HQC). [refs. 15 and 30].

tion.<sup>30,31</sup> The HPWFOR-group presented a similar analysis at this conference. They essentially come to the same conclusions.

The most abundant background is expected to come from 2//-events where one of the hadrons in the hadron shower decays into a muon. Monte Carlo simulations of this process give for the CDHS-sample  $\sigma_{ju\sim ju\sim ju}$  and 6.6  $p^+p^+p^-$  events. So all  $p^+p^+p^-$  events are compatible with background and the genuine  $f_{i\sim}(T p^+$  rate can be given as function of energy in Fig. 22. The rates are normalized to the single-// rate. The rates  $\sigma(3ju)/\sigma(lju)$  are given for all energies and for  $1s > 120$  GeV in Table 6.

Table 6.  $JU f_{j\sim}/\sigma(p^-)$ .

	All E	E > 120 GeV
CDHS $\nu$	$(3.0 \pm 0.4) \cdot 10^{-5}$	$(11 \pm 2.5) \cdot 10^{-5}$
" $\nu$	$(2.4 \pm 1) \cdot 10^{-5}$	
HPWFOR	$(6 \pm 2) \cdot 10^{-5}$	$(12 \pm 5) \cdot 10^{-5}$

At higher energies about  $10^{-4}$  of all charged current events are of the type  $3fi$ . The lower rates at lower energies can be easily explained to be due to the drop of acceptance.

Several mechanism may be thought to be responsible for the production of 3/z-events. These possibilities are depicted in Fig. 23.

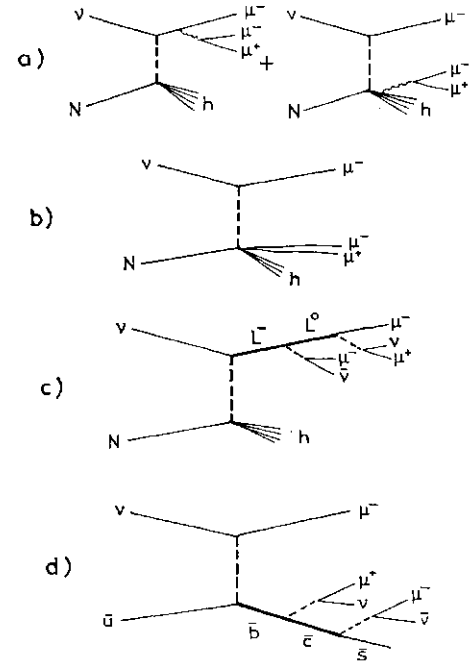


Fig. 23. Different processes leading to 3//-events. a) Electromagnetic mu-pair production (EMP) b) Hadronic mu-pair production (HMP) c) Heavy lepton cascade (HLC) d) Heavy quark cascade (HQC)

The first two are conventional processes whereas the two others invoke the production of new particles. Figure 23a represents electromagnetic mu-pair production (EMP) off the muon or off the quark and Figure 23b shows hadronic direct // -pair production (HMP) at the hadron vertex. In the heavy lepton cascade (Fig. 23c) (HLC) a  $L^-$  is produced which decays into a  $L^0$  and a muon. The  $L^0$  in turn decays into two muons. Figure 23d finally shows a heavy quark cascade (HQC) where a b-antiquark cascades down to a s-antiquark under emission of a  $ju^+$  and a  $f_{i\sim}$ . The third  $ju$  is produced at the lepton vertex.

The kinematical distributions will allow to discriminate between the above mentioned processes.

i) The invariant mass  $M_{23}$  of the two non-leading muons peaks at low masses as expected for the two conventional processes EMP and HMP (Fig. 24). The distributions of the invariant masses  $M_{12}$  and  $M_{13}$  of the leading muon with one of the nonleading muons however are much wider.

ii) Figure 25 gives the distribution of the transverse momentum  $p_{\perp}$  of the vector sum of the momenta of the nonleading muons with

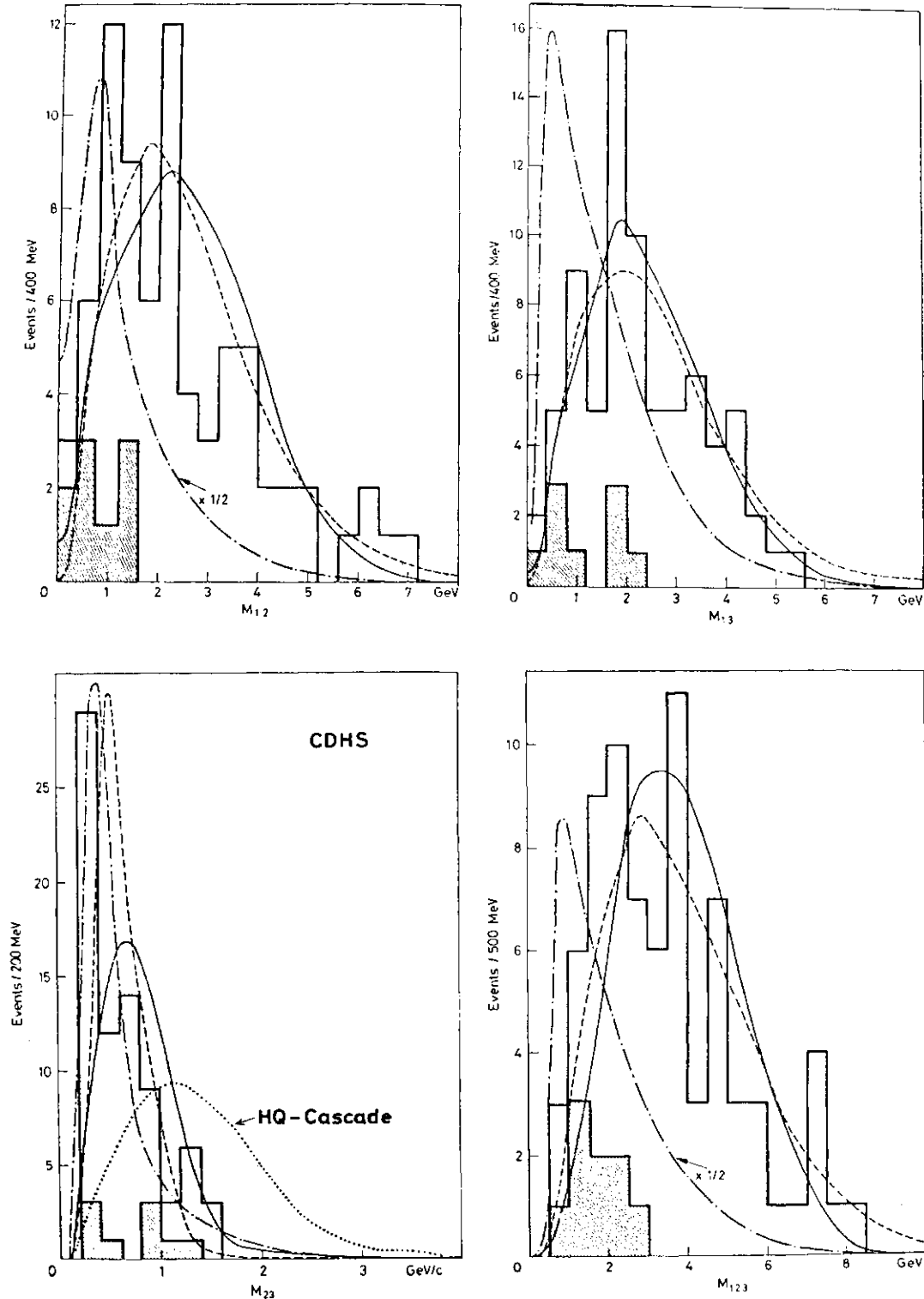


Fig. 24. Invariant mass distributions. Index 1 indicates the leading muon. The lines are model calculations (see caption of Fig. 23) [ref. 30].

respect to the axis of the hadronic shower. This distribution shows a limited  $p_z$  behaviour indicating that the two muons are hadron associated.

iii) In Figure 26 the angle between the vector sum of the two nonleading muons and the leading muon projected into the plane perpendicular to the neutrino direction is

shown. Most of the events are peaked back to back. Few are correlated at small angles.

All these distributions (and some others not presented here) can be well described by the processes EMP and HMP. The other two mechanism fail to explain the distributions. It is therefore concluded, that the  $3/j$ -events are primarily due to electromagnetic and

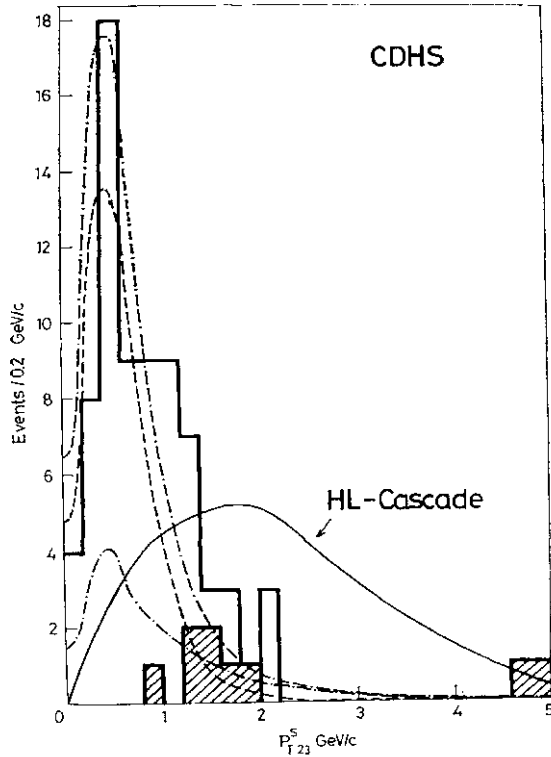


Fig. 25. Transverse momentum of the pair of non-leading muons with respect to the hadron shower. (For the lines see caption of Fig. 23) [ref. 31].

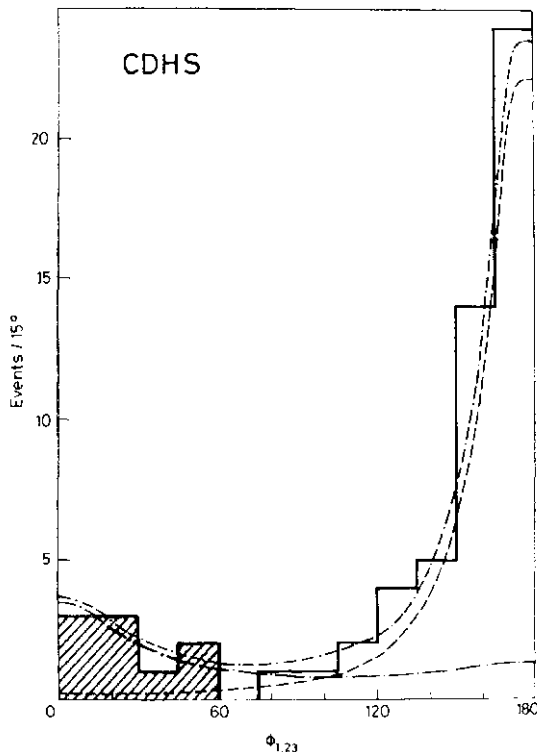


Fig. 26. Azimuthal angle between the leading muon and the nonleading pair. (For the lines see caption of Fig. 23.) [ref. 31].

hadronic  $\mu\mu$ -pair production. A fit to the  $01,23$ -distribution gives 25% contribution from EMP and 75% from HMP, consistent with a

Monte Carlo simulation of the two processes.

Limits can be given for HLC and HQC:

HLC: From the mass distributions on Fig. 24 values for the masses of  $L^\sim$  and  $L^\circ$  are extracted. They are chosen to  $m(L^\sim) \sim 9$  GeV and  $m(L^\circ) \sim 1.5$  GeV in order to minimize the disagreement with the distributions. It then follows from the  $\mu\mu$ -distribution of Fig. 25 that less than 17% of all  $3//$ -events could be due to a heavy lepton cascade (90% CL).

HQC: The  $M_{23}$ -massplot in Fig. 24 gives an upper limit for events having a heavy quark cascade as possible origin. With  $m(b) = 4.5$  GeV less than 10% of all  $3//$ -events are due to this process.

The two "superevents" of HPWF are still alive. These events have very energetic muons and are way outside of all distributions. Whether they represent tails in the distributions or a signature for new processes is still unresolved. The CDHS-sample also contains two unusual events with very high  $Q^2$  and the same argument applies here.

## 2. $ju\sim ju\sim$ -pairs

If heavy leptons or heavy quarks are produced in neutrino interactions they should be traced not only in  $3//$ -events, but also in two-lepton events. In this class of events they even should be almost ten times more abundant since the branching ratios for hadronic decays are much larger than those for semileptonic decays. Opposite sign dilepton events are not too well suited to search for new objects since the signal will be hidden under the much more copious charm decays. The  $///$ -events on the other hand may exhibit features indicative for new particles. Associated charm production where the charmed quark decays hadronically and the charmed anti-quark decays semileptonically—giving rise to a negative muon—will also contribute to this sample. The presently observed data sample is given in Table 7.

Table 7.  $\nu\bar{\nu} > \mu\mu$ -sample.

	$\mu^-\mu^-$ in $\nu$	calc. backgd.	$\mu^+\mu^+$ in $\bar{\nu}$	$p_{\mu}$ -cut
CDHS NBB <sup>82</sup>	47	$\sim 30$	9	4.5 GeV
CDHS WBB <sup>14</sup>	289	$\sim 200$	23	6.5 GeV
HPWFOR <sup>15</sup>	38	$\sim 18$	2	5.0 GeV

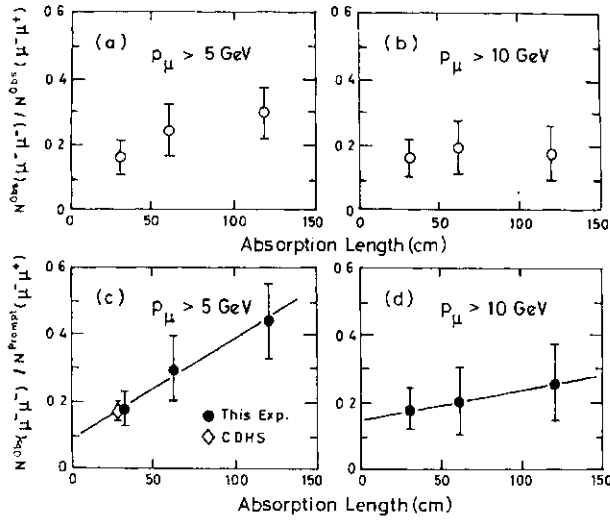


Fig. 27. Ratio of same sign dimuon events over opposite sign dimuon events as function of absorption length of the target (HPWFOR experiment) [ref. 15].

The main problem is the overwhelming background from ordinary charged current events where a *TZ* or *K* from the hadron shower decays into a negative muon plus anything. This background is calculated by Monte Carlo techniques. The uncertainty is estimated to be in the order of 25 %.

The HPWFOR-group has verified this calculation experimentally. They observe events in targets of different density. The decay probability for *7r*'s or *K*'s should be proportional to the absorption length of the target whereas the rate of the genuine signal should be independent of the density. Extrapolation from finite to infinite density should then lead to the prompt *yrfi*-rate. This is demonstrated in Fig. 27, where the rates  $N^{obs}(ju\sim/*\sim)/N^{prompt}$  are shown for muon momenta larger than 5 GeV/c and 10 GeV/c. The fitted slopes agree within the errors ( $\pm 40\%$ ) with the calculated slopes.

The results for  $R(ju\sim ju\sim)/R(pt\sim ju\sim)$  in neutrino interactions and for  $R(ju\sim JU+)/R(JU\sim ju\sim)$  in antineutrino interactions are quoted in Table 8.

Table 8. Prompt same sign dimuon rates.

	$R(\mu^-\mu^-)/R(\mu^-\mu^+)$	$R(\mu^+\mu^+)/R(\mu^+\mu^-)$	$p_{\mu^-}$ -cut
CDHS NBB	$(8 \pm 5)\%$	—	4.5 GeV/c
CDHS WBB	$< 7\%$ (66% CL)	$< 10\%$ (66% CL)	6.5 GeV/c
HPWFOR	$(12 \pm 5)\%$	no evidence	10 GeV/c

The results are not very conclusive. The

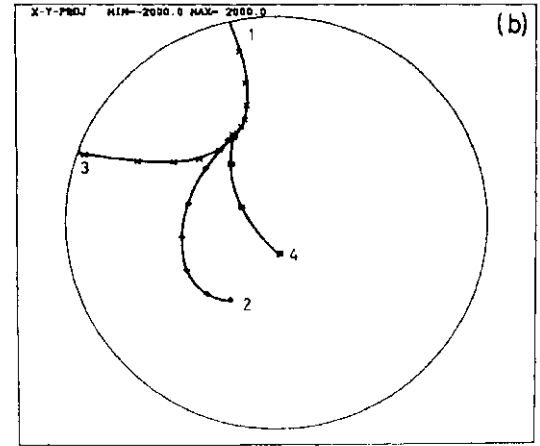
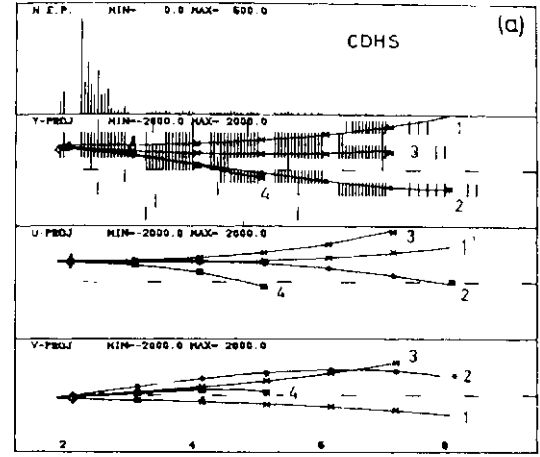


Fig. 28. 4-muon event of the CDHS collaboration at CERN-SPS [ref. 33].

question is even left open whether a prompt signal exists or not. Kinematical distributions are not significant. They mainly reflect the background. No evidence is found for unusual effect.

### 3. Four-lepton events

In December 1977 an event with four muons in the final state has been observed. The event was recorded in an exposure of the CDHS-detector to a wide-band neutrino beam at CERN.<sup>33</sup> Soon later two more events of this kind were reported: one by the HPWFOR-group<sup>16</sup> and one by the BFHSW-collaboration<sup>34</sup> in a bubble chamber exposure. The latter one contains *l**ju*, *Se\**, *IK*<sup>o</sup>, and *7fs*. The events are pictured in Figs. 28-30. Some of their characteristics are quoted in Table 9 and the corresponding rates in Table 10.

The ratio of neutrinos to antineutrinos in the beam of the BFHSW-experiment was 1:0.3. The rates are therefore quoted for

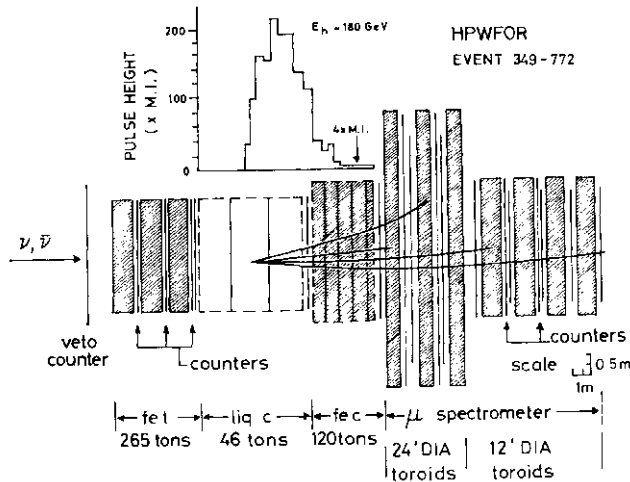


Fig. 29. 4-muon event of the HPWFOR collaboration at FNAL [ref. 15].

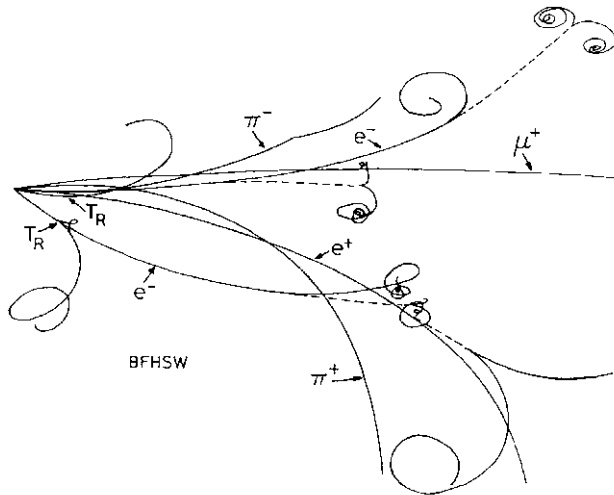


Fig. 30. 4-lepton event of the BFHSW collaboration at FNAL [ref. 34].

Table 9. 4-Lepton characteristics.

Event	Momenta [GeV/c]	$E_H$ [GeV]	$E_{vis}$ [GeV]
CDHS $\mu^- \mu^+ \mu^- \mu^+$	9/11/4.5/9	58	91
HPWFOR $\mu^- \mu^+ \mu^+ \mu^\pm$	44/60/4/3	178	289
BFHSW $\mu^+ e^- e^+ e^-$	22/2.3/2.0/0.9	5	32

Table 10. 4-Lepton rates.

	$R(4\mu)/R(3\mu)$	$R(4\mu)/R(2\mu)$	$R(4\mu)/R(1\mu)$
CDHS	$1.3 \cdot 10^{-2}$	$1.4 \cdot 10^{-4}$	$3 \cdot 10^{-7}$
HPWFOR	$2 \cdot 10^{-2}$	$2 \cdot 10^{-4}$	$7 \cdot 10^{-6}$
BFHSW			$16 \cdot 10^{-4}$ for $\bar{\nu}$ (or $2 \cdot 10^{-4}$ for $\nu$ )

both cases. It is however unlikely that the event originates from a neutrino interaction since the leading lepton is a muon with positive charge.

No convincing explanation has been found so far for these events. In the case of the counter experiments the most likely process might be a  $ju\bar{j}u$ -event (charm production), accompanied with a hadronic or radiative  $//$ -pair. In the CDHS-experiment, 0.2 events of this kind are expected. The bubble chamber event however resists all attempts of understanding. All processes, the authors have thought of, are on the level of  $10^{-7}$  or less. On the basis of so few events it will be difficult in any case to find the origin for the production of four leptons.

### Summary and Conclusions

Within the last year neutrino physics has achieved a remarkable progress. A big step forward has been made in understanding many of the open questions. Large data samples have been collected by the experimenters so that quantitative measurements of high accuracy and detailed comparisons to theory are now possible. All the experiments show a coherent picture, discrepancies are not visible.

The situation as exposed in this talk can be summarized in the following way:

i) Integral quantities like slope of the total cross section  $a_{tot}$ , the slope of average  $Q^2$ , ( $Q^2 y/E$ , or many others exhibit a significant energy dependence only for neutrino energies less or about 50 GeV. At higher energies only small variation with energy can be seen as it is expected from Quantum Chromo Dynamics. The concept of scaling can still be used, within a 10% limit, to study many features of neutrino interactions. Apart from a gap at intermediate energies data are now needed at higher energies, beyond 200 GeV, to eventually discover new thresholds or propagator effects due to the  $W_\pm$ .

ii) Scaling violation has definitely been demonstrated in particular now also at high  $g^2$ -values. The observed shrinkage of the structure function  $F_2(x, Q^2)$  can well be described by QCD. The analysis of the moments of the structure functions has provided a clean direct test of Asymptotically Free Gauge Theories. Quantitative agreement has been found. First attempts to extract a value for the cut-off parameter have been made. Now, more data with improved

accuracy and in particular at higher  $Q^2$  are needed. More refined analysis are necessary to test the predictions of QCD in detail. A precise value of  $A$  is needed, and the gluon distribution is almost completely unknown. These are some of the questions in this field waiting for a solution.

iii) Inclusive hadron production in neutrino interaction show at the first glance the same features as in hadron or electron scattering. But indications of QCD-effects have been observed. The near future might bring interesting results in this field.

iv) The origin of  $3//$ -events is now understood. These events are ordinary charged current events accompanied with a radiative or hadronic  $//$ -pair. Very little room is left for unconventional sources like production of heavy quarks or leptons. There is no evidence for such events at a level of the order of  $10^{-5}$  compared to the single- $//$  rate. And finally three four-lepton events have been observed. But so far no explanation could be found.

#### References

1. J. Steinberger: High-energy neutrino experiments, Proc. 1976 CERN School of Physics (report CERN 76-20, Geneva, 1976), p. 57.
2. D. H. Perkins: Inelastic lepton-nucleon scattering, Rep. Prog. Phys. **40** (1977) 409.
3. B.C. Barish: CalTech preprint CALT 68-621 (1977), to be published in Phys. Rep.
4. F. Dydak: High-energy neutrino experiments, Proc. 17th Internationale Universitätswochen für Kernphysik, Schladming, Austria, 1978.
5. C. Baltay: Neutrino reactions II, Plenary talk presented at this Conference.
6. C.H. Llewellyn Smith: Phys. Rep. **3C** (1972) 261.
7. O. Nachtmann: Weak interactions, Chapter VI, page 223, IN2P3 (1977).
8. T. Eichten *et al.*: Phys. Letters **46B** (1973) 281.
9. P.C. Bosetti *et al.*: Phys. Letters **70B** (1977) 273.
10. B. C. Barish *et al.*: Phys. Rev. Letters **39** (1977) 741, and paper submitted to this Conference.
11. A. J. Buras and K. J. F. Gaemers: Nucl. Phys. **B132** (1978) 249.
12. A. E. Asratyan *et al.*: Paper submitted to this Conference.
13. D. S. Baranov *et al.*: Measurement of the  $\nu$  N total cross section. . . , Paper submitted to this Conference.
14. D. Schlatter: Results of the CERN-Dortmund-Heidelberg-Saclay-Collaboration, Talk presented at this Conference.
15. A. K. Mann: Talk presented at this Conference.
16. P. C. Bosetti *et al.*: Oxford preprint 16/78, Oxford (1978) and submitted to Nucl. Phys. **B**; and J. H. Mulvey, Talk presented to this Conference.
17. E. M. Riordan *et al.*: SLAC-preprint, SLAC-PUB-1634 (1975).
18. H. Deden *et al.*: Nucl. Phys. **B85** (1975) 269.
19. R. E. Taylor: Talk presented at this Conference.
20. B. A. Gordon *et al.*: Phys. Rev. Letters **41** (1978) 615.
21. D.J. Fox *et al.*: Phys. Rev. Letters **33** (1974) 1504; Y. Watanabe *et al.*: Phys. Rev. Letters **35** (1975) 898; H. L. Anderson *et al.*: Phys. Rev. Letters **37** (1976) 4 and **38** (1977) 1450.
22. K. Schultze: Proc. Symposium on high energy lepton and photon interactions, Hamburg (1977).
23. D. H. Perkins *et al.*: Phys. Letters **67B** (1977) 347.
24. M. Gluck and E. Reya: Phys. Rev. **D16** (1977) 3242.
25. Argonne-Carnegie-Purdue-collaboration: paper submitted to this Conference.
26. FNAL-IHEP-ITEP-Michigan-collaboration: paper submitted to this Conference.
27. Aachen-Bonn-CERN-London-Oxford-Saclay-collaboration: Oxford-preprint 58/78 (1978).
28. R. O. Morrison: talk presented to this Conference.
29. M. Holder *et al.*: Phys. Letters **70B** (1977) 393.
30. T. Hansl *et al.*: Nucl. Phys. **B233** (1978) 381.
31. T. Hansl *et al.*: Phys. Letters **77B** (1978) 114.
32. M. Holder *et al.*: Phys. Letters **70B** (1977) 396.
33. M. Holder *et al.*: Phys. Letters **73B** (1978) 105.
34. R. J. Loveless *et al.* (Berkeley-FNAL-Hawaii-Seattle-Wisconsin-collaboration): C00-088-29, (1978).

P 7b

## Neutrino Interactions II: Neutral Current Interactions and Charm Production

C. BALTAY

*Columbia University, New York, NY. 10027*

### §1. Introduction

In the usual current-current theory of the weak and electromagnetic interactions, the interactions can be classified as:

a. The electromagnetic current, such as  $(e^-, e^+)$ ,  $(\nu, \bar{\nu})$ ,  $(p, \bar{p})$ ,  $(n, \bar{n})$ , etc., which is responsible for the electromagnetic interactions. The properties of this current are that it is charge conserving ( $dQ=0$ ), has a pure vector spatial structure ( $V$ ), and has isospin  $I=0$  and 1 parts.

b. The weak charged current, such as  $(e^-, \nu_e)$ ,  $(\mu^-, \nu_\mu)$ ,  $(\tau^-, \nu_\tau)$ ,  $(u, d)$ ,  $(c, s)$ , etc., which is responsible for the weak decay processes and the first neutrino interactions that were observed. This current is charge changing ( $J_Q=1$ ), has a V-A structure, and is isospin  $I=1/2$ .

c. The weak neutral currents, such as  $(e^-, e^+)$ ,  $(\nu, \bar{\nu})$ ,  $(p, \bar{p})$ , etc. This is a charge conserving ( $J_Q=0$ ) or "neutral" current. Its spatial ( $V, A, S, P, T$ ) and isospin ( $I=0, 1$ ) structure is the subject of a large portion of this talk.

Until 1971-72, the weak neutral currents were widely believed to be absent in nature, in part due to the low experimental limits on various processes such as  $K^+ \rightarrow \pi^+ e^+ e^-$  or  $K^0 \rightarrow \pi^0 e^+ e^-$ , or  $\nu p \rightarrow \nu p$ . However, in 1973-74 weak neutral currents were discovered experimentally in elastic neutrino interactions<sup>1</sup> and in single pion production processes by neutrinos.<sup>2</sup> In the past four years, a great deal of data on neutral currents has been accumulated, so that for the first time at this Conference, we can say that the main features of the neutral current interactions are understood.

The discovery of neutral currents was strongly motivated by the Weinberg-Salam model<sup>3</sup> (W-S), and this model together with the Glashow-Iliopoulos-Maiani<sup>4</sup> (G-I-M) charm scheme gives an adequate description of all of the experimental data. In §1. A of the talk,

the survey of the experimental situation, the experimental results will be compared with the prediction of the W-S model. In §1. B, the determination of the neutral current couplings, a "model independent" analysis will be followed, not assuming any specific model but using the experimental data to determine the relevant neutral current couplings. As we will see, the couplings obtained are just those of the W-S model.

In order to be able to discuss the predictions of the W-S model meaningfully, and introduce the terminology, we give here a very brief outline of some features of the model. The model introduces, among other things, four intermediate vector bosons:

Isotriplet	W	W <sup>0</sup>	W <sup>-</sup>
Isosinglet		B <sup>0</sup>	

The neutral members of these bosons mix to give the physical Z<sup>0</sup> and the  $\gamma$ :

$$\begin{aligned} Z^0 &= \cos \theta W^0 + \sin \theta B^0 \\ \gamma &= -\sin \theta W^0 + \cos \theta B^0, \end{aligned}$$

where  $\theta$  is a mixing angle (the Weinberg angle) to be determined by experiments. The W<sup>±</sup> mediate the usual charged current weak interactions, the Z<sup>0</sup> mediates the neutral current weak interactions, and the  $\gamma$  mediates the electromagnetic interactions.

The mixing angle can be expressed in terms of the coupling constants of the intermediate vector bosons to leptons:

$g$  — coupling constant of isotriplet to leptons,  
 $g'$  — coupling constant of isosinglet to leptons.  
 In terms of these coupling constants,

$$\sin \theta = \frac{g'}{\sqrt{g^2 + g'^2}}; \quad \cos \theta = \frac{g}{\sqrt{g^2 + g'^2}}.$$

The electromagnetic coupling constant is

$$e = \frac{gg'}{\sqrt{g^2 + g'^2}},$$

and the ratio of the electromagnetic to the weak coupling constants is

$$e^2/g^2 = \sin^2 \theta$$

The Fermi coupling constant  $G$  can be ex-

pressed in terms of the above coupling constants and the intermediate boson mass,  $M_w$ , as

$$G = \frac{\sqrt{2} g^2}{8M_w^2}$$

or

$$M_w^2 = \frac{\sqrt{2} g^2}{8G} = \frac{\sqrt{2} e^2}{8G \sin^2 \theta}$$

and similarly for the  $Z^0$ :

$$M_{Z^0}^2 = \frac{\sqrt{2}(g^2 + g'^2)}{8G} = \frac{M_w^2}{\cos^2 \theta}$$

Thus the masses of the intermediate bosons are given in terms of the known constants  $e$  and  $G$  and the single free parameter of the model,  $\sin^2 \theta$ . For values of  $\sin^2 \theta$  near 1/4, the masses are predicted to be

$$M_{W^\pm} \sim 75 \text{ GeV}$$

$$M_{Z^0} \sim 90 \text{ GeV}$$

This model predicted the existence of weak neutral currents. However, experimentally strangeness changing neutral currents were known to be absent in K decays. This motivated the G-I-M mechanism, in which a new hadronic quantum number, charm, was introduced to cancel out the strangeness changing neutral currents, while allowing strangeness conserving neutral currents. In quark language, this implies the introduction of a fourth quark to the still undiscovered triplet of quarks, as follows

Quark	Charge	Strangeness	Charm
u	+2/3	0	0
d	-1/3	0	0
s	-1/3	-1	0
c	+2/3	0	1

In order for this cancellation to work, the couplings between the quarks in terms of the Cabibbo angle must be

$$\begin{aligned} u \rightarrow +\cos \theta_c (d + \Lambda^+) + \sin \theta_c (s + W^+) \\ c \rightarrow +\sin \theta_c (d + W^+) + \cos \theta_c (s + W^+) \end{aligned}$$

The G-I-M charm scheme also predicted the existence of a new family of charmed hadrons. This seemed to be a problem until just recently when charmed particles were indeed found experimentally. Note that the above coupling scheme implies that charmed particles will decay predominantly into strange particles.

In the W-S model, the cross sections and

other properties of the weak neutral current processes are determined in terms of the single free parameter,  $\sin^2 \theta$ . For example, in the purely leptonic neutrino-electron scattering processes

$$\nu + e^- \rightarrow \nu + e^-,$$

the differential cross section is given by

$$\frac{d\sigma}{dy} = \frac{G^2 m_e E_\nu}{2\pi} [(g_V + g_A)^2 + (g_V - g_A)^2 (1-y)^2],$$

where  $y = E/E_0$ , the ratio of the energy of the final state electron to the incident neutrino energy. The constants  $g_V$  and  $g_A$  are, for the four processes:

Process	V-A Theory		Weinberg-Salam	
	$g_V$	$g_A$	$g_V$	$g_A$
$\nu_e + e^- \rightarrow \nu_e + e^-$	1	+1	$1/2 + 2\sin^2 \theta$	+1/2
$\bar{\nu}_e + e^- \rightarrow \bar{\nu}_e + e^-$	1	-1	$1/2 + 2\sin^2 \theta$	-1/2
$\nu_\mu + e^- \rightarrow \nu_\mu + e^-$	0	0	$-1/2 + 2\sin^2 \theta$	-1/2
$\bar{\nu}_\mu + e^- \rightarrow \bar{\nu}_\mu + e^-$	0	0	$-1/2 + 2\sin^2 \theta$	+1/2

Thus the purely leptonic processes are completely determined in terms of the single parameter,  $\sin^2 \theta$  and a theoretically unambiguous interpretation of the experiments is possible. For processes involving hadrons, however, uncertainties of varying degrees creep in due to hadronic form factors and other poorly understood features of hadronic interactions.

### §11. Neutral Current Interactions

#### A. Summary of the experimental situation

Table I summarizes briefly the neutral current processes that have been experimentally studied with some comment on the difficulty of the theoretical interpretation. Unfortunately the theoretically cleanest processes are the most difficult to study experimentally because of their very low cross sections.

We now proceed to a discussion of the experimental status of the processes listed in Table I.

#### 1. Purely leptonic processes

i. The process,  $\nu_e + e^- \rightarrow \nu_e + e^-$ , has been detected by Reines *et al.*<sup>5</sup> in an experiment at the Savannah River Fission Reactor using  $\nu_e$  with energies between 1 and 8 MeV. They obtained a result of

$$\sigma(\nu_e + e^- \rightarrow \nu_e + e^-) = (0.06 \pm 0.22) \times a_{\nu_e}$$

where  $G_{\nu_e} \sim A$  is the cross section predicted for this process by the V-A theory,  $0.54 \times 10^{-44}$



Table I. Experimentally studied N. C. processes.

Process	Comparison with theory
1. Purely leptonic $\nu_\mu + e^- \rightarrow \nu_\mu + e^-$ $\bar{\nu}_\mu + e^- \rightarrow \bar{\nu}_\mu + e^-$ $\bar{\nu}_e + e^- \rightarrow \bar{\nu}_e + e^-$	Very clean (No hadrons involved)
2. Elastic scattering $\nu_\mu + p \rightarrow \nu_\mu + \pi$ $\bar{\nu}_\mu + p \rightarrow \bar{\nu}_\mu + \pi$	Relatively straightforward. Some uncertainty due to proton form factors ( $M_A$ ).
3. Single pion production $\nu_\mu + N \rightarrow \nu_\mu + N' + \pi$ $\bar{\nu}_\mu + N \rightarrow \bar{\nu}_\mu + N' + \pi$	Model dependent due to hadronic vertex. Also nuclear physics corr.
4. Inclusive $\nu_\mu + N \rightarrow \nu_\mu + \dots$ $\bar{\nu}_\mu + N \rightarrow \bar{\nu}_\mu + \dots$	Quark-parton model Dependent.
5. Atomic physics $e^- + Bi \rightarrow e^- + Bi$	Large uncertainties due to atomic physics calculations.
6. Electron scattering $\bar{e}^- + d \rightarrow \bar{e}^- + \dots$	Quark-parton model dependent.

$E_e$  cm<sup>2</sup>/GeV. This process can proceed by either the standard charged current V-A interaction or by neutral currents. The theoretically predicted cross section for both the V-A interactions and the W-S model of the weak neutral currents, with the experimental detection efficiency folded in, is shown on Fig. 1 as a function of sin<sup>2</sup> θ. The experimental

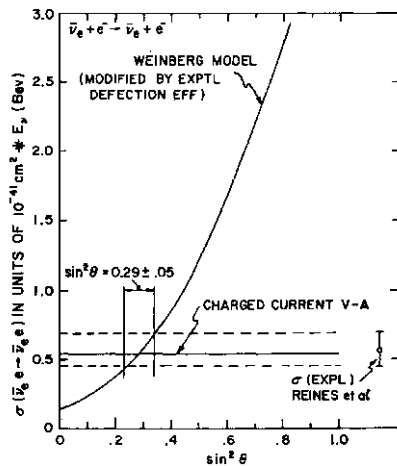


Fig. 1. Comparison of the experimental result on  $\langle j(\nu_e + e^- \rightarrow \nu_e + e^-) \rangle$  with the prediction of the W-S model.

result is in agreement with either the V-A theory or with the W-S model with

$$\sin^2 \theta = 0.29 \pm 0.05.$$

At this value of sin<sup>2</sup> θ, the total cross section for this process is very similar for the V-A theory and the Weinberg-Salam model. However the distribution in the electron

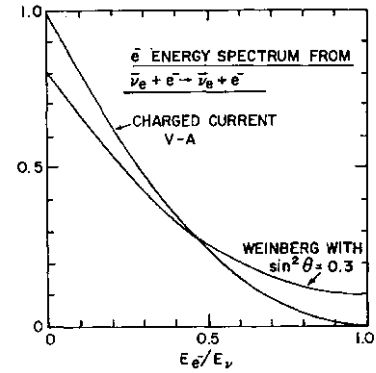


Fig. 2. Distribution in  $E_{e^-}/E_e$  for the process  $\nu_e + e^- \rightarrow \nu_e + e^-$  in the charged current V-A theory and the W-S model.

energy  $E_{e^-}$  is not the same in the two models, as shown in Fig. 2. The cross section for the W-S model is smaller than the V-A theory below  $E_{e^-}/E_e \sim 0.5$  and larger above.

The experimental cross sections when divided into low and high  $E_{e^-}$  regions are  
 $\sigma_{\text{expt}} = (0.85 \pm 0.25) \times 10^{-41} \text{ cm}^2$ ,  $1.5 < E_{e^-} < 3.0 \text{ MeV}$   
 $\sigma_{\text{pt}} = (1.70 \pm 0.44) \times 10^{-41} \text{ cm}^2$ ,  $3.0 < E_{e^-} < 4.5 \text{ MeV}$ .  
 This favors the W-S model, but the statistical significance is not conclusive.

ii. The experimental results on the process  $\bar{\nu}_e + e^- \rightarrow \bar{\nu}_e + e^-$  are summarized in Table II. In the low energy Gargamelle experiment<sup>6</sup> at the CERN PS, one candidate for this reaction was observed with a background of  $0.3 \pm 0.1$  events. The signal was not considered significant and an upper limit for the cross section was quoted. In the low energy Aachen-Padova spark chamber experiment<sup>7</sup> at the CERN PS, 32 events were seen with a rather large background estimated to be 21 events. The high energy Gargamelle experiment<sup>7</sup> at the CERN SPS published<sup>8</sup> a result for the cross section that was about five times larger than the prediction of the W-S model,

$$(7.3 \pm 1.0) \times 10^{-42} \text{ cm}^2 < \sigma < (8.2 \pm 1.0) \times 10^{-42} \text{ cm}^2,$$

based on 10 observed events in a sample of 24,000 charged current interactions. Soon thereafter a Columbia-Brookhaven experiment at Fermilab using the 15 ft bubble chamber filled with heavy neon published\*\* a result of

$$\sigma(\bar{\nu}_e + e^- \rightarrow \bar{\nu}_e + e^-) = (1.8 \pm 0.8) \times 10^{-42} \text{ cm}^2$$

based on 11 events found in a sample of

Table II.  $\nu + e \rightarrow \nu + e$

Experiment	Total sample of $\nu_\mu + N \rightarrow \mu^- + \dots$	Events observed	Background	Cross section $10^{-42} E_\nu \text{ cm}^2$
Gargamelle <sup>6</sup> CERN PS		— 1	$0.3 \pm 0.1$	—3
Aachen-Padova <sup>7</sup> CERN PS spark Chamber		32	21	$1.1 \pm 0.6$
Gargamelle <sup>8</sup> CERN SPS	41,000	9	$0.4 \pm 0.4$	$3.7 + 2.0$ to $4.2 + 2.2$ $-1.3$ $-1.7$
Columbia-NNL <sup>9</sup> Fermilab 15 ft chamber	160,000	11	$0.7 \pm 0.7$	$1.8 \pm 0.8$
Average				$1.7 \pm 0.5$

106,000 charged current interactions, not confirming the Gargamelle result, and in good agreement with the Weinberg-Salam model. At this conference the Gargamelle group reported a more recent value for the cross section of

$$(3.7^{+2.0}_{-1.5}) \times 10^{-42} E_\nu \text{ cm}^2 \leq \sigma \leq (4.2^{+2.2}_{-1.7}) \times 10^{-42} E_\nu \text{ cm}^2,$$

based on a scan of 75% more film with a combined 9 events in 41,000 charged current interactions. The agreement between the experiments shown on Table II, while not excellent, is no longer all that bad. The average of all the experiments is

$$\sigma(\nu_\mu + e^- \rightarrow \nu_\mu + e^-) = (1.7 \pm 0.5) \times 10^{-42} E_\nu \text{ cm}^2$$

where the average is obtained by adding the numbers of events observed in the experiments and dividing by the sum of the effective denominators.

The signal for this reaction in the high energy bubble chamber experiments is very clean. Figure 3 shows the plot of  $\theta_{e^-}$ , the lab

angle of the recoil electron, vs  $E_{e^-}$ , its lab energy, for the 11 Columbia-BNL events. All of the events are consistent with the kinematics of the reaction,  $\nu + e^- \rightarrow \nu + e^-$ , shown by the curves on Fig. 3. A nice variable to show this is  $E d\theta^-$ ; the kinematic limit for this reaction is  $E d\theta^- < 2 m_e$ , where  $m_e$  is the mass of

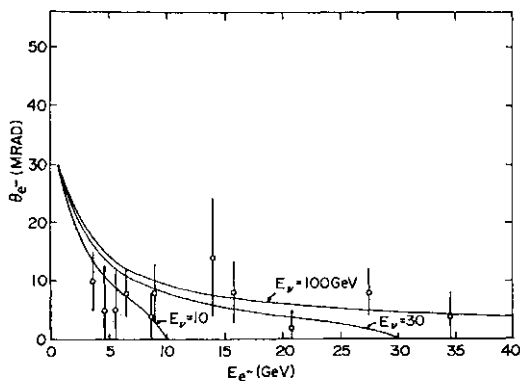


Fig. 3. Electron angle  $\theta_{e^-}$  vs electron energy  $E_{e^-}$  for the 11  $\nu\mu + Q \rightarrow \nu\mu + C$  events (from ref. 9).

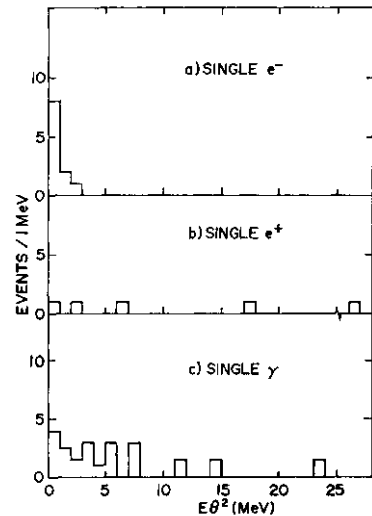


Fig. 4. Distribution in  $E d\theta^-$  for a) the single  $e^-$  events; b) the single  $e^+$  events and c) the single  $\gamma$  events (from ref. 9).

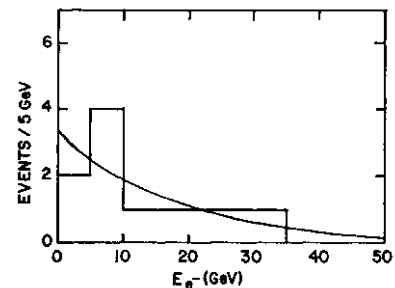


Fig. 5. Distribution in the electron energy  $E_{e^-}$  for the 11  $\nu + s \rightarrow \nu + G$  events (from ref. 9). The curve is the prediction of the W-S model for  $\sin^2 \theta = 1/4$ .

the target electron. Figure 4 shows the distribution in this variable. The single  $e^-$  events peak below 1 MeV with a small tail above 1 MeV consistent with the experimental resolution. The single  $e^+$  events, which are consistent with coming from the reaction  $\nu_e + p \rightarrow e^+ + n$ , and the single  $j$  events, are much more spread out in  $E_0$ , as expected. The distribution in the electron energy  $E_{e^-}$ , shown in Fig. 5, is consistent with the distribution predicted by the W-S model with  $\sin^2 \theta \sim 1/4$ , as shown by the curve on the figure.

The W-S model, with  $\sin^2 \theta = 0.23$ , predicts a cross section for this process of  $\langle \sigma \rangle = 1.5 \times 10^{-42} \text{ E}_\nu \text{ cm}^2$ . The average value of  $1.7 \pm 0.5$  for all of the experiments is in good agreement with this prediction. Conversely the average value can be used to obtain a mixing angle of  $\sin^2 \theta = 0.21 \pm 0.05$ .

There is also a solution at a large value of  $\sin^2 \theta$  as shown on Fig. 6a.

iii. The experimental results on the reaction  $\bar{\nu}_\mu + e^- \rightarrow \mu^+ + e^-$  are summarized in Table III. All five experiments find results which are consistent with the W-S model which predicts a cross section of  $\langle \sigma \rangle = 1.3 \times 10^{-42} \text{ E}_\nu \text{ cm}^2$  for this process for  $\sin^2 \theta = 0.23$ . The average of the two low energy experiments, where a signal is seen, is

$$\langle \sigma \rangle = (1.8 \pm 0.9) \times 10^{-42} \text{ E}_\nu \text{ cm}^2$$

This value corresponds to a mixing angle of

$$\sin^2 \theta = 0.3111$$

in the W-S model, as shown on Fig. 6b.

### 2. Elastic scattering on protons

The process,  $\bar{\nu}_\mu + p \rightarrow \mu^+ + p$ , has been observed in four experiments, and  $\bar{\nu}_\mu + p \rightarrow \mu^+ + n$  in one experiment, as listed in Table IV. The agreement between the experiments is good. The errors on the weighted averages shown on

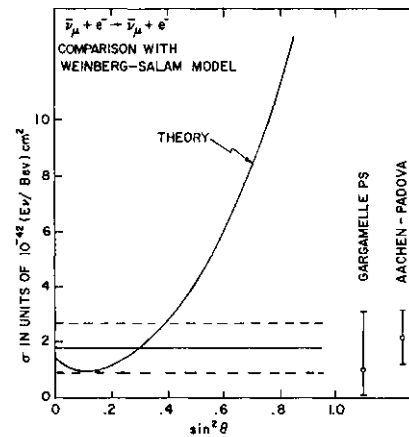
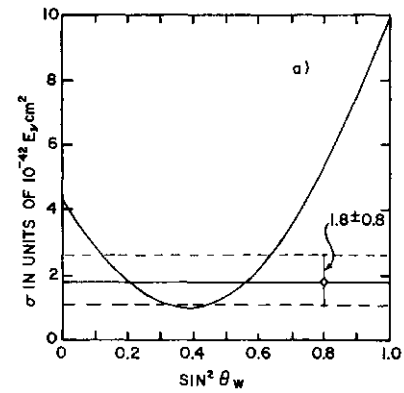


Fig. 6. Comparison of the experimental cross sections with the predictions of the W-S model for a) the reaction  $\bar{\nu}_\mu + e^- \rightarrow \mu^+ + e^-$ , and b) the reaction  $\bar{\nu}_\mu + p \rightarrow \mu^+ + p$ .

Table IV have increased by  $\sqrt{2}$  since the quoted errors in the experiments are statistical only. The agreement between the averaged ratios and the W-S model is good, as shown on Fig. 7. The best value of the mixing angle from the reaction is

$$\sin^2 \theta = 0.26 \pm 0.06$$

The  $q_\nu$  distribution for both the  $\bar{\nu}_\mu + p$  and  $\bar{\nu}_\mu + e^-$  scattering from the HPB experiment are shown in Fig. 8. Again the agreement with

Table III.  $\bar{\nu}_\mu + e^- \rightarrow \mu^+ + e^-$ .

Experiment	$\bar{\nu}_\mu + N \rightarrow \mu^+ + \dots$	Events observed	Background	Cross section $10^{-42} \text{ E}_\nu \text{ cm}^2$
Gargamelle <sup>10</sup>				+2.1
CERN PS		3	$0.4 \pm 0.1$	$1.0 - 0.9$
Aachen-Padova <sup>11</sup>				
CERN PS spark chamber		17	$7.4 \pm 1.0$	$2.2 \pm 1.0$
BEBC Wideband neon <sup>12</sup>				
CERN SPS	7,500	— 1	$0.4 \pm 0.2$	—3.5
Fermi-Mich-IHEP-ITEP <sup>13</sup>				
Fermilab 15 ft neon	6,300	0		—2.9
Gargamelle <sup>14</sup>				
CERN SPS	4,000	0		—3.3

Table IV. Elastic scattering on protons.

Experiment	$\nu_\mu + p \rightarrow \nu_\mu + p$			$\bar{\nu}_\mu + p \rightarrow \bar{\nu}_\mu + p$		
	Events observed	Back-ground	$\frac{\nu_\mu + p \rightarrow \nu_\mu + p}{\nu_\mu + n \rightarrow \mu^- + p}$	Events observed	Back-ground	$\frac{\nu_\mu + p \rightarrow \nu_\mu + p}{\bar{\nu}_\mu + p \rightarrow \mu^+ + n}$
Harvard-Penn-BNL <sup>15</sup> BNL counter detector	255	88	$0.11 \pm 0.02$	69	28	$0.19 \pm 0.05$
Columbia-III-Rock <sup>18</sup> BNL spark chamber	71	30	$0.20 \pm 0.06$			
Aachen-Padova <sup>17</sup> CERN PS S.C.	155	110	$0.10 \pm 0.03$			
Gargamelle <sup>18</sup> CERN PS	100	62	$0.12 \pm 0.06$			
Weighted average* <sup>†</sup>			$0.11 \pm 0.02$			$0.19 \pm 0.08$

\* Errors increased by  $\sqrt{2}$  since quoted errors statistical only.

† Caution—the experiments have slightly different  $Q^2$  cuts.

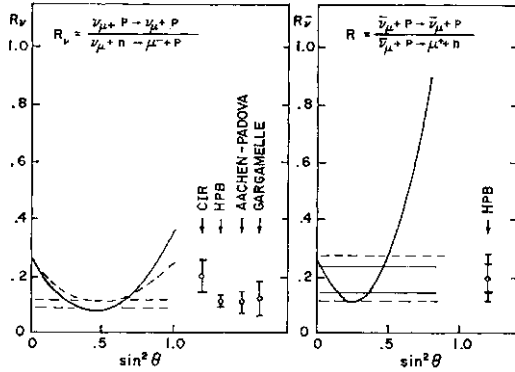


Fig. 7. Comparison of the experimental cross section ratios with the predictions of the W-S model for a) the reaction  $\nu_\mu + p \rightarrow \nu_\mu + p$  and b) the reaction  $\bar{\nu}_\mu + p \rightarrow \bar{\nu}_\mu + p$ .

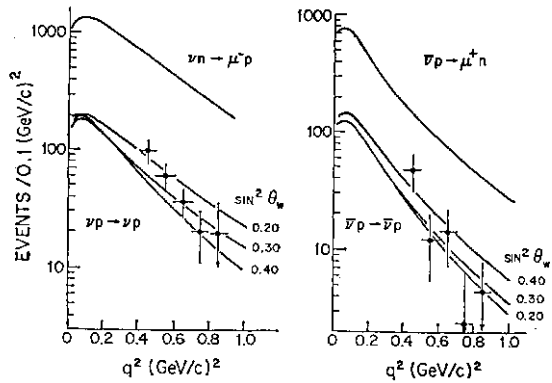


Fig. 8. Distribution in  $q^2$ , compared with the predictions of the W-S model for various values of  $\sin^2 \theta$ , for a)  $\nu_\mu + p \rightarrow \nu_\mu + p$  and b)  $\bar{\nu}_\mu + p \rightarrow \bar{\nu}_\mu + p$  (from ref. 15).

the predictions of the W-S model, shown by the curves on the figure, is good with values of  $\sin^2 \theta$  0-1/4.

### 3. Single pion production

The large amount of data that is available on the various neutral current single pion production processes is summarized in Table V. The predictions of the W-S model for these

reactions, listed in the last column on the table, are model dependent because of the form factors at the hadronic vertex. The model developed by Adler<sup>23</sup> is the basis for the numbers given in the table. The theoretical uncertainty on these is substantial, as indicated by the errors given on some of the numbers. There is an additional uncertainty on the ratios measured using complex nuclear targets due to the rescattering of the final state pion. In view of these uncertainties, the agreement between the experimental results and the model is satisfactory, as can be seen from a comparison of the last two columns on Table V.

The pion-nucleon mass distribution in the neutral current single pion production processes indicates that the  $J(1238)$ , the  $7=3/2$  pi-nucleon resonance is produced in these reactions. Figure 9 shows the  $p\pi^0$  and the  $p\pi^-$  mass distributions in the reactions  $J^+ + p \rightarrow \Lambda^+ + p + \pi^0$  and  $J^+ + n \rightarrow \Lambda^+ + p + \pi^-$ , respectively, in the Gargamelle propane experiment. This is significant because it shows in a model independent way that the neutral current is not pure isoscalar but has a sizeable isovector part to transform an  $7=1/2$  nucleon into an  $7=3/2$   $J(1238)$ . This conclusion is important in resolving the isoscalar-isovector ambiguity in the model independent analysis of the neutral current couplings.

### 4. Inclusive reactions

The neutral to charged current ratios for both  $\nu_\mu$  and  $\bar{\nu}_\mu$  induced inclusive reactions

$$R_\nu = \frac{\nu_\mu + X \rightarrow \nu_\mu + \dots}{\nu_\mu + X \rightarrow \mu^- + \dots}$$

$$R_{\bar{\nu}} = \frac{\bar{\nu}_\mu + X \rightarrow \bar{\nu}_\mu + \dots}{\bar{\nu}_\mu + X \rightarrow \mu^+ + \dots}$$

Table V. Single pion production.

Experiments	Ratio measured	Exptl. result	W-S $\sin^2 \theta \sim 1/4^{22}$
CIR <sup>18</sup> Aachen-Padova	$\{(\nu + X + \pi^0)\}/\{2(\mu^- + X + \pi^0)\}$	$0.21 \pm 0.07^*$	$0.24 \pm$
Gargamelle complex nuclei	$\{(\bar{\nu} + X + \pi^0)\}/\{2(\mu^+ + X + \pi^0)\}$	$0.46 \pm 0.10^*$	$0.30 \pm$
Argonne <sup>20</sup> 12 ft B.C. deuterium	$\{\nu + n + \pi^+\}/\{\mu^- + p + \pi^+\}$	$0.13 \pm 0.06$	$0.07 \pm$
	$\{\nu + p + \pi^0\}/\{\mu^- + p + \pi^+\}$	$0.40 \pm 0.22$	$0.17 \pm$
	$\{\nu + p + \pi^-\}/\{\mu^- + p + \pi^+\}$	$0.12 \pm 0.04$	$0.07 \pm$
Gargamelle <sup>21</sup> CERN PS propane	$\{(\nu p \pi^0) + (\nu n \pi^0)\}/\{2(\mu^- + p \pi^0)\}$	$0.45 \pm 0.08$	$0.42 \pm$
	$\{(\bar{\nu} p^0) + (\bar{\nu} n \pi^0)\}/\{2(\mu^+ + n \pi^0)\}$	$0.57 \pm 0.11$	$0.60 \pm$
	$\{\nu + p + \pi^0\}/\{\mu^- + p + \pi^0\}$	$0.56 \pm 0.10$	$0.42 \pm 0.13$
	$\{\nu + n + \pi^0\}/\{\mu^- + p + \pi^0\}$	$0.34 \pm 0.09$	$0.42 \pm 0.13$
	$\{\nu + p + \pi^0\}/\{\mu^- + p + \pi^0\}$	$0.45 \pm 0.13$	$0.28 \pm 0.08$
	$\{\nu + n + \pi^+\}/\{\mu^- + p + \pi^0\}$	$0.34 \pm 0.07$	$0.28 \pm 0.08$

\* Weighted average of three experiments. Agreement between experiments not very good. Errors calculated by  $\sqrt{\sum x^2/n} - 1$ . Average may not be valid!!

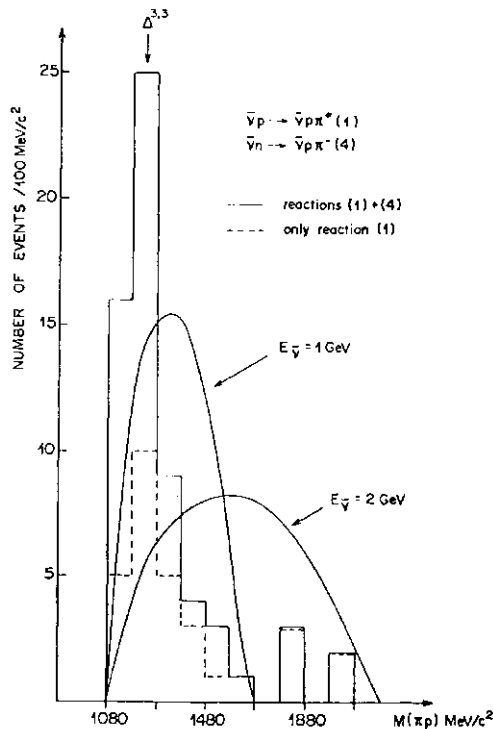


Fig. 9. Nucleon-pion mass distributions from the reactions  $\nu + p \rightarrow \ell + p + \pi^0$  and  $\nu + n \rightarrow \ell + p + \pi^-$  (from ref. 21).

have been measured in a large number of experiments. Their results are summarized in Table VI. The targets ( $x$ ) used were mostly heavy nuclei, so that the ratios are averages for approximately equal number of neutrons and protons. A cut on the visible hadronic energy has been used in all of the experiments. The raw ratios with the  $E_h$  cuts are listed in the table. The last two columns give the ratios extrapolated to  $E_h=0$ . The agreement be-

tween the experiments is very good, especially when one considers that the incident neutrino energies vary from a few GeV to a few hundred GeV in the various experiments. The measured ratios are also in good agreement with the predictions of the W-S model, as shown in Fig. 10. The weighted averages for the ratios are

$$\bar{R}_\nu = 0.29 \pm 0.01$$

$$\bar{R}_\mu = 0.35 \pm 0.025.$$

The ratio  $R_\nu$  implies a value of the mixing angle of

$$\sin^2 \theta = 0.24 \pm 0.02.$$

The determination of  $\sin^2 \theta$  from  $R_\nu$  is somewhat dependent on quark-parton model assumptions. However, the current understanding of the quark parton model is such that these uncertainties are not very large, and are estimated to be comparable to the quoted error on  $\sin^2 \theta$  of  $\pm 0.02$ . Paschos and Wolfenstein<sup>31</sup> have pointed out that the quark-parton model dependence cancels out in the ratio

$$R = \frac{\sigma_{NC}^\nu - \sigma_{NC}^{\bar{\nu}}}{\sigma_{CC}^\nu - \sigma_{CC}^{\bar{\nu}}} = 1/2 - \sin^2 \theta.$$

Using this method the BEBC narrow band experiment obtained<sup>32</sup>

$$\sin^2 \theta = 0.22 \pm 0.05.$$

##### 5. Parity violation in atomic bismuth

Due to the weak neutral current interaction between an atomic electron and the nucleus, parity violating effects at the  $10^{-11}$  level might

Table VI. Inclusive neutral current ratios.

Experiment	$E_\nu$ GeV	$E_h$ cut GeV	$R_\nu = \nu_\mu + N \rightarrow \nu_\mu + \dots / \nu_\mu + N \rightarrow \mu + \dots$			
			Raw Ratios		Corrected for $E_h$ Cut	
			$R_\nu$	$R_{\bar{\nu}}$	$R_\nu$	$R_{\bar{\nu}}$
Gargamelle <sup>24</sup> CERN PS	1-10	1	$0.25 \pm 0.04$	$0.56 \pm 0.08$	$0.26 \pm 0.04$	$0.39 \pm 0.06$
HPWF <sup>25</sup> Fermilab	30-200	4	$0.28 \pm 0.03$	$0.39 \pm 0.10$	$0.30 \pm 0.04$	$0.33 \pm 0.09$
CITF <sup>26</sup> Fermilab	30-200	12	$0.28 \pm 0.03$	$0.35 \pm 0.11$	$0.27 \pm 0.02$	$0.40 \pm 0.08$
CDHS <sup>27</sup> CERN SPS	30-200	12	$0.29 \pm 0.01$	$0.35 \pm 0.03$	$0.295 \pm 0.01$	$0.34 \pm 0.03$
BNL 7 ft B.C. <sup>28</sup> deuterium	1-10	0.4	$0.25 \pm 0.05$			
BEBC Narrowband <sup>29</sup> CERN SPS neon	30-200	15	$0.32 \pm 0.03$	$0.39 \pm 0.07$	$0.31 \pm 0.04$	$0.37 \pm 0.08$
Mariner <i>et al.</i> <sup>30</sup> Fermilab 15 ft neon	10-100	10	$0.35 \pm 0.06$			
Weighted average					$0.29 \pm 0.01$	$0.35 \pm 0.025$

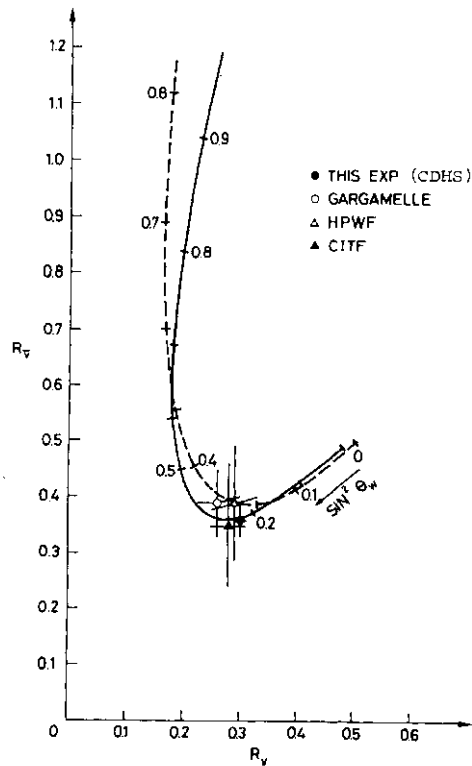


Fig. 10. Comparison of the experimental cross section ratios  $R_\nu$  and  $R_{\bar{\nu}}$  for the inclusive neutral current processes with the predictions of the W-S model with no antiquark contributions (dashed curve) and with the best estimate of the antiquark contribution,  $q/q=0.1$  (solid curve), from ref. 27.

be expected in heavy nuclei like Bismuth 209. The effect is due to the V-A interference term between the vector part of the hadronic current and the axial vector part of the leptonic neutral current. The experiments measure the optical rotation of the plane of polariza-

Table VII. Optical rotation in atomic bismuth.

Experiment	Transition Used	Observed optical rotation, $\times 10^{-8}$	Weinberg-Salam prediction, $\times 10^{-8}$
Seattle <sup>33</sup>	8757 Å	$-0.5 \pm 1.7$	-10 to -18
Oxford <sup>34</sup>	6480 Å	$-5 \pm 1.6$	-13 to -23
Novosibirsk <sup>35</sup>	6480 Å	$-19 \pm 5$	-13 to -23

tion of incident plane polarized laser light. A nonzero rotation measures a preferred direction (clockwise or counterclockwise) and is thus clearly parity violating. The results obtained in three experiments are summarized in Table VII. The agreement between the experiments is very poor. The predictions of the W-S model, listed in the last column of Table VII, have very large uncertainties due to the complex atomic physics calculations involved.<sup>36</sup> Bismuth has 83 atomic electrons, 3 valence and 80 in the core. The effects of the 80 core electrons are apparently very difficult to calculate. In view of these theoretical uncertainties and the disagreement between the three experiments, no conclusion seems warranted at this time, and one should not be too concerned about any possible discrepancies with the W-S model.

6. Parity violation in polarized electron scattering

Interference between the weak neutral current and the electromagnetic interactions can lead to parity violating effects in polarized electron scattering

$$e^- (\text{polarized}) + d \rightarrow e^- + \dots$$

An experiment to look for such effects has been carried out at SLAC.<sup>37</sup> The experiment measured the asymmetry between the cross sections of left and right handed polarized incident electrons

$$A = \frac{\sigma(\vec{e}) - \sigma(\bar{e})}{\sigma(\vec{e}) + \sigma(\bar{e})}$$

A nonzero value of  $A$  is clearly parity non-conserving.

At incident electron energies of 19.4 and 22.2 GeV,  $\langle 7^2 - 1.6 \text{ GeV}^2$ , and  $y = (E_{e^- \text{ out}} - E_{e^- \text{ in}}) / E_{e^- \text{ in}} = 0.21$ , a significant asymmetry was found

$$A/q^2 = (-9.5 \pm 1.6) \times 10^{-5} (\text{GeV})^{-2}.$$

For a given polarization of the electrons injected into the SLAC accelerator, the longitudinal polarization of the electrons hitting the deuterium target varied with  $E_e$  because of the precession of the spin. The observed asymmetry as a function of  $E_e$ , *i.e.*, the electron polarization, shown in Fig. 11, has the

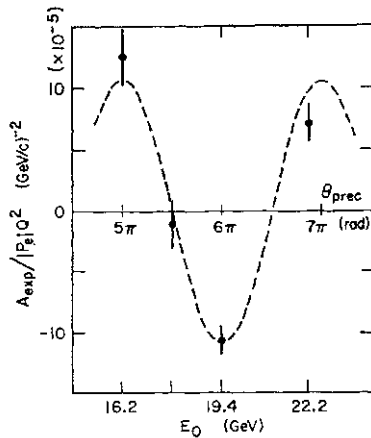


Fig. 11. Cross section asymmetry vs the electron beam energy in  $e^-$  (polarized) +  $d \rightarrow e^- + \dots$  (from ref. 37).

correct behavior for a spin dependent asymmetry. This as well as many other careful consistency checks make the experiment very convincing.

The agreement between this result and the prediction of the W-S model for values of  $\sin^2 \theta$  determined by the neutrino experiments is very good, as shown on Fig. 12. The best value of the mixing angle from this experiment is

$$\sin^2 \theta = 0.20 \pm 0.03.$$

This final conclusion is somewhat dependent

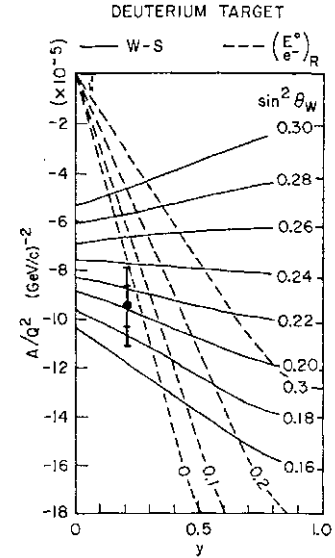


Fig. 12. Comparison of the experimental cross section asymmetry with the prediction of the W-S model for various values of  $\sin^2 \theta$  (from ref. 37).

on quark-parton model assumptions. However, the uncertainties introduced by these assumptions are not very significant.

### B. Determination of the neutral current couplings

In the previous section the experimental data were compared with the predictions of the W-S model. We saw that the data are consistent with these predictions. In this section we will discuss a "model independent" analysis in which no specific model is assumed at the outset. The experimental data will be used to determine the structure of the weak neutral currents in a general way. By structure of the weak neutral current we mean the space-time structure: vector (V), axial vector (A), scalar (S), pseudoscalar (P), or tensor (T) and the isotopic spin structure: isoscalar ( $I=0$ ) or isovector ( $I=1$ ). For the first time, at this conference, the experimental data are sufficient to produce a unique solution in a model independent analysis. As we will see, the resulting couplings are just those of the W-S model.

1. We start out by considering the general space-time structure.

(a) Any pure interaction (V, A, S, P, or T) must give the same neutrino and antineutrino cross sections for any given process. A difference in the  $\nu$  and  $\bar{\nu}$  cross section can only be caused by an interference between two different interactions with different  $C$  (like a VA

interference term). Experimentally, the results of the HPB experiment<sup>38</sup> for the elastic scattering process is

$$\frac{\sigma(\bar{\nu}_\mu + p \rightarrow \bar{\nu}_\mu + p)}{\sigma(\nu_\mu + p \rightarrow \nu_\mu + p)} = 0.53 \pm 0.17$$

and for the inelastic inclusive interactions the CDHS experiment<sup>39</sup> finds

$$\frac{\sigma(\bar{\nu}_\mu + N \rightarrow \bar{\nu}_\mu + \dots)}{\sigma(\nu_\mu + N \rightarrow \nu_\mu + \dots)} = 0.58 \pm 0.05.$$

These ratios are significantly different from unity so we can conclude that the neutral currents are not pure V, A, S, P or T.

(b) The distribution in  $y = (E_{\text{vis}} - E_{\text{miss}}) / E_{\text{vis}}$  for the inclusive neutral current process is sensitive to the space time structure of the interaction. For example,

$$\frac{d\sigma}{dy} \approx g(V-A) + g(V+A)(1-y)^2 + g(S, P)y^2$$

for  $\nu$  scattering on real quarks. The  $y$  distributions for various interactions are shown in Fig. 13. Several experiments have looked at

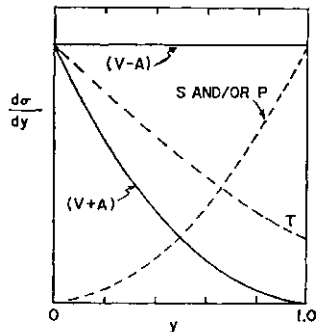


Fig. 13. Distributions in  $y = (E_{\text{vis}} - E_{\text{miss}}) / E_{\text{vis}}$  for the process  $i^+ + N \rightarrow i^+ + \dots$  for various possibilities for the space-time structure of the neutral current interaction (neglecting antiquark contributions).

the  $y$  distribution of the inclusive neutral current reaction, using narrow band neutrino beams where the incident  $\nu$  energy is known to some extent: the CITF experiment<sup>40</sup> at Fermilab, the CDHS experiment<sup>41</sup> at the CERN SPS, and the BEBC experiment<sup>42</sup> with a heavy neon fill at the CERN SPS. The conclusions are that:

i) S and/or P can be ruled out

$$\frac{g(V-A) + g(V+A)}{g(S, P)} = 0 \pm 0.03 \text{ BEBC} \\ = 0.02 \pm 0.07 \text{ CDHS}$$

(ii) Pure V, pure A, and pure (V+A) can be ruled out and pure (V-A) is unlikely

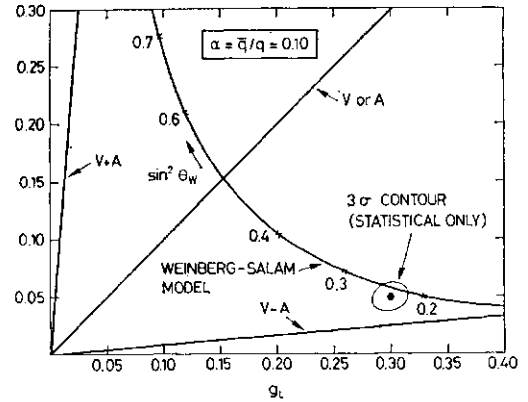


Fig. 14. Comparison of the experimental data for the V + A coupling ( $g_+$ ) vs the V-A coupling ( $g_-$ ) for various possibilities for the structure of the weak neutral current interaction (from ref. 41).

(see Fig. 14).

c) The parity violating asymmetry observed in polarized electron scattering at SLAC is due to an interference between the neutral currents and the electromagnetic interaction, which is a vector interaction. Thus the weak neutral current must have some V or A part to it.

2. In view of the above conclusions it seems reasonable to proceed with the analysis in terms of an arbitrary mixture of V and A interactions.

The various neutral current couplings between the leptons and the quarks are illustrated in Fig. 15. The purely leptonic processes,  $\nu + e \rightarrow \nu + e$  depend only on the V and A couplings of the electron,  $g_e$  and  $g_{e'}$ . In neutrino hadron scattering, isotopic spin is also relevant, so we have four couplings, V and A with  $I=0$  and  $I=1$  each. Sakurai<sup>43</sup> introduced the four couplings  $a$ ,  $\beta$ ,  $\gamma$  and  $\delta$  for (V,  $\tau=1$ ), (A,  $\tau=1$ ), (V,  $\tau=0$ ), and (A,  $\tau=0$ ), respectively. Sehgal<sup>44</sup> introduced an

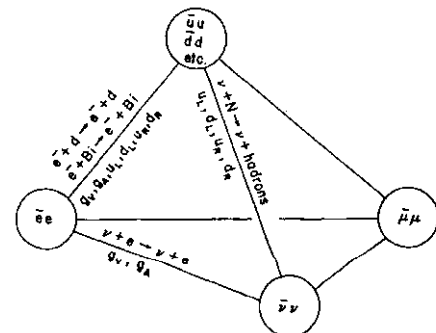


Fig. 15. Schematic diagram illustrating the various neutral current coupling constants (after ref. 43).



alternate four coupling constants  $u_L, d_L, u_R,$  and  $d_R$ . The subscript  $L$  and  $R$  are for  $(V-A)$  and  $(V+A)$  combinations, and the  $u$  and  $d$  are the isospin combination appropriate for the  $u$  and  $d$  quarks. The two sets of coupling constants are obviously just linear combinations of each other:

$$\begin{aligned} u_L &= 1/4(\alpha + \beta + \gamma + \delta) \\ d_L &= 1/4(-\alpha - \beta + \gamma + \delta) \\ u_R &= 1/4(\alpha - \beta + \gamma - \delta) \\ d_R &= 1/4(-\alpha + \beta + \gamma - \delta) \end{aligned}$$

The parity violating effects in atomic bismuth or polarized electron scattering depend on six coupling constants:  $g_A, g_V$  for the electrons, and  $u_L, d_L, u_R,$  and  $d_R$  for the quarks. At this point some theoretical assumptions have crept in. The fact that  $g_A, g_V$  for the last case are the same as  $g_A, g_V$  for  $\nu + e \rightarrow \nu + e$  scattering depends on the assumption that the same  $Z^0$  mediates both processes and that the neutrino couples to this  $Z^0$  with the normal  $V-A$  coupling.

3. Determination of the  $\nu$ -quark couplings. The analysis follows the work of Sehgal,<sup>44</sup> Hung and Sakurai,<sup>45</sup> Abbott and Barnett,<sup>46</sup> Sidhu and Langacker,<sup>47</sup> Paschos,<sup>48</sup> and Claudson, Paschos and Sulak.<sup>49</sup>

(a) The neutral to charged current ratios for the inclusive channel are used to determine

the overall strengths  $(u_L + d_L)$  and  $(u_R + d_R)$ . These are the circular bands on the  $u_L$  vs  $d_L$  and the  $u_R$  vs  $d_R$  planes, shown in Fig. 16.

(b) The charge ratios in inclusive pion production select four allowed solutions A, B, C, and D indicated on Fig. 16. The data used comes from the Gargamelle experiment<sup>50</sup> at the CERN PS.

$$\begin{aligned} \frac{\nu + N \rightarrow \nu + \pi^+ + \dots}{\nu + N \rightarrow \nu + \pi^- + \dots} &= 0.77 \pm 0.14 \\ \frac{\bar{\nu} + N \rightarrow \bar{\nu} + \pi^+ + \dots}{\bar{\nu} + N \rightarrow \bar{\nu} + \pi^- + \dots} &= 1.64 \pm 0.36. \end{aligned}$$

(c) Recent results on the exclusive channels,  $\nu + p \rightarrow \nu + p$  from the HPB experiment<sup>15</sup> at Brookhaven and  $\gamma + N \rightarrow \gamma + N + 7\pi$  from the Gargamelle propane experiment<sup>21</sup> at the CERN PS, select solution A as the only one allowed, as illustrated on Fig. 17.

The weakest part in this analysis is step (b), since the interpretation of the inclusive pion production data are quark-parton model dependent and the Gargamelle experiment was done at low neutrino energies. In a paper by Claudson, Paschos and Sulak<sup>49</sup> submitted to the Conference a similar analysis is carried out but the reliance on the inclusive pion ratios

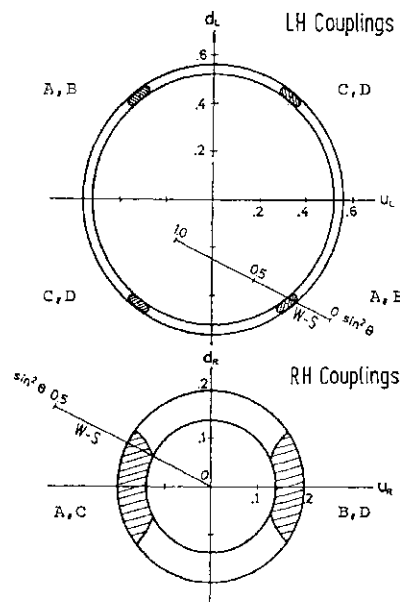


Fig. 16. Experimentally allowed values of the neutrino-quark neutral current coupling constants. A, B, C, and D indicate the solutions discussed in the text (from ref. 44).

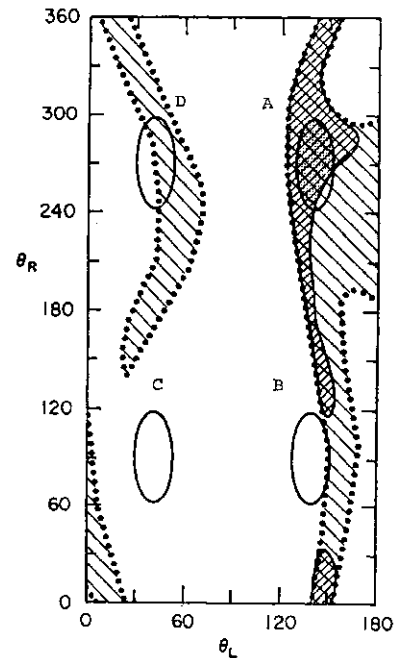


Fig. 17. The allowed angles in the  $L$  and  $R$  coupling planes of Fig. 16, with the solutions A, B, C, and D indicated. The shaded regions are those allowed by the elastic data. The doubly shaded region is that allowed by the single pion production data as well. Only solution A is consistent with all of the data (from ref. 46).

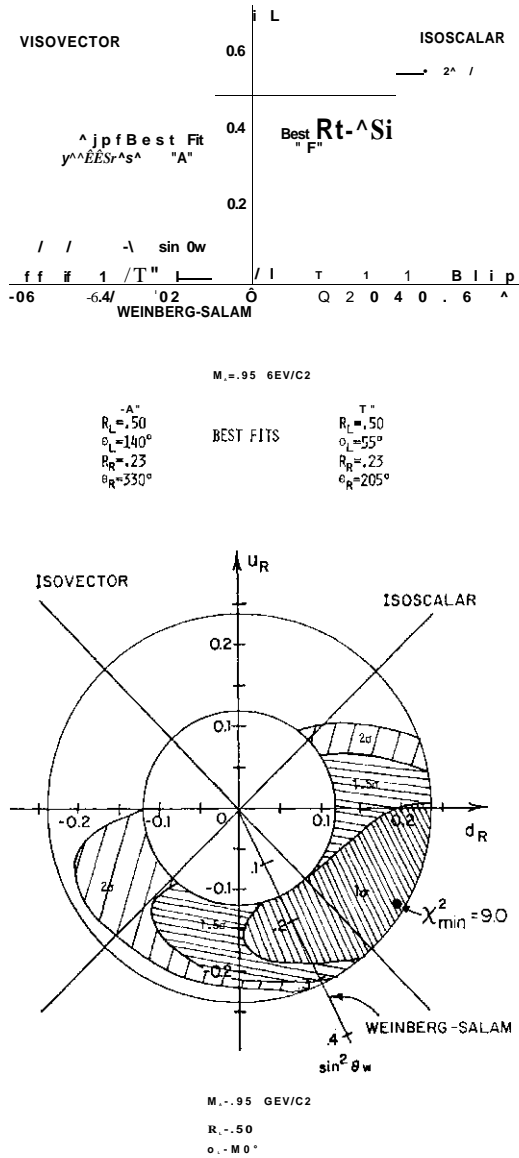


Fig. 18. Allowed regions in the  $u_R-d_L$  and the  $U_R-d_L$  coupling constant planes from the analysis of ref. 49.

is eliminated. The inclusive neutral current process is used to obtain  $(u|+dl)$  and  $(w|+</\mathcal{E})$ , as above. The improved  $i^+ + p - n^+ + P$  and  $i^+ + p \rightarrow iv + P$  data from the HPB experiment<sup>15</sup> is then used to obtain the solutions A and F shown on Fig. 18. Solution F, which is almost pure isoscalar, is ruled out using the fact that the J(1238) is produced in neutral current single pion production. This leaves solution A, which is essentially the same as solution A obtained by the analysis outlined above.

The values of the coupling constants for the unique solution are listed in Table VIII.

4. Determination of the  $\nu$ -electron couplings.

(a) The intersections of the regions allowed

Table VIII. Summary of the weak neutral current couplings.

Coupling constant	Value in Unique solution*	Weinberg-Salam	
		$\sin^2 \theta = 1/4$	As Function of $\sin^2 \theta$
$g_V$	$0.0 \pm 0.1$	0.0	$-1/2 + 2 \sin^2 \theta$
$g_A$	$0.55 \pm 0.1$	-0.5	-1/2
	$0.35 \pm 0.07$	0.33	$1/2 - 2/3 \sin^2 \theta$
$d_L$	$\sim 0.40 \pm 0.07$	-0.42	$-1/2 + 1/3 \sin^2 \theta$
$U_R$	$-0.19 \pm 0.06$	-0.17	$-2/3 \sin^2 \theta$
$d_R$	$0.0 \pm 0.11$	0.08	$1/3 \sin^2 \theta$

\* Using solution A of Abbott & Barnett.

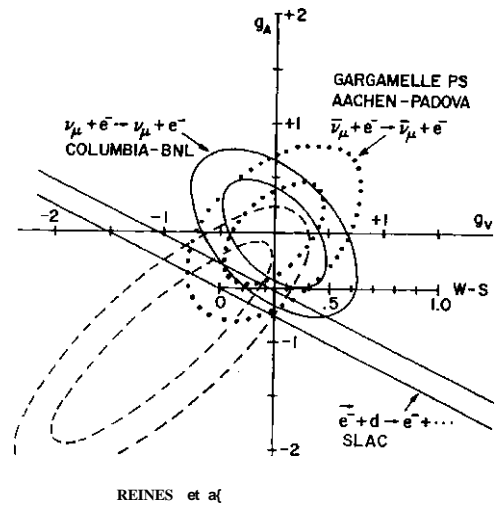


Fig. 19. Allowed regions in the neutrino-electron coupling plane,  $g_A$  vs  $g_V$ .

in the  $g_V-g_A$  plane by the cross sections for the processes,  $i^+ + e^- \rightarrow i^+ + e^-$  and  $\nu_e + e^- \rightarrow \nu_e + e^-$  produces two ambiguous solutions, one with  $g_V \sim 0, g_A \sim -1/2$ , the other with  $g_V \sim -1/2, g_A \sim 0$ , as shown in Fig. 19. The region allowed by the cross section for  $i^+ + e^- \rightarrow i^+ + e^-$  is consistent with these two solutions but does not distinguish between them.

(b) The region in the  $g_V-g_A$  plane allowed by the parity violating asymmetry in polarized electron scattering observed at SLAC<sup>37</sup> is also shown on Fig. 19. This region overlaps the solution near  $g_V \sim 0, g_A \sim -1/2$ , but not the other solution and thus resolves the ambiguity. The values of  $g_V$  and  $g_A$  with errors for this solution are also listed in Table VIII.

C. Summary of neutral currents

1. The "model independent" analysis now produces a unique solution. The values of the neutral current couplings for this solution are summarized in Table VIII. The

Table IX. Summary of neutral currents comparison with the Weinberg-Salam model.

Process	Experimental results	$\sin^2 \theta$	W-S Prediction with $\sin^2 \theta = 0.23$
1. Purely leptonic			
$\nu_e + e^- \rightarrow \nu_e + e^-$	$(5.7 \pm 1.2) \times 10^{-42} \text{ cm}^2$	$0.29 \pm 0.05$	5.0
$\nu_e + e^- \rightarrow \nu_e + e^-$	$(1.7 \pm 0.5) \times 10^{-42} \text{ cm}^2$	$0.21 \pm 0.05$	1.5
$\nu_e + e^- \rightarrow \nu_e + e^-$	$(1.8 \pm 0.9) \times 10^{-42} \text{ cm}^2$	$0.30 \pm 0.08$	1.3
2. Elastic scattering			
$\nu_e + p \rightarrow \nu_e + p$	$(0.11 \pm 0.02) \times 10^{-42} \text{ cm}^2$	$0.26 \pm 0.06$	0.12
$\nu_e + p \rightarrow \nu_e + p$	$(0.19 \pm 0.08) \times 10^{-42} \text{ cm}^2$	$< 0.5$	0.11
3. Single pion production			
$\nu_e + N \rightarrow \nu_e + N + \pi^+$	$(0.45 \pm 0.08) \times 10^{-42} \text{ cm}^2$	$0.22 \pm 0.09$	0.42
$\nu_e + N \rightarrow \nu_e + N + \pi^0$	$(0.57 \pm 0.11) \times 10^{-42} \text{ cm}^2$	$0.15 - 0.52$	0.60
4. Inclusive			
$\nu_e + N \rightarrow \nu_e + N + \text{hadrons}$	$(0.29 \pm 0.01) \times 10^{-42} \text{ cm}^2$	$0.24 \pm 0.02$	0.30
$\nu_e + N \rightarrow \nu_e + N + \text{hadrons}$	$(0.35 \pm 0.025) \times 10^{-42} \text{ cm}^2$	$0.3 \pm 0.1$	0.38

couplings in the W-S model are also listed on the table. The agreement is very good with a value of  $\sin^2 \theta \sim 1/4$ .

2. The experimental results on the neutrino induced neutral current processes are summarized in Table IX. The agreement with the W-S model is excellent in all cases, as can be seen by comparing the second and fourth columns on the table.

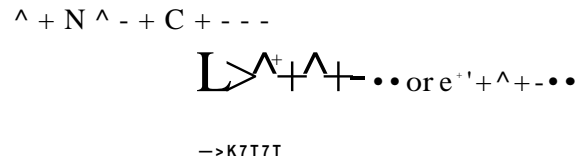
3. The values of  $\sin^2 \theta$  obtained from each reaction are listed in the third column of Table IX. These values are displayed on Fig. 20. They are in very good agreement with each other. The weighted average for all of

the reactions is

$$\sin^2 \theta = 0.23 \pm 0.02.$$

### §11. Charm Production by Neutrinos

The production of particles with the new hadronic quantum number, charm, has been observed in neutrino interactions both *via* the semileptonic and the hadronic decays of the charmed particles (C):



The signature of the first process is the presence of two charged leptons in the final state: *i.e.*, dilepton events, like  $pCp^+$  or  $p\sim\zeta^+$ . The signature of the second process is a  $pT$  and a visible strange particle decay such as  $K^0 \rightarrow \pi^+ \pi^-$  (*vee*) in the final state. In the first case there is an undetected  $\nu$  in the final state so that the mass of the charmed particle cannot be reconstructed from its decay products. The evidence that these dilepton events come from charm production is the correlation of these events with strange particle production and the consistency of the rate and other properties of the events with the GIM scheme. In the case of the hadronic decays, all of the decay products are seen and the charmed particle can thus be directly observed as a peak in a mass distribution.

#### A. Dimuon production in counter experiments

Dimuon production by neutrinos has first been observed by the HPWF experiment<sup>51</sup> at

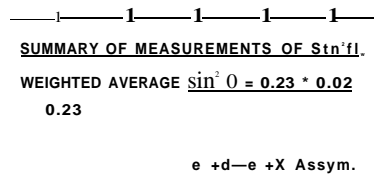


Fig. 20. Determination of the mixing angle,  $\sin^2 \theta$ , from the various neutral current reactions.

Table X. Dimuon production by  $\nu$  and  $\bar{\nu}$  in the large counter experiments.

Experiment	$\nu_\mu$ Induced		$\bar{\nu}_\mu$ Induced	
	Events*	$\mu^-\mu^+/\mu^-$	Events*	$\mu^+\mu^-/\mu^+$
HPWF <sup>51</sup> Fermilab	~160	$0.4 \pm 0.08\%$	~90	$0.27 \pm 0.09\%$
CITF <sup>52</sup> Fermilab	90	~1%	33	~1%
CHHS <sup>53</sup> CERN SPS	256	~1%	58	~1%

\* The numbers listed are the number of events published. All three experiments have much larger samples from recent runs which are being analyzed.

Fermilab, soon followed by the CITF experiment<sup>52</sup> at Fermilab and later by the CDHS experiment<sup>53</sup> at the CERN SPS. The results of these three experiments on opposite sign dimuons ( $\mu^-\mu^+$ ) are summarized in Table X. Like sign dimuon production and trilepton production has been discussed in the previous talk by Professor Tittel. The rates for the  $\mu^-\mu^+$  events relative to single  $\mu$  events are somewhat below 1%, as shown in Figs. 21 and 22 for the HPWF and the CDHS experiments, respectively. These rates seem to increase very rapidly with increasing  $E_\nu$ . However, this effect is now understood to be caused by

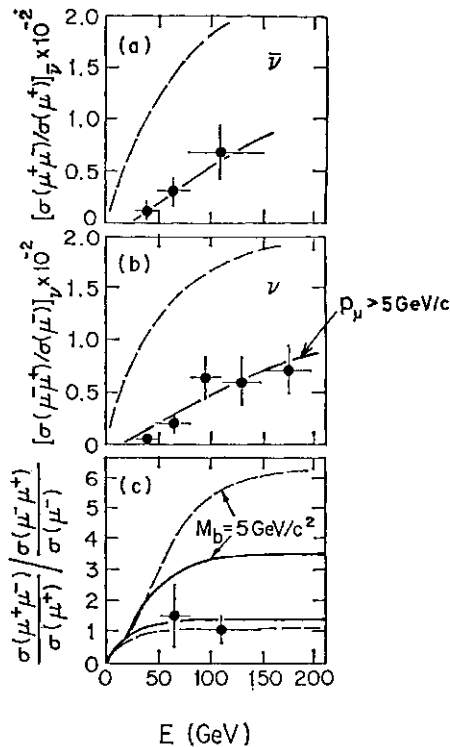


Fig. 21. The  $\mu^-\mu^+$  production rate relative to the total charged current cross section in the HPWF experiment (from ref. 51).

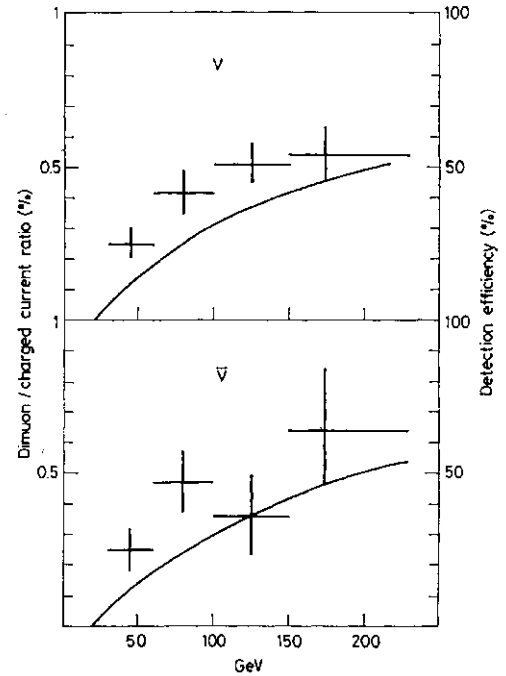


Fig. 22. The  $\mu^-\mu^+$  production rate relative to the total charged current cross section in the CDHS experiment (from ref. 53).

the severe cuts ( $p_\mu > 4$  or  $4\frac{1}{2}$  GeV/c) imposed on the muon momenta in these experiments. The  $x$  and  $y$  distributions for the dimuon events from the HPWF and the CDHS experiments are shown in Figs. 23 and 24, respectively.

B. Dilepton production in bubble chamber experiments

In the large bubble chambers filled with heavy liquids such as neon or freon the electron identification is very good and thus neutrino interactions,  $\nu_\mu + N \rightarrow \mu^- + e^+ + \dots$ ,

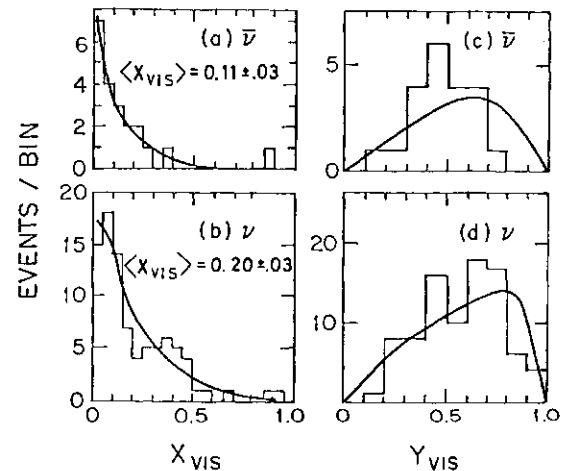


Fig. 23. Distribution in  $x=q/2mv$  and  $y=e/E$  for the  $\mu^-\mu^+$  events in the HPWF experiment (from ref. 51).

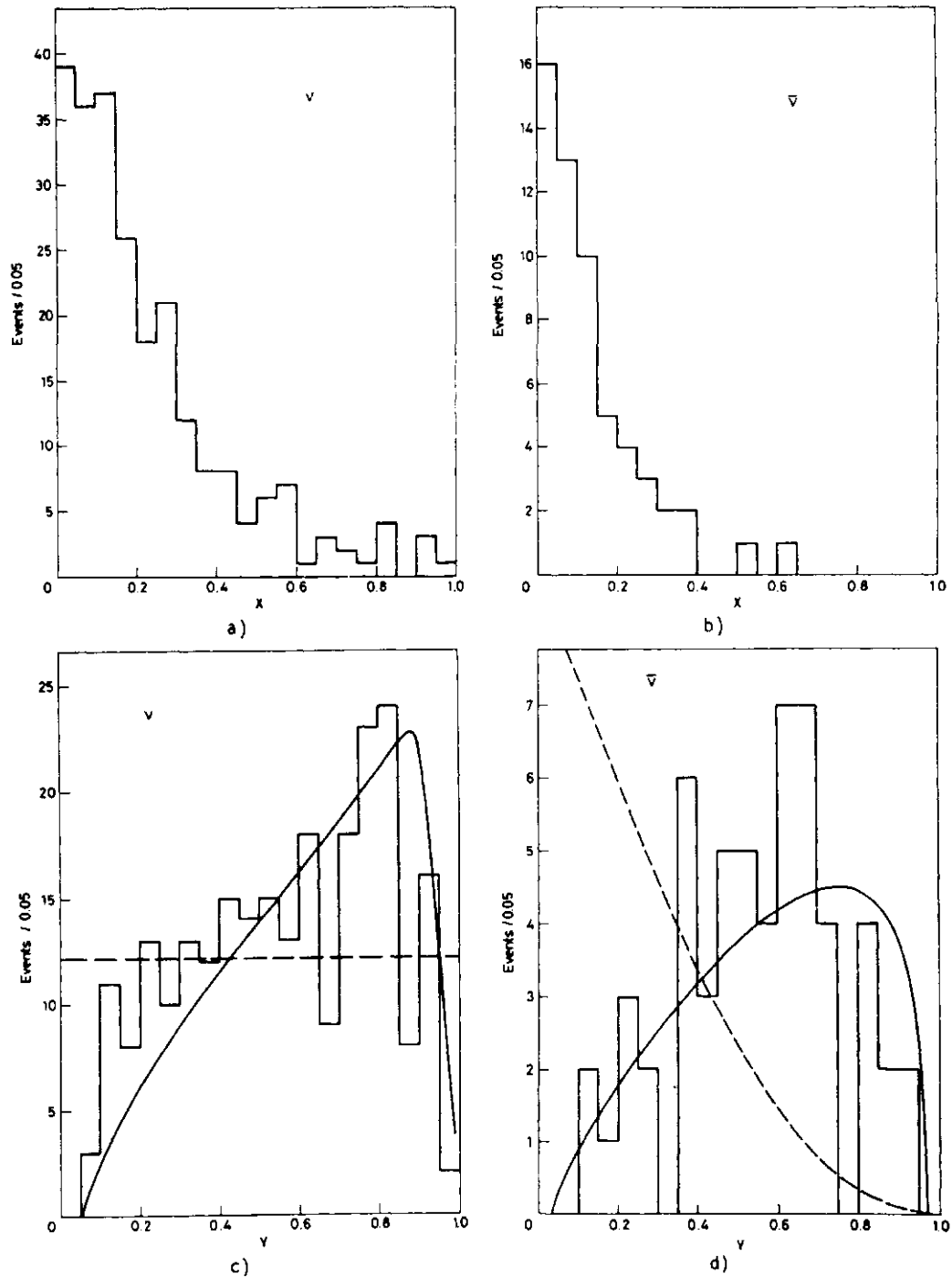


Fig. 24. Distribution in  $x$  and  $y$  for the  $|i f|$  events in the CDHS experiment (from ref. 53).

can be identified with very small backgrounds (typically 10-15%). Using external muon identifiers, production can also be isolated. The results of these experiments are summarized in Table XI for  $\nu_p$  experiments and in Table XII for experiments. In these experiments neutral strange particles can be detected *via* their decays  $K^0 \rightarrow \pi^+ \pi^-$  and  $A^0 \rightarrow p \pi^-$  ( $\nu$ es). The number of  $\nu$ es observed with these dilepton events is also listed on these tables. There is a significant correla-

tion with strange particle production. For example in the Columbia-BNL experiment<sup>56</sup> the visible  $\nu$  production in charged current (single  $JU^-$ ) events has been measured to be 6%. Thus  $\sim 15$   $\nu$ es would be expected with the 204  $/u\bar{e}^+$  events, but 43 were observed.

In the selection of the  $/u\bar{e}^+$  events much less stringent cuts were imposed on the lepton momenta than in the counter experiments. For example in the Columbia-BNL experiment no cut was imposed on  $P_{\nu^-}$ , and a 300

Table XI. Dilepton production by neutrinos in bubble chambers.

Experiment	$E_\nu$ GeV	Liquid	Events Obs.	VeCs Obs.	$\mu^-l^+/\mu^-$ Rate (%)
Gargamelle <sup>54</sup>	1-8	Freon	14	3	$0.31 \pm 0.13$
CERN PS			$\mu^-e^+$		
WISC-CERN-Hawaii-LBL <sup>55</sup>	~30	21% Ne	17	11	$0.8 \pm 0.3$
Fermilab E-28			$\mu^-e^+$		
Columbia-Brookhaven <sup>50</sup>	~30	64% Ne	204	43	$0.5 \pm 0.15$
Fermilab E-53			$\mu^-e^+$		
Berkeley-Seattle-LBL-Haw <sup>57</sup>	~30	64% Ne	6	1	$0.34^{+0.23}_{-0.13}$
Fermilab E-172			$\mu^-e^+$		
Fermilab-LBL-Hawaii <sup>58</sup>	~50	50% Ne	9	1	
Fermilab E-460			$\mu^-\mu^+$		
BEBC Narrowband <sup>59</sup>	~75	60% Ne	5	2	$0.7 \pm 0.3$
CERN SPS			$\mu^-e^+$		
BEBC Narrowband <sup>60</sup>	~75	60% Ne	11	6	$0.8 \pm 0.3$
CERN SPS			$\mu^-\mu^+$		
BEBC Wideband <sup>61</sup>	~30	60% Ne	17	6	$0.41 \pm 0.15$
CERN SPS			$\mu^-e^+$		
Fermi-Mich-IHEP-ITEP <sup>62</sup>	~30	64% Ne	6	1	$0 \pm 1/2$
Fermilab E-180			$\mu^-e^+$		
F-W-B-LBL-S <sup>63</sup>	~50	45% Ne	40	5	$0.54 \pm 0.14$
Fermilab E-546			$\mu^-\mu^+$		
Gargamelle <sup>64</sup>	~30	Freon	70	8	$0.62 \pm 0.18$
CERN SPS			$\mu^-\mu^+$		
SKAT <sup>65</sup>	2-30	Freon	3	1	$0.7 \pm 0.4$
Serpukhov			$\mu^-e^+$		
Totals			402	88	$0.5 \pm 0.1$

Table XII. Dilepton production by antineutrinos in the 15 ft bubble chamber.

Experiment	Liquid	Pictures	$\mu^+e^-$ Events	Background	Rae $\mu^+e^-/\mu^+$	VeCs
Fermilab-Serpukhov- Moscow-Michigan <sup>66</sup> E-180	21% Ne	74,000	— 1	$0.2 \pm 0.2$	$\leq 0.5\%$	
Berkeley-Hawaii- Seattle <sup>67</sup> E-172	64% Ne	59,000	4	0.6	$0.15^{+0.14}_{-0.08}$	2
Fermilab-Serpukhov- Moscow-Michigan <sup>68</sup> E-180	64% Ne	~150,000	12	—2	$0.22 \pm 0.07\%$	7
Total			16		$0.20 \pm 0.06$	9

MeV/c cut was imposed on  $P_{e^+}$ . Thus essentially the whole signal is observed, as shown in Fig. 25. The cuts used by the counter experiments throw out most of the signal, especially at low  $E_\nu$ . The rates observed for the dilepton events relative to single  $li$  events in the bubble chamber experiments are consistent with each other. The weighted average rate is  $(0.5 \pm 0.1)\%$  for neutrinos and  $(0.20 \pm 0.06)\%$  for antineutrinos. The energy dependence of the cross section for the  $jbt \sim e^-$  events, shown in Fig. 26, seems relatively constant or possibly rising gently relative to

the total charged current cross section in this energy range. The sharp rise observed by the counter experiments can be understood as an effect of the selection cuts on the muon momenta. For example, if the same cuts,  $P_{fi} > 4.5$  GeV/c, are applied to the  $JU \sim q^+$  events of the Columbia-BNL experiment, the rate is found to rise with  $E_\nu$  as shown in Fig. 27. For comparison the rates measured in the CDHS experiment for  $prJU^+$  events is also shown on this figure. The agreement is very good, indicating that the  $ll \sim e^+$  and the  $jll \sim \bar{li}$  events have the same origin.

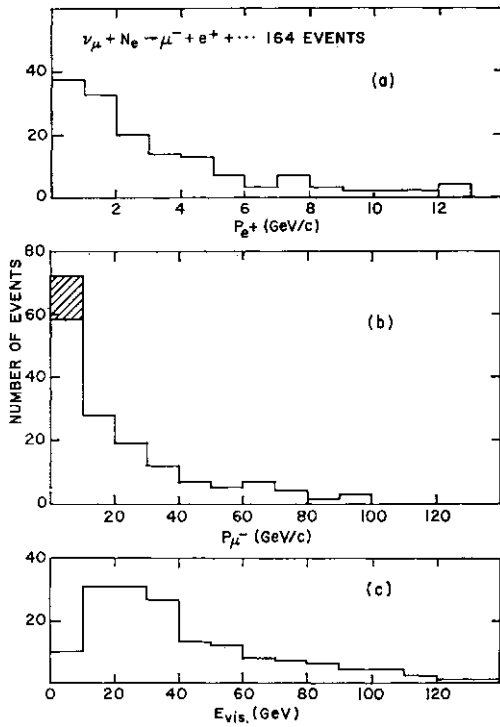


Fig. 25. Distributions in a) the positron momentum  $P_{e^+}$ , b) the muon momentum  $P_{\mu^-}$  and c) the total visible energy  $E_{vis}$  for the  $\bar{\nu}_\mu + e^+$  events in the Columbia-BNL experiment (from ref. 78).

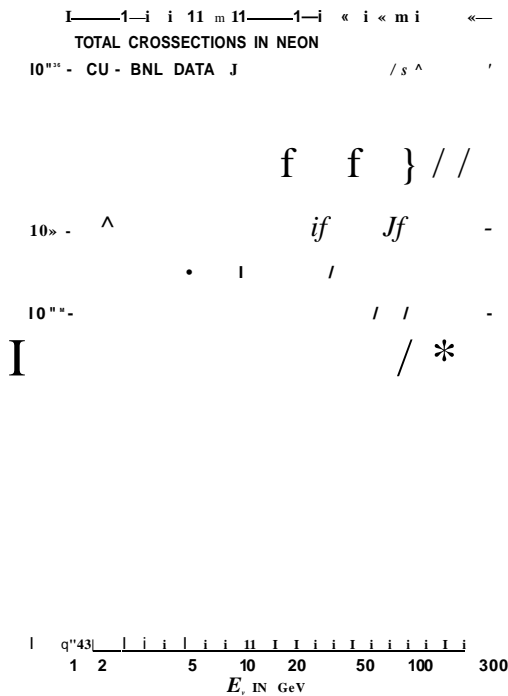


Fig. 26. Production cross section as a function of incoming neutrino energy  $E$ , for the  $f \bar{f}^*$  events relative to other neutrino interaction cross sections. The data points are from the Columbia-BNL experiment.

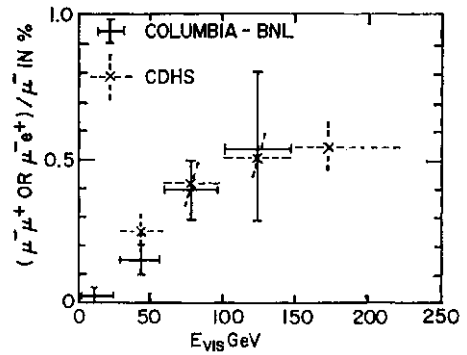


Fig. 27. Comparison of the relative production rates of the  $\mu^-$  and the  $\mu^+ / e^+$  events using the same  $p_{\mu^\pm} > 4.5$  GeV/c cut on both samples.

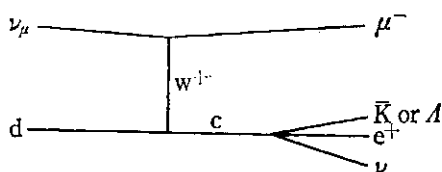
### C. Evidence that dilepton production is related to charm

The observed dilepton events are not consistent with being single  $p^-$  events with the second lepton, the  $\mu^+$ , or  $e^+$ , coming from  $n$  or  $K$  decay. The cross section for the dilepton events is too high by a factor of  $10^3$  to be due to the four fermion process  $\nu p C / u \nu p$  or  $\nu p \rightarrow j \bar{j} e^- \nu$ , in the Coulomb field of the target nucleus. These events, therefore, must be due to some new effect, such as the production and decay of a heavy lepton, an intermediate boson, or charmed particles. The interpretation as heavy lepton production followed by decay into  $u \bar{j} \nu$  or  $j \bar{u} e^-$  was ruled out by the observation that the  $p^-$  carried much more energy on the average than the  $JU^+$  or  $e^+$  (see Fig. 25), which is not what is expected for heavy lepton decay as pointed out by Pais and Treiman.<sup>69</sup> The interpretation as production and decay of an intermediate boson is inconsistent with the energy dependence of the cross section (see Fig. 26) and the high inelasticity of the dilepton events. The interpretation of these events as the production and semileptonic decay of charmed particles is consistent with all aspects of the data, as will now be discussed in more detail.

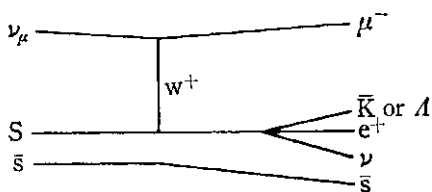
1. The rate of 1/2 to 1% of the total charged current cross section, with a semileptonic branching ratio around 1/10, indicates 5 to 10% charm production as expected from  $\sin^2 \theta_c$ .

2. The  $x$  and  $y$  distributions are consistent with the dominant charm production mechanisms:

i. For incident  $\nu_\mu$  :

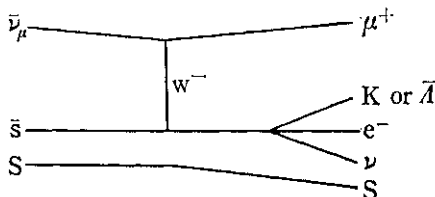


On valence quarks: Rate  $\sim d(x) \sin^2 \theta_c$  1 strange particle/event broad  $x$  distribution



On sea quarks: Rate  $\sim s(x) \cos^2 \theta_c$  2 strange particles/event narrow  $x$  distribution

ii. For incident  $\bar{\nu}_\mu$ , charm can be produced on sea quarks :



On  $s$  sea quarks: Rate  $\sim s(x) \cos^2 \theta_c$  2 strange particles/event narrow  $x$  distribution

We thus expect the  $x$  distribution for  $\bar{\nu}_\mu + N \rightarrow \mu^+ + N + c$  to be a combination of the valence and sea  $x$  distribution, while for  $\nu_\mu + N \rightarrow \mu^- + N + c$  to be narrow like the sea  $x$  distribution, as observed (see Figs. 23 and 24). For example in the Columbia-BNL

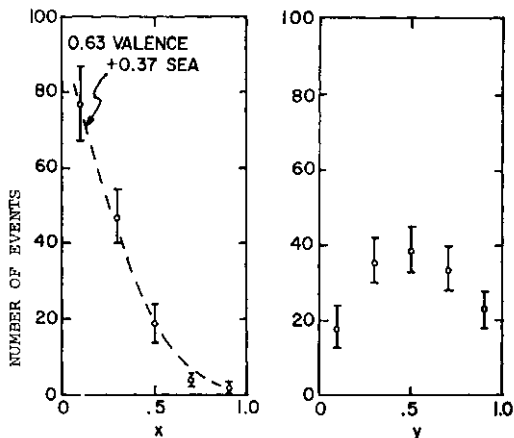


Fig. 28. Distributions in  $x$  and  $y$  for the  $\bar{\nu}_\mu + e^+$  events of ref. 56. The curve is the best fit of a combination of valence and sea quark  $x$  distributions to the data.

experiment, a fit to the  $x$  distribution to  $(1 - a) \text{ (sea)} + a \text{ (valence)}$  produced a good fit with  $a = 0.37 \pm 0.10$  (see Fig. 28) implying that charm production occurs about 1/3 of the time off sea  $s$  quarks and 2/3 of the time off valence quarks. Similar analyses, as well as the  $\nu/\bar{\nu}$  ratio for dilepton production, lead to the following estimates of the fraction of  $s$  or  $\bar{s}$  quarks relative to valence  $d$  quarks:

- $s$  or  $\bar{s}$  (sea)
- valence  $d$  quarks
- $= (3 \pm 2)\%$  Columbia-BNL,  $x$  distribution
- $= (5 \pm 2)\%$  CDHS,  $\nu/\bar{\nu}$  ratio
- $= (9.9 \pm 3.5)\%$  HPWF,  $x$  distribution
- $= (6.6 \pm 6A)\%$  HPWF,  $\nu/\bar{\nu}$  ratio.

3. Strange particle production. The visible  $\nu_e$  production ( $K^0 \rightarrow \pi^+ \pi^-$  and  $A \rightarrow p \pi^-$ ) in the dilepton events (see Table XI) is:  
 43  $\nu_e$ s in 204 events—Columbia-BNL  
 45  $\nu_e$ s in 198 events—all others combined  
 88  $\nu_e$ s in 402 events—Total;

or,  $\sim 21\%$  visible  $\nu_e$  production. Correcting for decay branching ratios, detection efficiencies, etc. Columbia-BNL obtain a rate of  $0.6 \pm 0.1$  total neutral strange particle production per  $\mu^+ \mu^-$  event. If the number of charged strange particles equal the number of neutral strange particles produced in these events, this rate leads to a total of

$\sim 1.2$  strange particles/event.

This agrees well with what we would expect from the G-I-M scheme, keeping in mind that from the fit to the  $x$  distribution we have 2/3 of the events on valence quarks with 1 strange particle per event plus 1/3 on sea quarks with 2 strange particles per event for a total expectation of 1 1/3 strange particles per event.

4. The detailed distributions of the dilepton events, such as the azimuthal angular distributions of the transverse momenta of the  $p^+$  or  $e^+$ , and the hadrons, the distributions in  $P$  and  $P_z$  of the leptons, and the total hadronic energies, etc. are all in good agreement with what is expected from charm production. The  $K^0 e^+$  mass distribution from the  $\bar{\nu}_\mu + N \rightarrow \mu^+ + N + c$  events, shown in Fig. 29, is in good agreement with the semileptonic decay of a  $D$  meson.

D. Direct observation of charm production via the hadronic decays  $D^0 \rightarrow K^+ \pi^-$   
 In the Columbia-BNL experiment<sup>70</sup> using



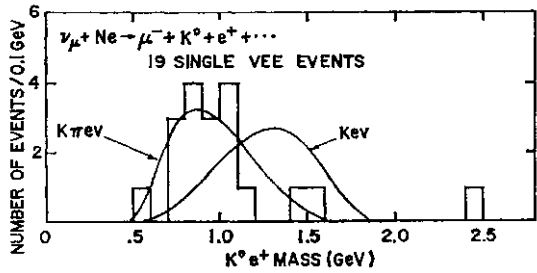


Fig. 29. Distribution in the  $K^0 e^+$  effective mass from the reaction  $\nu_\mu + Ne \rightarrow \mu^- + K^0 + e^+ + \dots$  in the Columbia-BNL experiment.

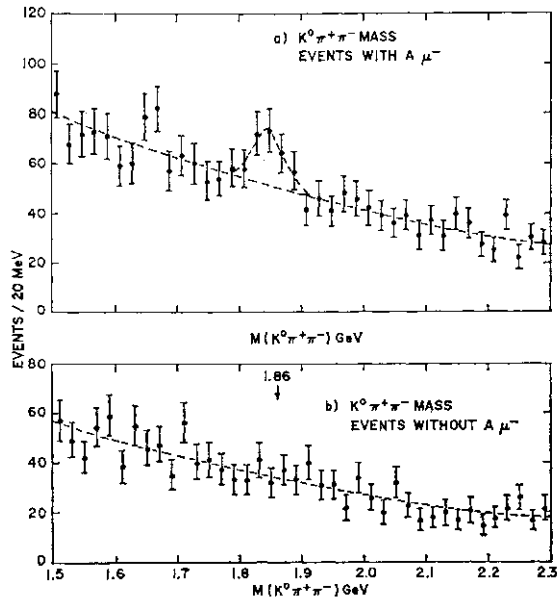


Fig. 30. Distribution in the  $K^0 \pi^+ \pi^-$  effective mass in the reaction  $\nu_\mu + Ne \rightarrow \mu^- + K^0 + \pi^+ + \pi^- + \dots$  in the Columbia-BNL experiment (from ref. 70).

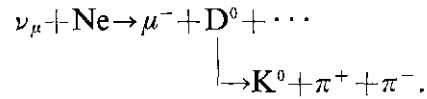
a heavy neonhydrogen mix in the Fermilab 15 ft chamber, a total of 1815  $\nu_\mu + Ne \rightarrow \mu^- + K^0 + e^+ + \dots$  and 1367  $\nu_\mu + Ne \rightarrow \mu^- + \pi^+ + \pi^- + \dots$  events have been measured. A peak in the  $K^0 \pi^+ \pi^-$  mass distribution is observed at the mass of the  $D^0$  discovered at SLAC, as shown in Fig. 30a. The signal is  $\sim 60$  events above background, with a statistical significance of four standard deviations. The mass and width of this peak are:

$$m = 1850 \pm 15 \text{ MeV}$$

$$\Gamma < 7 - 20 \pm 10 \text{ MeV.}$$

The observed width is consistent with the mass resolution of the experiment as expected for a very short-lived particle. No corresponding peak is observed in events without a  $\mu^-$  in the final state (Fig. 30b) consistent with the prediction of the G-I-M scheme that charm

changing neutral currents are absent. This effect is thus interpreted as the production and decay of a charmed D meson:



Correcting for  $K^0$  branching ratios and detection efficiencies, this effect corresponds to a  $D^0 \rightarrow K^0 \pi^+ \pi^-$  decay in  $(0.7 \pm 0.2)\%$  of all charged current  $\nu p$  interactions. The distribution in  $Z = E_p / E_{\text{HADRONIC}}$  the charm fragmentation function, from this sample is shown in Fig. 31.

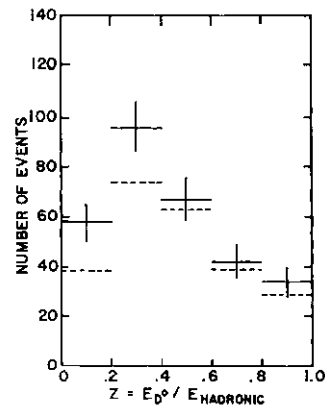
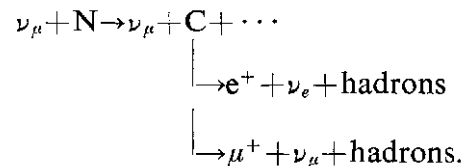


Fig. 31. Distribution in  $Z = E_p / E_{\text{HADRONIC}}$  for the  $\nu_\mu + Ne \rightarrow \mu^- + D^0 + \dots$   $D^0 \rightarrow K^0 \pi^+ \pi^-$  events in the Columbia-BNL experiment (from ref. 70).

E. Limits on charm changing neutral currents

Charm changing neutral current interactions were looked for both in production and decay processes.

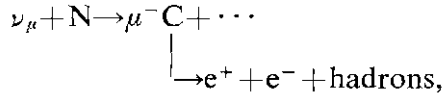
1. Charm production by neutrinos via neutral currents would lead to



The signature for this process would be events with an  $e^+$  or  $\mu^+$  in the final state but no  $\nu_\mu$ . Such a search has been carried out in the Columbia-BNL<sup>71</sup> and the Fermilab-Michigan-IHEP-ITEP experiments<sup>72</sup> at Fermilab looking for  $e^+$ , and in the CDHS experiment<sup>73</sup> at CERN looking for  $\mu^+$ , all with negative results. The best limit was obtained in the CDHS experiment

$$\frac{\sigma(\text{charm changing neutral currents})}{\sigma(\text{total neutral currents})} \leq 2.6\%.$$

2. Charm changing neutral currents would lead to decays of the type  $C \rightarrow e^+ + e^- + \text{hadrons}$  in analogy with the charm changing charged current decays,  $C \rightarrow e^+ + \nu_e + \text{hadrons}$ . The Columbia-BNL experiment has carried out a search for such decays in the process:



where the signature is a  $e^+ + e^- + \dots$  in the final state. No signal was found, and an upper limit was set, using the 204  $\nu_e$  events as normalization, of

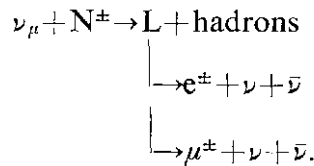
$$\frac{\text{Rate (charm changing neutral currents)}}{\text{Rate (charm changing charged currents)}} \leq 2\%$$

**§IV. Limits on Heavy Lepton Production**

Searches for heavy lepton production by neutrinos have been carried out *via* their decays into electrons or  $\mu^\pm + \pi^\pm$ , which will be discussed here. The search for heavy leptons in the tri-muon events observed in the counter experiments has been discussed by Professor Tittel in the previous talk.

*A. Charged heavy leptons*

Charged heavy leptons  $L^*$  could be seen in neutrino interactions *via* the production and decay processes



1. A search for  $L^*$  using this reaction, looking for events with a single  $e^*$  but no  $pT$ , was carried out by the Columbia-BNL experiment<sup>74</sup> with negative results. Their conclusions are:

(a) Muon type heavy leptons, if they exist, are heavier than:

$$m(L^-) \geq 7.5 \text{ GeV}$$

$$m(L^+) \geq 9.0 \text{ GeV}.$$

(b) The heavy lepton,  $r$  (1.8), discovered at SLAC is *not* muonlike.

(c) Any  $JU-T$  mixing is less than 2 1/2%.

2. Similar searches were carried out by the counter experiments by the CITF<sup>75</sup> and the CDHS<sup>76</sup> groups looking for events with a single  $LC^+$  but no  $\mu$  with negative results. The best limit on the mass of a muon-type

heavy lepton comes from the CDHS experiment

$$m(L^+) \geq 12 \text{ GeV}.$$

No limit is available from these experiments on  $m(L^-)$  since a single  $\mu^-$  signature from  $L^-$  decay cannot be distinguished from the dominant charged current  $\nu_\mu$  interactions.

*B. Neutral heavy leptons*

Several experiments have found evidence suggestive of neutral heavy lepton production by neutrinos. These effects, however, have not been confirmed in other experiments.

1. The Aachen-Padova experiment<sup>77</sup> has reported 7.2:3.7 events of the type  $i^+ + N^- \rightarrow \nu + e^+ + H$ —which they feel are not from charm production but might be due to heavy lepton decays. The rate for this effect is  $(1 \text{ to } 3) \times 10^{-4}$  depending on the  $E_\nu$  cut. This is at the CERN PS with incident neutrino energies of a few GeV.

The Columbia-BNL experiment<sup>78</sup> sees no evidence for such an effect. After cuts to separate  $L^0$  production from charm production in the  $pt \sim e^+$  events (the effects of these cuts are model dependent) set a limit of  $< 2 \times 10^{-4}$  on "non-charmlike"  $\mu \sim c^+$  events that could come from heavy lepton decays. This is at Fermilab energies where the cross section for the production of a light  $L^0$  would be expected to be much higher than at the energies of the Aachen-Padova experiment.

2. A heavy liquid bubble chamber experiment<sup>79</sup> at SKAT at Serpukhov has reported 1 or 2 events of the type  $i^+ + N^- \rightarrow \nu + e^+ + \dots$  where the  $\mu^-$  and the  $e^+$  originate from a common point which is not the neutrino interaction point (*i.e.*, there is a gap between the  $\nu$  interaction point and the beginning of the  $\mu^-$  and the  $e^+$  tracks). The possibility that these events might be due to the decay of a neutral heavy lepton has been suggested. These events are seen in a sample of  $\sim 500$  charged current neutrino interactions.

The Columbia-BNL experiment<sup>86</sup> has observed *no* such events in a sample of  $\sim 80,000$  charged current neutrino interactions.

3. Two experiments<sup>80</sup> in BEBC at the CERN SPS have presented evidence at the Oxford Neutrino Conference earlier this summer for a peak in the  $\nu \rightarrow \tau^+$  mass distribution

near 1.85 GeV in events of the type  $i^+ + N^* \rightarrow Z^0 + \tau^+ + \tau^- + H$ . In a similar sample of events, applying the identical selection criteria as used in the BEBC experiment, the Columbia-BNL experiment<sup>56</sup> at Fermilab sees no such effect with comparable statistics. The effect is also not seen in the BFHSW experiment<sup>81</sup> E-546 in the Fermilab 15 ft chamber. Two other experiments, the BHS (Expt. 172)<sup>82</sup> and the FIIM (Expt. 45)<sup>83</sup> in the Fermilab 15 ft chamber have data relevant to this question. At this conference the BEBC experiment (talk by D.R.O. Morrison) reported that the transverse momentum distribution of the  $TC^+$  from the events in the  $/U \sim K^-$  peak makes the interpretation of this effect as the decay of a heavy lepton unlikely.

In summary then, there appears to be no convincing evidence for either charged or neutral heavy lepton production in neutrino interactions.

#### References

1. F.J. Hasert *et al* (Gargamelle PS): Phys. Letters **46 B** (1973) 138; A. Benvenuti *et al* (HPWF): Phys. Rev. Letters **32** (1974) 800; B. C. Barish *et al* (CITF): Phys. Rev. Letters **34** (1975) 538.
2. S. J. Barish *et al* (Argonne): Phys. Rev. Letters **33** (1974) 448; W. Lee *et al* (CIR): Phys. Rev. Letters **38** (1977) 202.
3. S. Weinberg: Phys. Rev. Letters **19** (1967) 1264; A. Salam: in *Elementary Particle Theory*, ed. by N. Svartholm (Stockholm 1968), p. 367.
4. S. L. Glashow, J. Iliopoulos and L. Maiani: Phys. Rev. **D2** (1970) 1285.
5. F. Reines *et al*: Phys. Rev. Letters **37** (1976) 315.
6. J. Blietschau *et al*: Phys. Letters **73 B** (1978) 232.
7. H. Faissner *et al*: Phys. Rev. Letters **41** (1978) 213.
8. P. Alibrant *et al*: Phys. Letters **74 B** (1978) 422. M. Haguenaer: talk B6-5 at this Conference, and private communication.
9. A. M. Cnops *et al*: Phys. Rev. Letters **41** (1978) 357.
10. J. Blietschau *et al*: Nucl. Phys. **B114** (1976) 189.
11. H. Faissner *et al*: Phys. Rev. Letters **41** (1978) 213.
12. R. Armenise *et al*: Paper submitted to the Oxford Conference on Neutrino Physics, Oxford University (1978).
13. B. Roe *et al*: Paper submitted to the Oxford Conference on Neutrino Physics, Oxford University (1978).
14. M. Haguenaer: Talk no. B6-5 presented at this Conference.
15. H. H. Williams *et al*: Talk no. B5-3 presented at this Conference.
16. P. Sokolsky *et al*: Paper submitted to the Oxford Conference on Neutrino Physics, Oxford University (1978).
17. E. Radermacher: Talk no. B5-2 presented at this Conference.
18. M. Pohl *et al*: Phys. Letters **72 B** (1978) 488.
19. W. Lee *et al* (CIR): Phys. Rev. Letters **38** (1977) 202; T. Hansl *et al* (Aachen-Padova): *Proc. Int. Neutrino Conf.* (Aachen, 1976), p. 278; F. J. Hasert *et al* (Gargamelle); Phys. Letters **59 B** (1975) 485.
20. S. J. Barish *et al*: Phys. Rev. Letters **33** (1974) 448.
21. W. Krenz *et al*: Nucl. Phys. **B135** (1978) 45; O. Erriques *et al*: Phys. Letters **73 B** (1978) 350.
22. S. L. Adler, S. Nussinov and E. Paschos: Phys. Rev. **D9** (1974) 2125; E. H. Monsay: Argonne Rpt. ANL-HEP-PR-78-08 (1978); L. E. Abbott and R. M. Barnett: SLAC-PUB-2136 (1978).
23. S. L. Adler: Ann. Phys. **50** (1968) 189; see also ref. 22.
24. J. Blietschau *et al*: Nucl. Phys. **B118** (1977) 218.
25. P. Wanderer *et al*: HPWF-77/1 (to be publ. in Phys. Rev.).
26. F. S. Merritt *et al*: CALT 68-627 (to be publ. in Phys. Rev.).
27. M. Holder *et al*: Phys. Letters **71 B** (1977) 222; Phys. Letters **72 B** (1977) 254.
28. E. Cazzoli *et al*: Brookhaven Preprint NG-301.
29. P.C. Bosetti *et al*: Phys. Letters **76 B** (1978) 505.
30. J. Marriner: Ph.D. Thesis, LBL Rpt. LBL-6438 (1977).
31. E. A. Paschos and L. Wolfenstein: Phys. Rev. **D7** (1973) 91.
32. P.C. Bosetti *et al*: Phys. Letters **76 B** (1978) 505.
33. N. Fortson: Proceedings of Neutrinos 78, Purdue U. (1978).
34. P. G. H. Sandars: Recent result presented at the RIGA Conference (1978).
35. L. M. Barkov *et al*: Pisma Zh. Eksp. Fiz. (JETP Letters) **26** (1978) 379.
36. M. W. S. M. Brimicombe, C. E. Loving and P. G. H. Sandars: J. Phys. B. L. (1976) 237; E. M. Henley and L. Wilets: Phys. Rev. **A14** (1976) 1411; L.B. Kriplovich: JETP Letters **20** (1974) 315.
37. C. Y. Prescott *et al*: Phys. Letters **77 B** (1978) 347.
38. See ref. 15.
39. See ref. 27.
40. F. S. Merritt *et al*: Preprint CALT-68-600 (1977) 601.
41. M. Holder *et al*: Phys. Letters **72 B** (1977) 254.
42. Aachen-Bonn-CERN-LONDON-Oxford-Saclay Collaboration: paper no. 965, submitted to this Conference.

43. J. J. Sakurai: Invited paper presented at Neutrino-77, Elbrus, USSR, June 1977.
44. L. M. Sehgal: Phys. Letters **71 B** (1977) 99.
45. P. Q. Hung and J. J. Sakurai: Phys. Letters **72 B** (1977) 208.
46. L. F. Abbott and R. M. Barnett: Phys. Rev. Letters **40** (1978) 1303; SLAC Preprint SLAC-PUB-2136 (1978).
47. P. Langacker, D. P. Sidhu, Phys. Letters **74 B** (1978) 233; Phys. Rev. Letters **41** (1978) 732.
48. E. A. Paschos, Brookhaven National Laboratory, preprint no. BNL-24619 (1978).
49. M. Claudson, E. A. Paschos and L. R. Sulak: Paper no. 1158 submitted to this Conference.
50. H. Klutting, J. G. Morfin and W. van Doninck: Phys. Letters **71 B** (1977) 446.
51. A. Benvenuti *et al.*: Phys. Rev. Letters **34** (1975) 419; A. K. Mann: Talk no. B5-5, at this Conference.
52. B. C. Barish *et al.*: Phys. Rev. Letters **36** (1976) 939.
53. M. Holder *et al.*: Phys. Letters **69 B** (1977) 377.
54. J. Blietschau *et al.*: Phys. Letters **60 B** (1976) 207; H. Deden *et al.*: Phys. Letters **67 B** (1977) 474.
55. P. Bosetti *et al.*: Phys. Rev. Letters **38** (1977) 1248.
56. C. Baltay *et al.*: Phys. Rev. Letters **39** (1977) 62; R. B. Palmer *et al.*: Talk no. B6-2 at this Conference.
57. H. C. Ballagh *et al.*: Phys. Rev. Letters **39** (1977) 1650.
58. C. T. Murphy *et al.*: *Proc. XIIIth Rencontre de Moriond* (1977), p. 301.
59. P. Bosetti *et al.*: Phys. Letters **73 B** (1978) 380.
60. Same as ref. 59.
61. O. Erriques *et al.*: Phys. Letters **77 B** (1978) 227.
62. V. Ammosov *et al.*: Paper no. 907 submitted to this Conference.
63. V. Z. Peterson *et al.*: Paper no. 1122 submitted to this Conference.
64. M. Haguenaier: Talk no. B6-5 at this Conference.
65. D. S. Baranov *et al.*: Paper no. 942 presented at this Conference.
66. J. P. Berge *et al.*: Phys. Rev. Letters **38** (1977) 266.
67. H. C. Ballagh *et al.*: Phys. Rev. Letters **39** (1977) 1650.
68. V. Ammosov *et al.*: Paper no. 907 submitted to this Conference.
69. A. Pais, S. B. Triceman: Phys. Rev. Letters **35** (1975) 1206.
70. C. Baltay *et al.*: Phys. Rev. Letters **41** (1978) 73.
71. C. Baltay *et al.*: *Proc. Neutrino 78 Conf.*, Purdue University (1978).
72. V. Ammosov *et al.*: Paper no. 921 submitted to this Conference.
73. M. Holder *et al.*: Phys. Letters **74 B** (1978) 277.
74. A. M. Cnops *et al.*: Phys. Rev. Letters **40** (1978) 144.
75. B. C. Barish *et al.*: Phys. Rev. Letters **32** (1974) 1387.
76. M. Holder *et al.*: Phys. Letters **74 B** (1978) 277.
77. E. Radermacher: Talk 5B-2 at this Conference.
78. C. Baltay *et al.*: *Proc. Neutrino 78 Conf.*, Purdue University (1978).
79. D. S. Baranov *et al.*: Phys. Letters **70 B** (1977) 269; paper no. 942 at this Conference.
80. P. C. Bosetti *et al.*: *Proc. Oxford Neutrino Conf.*, Oxford University (1978).
81. V. Z. Peterson: Private communication.
82. H. Lubatti: Private communication.
83. B. Roe: Private communication.

P8: Theory of Weak Interactions and Models of Elementary Particles

*Chairman:* H. HARARI

*Speaker:* S. WEINBERG

*Scientific Secretaries:* K. FUJIKAWA  
Y. CHIKASHIGE

(Wednesday, August 30, 1978; 9: 00-10: 00)

S. WEINBERG

*Lyman Laboratory of Physics, Harvard University and  
 Harvard-Smithsonian Center for Astrophysics, Cambridge, Massachusetts 02138*

§1. Introduction

I will first offer a very brief review of the charged and neutral current weak interactions, and will then turn to some special topics in weak interaction physics.

§1.1. Charged Currents

We heard a review yesterday by Tittel<sup>1</sup> of the experimental information on the high energy charged-current weak interactions of neutrinos. In brief, everything here is in agreement with expectations based on the parton model and the simple gauge theory.<sup>2</sup>

First, there is no more "high-j anomaly." That is not to say that quantities like  $B = \int dx F_2(x) / F_1(x)$  and  $\langle y \rangle$  are strictly constant, but rather, that there is no evidence for an energy dependence which would not be accounted for by the corrections to scaling predicted by QCD. (I believe that this is a matter on which all groups are now in substantial agreement.) Thus there is no evidence now for a right-handed coupling of the  $u$  or  $d$  quarks to other quarks, and in fact one can use this data to put an upper limit on the strength of any such coupling. Barnett<sup>3</sup> finds in this way that any coupling  $g^0(u, b)$  of the right-handed  $u$  and  $b$  quarks must be less than a tenth of the usual coupling  $g(u, d)$ .

In addition, the total cross sections are behaving as they should. They are linear in neutrino lab energy, up to the highest energies studied ( $\sim 250$  GeV). According to an analysis<sup>4</sup> by the CalTech-Fermilab group, this implies a  $W$  mass greater than about 30 GeV.

Trimuons were also reviewed by Tittel.<sup>1</sup> These  $ipN \rightarrow \nu \mu \nu$  events are now essentially all explained by "conventional" mechanisms, including inner bremsstrahlung of  $p \bar{t} i u \nu$  pairs or associated  $D \bar{D} \nu$  production in  $\nu N \rightarrow p \bar{t} X$  reactions.<sup>5</sup>

Even though the word "nuclear" is no longer in the title of these Conferences, I

thought that I would also say a bit about classic weak interaction phenomena—that is, beta decay and allied low-energy charged current processes. Almost everything that we know about beta decay and allied charged-current processes is incorporated in an effective current-current Hamiltonian

$$\mathcal{H}_{\text{eff}} = \frac{1}{\sqrt{2}} G_F J_\lambda J^{\lambda\dagger} \quad (\text{i})$$

in which the current is the sum of leptonic and  $S=0, 1$  vector and axial-vector hadronic currents

$$\begin{aligned} J_\lambda = & \bar{e} \gamma_\lambda (1 + \gamma_5) \nu_e + \bar{\mu} \gamma_\lambda (1 + \gamma_5) \nu_\mu \\ & + \cos \theta_c [V_\lambda^{J^S=0} + A_\lambda^{J^S=0}] \\ & + \sin \theta_c [V_\lambda^{J^S=1} + A_\lambda^{J^S=1}]. \end{aligned} \quad (\text{2})$$

The hadronic currents are supposed to satisfy the chiral  $SU(3) \times SU(3)$  commutation relations of Gell-Mann; among other things, this fixes the normalization of the currents, and thus allows us to give a precise meaning to the Cabibbo angle  $\theta_c$ . In addition, the currents are supposed to satisfy CVC and PCAC; that is, they are all approximately conserved (nearly exactly for  $J^S=0$ ; rather poorly for  $J^S=1$ ), with the  $\rho$  and  $K$  serving as Goldstone bosons for the spontaneously broken symmetry associated with  $A^{J^S=0}$  and  $A^{J^S=1}$ . Finally, the  $J^S=0$  currents are supposed to be of first class with respect to their G-transformation properties

$$GV_\lambda^{J^S=0} G^{-1} = +V_\lambda^{J^S=0} \quad GA_\lambda^{J^S=0} G^{-1} = -A_\lambda^{J^S=0}. \quad (\text{3})$$

This whole body of classic weak interaction theory is a mathematical consequence of QCD plus the simple gauge theory of weak and electromagnetic interactions. In this framework, the gauge symmetry dictates that the  $W$  couples to the currents  $e_l (1 + f_s K) \gamma_\lambda (1 + \gamma_5) \nu_l$  and  $(d \cos \theta_c - s \sin \theta_c) j_\lambda + r s K$  just as gauge invariance in QED tells us that  $A_\lambda$  couples to  $e_l \bar{e}_l$ . The properties of these currents can

then be worked out by direct calculation, and one finds that they must satisfy all the established conservation, commutation, and  $G$ -conjugation rules. Thus, there continue to be deep connections between the classic part of weak interaction theory and high energy physics.

One aspect of classic weak interaction theory that has been studied experimentally in the last few years is the  $G$ -conjugation property of the axial-vector current. First-class terms in  $A_j^{i0}$  give nucleon matrix elements proportional to  $y_N$  or  $y_q$  (where  $q=k,-k$ ) while any second-class terms would give a matrix element of the induced-pseudotensor form  $i y_i(J_s g)$ . The conclusion reached on the basis of this experimental study is that there is no evidence for second-class currents, and good evidence that any second-class terms in the axial current must be quite small.<sup>6</sup> As a spin-off to this work, additional confirmation has also been found that "weak magnetism" has the value predicted by CVC.<sup>7</sup>

The absence of an induced pseudotensor term  $j^{\wedge}q^{\wedge}$  in the nucleonic matrix element of the axial-vector current is a nice counterpart to the very well known absence of an intrinsic Pauli moment term  $o_x q^r$  in the leptonic matrix element of the electromagnetic current, which would destroy the agreement between theory and experiment for  $g-2$  values in quantum electrodynamics. In both cases these terms would be allowed by current conservation, but are ruled out by the constraint of renormalizability, at least (for second-class currents) in the absence of strongly interacting scalar fields. The same reasoning also rules out any Konopinski-Uhlenbeck derivative coupling terms in the leptonic part of the weak current.

The current-current Hamiltonian (1) contains specific non-leptonic terms, but the difficulty of calculating effects of strong interactions at low energy has so far precluded quantitative calculations of non-leptonic weak processes. In particular, the  $AI=\sqrt{2}$  rule is not yet satisfactorily understood. Attention has recently focussed<sup>8</sup> on a previously neglected term of the form  $(s y_x T_a d) d F_i$  in the operator product expansion of two charged currents. (Here  $F_i$  is the Yang-Mills curl of the gluon field, and  $r_a$  is the color  $SU(3)$  generator.)

This is a pure  $AI=1/2$  term, but it remains to be seen whether its matrix elements are sufficiently enhanced to account for the  $JI=1/2$  rule.

## §HL Neutral Currents

Baltay<sup>9</sup> gave a comprehensive summary here of the experimental data on neutral currents, and its comparison with the gauge theory. There is not much that I need to add, and I will only make some disconnected remarks.

Our most detailed experimental information on neutral current weak interactions comes from data on  $\nu N$  and  $\bar{\nu} N$  reactions, including inclusive reactions  $\nu N \rightarrow \nu X$ ,  $\bar{\nu} N \rightarrow \bar{\nu} X$ ,  $\nu p \rightarrow \nu X$ ,  $\bar{\nu} p \rightarrow \bar{\nu} X$  elastic scattering  $\nu p \rightarrow \nu p$ ,  $\bar{\nu} p \rightarrow \bar{\nu} p$  semi-inclusive reactions  $\nu N \rightarrow \nu n X$ ,  $\bar{\nu} N \rightarrow \bar{\nu} n X$ , and exclusive reactions  $\nu N \rightarrow \nu n n$ ,  $\bar{\nu} N \rightarrow \bar{\nu} n n$ . It has been clear for more than a year now that the empirical cross sections for these reactions are in good agreement with the predictions of the simple gauge theory, and recent data has further improved the precision of the agreement here between theory and experiment.<sup>10</sup>

The data on neutrino-electron reactions is less precise than for neutrino-nucleon reactions, because at any given lab energy above a few GeV, the cross sections are smaller by a factor  $m_e/m_p$ . Within the experimental uncertainties, data on  $\nu e$ ,  $\bar{\nu} e$ , and  $\nu e$  scattering has for some time all been in agreement with the simple gauge theory. This spring, the Gargamelle group for a while observed an unexpectedly large rate of  $\nu e$  events, but some of these events have been withdrawn; the large event rate did not appear in analyses of further samples of Gargamelle data; and a much larger data sample of the Columbia-BNL group gave a  $\nu e$  cross section in good agreement with the simple gauge theory. As indicated here by Baltay,<sup>9</sup> an average of all data on  $\nu e$  scattering, including that from Gargamelle, gives a cross section of  $(1.7 \pm 0.5) \times 10^{-42} \text{ cm}^2/\text{GeV}$ , in excellent agreement with the gauge theory prediction of  $1.5 \times 10^{-42} \text{ cm}^2/\text{GeV}$ .

The electron-nucleon neutral currents have been difficult to study experimentally, because electrons interact with nucleons electromagnetically, so that one must look for effects that are characteristic of the weak interactions, and in particular, for a parity violation. The

first round of experiments on bismuth at Oxford and Seattle set upper limits on the optical rotation that were well below the level expected on the basis of the original atomic calculations using the simple gauge theory. However, subsequent atomic calculations revealed significant shielding corrections, leading to a large reduction in the theoretically expected circular polarization. Then the experimental situation itself became unclear, when the Novosibirsk group reported a circular polarization in bismuth in disagreement with the limit set at Oxford for the same frequency, but in agreement with the theoretical results as calculated by Novikov *et al* in the gauge theory. At this Conference, we have heard an indirect report from the Riga Conference that the Oxford group are now observing a parity violation of the expected sign, and some three standard deviations above zero, but still in disagreement with that seen at Novosibirsk.<sup>11</sup>

On the basis of this experience, even if one did not know of the specific gauge theory predictions, one could only conclude that experiments on heavy atoms like bismuth may be a good way to learn about heavy atoms, but they are not a good way to learn about neutral currents. The conflict between the experimental values of the circular polarization reported from Oxford and Novosibirsk shows that these are hard experiments, subject to systematic errors that are difficult to eliminate. And even if the experimental conflict is resolved, there is still the formidable difficulty of calculating the circular polarization to be expected in a complicated atom like bismuth, for which theoretical results have already changed by more than a factor of two.<sup>12</sup> Fortunately, this is a problem that may now be left to the atomic physicists to settle at their leisure, because a far cleaner way has been found to determine the electron-nucleon neutral current interaction, in high energy collisions of polarized electrons with nucleons.

The deep inelastic cross sections for  $eN \rightarrow eX$  with left- or right-handed electrons striking an isoscalar target differ by a fractional amount, given in the simple gauge theory as<sup>33</sup>

$$A \equiv \frac{\sigma_R - \sigma_L}{\sigma_R + \sigma_L} = -\frac{9G_F q^2}{20\sqrt{2}\pi\alpha}$$

$$\times \left[ 1 - \frac{20}{9} \sin^2 \theta + (1 - 4 \sin^2 \theta) \left( \frac{1 - (1-y)^2}{1 + (1-y)^2} \right) \right] \quad (4)$$

This asymmetry has now been measured in deuterium by a SLAC-Yale experiment, described here by Taylor.<sup>13</sup> At  $j=0.21$ , they find  $A^2 = (-9.5 \pm 1.6) \times 10^{-5} \text{ GeV}^{-2}$ . This result puts it beyond doubt that parity is violated in the neutral currents, and is quantitatively in good agreement with the simple gauge theory prediction (4), which, for values of  $\sin^2 \theta$  in the range 0.20 to 0.25 indicated by  $\nu N$  and  $\nu IV$  data, yields a theoretical value for  $A/q^2$  in the range  $(-9.7 \text{ to } -7.2) \times 10^{-5} \text{ GeV}^{-2}$  at  $j=0.21$ . A parity violation was also found in hydrogen, with a value also in agreement with theoretical expectations, but with a larger experimental uncertainty.

Apart from the gauge theory itself, the only theoretical input needed in deriving eq. (4) is the use of the parton model. Experience with deep inelastic electron and neutrino scattering at similar values of  $q^2$  and  $y$  suggests that the parton model should work well here. Nevertheless, it is of interest to judge theoretically how much of the parton model is actually needed here. This has been clarified by a recent analysis by Wolfenstein.<sup>14</sup>

First, note that the asymmetry consists of two terms  $A_{AV}$  and  $A_{VA}$ , with  $A_{AV}$  arising from the product of the axial-vector electron current and the vector nucleon current, and  $A_{VA}$  from the product of the vector electron current and the axial vector nucleon current. In the parton model, the term in (4) proportional to  $1 - (20/9) \sin^2 \theta$  gives  $A_{VA}$ , and the remaining term proportional to  $1 - 4 \sin^2 \theta$  gives  $A_{AV}$ . Now, without using the parton model, we know that  $A_{VA}$  vanishes at  $y=0$ , and vanishes for all  $y$  in the simple gauge theory if  $\sin^2 \theta = 1/4$ . As it happens, the SLAC-Yale experiment was carried out at a low value of  $y$ ,  $y=0.21$ , and we know that  $\sin^2 \theta$  is rather close to  $1/4$ , so in the simple gauge theory  $A_{VA}$  is expected to make a relatively small contribution to  $A$ . (In the parton model, at  $y=0.21$  and  $\sin^2 \theta=0.20$ , the  $A_{VA}$  term in eq. (4) contributes only 8% of the total asymmetry.) Thus, it would not matter if the use of the parton model did introduce rather large errors in  $A_{VA}$ ; the error introduced in  $A$  would still be



small.

The  $AV$  term in  $o_n - a_L$  involves an interference of the electromagnetic  $J_e \cdot J_N$  interaction with the  $A_e \cdot V_N$  weak neutral current interaction. The electromagnetic and weak neutral hadronic vector currents of the simple gauge theory are

$$J_\mu^{em} = \sum_n q_n \bar{Q}_n \gamma_\mu Q_n$$

$$V_\mu^{WK} = \sum_n q_n^Z \bar{Q}_n \gamma_\mu Q_n$$

with sums running over quark flavors, and

$$q_u = 2/3, \quad q_s = q_d = -1/3$$

$$q_u^Z = 1/2 - 4/3 \sin^2 \theta, \quad q_s^Z = q_d^Z = -1/2 + 2/3 \sin^2 \theta.$$

The  $AV$  term in  $o_n - G_L$  then takes the form

$$(\sigma_R - \sigma_L)_{AV} = -(2G_F/\sqrt{2})(e^2/q^2) \sum_{nm} q_n q_m^Z F_{nm}$$

where  $F_{nm}$  is a structure function appearing in the Fourier transform of the target expectation value of the product of the vector currents of the  $n$ th, and  $m$ th quarks. The same structure functions appear in the total  $eN$  cross section

$$\sigma_R + \sigma_L = (e^2/q^2)^2 \sum_{nm} q_n q_m F_{nm}.$$

The parton model would give  $F_{mm} = 0$  for  $ni = -m$ , because the collision of electrons with different quarks is supposed to lead to orthogonal final states. Of course, this is just an approximation, because recoiling quarks of different type *can* assemble themselves into the same final states, but it is a reasonable conclusion to abstract from any sort of parton model. In addition, the parton model suggests that for nuclear targets, we may neglect  $F_{nn}$ . With these two assumptions, the  $AV$  part of the asymmetry is

$$A_{AV} = A_0 \left[ \frac{q_u q_u^Z F_{uu} + q_d q_d^Z F_{dd}}{q_u^2 F_{uu} + q_d^2 F_{dd}} \right]$$

$$- A_0 \equiv 2G_F q^2 / (\sqrt{2} e^2) = G_F q^2 / (2\sqrt{2} \pi \alpha).$$

(5)

For scattering on an isoscalar target  $F_{nn} = F_{\bar{n}\bar{n}}$ , so without further use of the parton model Wolfenstein finds

$$A_{AV}^{(d)} = A_0 \left[ \frac{q_u q_u^Z + q_d q_d^Z}{q_u^2 + q_d^2} \right] = A_0 \left[ \frac{9}{10} - 2 \sin^2 \theta \right]$$

(6)

in agreement with eq. (4). On the other hand, for a proton target we need to use the parton model to estimate  $F_{nn} \sim 2F_{\bar{n}\bar{n}}$ ; Equation (5) gives in this case

$$A_{AV}^{(p)} = A_0 \left[ \frac{2q_u q_u^Z + q_d q_d^Z}{2q_u^2 + q_d^2} \right] = A_0 \left[ \frac{5}{6} - 2 \sin^2 \theta \right].$$

(7)

Finally, the neutral currents also contribute to a parity violation in the nucleon-nucleon interaction.<sup>15</sup> Unfortunately, even apart from the problems of dealing with complex nuclei, the difficulty of calculating soft gluon effects makes it impossible to predict the parity violation in  $NN$  or  $nN$  interactions that should be expected in the gauge theory.<sup>16</sup>

In all of the large number of cases where a comparison can reliably be made between theory and experimental data on charged and neutral current weak interactions, the results are found to confirm the simple gauge theory. It has been clear at this Conference that the simple gauge theory is in fact the correct theory of these interactions. In what follows, this theory will be used as a basis for the discussion of some topics of current interest in the physics of weak interactions.

#### §IV. New Leptons and Quarks

This section will deal with the weak interactions of the newest particles: the  $r$  lepton,  $b$  quark, and further leptons and quarks.

##### 1. $r$ Lepton<sup>19</sup>

The simplest assumption is that the  $r$  lepton is a "sequential" lepton; that is, that  $e^-$ ,  $\nu_e$ ,  $\mu^-$ , and  $\nu_\mu$  are in three left-handed  $SU(2) \times U(1)$  doublets

$$\begin{bmatrix} \nu_e' \\ e^- \end{bmatrix}_L, \quad \begin{bmatrix} \nu_\mu' \\ \mu^- \end{bmatrix}_L, \quad \begin{bmatrix} \nu_\tau' \\ \tau^- \end{bmatrix}_L \quad (8)$$

The primes indicate that if neutrinos have masses, then the  $\nu'$  are in general linear combinations of particles of definite mass. It has been pointed out<sup>17</sup> that the existence of a third neutrino is strongly indicated by the non-observation of the neutral-current processes  $r \rightarrow eee$ ,  $ee/u$ ,  $efi/u$ , or  $ju/iju$ . [If there were no  $r$  neutrino, then  $e^-$ ,  $\nu_e$ , and  $r^-$  would have to be in doublets with linear combinations of  $\nu_e$  and  $\nu_e r$  and mixing effects would give a total branching ratio for  $r \rightarrow eee$ , etc. of at least 5%, in contrast with an experimental upper limit of 1/2%.]

If the neutrinos are all massless, then the numbers of  $e$ ,  $ju$ , and  $r$ -type leptons are all

separately conserved. This is consistent with the observed absence<sup>60</sup> of processes like  $\nu^N \rightarrow r + X$ . As to direct measurements, we know that the neutral particles emitted in  $r$  decay are lighter than a few hundred MeV. Fritzsche<sup>18</sup> has pointed out that this leaves open the possibility that  $\nu_r$  is heavier than  $r$ , and that  $r$  decays by mixing effects into channels like  $\nu_i \bar{d}$ ,  $\nu_i \bar{u}$ ,  $\nu_i \bar{e}$ , etc., but in order to keep the mixing angles sufficiently small to be consistent with muon conservation and universality, the  $T$  would have to be rather long-lived. However, the observed limits on the  $r$  lifetime now rule out this possibility, so that the  $r$  neutrino is lighter than a few hundred MeV, and the  $r$  does decay into  $\nu_r$ .

The observed properties of  $r$  decay are all consistent with the simple picture that  $(\nu_r, r)_L$  forms a third  $SU(2) \times U(1)$  doublet. Measurements of the Michel parameter by the DELCO, SLAC-LBL, and PLUTO groups indicate a  $V$  minus  $A$  matrix element. Also, all  $r$  decay branching ratios are now in good agreement with theoretical expectations. In particular, the  $n \rightarrow \nu_r$  mode which seemed to be missing last summer is now observed to have a branching ratio compatible with the theoretical value.

The semileptonic modes  $r \rightarrow \nu X$  have been the subject of a number of recent papers,<sup>20</sup> including several submitted to this Conference. With  $(y, z)_L$  an  $SU(2) \times U(1)$  doublet, the differential rate for these modes is

$$\frac{d\Gamma(\tau \rightarrow \nu_r X)}{dQ^2} = \frac{G_F^2 \cos^2 \theta_c (m_\tau^2 - Q^2)^2 (m_\tau^2 + Q^2)}{32\pi m_\tau^3} \frac{1}{Q^2} \times [\rho_V(Q^2) + \rho_A(Q^2)] \quad (9)$$

where  $Q$  is the total energy of the hadrons "X" in their own center-of-mass system, and  $P_{V,A}(Q^2)$  &  $VZ$  the spectral functions of the vector and axial-vector currents of beta decay. In the "PCAC limit"  $m_u = m_d = 0$  of QCD, these functions satisfy the two spectral-function sum rules

$$\int [\rho_V - \rho_A] dQ^2 / Q^2 = F_\pi^2 \simeq (190 \text{ MeV})^2 \quad (10)$$

$$\int [\rho_V - \rho_A] dQ^2 = 0 \quad (11)$$

while  $\int \rho_V dQ^2$  diverges. When I discussed these sum rules at the Vienna "Rochester" Conference ten years ago, it was clear

that  $p(Q^2)$  could be measured from the rate  $e^+e^-$  annihilation into hadrons, but we could only dream of being able to measure  $p_A(Q^2)$ . Now, using  $r$  decay and eq. (9), we should be able to determine  $p_A$  as well as  $p_V$  from  $g^2 = ml$  to  $Q^2 = m_r^2$ . (To the extent that strange particles can be neglected, we can even determine  $p_V$  and  $p_A$  separately without using  $e^+e^-$  annihilation;  $p_V$  and  $p_A$  receive contributions only from states with even or odd numbers of pions, respectively.) At the present time the data only allows us to test a resonance-saturated form of eqs. (10) and (11); this yields<sup>20</sup> a branching ratio of 0.09 for  $T \rightarrow A \nu_r$ , in good agreement with the observed value of  $0.10 \pm 0.03$ .

## 2. $b$ Quarks<sup>\*</sup>

Though not definitely established, it seems reasonable to assume that the  $7^*(9400)$  and  $r'(10000)$  are bound states of a new quark of charge  $-1/3$  and its antiquark. The simplest assumption is that this  $b$  quark forms part of a third left-handed  $SU(2) \times U(1)$  doublet. As first described by Kobayashi and Maskawa,<sup>21</sup> the three quark doublets may be written as

$$\begin{bmatrix} u \\ d' \end{bmatrix}_L, \begin{bmatrix} c \\ s' \end{bmatrix}_L, \begin{bmatrix} t \\ b' \end{bmatrix}_L$$

where  $w, c,$  and  $t$  are quarks of definite mass and charge  $2/3$ , and  $d, s$  and  $b'$  are linear combinations of quarks of definite mass and charge  $-1/3$ :

$$\begin{aligned} d' &= C_1 d - S_1 C_3 s - S_1 S_3 b \\ s' &= S_1 C_2 d + (C_1 C_2 C_3 - S_2 S_3 e^{i\delta}) s \\ &\quad + (C_1 C_2 S_3 + S_2 C_3 e^{i\delta}) b \\ b' &= S_1 S_2 d + (C_1 S_2 C_3 + C_2 S_3 e^{i\delta}) s \\ &\quad + (C_1 S_2 S_3 - C_2 C_3 e^{i\delta}) b \end{aligned} \quad (12)$$

$$C_i \equiv \cos \theta_i \quad S_i \equiv \sin \theta_i \quad i=1, 2, 3$$

There is here a possibility that  $CP$  violation may be due to the complex phase  $e^{i\delta}$ , which for six quarks cannot be absorbed in a redefinition of the quark fields.

The mixing angles are constrained in various ways. From the success of the universality relations among leptonic and  $\Delta S=0, 1$  semileptonic decays, we know that  $S_1$  is essentially the sine of the Cabibbo angle  $\theta_c$ , and that  $S_3$  must be fairly small. Ellis, Gaillard, and Nanopoulos<sup>22</sup> have estimated that  $|S_3| \leq 0.24$ . More recently, on the basis of a new analysis

of universality relations, Shrock and Wang<sup>23</sup> have given a value  $|S_3| = 0.28$ . From the success of the Gaillard-5. Lee estimate<sup>24</sup> of the  $c$  quark mass from  $m(K^0) - m(K^+)$ , Ellis *et al*<sup>25</sup> estimate that  $|\xi_2| < 0.4$ . From experimental upper bounds on the reaction  $\nu_{\mu} + \mu \rightarrow \nu_e + e$ , Barnett<sup>3</sup> estimates that  $|\xi_1| < 0.3$ . Finally, if it is really true that  $CP$  violation arises from the phase angle  $\delta$ , then the observed rate of  $K_L \rightarrow \pi^0 \nu \bar{\nu}$  would indicate that<sup>25</sup>

$$|S_2 S_3 \sin \delta| \simeq 10^{-3}. \quad (13)$$

These estimates have important implications for the decay of hadrons containing the assumed  $Z$ -quark. Quigg and Rosner estimate the decay rates<sup>26</sup>

$$\Gamma(b \rightarrow uX) \approx S_1^2 S_3^2 / 1.3 \times 10^{-15} \text{ sec} \quad (14)$$

$$\Gamma(b \rightarrow cX) \approx |C_1 C_2 S_3 + S_2 C_3 e^{i\delta}|^2 / 4 \times 10^{-15} \text{ sec}. \quad (15)$$

If the observed  $CP$  violation does arise from  $\delta$ , then (13), (14), and (15) yield a bound on the total  $b$  decay rate

$$\Gamma(b) \geq 2 \times 10^{-11} \text{ sec}^{-1} \quad (16)$$

At present, all we know about  $b$  decay is that tracks of "bottom" particles are not seen at Fermilab,<sup>27</sup> so that if the cross section for producing these particles is comparable to that for the  $T$ , then their lifetime must be shorter than about  $5 \times 10^{-12}$  sec. Thus we do not yet know if  $b-d$  or  $b-s$  mixing is strong enough to account for the observed violation of  $CP$ .

In connection with the use of universality here, this is a good place to mention the work of Sirlin on radiative corrections.<sup>28</sup> In the Fermi theory of beta decay, photon exchange between protons and electrons would produce an ultraviolet divergence. This problem is cured in the gauge theory, for both  $j$  and  $Z^0$  exchange, by the natural ultraviolet cut-off provided by the  $j$  and  $Z^0$  masses. With  $m_c \sim 90$  GeV and a mean quark charge  $Q = 1/6$ , Sirlin finds a radiative correction of 3.4% to the ratio of the  $\Lambda^0$  and  $\Lambda^+$  decay rates, which yields a value of  $\sin \delta_c$  of 0.224, in good agreement with the values 0.22 to 0.23 derived from  $K_s$  and hyperon decay for small  $S$ . This radiative correction plays an essential role in checking universality; without it, the value of  $\sin \delta_c$  derived from  $\Lambda^0$  and  $\Lambda^+$  decay rates would be about 0.13! In his recent work, Sirlin has

been able to use current algebra to avoid the complications due to strong interactions in these calculations.

### 5. More neutrinos!

We do not know of any fundamental physical principle which determines the number of quark or lepton flavors, but at least it is possible to put experimental limits on the numbers of neutrino species. These limits are of two types, cosmological and terrestrial. In both cases, the limits exploit the property of neutral currents, that the  $Z^0$  couples equally to all types of neutrino, no matter how heavy are the charged leptons with which they are associated.

The cosmological limit arises from considerations of helium synthesis. If there had been a large number of neutrino flavors present during the first few seconds, then the energy density would have been greater, so the universe would have been expanding faster, less time would have been available for neutrons to turn into protons, and hence more helium would have been formed at the end of the first three minutes. In this way, Steigman, Schramm, and Gunn<sup>29</sup> find that for a cosmological helium abundance  $< 26\%$ , there cannot be more than 3 to 4 neutrino flavors.

It is important to be clear as to what particles are included as "neutrinos" in the above limit. The relevant particles are those which would have been about as abundant as  $\nu_e$ 's or photons during the first few seconds, when the temperature was above about 300 keV, and most of the conversion of neutrons into protons is believed to have taken place. Such particles can be of either of two exclusive types:

(a) Particles whose collision rate became less than the cosmic expansion rate at a "freezing" temperature  $T^* > 300 \text{ keV}$ . In this case, it is necessary that  $T^*$  be less than about 100 MeV to 1 GeV, because the annihilation of hadrons and muons at temperatures between 1 GeV and 100 MeV raised the temperature of the other particles ( $\gamma$ ,  $e^-$ ,  $e^+$ ,  $\nu_e$ , etc.), so that any particle that had frozen out of equilibrium before this annihilation occurred would afterwards have made a relatively small contribution to the total energy density. It is also necessary that these particles be massless or

have masses  $m < T^*$ , so that they would have been as abundant as photons and ordinary neutrinos when they froze out of equilibrium. Finally, it is necessary that they be stable or have lifetimes longer than a few seconds, so that they would have survived until  $n \rightarrow p$  conversion occurred.

(b) Particles whose collision rate remained greater than the cosmic expansion rate at least until the temperature dropped below about 300 keV. In this case, it is necessary that the particles have masses below about 300 keV, so that they would have been about as abundant as photons and ordinary neutrinos at the time of  $n \rightarrow p$  conversion. However, they could have any lifetime.

For instance, gravitons are not counted in the limit on "neutrino" types, because they froze out of thermal equilibrium very early, long before the ordinary hadrons and leptons began to annihilate. Semi-weakly-interacting particles could fall in category (b) if their mass is below 300 keV.

The known neutrinos  $\nu_e, \nu_\mu, \nu_\tau$  fall in category (a), because they all froze out of thermal equilibrium at  $T^* \sim 1$  MeV. (Even though it was much too cold then to allow charged current processes like  $\nu_e e \rightarrow \nu_e e$  or  $\nu_e e \rightarrow \nu_e e$ , thermal equilibrium would have been maintained down to  $T \sim 1$  MeV by neutral current processes like  $\nu_e e \rightarrow \nu_e e$ .) Note that if right-handed neutrinos existed, then they too would have to be included in the upper limit on neutrino flavors.<sup>30</sup> The only exception would be if they froze out of equilibrium at a temperature  $T^* > 100$  MeV to 1 GeV. The neutrino collision rate varies as  $T^5$ , while the cosmic expansion rate varies as  $t^2$ , so in order for neutrinos to have frozen out of equilibrium at  $T^* = 100$  MeV to 1 GeV instead of  $T^* = 1$  MeV, it could be necessary for their cross sections to be about  $10^6$  to  $10^9$  times smaller than usual. Putting aside this possibility, the cosmological upper limit on the number of neutrino flavors already makes it unlikely that there are right- as well as left-handed neutrinos.

There are also limits on the number of neutrino types, provided by purely terrestrial experiments. These limits again use the fact that the  $Z^0$  couples equally to all neutrino species, irrespective of how heavy the associated

charged leptons may be. Thus the rate for a neutral current transition  $A \rightarrow B \nu \bar{\nu}$  is proportional to the total number  $N_\nu$  of neutrino flavors, and may approach empirical limits if this number is large. For instance, Ma and Okada<sup>31</sup> estimate that the ratio of the rates for  $e^+ e^- \rightarrow \nu \bar{\nu}$  and  $e^+ e^- \rightarrow 3\gamma$  is of order  $(G_F^2 s^2 / \alpha^2 x^2) N_\nu$ , or  $2 \times 10^{-3} N_\nu$  for  $J_s = 10$  GeV. An upper limit of 10% on this ratio would set a limit  $N_\nu < 50$  on the number of neutrino flavors. Similarly, we could imagine sitting on the  $Y'$  resonance at PETRA, CESR, or PEP, and looking for the decay chain  $Y' \rightarrow Y \nu \bar{\nu}$ ,  $Y \rightarrow V \nu \bar{\nu}$ . The ratio of  $Y' \rightarrow \nu \bar{\nu}$  and  $Y' \rightarrow e^- e^+$  can be estimated as<sup>32</sup>

$$\frac{\Gamma_{Y' \rightarrow \nu \bar{\nu}}}{\Gamma_{Y' \rightarrow e^- e^+}} = \frac{9G_F^2 m_{Y'}^4 N_\nu}{16\pi^2 \alpha^2} \left[ \frac{1}{2} + \frac{2}{3} \sin^2 \theta \right]^2 \simeq 1.2 \times 10^{-4} N_\nu \quad (17)$$

This does not appear very useful as a means of providing a limit on  $N_\nu$ , but it might be more promising for bound states of even heavier quarks. At any rate, it is nice to know from the fact that  $\nu \bar{\nu}$  emission does not dominate over electromagnetic processes that there is *some* upper limit on the number of neutrino flavors.

### §V. Scalar Fields

Up to this point, I have left open the question of the number of doublets of scalar fields. No matter how many doublets there are, one still gets the same successful formula  $m_Z = m_j \cos \theta$  for the mass of the  $Z^0$ , which sets the scale of neutral current coupling strengths. The phenomenological differences between having one scalar doublet or several scalar doublets are more subtle; this section will deal with some of them.

#### (a) Higgs spectrum

For one scalar doublet, there is just one physical Higgs boson, a neutral particle  $H^0$ . For  $N$  scalar doublets, there are  $4N-3$  physical Higgs bosons, of which  $2N-2$  have charges  $\pm 1$ , and  $2N-1$  are neutral.

#### (b) Higgs masses

For one scalar doublet, vacuum stability sets a lower bound on the Higgs boson mass<sup>34</sup>

$$m_H > \frac{\alpha}{\sin^2 \theta} \left[ \frac{3(2 + \sec^4 \theta)}{16\sqrt{2} G_F} \right]^{1/2} \quad (18)$$

For  $\sin^2 \theta$  in the range of 0.20 to 0.25, this

lower bound is in the range of 7.4 to 6.1 GeV. With several scalar doublets, (18) only gives a lower bound on the mass of the *heaviest* Higgs boson; in fact if the scalar part of the Lagrangian happened to have an "accidental" symmetry which is not shared by the Yukawa couplings, then the corresponding pseudo-Goldstone Higgs boson would be quite light. Whether there is one or several scalar doublets, the Higgs boson masses must be below about 1 TeV in order to keep scalar self couplings weak.<sup>35</sup> If the Lagrangian is scale invariant, then for one scalar doublet the  $H^0$  has a mass given by  $\lambda T$  times the expression (18),<sup>36</sup> and even for arbitrary numbers of scalar doublets, there is one neutral boson, the "scalon," with the same mass.<sup>37</sup> Aside from this, it seems reasonable to expect that Higgs bosons generally have masses comparable to intermediate vector boson masses,<sup>38</sup> and in fact the Higgs bosons might be confused for  $W$ 's or  $Z$ 's in the first round of experiments on  $W$  or  $Z$  production.

(c) *CP and lepton flavor nonconservation*

For one scalar doublet, the Higgs couplings are uniquely given by the Lagrangian

$$\mathcal{L}_H = 2^{1/4} G_F^{1/2} H^0 \sum m \bar{\psi} \psi \quad (19)$$

the sum running over lepton and quark fields  $\psi$  of definite mass  $m$ . This coupling conserves  $C$ ,  $P$ ,  $T$  and all lepton and quark flavors, so effects of virtual Higgs bosons would be very difficult to detect. In particular, with massless neutrinos and one scalar doublet the simple gauge theory would automatically conserve all lepton flavors, so that processes like  $(i \rightarrow e \gamma)$  would be forbidden. Also, with one scalar doublet, the only mechanism in the simple gauge theory for  $CP$  violation is the complex phases in the quark mixing matrix, such as  $\delta$  in eq. (12), and in consequence the neutron electric dipole moment would be very small, of order  $10^{-30}$  ecm.<sup>22</sup> On the other hand, for several scalar doublets the Higgs couplings can be quite complicated, and could violate  $C$ ,  $P$ ,  $T$ , and/or flavor conservation. (However, the "scalon" mentioned above would have the same interaction (19) as in the case of one scalar doublet.) The violation of  $CP$  by Higgs boson exchange<sup>39</sup> is naturally "milliweak," and would give the neutron an electric dipole moment<sup>39,40</sup> of order  $10^{-24}$  ecm

to  $10^{-25}$  e cm. (The present experimental limits are  $(0.4 \pm 1.1) \times 10^{-24}$  e cm<sup>41</sup> and  $(0.4 \pm 0.75) \times 10^{-24}$  e cm.<sup>42</sup>) With several scalar doublets, Higgs exchange could produce lepton-flavor non-conserving processes. The present experimental limits on these processes are (at the 90 % confidence level):

$$\frac{\mu \rightarrow e \gamma}{\mu \rightarrow e \nu \bar{\nu}} < 3.6 \times 10^{-9} \quad \text{TRIUMF}^{43}$$

$$< 1.1 \times 10^{-9} \quad \text{SIN}^{44}$$

$$< 2.0 \times 10^{-10} \quad \text{LAMPF}^{45}$$

$$\frac{\mu N \rightarrow e N}{\mu N \rightarrow \nu X} < 1.6 \times 10^{-8} \quad \text{Ref. 46}$$

$$< 1.5 \times 10^{-10} \quad \text{SIN}^{47}$$

$$\frac{\mu \rightarrow 3e}{\mu \rightarrow e \nu \bar{\nu}} < 1.9 \times 10^{-9} \quad \text{Ref. 48}$$

(The phenomenology of other  $\mu \rightarrow e$  processes has been studied by Kakh.<sup>49</sup>) From these limits we can conclude either that there is only one scalar doublet, or that there is some selection rule which only allows one scalar doublet to couple to all the leptons, or that Higgs bosons are very heavy (above about 200 GeV), or that muon conservation is a fundamental symmetry principle.

In discussing  $CP$  violation, I have not taken into account the problem raised in QCD by instantons. I reviewed this in detail in my talk at the Neutrinos '78 Conference,<sup>50</sup> so I will not go into it further here.<sup>51</sup>

## §VL Grand Unified Theories

There is no experimental motivation for a gauge group of weak and electromagnetic interaction larger than  $SU(2) \times U(1)$ . Also, everything indicates that the strong interactions are described by QCD, with a gauge group  $SU(3)$ . But even though there is no experimental evidence for anything beyond  $SU(2) \times U(1) \times SU(3)$ , it is attractive to suppose that the weak electromagnetic and strong interactions are joined in a grand unified theory, based on a simple<sup>52</sup> gauge group  $G$ , which contains  $SU(2)$ ,  $U(1)$ , and  $SU(3)$  as subgroups. The larger group structure might fix those physical parameters that are still left free by  $SU(2) \times U(1) \times SU(3)$ . In a grand unified theory, the spontaneous breakdown of  $G$  into  $SU(3) \times SU(2) \times U(1)$  would be much stronger<sup>53</sup> than the breakdown of  $SU(2) \times U(1)$  into the

U(1) of electromagnetism, and hence the gauge bosons "X" associated with those generators of G that are outside the algebra of SU(3) x SU(2) x U(1) would be very heavy, with  $m_X \gg m_e$ . These superheavy gauge bosons would mediate a new class of "hyperweak" interactions, with effective couplings weaker than the usual weak interactions by factors  $m_e/m_X$ . The topic of grand unification was assigned to Salam's talk,<sup>54</sup> so I will only touch on some general aspects of the subject here.

An immediate question is, how large is the mass  $m_X$  of the superheavy gauge bosons of G? For a simple group, the couplings should all become equal (up to group theoretic factors of order unity) if measured at energies of order  $m_X$ . At ordinary energies, the strong coupling  $g_s$  is of course much larger than the "electroweak" couplings  $g$  or  $g'$  but it decreases logarithmically with the energy at which it is measured, so it can become of order  $g, g'$  at a very high energy. Hence  $m_X$  is expected to be quite large. Estimates in various sorts of grand unified gauge theory range from a "low" value<sup>55</sup>  $m_X \sim 10^4$  GeV up to<sup>56</sup>  $m_X \sim 10^{16}$  GeV, and beyond. In any case, it is clear that the hyperweak interactions will be very weak indeed, and may not be detectable at all.

As already mentioned, the larger group structure of a super-unified gauge theory might serve to fix some of the physical quantities which are at present free parameters. For instance

(a)  $Z^0$ -j mixing angle

A simple<sup>52</sup> grand unified gauge group can have only one free coupling parameter, so the ratio  $\tan \theta = g'/g$  is fixed. However, the group structure fixes this ratio at energies of order  $m_X$ ; at ordinary energies,  $\tan \theta$  is subject to very large renormalization effects. In one estimate,<sup>56</sup> with the best present value of  $g$ , the corrected value of  $\sin^2 \theta$  is 0.20.

(b) Quantization of  $e$

For any semi-simple grand unified group G, the ratios of the values of any given gauge coupling constant for different particles will be rational numbers. These ratios are unaffected by renormalization, whatever the value of  $m_X$ .

(c) Fermion Mass Matrices

A grand unified theory may in some cases

impose relations among the mass matrices of the quarks and leptons. One example of the sort of relation we would like to be able to derive is the well-known formula for the Cabibbo angle

$$\tan^2 \theta_c \simeq m_d/m_s \quad (20)$$

whose numerical success is so far not understood.<sup>57</sup>

(d) Small mass ratios

It is noteworthy that a number of otherwise identical leptons and quarks have extremely different masses

$$m_e/m_\mu = 4.8 \times 10^{-3}; \quad m_u/m_c \approx 4 \times 10^{-3}; \\ m_d/m_b \approx 1.5 \times 10^{-3}.$$

This might be explained in a grand unified gauge theory if some of the superheavy gauge bosons produce transitions<sup>58</sup>  $e \rightarrow \nu_j, u \rightarrow c, d \rightarrow b$  with couplings  $g_i$  of order  $e$ . In this case, if  $e, d, u$  were massless in zeroth order, then the emission and absorption of superheavy gauge bosons would give them masses of order

$$m_e/m_\mu \approx m_d/m_b \approx m_u/m_c \approx \alpha L/\pi$$

where  $L$  is a logarithm of superheavy gauge boson mass ratios. Since this depends only on the superheavy mass ratios, we can get reasonable orders of magnitude for the fermion mass ratio even if  $m_X$  is enormous. If the same superheavy gauge boson produced transitions  $e \rightarrow \nu$  and  $u \rightarrow c$  or  $d \rightarrow b$ , and if it is not too heavy, then it might produce observable rare decay processes like  $Z^0 \rightarrow e^+ e^-$  or  $(bd) \rightarrow iJL^+ e^+$ , with branching ratios of order  $m_e/m_X$ .

The hope is also sometimes expressed that a grand unified gauge theory might respect a left-right symmetry, which is broken when the grand gauge group breaks down to SU(3) x SU(2) x U(1). However, we know of no necessity for such a left-right symmetry, and in fact it leads to problems in dealing with neutrinos. If a left-right symmetric theory distinguishes fermions and antifermions, then for each left-handed neutrino  $\nu_l, \bar{\nu}_l$ , there must be a right-handed neutrino (as opposed to anti-neutrino) as well. This gives 6 neutrino species, which already exceeds the cosmological limits<sup>29,30</sup> discussed in Section 4. (However, as mentioned there, these limits would not apply if the cross sections of the right-handed neutrinos were less than usual neutrino

cross sections by a factor  $10^{-6}$  to  $10^{-9}$ , which would require that the interactions of right-handed neutrinos be mediated by gauge bosons with masses above  $10^2$  to  $10^3$  times  $m_w$ .) A left-right symmetric theory also risks giving the neutrinos masses in excess of present limits.<sup>59</sup> Perhaps we should be satisfied with TCP, as the only really essential symmetry between right and left.

#### Acknowledgements

I was greatly helped in preparing this report by conversations with many colleagues, especially M. Barnett and D. V. Nanopoulos.

#### References

1. K. Tittel, rapporteur's talk at this Conference. Where references are not given in this section, I believe that they can be found in Tittel's report.
2. The term "simple gauge theory" is used in Section 2-5 as an abbreviation for the simple specific gauge theory of weak and electromagnetic interactions, based on the gauge group  $SU(2) \times U(1)$ , which is spontaneously broken down to the  $U(1)$  of electromagnetic gauge invariance. The symmetry breaking is taken to occur in the simplest possible way, by the vacuum expectation values of any number of  $SU(2) \times U(1)$  doublets of scalar fields. There are any number of left-handed  $SU(2) \times U(1)$  doublets of leptons and quarks, and right-handed fermion fields are taken as singlets. Wherever relevant, the strong interactions are also assumed to be described by a gauge theory such as quantum chromodynamics (QCD). Although spontaneously broken, the  $SU(2) \times U(1)$  gauge symmetry is an *exact* property of the Lagrangian, which together with the requirement of renormalizability imposes tight constraints on the interactions. In consequence, all electromagnetic and charged and neutral-current weak interactions are described by the theory in terms of just a few free parameters:  $e$ ,  $G_F$ , the  $Z^0$ - $\gamma$  mixing angle  $\theta$ , and the mass matrices of the leptons and quarks. For a review of the gauge theory of weak and electromagnetic interactions, see E. S. Abers and B. W. Lee: *Phys. Rpt.* **9** (1973) 1. Its phenomenological implications were reviewed here by G. Altarelli and H. Fritzsch.
3. M. Barnett, talk at the Neutrinos '78 Conference, Purdue University, to be published.
4. B. C. Barish *et al.*: CALT 6S-605 (1977).
5. V. Barger, T. Gottschalk, and R. J. N. Phillips: Wisconsin preprint COO-881-32 (paper 402 submitted to this Conference); J. Smith *et al.*: Stony Brook preprint ITP-SB-78-31; M. Barnett, L.-N. Chang, and N. Weiss: *Phys. Rev.* **D17** (1978) 2266. It is not clear whether two very high energy events can be explained by conventional mechanisms, but no more such events have been seen, and these two events may well represent a statistical fluctuation. Even if these two events were due to cascade decay of some new quark, such as  $x \rightarrow d + \bar{t}$ ,  $t \rightarrow ii + \nu_{yb}$ ,  $b \rightarrow ii + \nu_{pc}$ , the rate of these very high energy events is still sufficiently small (less than  $10^{-5}$  to  $10^{-6}$  of all charged current events) that no conflict with universality would arise.
6. A comprehensive theoretical analysis of such experiments has been provided through the work of Morita and his colleagues at Osaka; see M. Morita, M. Nishimura, H. Ohtsubo, and J. Yamane: *J. Phys. Soc. Japan* **44** (1978) Suppl. 470 and earlier references quoted therein; M. Morita, M. Nishimura, and H. Ohtsubo: *Phys. Letters* **73B** (1978) 17; M. Kobayashi, N. Ohtsuka, H. Ohtsubo, and M. Morita: paper 205 submitted to this Conference. A search for effects that would be caused by an induced pseudotensor in the beta decay of polarized nuclei has been carried out for  $^{12}\text{B}$  and  $^{12}\text{N}$  at Osaka and for  $^{19}\text{Ne}$  at Princeton. After improvements in their apparatus, both groups now find no evidence of second-class currents: K. Sugimoto, reported at the International Conference on Nuclear Structure at Tokyo<sup>^</sup> September 1977, and F. Calaprice, private communication. For  $^{19}\text{Ne}$ , it is possible to set an upper limit of about 10% on any difference between the observed asymmetry parameter and that produced by weak magnetism, with no second-class currents. Similar results were also found in experiments on  $^{12}\text{B}$  at Louvain and ETH: see M. Steele *et al.*: *Proc. VI Int. Conf. High Energy and Nuclear Structure* (1975), and H. Brandle *et al.*: ETH preprint. (There is also evidence against second-class effects in a variety of other measurements, including the  $fi$ - $a$  correlation for  $A=8$ , the  $fi$ - $\nu$  correlation in  $^6\text{He}$ , the  $^{\wedge}\text{-}^{12}\text{C}$  capture rate\* and the  $^{12}\text{B}$  polarization in  $JLL\text{-}^{12}\text{C}$  capture.)
7. In the course of experiments on the G-conjugation properties of the axial current in  $^{12}\text{B}$  and  $^{12}\text{N}$  decay, the question was raised whether the experiment of Y. K. Lee, L. W. Mo, and C. S. Wu: *Phys. Rev. Letters* **10** (1963) 253 really gives a value for weak magnetism consistent with CVC when the correct Fermi function is used; see F. P. Calaprice and B. R. Holstein: *Nucl. Phys.* **273** (1976) 301. This experiment has recently been re-analyzed by C. S. Wu, Y. K. Lee, and L. W. Mo: *Phys. Rev. Letters* **39** (1977) 72, and by K. Koshigiri *et al.*: paper 206 submitted to this Conference, and repeated by W. Kaina *et al.*: *Phys. Letters* **70B** (1977) 411, with results in agreement with CVC.
8. M. A. Shifman, A. I. Vainshtein, and V. I. Zakharov: *Nucl. Phys.* **B120** (1977) 316.
9. C. Baltay: rapporteur's talk at this Conference. Where references are not given in this section, I believe that they can be found in Baltay's report.
10. For recent analyses, see L. Abbott and M. Barnett: *Phys. Rev. Letters* **40** (1978) 1303; **M.**

- Claudson, E. Paschos, and L. R. Sulak; Harvard preprint HUTP-78/A043, October 1978.
11. Post-Conference Note: A parity violation has now been found in bismuth also by the Seattle group, at the transition frequency previously studied by them; N. Fortson, private communication. The circular polarization has the expected sign, but its magnitude still appears smaller than would be expected from the Novosibirsk results. Parity violation has now also been found in thallium; E. Commins, private communication. The preliminary value of the circular dichroism in thallium agrees in sign and magnitude with the value expected on the basis of the simple gauge theory and numerical computations of thallium atomic structure.
  12. A possible uncertainty in these calculations is explored in the work of J. Hiller, J. Sucher, and G. Feinberg, paper 658 submitted to the Conference. They note that the circular polarization involves expectation values which are sensitive to poorly known details of the atomic wave functions near the nucleus. Using the Schrodinger equation, it is possible to transform the operator so that its vacuum expectation value depends on the wave function over a broader region. If the wave function were exact, there would be no difference, but Hiller *et al.* find that the results can be quite different when this procedure is applied to approximate variational wave functions, at least for the light atoms studied so far.
  13. R. Taylor: talk at this Conference; C. Y. Prescott *et al.*: Phys. Letters **77B** (1978) 347.
  14. L. Wolfenstein: Carnegie-Mellon preprint COO-3066-111.
  15. The phenomenology of parity violation in nuclear physics was discussed in papers submitted to this Conference by M. Konuma and T. Oka: No. 370; V. M. Dubovik and V. S. Zamiralov: No. 406; S. Marioka and T. Ueda: No. 578.
  16. Effects of hard gluons have been analyzed by G. Altarelli, R. K. Ellis, L. Maiani, and R. Petronzio: Nucl. Phys. **B88** (1975) 215.
  17. D. Horn and G. G. Ross: Phys. Letters **67B** (1977) 460; G. Altarelli, N. Cabibbo, L. Maiani, and R. Petronzio: Phys. Letters **67B** (1977) 463.
  18. H. Fritzsch: Phys. Letters **67B** (1977) 451.
  19. Where references on r and b decay are not given here, I believe that they can be found in the reports by G. Altarelli, C. Quigg and K. Fujikawa.
  20. T.N. Pham, C. Roisnel, and T.N. Truong: Phys. Rev. Letters **41** (1978) 371, and Ecole Polytechnique preprint, papers 718 and 719 submitted to this Conference; F. J. Gilman and D. H. Miller: Phys. Rev. **D17** (1978) 1846; N. Kawamoto and A. I. Sanda: Phys. Letters **76B** (1978) 446; D. A. Geffen and W. J. Wilson: U. Minnesota preprint, paper 327 submitted to this Conference; J.-L. Basdevant and E. L. Berger: Phys. Rev. Letters **40** (1978) 994, paper 577; K. Yamaniishi: Nagoya preprint, paper 353; M. P. Rokalo, A. P. Korsh and Y. P. Baranniki: Kharkov preprint, paper 353.
  21. M. Kobayashi and K. Maskawa: Progr. Theor. Phys. **49** (1973) 652; A. Pais and J. Primack: Phys. Rev. **D8** (1973) 3063; L. Maiani: Phys. Letters **68B** (1976) 183; S. Pakvasa and H. Sugawara: Phys. Rev. **D14** (1976) 305.
  22. J. Ellis, M. K. Gaillard and D. Y. Nanopoulos: Nucl. Phys. **B109** (1976) 213.
  23. R. E. Shrock and L.-L. Wang: Princeton preprint, August 1978.
  24. M. K. Gaillard and B. W. Lee: Phys. Rev. **D10** (1974) 897.
  25. J. Ellis, M. K. Gaillard, D. Y. Nanopoulos and S. Rudaz: Nucl. Phys. **B131** (1977) 285.
  26. C. Quigg and J. L. Rosner: LBL preprint 7961, July 1978.
  27. D. Cutts *et al.* (Brown-FNAL-III-Bari-MIT-Warsaw collaboration: Phys. Rev. Letters **41** (1978) 363; R. Yidal *et al.* (Col-FNAL-SUNY-UCB collaboration): Phys. Letters **77B** (1978) 344.
  28. A. Sirlin: Rev. mod. Phys. **50** (1978) 573, paper 185 submitted to this Conference, and earlier references quoted therein.
  29. G. Steigman, D.N. Schramm, and J. E. Gunn: Phys. Letters **66B** (1977) 202. Also see Y. P. Shvartzman: JETP Letters **9** (1969) 184; J. Yang, D. N. Schramm, G. Steigman, and R. T. Rood: EFINS preprint.
  30. This point has been especially emphasized by M. A. Beg, A. Marciano, and M. Ruderman, to be published.
  31. E. Ma and J. Okada: Phys. Rev. Letters **41** (1978) 287.
  32. A rough estimate of this ratio for the  $Jj < p$  decay was given by J. Rich and D. R. Winn: Phys. Rev. **D14** (1976) 1283. However, their estimate is considerably larger than would be given by replacing  $m_i$  with  $m_{i,p}$  in eq. (17).
  33. The asymmetry has been calculated by A. Love, D. Y. Nanopoulos, and G. G. Ross: Nucl. Phys. **B49** (1972) 513; E. Derman: Phys. Rev. **D7** (1973) 2755; W. W. Wilson: Phys. Rev. **D10** (1974) 218; S. M. Berman and J. R. Primack: Phys. Rev. **D9** (1974) 2171 and **D10** (1974) 3895; M. A. B. Beg and G. Feinberg: Phys. Rev. Letters **33** (1974) 606; S. M. Bilenkii *et al.*: Sov. J. Nucl. Phys. **21** (1975) 657; R. N. Cahn and F. J. Gilman: Phys. Rev. **D17** (1978) 1313; M. Yoshimura: Progr. theor. Phys. **59** (1978) 231; M. Klein and T. Riemann: Phys. Letters **76B** (1978) 79. Production of specific hadronic final states in deep inelastic scattering of polarized electrons on deuterons is considered by M. P. Rokalo, G. I. Gakh, and A. P. Rokalo, Kharkov preprint, paper 1022 submitted to this Conference.
  34. S. Weinberg: Phys. Rev. Letters **36** (1976) 294; A. D. Linde: JETP Letters **23** (1976) 64.
  35. B. W. Lee, C. Quigg, and H. B. Thacker: Phys. Rev. Letters **38** (1977) 888; Phys. Rev. **D16** (1977) 1519; C. E. Yayanakis: Athens preprint, May 1977; J. S. Kang: Maryland preprint 77-



254. With several scalar doublets and one extra-heavy Higgs boson  $H$ , the  $Z$ - $W$  mass ratio would be subject to a radiative correction of order  $\{g^2/32\pi^2\}(m_n^2/m_w^2)$  or 3% for  $w = 1\text{TeV}$ ; D. Toussaint: Princeton preprint.
36. S. Coleman and E. Weinberg: Phys. Rev. **D7** (1973) 1888. Also see S. Weinberg: Phys. Rev. **D7** (1973) 2887.
37. E. Gildener and S. Weinberg: Phys. Rev. **D13** (1976) 3333.
38. The Higgs boson would be required to have a mass of order  $m_w$  by considerations discussed by A. Salam and J. Strathdee, ICTP preprint.
39. T. D. Lee: Phys. Rev. **D8** (1973) 1226; Phys. Rpt. **9C** (1974) 143; S. Weinberg: Phys. Rev. Letters **37** (1976) 657.
40. A. A. Anselm and D. I. D'Yakonov: Leningrad Nucl. Physics Institute preprint N-394 (1978).
41. W. B. Dress *et al.* (ORNL-Grenoble-Harvard collaboration): Phys. Rev. **D15** (1977) 9.
42. I. S. Altarev *et al.*: Leningrad preprint submitted to this Conference.
43. P. Depommier *et al.*: Phys. Rev. Letters **39** (1977) 1113.
44. H. Povel *et al.*: Phys. Letters **72B** (1977) 183.
45. C. M. Hoffman *et al.* (LASL-Chicago-Stanford collaboration): paper 216 submitted to this Conference.
46. D. A. Brynam *et al.*: Phys. Rev. Letters **28** (1972) 1469.
47. A. Badertscher *et al.*: Berne preprint, paper 950 submitted to this Conference.
48. S. M. Korenchenko *et al.*: JETP **70** (1976) 3.
49. G. I. Kakh: Kharkov preprint, paper 1017 submitted to this Conference.
50. S. Weinberg: keynote talk at the Neutrinos '78 Conference at Purdue University, April 1978.
51. Several recent papers have strengthened the evidence against axions: A. E. Asratyam *et al.*: IHEP preprint, paper 288 submitted to this Conference; G. Micelmacher and B. Pontecorvo: JINR preprint, paper 135 submitted to this Conference; T. Hansl *et al.*: Phys. Letters **74B** (1978) 139; P. C. Bosetti *et al.*: Phys. Letters **74B** (1978) 143; E. Bellotti, E. Fiorini, and L. Zanotti: to be published.
52. By "simple" in Section VI, I mean either simple in the strict mathematical sense, or else a direct product of isomorphic simple groups connected by a discrete global symmetry.
53. It is not understood why there should be a "hierarchy" of scales of spontaneous symmetry breaking. It has been claimed that there are limits on the ratio of spontaneous breaking scales possible in such hierarchies: E. Gildener: Phys. Rev. **D14** (1976) 1667; also see K. T. Mahanthappa and D. G. Unger: preprint COLO-HEP-6, paper 255 submitted to this Conference. A contrary view is taken by R. N. Mohapatra and G. Senjanovic: preprint CCNY-HEP-78(6), paper 22 submitted to this Conference; I. Bars and M. Serdaroglu: preprint COO-3075-188. My conclusion is that there is no theorem which limits ratios of mass scales of spontaneous symmetry breaking, and plausible constraints can in fact yield very large mass ratios.
54. A. Salam: Rapporteur's talk at this Conference.
55. V. Elias, J. C. Pati, and A. Salam: Phys. Rev. Letters **40** (1978) 920.
56. H. Georgi, H. Quinn, and S. Weinberg: Phys. Rev. Letters **33**, (1974) 451.
57. There is an argument that eq. (20) cannot be derived from the addition of any set of discrete symmetries to  $SU(2) \times U(1)$ ; R. Barbieu, R. Gatto, and F. Strocchi: Phys. Letters **74B** (1978) 344, paper 753 submitted to this Conference. However, counter-examples have been proposed by D. Wyler: Rockefeller preprint COO-2232-B 157. For recent attempts to derive eq. (20) and related formulas in models with six quarks, see H. Fritzsch: Phys. Letters **73B** (1978) 317, paper 72 submitted to this Conference; T. Hagiwara, T. Kitazoe, B. B. Mainland, and K. Tanaka: paper 2382; T. Kitazoe and K. Tanaka: paper 441; H. Harari, H. Haut, and J. Weyers: paper 1084; G. C. Branco and R.N. Mohapatra: paper 954.
58. Illustrative models of this type have been considered by M. Horibe, J. Ishida and A. Sato: paper 687; T. Maehara and T. Yanagida: paper 528.
59. Limits on neutrino masses are surveyed in ref. 50.
60. A. M. Cnops *et al.* (Col-BNL collaboration): Phys. Rev. Letters **40** (1178) 1441.

## P9a: QCD and Related Problems

*Chairman :* C. N. YANG

*Speaker:* B. SAKITA

*Scientific Secretaries:* A. HOSOYA  
Y. HOSOTANI

## P9b: Unification Theories, Supergravity and New Ideas

*Chairman:* R. E. MARSHAK

*Speaker:* A. SALAM

*Scientific Secretaries:* H. TERAZAWA  
A. SUGAMOTO

B. SAKITA

*Department of Physics, The City College of the City University of New York,  
New York, NY. 10031*

### Introduction

I was asked to report on Sessions C1, C2, and C3, in which field theory aspects of quarks and gluons, especially quantum chromodynamics (QCD), are discussed. If I say something new in this report without quoting, these are all due to discussions with my colleagues, especially with J.L. Gervais.

The field theoretical investigations of QCD are a part of general studies of quanta! non-Abelian gauge field theories. Since the non-perturbative aspect is crucial for the large distance behavior of QCD, as I will explain later, I will include some technical developments on non-perturbative methods in quantum field theory in my report.

Quantum chromodynamics is a field theory model of colored quarks and gluons, which can be described by the Lagrangian:

$$\mathcal{L} = -\frac{1}{4}(F_{\mu\nu}^a)^2 - \bar{\psi}(\not{D}(A) + m)\psi \quad (1)$$

$$D_\mu(A) = \partial_\mu - ieA_\mu^a \frac{\lambda_a}{2} \quad (2)$$

$$F_{\mu\nu}^a = \partial_\mu A_\nu^a - \partial_\nu A_\mu^a + ef_{abc}A_\mu^b A_\nu^c \quad (3)$$

where  $\psi$  is a quark field,  $A_\mu^a$  is a Yang-Mills gauge field,<sup>1</sup> and  $X_a$  are the Gell-Mann SU(3) (color) matrices. We suppress the quark flavor indices. Since this Lagrangian is renormalizable, one can treat it by the standard Feynman-Dyson perturbation theory for small coupling. Although this Lagrangian has a similar form to that of QED, there is a great difference, at least at short distances. Namely, contrary to QED there is an anti-screening phenomenon in QCD. That is to say, if one probes closer and closer to a point charge the charge disappears, so that at short distances the quarks and gluons behave as free particles. This phenomenon is called the asymptotic freedom, noted by Gross and Wilczek,<sup>2</sup> and by Politzer,<sup>2</sup> and supports the parton model idea.<sup>3</sup> But since this has been

extensively discussed in the past years as well as in other sessions in this Conference, in this report I will omit subjects based on the perturbative calculations of QCD.

The concept of color was originally introduced by Greenberg<sup>4</sup> using the term "para-statistics of order 3," which mystified almost everybody including myself. However, it says essentially that there are three components for a quark field and only the totally anti-symmetric combination with respect to these components are observable. Another version<sup>5</sup> of color theory would be that there are three kinds of quarks for each flavor, which are specified by a new quantum number called color, and that there exists exact color SU(3) symmetry (each flavor of quark is a color triplet), together with an important ad hoc hypothesis that the physical states (hadrons) are color singlets. In this way one may obtain the same physical results as Greenberg's, without using para-statistics, at the expense of the additional ad hoc color singlet hypothesis. Once the new color degree of freedom is introduced, it provides the effects which can be checked experimentally, since the number of independent quarks is three-fold now. For example, since the hadronic production cross section in the  $e^+e^-$  colliding beam is proportional to  $N$ ,  $N$  being the number of colors, *i.e.*,  $N=3$ , it is a nice place to test the color idea. The present experiments support it.

QCD is a model<sup>6</sup> with color which has non-Abelian gauge fields coupled with the spinor quark field as shown in (1). The symmetry of the system is now the *local* color SU(3). The hope is that this large exact symmetry has the consequence that all the hadrons (the physical states) are color singlets, so that this conventional field theory reproduces the essence of "para-statistics." This hoped-for phenomenon is called "color confinement."<sup>7</sup> Since quarks, antiquarks, and gluons are not

singlets (being [3], [3\*], and [8] respectively), color confinement implies quark and gluon confinement.

Through the extensive investigations on  $S$ -matrix theory of hadrons in the 1960's a remarkable theory of strong interaction emerged based on the original Veneziano beta function formula\* for the four point amplitude. The progress of dual resonance theory<sup>9</sup> was discussed extensively in the past years, but once again I would like to stress that the dual resonance theory provides qualitatively for most of the phenomena in strong interaction physics. As noted by Nambu and Susskind,<sup>10</sup> the underlying physical picture of the dual resonance theory is the relativistic massless string. I should add at this point that the string theory is a version of nonlocal field theories, which have been extensively discussed by Yukawa<sup>11</sup> and others in this country. Most of the difficulties of the dual resonance theory, especially the difficulties in constructing local currents, are related to the lack of point like objects in the string theory on one hand and relativistic invariance on the other. As a phenomenological model one can naively imagine that the string binds quarks and anti-quarks, although within the framework of dual resonance theory this picture was not possible.

Around the time when people working in this field were frustrated, a more realistic model of hadrons was proposed by the MIT group, namely the MIT bag model,<sup>12</sup> which confines the constituent quarks in a bag. The model has had some phenomenological success. A natural guess would be that in QCD if the gluons and the quarks are confined the hadrons have the form of strings or bags.

**$A_0=0$  Canonical Formalism of Non-Abelian Gauge Theory**

In Table I, I present a comparison between a non-Abelian gauge theory in the gauge  $A_0=0$  and the system of a particle in a central potential. The table is self explanatory. In order to avoid confusions, I like to stress that  $A_0=0$  gauge does not imply the temporal gauge (*i.e.*  $d(A''(x, t))$  appearing in the Feynman path integral). Even if one proceeds with the canonical formalism starting with

Table I.

	Non-Abelian gauge theory ( $A_0=0$ )	Potential model
Lagrangian	$\mathcal{L} = \frac{1}{2}(A_i^a)^2 - \frac{1}{4}(F_{ij}^a)^2$	$L = \frac{1}{2}\dot{r}^2 - V(r)$
Canonical coordinate	$A_i^a(x)$	$r \equiv x, y$
Symmetry	Gauge symmetry	Rotation symmetry
Symmetry transformation	$A^{[A]} = u(A) \times Au^{-1}(A)$	$x(\theta) = x \cos \theta + y \sin \theta$
	$-\frac{i}{e}(\nabla u(A))u^{-1}(A)$	$y(\theta) = -x \sin \theta + y \cos \theta$
Convenient coordinates	(Gribov ambiguity)	Polar coordinates
Stable equilibria	Classical vacua	Minima of $V$
Tunnelings	Instantons meron pairs etc.	Tunnelings

the Lagrangian in Table I and then converting it to a Feynman path integral form (by constructing first the functional integration in the phase space and then by integrating the momenta out), one introduces collective coordinates to remove the zero frequency modes to make path integral meaningful. Depending on how to introduce collective coordinates, namely canonical or non-canonical in the sense of Jevicki,<sup>13</sup> one obtains various gauge conditions (including temporal gauge) as 5-conditions in the path integral.

**Tunneling in Potential Model**

First consider the dashed line potential in Fig. 1. The potential at the center is infinitely high, so that tunneling between the minima is impossible. If this is the case, the physical states are no longer eigenstates of the reflection operator  $P$ , *i.e.*, we have spontaneous symmetry breaking. On the other hand, in the case of the solid line potential tunneling occurs so that the physical states are eigenstates of  $P$ . The tunneling restores the reflection symmetry.

In the standard WKB method, the tunneling amplitude is given by

$$A_{\text{poce}} \sim e^{-S_0} \tag{4}$$

where  $S_0$  is the action of Euclidean classical solution (by a Euclidean classical solution I mean a solution of classical equation with

imaginary time)

$$S_0 = \int_{-\infty}^{\infty} d\tau (\dot{q}_{cl}(\tau))^2. \tag{5}$$

Since the Euclidean classical solutions are obtained by the solutions of mechanical systems of up side down potential (see Fig. 2). One can see intuitively that the solid line potential gives a finite action while the dashed line potential gives infinite action.

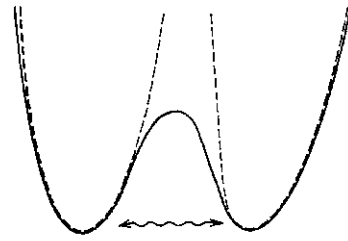


Fig. 1.

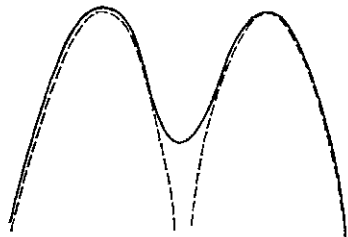


Fig. 2.

**Classical Vacua of Non-Abelian Gauge Theory**

The potential is given by

$$V[A] = \frac{1}{4} \int dx (F_{ij}^a)^2 \tag{6}$$

which is positive definite. Thus, the minima of  $V[A]$  are given by  $F \wedge 0$ , namely pure gauge.

The classification of non-singular gauge transformations has been studied by Jackiw and Rebbi.<sup>14</sup> By non-singular gauge transformations I mean that the gauge matrix  $u(x)$  (SU(3)) is continuous and differentiable and satisfies

$$u(x) \xrightarrow{|x| \rightarrow \infty} 1 \tag{7}$$

Then  $u(x)$  is a mapping from  $S^3$  to SU(3). The homotopy theory tells us the homotopy group is  $\pi_3(SU(3)) = \mathbb{Z}$ , where  $\mathbb{Z}$  is the additive group of the integers. This means that the gauge symmetry group  $G$  has disconnected components<sup>15</sup> and

$$G/G_{\text{conn.}} = \mathbb{Z} \tag{8}$$

The potential  $V[A]$  looks as shown in Fig. 3. The bold lines are classical ground states which are the orbits of pure gauge.

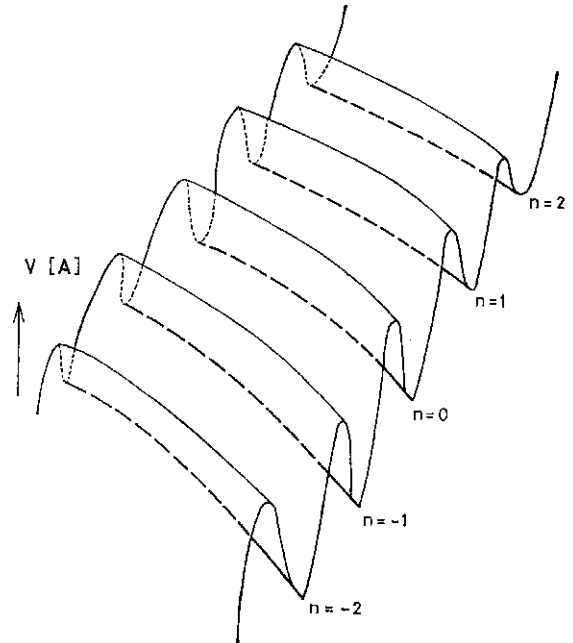


Fig. 3.

**0-Vacua<sup>16</sup>**

If the symmetry  $\mathbb{Z}$  is not broken, because of tunneling, the physical states are unitary representation of the symmetry group  $G$ . In particular, the physical vacuum satisfies

$$G_{\text{conn.}} |\text{phys. vac.}\rangle = |\text{phys. vac.}\rangle \tag{9}$$

Once the connected component of gauge symmetry is fixed by (9), the  $\mathbb{Z}$  symmetry is equivalent to the symmetry of a periodic potential. In general the unitary representation of  $\mathbb{Z}$  is specified by a parameter, say  $\theta$ .

$$K^n \in \mathbb{Z} \quad (n: \text{integers}) \tag{10}$$

$$K |\text{phys. vac}(\theta)\rangle = e^{i\theta} |\text{phys. vac}(\theta)\rangle \tag{11}$$

**Instanton Solution**

A Euclidean solution of the SU(2) Yang-Mills field equations with finite action has been found by Belavin, Polyakov, Schwartz and Tyupkin.<sup>17</sup> The solution has parameters (position of instanton) and  $\rho$  (size of instanton). In the  $y_4 = 0$  gauge, it has the properties

$$\lim_{r \rightarrow \infty} \hat{e}_i(r, x) = 0 \tag{12}$$

$$\lim_{r \rightarrow \infty} A_n(r, x) = \int_{\mathcal{F}} \mathcal{K}(x) \mathcal{K}^*(x) \quad (13)$$

where

$$\mathcal{K}(x) = \exp\left(\int_{\mathcal{F}} \mathcal{f} \Big|_{\mathcal{F}}\right) \quad (14)$$

and suffix *cl* implies the classical solution. Thus the solution changes its *n* value by 1 from  $T \rightarrow -\infty$  to  $r \rightarrow +\infty$ .

The reasons why instantons are important are following: (i) #-vacua which resolve<sup>18</sup> the famous  $U_1(1)$  problem.<sup>19</sup> (ii) In the Polyakov program,<sup>20</sup> QCD is expressed in terms of Euclidean functional integration and regarded as a four dimensional statistical mechanics. Then one keeps only a few important excitation modes. The instanton mode is one of the most important ones (see the discussion on Princeton bag below), (iii) In the semi-classical method in Minkowsky field theory,<sup>21</sup> the instanton solution determines the most probable path<sup>22</sup> of tunneling in configuration space, which is important for the WKB construction of wave functions in our method.

### Non-Perturbative Method

As I mentioned in Introduction, because of asymptotic freedom the short distance behavior of quarks and gluons is more or less predictable by perturbation calculations. Most of the successes in QCD are limited to short distance or equivalently large  $q^2$  phenomena, such as the scaling behavior and its breaking, in the deep inelastic e-p scattering experiments.<sup>23,24</sup> On the contrary, color confinement is a typical long range problem. Since QCD involves a zero mass vector field which interacts non-linearly with itself, the infrared problem as well as the non-linearity of the field interactions prevent us from discussing the long range properties of the theory in terms of standard perturbation theory.

The typical non-perturbative methods in ordinary quantum mechanics are the semi-classical method (WKB method) and the variational method. These methods were extended to quantum field theories, more specifically to the meson theory with static nucleon sources, already before the end of the second world war, in the strong coupling theory of Wentzel<sup>25</sup> and the intermediate coupling theory of Tomonaga.<sup>26</sup> The methods were

further developed in solid state physics and statistical mechanics and contributed to the great progress in the developments of the microscopic theories of critical phenomena and phase transitions, notably to the BCS theory of superconductivity.<sup>27</sup>

The use of semi-classical methods in field theories was revived by Dashen, Hasslacher and Neveu<sup>28</sup> in a modern form by using the stationary phase approximation for the Feynman path integral expression. This method has been applied to quantum solitons and instantons. In this development it became clear to us that the use of collective coordinates is extremely advantageous in the calculations.<sup>29</sup>

The essence of the method of collective coordinates is the following: When one wants to take into account field configurations which involve a few parameters, which we call collective coordinates, one treats the fluctuations, which are the small field configurations normal to the configuration under consideration, by perturbation theory. When the field configuration which one is interested in is a classical solution (for example, a soliton solution), the symmetry parameters of the system are the collective coordinates (for the soliton example the position of the soliton (translational symmetry)). The collective coordinates associated with the symmetry of the system as described above are called kinematical collective coordinates, otherwise they are called dynamical.<sup>30</sup> The dynamics of kinematical collective coordinates is trivial, while the dynamics of dynamical collective coordinates is non-trivial. The collective coordinates for the semi-classical calculations of solitons and instantons are all kinematical.

There are two ways of treating tunneling phenomena in quantum field theory: standard WKB wave function method and Euclidean instanton method. Let me explain these by taking an example of double well potential (Fig. 1).

In the standard WKB method that is given in the textbook, one constructs the wave function in the forbidden region and in the allowed region and connects them.

The Euclidean instanton gas method<sup>31</sup> is more involved. First the vacuum to vacuum transition in Euclidean metric is converted into

the Feynman-Kac functional integral form. Then the saddle point approximation to the functional integral is applied. Since the saddle points are the solution of Euclidean classical equation, one can obtain the solution using Fig. 2. The solutions look like in Fig. 4. The solid line represents an instanton, while the dashed line anti-instanton.

$$\begin{aligned} \langle 0 | e^{-HT} | 0 \rangle &\xrightarrow{T \rightarrow \infty} e^{-E_0 T} \\ &\downarrow \text{Feynman-Kac} \\ &\int \dots \int \mathcal{D}q(t) e^{-\int_0^T L dt} \\ &\xrightarrow{\text{Saddle pt. approximation}} \sum \frac{1}{n!} \int d\tau_1 \int d\tau_2 \dots \int d\tau_n e^{-n S_0} \quad (15) \end{aligned}$$

Expression (15) is equivalent to the grand partition function of a one dimensional instantons anti-instantons gas (see Fig. 5). So, one is reduced to a statistical problem of a one dimensional gas.

By choosing the parameter of most probable path in tunneling phenomena, more specifical-

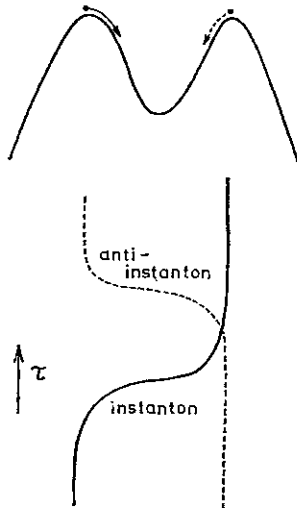


Fig. 4.

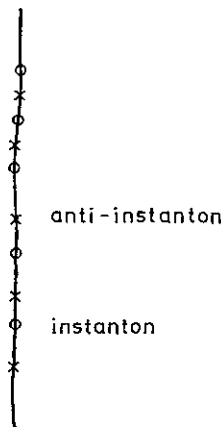


Fig. 5.

ly, the Euclidean time  $\tau$  of Euclidean classical solution, as a collective coordinate, Gervais and I were able to formulate instanton phenomena as standard tunneling phenomena in the canonical formalism,<sup>32</sup> *i.e.*, Minkowsky field theory. Since  $v$  has nothing to do with the symmetry of the system, this collective coordinate is dynamical and it is relevant to the tunneling. In this formalism we believe that the physical meaning of instanton phenomena becomes clear to the point that we all understand tunneling phenomena in quantum mechanics in terms of WKB method. More recent developments along this line on the two dimensional Higgs model were reported in the parallel session by de Vega. We obtained the result of dilute gas approximation of the Euclidean method. However, I must add that we are not yet in a position to be able to discuss the confinement problem of QCD in our formalism, because we have not succeeded yet in handling, the field degrees of freedom, which cause infrared problems in terms of collective coordinates.

**Gribov Problem**

Last summer some rather shocking news arrived, namely that Gribov<sup>33</sup> had proved that the Coulomb gauge does not fix uniquely gauge of the non-Abelian gauge field and he implied that this very non-uniqueness changes the infrared behavior of the theory in a way in favor of the confinement. Since then quite a few papers came to my attention, and several papers are contributed to this conference also.<sup>34</sup> Since I am going to discuss the confinement problem later let me first make a comment on the Gribov ambiguity.

The gauge theory Lagrangian in Table I is invariant under time independent gauge transformations. Therefore, there exists a large number of angular variables (cyclic variables) corresponding to the gauge transformations just like the polar coordinate  $\theta$  in the potential model (see Table I). In the case of central potential one can separate these angular variables using polar coordinates. What are the corresponding polar coordinates in non-Abelian gauge theory?

One can proceed as follows. First introduce the concept of orbits in the configuration space. In the ordinary potential problem in

two dimensions, one obtains a circle when one applies rotations to a point in the space. This circle is called an orbit. The orbits associated with rotations are the circles in this case. The orbits are specified in general by invariants, namely in this case by the radius. A point in space can be specified by the orbit on which the point lies and by the angle. The starting line of the angle is normally taken to be the positive axis, *i.e.*,

$$y=0, x>0. \tag{16}$$

Notice that the starting line given by eq. (16) intersects an orbit only once.

One can proceed in the same way for the more complicated case of non-Abelian gauge theories, provided one has an equation like (16), which we call the gauge condition. Notice that in this case the configuration space is an infinite dimensional functional space of  $A(x)$ . Moreover, it is not a vector space with respect to gauge transformations. What Gribov has shown is that the Coulomb gauge condition

$$\nabla \cdot A^a(x)=0 \tag{17}$$

intersects an orbit many times, so that one cannot draw the starting line uniquely.

Is this ambiguity universal? If so, is it really a crucial difficulty of the theory?

In this connection we remark on two published papers. One is by Amati and Rouet,<sup>35</sup> who showed that the Gribov ambiguity is irrelevant to the semi-classical calculations provided one uses the background gauge condition. The other is by the Berkeley mathematician, Singer,<sup>36</sup> who claims, that the Gribov ambiguities are not restricted to the Coulomb gauge condition but rather are a general feature of non-singular gauge conditions. (Non-singular gauge conditions are gauge conditions which do not fix the singular gauge transformations. In this respect, the axial gauge belongs to a singular gauge condition.)

Since in our investigation of WKB method in non-Abelian gauge field theories in canonical formalism,<sup>14</sup> Gervais and I came to the same conclusion as that of Amati and Rouet, I will use canonical formalism for the explanation. As I mentioned before in the semi-classical method one takes into account only the field configurations which are in a strip near the

classical configuration surface. (See Fig. 6.)

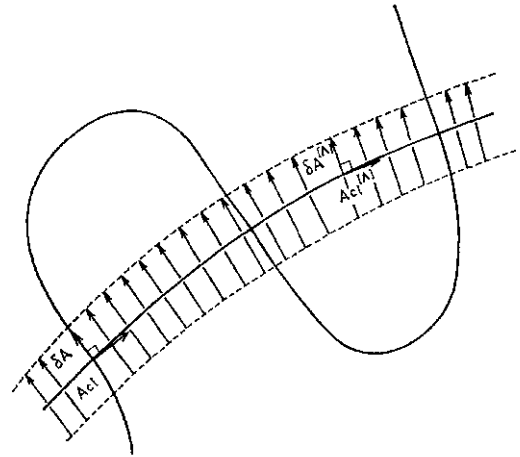


Fig. 6.

It is possible to draw the normal to the classical configuration anywhere in the strip, and it can be proven that the condition to be normal is gauge invariant.

$$\int \delta A_i^{[A]}(y) \cdot \frac{\delta A_{i_{cl}}^{[A]}(y)}{\delta A^a(x)} dy = 0 \tag{18}$$

$$\delta A_i^{[A]}(x) = A_i^{[A]}(x) - A_{i_{cl}}^{[A]}(x) \tag{19}$$

That is, eq. (18) can be shown to be independent of  $A$ . Figure 6 should be self-explanatory about the uniqueness of the coordinate system. Equation (18) has the following form after some calculations,

$$\nabla \cdot \delta A^a + ef_{abc} A_{cl}^b \cdot \delta A^c = 0 \tag{20}$$

which is nothing but the background gauge condition for the fluctuations.

The Singer paper is typical of mathematicians and is not understandable to me. But I believe in his results because of the following reason. If one replaces  $A_{cl}(x)$  in (20) by a general field configuration  $A(x)$  then (20) is the local condition that  $\nabla A^*(x)$  is normal to the orbit passing the point  $A^*(x)$ . Thus,  $\nabla A^*(x)$  can be considered as a segment of the starting line. If one can integrate this functional differential equation one obtains the equation for the starting line which intersects orbits normally all the way. Unfortunately, however, because of the second term of (20) the integrability condition is not satisfied. Thus, it is not possible to obtain an equation for a universal starting line (overall gauge condition).

Are Gribov ambiguities really the fundamental difficulty? From the geometrical point



of view I described, it is only a difficulty of setting up an overall coordinate system in the configuration space. As I explained before it is not a difficulty in the semi-classical calculation since one can always set up local coordinates (background gauge) which are gauge invariant. Thus, one solution for the Gribov ambiguity would be the following.<sup>37</sup> Start the perturbation calculation about a given field configuration, say  $A^{(1)}$  using the background gauge to obtain the Schrödinger wave function. The perturbation calculation would break down precisely at the field configurations  $A^{(2)}$ , at which Faddeev-Popov determinant becomes zero (see Fig. 7). The perturbation would be good in the region **2i** in this figure. Next use the field configuration  $A^{(2)}$  about which one proceeds new perturbation calculation with new background gauge to obtain the Schrödinger wave function for the region denoted by **2.**. There is an overlap region where wave function is connected by using a point canonical transformation to change the gauge in **2i** to that in **2.**. One may repeat this procedure successively to cover all the configuration space. The connection procedure I described is a generalization of the connection procedure in the WKB method; it is similar to Wu and Yang's section idea.<sup>38</sup>

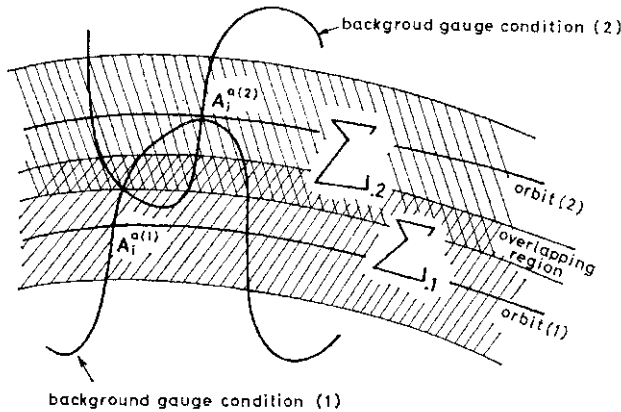


Fig. 7.

**Confinement**

Now let me come to the heart of QCD, namely color confinement. There are several interesting ideas proposed for the confinement mechanism in the past few years.

Let me first explain how to proceed with the discussion. The Lagrangian in Table I

can easily be cast into canonical form for quantization. Because of the gauge symmetry, the generators  $P \ll (x)$

$$P_a(x) = \frac{1}{e} \nabla \cdot E^a + f_{abc} E^b \cdot A^c \tag{21}$$

of the symmetry group commute with the Hamiltonian, so that one can diagonalize  $P_a(x)$  simultaneously with the energy where  $E^a$  is a canonical conjugate momentum of  $A^a$ .

The eigenvalues are color charge distributions, which correspond to Gauss' law in electrodynamics. One can show that the operator

$$M(x_1; x_2[A]) = P \exp \left( i \int_{x_2}^{x_1} dx \cdot A(x) \right) \tag{22}$$

has the property that it creates a color charge [3] at  $x_1$  and anti-charge [3\*] at  $x_2$ , from the color charge zero state  $|\wedge_0\rangle$

$$P_a(x) |\psi_0\rangle = 0. \tag{23}$$

Note that the operator  $M$  is in general path dependent. Thus, the energy eigenvalues also depend on the path of integration eq. (22), especially on the distance  $R$  between  $x_1$  and  $x_2$ .

$$HM |\psi_0\rangle = E(R, \dots) M |\psi_0\rangle \tag{24}$$

The confinement criterion is given by

$$\lim_{R \rightarrow \infty} E(R, \dots) = \infty. \tag{25}$$

Let us consider the expectation value of the evolution operator

$$\langle \psi_0 | M^+ e^{-HT} M | \psi_0 \rangle = e^{-ET} \tag{26}$$

The left hand side can be expressed in the form of a Feynman-Kac functional average of the Wilson loop integral

$$\langle \mathcal{W}(C) \rangle = \frac{\int \dots \int \mathcal{D}A_\mu \exp \left\{ - \int \mathcal{L}(A) d^4x \right\} \mathcal{W}(C)}{\int \dots \int \mathcal{D}A_\mu \exp \left\{ - \int \mathcal{L}(A) d^4x \right\}} \tag{27}$$

$$\mathcal{W}(C) = \text{Tr} P \exp \left( i \oint_C A_\mu(x) dx_\mu \right). \tag{28}$$

Most of the color confinement arguments hinge on whether or not the logarithm of the functional average eq. (27) is proportional to the area of the Wilson loop  $C$ .<sup>39</sup>

There are at least two versions of the QCD formulation, the lattice version<sup>40</sup> and the

standard continuum version given by eq. (1). In the lattice theory a la Wilson, the colors are confined in the strong coupling limit as shown by Wilson using the high temperature expansion techniques of statistical mechanics. However, as I explained before the most important aspect of QCD confirmed by experiments is asymptotic freedom, which is derived from the continuum theory by perturbation calculations. Thus, one must go to the continuum limit, for which it is necessary to make the bare coupling constant of lattice gauge theory zero. Therefore, if confinement is to hold, there must not occur any phase transition as the coupling varies from large to zero. There is a supporting discussion, due to Migdal,<sup>41</sup> who derived the lattice version of the Callan-Symanzik equation using an approximation (he checked the validity of the approximation on other solvable models, such as the Ising model) and concluded there are no phase transitions.

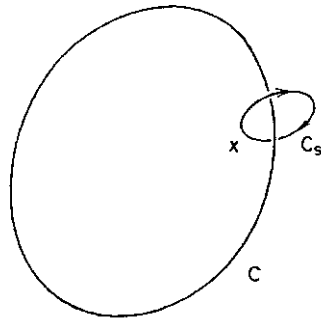


Fig. 8.

Last winter, 't Hooft wrote a paper<sup>42</sup> on confinement. It is a difficult paper to read but the results and implications are interesting and important. So, let me try to explain it. The Wilson loop operator defined by eq. (28) is a non-Abelian analogue of a magnetic flux operator, 't Hooft defines an analogue of electric flux by considering a singular gauge transformation operator  $\hat{\Lambda}(C)$ , which is defined as follows. Let  $C$  be a loop in 3+1 dimensional space. (See Fig. 8.) Consider the gauge SU(3) matrix at a point  $x$ ; it is such that when it goes around  $C$  along the path denoted by  $C$ , it changes by a factor  $e^{2\pi i/3}$  which is an element of  $Z(3)$ , the center of SU(3). Let  $\hat{\Lambda}(C)$  be an operator which causes such a singular gauge transformation. He then noticed that  $\hat{J}^{\Lambda}(C)$  and  $\hat{\Lambda}(C)$  satisfy an

algebraic relation

$$\hat{\Lambda}(C)\hat{B}(C') = \hat{B}(C')\hat{\Lambda}(C)e^{2\pi i n/3} \quad (29)$$

where  $n$  is the number of times the loop  $G$  winds through  $C$ . He then classified the representations of this algebra, assuming a cluster decomposition

$$\langle \hat{\Lambda}(C)\hat{B}(C') \rangle = \langle \hat{\Lambda}(C) \rangle \langle \hat{B}(C') \rangle \quad (30)$$

when  $C$  and  $C'$  are far apart, which is reasonable if there are no zero mass particles, which we assume. There are three representations i) Higgs mode; ii) Confinement mode; and iii) Higgs and confinement mode. The last one he thinks unlikely.

Higgs mode:

$$\langle \hat{\Lambda}(C) \rangle \propto e^{-L}, \quad \langle \hat{B}(C) \rangle \propto e^{-S}$$

Confinement mode:

$$\langle \hat{\Lambda}(C) \rangle \propto e^{-S}, \quad \langle \hat{B}(C) \rangle \propto e^{-L} \quad (31)$$

where  $S$  is the area of the loop  $C$ , and  $L$  is the circumference of the loop  $C$ .

Let me explain the Higgs mode and the confinement mode, taking the example of a superconductor. As you know superconductors expel magnetic fields (Meissner effect). So if you put a magnetic monopole in a superconductor, a magnetic flux line is formed. This is the Abrikosov-Nielsen-Olesen flux line.<sup>43</sup> Therefore if one puts a monopole and an anti-monopole in a superconductor a flux line (or you may say simply a string) is formed from the monopole to the anti-monopole. The energy of the system is mainly the magnetic field energy. However, since the magnetic lines are confined to a string (one dimensional) the energy is proportional to the distance between the monopoles. This confinement of magnetic charges is called the Nambu-Parisi analog model of confinement.<sup>44</sup>

We would like to have electric confinement rather than magnetic confinement. One can twist it around since ordinary (Abelian) electrodynamics is entirely symmetric with respect to the interchange between magnetic field and electric field together with the interchange between magnetic monopoles and electric charges. This interchange is called a dual transformation. After making the dual transformation if one makes a superdielectric (dual to superconductor) by the same mechanism one can confine a positive and negative charge, which one calls electric confinement.

The Higgs mode 't Hooft refers to corresponds to magnetic confinement (Nambu-Parisi), while the confinement mode corresponds to electric confinement<sup>45</sup> (Wilson-Kogut-Susskind). Notice that by the dual transformation weak coupling and strong coupling are interchanged because of the Dirac quantization condition :

$$ee' = 2\pi r.$$

The importance of dual transformations to the confinement is emphasized especially by Mandelstam<sup>46</sup> and 't Hooft.<sup>47</sup> The dynamical realization of 't Hooft's result has been attempted by Englert and Windey<sup>48</sup> and by Yoneya.<sup>49</sup> Since Englert's work is reported in these proceedings I will explain only Yoneya's work. He considered the lattice Z(3) model and proved that it is self-dual. From this he derived a critical coupling constant above which the system is in the confinement phase and below which is in the Higgs phase. He further tried to derive an effective Z(3) lattice gauge theory from Wilson's lattice QCD, but unfortunately there is a questionable point in the derivation.

Another attempt which addresses the dual transformation is by Sugamoto.<sup>50</sup> He considers the dual transformations only in the Abelian Higgs model. He points out that the dual transformation is similar to the ordinary Fourier transformation. Along this line he analyses the dual transformation in Abelian gauge theory, especially the Higgs model, and arrives at the conclusion that the dual transformed Higgs model is Kalb-Ramond-Nambu's relativistic hydrodynamic model.<sup>51</sup> This conclusion itself is not so significant, but I believe that the technique he developed in the paper is useful.

I should mention at this point two seemingly unrelated papers recently published in the literature. As Sugamoto and others noted, the dual transformations are kind of Fourier transformations in configuration space; in field theory that is a representation in which the conjugate momenta  $\mathbf{T}(\mathbf{X})$  (in gauge theory  $E$ ) are diagonal rather than the coordinates,  $\langle f(x) \rangle$  (in gauge theory vector potential,  $A(x)$ ). Goldstone and Jackiw<sup>52</sup> made the elimination of the gauge degrees of freedom precisely in this representation. Another is the work by Halpern.<sup>53</sup> He starts with the linear form of

non-Abelian gauge theory in path integral formalism. Then he integrates out the vector potential to obtain an expression entirely in terms of field strength  $F_{\mu\nu}$ . Since this procedure can be considered as a sort of a gauge invariant Fourier transform in functional space, one may regard this theory as a kind of dual transformed non-Abelian gauge theory. This is the reason why this formalism is not suitable for a weak coupling expansion. There is a possibility that these theories may be modified in such a way a strong coupling expansion is possible. If this is the case these works are interesting and important for the future investigations.

### Princeton Bag

This is a new work of Callan, Dashen and Gross<sup>54</sup> reported by D. Gross at the conference. They follow the Polyakov program I described earlier, keeping only the instanton excitations. Their calculations (and, as a matter of fact, all the calculations about the effects of instantons) depend heavily on 't Hooft's excellent calculation<sup>55</sup> for the quantum corrections about an instanton:

$$\begin{aligned} \langle 0 | e^{-HT} | 0 \rangle &\approx \int d^4x \int \frac{d\rho}{\rho} n(\rho), \\ n(\rho) &\sim c X^3(\rho) e^{-X(\rho)}, \\ X(\rho) &= \frac{8\pi^2}{g^2(\rho)}. \end{aligned}$$

This leads to the statistical mechanics of the instanton gas in four dimensions in the dilute gas approximation scheme. It is worth mentioning that the dilute gas approximation is valid only for the small coupling region, namely for  $p <$  typical hadron size. The Princeton authors make an analogy between the instantons and four dimensional permanent magnetic dipoles. Notice that the dipole moment of the instanton is proportional to  $p^2$  (apart from a  $\ln p$  factor):  $Docp^2$ . In the presence of the external field the interaction energy is given by  $\text{Energy} = 2x^2/g^2 \text{Tr } FD$  which provides the following Boltzman factor to the instanton statistical mechanics:

$$\exp\left(-\frac{2\pi^2}{g^2} \text{Tr } F \cdot D\right). \quad (32)$$

Because of this factor the large instantons are expelled from the color electric field which is produced by a quark and an anti-quark pair

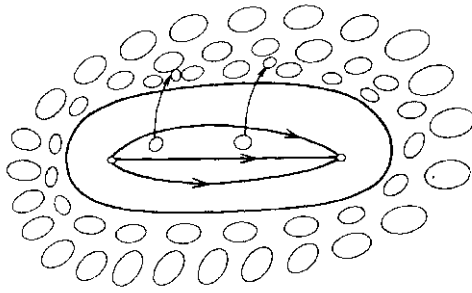


Fig. 9.

(see Fig. 9) and a sharp bag is formed. According to Gross this is due to a first order phase transition occurring at  $E=E_c$  so that the permeability changes from  $\infty$  to  $\# \ll \infty$ ; accordingly, a sharp bag. However, according to their calculation, small size instantons are stuck to the bag and make the thickness of the bag sizable, about  $1/10$  of the hadron size. If this is the case the instanton density inside the bag is not uniform, so that the effects of instantons for short distance phenomena are rather difficult to estimate.

In this theory  $\Lambda$ -mesons are Goldstone bosons and Callan, Dashen, and Gross think the  ${}^1S_0$   $qq$  state in the bag might be unstable, as pointed out first by Horn and Yankielowicz.<sup>56</sup>

### Phenomenological Lagrangian Approach

I believe in the color confinement, but it is fair to say that nobody has given a conclusive argument yet. I have tried to show you the different point of views shared among physicists concerning confinement in QCD. I believe that the difficulties are mostly technical in nature and with time and energy they will eventually be resolved.

Friedberg and Lee<sup>57</sup> view some of the QCD investigations in the following way. "The aim of most efforts in the current literature is to derive quark confinement from QCD directly. In this connection we may recall the relation between QED and the phenomena in superconductivity. A similarly direct attack would impel one to proceed by starting QED, using its short-range Coulomb force to establish the existence of crystals, then obtaining the electron-phonon interactions, extracting from them the BCS correlation energy, and finally deriving the BCS theory. As yet no one has succeeded through pure theoretical deduction even in the first step,

proving the existence of crystals from QED." This is an interesting but rather extreme view. Nonetheless let us take this view at this moment and seek phenomenological Lagrangian models, which can correctly describe hadrons in a simpler fashion.

Before going into the specific Lagrangian models let me make a remark based on the paper of Matsuyama and Miyazawa<sup>58</sup> who calculated the Van der Waals potential between hadrons assuming an attractive linear potential between a color singlet pair of a quark and an anti-quark. They obtained

$$V(R) = -2.8 \text{ MeV} (1/Rf) \quad (33)$$

where  $R$  is the nucleon separation distance in fermis, which is determined from hadron spectroscopy. This is a rather big long range force:  $V(R)$  is larger than the Coulomb interaction for  $r < 4.5$  fm, and dominates over the gravitational potential for  $r < 1$  km. By contrast, according to Matsuyama, Miyazawa and Kikkawa<sup>59</sup> the string model yields

$$K_{\text{str}}(1\hat{r}) = -1.26 M_0 V R e^{-2.58r} \quad (34)$$

These calculations implies that the naive potential model should be treated with care.

There are two approaches to the phenomenological Lagrangian method: (i) The Lagrangian contain string or bag coordinates to guarantee the confinement, ii) The strings or bags, accordingly the confinement, are derived from a solution of phenomenological Lagrangians.

The former approach is advocated by Kikkawa, who described their quark string model<sup>60</sup> in detail in his talk. (The MIT bag model belongs also to this category.) So I will not describe this approach further.

The latter approach includes the Friedberg-Lee model of a hadron as a non-topological soliton<sup>57</sup> and Ken Johnson's new Lagrangian formulation<sup>61</sup> of MIT bag model. In this new Lagrangian approach there is no solution for the empty bag, whose existence was considered as one of the defects of the original MIT bag model.

Another effective Lagrangian is a familiar Kogut-Susskind-'t Hooft type<sup>62</sup>

$$\mathcal{L} = -\frac{1}{4} Z(\phi) (F_{\mu\nu}^a)^2 - \frac{1}{2} (\partial_\mu \phi)^2 - V(\phi) \quad (35)$$

where  $\langle j \rangle$  is a real scalar field. Fukuda<sup>63</sup> reported his work in the parallel session, in

which he uses (35) as an effective Lagrangian. He and Kugo actually started with the fundamental Lagrangian and found a color singlet tachyon bound state of two gluons. He interprets this as a signal of the instability of the vacuum he started with and represents the tachyon as the quantum of a scalar field  $\langle f(x) \rangle$  whose effective potential  $V(f)$  has a double well form with two degenerate minima at  $\langle f \rangle = \pm \theta_e$ . He then argues that  $Z(\langle f \rangle) = 0$ , based on self-consistency. He assumes that  $Z(\theta) = (0 - 0_e / \zeta \theta)^{2\alpha}$  and deduces that  $\alpha > 1$  from vacuum stability. This is known to be sufficient for confinement.

**Nambu-Goto String from QCD**

Since Professor Kikkawa covered Nambu's work<sup>64</sup> in detail, I describe it only briefly. Nambu started with the Bethe-Salpeter type of sause invariant amplitude:

$$\psi_{\text{meson}} = \langle 0 | \bar{q}(x_1) M(x_1; x_2[A]) q(x_2) | \text{meson} \rangle \tag{36}$$

which is path dependent. He made a virtual variation of the path to derive an equation for  $\langle p \rangle$ . He obtained the relativistic massless string equation with the assumption

$$\langle F_{\mu t}^2 \rangle = C \quad C > 0 \tag{37}$$

He estimated  $C$  and found it equal but with opposite sign to the estimate by Shifman *et al*<sup>65</sup> (See below.) In our opinion the expectation value (37) should be the value inside the string, while the expectation value of Shifman *et al* is for the outside, namely electric inside and magnetic out side (which is reasonable).

**QCD and Resonance Physics**

Zakharov reported work<sup>65</sup> on sum rules based on QCD. The authors used Wilson's operator product expansion for  $TT(\#)$ , which is defined by

$$i \int e^{iq \cdot x} d^4x \langle 0 | T^*(j_\mu(x) j_\nu(0)) | 0 \rangle = (q_\mu q_\nu - g_{\mu\nu} q^2) \pi(q^2)$$

They determined the coefficients in front of operators such as  $(i \cdot \wedge)^2$ ,  $m_q \wedge \langle p \rangle$ ,  $\langle p F \rangle \langle p p F \rangle \langle p \rangle$  etc., as calculated using QCD in terms of the lowest order Feynman-Dyson perturbation theory. Using the dispersion relation for  $\gamma_T(\#)$  and a new technique of Borel transform,

they derived sum rules for the resonance parameters (masses, coupling constants, decay widths etc.) Unknown quantities appearing in the sum rules are  $\langle (F \wedge)^2 \rangle$  and  $\langle (p \langle p \rangle) \rangle$ . They obtained the value of  $\langle (F \wedge)^2 \rangle$  using the charmonium data, and estimated  $\langle p \langle p \rangle \rangle$  using Gell-Mann-Oakes-Renner theory. From the sum rules they obtain impressive results, such as

$$\frac{g_\rho^2}{4\pi} \simeq \frac{2\pi}{e} \simeq 2.3, \\ (m_\rho^2)_{\text{theor.}} \simeq (m_\rho^2)_{\text{exp.}}$$

where  $e$  is the base of natural logarithms.

**Conclusion**

Concluding my talk, I repeat that there are no decisive experimental tests of QCD nor any conclusive deduction of confinement yet. Nevertheless, I think all the circumstantial evidence points to the confirmation of QCD being the true theory of strong interactions.

**Acknowledgement**

In preparing this report I had great assistance from my students and colleagues, especially S. Wadia, A. Guha, T. Yoneya. I also had help from the scientific secretaries, A. Hosoya and Y. Hosotani, in reading some of the papers submitted later. I thank also K. Kikkawa, C. Callan, and D. Gross for valuable discussions and C. J. Goebel for valuable comments on the manuscript.

I acknowledge that this work is supported by U.S. National Science Foundation (PHY 77-03354) and by the Research Foundation of City University of New York (RF 11681).

**References**

1. C.N. Yang and R. L. Mills: Phys. Rev. **96** (1954) 191.
2. D. J. Gross and F. Wilczek: Phys. Rev. Letters **30** (1973) 1343; H. D. Politzer: Phys. Rev. Letters **30** (1973) 1346.
3. R. F. Feynman: Phys. Rev. Letters **23** (1969) 1415; J. D. Bjorken and E. A. Paschos: Phys. Rev. **185** (1969) 1975.
4. O. W. Greenberg: Phys. Rev. Letters **13** (1964) 598.
5. Y. Miyamoto: Progr. theor. Phys. Suppl. Extra Number 187 (1964); M. Y. Han and Y. Nambu: Phys. Rev. **B139** (1965) 1038; M. Gell-Mann; Acta Phys. Austriaca Suppl. **9** (1972) 733.
6. H. Fritzsch and M. Gell-Mann: *Proc. XVI Int.*

- Conf. High Energy Phys., Chicago, 1972*, vol. 2; S. Weinberg: Phys. Rev. Letters **31** (1973) 494; D.J. Gross and F. Wilczek: Phys. Rev. **D8** (1973) 3633; H. Fritzsch, M. Gell-Mann and H. Leutwyler: Phys. Letters **47B** (1973) 365.
7. D. J. Gross and F. Wilczek: Phys. Rev. **D8** (1973) 3633; S. Weinberg: Phys. Rev. **D8** (1974) 4482; K.G. Wilson: Phys. Rev. **D10**, (1974) 2445.
  8. G. Veneziano: Nuovo Cimento **57A** (1968) 190.
  9. M. Jacob, ed.: *Dual Theory*, (North-Holland Publishing Co., Amsterdam, 1974).
  10. Y. Nambu: *Proc. Int. Conf. Symmetry and Quark Models, Detroit, 1969* (Gordon and Breach, N.Y. (1970)) p. 269; L. Susskind, Nuovo Cimento 69A (1970) 457.
  11. H. Yukawa: Phys. Rev. **77** (1950) 219.
  12. A. Chodos, R. L. Jaffe, K. Johnson, C. B. Thorn and V. F. Weisskopf: Phys. Rev. **D9** (1974) 3471.
  13. A. Jevicki: Nucl. Phys. **B117** (1976) 365.
  14. R. Jackiw and C. Rebbi: Phys. Rev. Letters **37** (1976) 172.
  15. J. L. Gervais and B. Sakita: Phys. Rev. **D18** (1978) 453.
  16. C. G. Callan, Jr., R. F. Dashen and D. J. Gross: Phys. Letters **63B** (1976) 334; R. Jackiw and C. Rebbi: Phys. Rev. Letters **37** (1976) 172.
  17. A. Belavin, A. Polyakov, A. Schwartz and Y. Tyupkin: Phys. Letters **59B** (1975) 85.
  18. G. 't Hooft: Phys. Rev. Letters **37** (1976) 8.
  19. S. Weinberg: Phys. Rev. **D11** (1975) 3583.
  20. A. Polyakov: Phys. Letters **59B** (1975) 82.
  21. J. L. Gervais and B. Sakita: Phys. Rev. **D16** (1977) 3507; K. M. Bitar and S.-J. Chang: Phys. Rev. **D17** (1978) 486; H. J. de Vega, J. L. Gervais and B. Sakita: Nuclear Physics **B139** (1978) 20.
  22. T. Banks, C.M. Bender and T. T. Wu: Phys. Rev. **D8** (1973) 3346.
  23. H. Georgi and H. D. Politzer: Phys. Rev. **D9** (1974) 416; D. J. Gross and F. Wilczek: Phys. Rev. **D9** (1974) 980; D.J. Gross: Phys. Rev. Letters **32** (1974) 1071; See also H. D. Politzer, A12 report at this Conference.
  24. See E. Gabathuler P6 report at this Conference.
  25. G. Wentzel: Helv. Phys. Acta **13** (1940) 269.
  26. S. Tomonaga: Progr. theor. Phys. **1** (1946) 83.
  27. J. Bardeen, L.N. Cooper and J. R. Schrieffer: Phys. Rev. **108** (1957) 1175.
  28. R. F. Dashen, B. Hasslacher and A. Neveu: Phys. Rev. **D10** (1975) 4114.
  29. J. L. Gervais and B. Sakita: Phys. Rev. **D11** (1975) 2943.
  30. J. L. Gervais: 1978 Les Houches Winter School Lecture Notes.
  31. C. G. Callan, Jr., R. F. Dashen and D. J. Gross: Phys. Letters **63B** (1976) 334; A. M. Polyakov: Nuclear Physics **B121** (1977) 429.
  32. J. L. Gervais and B. Sakita: Phys. Rev. **D16** (1977) 3507.
  33. V.N. Gribov: Materials for the XII Winter School of Leningrad Nuclear Institute (1977).
  34. Contributed papers No. 279, 280, 366, 823, 851.
  35. D. Amati and A. Rouet: Phys. Letters **73B** (1978) 39.
  36. I. M. Singer: Comm. of Math. Phys. **60** (1978) 7.
  37. I thank S. Wadia for a discussion for this point.
  38. T. T. Wu and C.N. Yang: Nucl. Phys. **B107** (1976) 365.
  39. K. G. Wilson: Phys. Rev. **D10** (1974) 2445.
  40. K.G. Wilson: Phys. Rev. **D10** (1974) 2445; J. Kogut and L. Susskind: Phys. Rev. **D11** (1975) 395.
  41. A. A. Migdal: JETP 69 (1975) 810.
  42. G. 't Hooft: On the phase transition forwards permanent quark confinement, Utrecht preprint.
  43. A. A. Abrikosov: JETP **5** (1957) 1174; H. B. Nielsen and P. Olesen: Nucl. Phys. **B61** (1973) 45.
  44. Y. Nambu: Phys. Rev. **D10** (1974) 4262; G. Parisi: Phys. Rev. **D11** (1975) 970.
  45. K.G. Wilson: Phys. Rev. **D10** (1974) 2445; J. Kogut and L. Susskind: Phys. Rev. **D9** (1974) 3501.
  46. S. Mandelstam: Physics Reports **23C**, No. 3 (1976).
  47. G. 't Hooft: *Proc. EPS Int. Conf, Palermo, 1975*.
  48. F. Englert and P. Windey: Contributed paper No. 266.
  49. T. Yoneya: Contributed paper No. 323.
  50. A. Sugamoto: Contributed paper No. 470.
  51. M. Kalb and P. Ramond: Phys. Rev. **D9** (1974) 2273; Y. Nambu: in *Quark Confinement and Field Theory*, ed. by D. R. Stump and D. H. Weingarten (John Wiley, 1977); *Proc. Conf. Univ. of Rochester, Rochester, R.Y., 1976*.
  52. J. Goldstone and R. Jackiw: Phys. Letters **74B** (1978) 81.
  53. M. B. Halpern: Phys. Rev. **D16** (1977) 1798.
  54. C. G. Callan, Jr., R. F. Dashen and D. J. Gross: A theory of hadronic structure, Princeton preprint.
  55. G. 't Hooft: Phys. Rev. **D14** (1976) 3432; see also A. Belavin and A. Polyakov: Nucl. Phys. **B123** (1977) 429; F. Ore: Phys. Rev. **D16** (1977) 2577.
  56. D. Horn and S. Yankielowicz: Phys. Letters (to be published)
  57. R. Friedberg and T. D. Lee: Columbia University preprint CU-TP-118 (1978).
  58. S. Matsuyama and H. Miyazawa: Contributed paper No. 636; see also Y. Fujii and K. Mima: Contributed paper No. 591.
  59. See Kikkawa's report.
  60. K. Kikkawa and M. Sato, Phys. Rev. Letters **38** (1977) 1309; I. Bars and A. J. Hanson: Phys. Rev. **D13** (1976) 1744.
  61. K. Johnson: Contributed paper No. 1003.
  62. J. Kogut and L. Susskind: Phys. Rev. **D9** (1974) 3501; G. 't Hooft: *Quarks and Gauge Fields* in Proc. Collog. on Lagrangian Field Theories (CNRS, Marseille, 1974).
  63. R. Fukuda: Contributed paper No. 746.
  64. Y. Nambu: Contributed paper No. 956.  
T. Matsumoto: Contributed paper No. 369.
  65. M. A. Shifman, A. I. Vainshtein, V. I. Zakharov: Contributed papers No. 1041, 1042, 1043, 1044, 1045.

## P 9b Unification, Superunification and New Theoretical Ideas

A. SALAM

*ICTP, Trieste*

### §1. Introduction

The Organizers have kindly allotted to me five parallel sessions—nine hours of the Conference—to report to the plenary session on. These include sessions on 1) unification of strong, weak and electromagnetic interactions, 2) supersymmetry and supergravity, 3) quantum electrodynamics, 4) formal field theory and 5) new theoretical ideas. With my deepest apologies to those physicists whose beautiful work I will not be able to report, I have reluctantly decided, in view of the shortness of time, and the experimental interests of the majority of the audience, to structure my report around the theme of *unification ideas for the four basic forces*: strong, weak, electromagnetic as well as gravitational. For there is no question that after the unification implied by  $SU(2) \times U(1)$ , the unification of the other two forces with what may call the "electroweak force" is likely to be one of the most motivating concerns in particle physics and will affect the development of the subject. New theoretical ideas often take some five to ten years to mature. My concern will be not so much with the short-range but rather with the long-range aspects of unification over a perspective of ten to twenty years; in terms, if you like, of not just the LEP and the ISABELLE accelerators, projected for the late 1980's but their successors of 10 TeV centre of mass, projected for the later 1990's. The weak force will become comparable to the electromagnetic above 100 GeV. The question we shall be posing is this; is the unification with the strong likely to manifest itself directly at a relatively low energy like 10 TeV, or does it manifest itself only at the inaccessible energy in excess of  $10^{12}$  TeV?

#### *Standard unification ideas*

To unify weak, electromagnetic and strong, the standard renormalizable gauge model pro-

ceeds as follows:

a) Find an internal symmetry group  $G$ , simple or semi-simple (with discrete symmetries), which includes  $SU(2) \times U(1) \times SU(3)_c$  and whose fermionic representations describe the known (and predicted) quarks and leptons.

b) Write a *local* theory of this internal symmetry group  $G$ , with one coupling parameter  $g$  and with Yang-Mills spin-one gauge particles. (For a semi-simple group  $G$ , discrete symmetries can ensure that there is only one gauge coupling constant.) The gauge particles include octet of colour gluons corresponding to  $SU(3)_c$  and  $W^\pm, Z^0$  and  $\gamma$  corresponding to  $SU(2) \times U(1)$ . Assuming that the gauge theory is asymptotically free, the unifying constant  $g$  would manifest itself at low energies, through renormalization group considerations in the form  $a_s = g^2 / 4\pi$  for strong  $SU(3)_c$  symmetry and the fine structure constant  $a$  for the  $SU(2) \times U(1)$  "electroweak" force.

c) The descent from  $G$  to  $SU(3)_c$  on the colour and  $SU(2) \times U(1)$  on the flavour side determines the ratio  $a_s/a$ , in terms of the high unifying mass  $M$  (expressed in units of a low mass *ju-few* GeV) in accordance with the standard ideas of Georgi, Quinn and Weinberg. In most of the unification models considered, it is usually assumed that the unification mass  $M$  is realized physically as governing the masses of ultra-heavy gauge mesons.

d) There is spontaneous symmetry breaking (SSB) which is accomplished by introducing a set of Higgs-Kibble spin-zero representations of the group  $G$ , and a Higgs potential which gives rise to observed masses and other broken symmetry phenomena. With the Higgs multiplets, one introduces two sets of new coupling parameters:  $f$ 's coupling fermions and scalars and  $X$ 's describing the Higgs self-couplings. The Higgs sector is not as tightly controlled as the basic fermionic and the gauge sectors. Later we shall see that supersymmetry (Bose-Fermi symmetry) is

one way of controlling the arbitrariness of this sector.

e) To include gravity—a spin-2 *gauge* theory—a compact internal symmetry  $G$  cannot suffice. Einstein's gravity can be formulated as the gauge theory of Weyl's  $SL(2, C)$  symmetry. This group structure must then be included in the basic group together with the compact  $G$ .

f) To include gravity, a radically new and fascinating approach has been favoured. There are many ways to describe this—and a part of this talk will be concerned with these diverse approaches—but one of the simplest is to say that one brings gravity into a unified gauge scheme not just through  $SL(2, C) \sim O(3, 1)$ , but instead through the larger structure  $Sp(4)^0(3, 2)$ , which includes and reduces to  $SL(2, C)^0(3, 1)$  after a Wigner-Innonue contraction.

g) This structure  $Sp(4)$  permits of a rather special inclusion of internal symmetries of the type  $O(JV)$ , and the corresponding Yang-Mills particles, through the procedure of "grading". Grading is the adjoining of fermionic anti-commuting generators to  $Sp(4)$  to give what are known as ortho-symplectic structures  $Osp(4|A)$  which include  $Sp(4) \times SO(QV)$  "bosonic" generators. "Grading"—the Fermi-Bose supersymmetry—implies that all multiplets of the graded groups contain equal numbers of fermionic as well as bosonic components. For the particular case of  $Osp(4|8)$  (with  $O(8)$  internal symmetry), the basic multiplet contains one graviton (spin 2), eight gravitinos (spin 3/2), twenty-eight Yang-Mills (spin 1) particles, fifty-six spin 1/2 fermions and seventy Higgs scalar  $s$ . There are two distinct coupling parameters, the gravitational  $K^{\wedge} = An^{\wedge}$  Newtonian and the Yang-Mills  $g$ . Note that it is the *grading*, the Fermi-Bose supersymmetry, which makes the basic fermions (spin 1/2) come to belong to the same multiplet as the conventional gauge particles (spin-2 graviton, plus the Yang-Mills spin one objects) together with the spin-zero Higgs particles. This is a radically new type of unification where it is not so much the "*uni-constant*" aspect of gauge unification which is emphasized but the "*uni-multiplet*" aspect which is more to the fore.

This ambitious superunified approach

through supersymmetry is exceedingly constricting. It would have been pleasing (in van Nieuwenhuizen's phrase) if nature had "indeed been aware of our efforts". It does not seem to be on present evidence—or at least on present evidence as we interpret it now. Perhaps we need to re-examine, *ab initio*, the charge concept, questions like how many flavours, how many colours, how many quarks and leptons, why internal symmetry and why non-Abelian internal symmetry at all? In this respect, I shall finally touch upon some of the deepest ideas reported at this Conference, connected with space-time topology and internal symmetries. Thus there will be four parts to this talk.

1) The standard unification models utilizing "simple" or "semi-simple" gauge groups.

2) *Global supersymmetry*, unification of Fermi and Bose objects into one multiplet—the general aspects of unification through grading; extended supersymmetries; and their possible embedding in higher dimensional space-times; use of extended supersymmetries to unify gravity with matter.

3) *Local supersymmetry*; gauging of supersymmetry itself, leading to a theory of self-interactions of Einstein's gravitation, and of these with the spin 3/2 gravitinos as well as their supersymmetric interactions with other types of supersymmetric matter.

4) The search for internal symmetries within space-time *topological* ideas.

## PART I

### §11. The Standard Models of Strong plus Electro-Weak Unification *via* Exchanges of Spin-One Gauge Particles

As indicated in the introduction, one starts with a group  $G$  (simple or semi-simple)<sup>1</sup>

1)  $G$  includes  $SU(2) \times U(1) \times SU(3)_c$ ;

2) Its fermionic representations—and preferably the fundamental—should describe known and predicted quarks and leptons<sup>2</sup>;

3) We shall assume that the local (gauge) version of  $G$  spontaneously breaks into  $SU(2) \times U(1) \times SU(3)_c$  with essentially one heavy mass scale  $M$ ; all gauge bosons not contained within  $SU(2) \times U(1) \times SU(3)_c$  are ultra-heavy, their masses being of order  $M$ . This is follow-



ed by a second, more familiar breaking of  $SU(2) \times U(1) \times SU(3)_c$ , with a medium mass scale.

Surprisingly, there are not very many candidates for the unification<sup>3</sup> models. If  $G$  is "simple" the current choice is between  $G = SU(5)^4$  or  $SO(10)^5$  or  $E_6^6$ . For the "semi-simple" case<sup>1</sup> (with discrete left-right-colour-flavour symmetries guaranteeing one basic constant  $g$ ) the only offer is

$$G = [SU(4)]^4 = SU(4)_z \times SU(4)^*_{flavour} \\ \times SU(4)_x \times SU(4)^*_{colour}$$

(or more generally perhaps  $[SU(n)]^4$ ).

Except for quark and lepton spectra, the "simple" groups  $SU(5)$ ,  $SO(10)$  and  $E_6$  offer fairly similar dynamical predictions, so far as the high mass unification signals are concerned.

a) For "simple" groups the unification mass  $M$  is as a rule of the order of  $10^{12}$  TeV, as are the masses of all gauge particles not contained within  $SU(2) \times U(1) \times SU(3)_c$ . In this sense these groups predict the end of the directly experimentally accessible particle physics within a foreseeable future. For the semi-simple case, the situation is very different. Here  $M$  and therefore the ultra-heavy gauge particles have masses which can be as low as 10 TeV. [This is connected with the possibility of chiral colour—see below.] Thus direct tests of strong force unification with the "electroweak" force may be envisaged already at ISABELLE (c.o.m. energy 1 TeV) and possibly even at PETRA and PEP.

b) The semi-simple  $G$  offers a choice between liberated integer-charge quarks and confined fractional charge quarks.

The two tables summarize the salient features of these models. Several remarks are in order.

1) In the models based on the simple groups,  $SU(5)$ ,  $SO(10)$  and  $E_6$ , colour  $SU(3)$  as a good *global* symmetry appears to preclude integer-charge quarks. With fractional charges for quarks,  $SU(3)_{colour}$  gluons are neutral. With *exact*  $SU(3)_c$  they would remain massless. Since no massless gluons have been observed, there should be an exact confinement of these and possibly of all colour. On the other hand, the semi-simple  $[SU(4)]^4$  (or more generally  $[SU(\#)]^4$ ) model permits the alternative of

an electro-weakly broken global  $SU(3)_c$  admitting of *integer-charge* (vector and axial) gluons and quarks. Such particles do not need absolute but only partial confinement.

To motivate *partial confinement*, we remark that in the parton model language, the effective masses of quarks and gluons (inside the known hadronic bags) is rather small. There is no contradiction with medium or heavy physical masses, outside the bags for integer (or even fractional) charges.

The "Archimedes effect"—light quarks and gluons inside—and heavy outside—is well known in other branches of physics. (Electrons in a metal, nucléons in shell-model calculations, are examples of situations where the effective masses are different from physical liberated masses. The distinction between these examples and the case of the quarks and vector gluons is only quantitative. The Archimedes effect for quarks and gluons appears to be much stronger.)

In order to give an estimate of the ratio of the inside to the outside mass, we must have a theory of partial confinement. (For example, is it vector gluons which are responsible for particle confinement or is it tensor gauge particles—see below.) A formula based on possible partial confinement through vector gluons has been suggested by A. de Rujula, R. C. Giles and R. L. Jaffe (MIT preprint, CTP 637, June 1977). These authors surmise that  $m_{out} \sim m_v^2 C / 27 \pi a m_v$ . Here  $m_{out}$  is the outside mass of a colour multiplet with the Casimir operator  $C$ ,  $a$  is the Regge slope parameter and  $m_v$  is the vector gluon mass inside the bag. For  $m_v \rightarrow 0$ ,  $m_{out} \rightarrow \infty$ , i.e., one recovers exact confinement. For  $m_v \sim 10$  MeV one would obtain  $m_{out}$  for quarks  $\sim 10 \sim 15$  GeV.

2) The semi-simple  $G = [SU(4)]^4$  with left-right flavour colour symmetry must contain colour *axial*  $SU(3)$  gluons, in addition to vector  $SU(3)$  gluons. Let us assume that these axial objects are relatively light ( $m \ll 100$  GeV): so that  $SU_{c,1}(3) \times SU_{c,2}(3)$  is the low medium mass colour symmetry. It is this larger structure ( $SU_{c,1}(3) \times SU_{c,2}(3)$  vs  $SU(3)_c$ ) which provides the essential element for the semi-simple  $[SU(4)]^4$  to exhibit a unification mass  $M$  as low as 10 TeV.

The reason for this is simple; the grand

unification mass scale  $M$  is essentially controlled by a relation like<sup>7</sup>

$$\frac{1}{g_{\text{strong}}^2(\mu)} - \frac{1}{g_{\text{weak}}^2(\mu)} \approx [\beta^{\text{strong}} - \beta^{\text{weak}}] \ln \frac{M^2}{\mu^2},$$

where  $j_8 \ll 11/3 \times 1/16 \pi^2 \times \text{Casimir operator of the low-energy residual symmetry group}$ . The Casimir operator for a low-energy strong group like  $SU_{\text{cl}}(3) \times SU_{\text{c,r}}(3)$  is twice that for  $SU(3)_c$ . This means that for the same left-hand side, the unification mass  $M$  required for  $[SU(4)]^+$  descending into chiral colour is many orders of magnitude smaller than the unifying mass needed for the simple groups  $SU(5)$ ,  $SO(10)$  or  $E_6$ , which descend into vectorial colour  $SU(3)$ .

3) Together with the unifying mass scale,  $\sin^2 \theta$  can be determined by the standard techniques of ref. 7. The surviving candidate groups for unification are not sharply distinguished by the predicted values of  $\sin^2 \theta$ , except that  $E_7$ —a favourite at one time—seems implausible now.

4) There is, again, a sharp distinction between simple and semi-simple groups for the predicted proton lifetime. The distinction is important, not only in that the semi-simple  $[SU(4)]^+$  gives a lifetime near to the present experimental lower limit while the "simple" groups give substantially longer life scales. It is also important because the mechanism for proton decays are completely different.

For the "simple" groups this decay is a second-order process in the gauge coupling  $P \rightarrow g + (\# + ?) \rightarrow \# + X - * \text{ anti-lepton}$ . Since the (so-called lepto-quark) gauge meson  $X$  responsible for this decay must have a mass  $\sim M \sim 10^{15}$  GeV for the "simple" groups, the proton lifetime is generally in excess of  $10^{38}$  years. The (fractionally charged) quarks are themselves of course stable against decays into integer-charge leptons.

For the integer-charge semi-simple  $[SU(4)]^+$  model, the quarks themselves are unstable (the predominant decay mode is  $q \rightarrow \text{neutrinos} + \text{mesons}$ ). In contrast to the case of the "simple" groups, this decay, however, is a consequence of spontaneous symmetry breaking. (The decay mode  $q \rightarrow \text{anti-leptons} + \text{mesons}$  is forbidden by a selection rule.) With

a lepto-quark  $X$  mass of the order of  $10 M_0^3$  GeV, one obtains a lifetime for a 10 GeV quark of the order of  $10^{-13} - 10^{-15}$  sees or shorter. The proton decay in this model is a sixth order ( $g^6$ ) process;  $\text{proton} = qqq \rightarrow \text{three neutrinos} + \text{mesons}$ , the most favoured channel being three neutrinos plus one, two or three mesons.

The problem of the semi-simple  $[SU(4)]^+$  unification model is the converse of the one for the simple groups. Here we must guarantee that the proton lives long enough. (The present lower limit estimates of proton lifetime ( $10^{30}$  years) are essentially for the two-body mode,  $\text{protons} - * \text{ or } n^0$ ) (F. Reines and M. F. Crouch, Phys. Rev. Letters **32** (1975) 493.) It is important to note that this particular decay mode is forbidden in the basic model using  $[SU(4)]^+$ .

It is good to remind ourselves that proton stability is an *empirical* law, unmotivated by any fundamental theoretical reasons. This realization has been hammered into theoretical consciousness by the fine work of the group led by Professor Reines. Since the value of the proton lifetime parameter is now so decisive for distinguishing between simple and semi-simple unifying groups—and between high ( $10^{12}$  TeV) and low mass (10-100 TeV) unification, it seems important that this parameter is measured afresh, at least once more.

In a contribution to the Conference, M. Yoshimura had argued that the dominance of matter over antimatter in the present Universe is a consequence of baryon number non-conserving reactions in the very early fireball. His computations give a small ratio of baryon to photon number density of the same order as observed. This work has been extended by S. Dimpoulous and L. Susskind (SLAC preprint, 1978).

#### *The semi-simple option*

A. If the semi-simple  $[SU(4)]^+$  (or  $[SU(\text{rc})]^+$ ) is indeed the unifying group, one may list a number of further signatures for this theory. The rather low grand unification energy of around 10-100 TeV is the energy at which the quark-lepton distinction would disappear, and when the so-called strong interactions acquire their basic  $O(a)$  strength. This is the energy where leptoquarks ( $X$ ) of this theory, of masses

around 10-100 TeV, may begin to make their appearance. For example, for ISABELLE with 1 TeV in the c.o.m., we may expect a substantial contribution to  $pp \rightarrow p + \dots$  through the Drell-Yan  $pp \rightarrow qq + \dots \rightarrow \# + (X + /OH \rightarrow ju + \bar{ju}) + \dots$  with a lepto-quark  $X \rightarrow q + ju$  of 10 TeV mass. Likewise, in the converse reaction  $e^+ + e^- \rightarrow (\#H - X) + e^- + \bar{q} + q$  one will begin to feel the effects of X-particles at energies  $\sim m_X/30$ .

B. It can be shown that in an integer-charge liberated quark version of this theory the neutral axial SU(3) colour gluons (being companion particles to vector gluons) possess a direct effective interaction with  $e^+e^-$  and  $ju\bar{p}$  systems. Assuming that their masses lie in the PETRA-PEP energy range, one would expect asymmetries in the forward-backward  $e^+e^- \rightarrow ju\bar{ju}$  around these axial gluon masses. Then asymmetries will be sharply pronounced, provided the masses of the axial gluons and the vector gluons are propitiously related (see J. C. Pati & Abdus Salam ICTP preprint, August 1978). The main decay modes of axial gluons are into vector gluons plus  $\langle$ or  $ai$  $\rangle$ . Thus one may expect characteristic signals at PETRA and PEP of the type:

$$e^+ + e^- \rightarrow \text{axial gluons} + \text{vector gluons} + (\dots)$$

C. Regarding integer versus fractional charges for quarks, G. Rajasekharan and P. Roy (Pramana **6** (1976) 303) and J. C. Pati and Abdus Salam (Phys. Rev. Letters **36** (1976) 11) showed that for deep inelastic processes, a colour suppression mechanism is operative, such that the colour component of quark charges does not shine forth as a rule for deep inelastic eN. However, such suppression is not expected for Compton scattering. The data of D. O. Caldwell *et al* (Phys. Rev. Letters **33** (1974) 868) for deep inelastic Compton has recently been analysed by H. K. Lee and J. K. Kim (Phys. Rev. Letters **40** (1978) 485) who remark that the integer charges for quarks are favoured over fractional charges, in spite of uncertainties of the parton models for such a comparison.

D. Since in the [SU(4)]<sup>+</sup> integer-charge model, quarks decay into neutrinos+mesons, but not into anti-neutrinos, an excess of

neutrinos over anti-neutrinos in a beam-dump experiment would signal nucléon dissociation mechanism into quarks and their subsequent decays. There is also an expected asymmetry for  $\nu_e$  versus

Before closing this section, two general remarks are in order.

1) Some of us (Abdus Salam and J. Strathdee, ICTP, Trieste, preprint IC/77/153, to be published in Phys. Rev., P. Caldirola and E. Recami, M. Pavsic, Phys. Letters 66A (1978) 9 and F. W. Hehl, Y. Neeman, J. Nitsch and P. Von der Heyde, submission to this Conference) have argued that confinement—partial or exact—may have as its origin the interaction of quarks and gluons with spin-2 gauge particles (strong gravitons). These are described for example by the Einstein equation for a strong tensor field with the Newtonian constant  $G_N$  replaced by a strong constant  $G_{\#} m^2 \dots i e o i i \sim 1$ . If there is, in addition, a cosmological term with a parameter  $X$ , (replacing the conventional cosmological parameter  $X_0$ ), where  $A/A_0 \sim G/G_N \sim z/10^9$ , the spin-2 Einstein-de-Sitter equation possesses a classical solution describing a "closed" de-Sitter micro-Universe of radius  $i^?_{\dots} c r o - (\wedge \wedge / 6) - 1/2 \wedge 10^{-13}$  cms. [The  $f_{00}$  component of the strong tensor equals  $f_{00} = l r G \dot{\wedge} / 6 r^2 + 2ju/r$ . Here  $ju$  is the mass parameter for the source quark. Note the  $r^2$  confining term in the potential.] A test quark of mass  $ju$ , in the strong gravity field is described by a Klein-Gordon equation  $(\sim f)^{-1/2} \Delta f + f A = 0$ . This equation possesses  $0(3, 2)$  symmetry and gives an energy spectrum,  $co = l/R - (2n+1+3/2+V9/4+ju^2)$ . The system exhibits discrete levels only and no continuum. There is *exact* confinement of the quarks inside a hadronic bag of radius  $i^? \wedge 10^{-13}$  cms.

One can introduce SU(3) of colour and show that with an appropriate choice of parameters the resulting octet of spin-2 gauge mesons produce confinement for colour singlet states only. From this point of view, a theory<sup>\*</sup> unifying the strong and the electro-weak forces, without taking into account strong gravitons (spin-2 gauge particles) is incomplete.

The appropriate group which describes eight coloured spin-2 gravitons together with nine Yang-Mills spin-one objects is SL(6, C) which contains SL(2, C) x SU(3). If strong as well

Table I. *Simple* "Unifying" Groups.

$G$	SU(5)	SO(10)	$E_6$
Favoured basic fermionic (two-component) multiplets	5+10	16	27
Quarks (four-component) including colour in the basic multiplet	6	6	9
Replications of the basic multiplet already observed	(u,d); (c,s); (t,b); ...	(u,d); (c,s); (t,b); ...	(u, d, b); (c, s, b') ; notice, no t-quarks with charge 2/3; instead b of charge -1/3
Leptons (charged) (neutral)	1 one two-component $\nu_e$	1 one four-component	2 two four-component plus three two component
Replications	( $\nu_e, e$ ); ( $\nu_\mu, \mu$ ); ( $\nu_\tau, \tau$ )	same as SU(5)	( $e, E=\tau$ ) and ( $\mu, M$ ) are replications of the basic multiplet
Number of gauge particles	24	45	78
Possible low-energy symmetry	SU(2) $\times$ U(1) $\times$ SU(3) <sub>c</sub>	SU <sub>L</sub> (2) $\times$ SU <sub>R</sub> (2) $\times$ U(1) $\times$ SU <sub>c</sub> (3)	[SU(2) $\times$ U(1)] $\times$ SU(3) <sub>c</sub> or [SU(2) $\times$ U(1)] <sup>2</sup> $\times$ SU(3) <sub>c</sub>
"Grand" unification mass	$\geq 2 \times 10^{16}$ GeV	$\geq 10^{16}$ GeV	$\geq 10^{15}$ GeV
$\sin^2 \theta$	$\approx 0.20$	$\approx 0.20$	$\approx 0.25$ ( $E_7$ excluded because predicted $\sin^2 \theta \approx 3/4$ )
$\tau_{\text{proton}}$ (with renormalization group corrections)	$\geq 10^{33}$ years	same as SU(5)	same as SU(5)

The major distinction between SU(5) and SO(10) lies in the four-component neutrino in the latter and left-right symmetry.

None of the groups above permit of *chiral* colour.

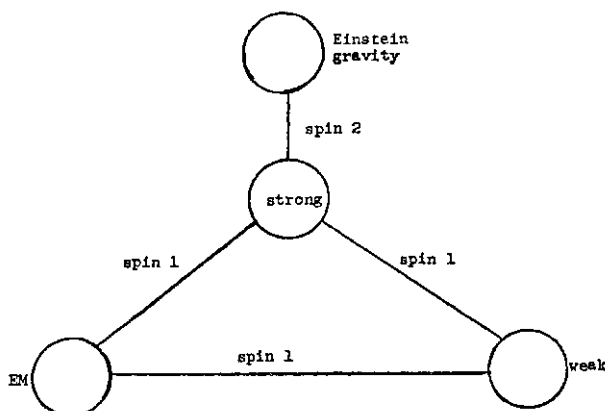
Table II. Semi-simple [SU(4)]<sup>4</sup> with discrete left-right-flavour-colour symmetry.

Basic fermionic multiplets	(4, 1, 4, 1)+(1, 4, 1, 4)	Remarks Possibility of liberated integer-charge quarks and gluons
Number of quarks (four component)	12+12 "mirror"	(u, d, s, c)+(e, $\mu$ ) and (t, b, b', t')+(E, M) may belong to the basic multiplet (including the mirror). A new replication of the basic multiplet is needed to accomodate the $\tau$ -lepton. Alternatively the group may be [SU(6)] <sup>4</sup> .
charged leptons ( " )	2+ 2 "mirror"	
neutral leptons ( " )	2+ 2 "mirror"	
gauge particles	60	
Possible low-energy symmetries	[SU(2) $\times$ U(1)] $\times$ SU <sub>cL</sub> (3) $\times$ SU <sub>cR</sub> (3) or [SU(2) $\times$ U(1)] <sup>2</sup> $\times$ SU <sub>cL</sub> (3) $\times$ SU <sub>cR</sub> (3)	
Unification mass	$10^4$ - $10^5$ GeV	The low unification mass is a consequence of axial colour.
$\sin^2 \theta$	$\approx 0.25$ - $0.27$	
$\tau_p$	$\approx 10^{28}$ - $10^{32}$ years	This is for the integer-charge quarks, where quarks decay into neutrinos+mesons.

as Einstein gravity must be included together, for example, with the unifying compact group (r=SU(5), one should be considering the structure SL(2, C)xSL(10, C).

2) The second general remark concerns the proliferation of quarks and leptons. This is the most serious problem which model builders must face. If one is thinking in terms of

fundamental entities of which all other particles are composed, one would like to introduce only the fundamental representation of the unifying group. As can be seen from Tables I and II this is already no longer true, for any of the groups proposed. At the very least, there is a replication of the representations- which implies that the group structure is not



describing those quantum numbers which differentiate one basic multiplet from another.

Assuming that the numbers of flavours and colours, etc. is not infinite—increasing with the energy range experimentally explored—the only answer to this situation would be to set up gauge theories in terms of pre-quarks ("preons") or sub-quarks or sub-stratons<sup>9,10</sup>—basic entities which might carry the *individual* basic quantum numbers. (Quarks carry two quantum numbers: colour and flavour. "Preons" would carry only one.) At the present time all known quarks and leptons may be considered as made of nine (hypothetical) entities—five carrying flavour and four carrying colour (the fourth colour representing lepton number). This number, nine, of independent quantum numbers, may possibly be reduced, but not very much. It is conceivable that for energies above 10-100 TeV or so, quarks and leptons can no longer be considered as point particles and their form factors must be taken seriously. The "preon" notion will then come into its own.

Concluding the discussion of how many quarks and how many leptons there may be, one may remark the following.

If the flavour and colour quantum numbers really are manifestations of topological structure of space-time, as I shall discuss later, it is fully conceivable that the flavour and colour quantum numbers increase with the energies considered when we probe deeper into the structure of the space-time manifold. Glashow (Report to the Oxford Conference, July 1978) has studied such a situation and he concludes that in such a situation

- i) neutrinos would in general be massive,
- ii) the masses of new quarks  $m_n$  increases faster than  $N^n$ , any  $j$ ?

iii) there must be an infinity of Higgs particles as well.

The restriction that neutrinos should be massive comes from cosmological considerations which limit the number of massless neutrinos to something like three or four, this number depending on the figure for helium abundance. The limitations on mass increase comes from  $(g-2)$  limitations for electrons and muons. There are also limitations from asymptotic freedom—*e.g.*, the celebrated limitation of  $16(1/2)$  quark flavours from asymptotic freedom of SU(3) of colour.

3) A final remark; as mentioned before, besides the basic gauge coupling parameter, there are the set of the Higgs-fermion coupling parameters ( $f$ ) and the Higgs self-coupling parameters ( $X$ ) in the theory. It is important that one should find theoretical reasons to decrease the arbitrariness implied by these constants. Based on a demand for asymptotic freedom, two suggestions have been made to evaluate these in terms of the gauge parameter  $g$ —

a) Abdus Salam and J. Strathdee (IC/78/44, Phys. Rev. to be published) have used an improved perturbation theory (where Dyson's irreducible graphs for gauge Higgs interactions are modified with line and vertex insertions—the effect of these insertions being estimated by using the running coupling parameter  $g(k)$  in the irreducible graphs). They show that the effective  $\Lambda$ 's thus computed are finite, (provided the bare  $\Lambda$ 's vanish) and equal  $\Lambda (= g^2/b$  times a group-theoretic factor. Here  $b$  is the parameter which appears in the renormalization group formula

$$\frac{g^2(k^2)}{g_R^2} \approx \left[ 1 + \frac{b}{16\pi^2} g_R^2 \log k^2 \right]^{-1}.$$

Since  $\Lambda_{\text{effective}} \propto g^2$  (rather than  $\Lambda \propto g^4$ ) the Higgs masses are thus of the same order of magnitude as the gauge masses. Salam and Strathdee also show that the theory is asymptotically free.

b) In a communication to this Conference, N. P. Chang and J. Perez Mercader have studied a class of SO( $iV$ ) grand unified theories where the Yukawa set of couplings and Higgs self-couplings are fixed by the eigenvalue conditions for asymptotic freedom. (The eigenvalue conditions require the existence of con-

starts  $\lambda$ ,  $I$ ,  $A$ , where the running parameters are all expressed as functions of the running gauge constant  $g(t)$ ; for example  $f(t)=fg(t)$ ,  $X(t)=Ig(t)$  and  $A(t)=Ag(t)$ . Here  $t=\log k'$ .

The technique used was originally studied by N. P. Chang, Phys. Rev. **D10** (1974) 2706; M. Suzuki, Nucl. Phys. **B83** (1978) 269; E. Ma, Phys. Rev. **D11** (1975) 322 and E. S. Fradkin and O.K. Kalshnikov, J. Phys. **A8** (1975) 1814. But the major new result is that, though replications of the basic Fermi families are needed, the number is limited and depends on the particular group  $SO(iV)$ .

c) Finally, before concluding this section I must mention some nice ideas of H. Terazawa, K. Akama, Y. Chikashige and T. Matsuki, who have considered unified models of the Nambu-Jona-Lasinio type for all elementary particles (including gravity).<sup>10</sup> They start with a non-linear Heisenberg type Lagrangian and from this construct an effective Lagrangian which combines  $SU(2)\times U(1)$  with  $SU(3)$  of colour. The photon,  $W$ ,  $Z^0$  and physical Higgs appear as collective excitations of lepton-antilepton pairs or quark-anti-quark pairs. They obtain mass formulae for  $W$  and  $Z$  particles. Extending their work to gravity theory they obtain a relation like  $a=3TT/(HQ^2) \approx 4\pi/3c^2 N_c G m^2$  where  $N_c$  is the number of quark flavours. They predict on this basis that there exist a dozen leptons (six neutrinos and six charged leptons) and a dozen flavours and three colours of quarks.

#### References and Footnotes to Part I

There is a number of fine reviews of the material covered in this lecture. I shall in general use these for purposes of referencing and not refer to individual papers unless a particular paper needs identification, or has not been included in the reviews.

1. I believe one of the first models attempting to unify strong with electro-weak forces was that of I. Bars, M. B. Halpern and M. Yoshimura (BHY), Lawrence Lab. Report LBL-990 (1972). Unhappily at the time the model was proposed, the role of gauged colour  $SU(3)_c$  QCD, mediating strong interactions through the operation of a group structure and *commuting* with  $SU(2)\times U(1)$  was not sufficiently recognized. This was achieved in the  $SU(2)\times U(1)\times SU(3)_c$  model of strong and electroweak unification by J. C. Pati and Abdus Salam (reported in the Proceedings of the Batavia Conference, Vol. 2, Sept. (1972) p. 304, Review talk by J. D. Bjorken and Phys. Rev. **D8** (1973) 1240). Pati and Salam also introduced the idea of grouping leptons and quarks in the same multiplet. A gauging

of such a multiplet inevitably (J. C. Pati and Abdus Salam, Phys. Rev. Letters **31** (1973) 661) gave rise to lepto-quarks (superheavy gauge particles) and a fundamental unification around the superheavy mass. These three ideas of Pati and Salam, ie,

- a) gauging  $SU(3)_c$  for colour and thereby generating strong interactions (in addition to  $SU(2)\times U(1)$  for the electroweak), in the contest of grand unification
- b) grouping quarks and leptons in the same multiplet of a basic symmetry group
- c) and the inevitability of lepto-quarks through the gauging of this group, are the cornerstones of all current unified gauge models of strong and electroweak forces.

Whereas the model of Pati and Salam was based on a "semi-simple" non-Abelian  $SU(4)_c \times SU(4)_l$  group structure, with discrete symmetry  $F \leftrightarrow C$  in contrast the next unifying model—that of H. Georgi and S. L. Glashow (Phys. Rev. Letters **32** (1974) 438) which incorporated the features listed above, was "simple." Another distinction between these prototype models was left-right symmetry which was a part of the Pati-Salam model, but abandoned in the Georgi-Glashow model.  $SO(10)$  and  $E_6$  however can admit of left-right symmetry. For complete references see J. C. Pati, submissions to this Conference 971, 972 and 973.

2. Ideally it should be the fundamental representation of the group, since other representations can be constructed out of it and particles corresponding to these other representations are composites. In practice, as we shall see, this is seldom the case for the groups now being considered. This is because we appear to have been caught almost unawares by the problem of quark and lepton explosion after the  $b$  quarks and  $r$  leptons have been discovered.

3. M. Gell-Mann, P. Ramond and R. Slansky: Rev. mod. Phys. (to be published) have attempted to limit the choice of permissible groups  $G$  by imposing *additional requirements*. For example, by requiring that colour conserves parity *exactly*, they are limited to groups which are vector-like in colour and permit chirality in the flavour sector only. By making the standard requirement that colour be an absolutely *exact* symmetry, they motivate fractional charges for quarks and thus confinement; by requiring further that the group structure relate the lepton and quark charges, they come to limit themselves to  $SU(5)$  or the three exceptional groups  $F_4, DSU(3)\times SU(3)_c, E_6, DSU(3)\times SU(3)\times SU(3)_c, E_7, SU(6)\times SU(3)_c$ .

4. H. Georgi and S. L. Glashow: Phys. Rev. Letters **32** (1974) 438; A.J. Buras, J. Ellis, M. K. Gaillard and D. V. Nanopoulos: Nucl. Phys.

5. H. Fritzsch and P. Minkowski: Ann. Phys. (NY) **93** (1975) 193; Nucl. Phys. **B103** (1976) 61; H. Georgi: *Particles and Fields* (APS/DPF Williamsburg), Ed. C. E. Carlson (AIP, New York 1975), p. 575.

6. F. Gursev, P. Ramond and P. Sikivie: Phys. Letters **60B** (1976) 177; F. Gursev and M. Serdareglu, Yale preprint COO-3075-180 (1978); Y. Achiman and B. Stech, Heidelberg preprint, HD-THEP 78-6; Q. Shaft, University of Freiburg preprint (1978).

7. H. Georgi, H. R. Quinn and S. Weinberg: Phys. Rev. Letters **33** (1974) 451.

8. C.J. Isham, Abdus Salam and J. Strathdee: Phys. Rev. **D3** (1971) 867; *ibid.*, **D8** (1973) 2600 and 1.1. Rabi 70<sup>th</sup> Birthday Volume (American Academy of Sciences, New York 1977), Series II, Vol. 38, p. 77; and references therein.

9. J. C. Pati, Abdus Salam and J. Strathdee: Phys. Letters **59B** (1975) 265-268 and references therein, in particular, the work of W. Greenberg.

10. H. Terazawa, Y. Chikashige and K. Akama: Phys. Rev. **D15** (1977) 480; H. Terazawa, Y. Chikashige, K. Akama and T. Matsuki: *ibid.*, **D15** (1977) 1181; H. Terazawa: *ibid.*, **D16** (1977) 2373.

PART II

Supersymmetry and Supergravity

§111. Global Supersymmetry

The unification we have discussed above has no arbitrariness in respect of the gauge multiplet, once the group structure is specified. It is unique. There is also no arbitrariness in respect of the fermionic multiplet, if it is stipulated that we shall only use the fundamental representations—all other representations referring to composite particles. There is however arbitrariness regarding Higgs scalars. This can be cured if, for example, the Higgs scalars were tied to the fermions. This is what supersymmetry does. Supersymmetry is Fermi-Bose symmetry introduced into particle physics by Y. A. Golfand and E. P. Lichtman (JETP Letters **13** (1971) 323) and rediscovered by J. Wess and B. Zumino (Nucl. Phys. **B70** (1974) 39). In its simplest global form, it forces the Higgs scalars to belong to the same representation of the internal symmetry group as the fermionic multiplet. In the so-called *extended super symmetries* ^ the next unification is achieved; the Yang-Mills as well as the basic fermions, as well as the Higgs, could all belong to the same multiplet of the internal symmetry. In its final form, *extended local supersymmetry* the same multiplet contains the spin-2 graviton, the Yang-Mills fields, the basic fermions as well as the Higgs scalars, and there is a unification of gravity with matter.

Global aspects

In its most direct form supersymmetry should be viewed as an extension of the symmetry of

space-time. Its algebra contains new generators  $Q_\alpha$  which are on the same footing as the Poincaré generators and  $J^\wedge$ . In particular, there is the fundamental relation

$$\{Q_\alpha, Q_\beta\} = -P_\mu (\gamma^\mu C)_{\alpha\beta}.$$

It is natural to attempt to see this symmetry as acting in an enlarged space-time. In fact, by adjoining the anti-commuting Majorana spinor co-ordinates  $d^r$  to the Minkowski , one can realize the "supertranslations" which are generated by  $Q_\alpha$ .

$$\delta\theta^\alpha = \varepsilon^\alpha, \delta x^\mu = \frac{i}{2} \bar{\theta} \gamma^\mu \varepsilon.$$

A non-trivial feature of this flat super-space-time on which the extended Poincaré symmetry acts is its non-vanishing torsion (see below).

Supersymmetric systems are characterized by a balancing of fermionic and bosonic states. The spin content of the irreducible unitary representations is

$$J, J - \frac{1}{2}, J + \frac{1}{2}, J \text{ (timelike)}$$

or

$$J, J - \frac{1}{2} \text{ (lightlike),}$$

where / is some integer or half-integer.

The balancing of Fermi and Bose components in supermultiplets is reflected in the suppression of quantum fluctuation effects. This is brought about by cancellations between Fermi and Bose contributions. One of the most striking features of supersymmetric dynamics is the absence of certain ultraviolet divergences: for example, (1) absence of coupling constant and mass renormalizations, (2) vacuum energy density, (3) the absence—at least at the one-loop level, of quantum corrections to the classically computed energy of a monopole solution in a supersymmetric version of the Georgi-Glashow model, (4) the finiteness of supergravity and extended supergravity for one- and two-loop diagrams and (5) the impossibility of breaking supersymmetry spontaneously through quantum loops, if it has not been broken at the tree diagram level. It would appear that, owing to cancellations among quantum fluctuations, supersymmetric theories are particularly well suited to a semi-classical treatment. Paradoxically then, balancing of bosons with fermions in a

supersymmetric manner appears to bring quantum theories nearer to the classical.

*Examples of renormalizable supersymmetric field theories*

(1) First, the self-interacting chiral scalar multiplet comprising the complex: scalars  $A_+, F_+$  and the left-handed spinor  $\psi_+$ . The Lagrangian is

$$\begin{aligned} \mathcal{L} = & |\partial_\mu A_+|^2 + \bar{\psi}_+ i \not{\partial} \psi_+ + |F_+|^2 \\ & + m \left( A_+ F_+ + \frac{1}{2} \psi_+^T C^{-1} \psi_+ + \text{h.c.} \right) \\ & + h (A_+^2 F_+ + \psi_+^T C^{-1} A_+ \psi_+ + \text{h.c.}), \end{aligned}$$

where  $m$  denotes the common mass and  $h$  is a dimensionless coupling. This Lagrangian is invariant (up to a 4-divergence) under the infinitesimal supertransformations

$$\begin{aligned} \delta A_+ &= \bar{\epsilon} \psi_+ \\ \delta \psi_+ &= F_+ \epsilon_+ - i \not{\partial} A_+ \epsilon_- \\ \delta F_+ &= -\bar{\epsilon} i \not{\partial} \psi_+. \end{aligned}$$

The complex scalar  $F_+$  is an auxiliary field: its equation of motion is purely algebraic and it can easily be eliminated from the Lagrangian. A result of this elimination is the appearance of a quartic coupling term  $-h^2 |A_+|^4$  among others. (This term, representing a Higgs potential, has a coefficient ( $h^2$ ) related in a definite well-defined manner to the coefficient of the Fermi-Bose coupling  $term h \psi_+^T C^{-1} A_+ \psi_+$ .) However, if this elimination of the  $F_+$  field is performed, the manifest symmetry, as reflected in the linear transformation rules would be lost. The transformations would become non-linear and the algebra would fail to close without the intervention of field equations. The auxiliary field  $F_+$  therefore plays a decisive role in the closing of the supersymmetric algebra and in the construction of supersymmetric Lagrangians. (Note the fields  $A_+, \psi_+$  can carry indices ( $\mu, \nu$ ) corresponding to an appropriate internal symmetry. Clearly global supersymmetry and internal symmetry are commuting operations.

(2) The second example is the supersymmetric Yang-Mills Lagrangian containing the usual vectors  $A_\mu^a$  and, in addition, a Majorana spinor  $\lambda^a$  and scalar  $D^a$

$$\mathcal{L} = -\frac{1}{4} F_{\mu\nu}^a F_{\mu\nu}^a + \frac{1}{2} \bar{\lambda}^a i \not{\partial} \lambda^a + \frac{1}{2} D^a D^a.$$

All of these fields belong to the adjoint re-

presentation of the internal symmetry which commutes with supersymmetry. The infinitesimal supertransformations are

$$\begin{aligned} \delta A_\mu^a &= -\frac{i}{\sqrt{2}} \bar{\epsilon} \gamma_\mu \lambda^a \\ \delta \lambda^a &= -\frac{i}{\sqrt{2}} \left( i \gamma_5 D^a + \frac{1}{2} \sigma_{\mu\nu} F_{\mu\nu}^a \right) \epsilon \\ \delta D^a &= -\frac{i}{\sqrt{2}} \bar{\epsilon} \not{\partial} \gamma_5 \lambda^a. \end{aligned}$$

Again an auxiliary field  $D^a$  is needed to close the algebra. The gauge supermultiplet may be coupled to a matter supermultiplet by a generalized version of the minimal principle. For example,

$$\begin{aligned} \mathcal{L}_{\text{matter}} = & |D_\mu A_+|^2 + \bar{\psi}_+ i \not{\partial} \psi_+ + |F_+|^2 \\ & + (ig \sqrt{2} A_+^\dagger \bar{\lambda}_- \psi_+ + \text{h.c.}) + g A_+^\dagger D A_+, \end{aligned}$$

where  $g$  denotes the Yang-Mills coupling constant. Note once again, that the elimination of the auxiliary field  $D$ , results in a quartic (Higgs) self-coupling of the field  $A_+$  with a coefficient which is tied to the gauge coupling  $g$  as well as to the Yukawa coupling constant in the term  $ig A_+^\dagger \bar{\lambda}_- \psi_+$ . To complete the enumeration of the Lagrangians for spin-1 gauge unification purposes, the matter Lagrangian may also contain self-couplings associated with parameters  $1/z$ , as discussed above, provided these are compatible with the internal symmetry.

To summarize, globally supersymmetric renormalizable theories with any internal symmetry, e.g.,  $SU(w)$  can be written down using the two types of Lagrangians shown above. (The second example is locally  $SU(w)$  symmetric, though still globally supersymmetric.) The chief characteristics of these Lagrangians are:

- 1) scalar (Higgs) fields (the  $A_+$ s) necessarily belong to the same internal symmetry multiplets as the matter fermions ( $\psi_+$ ).
- 2) Besides the internal symmetry gauge spin-one particles, there appear in the theory, *gauge fermions* (named "gluinos" by Fayet) in the adjoint representation of the internal symmetry.
- 3) The self-couplings of the scalar Higgs fields (the  $A_+$ s) and the fermion-Higgs couplings are tied to each other.
- 4) Since the Higgs potentials are so strongly restricted both in form and in the values of



the coupling parameters, *realistic* SSB is in practice hard to achieve. One may break internal symmetry spontaneously somewhat easily, but the spontaneous breaking of supersymmetry itself (needed to generate mass differences between fermions and bosons) usually presents considerable difficulties. As noted before, there is a theorem due to Weinberg which states that if global supersymmetry does not break at the tree level, it cannot do so radiatively.

5) Finally, spontaneous breaking of global supersymmetries is accompanied by an appearance of Goldstone fermions (Goldstinos) and (usually unwanted) low-energy theorems. (Later we shall see that when supersymmetry itself is gauged, spin 3/2 gauge objects are mandatory and a genuine Higgs effect can be motivated, whereby the "Goldstoninos" disappear from the theory, giving a mass to the corresponding spin 3/2 objects *[cf. presentation at the Conference by J. Scherk.]*)

6) It has been advocated that for realistic models, supersymmetry may be broken by addition of soft non-supersymmetric mass terms (*e.g.*, for fermions alone). This procedure is not only aesthetically non-pleasing; it is also likely to destroy the fine features of cancellations of quantum fluctuations noted above.

Application of globally supersymmetric ideas to weak and electromagnetic phenomena has been made but is not promising. A supersymmetric version of SU(2)xU(1) theory would require a large number of new and as yet unseen states. First, the leptons acquire scalar partners and the gauge vectors acquire spinor partners. Unless the symmetry is very badly broken the leptonic scalars would have to be light (~1 MeV) and the gauge spinors heavy (~100 GeV) except, of course, for the photonic spinor which should be light or even massless. Second, in order to generate masses there must be a Higgs doublet of scalars and this will acquire spinor partners. However, if supersymmetry is to break spontaneously as well as SU(2)xU(1) then the Higgs system will have to be even larger. The supersymmetry will have to break if only to make heavy the electron's scalar partner. One might prefer to do this explicitly rather than spontaneously although on aesthetic grounds that

is not a desirable prospect. If a spontaneous mechanism is used then a Goldstone spinor must arise. This could be the photon's partner but it is unlikely to be a neutrino since its low-energy coupling tends to vanish.

SU(2)xU(1) globally supersymmetric models have been constructed by Fayet, Kummer, Capper, Sohnius and others. In the model of Sohnius it was found necessary to introduce nine chiral spinors in addition to the three physical  $\nu$ ,  $e$ ,  $e^c$  for a model not yet containing muons and quarks. The main feature of the model is the expected appearance of leptons with masses of the order of  $W$  and  $Z^0$  masses. If found, these objects will provide the first empirical motivation for supersymmetry.

#### §IV. Extended Supersymmetries

Supersymmetry, an extension of Poincaré symmetry, may itself be extended. This is brought about by enlarging the number of spinor generators  $Q_{\alpha} + Q_{\alpha c}$   $i=1,2, \dots, N$ . (This may or may not be associated with an increase in the number of Bose dimensions: see below.) The basic anticommutator becomes

where  $C_{ij}$  and  $V_{ij}$  are central charges. (As pointed out by Haag, Lopuszanski and Sohnius the algebra will admit a set of  $O(N)$  generators, *its* which have dimension of mass. The central charges are in a sense commuting contractions of the  $O(N)$  non-Abelian charges.) The point about extended supersymmetries is that the spin content of the particles comprised in a multiplet possesses a wider range. For example, for  $N=4$ , and for lightlike one of the multiplets comprises one state of helicity  $\pm 1$ , four of helicity  $\pm 1/2$  and six of helicity zero. Thus there is the possibility of a unimultiplet of combined  $N=4$  extended supersymmetry (and if desired an internal symmetry SU( $\ll$ )) which contains Yang-Mills particles plus the basic fermions plus the Higgs scalars, all in one multiplet.

Renormalizable Lagrangian models have been devised which realize some of these extended symmetries. In particular  $N=2$  (complex supersymmetry) and  $N=4$ . The

latter example also illustrates a deeper mechanism at work in that it finds its most natural formulation as a supersymmetric pure Yang-Mills theory in a *ten-dimensional space-time* just as the  $N=2$  extended supersymmetry may be realized in a six-dimensional space-time. For  $N=4$ , the ten-dimensional space-time symmetry is broken down explicitly by restricting all momenta to the physical four-space so that the extra dimensions contribute only to the "internal" quantum numbers. But there survives a global internal  $O(6) \wedge SU(4)$  corresponding to rotations in the extra dimensions.

The supersymmetry generators  $Q_m$  comprise a sixteen-component Weyl-Majorana spinor with respect to the underlying space-time symmetry  $O(9, 1)$ . They decompose into four four-component Majorana spinors of  $O(3, 1)$ . The Yang-Mills Lagrangian is

$$\mathcal{L} = -\frac{1}{4} F_{\hat{\mu}\hat{\nu}}^\alpha F_{\hat{\mu}\hat{\nu}}^\alpha + \bar{\lambda}^\alpha i \Gamma_{\hat{\mu}} \not{V}_{\hat{\mu}} \lambda^\alpha,$$

where  $F_{\hat{\mu}\hat{\nu}}^\alpha$  is made out of the ten vectors  $A^a$  and  $X^a$  is a sixteen spinor. (The index  $a$  refers to any internal *local* symmetry, e.g.,  $SU(n)$  of the conventional type which can be operative independently.) The Lagrangian is invariant under the transformations

$$\delta A_{\hat{\mu}} = -i \bar{\epsilon} \Gamma_{\hat{\mu}} \lambda, \quad \delta \lambda = \frac{1}{4} \Gamma_{\hat{\mu}\hat{\nu}} [\Gamma_{\hat{\mu}}, \Gamma_{\hat{\nu}}] \epsilon.$$

The field content with respect to the unbroken subgroup  $O(3, 1) \times O(6)$ , or, rather, its covering,  $SL(2, C) \times SU(4)$  is

$$A_{\hat{\mu}} = (2, 2; 1) + (1, 1; 6) \\ \lambda = (2, 1; 4) + (1, 2; 4^*)$$

all of which belong to the adjoint representation of whatever additional conventional local internal symmetry  $SU(nc)$  which is being gauged. Among the Bose components are six space-time scalars and a four vector. The fermions comprise a left-handed 4 together with a right-handed  $4^*$ .

It is possible to break the global internal symmetry from  $O(6)$  to  $O(2)$  (complex supersymmetry) by introducing a mass term. With respect to complex supersymmetry the multiplet is yet irreducible. It contains only one coupling constant—the constant pertaining to the local  $SU(\#)$ . The model is remarkable in that this coupling is two-loop finite (as shown

by E. Poggio, H. N. Pendleton and by D. R. T. Jones: another example of the cancellations between fluctuations in supersymmetric theories. Since all other possible infinities in the model refer to wave-function renormalization and since these presumably can be eliminated by suitable choices of gauge parameters, this model (up to the two-loop level) can claim to be the only known finite field theory of the conventional type.

The  $N=2$  supersymmetric model (a supersymmetric version of the Georgi-Glashow model) is also very intriguing as has been shown by A. D'Adda, R. Horsley and P. Di Vecchia, Phys. Letters **76B** (1978) 298; A. D'Adda and P. Di Vecchia, Phys. Letters **73B** (1978) 162 and E. Witten and D. Olive (HUTP 78/A013). The two central charges in this theory can be identified with electric ( $Q$ ) and the magnetic charges ( $M$ ) defined as appropriate surface integrals. Witten and Olive show that  $Q$  and  $M$  may be regarded as fifth and sixth spatial components of a light-like six-momentum—a refinement of the Kaluza-Klein theory.

**§V. Local Supersymmetry and Supergravity**

Local supersymmetry is obviously the next extension. Before one considers approaches based on a geometrization of the superspace manifold, one may mention the graded algebraic approach due to Chamseddine and West, MacDowell and Mansouri and Neemann and Regge. Here Weyl's  $SL(2, C)$  internal symmetry which on gauging gives rise to the theory of a spin-2 field is replaced by the orthosymplectic  $OSp(4, 1)$ , which after gauging gives rise to a field theory of spin-2 and spin 3/2 fields. Just as for the case of Weyl's  $SL(2, C)$ , there is no compulsion to introduce general covariance in the context of graded  $OSp(4, 1)$ . However, this can be done, and by a further process of constraint and contraction, a generally covariant supersymmetric theory of spin-2 and spin-3/2 fields is constructed which agrees with the Stony Brook-CERN supergravity (see below).

To go back to the alternative superspace approach to local supersymmetry, just as the bosonic co-ordinates  $x^m$  undergo general coordinate transformations, one expects the combined superspace co-ordinates  $(x^m, d^{\#}) =$

$Z^u$  to do likewise. The natural extension of supertranslations in flat superspace is the group of general co-ordinate transformations in eight-dimensional curved superspace. One then tries to set up a graded Einstein-Cartan theory using frames and connections. The basic superfields are the one-form

$$E^A = dZ^M E_M^A \text{ and } \Phi_B^C = dZ^M \Phi_{MB}^C (= E^A \Phi_{AB}^C),$$

where the  $8 \times 8$  matrix  $E_M^A(z)$  includes the original vierbein  $e_m^a(x)$  together with many other components and  $\omega_m^{ab}(z)$  includes the spin connection  $\omega_m^{\alpha\beta}(x)$ .

in addition to the superspace general co-ordinate transformations—which are inevitable—one must choose an appropriate generalization of the local Lorentz transformation, or frame rotations, of Cartan and Weyl. Two suggestions have been made. These are  $OSp(4, 3+1)$  advocated by Arnowitt and Nath and  $SL(2, C)$  suggested by Wess and Zumino. There is a third approach due to Brink, Gell-Mann, Ramond and Schwarz, which, using 126 auxiliary fields of Breitenlohner, relies on the local group being  $OSp(4, 1)$ . Of these, the first corresponds to super-Riemannian geometry—the claim is that nothing is lost in replacing the super-vierbein  $E_M^A$  by the super-metric

$$g_{MN} = E_M^A \eta_{AB} E_N^B (-)^{B+BN},$$

where  $rj$  denotes the  $OSp(4, 3+1)$  invariant metric. The second alternative allows more independent components in the super-vierbein and corresponds to a non-Riemannian geometry.

Out of the primary objects  $E$  and  $\Phi$  of Wess and Zumino, it is possible to construct curvature and torsion two-forms

$$R_A^B = d\Phi_A^B - \Phi_A^C \Phi_C^B, \\ T^A = dE^A - E^B \Phi_B^A,$$

which contain all possible covariant combinations involving one derivative of  $E$  or  $\Phi$ . In detail

$$R_C^D = \frac{1}{2} E^B E^A R_{ABC}^D \\ = E^B E^A \left( D_A \Phi_{BC}^D + (-)^{B(C+E)} \Phi_{AC}^E \Phi_{BE}^D \right. \\ \left. + \Phi_{AB}^E \Phi_{EC}^D + \frac{1}{2} T_{AB}^E \Phi_{EC}^D \right),$$

$$T^C = \frac{1}{2} E^B E^A T_{AB}^C \\ = -E^B E^A (D_A E_B^M E_M^C + \Phi_{AB}^C),$$

where the derivatives are defined by

$$d = dZ^M \frac{\partial}{\partial Z^M} = E^A D_A, \text{ i.e., } D_A = E_A^M \frac{\partial}{\partial Z^M}$$

The main problem is to impose sufficient constraints so as to reduce the set of independent components to a realistic number. This has been solved by Wess and Zumino by restricting the torsion

$$T_{\alpha\beta}^\gamma = T_{\alpha b}^c = T_{ab}^c = 0 \quad (\alpha, \beta, \dots = \text{Fermi}) \\ T_{\alpha\beta}^c = i(\gamma^c C)_{\alpha\beta}, \quad a, b, \dots = \text{Bose}$$

while leaving free the components  $T_{ab}^c$  and  $T_{ab}^{\alpha\beta}$ . Three remarks are in order. First the local group is  $SL(2, C)$  and, with respect to this group, these constraints are covariant. Second, the constraint  $T_{ab}^c = 0$  is a direct generalization of the one usually imposed in Einstein-Cartan gravity: it solves to give the spin connection  $\omega_{ab}^c$  in terms of  $E$  and  $dE$ . Third, the non-vanishing (but fixed) values of  $T_{\alpha\beta}^c$  are what is needed to reproduce global supersymmetry as the flat space limit.

Global supersymmetry corresponds to the one forms

$$\Phi_A^B = 0, \quad E^a = d\theta^a, \\ E^a = dx^a + \frac{i}{2} d\theta^\mu (\gamma^a C)_{\mu\nu} \theta^\nu$$

which should emerge as solutions of the supergravity equations of motion.

The constraints on  $T$  reduce the number of independent superfields among  $E$  and  $\Phi$  to just give,  $v_a$  and  $u$  (of which the latter may be gauged away completely along with certain components of the former). The well-defined linear transformation rules for  $E_M^A$  and  $\Phi_{AB}^C$  corresponding to general co-ordinate and local Lorentz transformations should be realized through a non-linear group action on the fields  $v_a$  and  $u$ . The Lagrangian for the independent fields is given by the extremely elegant expression

$$\int d^4x d^4\theta \det E(\partial v, u, \partial u).$$

The corresponding equations of motion are covariant

$$G_a = 0, \quad R = 0.$$

where  $G_a$  and  $R$  are covariant objects contained among the surviving components of  $R_{abc}^d$  and  $T_{ab}^c$ . For example, they can be extracted from  $T_{ab}$  since

$$G_a = \frac{1}{4} \left( \gamma_a \gamma^b \frac{1+i\gamma_5}{2} \right)_\gamma^\alpha T_{ab}^\gamma,$$

$$R^* = \frac{1}{4} \left( \gamma^b \frac{1+i\gamma_5}{2} \right)_\gamma^\alpha T_{ab}^\gamma.$$

Since  $u$  can be removed by a gauge transformation, it follows that the equation  $R=0$  is simply a consequence of  $G_a=0$ . The latter must contain all the independent dynamical information.

In their communication to the Conference Wess and Zumino show how the constraints they have imposed, solve to give an expression for  $E$  (after gauge fixing) in terms of two (#-space) derivatives of the field  $v_a$ . Thus the Lagrangian expression  $\det E$  is expressed directly in terms of the field  $v_a$ . Since later we shall see that the super-field  $v_a$  contains nothing but the field components of Stony Brook-CERN formulation of supergravity as modified by the groups working at Imperial College, CERN and Lebedev Institute, we obtain a direct connection between the super-space geometrical approach and the "component" approach of the next section §VI.

A somewhat different approach is followed by Arnowitt and Nath who choose  $OSp(4, 3+1)$  as the local group. They eliminate the connections  $\langle j \rangle_{ab}^c$  as independent variables by imposing the  $OSp(4, 3+1)$  covariant constraints

$$T_{ab}^c = 0.$$

Their geometry is Riemannian. Spontaneous symmetry breaking (at least at the tree level) yields

$$\phi_{\alpha\beta}^c = -i(\gamma^c C)_{\alpha\beta}$$

which possesses global supersymmetry as the flat space. Stony Brook-CERN supergravity arises as a limit of the Arnowitt-Nath gauge supersymmetry in the following way. A metric  $g_{mn}$  is constructed to  $O(\#^2)$  (which is sufficient to deduce field equations) depending only on the supergravity fields  $e_a^\mu(x)$  and  $\hat{\Lambda}(x)$ , such that the gauge change of  $g_{mn}(z)$  correctly deduces the Stony Brook-CERN supergravity transformations on  $e_a^\mu$  and  $\hat{\Lambda}$ . The authors call this the "gauge complete" metric. The gauge supersymmetry field equations are

$$R_{MN} = \frac{8}{k^2} g_{MN}$$

(Here  $k$  enters in the vacuum metric arising in the spontaneous breakdown.) These field equations are then seen to produce the supergravity equations in the limit  $k \rightarrow 0$ . Two additional results have been stated (see talk by P. Nath and NUB 2361, June 1978): First, when the Wess-Zumino or CALT supervierbein  $E_m^a$  are combined to form the metric  $g_{mn}$ , this metric is identical to the above gauge complete metric when field equations are imposed, *i.e.*, modulo the supergravity field equations, the vierbein and metric spaces are identical. Second, Arnowitt and Nath have also gauge completed the vierbein to  $O(\#^2)$  without auxiliary fields by expanding the tangent group to include elements of  $OSp(4, 3+1)$ . These vierbein then reproduce their metric without the limit  $k \rightarrow 0$ .

However, Arnowitt and Nath suggest that the limit  $k \rightarrow 0$  should not be taken as  $e$  (the vector gauge coupling constant) is proportional to  $k$  in their theory. Thus  $k \neq 0$  allows for the existence of minimal couplings in gauge supersymmetry without the difficulty found in supergravity of a concomitant cosmological constant. The authors have examined the  $k \neq 0$  theory under the hypothesis that the spontaneous breaking preserves global supersymmetry and have obtained the following results (see talk by P. Nath and NUB 2343, 2344). First, at the one and two loop level the authors calculate that all w-point propagators are finite for  $N > 2$  (not just the S-matrix elements as in supergravity). Second, the symmetry breaking was found to spontaneously break all gauges of the theory except (i) Einstein general covariance, (ii) a supergravity gauge and (iii) a set of vector meson gauges (Yang-Mills and/or Abelian) determined by the symmetry breaking equations. These unbroken vector gauges can be characterized by the Dirac and internal space matrix  $JH$  which appears in the spontaneously broken vacuum metric;  $g^{TM} = \dots$ ,  $\hat{\Lambda} = -\hat{\Lambda}(\hat{\Lambda})$ ,  $g^{\%} = k(-C \sim \hat{\Lambda}^r(\hat{O}r)_{\mu a}(dr)_{\mu})p$ . The preserved gauges with generators  $M$  are then the subgroup of  $O(N)$  for which

$$[I^\mu, M] = 0.$$

This result is shown to hold when all quantum

corrections are included. It is a direct prediction of the  $k^{\wedge}O$  gauge invariance since supersymmetry leaves no arbitrariness in the Higgs potential. An additional analysis shows further that the set of unbroken vector meson gauges must be non-empty. Arnowitt and Nath suggest that this might offer a theoretical explanation of why some gauges in nature seem to be perfectly preserved (e.g., Maxwell and colour).

The full field content of gauge supersymmetry has now been obtained by the authors (and characterized in terms of unbroken gauge fields, broken gauge fields, fictitious Goldstone fields and Higgs fields, NUB 2344). The outstanding unresolved question of the theory is whether it has ghosts. This is particularly pressing in view of the finiteness of the propagators mentioned above.

The superspace approach followed by Brink, Gell-Mann, Ramond and Schwarz at Caltech and MacDowell at Yale has also reported considerable progress at Tokyo. In this approach too the tangent space group is  $SL(2, C)$ ; the primary quantities are again the supervierbein  $E$  and the super-connection  $\theta$ . Gell-Mann, Ramond and Schwarz have exhibited an expression, variations of which with respect to the 112 independent quantities contained in  $E$  and  $\theta$ , give rise to a set of 112 equations of motion. These then reproduce the content of the Stony Brook supergravity. The approach has the merit that it can be extended to *extended supergravities*  $N=2, 3$  (see below).

These various approaches, Karlsruhe-CERN, Caltech-Göteborg, Yale and Northeastern will doubtless converge still further during the next few months when their interrelations are better understood.

### §VL The Stony Brook-CERN Supergravity: The Imperial College-CERN-Lebedev Approach

The elegant geometric structures considered above hold out the expectation of a deep and aesthetically pleasing conception of extended spacetime. As it stands at present, however, the geometrical approach is burdened with the difficult problem of constraints. When the constraints have all been solved and the very numerous redundancies eliminated, we are left with a residue of manageable com-

ponents: the fields of Stony Brook-CERN supergravity.

The principal dynamical fields are the vierbein and the Rarita-Schwinger  $\langle p^{\wedge}(x)$ , introduced by the Stony Brook group and by Deser and Zumino at CERN. This formulation however suffers from the shortcoming that the supersymmetry algebra does not close, except when equations of motion are used. In the recent work of Stelle and West at Imperial College, of Ferrara and van Nieuwenhuizen at CERN and Fradkin and Vasiliev at Lebedev, this has been remedied by an introduction of auxiliary fields. These auxiliary fields designated as  $M, N$ , at Imperial College and  $S, P, A?$  at CERN, are necessary in order to close the algebra. Thus, all one needs in order to make gravity supersymmetric, is to introduce a spin-3/2 particle to go with the spin-2 graviton plus the non-propagating auxiliary fields. The Lagrangian is

$$\mathcal{L}_{\text{s.g.}} = \frac{e}{4K^2} R - \frac{ie}{2} \bar{\psi}_{\mu} R^{\mu} + \frac{e}{3} (b_{\mu} b^{\mu} - M^2 - N^2),$$

where  $e = \det(e_{\mu}^a)$  and

$$R = e_b^{\mu} e_a^{\nu} (\partial_{\mu} \omega_{\nu}^{ab} + \omega_{\mu}^{ac} \omega_{\nu c}^b - (\mu \leftrightarrow \nu))$$

$$e R^{\mu} = \varepsilon^{\mu\nu\rho\sigma} \gamma_{\nu} \gamma_{\rho} \left( \partial_{\sigma} + \frac{1}{2} \omega_{\rho a} \sigma^{ab} \right) \psi_{\sigma}.$$

It is understood that  $co$  is to be expressed in terms of  $e$  and  $\langle p$  by solving the algebraic equations  $d^{\wedge}f/00=0$ ,

$$\omega_{\mu ab} = \omega_{\mu ab}(e) + \frac{iK^2}{4} (\bar{\psi}_{\mu} \gamma_a \psi_b - \bar{\psi}_{\mu} \gamma_b \psi_a - \bar{\psi}_a \gamma_{\mu} \psi_b).$$

The torsional contribution to  $co$  is characteristic of supersymmetry and plays an essential role in establishing the invariance of  $\mathcal{L}f$  under supertransformations. The action of local supertransformations is given by

$$\delta e_{\mu}^a = ik \bar{\varepsilon} \gamma^a \psi_{\mu}$$

$$\delta \psi_{\mu} = 2k^{-1} D_{\mu} \varepsilon + \gamma_5 \left( b_{\mu} - \frac{1}{3} \gamma_{\mu} b \right) \varepsilon - \frac{1}{3} \gamma_{\mu} (M + \gamma_5 N) \varepsilon$$

$$\delta M = -\frac{i}{2} \bar{\varepsilon} \gamma \cdot R - \frac{i}{2} k \bar{\varepsilon} \gamma_5 b^{\nu} \psi_{\nu}$$

$$-\frac{i}{2} k \bar{\varepsilon} \gamma \cdot \psi M + \frac{i}{2} k \bar{\varepsilon} \gamma_5 \gamma \cdot \psi M$$

$$\begin{aligned} \delta N &= -\frac{i}{2}\bar{\epsilon}\gamma_5\gamma\cdot R + \frac{i}{2}k\bar{\epsilon}b^\nu\psi_\nu \\ &\quad -\frac{i}{2}k\bar{\epsilon}\gamma\cdot\phi N + \frac{i}{2}k\bar{\epsilon}\gamma_5\gamma\cdot\phi M \\ \delta b_\mu &= \frac{3i}{2}\bar{\epsilon}\gamma_5\left(R_\mu - \frac{1}{3}\gamma_\mu\gamma\cdot R\right) + ik\bar{\epsilon}\not{b}\psi_\mu \\ &\quad -\frac{i}{2}k\bar{\epsilon}\gamma\cdot\phi b_\mu - \frac{i}{2}k\bar{\phi}_\mu(M + \gamma_5 N)\gamma_5\epsilon \\ &\quad -\frac{i}{4}k\epsilon_\mu{}^{abcd}b_b\bar{\epsilon}\gamma_5\gamma_c\psi_d, \end{aligned}$$

where

$$D_\mu = \partial_\mu + \frac{1}{2}\omega_{\mu ab}\sigma^{ab}.$$

The auxiliary fields  $M$ ,  $N$  and all vanish when the action of pure supergravity is extremized. In this they resemble the fields  $D$  of pure Yang-Mills and also in that they play an essential role in closing the algebra, greatly simplifying the coupling of the gauge system to matter supermultiplets. The anticommutator of two local supertransformations  $e_\nu, e_\lambda$  takes the form

$$\begin{aligned} [\delta_g(\epsilon_1), \delta_g(\epsilon_2)] &= \delta_G(t^\lambda) + \delta_L(t^\lambda\omega_{\lambda ab}) \\ &\quad + \delta_S\left(-\frac{k}{2}t^\lambda\psi_\lambda\right), \end{aligned}$$

where  $t = 2\delta_{\nu\lambda}e_\nu e_\lambda$ , and  $\delta_\omega, \delta_\nu, \delta_S$  denote general co-ordinate, local Lorentz and local supersymmetry transformation, respectively.

Any globally supersymmetric matter system can be coupled to supergravity with the help of auxiliary fields. This is based on a "tensor calculus" of matter multiplets which includes the following operators :

- i) multiplication of same chirality scalars
- ii) multiplication of opposite chirality scalars  $\theta X\theta' L = \theta''$ ,
- iii) construction of F-type density for  $\theta_\nu$
- iv) construction of D-type density for  $\theta_\nu$

where  $\theta_\nu$  denotes the scalar multiplet ( $A, B, X, F, G$ ) and  $\theta$  is the vector multiplet ( $C, C, H, K, V_\nu, I, D$ ). The global behaviour of these components is fixed by the superfield expressions

$$\begin{aligned} \Phi_+ &= \exp\left(-\frac{1}{4}\bar{\theta}\partial\gamma_5\theta\right)\left[\frac{A+iB}{\sqrt{2}} + \bar{\theta}\frac{1+i\gamma_5}{2}\chi\right. \\ &\quad \left. + \frac{1}{2}\theta\frac{1+i\gamma_5}{2}\bar{\theta}\frac{F+iG}{\sqrt{2}}\right] \end{aligned}$$

$$\begin{aligned} \Phi &= C + \frac{1}{2}\bar{\theta}\gamma_5\zeta + \frac{1}{4}\bar{\theta}(H + \gamma_5 K + i\gamma_a\gamma_5 V_a)\theta \\ &\quad - \frac{1}{2}\bar{\theta}\theta\bar{\theta}\gamma_5(\lambda + i\bar{\theta}\zeta) + \frac{1}{32}(\bar{\theta}\theta)^2(D - \partial^2 C). \end{aligned}$$

The product rule for "same" chirality scalars is exactly the same in supergravity as for global supersymmetry—no dependence on the gravitational constant  $K$  enters this rule. The product rule for opposite chirality scalars is modified to the extent that ordinary derivatives are replaced by the following "covariant" forms :

$$\begin{aligned} \hat{D}_a A &= \partial_a A - \frac{ik}{2}\bar{\phi}_a\chi \\ \hat{D}_a B &= \partial_a B - \frac{ik}{2}\bar{\phi}_a\gamma_5\chi \\ \hat{D}_a \chi &= \left(D_a - \frac{k}{2}b_a\gamma_5\right)\chi \\ &\quad - \frac{k}{2}(\hat{D}(A + \gamma_5 B) + (F + \gamma_5 G))\phi_a. \end{aligned}$$

Finally, the supercovariantization of the  $F$ -type and  $D$ -type densities, whereby the problem of giving global  $F$ 's and  $D$ 's and how to write supercovariant Lagrangians, is solved by the following expressions :

$$\begin{aligned} e\left[F + i\frac{k}{2}\bar{\phi}\cdot\gamma\chi + \frac{k^2}{2}\bar{\phi}_\mu\sigma^{\mu\nu}(A - i\gamma_5 B)\phi_\nu\right. \\ \left. + k(MA + NB)\right] \end{aligned}$$

and

$$\begin{aligned} e\left[D + \frac{ik}{2}\bar{\phi}_\mu\gamma_5\gamma^\mu\lambda - \frac{2}{3}k(NH - MK)\right. \\ \left. - \frac{2}{3}k\left(b^\nu + \frac{3}{8}i\frac{k}{2}\epsilon^{\mu\rho\nu\tau}\bar{\phi}_\rho\gamma_\tau\phi_\mu\right)V_\nu\right. \\ \left. - \frac{i}{2}k\bar{\zeta}\left(\gamma_5 R + \frac{3}{8}i\frac{k^2}{e}\epsilon^{\mu\rho\nu\tau}\phi_\nu\bar{\phi}_\rho\gamma_\tau\phi_\mu\right)\right. \\ \left. - \frac{2}{3}k^2\frac{C}{e}\mathcal{L}_{s.g.}\right], \end{aligned}$$

respectively. Once again note that for  $c=0$  these expressions reduce to those for global supersymmetry. With the help of these rules one can make any globally supersymmetric system into a locally supersymmetric one. These rules are seen therefore as the graded extension of the well-known minimal principle, whereby flat space systems are "covariantized" by coupling to the gravitational field.

One simple application of these rules would be to make a "cosmological" density by inserting in the F-type density the constant chiral field

$$\Phi_+ \sim \left( \frac{\lambda}{\kappa}, 0, 0, 0, 0 \right)$$

thereby obtaining the term

$$\lambda e \left( M + \frac{k}{2} \bar{\psi}_\mu \sigma^{\mu\nu} \psi_\nu \right).$$

Another application would make use of a self-coupled scalar multiplet to generate spontaneous breakdown of the local supersymmetry. The associated Higgs effect has been shown to eliminate the Goldstone spinor from the physical spectrum while giving mass to the spin 3/2 field. This was shown in the presentation to the Conference in the lecture of J. Scherk.

This clarification of the structure of Stony Brook supergravity by the introduction of auxiliary fields is one of the most important achievements in the supersymmetry field in the last year. The theory thus arrived at provides the irreducible basis upon which all the geometrical formulations based on supermetrics and super-vierbeins, etc. must be founded. In particular the field  $v_\alpha$  of Wess and Zumino must after gauge-fixing comprise the set  $e/, (p^\wedge Ap, S$  and  $P$ .

The coupling of matter, including systems with local internal symmetries, has been given an elegant formulation in the non-Riemannian supergeometry of Wess and Zumino. First, the Lagrangian density for a U(1) gauge superfield  $V$  is given (in the notation of 2-component spinors) by

$$\mathcal{L}_V = E(W^\alpha \mathcal{D}_\alpha V + W_\alpha \mathcal{D}^\alpha V),$$

where  $E = \det E_m^\alpha$  and the superfield strength  $W_\alpha$  is defined by

$$W_\alpha = (\mathcal{D}_\alpha \mathcal{D}^\alpha - 8R) \mathcal{D}_\alpha V.$$

In these formulae, the supercovariant derivative  $\mathcal{D}^\alpha A$  appears. It is defined by, for example,

$$\mathcal{D}_A v_B = D_A v_B - \Phi_{AB}{}^C v_C,$$

where  $\Phi_{AB}{}^C$  denotes the superconnection. (In a suitable gauge the components of  $Sf\nu$  agree with those defined by Ferrara and van Nieuwenhuizen and Stelle and West.)

The concept of chiral superfield can be given a meaning in this non-Riemannian

geometry. For example the positive chirality field  $\theta$ , satisfies

$$\mathcal{D}_\alpha \Phi_+ = 0$$

and it can be represented in the form

$$\Phi_+ = (\mathcal{D}_\alpha \mathcal{D}^\alpha - 8R)U,$$

where  $U$  is defined up to a kind of gauge transformation

$$U \rightarrow U + \mathcal{D}_\alpha A^\alpha.$$

(Note that the field strength  $W_\alpha$  is chiral in this sense.) The rule for constructing a scalar density out of  $\Phi_+$  is then obtained as follows :

$$\begin{aligned} & \int d^4x d^4\theta E U \\ &= \int d^4x d^4\theta E \left( -\frac{1}{8R} \right) (\Phi_+ - \mathcal{D}_\alpha \mathcal{D}^\alpha U) \\ &= -\frac{1}{8} \int d^4x d^4\theta \frac{E}{R} \Phi_+ \\ &= -\frac{1}{8} \int d^4x d^2\theta E \Phi_+, \end{aligned}$$

where  $E$  denotes a chiral density which in a special (chiral) gauge is given by

$$E = \frac{1}{R} \partial_\alpha \partial^{\dot{\alpha}} E.$$

The Lagrangian given above for the U(1) gauge superfield can be given also in the chiral form

$$\mathcal{L}_{V(\text{chiral})} = E W^\alpha W_\alpha.$$

The Lagrangian for a self-interacting scalar supermultiplet coupled to supergravity is given by Zumino in the form

$$\begin{aligned} \mathcal{L}_\phi &= \int d^4x d^4\theta \\ &\times \left[ E |\phi|^2 + \frac{1}{2} \frac{E}{R} V(\phi) + \frac{1}{2} \frac{E}{R^*} V(\phi^*) \right] \end{aligned}$$

with the chirality of  $\langle j \rangle$  being allowed for by writing

$$\phi = (\mathcal{D}_\alpha \mathcal{D}^\alpha - 8R)Z.$$

Variation of  $Z$  yields the equations of motion

$$(\mathcal{D}\mathcal{D} - 8R^*)\phi - 4V'(\phi^*) = 0.$$

Corresponding to this the equations of supergravity acquire right-hand sides

$$G_{\alpha\dot{\alpha}} = \kappa J_{\alpha\dot{\alpha}}, \quad R = \kappa S,$$

where  $J$  is a generalized supercurrent

$$J_{\alpha\dot{\alpha}} = i\phi(\overrightarrow{\mathcal{D}}_{\alpha\dot{\alpha}} - \overleftarrow{\mathcal{D}}_{\alpha\dot{\alpha}})\phi^* + \frac{1}{2}\mathcal{D}_{\alpha\dot{\alpha}}\phi\mathcal{D}_{\dot{\alpha}\alpha}\phi^* + 2G_{\alpha\dot{\alpha}}\phi\phi^*$$

It satisfies the conservation law

$$\mathcal{D}^{\alpha}J_{\alpha\dot{\alpha}} = \mathcal{D}_{\dot{\alpha}}S^*$$

with

$$S^* = 3V(\phi^*) - \phi^*V'(\phi^*)$$

It contains the energy momentum tensor, the spinor supercurrent and an axial vector current.

An interesting new contribution to the understanding of supergravity is due to Ogievetsky and Sokatchev. They consider the group of volume preserving general co-ordinate transformations in four complex Bose+two complex Fermi dimensions  $(z^{\mu}, \theta^i)$ . In some sense this corresponds to a subgroup in the general co-ordinate transformations in eight real boson+four real Fermi dimensions. The idea of Ogievetsky and Sokatchev is to pick out a submanifold in this space by specifying four of the Bose co-ordinates in terms of the remaining Bose and Fermi variables.

$$z^{\mu} = x^{\mu} + iH^{\mu}(x, \theta, \bar{\theta})$$

with  $x^{\mu}$  and  $\theta^i$  real. They show that by imposing suitable co-ordinate conditions, *i.e.*, fixing the gauge the components of  $H^{\mu}$  can be set into correspondence with the variables of simple supergravity:  $e^{\mu}, b^{**}, M$  and  $N$ . Moreover, a consistent algebraic structure is ensured by this construction. (It is interesting to note that the group of general co-ordinate transformations from which they start contains only twenty real Bose and twenty real Fermi functions of  $z^{\mu}$ . This is more restricted than the sixty-four real Bose+sixty-four real Fermi functions of  $(x, \theta)$  which enter the general co-ordinate transformations of real superspace.)

In spite of the brilliance of this idea, as yet the geometry of this manifold is obscure and we need rules for constructing covariant objects, Lagrangian densities, etc.

To summarize, the Ogievetsky and Sokatchev superfield  $H_{\mu}(x, \theta)$  is the object nearest to the I.C.-CERN-Lebedev set of fields, in terms of which the Stony Brook supergravity is recovered. Wess and Zumino show how their constraints can lead the supergeometric quantities used by them ( $E^{\mu}, \theta^{ab}, T^{\mu}$ ) to be

expressed in terms of  $H_{\mu}(x, \theta)$  ( $=v_{\mu}$  in the notation of Wess and Zumino). The Göteborg-Caltech approach uses the Breitenlohner fields  $B_{\mu}(x, \theta)$ ,  $B_{\mu\dot{\alpha}}(x, \theta)$  and  $B_{\dot{\alpha}\mu}(x, \theta)$ , among which are included the components of  $H_{\mu}(x, \theta)$ . They express  $E^{\mu}$ ,  $\theta^{ab}$  and  $T^{\mu}$  in terms of the Breitenlohner fields, which themselves are shown to depend on components of  $H_{\mu}(x, \theta)$ . Arnowitt and Nath work with metrical quantities  $g_{\mu\nu}(x, \theta)$ . They show that the Göteborg-Caltech formulation of supergravity equations is equivalent to their metric tensor formulation on physical mass-shell. Their formulation contains one extra parameter  $k$ ; the limit  $k \rightarrow 0$  is necessary to obtain Stony Brook supergravity (and the flat superspace when the Newtonian constant vanishes).

Wess and Zumino give a Lagrangian. When their additional covariant constraints on  $E$  and  $\theta$  are solved, and the result is substituted with their Lagrangian, the final Lagrangian coincides with that of the Imperial College-CERN-Lebedev workers. The approach of Göteborg-Caltech and also of MacDowell reported at the Conference relies on formulating equations of motion and working with these for the  $E$  and  $\theta$  fields. The approach can be used for extended supergravity also for the cases  $N=1, 2, 3$  (see below).

### §VII Prospects for a Physical Theory

To construct a physical theory, one may take the view that all we need from the spin-2 graviton and the spin 3/2 gravitino (with the Newtonian coupling parameter) is to supercovariantize a given globally supersymmetric Lagrangian. In this approach the graviton and the gravitino stand apart from the matter (including Yang-Mills gauge) supermultiplets. One may be more ambitious and consider extended supergravity theories in which the graviton is accompanied by a number  $N < \infty$  of spin-3/2 gravitinos and the system admits a global internal  $O(N)$  symmetry. Also included in the graviton supermultiplet are states with successively lower helicities which transform as antisymmetric tensors of  $O(N)$ . Physical states—assumed massless—are conveniently tabulated according to helicity  $\lambda$ . For a set of values of  $N$  their multiplicities are as follows:



$N$	1	2	3	4	5	6	7	8
2	1	1	1	1	1	1	1	1
3/2	1	2	3	4	5	6	7+ 1	8
1		1	3	6	10	15+ 1	21+ 7	28
1/2			1	4	10+ 1	20+ 6	35+21	56
0				1+1	5+ 5	15+15	35+35	70
-1/2			1	4	1+10	6+20	21+35	56
-1		1	3	6	10	1+15	7+21	28
-3/2	1	2	3	4	5	6	1+ 7	8
-2	1	1	1	1	1	1	1	1

Explicit expressions for Lagrangians for  $N < 4$  have been given (see D. Z. Freedman's report, this Conference) but only partial results are available for the larger values of  $N$ . (The global symmetry in these cases can be extended from  $O(N)$  to  $U(iV)$ , by separating the spinors into chiral pieces. For example, in the case  $JV=3$ , the three Majorana-Rarita-Schwinger spinors of spin  $3/2$  decompose into a left-handed  $3$  and a right-handed  $3^*$ . There are three vectors,  $A^\mu$  out of which three field strengths can be made. The self-dual and anti-self-dual pieces of these transform as  $3$  and  $3^*$  under  $SU(3)$ .)

For a general  $JV < 8$ —this restriction being needed in order that no helicities higher than  $2$  occur—there are  $N(N-1)/2$  spin-1 vector fields  $A_j^\mu$  in the same multiplet with the graviton field, but they do *not* gauge  $O(N)$ . Rather, they gauge (non-minimally) a set of central charges  $Z^{ij}$  with respect to which the graviton is neutral. Hence there are only magnetic moment type couplings of  $A_j^\mu$  to this multiplet. It is possible, however, to introduce matter multiplets with non-vanishing central charges. To these the  $A_j^\mu$  couple in the usual minimal fashion with strength  $g = \text{tern}$ , where  $\text{ra} = \text{mass of matter multiplet}$ .

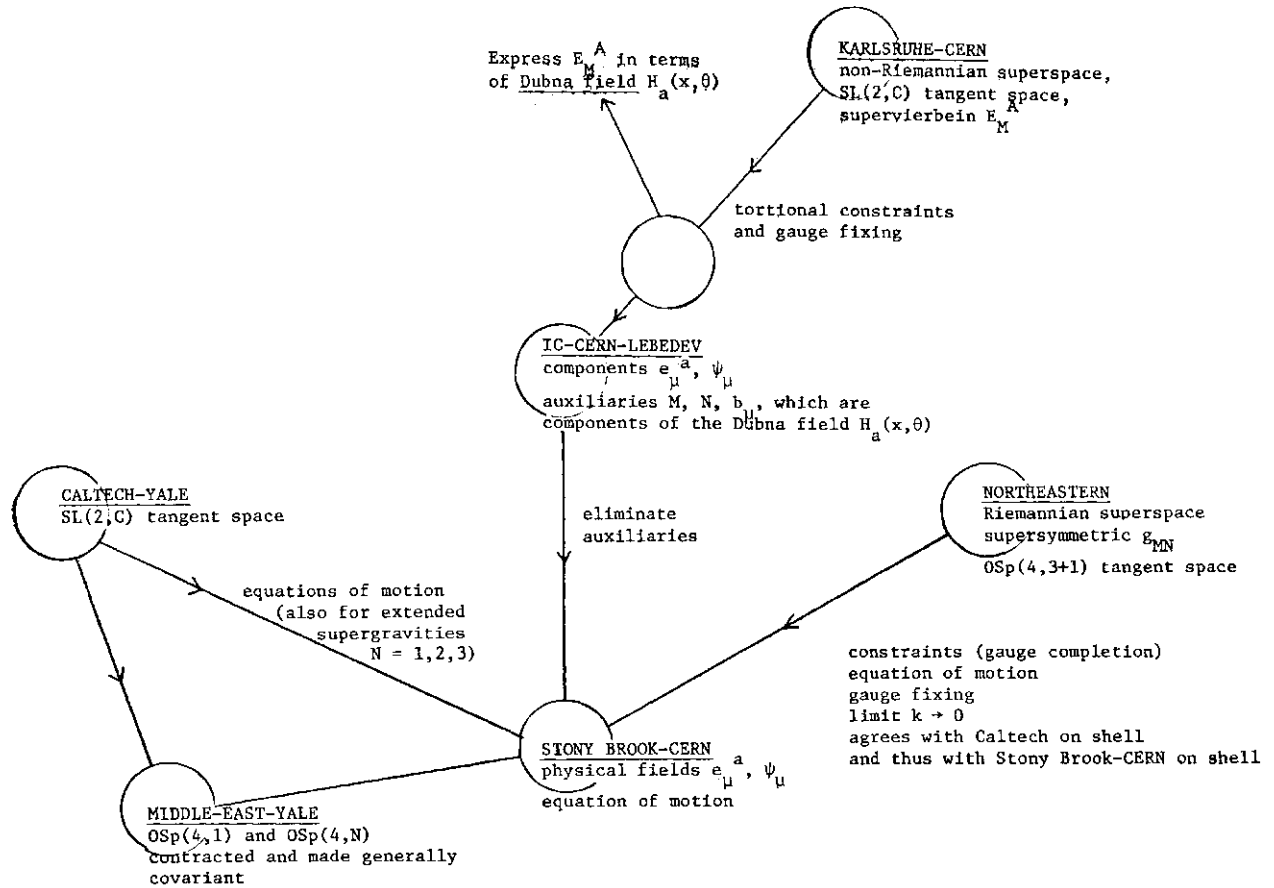
It is possible to turn the global  $O(N)$  into a local symmetry with the  $A_j^\mu$  as gauge fields by adjoining various terms to the Lagrangian including a cosmological term and a spin-3/2 mass term. The  $O(N)$  gauge coupling is given by  $g \sim tc/\sqrt{\Lambda}$ , where  $\Lambda$  denotes the cosmological constant. These models can perhaps best be approached by a process of gauging the graded de-Sitter group  $OSp(4, N)$  and then Wigner-Innonue contracting it. There are thus two independent couplings in extended supergravity Yang-Mills  $g$  and Newtonian  $\mu/c$ , or  $fc$  and the cosmological constant  $\Lambda$ .

Finally, we must raise the question of how

near to physical reality theories like extended  $O(N)$  supergravities are likely to be. Starting with one (Einstein) graviton, we are perhaps dealing for the  $O(8)$  case with 8 spin  $3/2$  gravitinos, which for  $SU(3)$  of colour (embedded in  $O(8)$ ) split into  $(3+3^*+1+1)$ , 28 spin-1 particles (a colour octet of gluons+ two electrically neutral singlets (photon+ $Z^0$ ) and  $9+9$  fractionally charged ( $\pm 1/3, \pm 1/3, +2/3$ ) perhaps superheavy bosons; plus 56 spin-1/2 objects, comprising  $3+3+3+3$  quarks of charges  $2/3, -1/3, -1/3, 2/3$ , a neutral octet (of gluinos) a singlet of charge  $-1$  (the electron), a colour six-fold of charge  $-1/3$  and two Majorana neutrinos. There is no place for any  $W$  (since  $O(8)$  cannot accommodate  $SU(3)_c$  as well as  $SU(2) \times U(1)$ ) nor for the muon, nor for the  $\tau$  lepton. There are two coupling constants, the Yang-Mills  $g \sim e$ , and the Newtonian  $K$ , together with the inevitable cosmological term. (The cosmological constant  $3e^2/\mu c^2$  is  $10^{118}$  times larger than the astrophysical limit—in Freedman's words "the record for the worst comparison of theory and experiment"). There is hope from some of S. Hawking's recent work that this large cosmological constant may turn into a virtue of the theory; such a constant apparently implies that space-time is made up of extremely tiny granules of de-Sitter black-holes.

An elegant way of writing the  $O(8)$  extended supergravity has been suggested by E. Cremmer and J. Scherk, who show that if one extends space-time to eleven dimensions, a dimensional compactification from eleven to four dimensions gives a theory with eight spins or charges (gravitinos).

Another avenue for realizing a physical theory may lie along conformal supergravity. In this report I have not mentioned conformal supersymmetry, or conformal supergravity.



If the Poincaré group is extended to the 15-component conformal group, the grading needs eight rather than four fermionic generators. To close the algebra, one also needs one further pseudoscalar bosonic generator (connected with chiral transformations), making for a total set of 24 generators constituting a graded  $SU(2, 2; 1)$ , instead of the 14 generators in the Poincaré case with its contracted de-Sitter ancestry through  $OSp(4, 1)$ . In addition to the simple conformal supersymmetry, extended conformal supersymmetries can also be constructed corresponding to a graded  $SU(2, 2, N)$ . These structures have the merit of incorporating an internal  $SU(A_0)$  instead of the internal  $O(N)$  as is the case for the graded  $OSp(4, N)$ . In this sense (of incorporating  $SXJ(N)$ ) this theory is an advance over the Poincaré case.

So much for the global conformal supersymmetry theory. The local version of this theory (conformal supergravity) has been constructed—the Lagrangian having been written down by the groups working at Stony Brook, City College New York, and CERN. The Lagrangian describes the propagation of spin-2 dipole objects (quartic propagators

$1/p^2$ ) [through the Lagrangian  $(WR^{\wedge} - l\hat{f}R^2)$ ] together with the spin 3/2 gravitinos (two of positive and one with negative metric) plus a spin-1 axial particle. There is no cosmological term.

On account of the soft propagator ( $1/p^4$  for gravitons), theories of this variety—even when conformal symmetry is broken (spontaneously or otherwise) by the addition of the Poincaré supergravity Lagrangian—are known to be renormalizable. One can set up a renormalization-group scheme—this has been done by Salam and Strathdee (IC/78/12, to be published in Phys. Rev.) and independently by J. Juive and M. Tonin (Padua preprint, IFPD 2/78). These authors claim to show that the massive unphysical spin-2 ghost in theories with Lagrangians  $(1/c^2)\hat{f}\hat{f} + (1/g^2)\hat{f}\hat{f}^{\wedge} + (1/g^e)R^2$ , is innocuous so far as unitarity difficulties are concerned, provided the constants  $g$  and  $g'$  have values for which the gravity propagator shows an anomalous dimension. They give criteria for this to happen.

Such explorations are important, even without supersymmetry, particularly in view of the feeling that supergravities are not likely, in three or higher loop diagrams, to prove finite

on shell, as had once been fondly hoped for from the example of one or two loops (for details of these calculations, see the report to the Conference by D. Z. Freedman). Even if supergravities had proved finite, the fact that the high-energy behaviour increases like  $K^{\epsilon} t^{\epsilon}$  ( $K t^{\epsilon} Y^{\epsilon}$  for an  $\#$ -loop graph with  $E$  external gravitons, implies that unless a summation technique is devised, there is no hope of gravity theory exhibiting Froissart boundedness. In this connection Salam and Strathdee have surmised that if gravity theory is asymptotically free—as suggested by Fradkin and Vilkovisky—the running parameter  $K(tc)$  may fall as  $1/fc$ . This implies, not only that the high-energy behaviour is Froissart ( $\sim t^{\epsilon}$ ) but also a possible renormalization technique for loop calculations, when one starts with Dyson's irreducible graphs in a first-order Palatini formulation of Einstein's gravity and uses the running constant  $K(tc) \sim 1/fc$  in place of  $A$ ; to obtain an estimate of infinity behaviour of the insertions in lines and vertices.

To summarize the prospects of supersymmetric and supergravity theories, my personal feeling is this. Spontaneously broken global supersymmetry may prove to be an important principle for constructing physical Lagrangians. This will find confirmation or otherwise if the  $W^{\pm}$  and  $Z^0$ 's are accompanied by correspondingly heavy leptons. If confirmed, one will need simple supercovariantization of such a unified globally supersymmetric theory and a possible Higgs effect, whereby the Goldstones give mass to the gravitinos. The prospects of renormalizability for such a theory are unlikely to depend on its supersymmetric character. These will probably be settled by incorporating techniques like the use of running coupling constants or the asymptotic safety ideas of Weinberg.

It would be good to have a complete superspace formulation for such supercovariantization; superspace is an important extension of space-time, one where no problems of direct measurability arise for the extra fermionic dimensions of space-time. Regarding extended supergravities, my own feeling is that they will prove their relevance for strong supergravity, perhaps in a spontaneously broken extended superconformal form, before one uses them for unifying Einstein's gravity with

matter.

## References to Part II

Most of this section of the report was written in collaboration with Dr. J. Strathdee.

For supersymmetry a number of reviews exist:

P. Fayet and S. Ferrara: Phys. Reports **32** (1977) C5.

Abdus Salam and J. Strathdee: Fortschr. Phys. **26** (1978) 57.

For various aspects of supergravity see the excellent reports to this Conference by D. Z. Freedman (Stony Brook), J. Schwartz (Göteborg-CALTECH), B. Zumino (CERN and Karlsruhe) and P. Nath (Northeastern). The groups not represented directly at the Conference are the Imperial College group, K. S. Stelle and P. C. West, Imperial College, London, preprint ICTP/77-78/6, S. Ferrara, P. van Nieuwenhuizen, CERN preprint TH. 2463, E. S. Fradkin and M. A. Vasiliev, IAS-788-3PP (1978) and V. Ogievetsky and L. Sokatchev, Dubna preprint E-2-11702 (1978).

## PART III

### §VIII. Topological Ideas and the Origin of the Internal Symmetries

The central problem—made the more serious by the quark and lepton explosion situation—is the problem of understanding the charge concept in a fundamental manner. To make "fundamental understanding" more precise one may use the analogy of the gravitational charge (mass). Einstein succeeded in linking it with the curvature of space-time. Can we hope that a similar fundamental understanding will be achieved for the other charges? Perhaps this way we shall understand the secret of how many charges (flavours and colours) there are, of the symmetries they are associated with, and why these symmetries appear to give rise to non-Abelian group structures.

There is the conjecture made already in the 1950's by Wheeler, Shönberg and others that it is the topological structure of space-time—both in the large and the small—which gives rise to the charge concept. If this conjecture is correct, one may ask, what is the origin of the Lie group symmetries (even of the humblest  $SU(2) \times U(1)$ ) within the context of topological ideas?

Topological ideas have recently played a crucial and a central role in Yang-Mills theory, with the discovery of the 't Hooft-Polyakov monopole and the instanton-meron solutions.

In fact a conjecture has been made by D. Olive based on the celebrated equivalence of Sine-Gordon theory in 1+1 dimensions with the Thirring model. What looks like as a topological charge in one formalism, may appear as an internal symmetry Noether charge in the other. Could this be the prototype for an understanding of *all* Noether charges?

My own feeling is that this is unlikely to be the case. Normal instanton or soliton physics is done on  $S^1$  or  $S^3$ . This is obtained as the one point compactification of Euclidean space. Technically, for example, the different instanton sectors for a gauge group  $G$  correspond to different principal fibre bundles with fibre  $G$  over  $S^4$ . Now the classification of bundles over spheres is rather easy. In fact the set of all  $G$  bundles over  $S^n$  is in (1, 1) correspondence with  $\pi_{n-1}(G)$  and in particular on  $S^4$  the bundles are classified by  $\pi_3(G)$ . However, for every simple, connected Lie group

$$\pi_3(G) \approx Z(\text{integers})$$

and hence bundles are always labelled by an integer (the "winding" number) which can be related to the Yang-Mills fields (connections) by the well-known Pontryagin-Chern formula

$$n \propto \int_{S^4} F^{\mu\nu} F^{\alpha\beta} \epsilon_{\mu\nu\alpha\beta}.$$

We started from a gauge group  $G$  and have progressed from  $G$  to classes of integers ( $Z$ ) for compactified space-time manifolds  $M$ . Can the rather humble  $Z$ 's lead one back to the non-Abelian group  $G$  itself?

In this respect an important suggestion has recently been made by Hawking and Pope and Back and Freund. Let us go back to the characteristic classes—and in particular to the second Pontryagin and Euler classes of a general space-time with no gauge field except the gravitational. These classes are represented by the curvature tensor in a well-known manner, with the celebrated Atiyah-Singer index theorem stating that for such a situation:

$$n_R - n_L = -\frac{1}{384\pi^2} \int R_{\mu\nu\alpha\beta}^* R^{\mu\nu\alpha\beta} \sqrt{g} d^4x,$$

where  $n_R$  and  $n_L$  are the numbers of zero mass spin states of right and left helicities.

Consider now a compact space without boundary, for example  $CP^2$ . The complex

projective two-space  $CP^2$  can be given a positive definite Riemannian metric for which  $\int RR^* d^4x = 48\pi^2$ . The index theorem would then seem to imply that  $n_R - n_L = -1/8$ , which is absurd. The reason that one appears to get a non-integer contribution to the index is that  $CP^2$  does not have a spin structure; one cannot consistently define spinors on  $CP^2$ .

How does one correct this situation? Hawking and Pope in a beautiful paper in Phys. Letters have answered this question. They point out that there exists a covariant constant two form which can be taken as associated with the U(1) symmetry and with the inclusion of this  $F^\wedge$ , the Atiyah-Singer theorem reads:

$$n_R - n_L = -\frac{e^2}{16\pi^2} \int F_{\mu\nu} F^{*\mu\nu} \sqrt{g} d^4x - \frac{1}{384\pi^2} \int RR^* \sqrt{g} d^4x.$$

The contribution of the first term depending on  $F^\wedge$  can be computed. This contribution is precisely  $ra(ra+1)+1/8$ . Peace is restored if both terms are added;  $n_R - n_L$  is indeed an integer.

Now what is the moral of this. The moral is that a compact space-time structure  $CP^2$ , would be unacceptable physically unless it was supplemented with an "internal" U(1) symmetry. The U(1) is motivated by space-time topology. From this observation, Hawking and Pope argue that there may be a connection between the topology of space-time and the spectrum of elementary particles.

This theme has been taken further by Allen Back and P. G. O. Freund in a contribution to the Conference. They rebel against the starting point of Hawking and Pope. Why the compact  $CP^2$  from which Hawking and Pope start? Freund himself was one of the first to suggest consideration of  $CP^2$  in the context of gravitational anomalies. However, there has to be some dynamical reason for this. Back and Freund instead start with general (pseudo) Riemannian space-times and show that all matter fields must appear in suitable multiplets of a gauged symmetry in order to permit the definition of a generalized spin structure. (They argue that one cannot *a priori* restrict oneself to manifolds that have a

spin structure; this would be an unacceptable restriction for example in a standard functional integral formalism for quantum gravity.) The simplest choice, they discover, for the gauge structure for a general Riemann manifold is  $SU(2)$ —the first indication of a non-Abelian structure from space-time topology. With a gauged internal  $SU(2)$  symmetry one can define spinors of any four-dimensional Riemann manifold. Physically one may attempt to identify this  $SU(2)$  with the universal weak isospin  $SU(2)$  factor of the unified electroweak group. The corresponding weak isospin statistics connection they discover requires bosons (fermions) to possess integer ( $1/2$  odd integer) weak isospin. This unfortunately will not accommodate the simplest Higgs structure currently utilized in  $SU(2) \times U(1)$ . However, one might generalize weak isospin to  $SU_i(2) \times SU^{\wedge}$  with two quantum numbers  $(k_i, k_r)$ , such that fermions carry half odd values of  $k_i \pm k_r$  and bosons carry integer  $k_i + k_r$ .

This is powerful stuff—space-time Riemannian topology dictating (at least partially) internal gauge symmetries, plus an internal charge-statistics relation restricting the types of multiplets one may contemplate. It is suggestive; it is deep, could this be the whole story?

Though not directly relevant to the question of where the internal symmetries come from, there are still other directions into which the delicate interplay of space-time and group topologies can lead us into. For example, remark that the classification of  $G$  bundles in general space-times is *different* for different Lie groups. While for a four-dimensional manifold  $\wedge^4$  and for any simply connected groups  $G$  (e.g.,  $SU(\infty)$ ,  $Sp(w)$ ,  $G_2$ , etc.)

$\{G \text{ bundles}\}^{\wedge^4 H^1(\wedge, Z)} = Z$  if  $\wedge^4$  is compact and oriented

$\neq 0$  if  $\wedge^4$  is non-compact,

the situation is richer for  $U(\#)$ 's or  $SO(\infty)$ 's. For example, for  $SO(n)$ , with a non-compact  $\wedge^4$   $\{SO(a) \text{ bundles}\}^{\wedge^4 H^1(\wedge, Z)}$  so that the classifying element is the second Stieffel-Whitney class ( $W_2$ ). It is noteworthy that although the Pontryagin class of an  $SO(n)$  bundle can be expressed in terms of the Yang-Mills fields this is apparently not true

of  $W_2$ . Hence the Stieffel-Whitney class corresponds to some new type of quantum number whose physical significance has not yet been elucidated. (For details see S. Avis and C. J. Isham, Cargese lectures 1978, IC preprint ICTP/77-78/23) Another example is the mobility or twistedness quantum number (C. J. Isham, Proc. Roy. Soc, in press) which can be assigned to scalar or spinor fields which correspond to cross sections of  $G$ -bundles when  $G=Z_2$ . (The number of inequivalent  $Z_2$  bundles is equal to the number of elements in the group  $H^1(\wedge, Z_2)$ .)

J. Kiskis has tried to relate these ideas to the basic concept of how to define the signs of charges (including that of the electric charge) when a gauge group is enlarged to include certain discrete symmetries, such as charge conjugation in a space-time which is not simply connected. He concludes that in a space-time with a handle, for example, such a definition is not possible and there exists a mechanism for global violation of charge conservation. Kiskis makes the remark that we know nothing about global topology of real space-times on a cosmological scale, nor do we know anything about space-time topology at distances shorter than  $10^{-16}$  cms. However, the problem about exotic topologies will always be, what is the dynamical mechanism which produces "handles" for example in space-time?

There is yet one more approach to the "explanation" of internal symmetries. I have always been very impressed by a remark which 'Res Jost made in his lecture on *New Theoretical Ideas* at the Sienna Confernece in 1963. Jost said; given a number of choices, he believed nature always made the brashest, the least subtle and from one point of view the "least imaginative" choice. To solve the  $r, Q$  puzzle of 1956, nature did not resort to a use of parity-conserving density matrices between accidentally nearly degenerate states. It chose instead, the brash, bold, expedient of parity violation. Likewise in our times for neutral currents, in the low-energy regime, nature has chosen the simplest structure it could, the  $SU(2) \times U(1)$ .

The least imaginative—though perhaps the brashest—resolution to the problem of internal symmetries is to assume that what we are

witnessing is the structure of extra space-time dimensions. We really do live in an extended space-time. If space-time does possess extra dimensions (perhaps all spacelike) and if the curvature pertaining to these happens to be so large that these fold upon themselves, with dimensions much smaller than  $10^{-16}$  cms (and perhaps with a hierarchy even approaching Planck length  $10^{-33}$  cms), we would not apprehend them, except indirectly. The so-called internal symmetry quantum numbers are then the only (indirect) window we possess for apprehending these extra dimensions.

The idea is not new: it started with the Kaluza-Klein introduction of the 5<sup>th</sup> dimension and its connection with electric charge. It was pursued in the 1950's by Abraham Pais and in the 1960's by T. Takabayashi (see Proceedings of the 8<sup>th</sup> Nobel Symposium, Ed. N. Svartholm, 1978 (Almqvist and Wiksell), p. 157) following an earlier work of H. Yukawa, Phys. Rev. **91** (1953) 415, 416. What is however new is a recent attack on this problem by Cremmer, Scherk, Schwarz and others (reviewed in this Conference by Scherk), taking their cue from dual models in ten space-time dimensions (Nucl. Phys. **B108** (1976) 409, where the "compactification" of the extra dimensions is seen as a spontaneous symmetry-breaking phenomena, through which the highest unification mass (Planck mass) enters particle physics). Although topological ideas were already introduced by Cremmer and Scherk in order to motivate stability of structures in extra-dimensions, a new twist has been given to these ideas by Horvath and Palla who seek the masslessness of the neutrino through a use of the *Atiyah-Singer theorem as applied to extended space-time*. Thus the notions of curvature and topology of extra space-time dimensions motivate the charge concept, the non-Abelian symmetries, the highest unification energy and the relatively low masses of physical objects we are dealing directly with, including the masslessness of the neutrinos. The major unsolved problem then is: how many extra dimensions and why that many?

In the next section we examine these ideas of spontaneous compactification in some more detail.

## §IX. Spontaneous Compactification

The idea seems to be due originally to Cremmer and Scherk (Nucl. Phys. **B108** (1976) 409) who were looking for an interpretation of the extra dimensions in dual models. As a bonus this mechanism may explain the super-heavy scale in grand unified schemes. Since the dual models are supposed to be renormalizable, one is able to incorporate gravity as well as all other forces in a renormalizable framework. For the compactification discussion, however, the dual model is replaced by a "low-energy approximation" in the form of a classical Lagrangian containing local fields and satisfying general covariance, gauge invariance, etc.

The Lagrangian contains a  $4+N$  dimensional metric tensor  $g_{\mu\nu}$  and a set of gauge vectors for an internal symmetry group, which to start with at least has a non-geometrical origin. These fields couple with a strength  $e$ . The Lagrangian may or may not have scalars. It is conjectured that the ground state solution may have non-trivial topology—in both metric and group spaces, *i.e.*,  $(g^{\mu\nu})^{\wedge}$  and  $(A^a)^{\wedge} \neq 0$ . (Cremmer and Scherk in treating the  $N=2$  case assumed a monopole form for  $A_p$  on the sphere  $S^2$ .)

A non-vanishing Chern class for  $(Af)$  implies obviously that some components of  $(A^a)^{\wedge}$  are non-zero and so must contribute to  $Tf_c$  on the right-hand side of Einstein's equations. Hence one expects  $(g^{\mu\nu})^{\wedge}$  not to be flat. The non-trivial topology is supposed to stabilize this situation.

The simplest non-trivial topology that can be imagined in  $[4+N]$  is  $i\hat{t} \times S^N$  and the most symmetrical (and therefore lowest) solution with this topology would be the product of Minkowski 4-space with an  $iV$ -sphere. The group of motions would then be Poincaré  $\times$   $SO(N+1)$ . Corresponding to this, the 4-space components of the gauge vector must vanish, but the remaining  $N$  components need not—at least if the gauge group contains  $SO(N+1)$ . If the  $N/2$  Chern class is non-vanishing then the gauge vector cannot vanish and the situation is self-sustaining. (According to Horvath and Palla, ICTP, Trieste, preprint IC/78/37, submitted to this Conference, the gauge group

$G$  need not be so large as  $SO(iV+1)$ . The main need is that the groups allow gauge field configurations on  $S^n$  with non-vanishing  $N/2$ 'th Chern class and for this  $TT^{\wedge}_I(G)$  should be nontrivial. To close the cycle, it has been shown by G. F. Luciani that the  $S0(A4-1)$  symmetry is itself local and may possibly be identified with the non-geometrical gauge group we started with.

The main check on the consistency of this idea is a computation of the excitation spectrum; *i.e.*, one must expand the background values showing that the first-order terms cancel while the second-order terms are positive definite.

At the strictly classical level one could perhaps verify the stability against small perturbations by computing the mass spectrum but one does not know if the possibility of tunnelling can be excluded.

In the papers of Cremmer and Scherk, Higgs' fields are included and a monopole solution of the 't Hooft type is conjectured in the extra dimensions. In their paper with Horvath and Palla (Nucl. Phys. **B127** (1977) 57) the Higgs is absent and a Wu-Yang type monopole is assumed.

For  $N=2$  the ansatz takes the form (with  $G=SO(3)$ ):

$$\langle g_{i\bar{i}} \rangle dx^{\bar{i}} dx^i = -dx_0^2 + dx^2 + R_0^2(d\theta^2 + \sin^2 \theta d\varphi^2)$$

$$\langle \vec{W}_\mu \rangle = 0$$

$$\vec{W}_\theta = \frac{1}{e}(-\sin \varphi, \cos \varphi, 0)$$

$$\vec{Q} = (\cos \varphi \sin \theta, \sin \varphi \sin \theta, \cos \theta)\rho,$$

where  $i, \bar{i}$  and  $p$  are constants. They are obtained rather trivially since the field equations reduce to an algebraic form. There is also a cosmological term since the Higgs potential is taken in the form

$$V(Q) = \frac{\lambda}{4}(\vec{Q}^2 - F^2)^2 + V_0.$$

By a careful (and therefore possibly an unnatural) adjustment of  $K_0$ , there is the possibility of the model giving a possible explanation of the large unification masses of the order of Planck mass for the "simple" unified

groups.

After the spontaneous compactification, all fields can be expanded in series of hyperspherical functions defined on the internal space with coefficients dependent on the first four co-ordinates. In effect the effective action has the form of an infinite component field theory, but the masses of the components are different and depend both on the indices of the hyperspherical functions and the representation the components belong to. All the non-zero masses turn out to be of the order of Planck's mass. Thus at low energies only the zero mass components have physical relevance in the sense that either they remain exactly massless or they obtain their non-zero physical masses by some other mechanism.

It is in the question of zero mass fermions that topologically non-trivial compactification of gauge fields plays an important role. This is with the use of the Atiyah-Singer index theorem which relates the zero-energy eigenspace of the Dirac operator to the topological invariants characterizing the global gauges, among which are the gauges referring to the compactified space. *Thus the number of zero mass objects (neutrinos) may be connected with the topology of the internal space.*

### Concluding remarks

Some of the ideas I have spoken of above appear at this time simply crazy. The question, over the perspective of twenty years—the time for such theoretical idea to be worked out and then possibly tested—is not if an idea is crazy. One should rather ask with Niels Bohr; is the idea crazy enough? I wish to conclude with a quotation from a very great physicist whom many of us here were privileged to know; predicting, in his opinion, the future course of physics,

“Physics will change even more. If it is radical and unfamiliar and a lesson that we are not likely to forget, we think that the future will be only more radical and not less, only more strange and not more familiar, and that it will have its own new insights for the inquiring human spirit.”

J. R. Oppenheimer

## **P10: ICFA**

*Chairman:* **Y. YAMAGUCHI**

*Speaker:* **E. L. GOLDWASSER**

*Scientific Secretaries:* **Y. KIMURA**  
**Y. ASANO**



## **P 10b**                      **Report on the Status and Plans of the International Committee on Future Accelerators**

E. L. GOLDWASSER

*FNAL*

Over the past years a series of informal meetings has been held by small groups of high energy physicists from the Soviet Union and the Dubna member states, from Western Europe and from the USA in order to discuss the future of high energy physics and questions of international collaboration. The series began with meetings between European and Soviet physicists emerging from the CERN-Dubna and CERN-Serpukhov Collaborations; it was then extended to include USA physicists. Meetings were held in 1967 in Riga, then in 1968 in Semmering, in 1969 in Tbilisi and in 1971 in Morges.

No further meeting in that series was held until March 1975 when a seminar was held in New Orleans entitled "Prospectives in High Energy Physics." The meeting was international in character and presented a forum for discussion of the status of international collaborations in high energy physics as well as for the planning of possible future expansion of those collaborations.

During the course of that meeting it was noted that the progress of high energy physics would almost certainly lead to a requirement for an accelerator and for facilities so large that they would be beyond the reach of any individual nation or any individual region. It was recognized that not only would the technical problems of creating such a facility be enormous, but also that the organizational, economic and political problems connected with the formation of an international collaboration would also be formidable. It was agreed that it was not too early to begin to study some of those problems although it was also agreed that such studies should be undertaken in a manner that would not jeopardize nor slow down progress toward the realization of a number of national and regional projects which were already underway or in a planning stage. A time scale of about

ten years was suggested as one within which plans for such a large facility might be developed. The rather unimaginative name, Very Big Accelerator (VBA) was suggested for the new facility. It was agreed that meetings should be organized to study the problems associated with the creation of such a facility.

At New Orleans it was agreed to hold a first organizational meeting at CERN in October, 1975, with the understanding that the main purpose of that meeting would be to establish an agenda for a second meeting which would be held in Serpukhov, in May, 1976. A third meeting might later be held in the United States. It was further agreed that the studies would be initiated with participation from Eastern Europe, Japan, USA, USSR, and Western Europe. Scientific authorities in each of those regions were to be asked to nominate scientists to participate in the study group.

In CERN, in October of 1975, the organizing meeting was attended by V. Yarba representing the USSR; K. Lanius representing other nations of Eastern Europe; J. Adams, M. Conversi, and W. Jentschke representing Western Europe; L. Lederman, K. Strauch, and R. R. Wilson representing the USA; and V. Weisskopf as the Chairman of the New Orleans meeting at which an initial agreement had been reached to proceed with a study problems associated with a VBA.

Official participants in the Serpukhov meeting were: A. Logunov, A. Vassilyev, M. Markov, V. Glukhikh, L. Soloviev, I. Chuvilo, and V. Yarba from the USSR; K. Lanius and V. Dzhelepov representing JINR member states; Y. Yamaguchi from Japan; V. Weisskopf, R. R. Wilson, L. Lederman, M. Barton, R. Diebold and J. Bjorken from the USA; and G. von Dardel, U. Amaldi, D. Husmann, K. Johnsen, A. Rousset, and D. Thomas from CERN member states.

At the Serpukhov meeting the general scale for a VBA was discussed. It was tentatively decided that something equal to or greater than a 10 TeV fixed target accelerator would be the smallest facility appropriately to be considered. It was further decided that a minimum energy of 100 GeV would establish a scale for a pair of  $e^+e^-$  storage rings.

In the report of the meeting a set of three conclusions was stated:

A) The present status of the science of the structure of matter poses fundamental problems which require a new generation of facilities. . . Such facilities are within the capabilities of the individual regions and are needed for continued progress of this field of research.

B) The success of regional and interregional collaboration in the past provides a good basis for extending and strengthening this collaboration in the new generation of regional facilities.

C) Looking beyond this new generation of regional accelerators we foresee the need for an accelerator complex (VBA) which will require international collaboration of all regions concerned.

Finally four recommendations were formulated at the Serpukhov meeting:

1. Efforts should be made to coordinate the design and construction of new regional facilities. Consultations and exchange of experiences should be encouraged in order to optimize the diversity of facilities and to enhance the efficiency of construction and operation. The study group also recommends joint studies of new technology (*e. g.*, superconductivity, new detectors and other experimental apparatus) and joint design and/or construction of components of regional projects.

2. Joint utilization of regional facilities by scientists of different regions should be organized on the basis of present and future arrangements or agreements. The general availability of regional installations is essential to enable scientists of different regions to take advantage of facilities with complementary research potentialities.

3. International collaboration should provide for studies leading towards the realization of a next generation of superhigh energy facilities, following the regional projects referred to above. It is expected that these facilities will be so large that their realization will be

possible only by pooling the resources of all regions concerned into common international projects.

Creation of a superhigh energy accelerator complex (VBA) involves especially complicated scientific, technical and organizational problems. These will require several years of continuing studies and discussions. The Study Group recommends that these discussions begin in the near future leading to the start of the design of the VBA in about 10 years.

4. In view of the need for these extensions of international collaboration, the Study Group suggests to the IUPAP Division of Particles and Fields to initiate these activities in an appropriate form, for example, by appointing a sub-committee for the purpose of organizing working groups and future meetings such as the present one.

In response to Recommendation #4, stemming from the Serpukhov meeting, the subject of IUPAP sponsorship of the new study project was placed on the agenda of the meeting of the IUPAP Commission on Particles and Fields which was held in Tbilisi on July 20, 1976. At that meeting it was agreed that the IUPAP Commission should serve as sponsor of the activities of the proposed new committee which was there officially named the International Committee on Future Accelerators (ICFA).

There was considerable discussion about the appropriate membership of the new Committee and about the charge which would be presented to the new committee by the IUPAP Commission. It was recognized that if the activity was now to be formalized by IUPAP sponsorship, IUPAP must assume a substantial responsibility for the direction in which ICFA might go and for the procedures through which ICFA would operate.

Accordingly at Tbilisi the IUPAP Commission adopted a scheme of representation on the new committee consisting of two members from Western Europe, two members from Eastern Europe, two members from the USA, one member from Japan and the Chairman of the IUPAP Commission, serving in an *ex-officio* capacity, with an explicit responsibility to represent the interests of the "other countries."

Following the Tbilisi meeting certain objections were raised regarding the formula that had been adopted by the IUPAP Commission. In an effort to resolve that problem and in preparation for the first official meeting of ICFA, Bernard Gregory, who was then Chairman of the IUPAP Commission, had a series of discussions with the interested parties. In the course of those discussions, Dr. Gregory formulated a substitute suggestion for ICFA membership which appeared to be generally acceptable. The suggested composition of the committee was: three members from CERN member countries, three from the Soviet Union, three from the USA, one from Japan, and one from Dubna member states other than the Soviet Union. The Chairman of the IUPAP Commission on Particles and Fields was still designated to be a member, *ex officio*, as before.

During the winter of 1976-77, the IUPAP Commission agreed, by correspondence, on a stipulation of ICFA responsibilities as follows:

"To organize workshops for the study of problems related to an international super high energy accelerator complex (VBA) and to elaborate the framework of its construction and of its use."

"To organize meetings for the exchange of information on future plans of regional facilities and for the formulation of advice on joint studies and uses."

No official IUPAP action on the revised suggestion for ICFA membership was planned to be taken prior to the annual Commission meeting scheduled for August 31, in Hamburg, and since a first meeting of the ICFA Committee had been scheduled to take place on August 30, it was agreed that the scheduled ICFA meeting would be held but would be provisional in character, its official status pending approval, on the next day, by the IUPAP Commission, of the constituency of the ICFA Committee.

For the provisional first meeting of ICFA the membership was as follows: J. Adams, G. von Dardel, and W. Paul from Western Europe; L. Lederman, V. Weisskopf, and R. Wilson from the USA; V. Dzhelepov, K. Mishnekov and V. Yarba from the USSR; K. Lanis from the Dubna member states; Y. Yamaguchi from "Other Countries" (Japan); and B.

Gregory, *ex officio*, as Chairman of the IUPAP Commission. A. Rousset, of France, also attended as Committee Secretary.

At this first provisional meeting of ICFA Bernard Gregory, chairman of the IUPAP Commission, was elected to serve also as Chairman of ICFA. At his request, A. Rousset was appointed to assist him in his task. Gregory presented the stipulation of ICFA responsibilities, as formulated by the IUPAP Commission and as stated above. The ICFA members proposed to interpret those instructions as being identical to the more detailed recommendations which had been forthcoming from the organizing meeting at Serpukhov. Those recommendations placed more emphasis on the coordination of present regional activities and somewhat less emphasis on activities specifically oriented toward the study and organization of the VBA. Gregory was asked to report on that point to the IUPAP Commission.

At the provisional ICFA meeting it was also decided to create a "Regional Facilities Collaboration Study Group" (Group 1). That Group was to deal with problems of collaboration on design, construction and use of all accelerators.

It was further decided to create a "Super High Energy Facility Study Group" (Group 2). That study group was to cover all scientific, technical and organizational problems pertaining to a super high energy accelerator (VBA).

Questions were raised during the discussion regarding the possible existence of limits on design parameters of very high energy machines. To address those questions, it was decided that Group 2 should hold a seminar on "Technical Possibilities and Limitations of Accelerators and Detectors" at Fermilab in the middle of 1978.

In order to set up the two study groups, three members of the ICFA Committee (Adams, Wilson and Yarba) were nominated to send proposals on terms of reference, working methods, topics, agendas and memberships to Gregory before 31 October 1977. A final decision was to be taken by exchange of telex or by a meeting in January of 1978 at CERN.

Finally it was agreed that an ICFA meeting

should be held during the next International Conference on High Energy Physics at Tokyo (24-30 August, 1978). It was agreed that a report of ICFA activities should be made at that conference.

On the day following the first provisional meeting of ICFA, described above, the IUPAP Commission met in Hamburg and approved the revised membership of the ICFA Committee, thus officially constituting the prior day's meeting as the first meeting of ICFA. There was an extended discussion of the preferences that had been expressed by ICFA members concerning the charge under which ICFA would operate. However the IUPAP Commission retained its previous statement of ICFA responsibilities, preferring to maintain a strong emphasis on a VBA rather than on the coordination of the design, construction and use of regional facilities. The IUPAP Commission did favor an organized exchange of information about the progress and plans of regional facilities, but the members believed that to be covered in the second part of their charge to ICFA.

Since the IUPAP Commission has the tradition of meeting on an annual basis, it was agreed that a report should be submitted by the ICFA Committee to the IUPAP Commission each year, at the latter's regular meeting.

Last autumn and winter, Gregory, working together with Rousset, was making preparations for a second meeting of ICFA at CERN in January. Then, at Christmas time, Bernard Gregory's sudden and tragic death ended his brilliant and dedicated career. He was a man of great talent and unusual insight. He had a deep commitment to the furthering of international cooperation. He was a principal moving force behind the initiative that was taken at New Orleans. Without his leadership, tact and diplomacy no agreement could have been reached, and his guidance and judgment will be missed in the ICFA enterprise as it has been and will be in many other activities which are important both to high energy physics and to France. The most fitting tribute we can pay to him will be to assure that his dream of increasing international cooperation flourishes.

After Gregory's death, Larkin Kerwin, Secretary General of IUPAP, asked me, as

Secretary of the IUPAP Commission on Particles and Fields, to assume responsibility for the remainder of Gregory's term as Chairman. As Acting Chairman of that Commission, I also became the IUPAP ex-officio member of ICFA, and with that, temporarily assumed Gregory's elected position as Chairman of ICFA.

I immediately contacted Andre Rousset and we began putting together the pieces that he and Gregory had been working on in preparation for an ICFA Meeting in January. Our first task was to arrange for replacements for three of the original ICFA members who had submitted their resignations. A von Dardel and W. Paul had submitted resignations by reason of the fact that their respective terms as Chairman of ECFA and as Chairman of the CERN Science Policy Committee had expired. Leon Van Hove, the designated responsible authority for Western European representation, recommended M. Vivargent and G. Stafford, successors to von Dardel's and Paul's previous responsibilities, as replacement members of ICFA. A mail ballot to the IUPAP Commission Membership obtained unanimous agreement to those two suggested appointments.

Last winter I also regretfully received Victor Weisskopf's resignation from ICFA. Although he expressed his continuing enthusiasm for the project, he indicated that he was no longer able to undertake the strenuous travel that would be involved. The vacancy created by Dr. Weisskopf's resignation was only filled a few days ago when, by action of the IUPAP Commission, B. Richter was appointed to fill that vacancy in the U. S. representation.

At the IUPAP Commission meeting in Hamburg the Commission had expressed its wish that its Chairman should serve on ICFA only in an ex officio capacity and should not normally have a position of responsibility on the ICFA Committee. The Chairman of ICFA was to be elected annually by action of the ICFA Committee from among its directly appointed members. Accordingly, prior to the January ICFA Meeting, I informed Committee members that I was withdrawing my name from consideration for the ICFA chairmanship.

In Hamburg, the IUPAP Commission **had**

Table I.

Name and (location) of project	Particles	Energy (GeV in c.m.)	Luminosity ( $\text{cm}^{-2} \text{s}^{-1}$ )	Other options	Status and/or dates
PETRA (DESY)	$e^-e^+$	38	$10^{32}$ at 30 GeV	—	Starting operation ~1980 Depends on tests of superconducting cavities in 1979 (CERN-DESY- KARLSRUHE)
	—	45	$1.5 \times 10^{32}$ at 38 GeV	—	
	—	>60	$\sim 10^{31}$	—	
PEP (SLAC)	—	8-36	$10^{32}$ at 30 GeV	ep and/or increase energy to 48 GeV	~ Oct. 79
CESR (Cornell)	—	16-20	$10^{32}$	—	1979 Completion
ALA (Frascati)	—	2.4	$2 \times 10^{30} \sim 2 \times 10^{31}$	—	Approved for construction starting 1979
LEP (CERN)	—	80-200	$\sim 10^{32}$ max	ep if LEP is close to SPS Polarized beams	Design study under way-project not yet approved After PETRA has run DESY will study $2 \times 100$ GeV possibility DESY-CERN will coordinate on single project
(DESY)	—	—	—	—	

empowered me, as Secretary, to provide for a rotation of terms on the ICFA Committee, based on a three year cycle. Terms are normally to start on January 1 of any given year and to end on December 31. Individual members will be eligible for reappointment for a second term, but normally will not be eligible for appointment for a third term.

The present ICFA membership together with the dates of termination of present appointments is as follows:

Adams (1979)	Dzhelepov (1979)
Vivargent (1980)	Mishnekov (1980)
Stafford (1981)	Yarba (1981)
Lederman (1979)	Lanius (1980)
Richter (1980)	Yamaguchi (1979)
R. R. Wilson (1981)	Goldwasser (1978)
	( <i>ex officio</i> as Acting Chairman of IUPAP)

The second meeting of ICFA convened at CERN on the 27th of January, 1978. The first order of business was the election of a new ICFA Chairman, and John Adams was unanimously chosen.

At that meeting it was decided to accept the stipulation of ICFA responsibilities as formulated by the IUPAP Commission. It was further agreed that there was no need, at

the present time, to set up standing working groups as had been suggested at the previous meeting in Hamburg. However it was agreed that there was a clear need to organize a number of workshops on topics related to an eventual VBA Project and on topics related both to existing regional facilities and to the realization of a VBA. It was agreed that there were four main areas of interest relating to the VBA.

1. The physics needs.
2. Accelerator possibilities and limitations.
3. Detector possibilities and limitations.
4. How to build and use a VBA.

It was agreed to organize a first workshop on "Possibilities and Limitations of Particle Accelerators and Detectors" at Fermilab from October 9-19, 1978. It was further agreed that there should be about forty participants in all, ten each to be designated by the three major regions, two from Japan and the others to be chosen by the workshop's Organizing Committee to round out the technical competence of the group. Fermilab was asked to take responsibility for the organization of the workshop. It was agreed that a meeting of ICFA, itself, should be held in conjunction with the Fermilab workshop and that there was no need

Table II.

Name and (location) of project	Particles	Energy (GeV)		Luminosity ( $\text{cm}^{-2} \text{s}^{-1}$ ) or intensity	Other options	Status and/or dates
Tristan (KEK)	ep	15 <sup>e</sup>	50-200 <sup>p</sup>	$6-9 \times 10^{31}$	$e^+e^-$ pp 400 GeV (supercond.)	None approved
Cheep (CERN SPS)	—	25	270	$5 \times 10^{31}$	Trade off energy and luminosity	
Proper (DESY PETRA)	—	10	175	$4 \times 10^{32}$		
LEP Option (CERN)	—	17	280	$1 \times 10^{32}$		
Fermilab	—	60	400	$6 \times 10^{31}$	—	
		12	1000	$10^{32}$		

for an ICFA meeting at the time of the Tokyo Conference.

It was tentatively agreed to hold a second workshop on "Superconducting Magnets and Cavities" at IHEP, Serpukhov, in the Spring of 1979. A final decision whether or not to hold this workshop will be made at the next meeting of the full ICFA Committee which will follow the workshop at Fermilab on October 20, 1978.

The question of whether or not to hold a workshop on the physics needs for a VBA, perhaps also in 1979, will be discussed at the next ICFA Meeting.

It was agreed that there were three topics of interest related to the current regional facilities; (1) the physics reasons for building the new regional facilities such as LEP, UNK, ISABELLE, etc., (2) the technology required for building these regional facilities and (3) the experience gained in the present joint utilization of regional facilities.

Finally, it was agreed that I should report on ICFA activities at the Tokyo High Energy Physics Conference. That I am doing today.

Plans are proceeding well toward the convening of a workshop in October at Fermilab. The Organizing Committee consists of Lee Teng, Chairman; Jack Sandweiss, Associate Chairman; Burt Richter, Jim Sanford and Bill Willis. The meeting is to start on October 15 and extend through October 21. One concern of the workshop will be with problems related to various types of accelerators and accelerator configurations, —technical limitations, approximate cost, and so forth. The second concern of the workshop will be with problems relating to detector designs, capabili-

ties and limitations.

My own term on IUPAP expires next month and with it will expire my membership on ICFA. I believe now, as I did at New Orleans, that the concept of an international laboratory is one which must be developed with inspiration and nurtured with wisdom. Its role in the future development of high energy physics and its role in the development of a new dimension of international collaboration could both be of enormous importance.

The problems are sufficiently difficult that they will be met only if the need for such a laboratory is a real one. That condition will be satisfied only if the scope of the laboratory, the dimensions of the facility and the cost of the construction and operation are such that they require a world collaboration.

The time scale on which the physics demand for such a facility will become pressing is likely to be about a decade. That time scale might lead some to an attitude of complacency and inaction. However the problems are so complex that if we are to know how to start to address them, even ten years from now, we must begin to try to understand them immediately.

We are not likely to choose the design of a VBA today or tomorrow. But it is not too early to try to understand the physics needs, the technical limitations and the economic and political problems. I am sure that you will all join in wishing your IUPAP and ICFA representatives the best of luck in pursuing this dream.

In closing I cannot help remembering Steve Weinberg's closing remarks this morning when he expressed his hope that today's outstanding

Table III.

Name and (location) of project	Particles	Energy (GeV)	Luminosity (cm <sup>-2</sup> s <sup>-1</sup> ) or intensity	Other options	Status and/or dates
$\bar{p}p$ (CERN)	$\bar{p}p$	540	10 <sup>30</sup>		Under construction '78-'81
Tevatron (Fermilab)	p	1000	5 × 10 <sup>13</sup> ppp		"
	pp	1000 on 250	4 × 10 <sup>30</sup>		"
	$\bar{p}p$	250 on 250	2 × 10 <sup>28</sup>		electron cooling experiment in progress
Isabelle	$\bar{p}p$	1000 on 1000	10 <sup>30</sup>		"
	pp	400 on 400	~ 5 × 10 <sup>32</sup>	$\bar{p}\bar{p}$ ep	Construction starts 1979 Completion ~ 1986
Institute for High Energy Physics (Peking)	p	50	1-2 × 10 <sup>13</sup> ppp	Booster could increase intensity (Phase 2 ? TeV)	'78-'83 '84-'89
UNK (Serpukhov)	p	3000	6 × 10 <sup>14</sup> ppp	$\bar{p}\bar{p}$	Development started-
	pp	2100 + 1100	10 <sup>32</sup>		construction not yet approved
Tristan (KEK)	pp	200 + 200	10 <sup>34</sup>	$\bar{p}\bar{p}$ or 400+400 (supercond.)	Not yet approved

questions might all be answered by the time of the next conference, but also his doubt that we would be so skillful or lucky, I join him on both counts, and, in that connection, I would like to share with you the only great disappointment I have had at this conference.

From the Eight-fold Way we are all used to relying on the teachings of Buddha for our insights in elementary particle physics. It therefore was with some pleasure and anticipation that I roused through the book on the Teachings of Buddha which I found in my hotel room. As I hastily scanned the pages it was not long before I thought I had found exactly what I had half expected. I thought I read:

#### Search For Truth

In the search for truth there are certain questions that are important.

Of what material is the universe constructed?

Is the universe eternal?

Are there limits or not to the universe?

In what way is this human society put together?

What is the ideal form of organization for human society?

Reading this I was gratified to find this ringing support for the pursuit of political science,

sociology, cosmology, and high energy physics.

You can then imagine my shock when I went back to read the passage more carefully. What it really says, by way of introduction, is:

"In the search for truth there are certain questions that are unimportant."

And in concluding that passage, the Teachings go on to say:

"If a man were to postpone his searching and practicing for Enlightenment until such questions were solved, he would die before he found the path."

Let us hope that not all of us will die before we take at least a few more steps along the path for which we are searching.

The report I was originally requested to present at this conference was supposed only to inform you about the birth, purpose and progress of a new committee which is intended to represent you and to concern itself primarily with problems pertaining to the long range future for the study of high energy physics. At first I had doubts that such a report would be useful, but, in light of the many questions I have been asked, during this conference, about the letters ICFA which appear at this point in the program, it is clear that not much is known about this new com-

mittee and that even less is known about its activities.

Some of my friends have suggested that perhaps ICFA stands for International Conference for Future Administrators, a possibility that might concern me as I leave Fermilab. However, in fact, it stands for International Committee on Future Accelerators and I shall tell you more about it in a few moments.

First, however, some of you may remember that in one of the earlier Conference Programs there was listed a session on Future Facilities. That session has been cancelled but during the first few days of the Conference, coincident with the parallel sessions an International Symposium on Future Perspectives in High

Energy Physics was held. At its conclusion a summary of the projects which had been described was presented by Professor Nishikawa. I have been asked to fill in some of the cancelled plenary session by summarizing the substance of last week's Symposium. The following three transparencies are taken mostly from Dr. Nishikawa. They summarize the states of short-range future accelerator projects and provide a bridge of reality to the ICFA dream which I shall describe in the few minutes.

So much for the world of reality and perhaps a little beyond, I would now like to step into the world of pure dreams.



## P11: Concluding Talk

*Chairman:* G. TAKEDA

*Speaker:* Y. NAMBU

*Scientific Secretaries:* J. ARAFUNE  
M. YOSHIMURA

(Wednesday, August 30, 1978; 14: 30–15: 30)

Y. NAMBU

*University of Chicago*

It is now my task to look back with you, at the six days of eventful sessions that we have had, take stock of our accomplishments, summarize them, and put them in perspective. However, you will understand that it is not possible for me to cover all the subjects uniformly. Nor would it be desirable. I will focus on what I think are the main themes, and devote the rest of my time to a bit of palm reading into the future.

§I.

Almost four years have passed since that november of 1974, and it thrills us to think about the long strides high energy physics has made within that short span of time. I will start by showing a chronological list of representative classes of new particles (Table I).\*

Table I. A chronological list of representative classes of particles. The numbers in the parentheses are the years of discovery.

$J/\psi$	(1974)
$\chi$	(1975)
$\tau$	(1975)
D	(1976)
$\Upsilon$	(1977)

These particles belong to new classes because, first of all, they have high masses and yet are relatively stable. In other words, a new scale of mass or level spacing larger than the known hadronic mass scale seems to exist. Remarkably, the leptons are also beginning to show a parallel trend. These discoveries are a direct result of the development of a new generation of high energy accelerators. It is gratifying that going to the next level of energy range one should immediately be rewarded with such a wealth of exciting new phenomena. One can always question the value and wisdom of pursuing ever increasing energy with ever increasing cost and effort. But I doubt that

\* More detailed data will be found in the talks of the corresponding speakers of the plenary sessions of this Conference, Flüge, Hara, Lederman and Feldman.

anyone is hesitant or doubtful about it now.

The real significance of the experimental discoveries, however, can be appreciated only when they are combined with theoretical developments. It is in fact remarkable that the theorists had more or less anticipated the general scenario according to which the events seem to be unfolding. But this scenario is naturally not unique. In order to make progress, one has to narrow down one by one the various alternative possibilities by means of crucial tests. If I have to summarize the Conference in one sentence, I will say that this is the year when a significant advance was made in the narrowing down process thanks to the completion of a large number of precision experiments, which are impressively consistent with each other and with a particular theoretical framework. The agreement is a quantitative one, and hence it is a real and definite step forward.

I am here talking, primarily, about the Weinberg-Salam theory<sup>1</sup> of unified weak and electromagnetic interactions, and the comparison is between the original model and the generalized and more complicated versions of it. As usual, the latter were motivated either by the earlier confusion in experimental data, or by a desire to improve on the theory. Very often, however, one ends up spoiling everything in the process. So it is reassuring to find out that nature likes simplicity after all; according to the developments in very recent months, the original Weinberg-Salam version seems to be the sole survivor of the various "low energy" tests. I use the word "low energy" only in a relative sense. Crucial in this sudden narrowing down of options are the beautiful SLAC results on parity violation in electron-deuteron and electron-proton scattering.<sup>2</sup> Also important is the impressive consistency shown by numerous neutrino reaction experiments.<sup>3</sup> Indeed, the neutrino physics has come of age. So we now seem to be in a situation in which all the low energy weak

processes, that is to say, the processes that do not involve production of  $W$ 's,  $Z$ 's or  $H$ 's (Higgs), are consistently described with just one parameter.

In a more phenomenological approach, the neutral weak current has the form

$$J_{L,R}^0 = \rho(I_3 - Q \sin^2\theta_w)_{L,R}$$

where  $\rho$  measures the ratio of neutral to charged current. We now know that

- a)  $\rho \approx 1$  ( $0.98 \pm 0.05$ ) (ref. 3)
  - b)  $\sin^2\theta_w \approx .2 \sim .3$  ( $.24 \pm .02$ ) (ref. 3)
  - c) left-handed  $q$  and  $l$  are (weak) doublets, and right-handed  $q$  and  $l$  are singlets.
- In other words, the gauge group is  $SU(2)_L \times U(1)$ .

Remarkably, a) and c) were already built into the specific model of Weinberg and Salam. Combining a) and b), one makes the prediction

$$m_W \approx 75 \text{ GeV},$$

$$m_Z \approx 85 \text{ GeV}.$$

So, we should be satisfied that the rather simple and even naive synthesis of electromagnetic and weak currents, with which are associated such names as Schwinger, Glashow, Salam and Weinberg, has been indicated. Following Salam's suggestion in his talk today, I will from now on refer to the two unified interactions as electroweak interaction. It sounds a bit awkward, but certainly does simplify the terminology.

One may also view the above development as a further success of the quark and quark-parton model. The charmed quark, which was an essential ingredient in the development of the theory of weak interactions, is now firmly established as more and more data accumulate regarding the charmed particles. But here nature is playing a little trick with us. The four quarks and four leptons do not seem to be enough, as the minimum theory of weak interactions would have demanded. We have now the  $\tau$  and the  $Y$ .

The  $Y$  has been observed in p-p as well as  $e^+e^-$  interactions, as in the earlier case of the  $J/\psi$ . The new lepton  $\tau$  is so far known only in electron reactions. These "undesirable" particles tell us in unmistakable terms that the world of leptons and quarks is bigger than we thought, quite possibly a lot bigger, and both theorists and experimentalists will

face a busy future in search of more particles and more theories. I will come back to these problems of the future, but let me next turn to the status of strong interaction physics.

The strong interactions affect not only the hadronic reactions, but also semi-leptonic processes that involve electroweak interactions I have just discussed. One of the tests of the quantum chromodynamics (QCD) has to do with the characteristic deviations from the scaling law, *i.e.*, from the naive quark-parton model. Such deviations have been seen for some time, and at least qualitatively they have been showing agreement with QCD predictions. I am impressed by the fact that these deviations seem to be even in quantitative agreement with the predictions of QCD as expressed, for example, by the  $q^2$  dependence of the parton  $x$  distribution, although one may still have to regard it as tentative.<sup>4</sup> Other aspects of QCD, like the presence of jets with computable characteristics, also are beginning to be tested. So one may say that, as far as the high energy or short distance behavior is concerned, QCD with its asymptotic freedom is gaining more and more credentials as the basis for strong interaction dynamics. But, for really critical tests, one would have to go to still higher energies. There is, however, the problem that it is not possible to completely separate strong interaction phenomena into high and low energy, or short and long distance, regimes, and unfortunately the low energy properties of QCD are a greatly more difficult problem over which we do not yet have a firm control. Nonetheless, we are witnessing a great deal of activity in this long distance and strong coupling regime of QCD.

The central question is the dynamics of quark confinement, assuming as one does that confinement is true. It might not be true, as is held by a minority of people, but there is no question about at least a partial confinement. In the meantime, what we have now for low energy hadron dynamics are the string and bag models. Actually one may safely regard these two as representing different aspects of one and the same basic model, namely a thick string = a deformable bag. But when it comes to the details, several different variants emerge.

At the phenomenological and qualitative level, these models seem to be working rather

well in general. We have heard more and more evidence for exotic mesons and baryons having chemical compositions  $q^2\bar{q}^2$ ,  $q^4\bar{q}$ ,  $q^6$ , etc.<sup>5</sup> So those quark compounds that are expected to exist do actually seem to exist. The string-bag models can explain their relative stability by assigning them specific molecular or bond structures. This represents an amusing and welcome return of the intuitive chemistry. At the moment, however, there are various different versions or hypotheses competing with each other, and none of them are yet capable of making quantitatively reliable predictions. If that is asking too much, at least one would like a well defined model to emerge as the most successful one. The different versions can be illustrated by the following examples (Fig. 1).

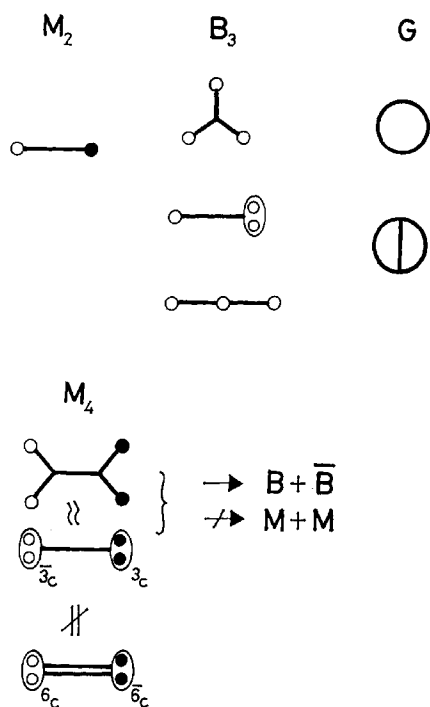


Fig. 1. Different versions for the phenomenological models of hadrons. White circle and black circle represent quark and antiquark, respectively. M, B and G stand for meson, baryon and meson without quarks, respectively. The subscript is the number of quarks and antiquarks in the hadron.

So, roughly speaking, this is what we know about the quarks, leptons and their weak, electromagnetic and strong interactions. In addition to the table of new particles I have

\* The factor 1.5 is an approximate representation of a theoretical and flavor dependent ( $n_f \approx 3$ ) number, not an experimental determination.

shown, there are a few numbers that symbolize our knowledge

$$\sin \theta_c \approx 0.22 \text{ (ref. 6)}$$

$$\sin^2 \theta_w \approx 0.24 \text{ (ref. 3)}$$

$$1/\alpha = 137.035987(29) \text{ (ref. 7)}$$

$$1/\alpha_s \approx 1.5 \ln(Q/\Lambda)^2, * (Q/\Lambda \gg 1,$$

$$\Lambda \approx .4 \sim .8 \text{ GeV) (ref. 4)}$$

$$1/\alpha' \approx 1.1/\text{GeV}^2$$

The last one is the common Regge slope of ordinary hadrons. You will notice that there is a remarkable simplicity in the numbers as well as symbols. But I am also a bit disappointed by the physicists' lack of imagination in the use of symbols.

## §II.

I would next like to come to mainly theoretical problems confronting us, and discuss some of the recent developments in this regard that have been reported at this Conference.

I think it is safe to start from the set of propositions:

a) The leptons and quarks are the elementary constituents of today; that is, particles which are pointlike, and make up the material particles — leptons and hadrons — that are known at the present energy range.

b) There are four kinds of interactions; gravitational, weak, electromagnetic, and strong.

There may well be new kinds of constituents and new kinds of interactions, but we do not know for sure. The leptons and quarks might not be elementary at much higher energies, although the definition of elementarity is never a clear and precise one. There are four flavors coming in two doublets of well established leptons and quarks, plus a fifth lepton  $\tau$ , and a fifth quark indicated by the  $\gamma'$ . It would be safe to supplement the latter two with  $\nu_\tau$  and  $t$  so that there are six flavors or three doublets. The parallelism between the number of leptons and the number of quarks seems interesting, and points to some regularity or symmetry which was emphasized by Gamba, Marshak, Okubo<sup>8</sup> at a time when only three flavors were known. But how many of them will there be eventually? One can only speculate at the moment.

In any case, the existence of at least three flavor doublets makes life interesting. For one thing, the CP violation can be generated through a complex mass matrix as was first noted by Kobayashi and Maskawa.<sup>9</sup> It also poses an intriguing question: What are the masses of  $\nu_\tau$  and  $t$ ?

If  $\nu_\tau$  is massless, it raises the specter (or maybe a welcome thing) of all neutrinos being massless, including those associated with the possible 4th, 5th, . . . generations of lepton doublets. On the other hand, there are cosmological arguments<sup>10</sup> that the number of low mass neutrinos should not be too large ( $\leq 4$  helicity doublets), lest they disturb the scenario for nucleosynthesis. Also there is a nice observation that the number of neutrinos may be determined from the process,<sup>11</sup>  $e^+ + e^- \rightarrow \gamma + \nu + \bar{\nu}$ , and this could give us an answer about low mass neutrinos. If, on the other hand, the  $\nu_\tau$  has a nonzero mass, there is no reason for  $\nu_e$  and  $\nu_\mu$  to be strictly massless and two-component. This would also have significant experimental and theoretical implications. As for the  $t$  quark, it is probably heavier than the  $b$  because lower resonances are not found. Then in both  $(c, s)$  and  $(t, b)$  doublets the first member is the heavier one, in contrast to the  $(u, d)$  doublet, and the leptons. Why? I do not know.

Now if the number of leptons and quarks keeps increasing with energy, we will have to question our premises regarding their elementarity. On the other hand, the number may be finite, and reasonably small, like 6, 8, etc., as some people would like to believe. If it is finite, one would like to know if there is a sensible reason why it is a particular number. Operationally, the number I am talking about is the number of repetitions of the events I have listed in Table I, as we sweep higher and higher energies with bigger and bigger accelerators.\*

But probably the situation will not be that simple. The weak interaction is getting stronger with energy, and will become comparable to the electromagnetic interaction in the 100 GeV center of mass energy range. So some new phenomena are certainly going to happen

\* One can also ask the hypothetical question: What if the ratio  $R = \sigma(e^+e^- \rightarrow X) / \sigma(e^+e^- \rightarrow \mu^+\mu^-)_{\text{QED}}$  should drop to a low value after a series of rises?

beside the afore-mentioned possible repetitions. Our question regarding the number of leptons and quarks might get mired in the confusion, if such repetitions should continue until then.

Let me next turn to the interactions among these constituents. The prevailing assumptions are that

1) All the known interactions are manifestations of gauge fields. A gauge field is characterized by a perfect symmetry principle and long range forces associated with conserved charges.

2) The fact that weak and strong interactions do not seem to show these characteristics is attributed to spontaneous breakdown of symmetry, charge screening (plasma formation), and other special effects. In other words, one regards the vacuum as a complicated medium capable of showing many faces.

3) The gauge fields are considered to be elementary and most desirably renormalizable in the context of quantum field theory, although this last point has not yet been achieved for gravity.

I might also add a fourth and rather popular proposition:

4) It is theoretically desirable, if not necessary, that the different gauge fields be unified under a single large group structure (grand and supergrand syntheses), which is broken down to the observed symmetries in a hierarchy of steps.

The remarkable progress of recent years is certainly due to the success in combining the first three important concepts that are among our theoretical heritages. We have just seen the vindication of the electroweak gauge principle, and the evidence is all pointing towards the validity of the general picture. One can look forward to the next generation of accelerators to produce the weak bosons, follow the QCD predictions, and explore other ingredients of our theoretical framework.

At this point I would like to touch on two different schools of thought regarding strong interactions, although this belongs to the problem of grand synthesis of electroweak and strong interactions to be discussed later. There is a dominant school which postulates

a) Conventional plasma medium for flavor, that is, for the electroweak interactions. The group is  $SU(2)_L \times U(1)$ .

b) A special symmetric SU(3) medium for color, with asymptotic (or maybe temporary) freedom and quark confinement. This is the standard QCD.

A small minority school, of which Pati and Salam are the most ardent advocates, asserts:

a) Same as above.

b) Color symmetry is also broken in a plasma phase, so flavor and color mix. If this happens for the photon, the quarks become integrally charged.

c) Confinement is naturally imperfect; the leptons are quarks of the fourth color. Quarks and gluons exist as real particles, and their masses may not be very high.

To decide experimentally between the two alternatives is not as easy a task as you might think. The nice properties of gauge theory are already incorporated in both. A crucial test of the second model would be of course to find colored states—quarks and gluons, but such a test has to rely on some details of the theory. My personal position on this matter is somewhat ambiguous because I have a little stake in either of the alternatives. The main problem with me is the confinement question. Recently I have been leaning toward the first alternative because: a) We do not see signs of colored excitations; and b) with plasmatic gluons it seems difficult to achieve an imperfect but high degree of confinement implied by the validity of the string model. But this really depends on how convincing is the theoretical derivation of a confinement mechanism. It is possible to produce models of confinement, like models in lower dimensions, or models using magnetically charged quarks placed in a superconducting medium.<sup>12</sup>

Originally, confinement was suggested to be a result of infrared slavery.<sup>13</sup> But we do not know for sure what exactly happens in QCD at long wave lengths. Basically, we need a magnetic and non-Abelian analog of superconductivity in order to trap the quarks. The difficulties lie in mathematically realizing such a medium, especially within the boundaries of the standard QCD. A recent popular idea is to attribute confinement to the workings of instantons and/or merons that may populate the vacuum, as has been most vigorously pursued by the Princeton group.<sup>14</sup> They do not claim to have proven confinement, but

the physical picture is that of an instanton-filled medium in which the dielectric constant tends to zero away from color charges. There is also another model which is closer in spirit to magnetic superconductivity, in a monopole-filled medium. This was originally, advocated by Mandelstam<sup>15</sup> and recently studied by 't Hooft<sup>16</sup> in a quite general context. Unfortunately the relation between this and the Princeton theory based on instanton vacuum is obscure at the moment.

I will next turn to observations of more general nature about gauge theories. One of the remarkable developments in the past few years is the realization that gauge theories are rich in topologically nontrivial configurations. Another related problem which was triggered by the recent work of Gribov,<sup>17</sup> is that non-abelian gauge fields possess a very complex and large phase space, and therefore a very large entropy. By this I mean that the gauge degrees of freedom cannot be factored out in quantum action function by simple gauge fixing, and hence the entropy of the gauge degrees of freedom may play a very important role in determining the nature of the vacuum which corresponds to the minimum of free action density,

$$\Theta = -L - g^2 S,$$

rather than action density  $-L$  as would be the case in classical theory. The coupling constant  $g^2$  plays the role of temperature in this thermodynamic analogy. The usual quantum theory starts from the classical vacuum  $L=0$ , and computes  $S$  due to quantum fluctuations around it. But nontrivial topological configurations with  $-L > 0$ , could lead to a lower action because of the large entropy associated with them, especially at high “temperatures.” So one can talk about “phase transitions” between different vacua as the temperature varies. The significance of various topological configurations or solitons, however, is still in a very early stage of exploration. Among other physical effects caused by instantons are the problem of CP violation and axion.<sup>18</sup> As for the monopoles and strings, their existence as finite energy objects requires the presence of Higgs fields. Besides, the details of all these phenomena depend sensitively on the gauge group and its representation.

This brings me to ultra high energy physics and the grand unification schemes of electroweak and strong interactions. Here I am particularly concerned about the nature of Higgs fields. In the currently prevailing strategies of model building, the most arbitrary and obscure elements are the Higgs fields, which spoil the compelling simplicity of gauge theories. Right now only one doublet of Higgs is called for, which is simple enough. But their Yukawa couplings to quarks and leptons are purely phenomenological. In a grand synthesis, moreover, one would need a large number of Higgs in order to achieve required patterns of symmetry breaking.

The basic reason for this awkward situation seems to me that we do not yet understand the origin of masses; the masses of leptons and quarks do not yet reveal to us any regularity, as did the energy levels of hydrogen and the Regge trajectories of hadrons. In my view, the Higgs fields represent only a phenomenological way of driving masses in gauge theories. We are only at the level of the Ginzburg–Landau description of superconductivity, but not at the level of the BCS theory. To be sure, the G–L theory is enormously useful; besides, renormalizability of Higgs-type theories is an important element which is unique to the relativistic problems. Nevertheless, to bring in more and more Higgs fields, just to achieve a hierarchy of symmetry breaking, looks to me like drawing more and more epicycles. Even if it turns out that only a few Higgs fields are needed, I think one can rightfully ask whether there is a BCS theory behind it. What is a Higgs field a Cooper pair of? Most naively one would say it is a pair of leptons and quarks, especially of heavy ones since they are more strongly coupled to it, but maybe it is made up of new objects with new interactions and new Regge trajectories, as was recently suggested by Susskind.<sup>19</sup>

Let me therefore indulge in a bit of day-dreaming. The time of the scene is not certain, but you can guess from the list\* of future accelerators shown by the previous speaker E. L. Goldwasser.—We have already found several flavors of quarks and leptons with the PETRA and PEP machines. An

\* See the report of E. L. Goldwasser in this Conference.

assortment of multi-100 GeV class proton accelerators of various kinds have also begun operation. People are finding heavy vector and scalar mesons, which appear to fit the characteristics of the  $W$ ,  $Z$  and  $H$ , with masses in the 100 GeV range. As one goes up to higher energies, however, there is a surprise. Invariant mass distributions of clusters of  $W$ 's,  $Z$ 's and  $H$ 's reveal the existence of a series of massive objects reaching into the TeV's. It looks as if the whole pattern of hadron spectrum is being repeated. Some theorists recall that there was a prediction<sup>20</sup> that topological solitons consisting of monopole and string configurations of the  $Z^0$  and  $H$  fields should exist in the form of a Regge sequence of rotating dumbbells and also doughnut states (Fig. 2). Other theorists

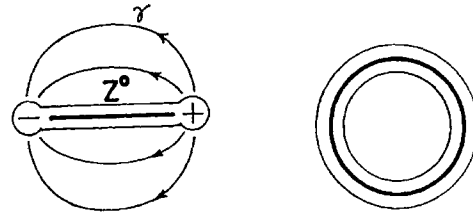


Fig. 2. Dumbbell and Doughnut.

revive Susskind's idea and begin to introduce new heavy constituents with new interactions. Compared to them, the old hadrons and leptons simply become generalized leptons. The  $H$ 's (there may be several kinds) are the lowest  $J=0$  composites in this model. The  $W$ 's and  $Z$ 's are  $J=1$  composites. Thus one repeats all over again Sakurai's vector dominance game. One may feel uneasy about the smallness of the gauge coupling constants and about the status of the photon, (can it be composite?) but let's leave the problems for the future. The spirit of gauge theory is not spoiled because it is primarily a statement of symmetry principle. One may also repeat the chiral symmetry game with analogs of  $\pi$  and  $\sigma$ , the latter being the  $H$ . Are there "low mass" pseudoscalars? Certainly the TeV physics looks exciting.

### §III.

Now, let us come back to other theoretical speculations. Actually they encompass a whole hierarchy of theories leading to the ultimate ones which would unify all the known

and unknown particles and fields in one sweep.<sup>21</sup> One may classify them into three broad categories:

1. Enlargement of flavor group and its representation content.  $SU(2)_L \times U(1) \subset G_f$
2. Grand synthesis of color and flavor groups.
3. Supergrand synthesis of all boson and fermion fields from gravity to Higgs.

The first one is partly motivated by the increasing number of flavors. One may also ask the questions: Why do the left and the right behave so differently in the flavor sector? Shouldn't there be some left-right symmetry, and shouldn't there be only one coupling constant for a unified theory?

From a theoretical point of view, probably it is impossible to separate flavor and color; one must go to the grand or supergrand unification scheme in order to understand either of them. There is indeed a possibility of a large unifying group with a single coupling constant, to which all the effective coupling constants converge at a huge unification energy. Minimum theories that have been proposed include  $SU(5)$ ,  $SU(6)$ ,  $SO(10)$  and  $E_6$  groups.<sup>21</sup> Here the basic properties of renormalizable field theories, especially the concept of running coupling constants, are pushed to their logical conclusion, as was first done by Landau.<sup>22</sup> The unification energy is usually of the order (on a logarithmic scale) of the Planck mass  $\sim 10^{19}$  GeV (or  $10^{-5}$  g), which gives one an incentive to unify gravity as well. In some theories such as the one advocated by Salam and Pati, it is only  $\sim 10^4$  GeV. In this case the proponents may have a hope of seeing their dreams come true or be shattered within their lifetimes.

Any such grand unification scheme naturally invites the possibility of baryon number non-conservation. For there is no evidence for a long range gauge field coupled to baryon number, as was once pointed out by Lee and Yang.<sup>23</sup> Thus, the baryon number must correspond to a broken local (gauged) symmetry or a global (non-gauged) symmetry. In either case the conservation may be violated. The present limit of proton lifetime<sup>24</sup> is  $\sim 10^{30}$  years. It seems possible to arrange a theory to yield a finite yet long enough lifetime. It should be an exciting event if the lifetime

turned out to be indeed finite and measurable. Another intriguing question concerns the total baryon number of the universe. Why does the number appear to have an asymmetry  $\sim 10^{80}$ , which is numerically huge, but is a small fraction ( $\sim 10^{-9}$ ) of the number of photons. The question may be answerable within the gauge theory framework.<sup>25</sup>

At this level of unification, what else can one say? The Weinberg angle is calculable because it depends on the way the quarks decompose under the chain  $G_{\text{flavor}} \rightarrow SU(2)_L \times U(1)$ , apart from renormalization corrections away from the unification energy. Basically, the value for  $\sin^2 \theta_w$  should not be too far away from 1/4. If all left-handed fermions form  $SU(2)$  doublets and all right-handed fermions are singlets, one has<sup>26</sup>

$$\sin^2 \theta_w \approx 3/8 = 0.375,$$

which may be acceptable, considering the renormalization effects. If integer charges are effectively assigned to the four flavors at low energies,<sup>27</sup> one has

$$\sin^2 \theta_w \approx 1/4,$$

which looks nice.

As I have already said, the basic problem is our ignorance of the dynamics of mass spectrum generation, that is, why the spectrum looks the way it does, with no obvious regularities. In current gauge theories one is simply trading Higgs parameters for fermion masses. A more satisfying way might be found by considering both fermions and Higgses in a unified fashion.

Composite models of Higgses and perhaps also of quarks and leptons are, of course, a possibility which I have already discussed. In particular, all bosons are reduced to fermion composites in the Fermi-Yang-Heisenberg-Sakata type theories. They represent a monistic point of view in contrast to the dualism which separates particles and fields. The prevalent view as well as my own has been along the latter line. This is because the fields have a universal guiding principle, that is, the gauge theory, whereas the material part does not have one, and looks terribly complicated and arbitrary. This situation was already present in Einstein's observation concerning his equation

$$R_{\mu\nu} - 1/2 g_{\mu\nu} R = -T_{\mu\nu}.$$



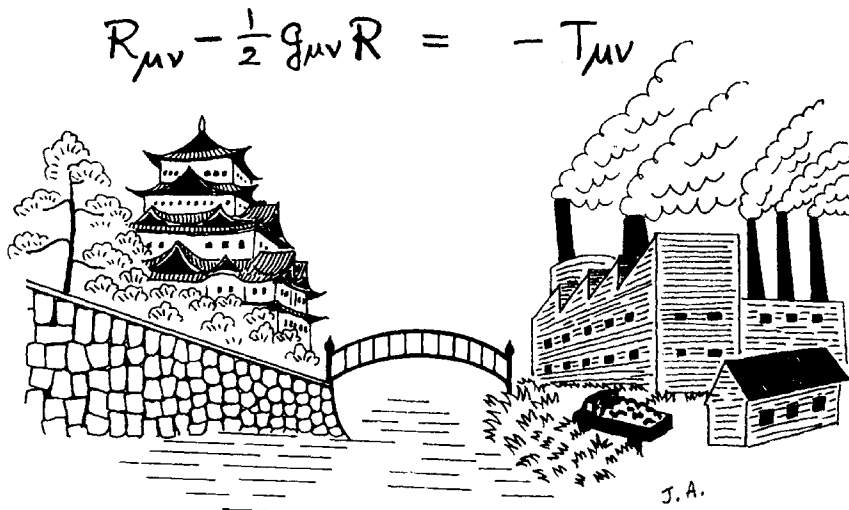


Fig. 3.

To quote: “[the equation] is similar to a building, one wing of which is made of fine marble, but the other wing of which is made of low grade wood.”<sup>28</sup> The following is a pictorial rendition of Einstein’s theme by Dr. Jiro Arafune, the house cartoonist at KEK (Fig. 3). From this point of view, the Heisenberg–Sakata approach is an attempt to make the whole building symmetric by replacing marble with wood everywhere. But it may have its own appeal, and there are quite a few people pursuing this road. Probably I contributed to this trend unwittingly when Jona-Lasinio and I proposed the superconductivity model<sup>29</sup> borrowing the mathematical techniques of BCS and Heisenberg.

An alternative approach, which amounts to building everything with marble, and about which we have heard the latest developments at this Conference, is the unification via supersymmetry and supergauge principle. This has the capacity to hold all bosons and fermions from spin 2 down to 0, which include gravitons, gravitinos, gauge bosons, quarks and leptons, and Higgses. The only new appearance is the spin 3/2 gravitino field. One of the attractive features of this framework, beside the obvious ones, has been the possibility of making everything renormalizable, gravity included. Unfortunately, this hope seems to be on rather shaky grounds at the moment. Furthermore, the problem of mass still persists. Since a gauge theory, whether ordinary or supersymmetric, is a theory of massless fields to begin with, it is not easy to predict the patterns of mass spectra that can be

dynamically generated. I am not sure that this noble goal of a unification of field and matter, whether in terms of marble, or in terms of wood, can be achieved in a really meaningful way. There is no doubt, however, that the gravity must become an essential ingredient in particle physics, and vice versa. For example, the topological solitons are already being studied in these extended gauge theories. One might speculate that the geometrical richness of gauge principle will lead to interesting and detectable consequences in quantum gravity. I remind you that gravitational waves, not to speak of gravitons, are yet to be detected. Our road is rosy, but surely it will be a long one. I will close my talk with a quotation which I believe should represent the spirit of a gathering such as the one we have just gone through:

“Our science, which we loved above everything, had brought us together. It appeared to us as a flowering garden. In this garden there were well-worn paths where one might look around at leisure and enjoy oneself without effort, especially at the side of a congenial companion. But we also liked to seek out hidden trails and discovered many an unexpected view which was pleasing to our eyes: and when the one pointed it out to the other, and we admired it together, our joy was complete.”

—David Hilbert (memorial address for Hermann Minkowski)<sup>30</sup>

#### References

1. S. Weinberg: *Phys. Rev. Letters* **19** (1967) 1264;

- Phys. Rev. **D5** (1971) 1412; Abdus Salam: *Elementary Particle Theory*, edited by N. Svartholm (Almqvist and Wiksell Stockholm, 1968) p. 367.
2. R. E. Taylor: a talk in this Conference.
  3. G. Altarelli: a talk in this Conference, and C. Baltay: a talk in this Conference.
  4. See the reports of E. Gabathuler and K. Tittel in this Conference, for example.
  5. See the report of Y. Hara in this Conference, for example.
  6. See Weinberg's report in this Conference, and R. E. Shrock and L. L. Wang, Princeton Univ. preprint.
  7. See the report of T. Kinoshita in this Conference.
  8. A. Gamba, R. E. Marshak and S. Okubo: Proc. Nat. Acad. Sci. **45** (1959) 881.
  9. M. Kobayashi and T. Maskawa: Progr. theor. Phys. **49** (1973) 652.
  10. G. Steigman, D. N. Schramm and J. E. Gunn: Phys. Letters **66B** (1977) 202. See also the report of S. Weinberg in this Conference.
  11. E. Ma and J. Okada: Phys. Rev. Letters **41** (1978) 281; D. N. Schram: Enrico Fermi Inst. preprint 78-25. See also the report of S. Weinberg in this Conference.
  12. See the report of B. Sakita in this Conference.
  13. S. Weinberg: Phys. Rev. Letters **31** (1973) 494.
  14. C. G. Callan and also D. J. Gross: talks in this Conference.
  15. S. Mandelstam: in *Extended Systems in Field Theory* (edited by J. L. Gervais and A. Neveu, Phys. Rep. **23C** (1976) 237).
  16. G.'t Hooft: Utrecht preprint (1977).
  17. V. N. Gribov: Nucl. Phys. **B139** (1978) 1. See also ref. 12.
  18. R. Peccei and H. Quinn: Phys. Rev. Letters **38** (1977) 1440; Phys. Rev. **D16** (1977) 1791; S. Weinberg: Phys. Rev. Letters **40** (1978) 223; F. Wilczek: *ibid.* **40** (1978) 279.
  19. L. Susskind: SLAC preprint SLAC-PUB-2142 (1978).
  20. Y. Nambu: Nucl. Phys. **B130** (1977) 505; M. B. Einhorn and R. Savit: Phys. Letters **77B** (1978) 295.
  21. See the report of A. Salam in this Conference.
  22. L. D. Landau: *Niels Bohr and the Development of Physics*, ed. W. Pauli (McGraw-Hill Co., New York, 1955) p. 52.
  23. T. D. Lee and C. N. Yang: Phys. Rev. **98** (1955) 1501.
  24. F. Reines and M. F. Crouch: Phys. Rev. Letters **32** (1974) 493; L. Bergamasco and P. Picchi: Letters Nuovo Cimento **11** (1974) 636.
  25. For an attempt along this line, see M. Yoshimura: Phys. Rev. Letters **41** (1978) 281.
  26. See for example H. Georgi and S. L. Glashow: Phys. Rev. Letters **32** (1974) 438.
  27. J. C. Pati and A. Salam: Phys. Rev. Letters **31** (1973) 661. See also ref. 19.
  28. A. Einstein: *Out of My Later Years* (Philosophical Library, Publishers, New York, 1950) p. 83.
  29. Y. Nambu and G. Jona-Lasinio: Phys. Rev. **122** (1961) 345.
  30. As quoted by S. Chandrasekhar: in *Shakespeare, Newton, and Beethoven, or Patterns of Creativity*, the Nora & Edward Ryerson Lecture, 1975, Univ. Chicago.
-